

Cyclo- and Cyclized Diene Polymers. IV. Infrared Spectra of Cyclopolyisoprenes and Cyclized Polyisoprenes*

I. KÖSSLER, J. VODEHNAL, and M. ŠTOLKA, *Institute of Physical Chemistry, Czechoslovak Academy of Sciences, Prague, Czechoslovakia*

Synopsis

The infrared absorption bands which appear in cyclized polyisoprenes (*cis*-1,4-, *trans*-1,4-, and 3,4-) and in ladder cyclopolyisoprenes have been divided into three groups: (1) absorption bands typical of six-membered saturated rings, (2) bands characteristic of endgroups, and (3) absorption bands which have their origins in chemically bound solvent from transfer reactions. The assignment of these bands to probable modes of vibration has been made.

INTRODUCTION

Cyclization of polyisoprenes²⁻⁴ and direct cyclopolymerization of isoprene^{1,4-8} lead to the formation of cyclic structural units with single or fused six-membered rings. The cyclic segments are sometimes separated by linear segments.

In this paper an attempt is made to interpret the infrared spectra of both the cyclopolyisoprenes and of the cyclized units in a copolymer of linear and cyclic structures.

EXPERIMENTAL

Polymers

Polymers with cyclic units were obtained by cyclization of *cis*-1,4-polyisoprene (hevea), *trans*-1,4-polyisoprene (balata), and 3,4-polyisoprene³ or by cyclopolymerization of monomeric isoprene.^{1,4-8}

Infrared Spectra

Infrared spectra were recorded on a Zeiss UR-10 spectrometer provided with a lithium fluoride prism (3500-1800 cm^{-1}), a sodium chloride prism (1800-700 cm^{-1}), and a potassium bromide prism (700-400 cm^{-1}). Samples were prepared by the potassium bromide pellet technique. The amount of polymer in a 13-mm. diameter pellet was approximately 3 mg. in 300 mg. of potassium bromide.

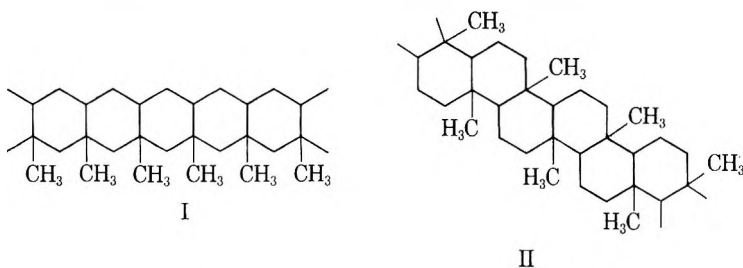
* Part III, see Kössler, Štolka, and Mach.¹

Chemical Treatment of Cyclopolymers

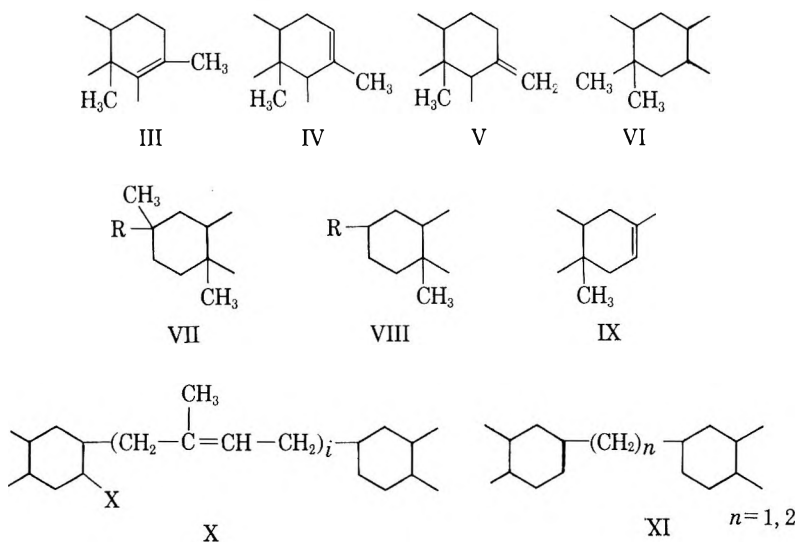
The polymers were exposed to bromine vapor for 4 days at 10°C. Hydrogenation was accomplished in solution with the use of Raney nickel catalyst at 200°C. and 200 atm.

RESULTS AND DISCUSSION

Two principal structures may exist in double-chain cyclopolymers: a perhydroanthracene type (I) or a perhydrophenanthrene type (II).



The infrared spectra of these structures will be characterized by a series of absorption bands of CH vibrations. In addition to the absorption bands which are characteristic for the structural forms I and II, absorption bands for different endgroups III-IX where R is alkyl, aryl, or alkenyl will appear in the infrared spectra.



The structures III, IV, and V are expected in cyclized 1,4-poly-isoprene. Corresponding structures with di-, tri-, and tetrasubstituted carbon-carbon double bonds are also to be expected in cyclized 3,4-polyisoprenes. The structures VII, VIII, and IX may be expected in cyclopolymers. The structure VI appears in cyclized 3,4-polyisoprene.

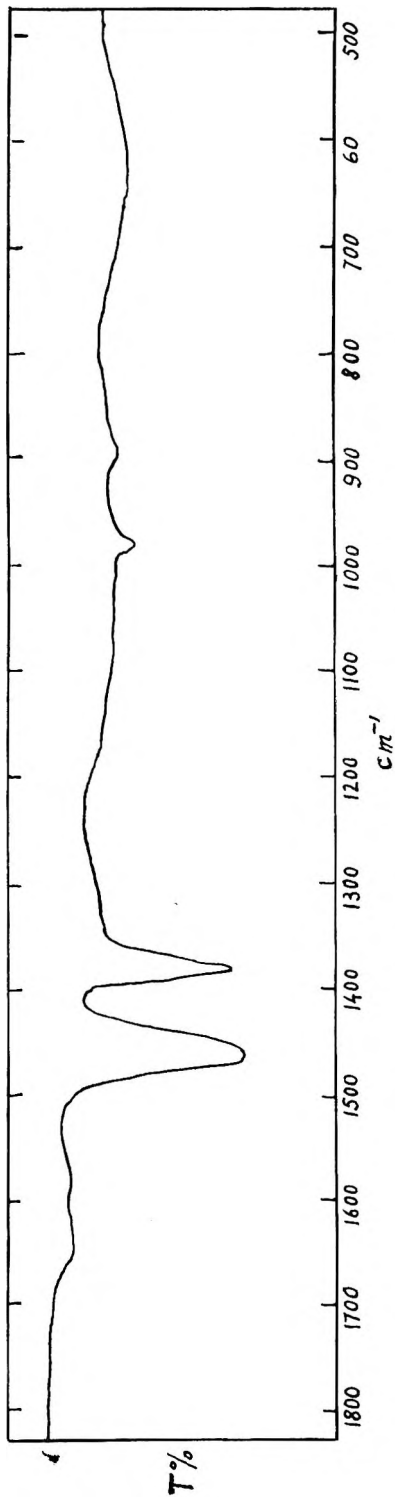


Fig. 1. Infrared spectrum of cyclopolyisoprene.

Cyclized segments may be connected through segments of linear polyisoprene or by other linear groups. Polyisoprene linear units may be of either the 1,4- or 3,4- (1,2-) type. Other absorption bands may appear when cyclopolymerization or cyclization is carried out in solution. These are due to the solvent molecules (X) chemically bound into the polymer⁶ and there may be more than one of these groups per polymer chain (see structure X).

The spectrum of cyclopolyisoprene with the lowest content of structures other than fused cyclic structures is shown in Figure 1. The wave numbers of absorption bands and their assignment to the vibration modes are listed in Table I. At the concentration of polymer in the KBr pellet indicated in the experimental section, no other absorption bands are observed.

TABLE I
Wave Numbers of Absorption Bands for CH and C—C
Vibrations in Cyclic Segments

| Band wave number, cm.^{-1} | Mode of vibration |
|-------------------------------------|--|
| 2950 | CH stretching of $-\text{CH}_3$, asymmetrical |
| 2920 | CH stretching of $-\text{CH}_2$, asymmetrical |
| 2900 | CH stretching of $-\text{CH}$ |
| 2865 | CH stretching of $-\text{CH}_3$, symmetrical |
| 2850 | CH stretching of $-\text{CH}_2$, symmetrical |
| 1465 | CH deformation of $-\text{CH}_2$ and $-\text{CH}_3$, asymmetrical |
| 1382 | CH deformation of $-\text{CH}_3$, symmetrical |
| 985 | C—C stretching of $-\text{C}-\text{CH}_2$ in ring (?) |

Of the C—H stretching vibrations, the strongest is the 2920 cm.^{-1} band. The intensities of the 2950 , 2865 , and 2850 cm.^{-1} bands are much weaker. Only a trace of the 2900 cm.^{-1} band appears.

The 2920 cm.^{-1} C—H stretching vibration band (asymmetric) in the $-\text{CH}_2-$ group is at the same wave number as in linear 1,4- and 3,4-polyisoprenes. The band of the asymmetric $-\text{CH}_3$ stretching vibration is at 2950 cm.^{-1} and of the symmetric vibration at 2865 cm.^{-1} . The 2950 cm.^{-1} band is shifted to lower wave numbers when compared to its usual position in linear polyisoprenes, i.e., 2960 cm.^{-1} . Ciampelli⁹ gives the following values: 2959 – 2976 cm.^{-1} for $-\text{CH}_3$ asymmetric and 2865 – 2874 cm.^{-1} for $-\text{CH}_3$ symmetric vibrations, all in carbon tetrachloride solution. The 2850 cm.^{-1} C—H stretching band (symmetric) in the $-\text{CH}_2-$ group is at approximately the same position as in linear polymers. The 2900 cm.^{-1} band of tertiary carbon C—H stretching is so small that it appears only as an indication on the shoulder of the 2920 cm.^{-1} band.

The very strong band at 1465 cm.^{-1} is assigned to two deformation vibrations, i.e., of $-\text{CH}_2-$ (higher wave number) and of $-\text{CH}_3$ (lower wave

TABLE II
Ratio of Optical Densities of CH_2/CH_3 Vibrations in Rings and Linear Chains

| Polymer | $D(1460)/D(1380)$ | Maximum wave number, cm^{-1} |
|-------------------|-------------------|---------------------------------------|
| <i>cis</i> -1,4 | 1.66 | 1450 |
| <i>trans</i> -1,4 | 1.67 | 1450 |
| 3,4- | 1.14 | 1455 |
| Cyclopolymer | 1.20 | 1460 |

number). The frequency of the $-\text{CH}_2-$ vibration in a ring is higher than that in a linear chain. As shown in Table II, the ratio of the optical densities at 1380 cm^{-1} and approximately 1460 cm^{-1} is lowered.

The wave number of the $-\text{CH}_3$ symmetric deformation vibration on a quaternary carbon, as in structures I and II, is slightly shifted to higher wave numbers in all cyclized polyisoprenes and cyclopolyisoprenes as compared with linear *cis*-1,4-polyisoprene.

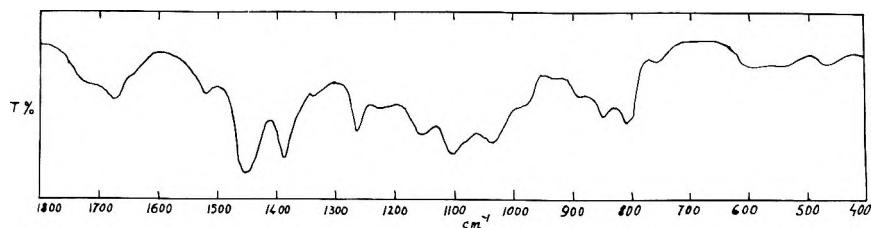


Fig. 2. Infrared spectrum of cyclized balata.

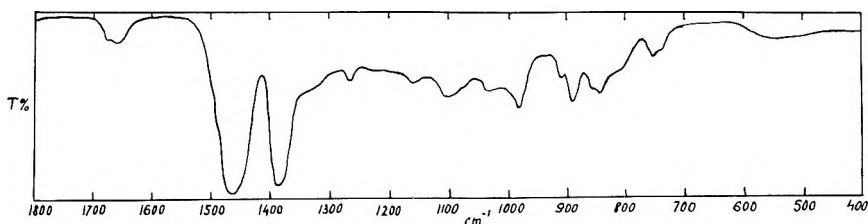


Fig. 3. Infrared spectrum of cyclopolyisoprene with high amount of endgroups.

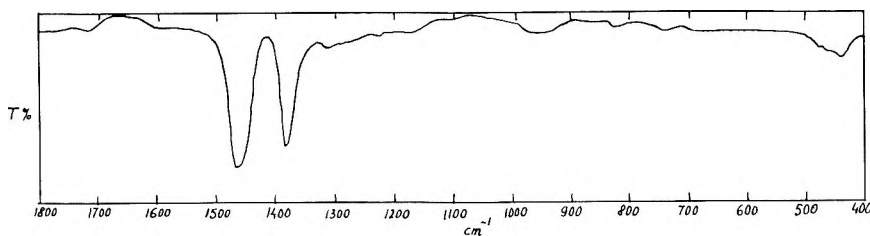


Fig. 4. Infrared spectrum of hydrogenated cyclopolyisoprene.

The 985 cm.^{-1} band appears as a more or less intense band in almost all polymers with several fused rings. It is weak in the case of cyclized 3,4-polyisoprene and cyclopolymers but is more intense in the case of cyclized 1,4-polyisoprene. It disappears on bromination and increases in width on hydrogenation. It appears in the spectrum of liquid decalin (972 cm.^{-1}), 1,9-octalin (990 cm.^{-1}), *trans*-1,2-octalin (980 cm.^{-1}), and *cis*-1,2-octalin (962 cm.^{-1}).

To decide on the basis of infrared examination whether the polymer is of perhydroanthracene type (I) or perhydrophenanthrene type (II) structure or whether the rings in these structures are of *cis* or *trans* (boat or chair) conformation is at present impossible.

The values of wave numbers of absorption bands typical of vibrations of the endgroups are listed in Table III. These bands are very distinct in the cyclized polymers³ (Fig. 2) and in some cyclopolymers (Fig. 3) but they disappear on bromination and hydrogenation of the polymer (Fig. 4).

The very weak 3070 cm.^{-1} C—H stretching vibration for the $=\text{CH}_2$ group appears in cyclized polyisoprenes and is accompanied by the 890 cm.^{-1} band. The $=\text{CH}_2$ group appears in the endgroup structure (V) as an exomethylene group. This 3070 cm.^{-1} band is present in the spectrum of methylenecyclohexane, but its intensity as well as that of the 890 cm.^{-1} band is less than that of isopropenyl groups. The $=\text{CH}_2$ group should also be present as an endgroup in VII and VIII when R is vinyl or isopropenyl.

The 1665–1670 cm.^{-1} bands are assigned to C=C stretching vibrations of a tri- or tetrasubstituted ethylenic double bond. The 1670 cm.^{-1}

TABLE III
Wave Numbers of Absorption Bands Typical of Endgroup Structures

| Band wave number, cm.^{-1} | Mode of vibration |
|-------------------------------------|--|
| 3070 | CH stretching of $=\text{CH}_2$ (exomethylene) |
| 1670 | C=C stretching of $\text{R}_1\text{R}_2\text{C}=\text{CR}_3\text{R}_4$ |
| 1665 | C=C stretching of $\text{R}_1\text{R}_2\text{C}=\text{CR}_3\text{H}$ |
| 1650 | C=C stretching of $\text{C}=\text{CH}_2$ |
| 1410 | CH in plane deformation of $\text{C}=\text{CH}_2$ |
| 1370 } 1385 } | Doublet of CH deformation of two $-\text{CH}_3$ groups on the same carbon |
| 1330–1350 | |
| 1265 | |
| 1160 | C—C stretching in $=\text{C}-\text{CH}_2-$ in ring |
| 1100 | C—C stretching in $=\text{C}-\text{CH}_3$ |
| 1040 | $-\text{CH}$ rocking in $=\text{C}-\text{CH}_3$ |
| 985 | |
| 910 | Out-of-plane $=\text{CH}_2$ deformation in $\text{CH}_2=\text{CH}-$ |
| 890 | Out-of-plane $=\text{CH}_2$ deformation in $\text{CH}_2=\text{CR}_1\text{R}_2$ |
| 850–860 | Out-of-plane $-\text{CH}$ deformation in $-\text{C}(\text{CH}_3)=\text{CH}-$ |
| 810 | |

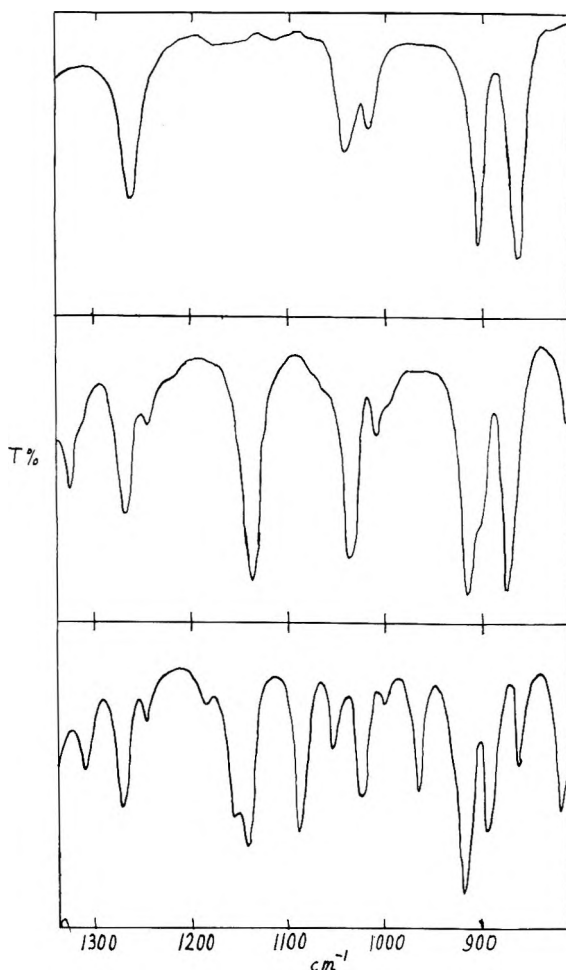


Fig. 5. Infrared spectra of (a) cyclohexane, (b) cyclohexene, (c) methylcyclohexene.

band appears in partially cyclized hevea and balata and is characteristic of the endgroup III and IV. The 1650 cm.^{-1} band is assigned to exomethylene >C=CH_2 in the endgroup V. In methylenecyclohexane it is situated at 1652 cm.^{-1} and is accompanied by the 890 and 3070 cm.^{-1} bands.

The 1410 cm.^{-1} band is very weak in intensity and is ascribed to the C—H in plane deformation vibration in the C=CH_2 group. It appears in cyclized balata and is accompanied by the 890 and 1650 cm.^{-1} bands.

The band for the C—H deformation vibration in —CH_3 groups in the spectrum of cyclized 3,4-polyisoprene splits into a doublet with maximum absorptions at 1370 and 1385 cm.^{-1} . This split is a result of the formation of the initial segment of the chain (VI).

In the infrared spectra of samples which are characterized by strong absorption bands typical of endgroups III–IX, new weak absorption

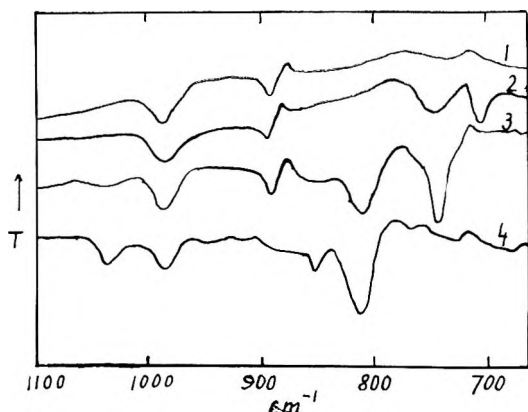


Fig. 6. Infrared spectra of cyclopolyisoprene prepared in (1) heptane (2) benzene, (3) toluene, (4) xylene.

bands appear in the range of 1330–1350 cm^{-1} . These belong to various C—H vibrational modes in connection with the C=C group.

The 1265 cm^{-1} band appears in all cyclized polyisoprenes and in some cyclopolyisoprenes. In the spectra of linear polymers as well as cyclopolyisoprenes in which the 800–920 cm^{-1} bands of endgroups are absent, the 1265 cm^{-1} band is also absent. Therefore it is assigned to some vibration in a monocyclic structure.

In the region of C—C stretching and C—H rocking vibrations, 1160, 1100, and 1040 cm^{-1} bands appear. This is especially so in samples which had been cyclized to a relatively small degree and in which several types of endgroups are present, i.e., III and IV. The 1160 cm^{-1} absorption

band is assigned to a C—C stretching vibration in the $-\text{CH}_2-\overset{\text{C}}{\text{=}}$ group. Binder¹⁰ has found this band in diprene and dipentene (8.6 μ). The corresponding bands in linear polyisoprenes are at 1150 cm^{-1} (*trans*) and 1130 cm^{-1} (*cis*) which we have assigned to the same vibration rather than to a $=\text{C}-\text{CH}_3$ vibration.

The 1100 cm^{-1} band is assigned to a C—C stretching vibration in the $=\text{C}-\text{CH}_3$ group, and the 1040 cm^{-1} band to $-\text{CH}_3$ rocking in the same group. These groups are found in the endgroups III and IV. Binder¹⁰ finds similar bands between 9 and 9.8 μ (1020–1100 cm^{-1}).

Assignment of vibrations to the bands mentioned above is in accord with absorption bands found in cyclohexane, cyclohexene, and methylcyclohexene (Fig. 5). Introducing one C=C group into a saturated ring gives rise to new vibrations of $-\text{CH}_2-\text{C}=\text{}$ and thus the band at 1140 cm^{-1} . Introducing a methyl group then induces new bands at 1055 and 1090 cm^{-1} and the splitting of the 1140 cm^{-1} band into two bands, at 1140 and 1160 cm^{-1} .

The 1160, 1100, and 1040 cm^{-1} absorption bands are accompanied by out-of-plane =CH vibration bands. These vibrations are characterized

by bands at 910, 890, and 850–860 cm^{-1} , respectively. The 910 cm^{-1} band is virtually absent in all cyclopolymers. It is due to the CH_2 out-of-plane vibration of the $-\text{CH}=\text{CH}_2$ group, which may occur in the endgroup VII or in uncyclized 1,2-linear units between cyclic segments.

The 890 cm^{-1} band which is typical of the same vibration of the $\text{CH}_2=\text{C}$ group appears more frequently. This appears in endgroups V and VIII where R is isopropenyl. The 850–860 cm^{-1} band is assigned to the CH out-of-plane vibration in the $-\text{C}(\text{CH}_3)=\text{CH}-$ group in the ring, as in endgroup IV. It is shifted about 10–20 cm^{-1} to higher wave numbers as compared with linear 1,4-polymers.

In Table IV are listed the wave numbers of typical absorption bands which result from solvent molecules chemically bound to the polymer molecule. Solvent molecules participate in chain transfer reactions in cyclopolymerization^{1,6} and in cyclization.³

TABLE IV
Wave Numbers of Absorption Bands Due to Solvent Incorporation in Chain

| Solvent | Typical absorption bands, cm^{-1} | | | | |
|---------|--|------|-----|------|------|
| Benzene | 700 | 740 | | | |
| Toluene | | ~740 | 810 | 1515 | 1610 |
| Xylene | | | 805 | 1510 | 1615 |

The infrared spectra of cyclopolyisoprenes polymerized in aromatic solvents are presented in Figure 6.

The alternation of cyclic and linear segments (see structure X), when $i > 4$ gives rise to absorption bands which are known from the infrared spectra of linear polyisoprenes. If number of units in the linear segment is small ($i < 4$), it is possible that a shift of some absorption bands may occur.¹¹ The presence of $-\text{CH}_2-$ groups in the ring and in linear segments causes broadening and deformation of the 1450–1465 cm^{-1} band, as well as slight deformation of the 1380 cm^{-1} band.

References

1. Kössler, I., M. Štolka, and K. Mach, *J. Polymer Sci.*, **C4**, 977 (1963).
2. Golub, M. A., and J. Heller, *Can. J. Chem.*, **41**, 937 (1963).
3. Štolka, M., J. Vodehnal, and I. Kössler, *J. Polymer Sci.*, **A2**, 3987 (1964).
4. Gaylord, N. G., I. Kössler, M. Štolka, and J. Vodehnal, *J. Am. Chem. Soc.*, **85**, 641 (1963).
5. Gaylord, N. G., I. Kössler, M. Štolka, and J. Vodehnal, *J. Polymer Sci.*, **A2**, 3969 (1964).
6. Štolka, M., unpublished results.
7. Kössler, I., and I. Dolezal, in preparation.
8. Matyska, B., K. Mach, J. Vodehnal, and I. Kössler, *Collection Czech. Chem. Commun.*, in press.
9. Ciampelli, F., and I. Manovicu, *Gazz. Chim. Ital.*, **91**, 1045 (1961).

10. Binder, J. L., K. C. Eberly, and G. E. P. Smith, Jr., *J. Polymer Sci.*, **38**, 229 (1959).

11. Kössler, I., and J. Vodehnal, *J. Polymer Sci.*, **B1**, 415 (1963).

Résumé

Les bandes d'absorption infra-rouges, qui apparaissent dans les polyisoprènes cycliques (*cis*-1,4-, *trans*-1,4-, et 3,4-) et les cyclopolyisoprènes en échelle, ont été classées en 3 groupes. (1) les bandes d'absorption caractéristiques des noyaux saturés à six membres; (2) celles caractéristiques des groupes terminaux (3) celles qui ont pour origine le solvant lié chimiquement par réaction de transfert. On a attribué ces bandes d'absorption aux modes probables de vibration.

Zusammenfassung

Die Infrarotabsorptionsbanden, die bei cyclisierten Polyisoprenen (*cis*-1,4-, *trans*-1,4-, und 3,4-) und bei Leitercyklopolyisoprenen auftreten, wurden in drei Gruppen eingeteilt: (1) Typische Absorptionsbanden für sechsgliedrige gesättigte Ringe, (2) charakteristische Endgruppenbanden und (3) Absorptionsbanden, die auf chemisch gebundenes Lösungsmittel aus Übertragungsreaktionen zurückgehen. Die Zuordnung dieser Banden zu wahrscheinlichen Schwingungen wurde durchgeführt.

Received October 27, 1964
(Prod. No. 4570A)

Structural Study of Phenol-Formaldehyde Polymers with Proton Magnetic Resonance*

ROBERT C. HIRST,† DAVID M. GRANT, RAYMOND E. HOFF,‡
and WILLIAM J. BURKE,§ *Department of Chemistry, University of Utah,
Salt Lake City, Utah*

Synopsis

Proton magnetic resonance spectra were obtained for a number of representative phenol-formaldehyde dimers and trimers of known structure and for related compounds having methyl or chloro substituents on the aromatic ring. The data thus obtained, particularly for the methylene protons, were used in the interpretation of the structure of well characterized, linear phenol-formaldehyde polymers and the corresponding halogenated polymers prepared by the condensation of *o*- and *p*-chlorophenol with formaldehyde. In all cases there was a shift to lower field as the methylene linkage was varied from *para-para* to *ortho-para* to *ortho-ortho*, although in certain instances the *ortho-para* and *ortho-ortho* peaks moved very close together. The spectra obtained indicated that the condensation of *o*-chlorophenol with formaldehyde proceeds in an essentially random manner, since the ratio of *ortho-ortho* to *ortho-para* to *para-para* methylene linkages was found to be 1:2:1, within the limits of experimental error. The preliminary results obtained in this work clearly demonstrate the potential utility of PMR as a valuable tool in the characterization of the highly complex products obtained from phenol-formaldehyde systems.

INTRODUCTION

Considerable progress has been made in elucidating the structure of phenol-formaldehyde polymers and the nature of the complex reactions leading to their formation. Much of this work^{1,2} has involved the use of substituted phenols in model reactions as a route to well defined intermediates which could be characterized. The complexity of the structure of phenol-formaldehyde polymers is indicated by the enormous number of possible relatively low molecular weight products. For example, with a novolac having only nine phenolic units (MW 942) there are approximately 85,000 isomers, 4401 of which are linear.

In work directed toward the correlation of structural features with important physical and chemical properties, several types of linear phenol-formaldehyde polymers were prepared and characterized in this labora-

* Presented in part at the Conference on Analytical Chemistry and Applied Spectroscopy in Pittsburgh, Pa., March, 1962.

† Present address: Socony Mobil Oil Company, Princeton, New Jersey.

‡ Present address: B. F. Goodrich Company, Cuyahoga Falls, Ohio.

§ Present address: Arizona State University, Tempe, Arizona.

tory.³⁻⁶ Infrared spectra proved to be most useful in these studies since specific absorption bands were readily associated with important types of repeating units in the polymers. For example, the presence of relative amounts of 2,4-, 2,6-, and 2,4,6-substituted phenolic repeating units in the polymers were readily detected, and at least a rough comparison of molecular weights was possible through a study of bands resulting from the presence of 2- or 4-substituted endgroups. In addition, study of the reactions of these polymers such as their nitrosation and nitration was greatly facilitated by noting changes in the infrared spectra as the reaction proceeded.⁷

The use of infrared data has contributed extensively to a better understanding of the structure of phenol-formaldehyde polymers, particularly with respect to the various positions substituted on the individual repeating phenolic units. However, these studies have not provided information on the relative distribution of the methylene bridges between *ortho-ortho*, *ortho-para*, and *para-para* positions of adjacent phenolic linkages in the polymers, except for the all *ortho-ortho* substituted series.

EXPERIMENTAL APPROACH

Proton magnetic resonance spectroscopy has proved to be a valuable tool in the determination of structure of a wide variety of complex molecules including stereoregular polymers, since minute differences in the electronic structure give rise to characteristic chemical shifts in the spectra. Accordingly, a proton magnetic resonance study of phenol-formaldehyde dimers and trimers of known structure and of well characterized linear phenol-formaldehyde polymers was undertaken with the intent of relating the specific molecular structure of the methylene groups with a corresponding value for the chemical shift. The availability in this laboratory of a number of model compounds of previously determined structure greatly facilitated the establishment of criteria upon which future structural assignments may be based.

RESULTS AND DISCUSSION

Phenol-Formaldehyde Dimers and Trimers

Condensation of phenol with formaldehyde under acidic conditions at elevated temperatures results in the introduction of a methylene bridge between one of the highly reactive *ortho* or *para* positions on one phenol molecule and an *ortho* or *para* position on the next phenolic unit.¹ A given methylene bridge is designated as *para-para* (I), *ortho-para* (II), or *ortho-ortho* (III) depending upon the position of hydroxyl groups on adjacent aromatic rings relative to the methylene bridge. The results of this study have shown that there are small but characteristic chemical shifts for each of these three different configurations in dimers and trimers and also in various linear polymers.

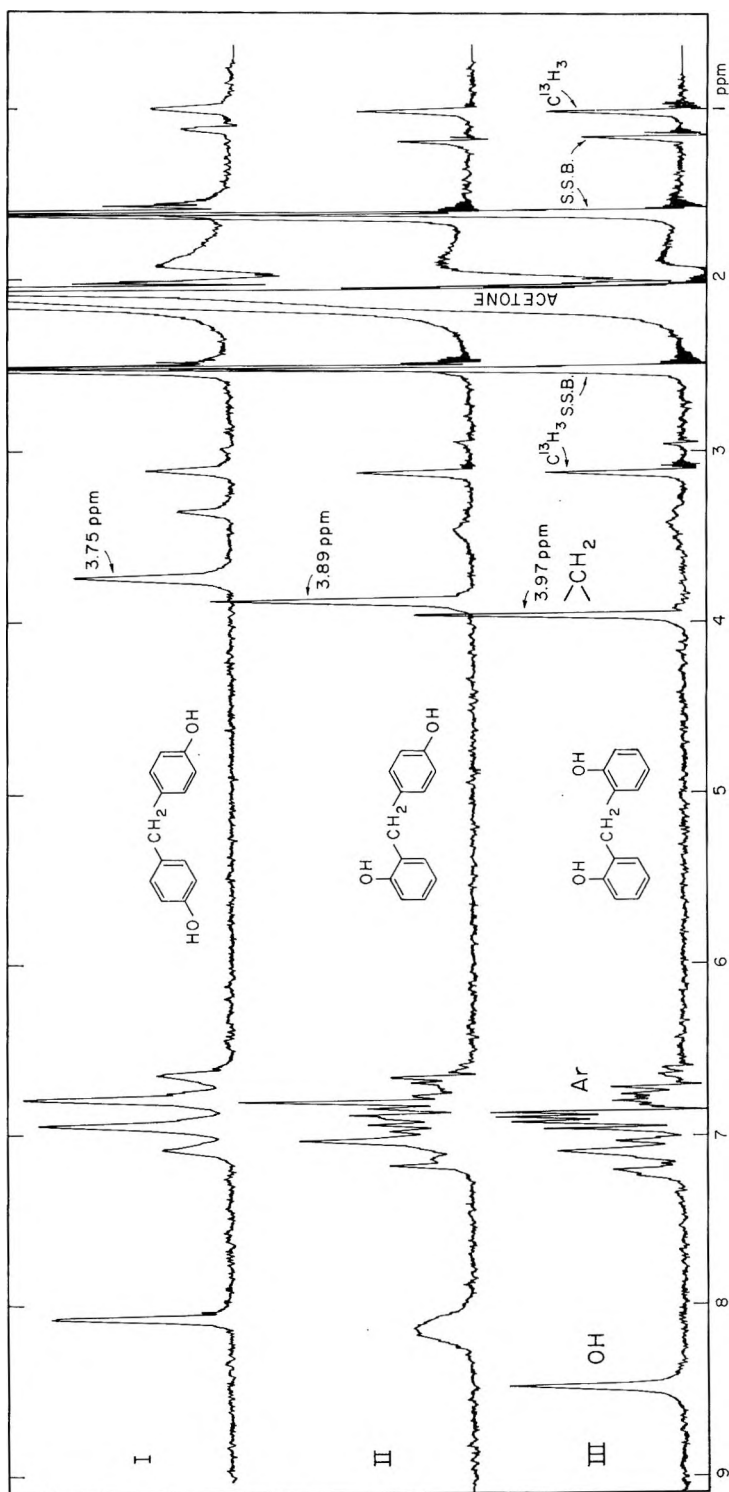


Fig. 1. PMR spectra of phenol-formaldehyde dimers.

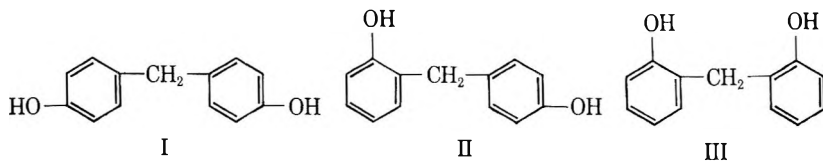


Figure 1 contains the 60 Mcycle/sec. spectra of the three possible phenol-formaldehyde dimers^{2b} showing clearly hydroxyl, aromatic, and methylene resonance peaks, which are well separated and easily assigned. In addition to the phenol-formaldehyde peaks, spectral components due to acetone, its C^{13} satellites and several spinning side bands (SSB) are labeled. Fortunately line positions of the two components do not overlap, and the much larger acetone peaks have not obscured the analysis of the desired phenol-formaldehyde spectra. In fact the downfield C^{13} satellite, which results from spin-spin coupling to the 1.1% naturally occurring C^{13} magnetic nuclei, is a very convenient fiducial mark for measuring accurately the relative chemical shifts of the closely positioned methylene peak. The downfield C^{13} satellite at 60 Mcycle/sec. has a chemical shift of 3.12 ppm from tetramethylsilane (TMS), a value which can be added to the separation between the $C^{13}H_3$ and CH_2 peaks to give the chemical shift of the latter group. The relative areas of the $C^{13}H_3$ and CH_2 peaks also may be used to obtain a convenient measure of the relative concentration of the phenol-formaldehyde condensates in the acetone solution.

Only the methylene proton chemical shifts will be discussed in detail, although conceivably the hydroxyl and aromatic resonance positions also could be of use in some studies. The greater complexity of the aromatic multiplets and the extreme sensitivity of the OH resonance position to shifts resulting from solvents and impurities, however, are factors which would have to be taken into consideration. A slight concentration dependence is noted for the various methylene resonances, with these peaks shifting up to 3 cycle/sec. for a threefold change in concentration. Therefore, all of the model compounds were investigated at the same effective concentration which was selected to correspond roughly with typical saturation concentrations of available polymeric materials. As conditions may vary from one polymer batch to another, it probably would be desirable that control samples be established in any future studies. This work, however, elucidates the type of data which may be obtained and gives the relative chemical shifts determined for various types of methylene groups even though solvent and impurity corrections may be required to secure actual chemical shift values in any specific solution.

The chemical shifts of 3.75, 3.89, and 3.97 ppm observed for the methylene resonance in I, II, and III, respectively, are typical for larger moieties, and they form a basis for interpreting the remaining data given in this paper. The shift to lower field as the linkage is varied from *para-para* to *ortho-para* and finally to *ortho-ortho* was found in every case, although in some instances the *ortho-para* and *ortho-ortho* peaks move very close to-

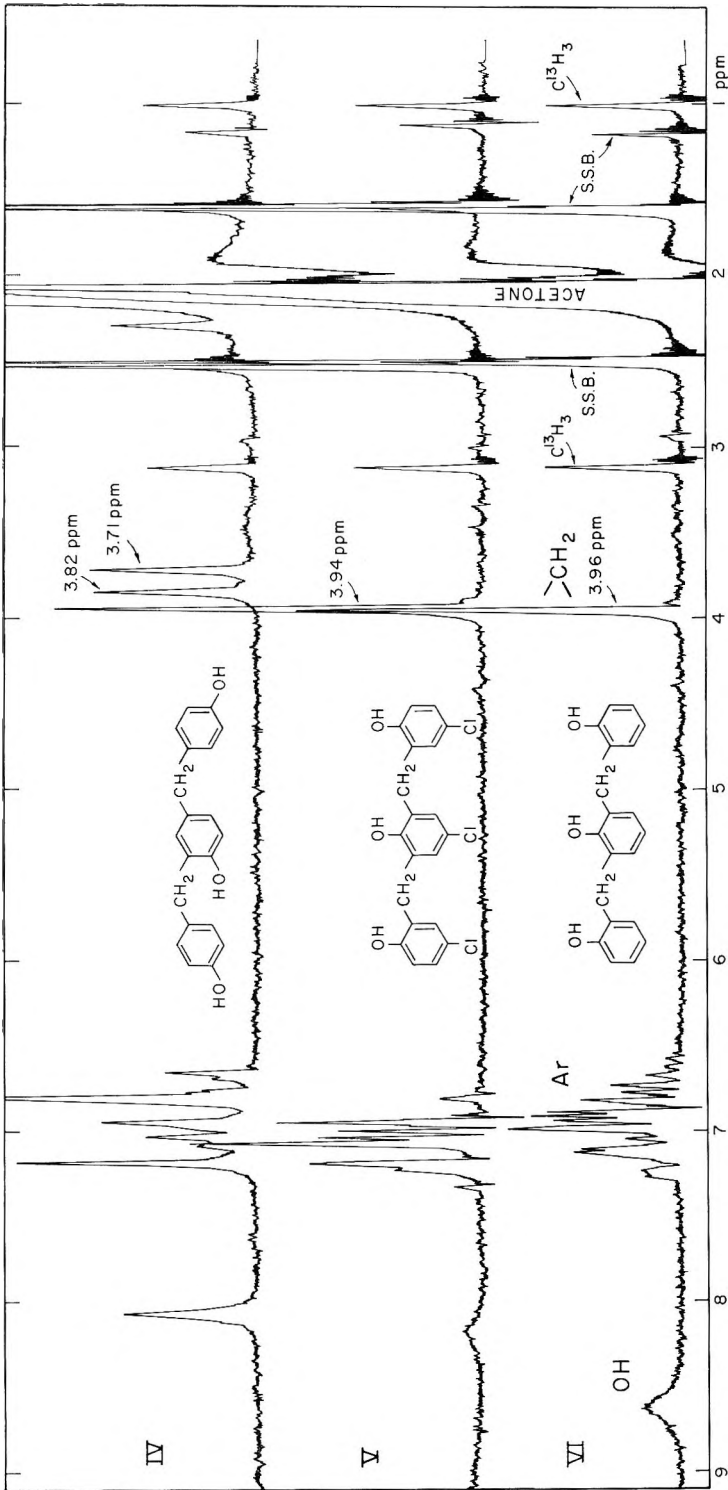
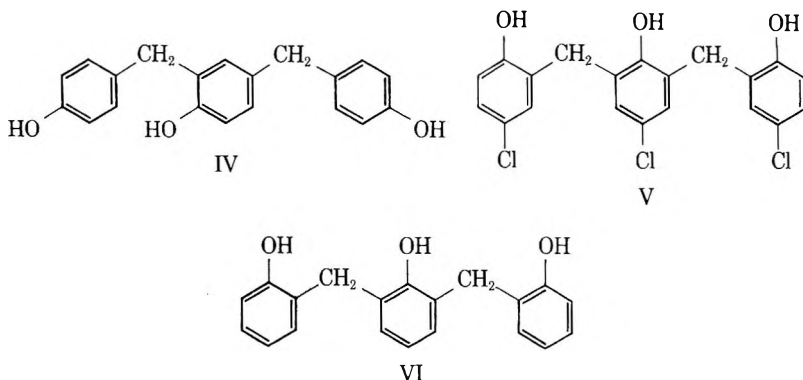


Fig. 2. PMR spectra of phenol-formaldehyde trimers and a *p*-chlorophenol-formaldehyde trimer.

ห้องสมุด กรมวิทยาศาสตร์

gether. Confirmation of this trend in chemical shifts is observed in Figure 2, which shows the spectra of three trimers. The *ortho-ortho-ortho-ortho* trimer (VI) appears at a field (3.96 ppm), only slightly above that for III, but sufficiently below that of II so that a clear distinction can be made. It is interesting to note that for the all-*ortho* trimer (V),⁸ which contains a chlorine *para* to each hydroxyl group, the methylene resonance (3.94 ppm) is in good agreement with the corresponding nonhalogenated trimer (VI). This lack of any appreciable shift as a result of the presence of chloro substituents was found to be typical for several of the model compounds which contained chlorine. Two methylene peaks are observed for the *para-ortho-para-para* trimer (IV) at 3.71 ppm and 3.82 ppm corresponding to *para-para* and *ortho-para* methylenes, respectively. These shifts correspond reasonably well with the respective values found for dimers I and II.



Spectra presented in Figure 3 of three substituted dimers indicate the type of difficulties which have been encountered when substituents alter the chemical shift slightly. In the dimethyl *para-para* dimer⁹ (VII) and the dimethyl *ortho-ortho* dimer⁹ (IX), a 2–3 cycle/sec. shift to higher field was observed in the respective methylene resonance peaks. This shift is attributed to methyl substituents *meta* to the methylene bridge. In the case of VII the peak at 3.69 ppm has moved upfield away from other typical methylene positions and can be assigned with no difficulty. The methylene resonance position for IX, however, occupies a position (3.93 ppm) which is intermediate between the values found for II and III, and care is required in making a proper assignment. The dimethyl dimers VII and IX in many respects simulate more closely a phenol-formaldehyde polymer than do structures I and II, as the methyl substituents are similar to methylene groups. Therefore, as might be expected, the upfield shifts are somewhat characteristic of those found in the larger polymeric species. The trichloro dimer (VIII)¹⁰ exhibits an *ortho-para* chemical shift (3.90 ppm) which agrees very well with the value for II (3.89 ppm), indicating again that chloro substituents have little effect in the spectra of the structures under consideration. The chemical shift values of the model dimers

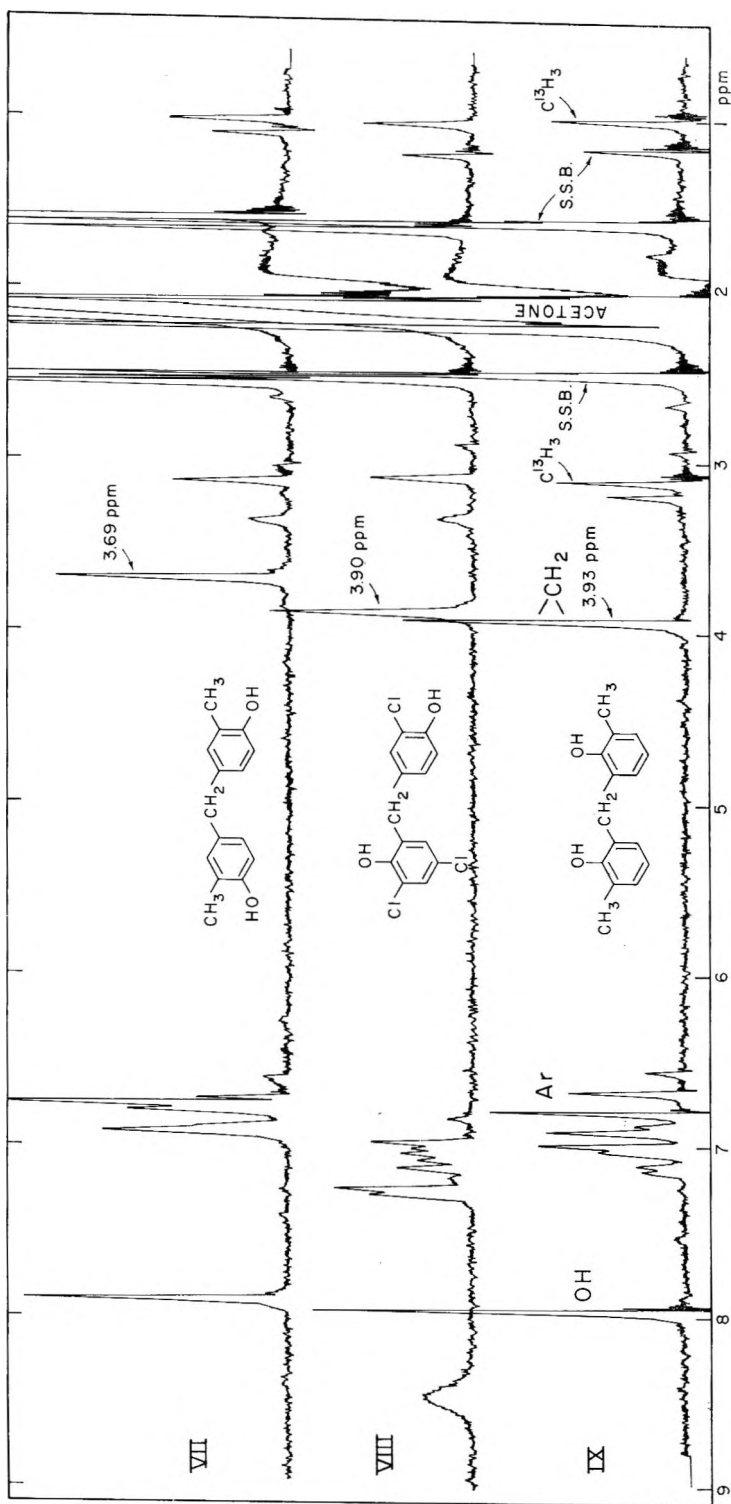


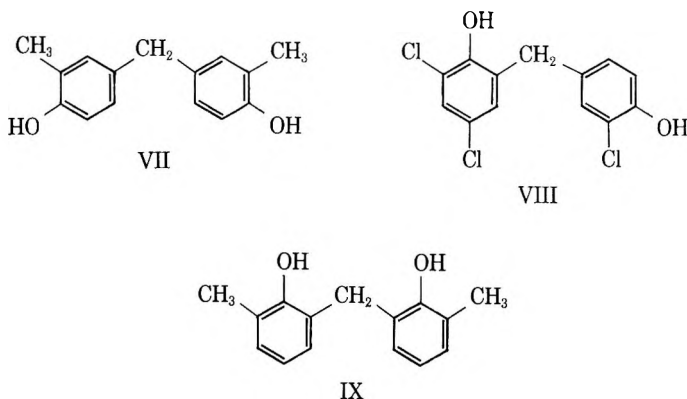
Fig. 3. PMIR spectra of substituted phenol-formaldehyde dimers.

TABLE I

| | Chemical shift from TMS, ppm | | |
|--------------------|------------------------------|---------------------|--------------------|
| | <i>para-para</i> | <i>ortho-para</i> | <i>ortho-ortho</i> |
| Dimers and Trimers | | | |
| I | 3.75 | — | — |
| II | — | 3.89 | — |
| III | — | — | 3.97 |
| IV | 3.71 | 3.82 | — |
| V | — | — | 3.94 |
| VI | — | — | 3.96 |
| VII | 3.69 | — | — |
| VIII | — | 3.90 | — |
| IX | — | — | 3.93 |
| Linear polymers | | | |
| X | — | — | 3.92 |
| XI | — | — | 3.96 |
| XII | 3.69 | 3.81 | 3.88 |
| XIII | 3.71 | 3.85 | 3.98 |
| XIV | 3.70 | (3.84) ^a | 3.90 |
| XV | 3.70 | (3.85) ^a | 3.98 |

^a While not anticipated for this polymer, a definite peak was observed in the *ortho-para* region of the spectrum. Some rearrangement of *ortho-ortho* and *para-para* methylene linkages under the conditions of polymerization was assumed.

and trimers used in this study are tabulated in Table I along with the values recorded for characteristic linear polymers.



Linear Phenol-Formaldehyde Polymers

When compared with the methylene resonance peaks in the dimers and trimers, the corresponding peaks for higher molecular weight polymers are broadened appreciably. This can be attributed to a lack of complete equivalence of all methylene groups in a polymeric chain and possibly to the larger molecular size which may limit complete motional narrowing of the line width. Excessive broadening by very small amounts of paramagnetic impurities such as Fe^{+3} in crude polymers also may be important

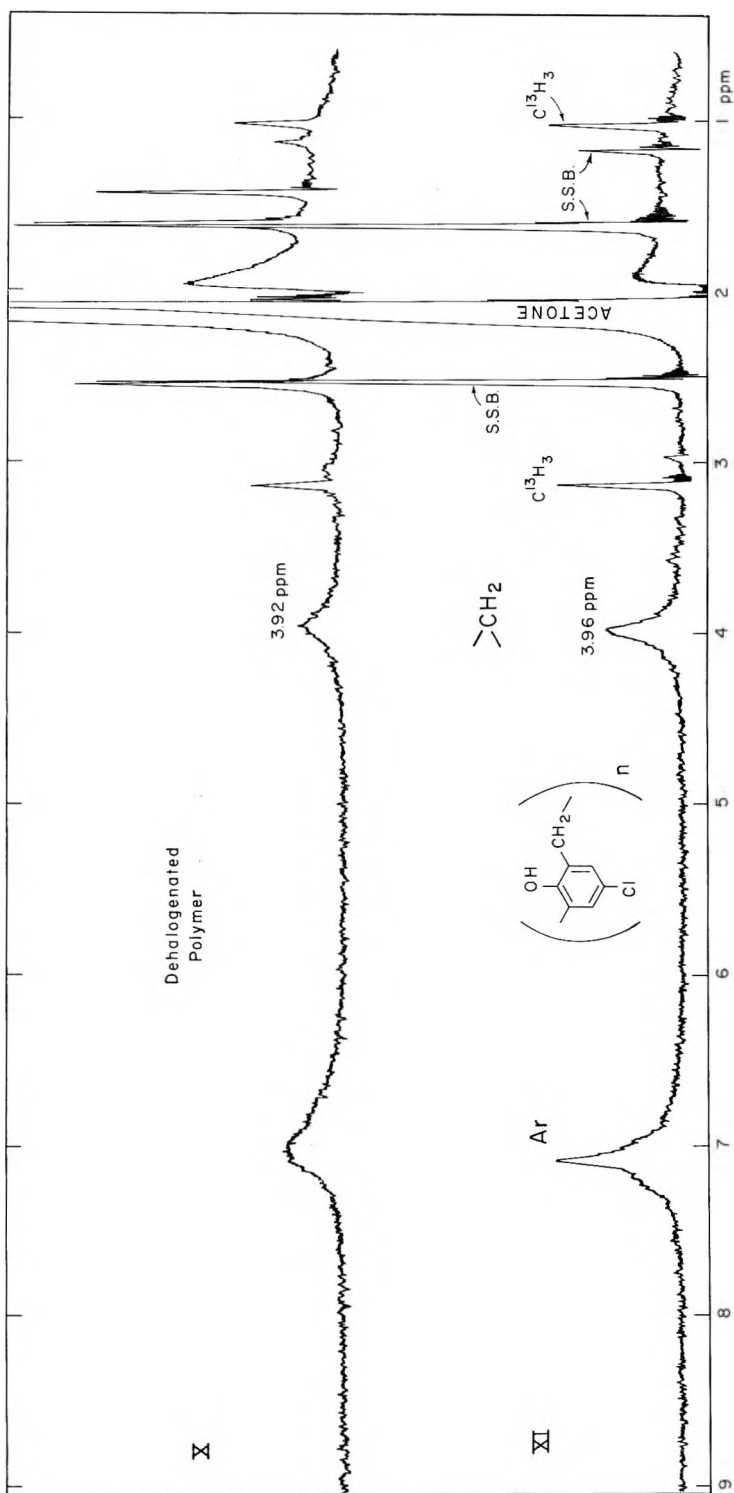
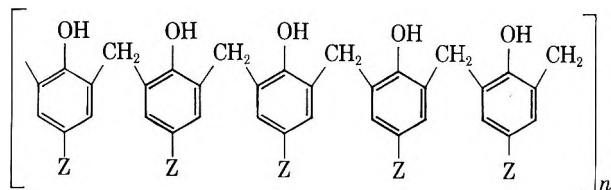


Fig. 4. PMR spectra of a *p*-chlorophenol-formaldehyde polymer (XI) and the corresponding dehalogenated polymer (X).

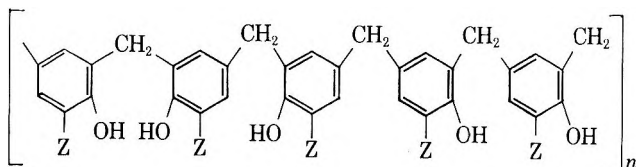
in some cases. Preliminary spectra obtained in this laboratory were of polymers which had been precipitated in tap water that contained Fe^{+3} ions. Although the polymers were washed with distilled water, the peaks in the spectra, including the acetone peaks, remained very broad. This suggested the possibility that small amounts of the paramagnetic impurity were not washed out and, presumably, were chelated by the phenolic groups. All polymers used in this study, therefore, were prepared under conditions designed to avoid inclusion of paramagnetic ions. Appreciably narrower line widths were observed for these samples.

Procedures previously described^{11,12} were used in the condensation of *p*-chlorophenol and *o*-chlorophenol with formaldehyde as a source of polymers having the structural features shown in XI and XIII, respectively. The corresponding dehalogenated polymers^{4,5} are designated X and XII, respectively. *p*-Chlorophenol was used with a view to obtaining a relatively simple structure (XI) in which all of the methylene groups are joined to *ortho* positions. The proton magnetic resonance spectra of X and XI are given in Figure 4. As expected, only a single methylene peak is observed in each spectrum, and the chemical shift value corresponds to the range of values found for *ortho-ortho* linkages in the dimers and trimers. A small shift of the methylene peak noted when compound VIII is compared with dimer II is reproduced again in X and XI



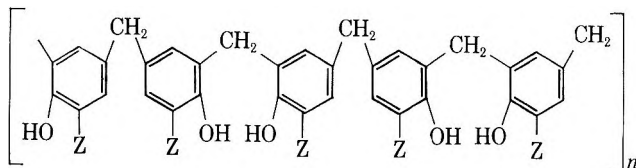
X Z = H

XI Z = Cl



XII Z = H

XIII Z = Cl



XIV Z = H

XV Z = Cl

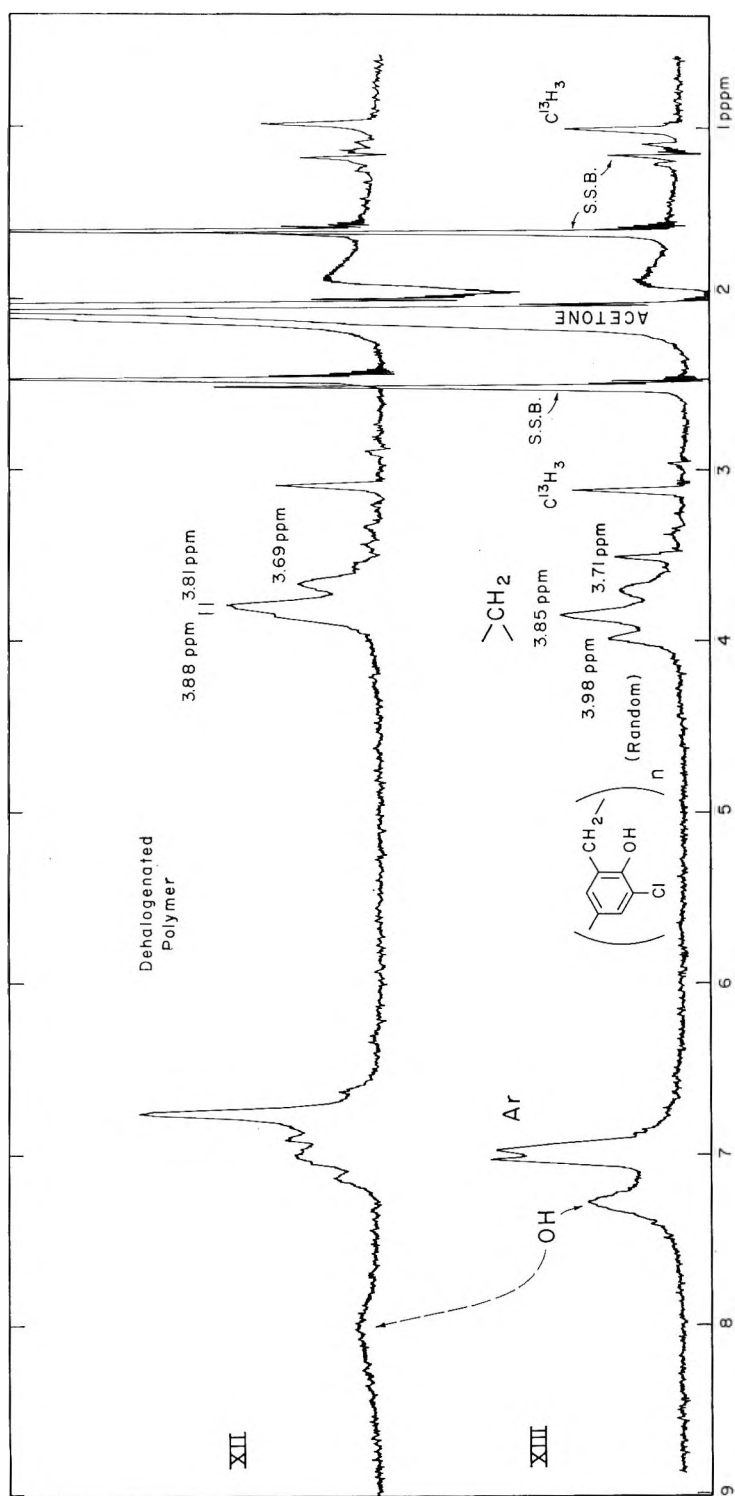


Fig. 5. PMR spectra of an *o*-chlorophenol-formaldehyde polymer (XIII) and the corresponding dehalogenated polymer (XII).

with the removal of chloro substituents. Deviations in the chemical shifts obtained from Figure 4 from the expected *ortho-ortho* value are within the experimental deviations noted for the dimers and trimers.

Among the three general types of polymers studied XIII and the corresponding dehalogenated form XII have the possibility of being the most random. Connective links through both an *ortho* and a *para* position are possible for a polymer from *o*-chlorophenol, which has an equal number of free *ortho* and *para* positions. If the polymerization mechanism is completely random for such a system, then the statistical ratio of the various types of methylene linkages would be *para-para:ortho-para:ortho-ortho* = 1:2:1. If during polymerization, however, an *o*-hydroxymethyl group reacted only at an *ortho* position in the second phenol ring and likewise if *p*-hydroxymethyl groups were to couple only at a *para* position, a polymer would be formed which contained only *ortho-ortho* and *para-para* methylene groups in equal number. Various other populational ratios for the several types of linkages would be predicted depending upon the relationships existing between the specific rate constants governing the several kinetic sequences of polymerization. Under any condition, however, the principle of detailed balance requires that the number of *ortho-ortho* and *para-para* linkages be equal. The spectra of XII and XIII in Figure 5 shows clearly that three types of methylene bridges are present in the polymers. In the dehalogenated polymer XII, the *ortho-ortho* resonance is observed as a shoulder on the *ortho-para* peak but for the chloro substituted polymer XIII these two peaks are resolved. In order to measure accurately the relative areas of the three methylene peaks in XIII, this region was expanded by five fold. Symmetrical curves were sketched in for the three peaks, and the relative areas, which were measured graphically, were found to be 0.23, 0.51, and 0.26 for the *ortho-ortho*, *ortho-para*, and *para-para* methylene groups, respectively. Within the limits of error these values correspond to the 1:2:1 ratio expected for a completely random polymerization. No other existing data establish this pertinent conclusion in such a forceful manner. In the spectrum of the dehalogenated polymer XII, the relative area of the combined *ortho-ortho* and *ortho-para* peaks was measured to be 0.76 when compared with a value of 0.24 for the resolved *para-para* peak. This result is consistent with the results with XIII that the polymerization is random.

The polymerization of the dimer bis(3-chloro-4-hydroxyphenyl)methane^{2b} with formaldehyde was studied earlier¹³ as a possible approach to a polymer having alternating *ortho-ortho*, *para-para* linked methylene bridges in its structure (XV). This appeared reasonable if it is assumed that the *para-para* methylene linkages present in the dimer are stable, since further polymerization could be expected¹¹ to proceed through the two free *ortho* positions. The existence of a resonance peak in the spectra of XIV and XV (Fig. 6) in the region associated with an *ortho-para* linked methylene group suggested that the above assumption regarding the stability of the *para-para* linkages is not tenable. While the peak in the *ortho-para* region falls far

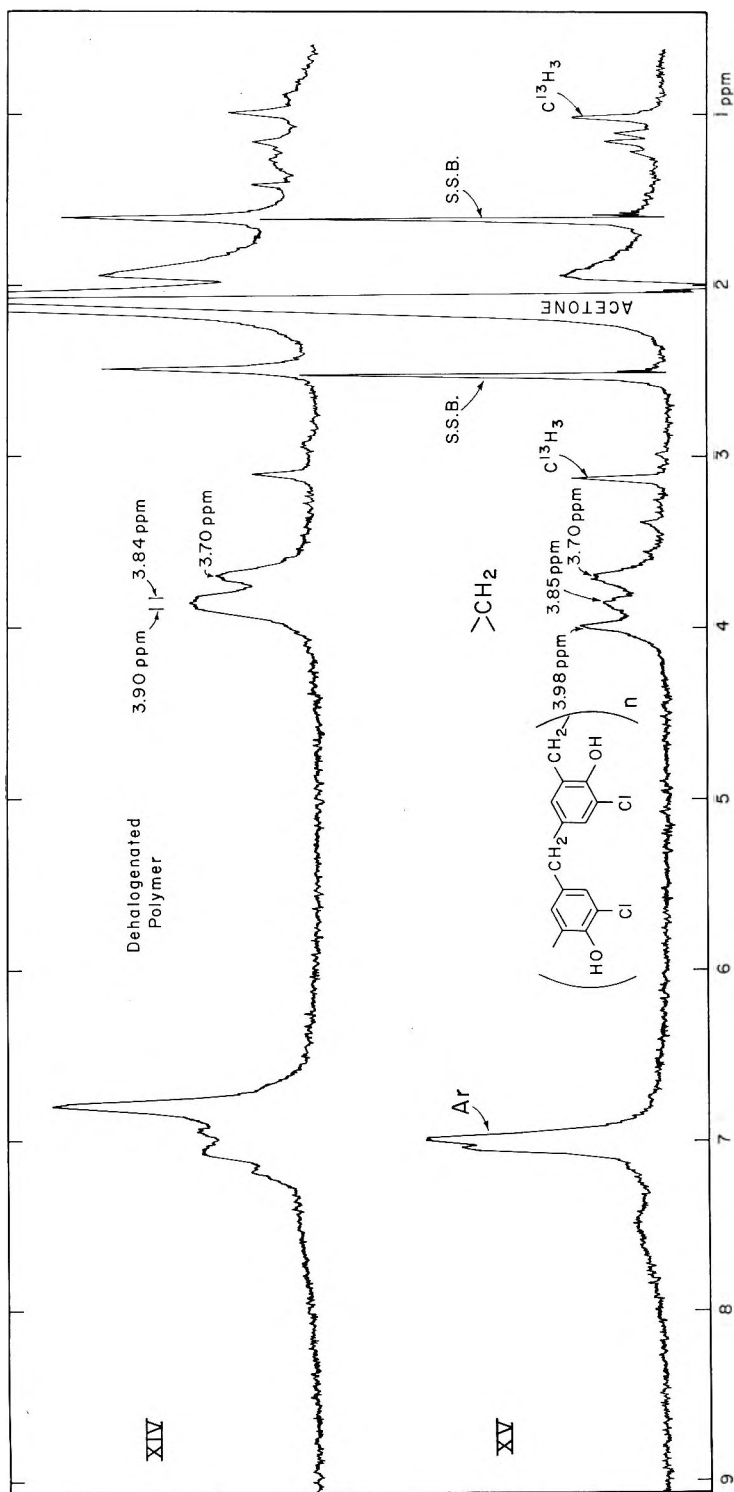


Fig. 6. PMR spectra of a polymer prepared from bis(3-chloro-4-hydroxyphenyl)methane and formaldehyde (XV) and the corresponding dehalogenated polymer (XIV).

below the 50% relative intensity expected for a completely random polymer, its intensity in XV would indicate that approximately one-fourth of all methylene linkages are *ortho-para*. This finding requires that some bond breaking and subsequent rearrangement are involved during the polymerization reaction. Chain breaking of the chlorinated polymer (XV) under polymerization conditions as well as the splitting of the dimer could lead to *ortho-para* links. It appears reasonable to assume that both effects combine to account for the data shown in Figure 6. Once again the *ortho-ortho* and *ortho-para* peaks move together (Fig. 6) in the dehalogenated polymer XIV as was noted with the dehalogenated polymer XII (Fig. 5).

EXPERIMENTAL

All spectra were obtained at 60 Mcycles/sec. on a Varian A-60 console operating in conjunction with a Varian 12-in. high-resolution magnet. Samples were dissolved in acetone solution and contained in Varian precision ground sample tubes. The samples were not degassed, but sharp acetone peaks in each case indicated that broadening in the phenol-formaldehyde spectrum was not due to the presence of oxygen.

References

1. Megson, N. J. L., *Phenolic Resin Chemistry*, Academic Press, New York, 1958.
2. (a) R. W. Martin, *The Chemistry of Phenolic Resins*, Wiley, New York, 1956; (b) *ibid.*, p. 64.
3. Burke, W. J., G. A. Short, and H. P. Higginbottom, *J. Polymer Sci.*, **43**, 49 (1960).
4. Burke, W. J., S. H. Ruetman, and H. P. Higginbottom, *J. Polymer Sci.*, **38**, 513 (1959).
5. Burke, W. J., S. H. Ruetman, C. W. Stephens, and A. Rosenthal, *J. Polymer Sci.*, **22**, 477 (1956).
6. Burke, W. J., B. A. Barton, P. D. Gardner, and J. D. Lewis, *J. Am. Chem. Soc.*, **80**, 3438 (1958).
7. Burke, W. J., and H. P. Higginbottom, *J. Polymer Sci.*, **A1**, 3617 (1963).
8. Finn, S. R., J. W. James, and C. J. S. Standen, *J. Appl. Chem. (London)*, **4**, 497 (1954).
9. Higginbottom, H. P., Ph.D. Thesis, University of Utah, 1962, pp. 78, 79.
10. Bullough, V. L., Ph.D. Thesis, University of Utah, 1955, p. 92.
11. Burke, W. J., W. E. Craven, A. Rosenthal, S. H. Ruetman, C. W. Stephens, and C. Weatherbee, *J. Polymer Sci.*, **20**, 75 (1956).
12. Burke, W. J., and S. H. Ruetman, *J. Polymer Sci.*, **32**, 221 (1958).
13. Ruetman, S. H., Ph.D. Dissertation, University of Utah, 1957, p. 42.

Résumé

On a tiré les spectres de résonance magnétique protonique d'un certain nombre de composés représentatifs dimères et trimères du phénolformaldéhyde et de structure connue ainsi que des composés s'y rattachant portant des substituants méthyl- et chlor- sur le noyau. Les résultats obtenus ainsi, particulièrement pour les protons méthyléniques, ont été utilisés pour l'interprétation de la structure des polymères linéaires phénol-formaldéhyde et des polymères halogénés y correspondant, préparés par condensation de l'*o*- et du *p*-chlorophénol avec le formaldéhyde, tous ces composés étant bien caractérisés. Dans tous les cas, on a observé un déplacement vers les champs plus

faibles lorsque le lien méthylénique passait de *para-para* à *ortho-para* puis à *ortho-ortho*, quoique dans certains cas les pics *ortho-para* et *ortho-ortho* se rapprochaient très fortement les uns des autres. Les spectres obtenus révélèrent que la condensation de l'*o*-chlorophénol avec le formaldéhyde suit un processus entièrement statistique, les liens méthyléniques *ortho-ortho*, *ortho-para* et *para-para* étant dans des rapports respectifs de 1/2/1, dans les limites des erreurs expérimentales. Les résultats préliminaires obtenus dans ce travail démontrent clairement l'utilité potentielle de la RMP comme instrument valable de caractérisation des produits de complexité élevée obtenu au départ des systèmes phénol-formaldéhyde.

Zusammenfassung

Protonmagnetische Resonanzspektren wurden für eine Anzahl repräsentativer Phenol-Formaldehyddimerer und -trimerer von bekannter Struktur und für verwandte Verbindungen mit Methyl- oder Chlorsubstituenten am aromatischen Ring erhalten. Diese Daten, besonders diejenigen für die Methylenprotonen, wurden zur Interpretierung der Struktur gut charakterisierter linearer Phenol-Formaldehydpolymerer sowie der entsprechenden, halogenierten, durch Kondensation von *o*- und *p*-Chlorphenol mit Formaldehyd dargestellten Polymeren verwendet. In allen Fällen trat bei Veränderung der Brücke von *para-para* zu *ortho-para* zu *ortho-ortho* eine Verschiebung zu niedrigerer Feldstärke auf, obwohl sich in gewissen Fällen die *ortho-para* und *ortho-ortho*-Maxima sehr nahe zueinander verschoben. Die erhaltenen Spektren zeigten, dass die Kondensation von *o*-Chlorphenol mit Formaldehyd im wesentlichen statistisch verläuft, da das Verhältnis von *ortho-ortho* zu *ortho-para* zu *para-para*-Methylenbrücken innerhalb des Versuchsfehlers zu 1:2:1 gefunden wurde. Die vorläufigen Ergebnisse dieser Arbeit beweisen die potentielle Brauchbarkeit von PMR als wertvolles Werkzeug zur Charakterisierung der hochgradig komplexen, in Phenol-Formaldehydsystemen erhaltenen Produkte.

Received October 5, 1964
(Prod. No. 4571A)

Aromatic Polybenzoxazoles

W. W. MOYER, JR.,* CARL COLE,† and T. ANYOS, *Marbon Chemical Division, Borg-Warner Corporation, Washington, West Virginia*

Synopsis

The polymerization of 3,3'-dihydroxybenzidine with the phenyl esters of phthalic, isophthalic, terephthalic, and 5-chloroisophthalic acids yielded a series of aromatic polybenzoxazoles exhibiting high thermal stability. Melt polymerization afforded these polymers in quantitative yield with inherent viscosities in the range of 0.20-1.04 and thermal stability very similar to those obtained with the aromatic polybenzimidazoles. Homopolymerization of 3-amino-4-hydroxybenzoic acid and 4-amino-3-hydroxybenzoic acid was achieved through the preparation of an intermediate poly(ester-amide) followed by thermal cyclization (at 250-300°C.) to the benzoxazole unit. Six model compounds containing the benzoxazole unit were prepared for use as standards of reference. These were 2-phenylbenzoxazole, 2,2'-*p*-phenylene-bisbenzoxazole, 2,2'-*m*-phenylene-bisbenzoxazole, 2,2'-*o*-phenylene-bisbenzoxazole, 2,2'-(5-chloro-1,2-phenylene)-bisbenzoxazole, and 2,2'-(diphenyl)-6,6'-bibenzoxazole.

I. INTRODUCTION

The interest in thermally stable organic polymers has generated a great deal of work on the synthesis of new, fully aromatic or pseudoaromatic systems. Condensation polymerization techniques to give polymers having heterocyclic units in their backbones has been shown to be one of the easiest and most versatile routes to these fully aromatic polymers. To date, of this new class of heterocyclic polymers, polybenzimidazoles,^{1,2} polythiazoles,³ polybenzborimidazolines,⁴ polyoxadiazoles,⁵ polytriazoles,^{5,6} polydithiazoles,⁷ polybenzothiazoles,⁸ polytetrazopyrenes,⁹ and polyquinoxalines¹⁰ have been reported. This report concerns the preparation and properties of still another fully aromatic, polymeric heterocyclic system, polybenzoxazoles.

II. DISCUSSION

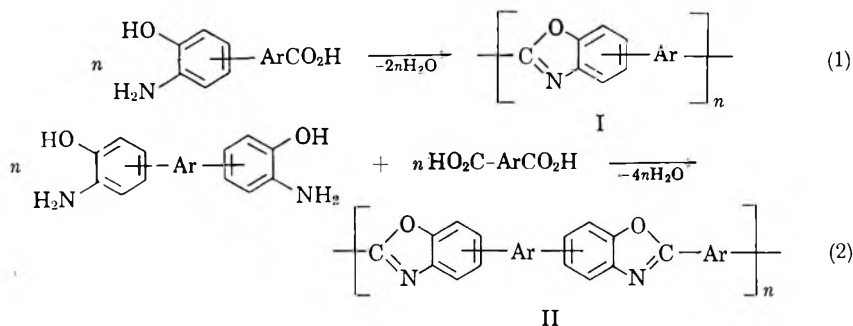
Benzoxazoles are generally formed by the reaction of a carboxylic acid or a carboxylic acid derivative with an *o*-aminophenol.¹¹ That reactions of this type are suitable to high polymer formation was demonstrated by Brinker, Cameron, and Robinson,¹² who prepared benzoxazole containing

* Present address: Daubert Chemical Co., Chicago, Illinois.

† Present address: Department of Chemistry, Northwestern University, Evanston, Illinois.

polymers by the reaction of bis-*o*-aminophenols with aliphatic dicarboxylic acids and by the self-condensation of ω -*o*-aminophenol-aliphatic carboxylic acids. Using this same polymerization reaction but with monomers in which the aliphatic units have been eliminated or replaced by aromatic groups, the fully aromatic polybenzoxazoles can be formed.

There are essentially two classes of aromatic polybenzoxazoles: those derived from self-contained "homomonomers",¹ i.e., *o*-aminohydroxybenzoic acid derivatives and those derived from complementary comonomers,¹¹ i.e., bis-*o*-aminophenols and dicarboxylic acids or their derivatives. The generalized reaction scheme and structures are shown in eqs. (1) and (2):



where Ar is an aromatic nucleus or a single bond.

Examples of both types of polymers have been prepared and characterized. Additionally, several model compounds have been synthesized for the purpose of establishing structure-property relationships.

A. Polybenzoxazoles Derived from Comonomers

The bis-*o*-aminophenol used in this work was 3,3'-dihydroxybenzidine which was prepared in one step from dianisidine. The acid comonomers were phthalic, isophthalic, terephthalic, and 5-chloroisophthalic acids. For the polymerizations the phenyl esters of the acids were found to work best, in agreement with the findings of Vogel and Marvel,¹ and were generally used. Less satisfactory polymerization results were achieved when the methyl esters, acid chlorides, or acids themselves were used.

All polymerizations were conducted in essentially the same manner. Equimolar quantities of the comonomers were carefully weighed out, mixed thoroughly by grinding in a mortar, and transferred quantitatively to a reaction vessel. Heating the mixture in an inert atmosphere to about 250–330°C. brought about reaction. The condensation polymerizations generally proceeded smoothly and rapidly as evinced by the simultaneous evolution of water and phenol (when the phenyl esters were used). Reaction periods of 4–28 hr. were usually sufficient.

Reduced pressure had little influence on the reaction rate or final molecular weights. Except for a brief period at the beginning of the reactions,

TABLE I
Polybenzoxazoles Derived from Comonomers

| Reactants | Polymer recurring unit | Reaction time, hr. | Reaction temp., °C. | η_{inh}^a | Solubility in H_2SO_4 , % |
|--|------------------------|--------------------|---------------------|----------------|-----------------------------|
| 3,3'-Dihydroxybenzidine Diphenyl isophthalate | | 6 | 300-330 | 0.43 | 99 |
| 3,3'-Dihydroxybenzidine Diphenyl terephthalate | | 24 | 250-330 | 0.93 | 100 |
| 3,3'-Dihydroxybenzidine Diphenyl phthalate | | 48 | 280-310 | 0.20 | 75 |
| 3,3'-Dihydroxybenzidine Diphenyl 5-chloroisophthalate | | 26 | 220-280 | 0.25 | 77 |

^a Concentration 0.2 g. sample/100 ml. concentrated sulfuric acid, 25°C.

the polymerizations proceeded entirely in the solid state. A summary of the comonomer polymerizations is given in Table I.

The extent of polymerization, and therefore molecular weight, is presumed to be primarily a function of the stoichiometry. This assumption is based on the facts that additional reaction time has little or no effect on the molecular weights of the products (other than to decrease the amount of soluble polymer) but that the addition of trace amounts of one of the comonomers (opposite to that which constitutes the endgroups) to the reaction mass can significantly increase their molecular weight. Generally, polymers having a predominance of aminophenol endgroups are isolated. This is due to the fact that trace amounts of the diphenyl esters are lost during the reaction because of their greater volatility. The effect of added comonomers on the molecular weight of certain polybenzoxazoles is summarized in Table II.

TABLE II
Effect of Added Comonomers on Polybenzoxazoles

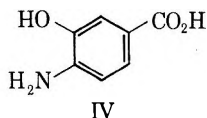
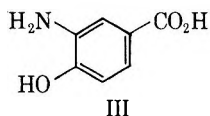
| Polymer | Presumed endgroup | η_{inh}^a | Added comonomer | Reaction conditions | | η_{inh} after reaction ^b |
|---|-------------------|----------------|----------------------------------|---------------------|------------|--|
| | | | | Time, hr. | Temp., °C. | |
| Poly-2,2'-(<i>p</i> -phenylene)-6,6'-bibenzoxazole | Amino-phenol | 0.28 | Diphenyl terephthalate, 2 wt.-% | 17 | 270-280 | 0.43 |
| Poly-2,2'-(<i>p</i> -phenylene)-6,6'-bibenzoxazole | Phenyl ester | 0.43 | 3,3'-Dihydroxybenzidine, 1 wt.-% | 14 | 275-285 | 0.79 |
| Poly-2,2'-(<i>o</i> -phenylene)-6,6'-bibenzoxazole | Amino-phenol | 0.13 | Diphenyl phthalate, 2 wt.-% | 6 | 270-300 | 0.20 |

^a Concentration 0.2 g. sample/100 ml. concentrated sulfuric acid, 25°C.

^b Final viscosity of polymer after treatment with comonomer under conditions indicated.

B. Polybenzoxazoles Derived from Homomonomers

The "homomonomers" studied were 3-amino-4-hydroxybenzoic acid (III) and 4-amino-3-hydroxybenzoic (IV).

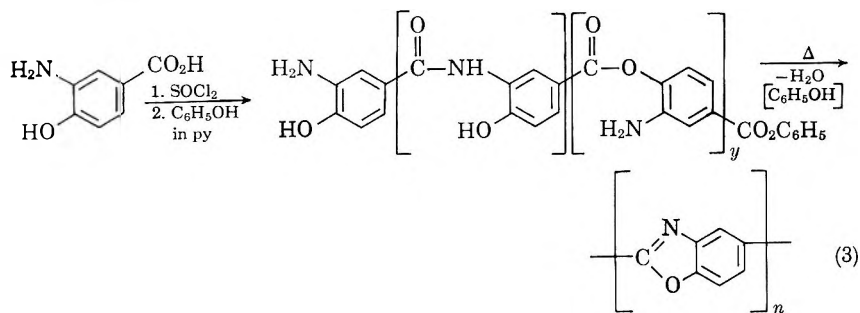


Direct polymerization of these monomers was not possible. The monomers underwent decarboxylation at the temperature required for polymerization (210°C.). Solution condensation techniques likewise were unsuccessful. The methyl ester of 3-amino-4-hydroxybenzoic did give a low molecular weight polymer but decomposition products also were formed.

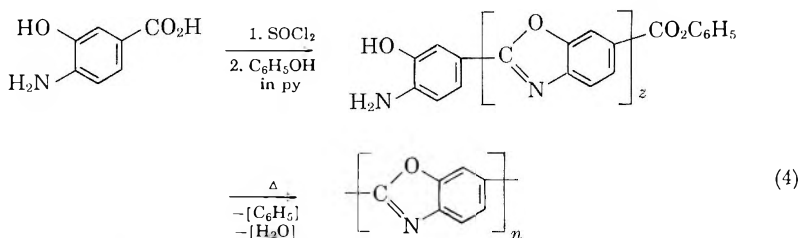
Satisfactory polymerizations of these two monomers were achieved by a somewhat indirect method. The preferred reactants are the phenyl esters. However, the simple phenyl esters could not be prepared. Attempts at the preparation of these esters gave only low molecular polymers formed from the polymerization of these esters of the aminohydroxycarboxylic monomers. The desired high molecular weight polybenzoxazoles were then formed by subjecting these intermediate polymers to thermal polymerization conditions.

The infrared spectra of the intermediate polymers derived from 3-amino-4-hydroxybenzoic acid indicated that they were essentially poly(ester-amides) since they had strong carbonyl absorption bands at 5.75 and 6.05 μ . The infrared spectra of the intermediate polymers derived from 4-amino-3-hydroxybenzoic acid contain no strong carbonyl absorption bands or absorption in the 5.0–6.05 μ region, indicating that nearly complete benzoxazole ring closure occurs. A possible explanation for the greater tendency of the 4-amino-3-hydroxybenzoate derivative to form benzoxazole units compared to the 3-amino-4-hydroxy isomer is the increased conjugation in the poly-2,6-benzoxazole resulting from the 4-amino-3-hydroxy isomer. The 3-amino-4-hydroxy isomer gives the poly-2,5-benzoxazole in which direct classical conjugation is limited to single benzoxazole units. In either case the endgroups of the low molecular weight polymers are presumed to be aminophenol and phenyl ester.

Heating these intermediate polymers in an inert atmosphere at 250–300°C. gave the high molecular weight polybenzoxazoles with inherent viscosities up to 1.0. The polymerization scheme is indicated in eqs. (3) and (4).



3-Amino-4-hydroxybenzoic acid (III) Poly-2,5-benzoxazole

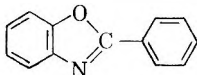
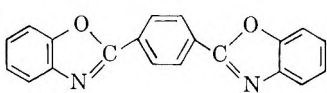
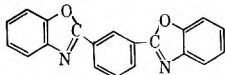
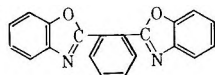
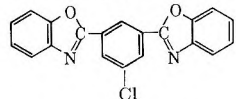
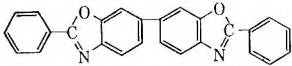


4-Amino-3-hydroxybenzoic acid (IV) Poly-2,6-benzoxazole

C. Model Compounds

Six model compounds were synthesized to serve as standards of reference: 2-phenylbenzoxazole (V), 2,2'-*p*-phenylene-bisbenzoxazole (VI), 2,2'-*m*-phenylene-bisbenzoxazole (VII), 2,2'-*o*-phenylene-bisbenzoxazole (VIII), 2,2'-(5-chloro-1,3-phenylene)-bisbenzoxazole (IX), and 2,2'-(diphenyl)-6,6'-bibenzoxazole (X). The structure and general properties of these compounds are given in Table III.

TABLE III
Benzoxazole Model Compounds

| | Structure | Melting point, °C. | Appearance | Solubility |
|------|---|--------------------|--------------------|--|
| V |  | 99-101 | White, crystalline | Sol. most solvents: DMF, THF, benzene, MEK, CHCl ₃ |
| VI |  | 353-355 | Gold, crystalline | Sl. sol. DMF, THF, benzene, CHCl ₃ , MEK; sol. conc. H ₂ SO ₄ |
| VII |  | 227-228 | Tan powder | Sl. sol. most org. solv.; sol. conc. H ₂ SO ₄ |
| VIII |  | 202-204 | Gold powder | Sol. most org. solvents; DMF, THF, benzene, MEK, CHCl ₃ |
| IX |  | 288-289 | White, crystalline | Sol. most org. solvents; DMF, THF, C ₆ H ₆ , MEK, CHCl ₃ , H ₂ SO ₄ |
| X |  | 330-332 | Gold-green powder | Insoluble most solvents; sol. hot chlorobenzene, conc. H ₂ SO ₄ |

It is evident that the melting points of aromatic benzoxazole systems increase rapidly as the number of aromatic rings increase, with molecular structure also having a significant influence. The solubilities follow a similar pattern; solubility decreases with increasing molecular weight and increases with molecular dissymmetry. The compounds have a tendency to be colored. From these observations it is predicted that high molecular weight, totally aromatic polybenzoxazoles, as a class, will be nonfusible, colored, and soluble only in concentrated sulfuric acid.

D. Polybenzoxazole Properties

General Physical Properties. The physical properties of fully aromatic polybenzoxazoles are much the same. They are tan- to brown-colored friable resins which are nonfusible and insoluble in all common solvents

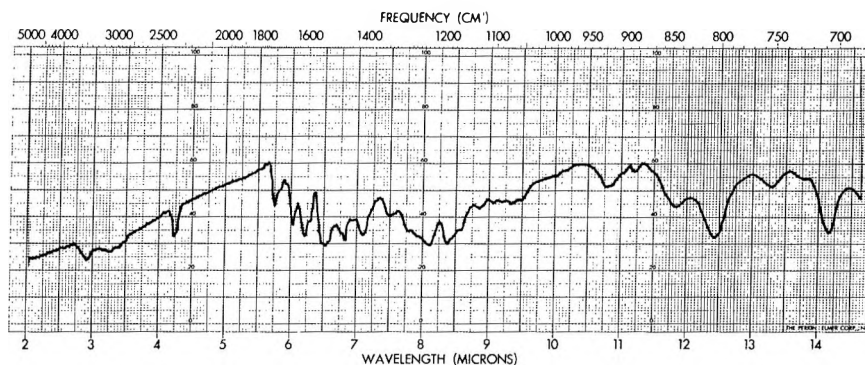


Fig. 1. Infrared spectrum of poly-2,2'-(*m*-phenylene)-6,6'-bibenzoxazole.

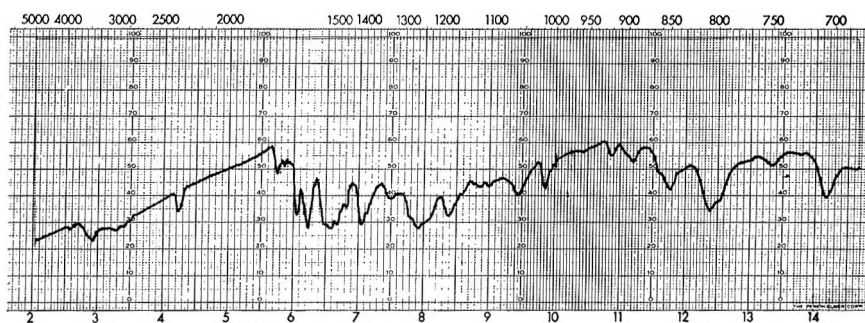


Fig. 2. Infrared spectrum of poly-2,2'-(*p*-phenylene)-6,6'-bibenzoxazole.

except sulfuric acid. The polymers derived from 3,3'-dihydroxybenzidine and isophthalic and terephthalic acids were crystalline as determined by x-ray analysis. All of the other polymers were amorphous. Chemically the resins are very stable; however they are decomposed by hot concentrated nitric acid and boiling caustic solutions. The poly-2,5-benzoxazole and the 2,6-isomer are completely nonflammable, while the comonomer-derived polymers are consumed slowly when exposed to a direct flame. Within the molecular weight range studied ($\eta_{inh} = 0.1-1.0$, H_2SO_4), the physical properties are constant with the possible exception of thermal stability which seems to improve with increasing molecular weight.

Infrared Spectra. Representative spectra of three of the polymers and the 2,2'-*m*-phenylene-bisbenzoxazole model compound are given in Figures 1-4. In general both the polymers and model compounds show five characteristic bands in the 6-7 μ region of varying intensities, depending on the specific structures. Traces of uncyclized units (ester and amide groups) or ester endgroups occasionally are detected in the polymers by the absorption in the 5.75-6.00 μ region. It should be noted, however, that even in the cases of the pure model compounds there is some absorption in this carbonyl region. Unfortunately it has not been possible to identify the endgroups of the polymers by infrared techniques.

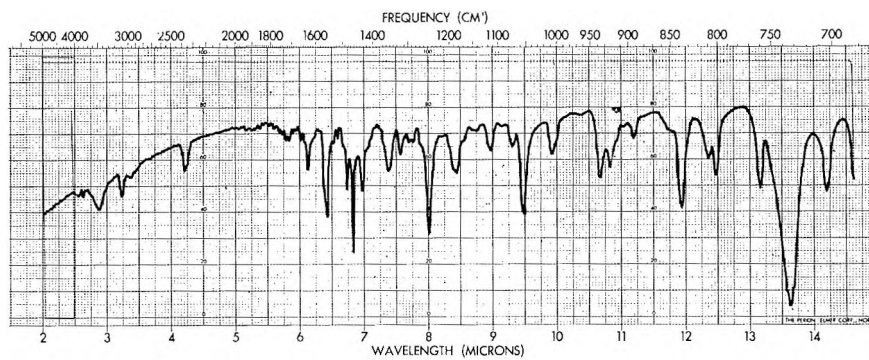
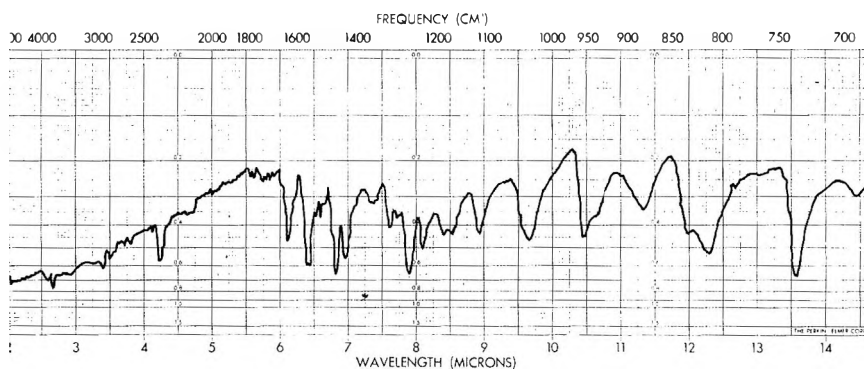
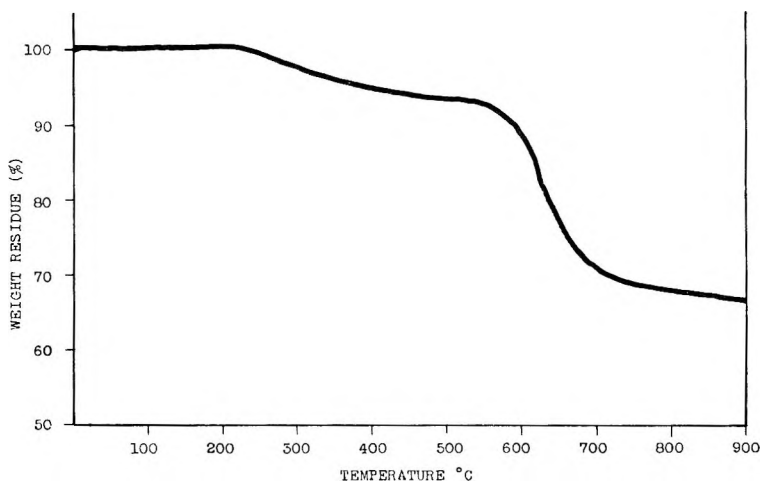
Fig. 3. Infrared spectrum of 2,2'-*m*-phenylene-bisbenzoxazole.Fig. 4. Infrared spectrum of poly-2,2'-(*o*-phenylene)-6,6'-bibenzoxazole.

Fig. 5. Thermogravimetric analysis of poly-2,5-benzoxazole.

TABLE IV
 Ultraviolet Spectral Properties of Benzoxazoles

| Compound | Max. m μ ^a | Absorb- ance | |
|---|------------------------------|-----------------|---|
| | | K ^b | E _{1 cm.} ^{1%} ^c |
| 2-Phenylbenzoxazole | 310 | 110 | 2010 ^d |
| 2,2'- <i>p</i> -Phenylene-bisbenzoxazole | 367 | 118 | 2160 |
| 2,2'- <i>m</i> -Phenylene-bisbenzoxazole | 318 | 124 | 2270 |
| 2,2'-(5-chloro-1,3-phenylene)-bisbenzoxazole | 320 | 118 | 2160 |
| 2,2'-(Diphenyl)-6,6'-bibenzoxazole | 281 | 65 | 1190 |
| | 250 | 61 | 1120 |
| Poly-2,5-benzoxazole | 380 | 180 | 3300 |
| Poly-2,6-benzoxazole | 375 | 193 | 3530 |
| Poly-2,2'-(<i>m</i> -phenylene)-6,6'-bibenzoxazole | 348 | 77 | 1410 |
| | 238 | 100 | 1830 |
| Poly-2,2'-(<i>p</i> -phenylene)-6,6'-bibenzoxazole | 390 | 45 | 824 |
| Poly-2,2'-(5-chloro-1,3-phenylene)-6,6'-bibenzoxazole | 343 | 68 | 1240 |
| | 236 | 106 | 1950 |

^a Concentrated sulfuric acid solutions were used in all cases.

^b K = absorbance/g./l. (measured in a 1 cm. cell).

^c E_{1 cm.}^{1%} = 1% solution in 1 cm. cell.

^d Log E_{max.} = 4.34. This value corresponds well with the reported value determined in ethanol solution.¹³

Ultraviolet Spectra. The ultraviolet spectra of the polybenzoxazoles and model compounds have been determined in sulfuric acid solution. The data are given in Table IV. All of the benzoxazoles studied show very intense absorptions over broad ranges; the spectra of the polymers having the broader ranges of absorption and exhibiting a bathochromic shift of 20-80

 TABLE V
 Weight Loss of Polybenzoxazoles Heated at Various Temperatures

| Polymer | Sam- ple No. | η_{inh} | Atmos- phere | Weight loss after 1 hr. at various temperatures, % | | | | |
|--|--------------------|--------------|-----------------|---|------------|------------|------------|-------|
| | | | | 400° C. | 450° C. | 500° C. | 550° C. | Total |
| Poly-2,5-benzoxazole | A | 1.04 | Nitrogen | 2.0 | 1.1 | 0.4 | 1.1 | 4.6 |
| Poly-2,5-benzoxazole | B | 0.71 | Nitrogen | 1.0 | 0 | 1.9 | 0.6 | 3.5 |
| Poly-2,5-benzoxazole | B | 0.71 | Air | 2.6 | 3.1 | 3.7 | 10.7 | 20.1 |
| Poly-2,5-benzoxazole | C | 0.33 | Nitrogen | 2.3 | 1.2 | — | 0.1 | 3.6 |
| Poly-2,5-benzoxazole | C | 0.33 | Air | 2.8 | — | 5.7 | 4.0 | 12.6 |
| Poly-2,6-benzoxazole | D | 0.32 | Nitrogen | 5.4 | 2.2 | — | 4.6 | 12.2 |
| Poly-2,2'-(<i>m</i> -phenylene)- 6,6'-bibenzoxazole | E | 0.22 | Nitrogen | 8.6 | 1.7 | 1.5 | 0.1 | 11.9 |
| Poly-2,2'-(<i>p</i> -phenylene)- 6,6'-bibenzoxazole | F | 0.28 | Nitrogen | — | 8.7 | 1.0 | 1.9 | 11.6 |
| Poly-2,2'-(5-chloro-1,3- phenylene)-6,6'-bibenz- oxazole | G | 0.25 | Nitrogen | 5.2 | — | 5.1 | 0.7 | 11.0 |

$m\mu$. Except for the polymer made from 5-chloroisophthalic acid and 3,3'-dihydroxybenzidine the other polymers and model compounds show virtually no absorption in the visible region. It was observed that the absorption maxima of the polymers would vary for different samples of the same polymer. This phenomenon has been observed by others.¹

Thermal Stability. The thermal stabilities of the polybenzoxazoles were determined by measuring the weight loss in both air and nitrogen after 1-hr. heating periods at 300, 400, 450, 500, and 550°C. The weight obtained after the first hour at 300°C. was taken as the base weight. The results are given in Table V. A thermogravimetric analysis* on a poly-2,5-benzoxazole (nitrogen atmosphere, heating rate of 150°C./hr.) also was run (Fig. 5). These thermal studies show that the polybenzoxazoles have stabilities in air and nitrogen similar to those obtained on the polybenzimidazoles.

III. EXPERIMENTAL

A. Monomers

3,3'-Dihydroxybenzidine. This monomer was prepared from dianisidine by the method of Burkhardt and Wood.¹⁴ Yields of the white powdery product were in the range of 40–77% with melting points in the range of 285–288°C. (reported yield¹⁴ 90%; m.p. 292°C.).

Diphenyl 5-Chloroisophthalate. To a solution of 20.7 g. (0.22 mole) phenol and 16.6 g. (0.21 mole) pyridine in 100 ml. of methylene chloride was added a solution of 23.8 g. (0.10 mole) 5-chloroisophthaloyl chloride in 150 ml. methylene chloride with stirring over a period of 30 min. while maintaining a temperature of $25 \pm 3^\circ\text{C}$. A gelatinous precipitate of pyridine hydrochloride formed toward the end of the addition. After standing at room temperature for 3 hr., the mixture was filtered and the filtrate washed successively once with 100 ml. water, twice with 100 ml. 5% sodium hydroxide solution, and twice with 150 ml. water. After evaporation of the solvent, the crude diphenyl ester was recrystallized twice from 95% ethanol, giving 23.0 g. (65%) of white crystals; 105–106.5°C.

ANAL. Calcd. for $\text{C}_{20}\text{H}_{13}\text{Cl}$: C, 68.9%; H, 3.69%; Cl, 10.06%. Found: C, 68.14%; H, 3.71%; Cl, 10.08%.

4-Amino-3-Hydroxybenzoic Acid. This monomer was synthesized in two steps starting from *m*-hydroxybenzoic acid by way of the 4-nitro derivative. *m*-Hydroxybenzoic acid was nitrated by the method of Froelicher and Cohen.¹⁵ A suspension of 50.0 g. (0.36 mole) *m*-hydroxybenzoic acid in 175 ml. nitrobenzene was treated slowly with stirring with a solution of 25.5 g. fuming nitric acid (specific gravity 1.5, 90%, 0.365 mole) dissolved in 17 ml. nitrobenzene while maintaining a temperature of 35–40°C. The reaction was stirred 3 hr. after the addition was complete. The crude

* We are indebted to Dr. G. F. L. Ehlers, Wright Air Development Division, Wright-Patterson Air Force Base, Ohio, for this determination.

product was isolated by filtration, washed with carbon tetrachloride, then recrystallized from 25% ethanol. A yield of 12 g. (18%) of yellow crystals was obtained; m.p. 225–228°C. (reported¹⁵ m.p. 227–228°C.).

Reduction of the nitro derivative to give the monomer was accomplished by the method of Einhorn.¹⁶ Mossy tin, 75 g. was slowly added to a water bath heated mixture of 25 g. (0.14 mole) of 3-nitro-4-hydroxybenzoic acid in 500 ml. concentrated hydrochloric acid. After the tin had dissolved the reaction mixture was allowed to stand 1 hr. The reaction products were separated by filtration and dissolved in 500 ml. warm water. Hydrogen sulfide was passed into this solution until all of the tin was precipitated. After filtering, the filtrate was concentrated under reduced pressure. At the saturation point a concentrated solution of sodium acetate was added until pH 6 was reached. The pale yellow crystalline product precipitated from the solution. A yield of 11 g. (53%) was obtained; m.p. 230–232°C., (reported¹⁶ 60% yield; m.p. 216–217°C., dec.).

ANAL. Calcd. for $C_7H_7NO_3$: C, 54.89%; H, 4.61%; N, 9.16%. Found: C, 54.70%; H, 4.66%; N, 9.10%.

3-Amino-4-hydroxybenzoic Acid. The previously described procedure was also used to prepare the 3-amino-4-hydroxy derivative by using *p*-hydroxybenzoic acid as starting material. From 250 g. of *p*-hydroxybenzoic acid, a yield of 216 g. (87%) of the yellow crystalline *m*-nitro intermediate was obtained; m.p. 182°C. (reported¹⁷ 184°C.). The tin reduction of the nitro compound was effected in 78% yield giving the desired 3-amino-4-hydroxybenzoic acid; m.p. 200–202°C., dec. (reported¹⁷ m.p. 201–202°C., dec.).

ANAL. Calcd. for $C_7H_7NO_3$: C, 54.89%; H, 4.61%; N, 9.16%. Found: C, 54.99%; H, 4.65%; N, 9.28%.

Methyl 3-Amino-4-hydroxybenzoate. The general procedure of Clinton and Laskowski¹⁸ was used. A 10-g. portion of 4-hydroxy-3-nitrobenzoic acid, 16 ml. of methylene chloride, 7 ml. of methanol, and 1 ml. of concentrated sulfuric acid were charged to a 50-ml. round-bottomed flask and heated under reflux for 17 hr. The resulting solution was washed with water, 5% sodium bicarbonate solution, and again with water. After stripping of the solvent under reduced pressure, the product was recrystallized from 25% acetic acid solution. The yield of methyl 4-hydroxy-3-nitrobenzoate was 7.0 g. (65%); m.p. 69–71°C. (reported¹⁷ 74°C.). Reduction of this nitro intermediate was effected in the previously described manner, giving 1.8 g. (43%) methyl 3-amino-4-hydroxybenzoate; m.p. 104–107°C. (reported¹⁹ 110–111°C.).

ANAL. Calcd. for $C_8H_9NO_3$: C, 57.48%; H, 5.43%; N, 8.38%. Found: C, 57.18%; H, 5.28%; N, 8.42%.

B. Model Compounds

2-Phenylbenzoxazole (V). To a sidearm test tube fitted with a nitrogen inlet tube were charged 2.18 g. (0.02 mole) *o*-aminophenol and 3.96 g.

(0.02 mole) phenyl benzoate. The tube was flushed with nitrogen and a slow stream maintained during the reaction. The tube was slowly heated from 160 to 190°C. over a 4-hr. period. During this time a white sublimate of the pure compound formed in the upper part of the tube; m.p. 99–101°C. (reported²⁰ 101–103°C.). The crude product remaining in the tube could not be recrystallized satisfactorily.

ANAL. Calcd. for $C_{13}H_9NO$: C, 79.98%; H, 4.65%; N, 7.18%. Found: C, 79.73%; H, 4.40%; N, 6.78%.

2,2'-*p*-Phenylene-bisbenzoxazole (VI). The procedure was essentially the same as described above using 4.77 g. (0.015 mole) diphenyl terephthalate and 3.27 g. (0.03 mole) *o*-aminophenol. The mixture was heated from 150 to 230°C. over a 5-hr. period (water and phenol were expelled), yielding 4.75 g. (101%) gold-colored crystals. The crude product was recrystallized from 150 ml. of pyridine, yielding 2.25 g. (48%) pale gold crystals; m.p. 353–355°C. (reported²¹ m.p. 355–356°C.).

ANAL. Calcd. for $C_{20}H_{12}N_2O_2$: C, 76.91%; H, 3.87%; N, 8.97%. Found: C, 76.63%; H, 3.55%; N, 8.60%.

2,2'-*m*-Phenylene-bisbenzoxazole (VII). The procedure was the same as in the previous preparation, 4.77 g. (0.015 mole) diphenyl isophthalate and 3.27 g. (0.03 mole) *o*-aminophenol being used. The mixture was heated at 215–220°C. for 16 hr. A crude yield of 4.53 g. (97%) was recovered. The product was recrystallized first from dioxane and then from isobutanol, yielding 1.4 g. (31%) light brown powder, m.p. 227–228°C. (reported²¹ m.p. 229°C.).

2,2'-*o*-Phenylene-bisbenzoxazole (VIII). The procedure used was the same as that in the previous preparation, 1.09 g. (0.02 mole) of *o*-aminophenol and 3.18 g. (0.01 mole) of diphenyl phthalate being used. The mixture was heated at 200–300°C. for 7 hr. under nitrogen. The crude yield was 3.00 g. (95%) gold powder. The product was reprecipitated from DMF/H₂O to yield a fine gold-colored powder, m.p. 180–182°C., (reported²¹ m.p. 177°C.).

ANAL. Calcd. for $C_{20}H_{12}N_2O_2$: C, 76.91%; H, 3.87%; N, 8.98%. Found: C, 76.88%; H, 3.67%; N, 9.17%.

2,2'-(5-Chloro-1,3-phenylene)-bisbenzoxazole (IX). The same procedure as used previously was employed, with the use of 3.53 g. (0.01 mole) diphenyl 5-chloroisophthalate and 2.18 g. (0.02 mole) *o*-aminophenol. The mixture was heated from 130 to 195°C. over a 7-hr. period. The crude yield of brown powdered product was 3.40 g. (98%). The product was recrystallized from 95% ethanol, then sublimed under reduced pressure to give the pure new compound; white crystals; m.p. 288–289°C.

ANAL. Calcd. for $C_{20}H_{11}N_2O_2Cl$: C, 69.27%; H, 3.20%; N, 8.08%; Cl, 10.23%. Found: C, 69.39%; H, 3.31%; N, 7.81%; Cl, 10.93%.

2,2'-(Diphenyl)-6,6'-bibenzoxazole (X). The procedure was essentially the same as described, 0.54 g. (0.0025 mole) of 3,3'-dihydroxybenzidine

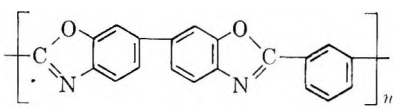
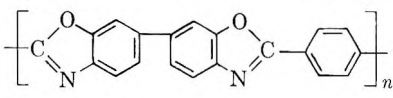
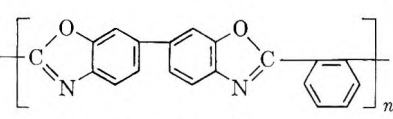
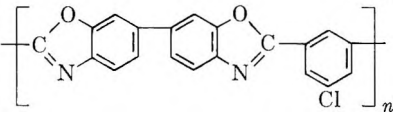
and 1.0 g. (0.005 mole) of phenyl benzoate being used. The mixture was heated from 230 to 270°C. for a 12-hr. period. The crude yield of yellow green powdered material was 1.31 g. (96%). The product was reprecipitated from DMF/H₂O and dried under reduced pressure to give the pure new compound gold-green powder, m.p. 330–332°C.

ANAL. Calcd. for C₂₆H₁₆N₂O₂: C, 80.41%; H, 4.12%; N, 7.22%. Found: C, 79.40%; H, 4.32%; N, 7.02%.

D. Polymerization

Polybenzoxazoles derived from comonomers were all prepared as described below. The yields were in the range of 100–108%, depending upon the degree of polymerization. Results of analyses are given in Table VI.

TABLE VI
Analytical Results for Polybenzoxazoles Derived From Comonomers

| Polymer recurring unit | Calculated | | | Found | | |
|---|------------|------|------|-------|------|------|
| | C, % | H, % | N, % | C, % | H, % | N, % |
|  | 77.42 | 3.23 | 9.03 | 77.08 | 3.70 | 8.77 |
|  | 77.42 | 3.23 | 9.03 | 77.13 | 3.52 | 8.89 |
|  | 77.42 | 3.23 | 9.03 | 77.06 | 3.60 | 8.75 |
|  | 69.67 | 2.61 | 8.13 | 69.43 | 2.55 | 7.97 |

Poly-2,5-benzoxazole. A 5-g. portion (0.033 mole) of 3-amino-4-hydroxybenzoic acid and 25 ml. of thionyl chloride were heated under reflux for 3 hr., hydrogen chloride and sulfur dioxide were evolved. The excess thionyl chloride was stripped under reduced pressure, and the yellow residue was dispersed in 25 ml. of benzene. This dispersion was slowly added to a solution of 3.5 g. phenol and 3.0 g. pyridine in 25 ml. benzene. The mixture was refluxed for 1 hr. The resulting residue was separated by filtration and washed with benzene and water giving, after drying 3.3 g. of yellow resin, m.p. >300°C., η_{inh} 0.075 (0.2 g./100 ml. conc. H₂SO₄, 25°C.). The infrared spectrum of this intermediate showed significant bands at 5.75, 6.05, 6.22, 6.46, 6.60, and 6.90 μ which is indicative of ester, amide, as well as benzoxazole groups. This intermediate polymer was

then heated in an inert atmosphere at 270°C. for 16 hr. The resulting polybenzoxazole was a light brown powder, η_{inh} 1.04 (0.2 g./100 ml. conc. H₂SO₄, 25°C.).

ANAL. Calcd. for (C₇H₃NO)_x: C, 71.79%; H, 2.58%; N, 13.66%. Found: C, 71.51%; H, 2.38%; N, 13.43%.

A larger run with 20 g. (0.13 mole) of 3-amino-4-hydroxybenzoic acid gave 10.4 g. (68%) of poly-2,5-benzoxazole; η_{inh} 0.65. The x-ray diffraction pattern showed two amorphous halos at $d = 6.2$ Å. (intensity 35) and $d = 3.4$ Å. (intensity 39).

Poly-2,6-benzoxazole. This polymer was prepared by the previously described procedure with the use of 5.0 g. (0.033 mole) 4-amino-3-hydroxybenzoic acid. The intermediate polymer was dark yellow in color and had an η_{inh} of 0.08 in sulfuric acid. The infrared spectrum showed no significant absorption below 6 μ and was very similar to that of the final powder; yield 72%, η_{inh} 0.22 (0.2 g./100 ml. conc. H₂SO₄, 25°C.). The x-ray diffraction pattern had two amorphous halos at $d = 6.2$ Å. (intensity 47) and $d = 3.4$ Å. (intensity 43).

ANAL. Calcd. for (C₇H₃NO)_x: C, 71.79%; H, 2.58%; N, 13.66%. Found: C, 71.66%; H, 2.46%; N, 13.56%.

References

1. Vogel, H., and C. S. Marvel, *J. Polymer Sci.*, **50**, 511 (1961).
2. Vogel, H., and C. S. Marvel, *J. Polymer Sci.*, **A1**, 1531 (1963).
3. Mulvaney, J. E., and C. S. Marvel, *J. Org. Chem.*, **26**, 95 (1961).
4. Mulvaney, J. E., J. J. Bloomfield, and C. S. Marvel, *J. Polymer Sci.*, **62**, 59 (1962).
5. Abshire, C. J., and C. S. Marvel, *Makromol. Chem.*, **44-46**, 388 (1961).
6. Lilyquist, M. R., and J. R. Holston, paper presented at 145th American Chemical Society Meeting, New York, September 1963; *Polymer Preprints*, **4**, 6 (1963).
7. Longone, D. T., and H. H. Un, paper presented at 145th American Chemical Society Meeting, New York, September 1963; **4**, 49 (1963).
8. Hergenrother, P. M., W. Wrasidlo, and H. H. Levine, paper presented at 147th American Chemical Society Meeting, Philadelphia, April 1964; *Polymer Preprints*, **5**, No. 1, 153 (1964).
9. Marvel, C. S., paper presented at 147th American Chemical Society Meeting, Philadelphia, April 1964; **5**, No. 1, 167 (1964).
10. Stille, J. K., and J. R. Williamson, paper presented at 147th American Chemical Society Meeting, Philadelphia, April 1964; *Polymer Preprints*, **5**, No. 1, 185 (1964).
11. Cornforth, J. W., in *Heterocyclic Compounds*, Vol. 5, R. C. Elderfield, Ed., Wiley, New York, 1957, pp. 418-451.
12. Brinker, K. C., D. D. Cameron, and I. M. Robinson, U. S. Pat. 2,904,537 (1959).
13. Passerini, R., *J. Chem. Soc.*, **1954**, 2256.
14. Burkhardt, G. N., and H. Wood, *J. Chem. Soc.*, **1929**, 151.
15. Froelicher, V., and J. B. Cohen, *J. Chem. Soc.*, **119**, 1425 (1921).
16. Einhorn, M., *Ann.*, **311**, 43 (1900).
17. Cavill, G. W. K., *J. Soc. Chem. Ind.*, **64**, 212 (1945).
18. Clinton, R. O., and S. C. Laskowski, *J. Am. Chem. Soc.*, **70**, 3135 (1948).
19. Lange, N. A., Ed., *Handbook of Chemistry*, Handbook Publishers, Sandusky, Ohio, 1949, p. 562.

20. Hein, D. W., R. J. Alheim, and J. J. Leavitt, *J. Am. Chem. Soc.*, **79**, 427 (1959).
21. Nyilas, E., and J. L. Pinter, *J. Am. Chem. Soc.*, **82**, 609 (1960).

Résumé

La polymérisation de la 3,3'-dihydroxybenzidine avec les esters phénylés des acides phtalique, isophtalique, téréphtalique et 5-chloroisophtalique, fournit une série de polybenzoxazoles aromatiques possédant une stabilité thermique élevée. La polymérisation à l'état fondu a fourni ces polymères avec un rendement quantitatif, polymères possédant des viscosités inhérentes de l'ordre de 0.20-1.04 et de stabilité thermique très semblable à celles obtenues avec les polybenzimidazoles aromatiques. L'homopolymérisation de l'acide 3-amino-4-hydroxybenzoïque et de l'acide 4-amino-3-hydroxybenzoïque a été effectuée en préparant un intermédiaire poly(ester-amide) suivi de la cyclisation thermique (à 250-300°C) en l'unité benzoxazole. Six produits modèles contenant l'unité benzoxazole furent préparés comme standards de référence; à savoir le 2-phénylbenzoxazole, le 2,2'-p-phénylène-bis-benzoxazole, 2,2'-m-phénylène-bis-benzoxazole, le 2,2'-o-phénylène-bis-benzoxazole, le 2,2'-(5-chloro-1-2-phényline)-bis-benzoxazole et le 2,2'-(diphényl)-6,6'-bibenzoxazole.

Zusammenfassung

Die Polymerisation von 3,3'-Dihydroxybenzidin mit den Phenylestern von Phthal-, Isophthal-, Terephthal- und 5-Chloroisophthalsäure lieferte eine Reihe von aromatischen Polybenzoxazolen mit hoher thermischer Stabilität. Bei der Schmelzpolymerisation wurden diese Polymeren mit Viskositätszahlen im Bereich von 0,20-1,04 und einer thermischen Stabilität sehr ähnlich derjenigen von aromatischen Polybenzimidazolen in quantitativer Ausbeute erhalten. Homopolymerisation von 3-Amino-4-hydroxybenzoesäure und 4-Amino-3-hydroxybenzoesäure wurde durch Darstellung eines intermediären Poly(esteramids) mit darauffolgender thermischer Zyklisierung (bei 250-300°C) zu Benzoxazolbausteinen erreicht. Sechs Modellverbindungen mit dem Benzoxazolbaustein wurden zur Verwendung als Bezugsstandards dargestellt. Diese waren 2-Phenylbenzoxazol, 2,2'-p-Phenylen-bis-benzoxazol, 2,2'-m-Phenylen-bis-benzoxazol, 2,2'-o-Phenylen-bis-benzoxazol, 2,2'-(5-Chlor-1,2-phenylen)-bis-benzoxazol und 2,2'-(Diphenyl)-6,6'-bis-benzoxazol.

Received July 16, 1964

Revised November 20, 1964

(Prod. No. 4579A)

Test of Theories of Flory, Ptitsyn, and Kurata for Dilute Polymer Solutions

R. S. PATEL and R. D. PATEL, *Chemistry Department,
Sardar Vallabhbhai Vidyapeeth, Vallabh-Vidyanagar, Gujarat, India*

Synopsis

The linear expansion factor α for the fractions of amylose acetate in various solvent-nonsolvent mixtures at different temperatures have been determined using Kurata's relationship. The validity of the Flory, Kurata, and Ptitsyn theories has been tested in terms of the dependence of the function of α on molecular weight. It has been found that Flory's theory is not applicable while the Kurata and Ptitsyn theories are in good agreement.

INTRODUCTION

Size and other properties of linear polymer molecules are affected by the excluded volume effect which is due to the interactions of segments of the chain approaching one another at random. Flory¹ assumed that the distribution of the polymer segments is similar to that without these interactions if all the linear dimensions are increased by a factor α , known as linear expansion factor. Considering the thermodynamic interaction between polymers and solvent or between segments of the same polymer molecule through the consideration of heat of mixing and entropy of mixing, he derived an expression giving an approximate quantitative relation of the interaction by α as

$$\alpha^5 - \alpha^3 = CN^{1/2} \quad (1)$$

where C is a temperature-dependent parameter related to thermodynamic interactions between segments and solvent and N is the number of segments of the chain. In Flory's theory the macromolecule is replaced by a cluster of segments for which there is a Gaussian distribution of the centers of mass. However, an extensive study of Flory's equation has shown^{2,3} that the value of C is affected by the type of distribution, and thus eq. (1) is approximate. Especially the value of $(\alpha^5 - \alpha^3)/N^{1/2}$ is not constant but increases with N ^{4,5}.

While giving a rigorous treatment to excluded volume effect and achieving a refinement of the original theory proposed by one of them, Kurata, Stockmayer, and Roig⁶ derived the following relationship by using an equivalent ellipsoid model instead of a spherically symmetrical model,

$$(1 - \alpha^{-2})(\alpha^2 + 1/3)^{3/2} = C'N^{1/2} \quad (2)$$

where C' is a constant, the value of which depends upon the effective bond length, and β , the binary cluster integral of each chain element. This equation gives a much better fit than eq. (1) to the results of Wall and Erpenbeck's Monte Carlo calculations⁷ of the dimensions of chains on a diamond lattice. Recently, Kurata and Stockmayer⁸ have used it to obtain unperturbed dimensions of a large number of polymers from their intrinsic viscosities. However, eq. (2) is derived for a Gaussian chain, and its use for chains with volume effects means that the latter increases only the distance between the ends of the chain and has no effect on its cross-sectional dimensions. This is contrary to experiment.⁹

Recently Ptitsyn¹⁰ has proposed an approximate theory which takes into account the interaction between segments of the chain roughly but leads to an equation differing substantially from that of Flory. Taking into consideration the non-Gaussian distribution functions for α , he derived the equation

$$[(4.68\alpha^2 - 3.68)^{2/3} - 1] = C'N^{1/2} \quad (3)$$

The validity of the theories of Flory,¹ Kurata et al.,⁶ and Ptitsyn¹⁰ is tested in this paper by the examination of eqs. (1), (2), and (3) in terms of accurate values of α obtained experimentally for solutions of well defined fractions of amylose acetate in different solvents of varying solvent power at different temperatures. A similar study of eqs. (1) and (2) has been reported by Fujita et al.¹¹ on polystyrene fractions. However, their conclusions are not very convincing and are slightly ambiguous.

EXPERIMENTAL

Amylose was obtained from freshly prepared potato starch by precipitation from its solution in 0.1M NaCl as the thymol complex. The amylose-thymol complex was dissolved in hot 0.1M NaCl solution and reprecipitated with *n*-butanol. Reprecipitation was carried out till the amylose-butanol complex when treated with ethanol yielded amylose having a purity of about 99%. Acetylation of amylose dispersed in formamide and pyridine was carried out with acetic anhydride according to the method of Potter and Hassid.¹²

Fractionation of amylose acetate was carried out by the precipitation method. The acetate was dissolved in nitromethane to give 0.2% solution and the solution was maintained at 30°C. Methanol was added slowly with stirring until the solution was cloudy. The temperature was raised to 35°C. and the solution stirred until the turbidity disappeared, then allowed to cool slowly to 30°C. and left overnight. The precipitates which formed settled to the bottom of the container and the supernatant liquid siphoned off. The precipitates were dissolved in nitromethane and reprecipitated into methyl alcohol. Sixteen samples were obtained by repeating the above process fifteen times. Four suitable fractions were selected for the present work.

All solvents used for the viscosity measurements were purified in accordance with standard procedures and used for light-scattering measurements to evaluate weight-average molecular weight (\bar{M}_w). The refractive index increment (dn/dc) was determined by the Brice-Phoenix differential refractometer.

Determination of α

The linear expansion factor α for any linear polymer has been correlated with intrinsic viscosity $[\eta]$ by the Flory-Fox¹ relationship,

$$[\eta] = KM^{1/3}\alpha^3 \quad (4)$$

where K is a characteristic constant of short-range interaction of chain segments and depends to small extent on temperature but is independent of the solvent.

K of eq. (4) is determined by a modified relationship proposed by Kurata et al.:¹⁷

$$[\eta]^{2/3}/M^{1/3} = k^{2/3} + 0.363 \Phi_0 B [g(\alpha_n)(\bar{M}^{2/3}/[\eta]^{1/3})]$$

where

$$\begin{aligned} \Phi_0 &= 2.87 \times 10^{21} \\ B &= \beta/m_0^2 \end{aligned}$$

in which β represents the binary cluster integral and m_0 is the molar weight of a polymer segment, and

$$g(\alpha_n) = 8\alpha_n^3(3\alpha_n^2 + 1)^{-2/3}$$

The values of K were determined at 15, 30, 40, 50, and 60°C. as given in Table I, according to the procedure followed by Kurata et al.¹⁷ Measurements¹⁸ of intrinsic viscosity under essentially theta conditions in nitromethane-methanol mixtures at 30 and 40°C. have confirmed these values of K , which may therefore be regarded as essentially independent of the fact that the method presently used assumes the correctness of eq. (2).

From the knowledge of K and $[\eta]$ at different temperatures and the molecular weight determined by light-scattering measurements, α was calculated from eq. (4).

RESULTS AND DISCUSSION

Table II gives the experimental values of $[\eta]$ of amylose acetate fractions in different solvents at different temperatures and weight-average molecular weights.

Intrinsic viscosities are obtained by plotting η_{sp}/c against c and $\ln \eta_r/c$ against c and extrapolating them to zero concentration. Generally there is a decrease in $[\eta]$ with the increase in temperature in all the solvent-nonsolvent mixtures. This behavior is similar to that of cellulose which also has a similar structure. In fact, amylose and cellulose can be con-

TABLE I
Values of K for Amylose Acetate Fractions at Different Temperatures

| Temperature, °C. | $K \times 10^3$ |
|---------------------|-----------------|
| 15 | 1.27 |
| 30 | 1.20 |
| 40 | 1.15 |
| 50 | 1.10 |
| 60 | 1.05 |

TABLE II
Experimental Values of Intrinsic Viscosities $[\eta]$
in Various Solvents at Different Temperatures

| Frac- tion | \bar{M}_{10} $\times 10^{-5}$ | Solvent | | $[\eta]$ | | | | |
|---------------|------------------------------------|---|------------------|----------|-------|-------|-------|-------|
| | | System | Compo- sition | 15°C. | 30°C. | 40°C. | 60°C. | 60°C. |
| 1 | 10.30 | CHCl ₃ -C ₆ H ₁₂ | 100:0 | 7.00 | 6.30 | 5.80 | 5.30 | |
| | | | 80:20 | 6.60 | 6.00 | 5.40 | 5.05 | |
| | | | 65:35 | 5.98 | 5.47 | 4.72 | 4.52 | |
| | | | 50:50 | 4.87 | 4.15 | 3.65 | 3.30 | |
| | | | | | | | | |
| 2 | 6.31 | | 100:0 | 4.55 | 4.05 | 3.75 | 3.25 | |
| | | | 80:20 | 4.35 | 3.80 | 3.50 | 3.13 | |
| | | | 65:35 | 3.95 | 3.54 | 3.10 | 2.90 | |
| | | | 50:50 | 3.35 | 2.75 | 2.47 | 2.25 | |
| | | | | | | | | |
| 3 | 4.57 | | 100:0 | 3.45 | 3.12 | 2.80 | 2.56 | |
| | | | 80:20 | 3.35 | 2.95 | 2.66 | 2.43 | |
| | | | 65:35 | 3.02 | 2.70 | 2.39 | 2.22 | |
| | | | 50:50 | 2.41 | 2.10 | 1.88 | 1.72 | |
| | | | | | | | | |
| 5 | 2.10 | | 100:0 | 1.78 | 1.62 | 1.48 | 1.36 | |
| | | | 80:20 | 1.77 | 1.54 | 1.42 | 1.29 | |
| | | | 65:35 | 1.62 | 1.43 | 1.27 | 1.20 | |
| | | | 50:50 | 1.37 | 1.19 | 1.08 | 0.95 | |
| | | | | | | | | |
| 1 | 10.30 | CH ₃ NO ₂ -CH ₃ OH | 100:0 | | 3.65 | 3.50 | 3.35 | 3.16 |
| | | | 75:25 | | 3.80 | 3.61 | 3.51 | 3.24 |
| | | | 50:50 | | 3.15 | 3.09 | 3.08 | — |
| | | | 35:65 | | 2.10 | 2.24 | 2.30 | — |
| | | | | | | | | |
| 2 | 6.31 | | 100:0 | | 2.54 | 2.38 | 2.24 | 2.19 |
| | | | 75:25 | | 2.59 | 2.48 | 2.35 | 2.22 |
| | | | 50:50 | | 2.13 | — | — | 2.03 |
| | | | 35:65 | | 1.48 | 1.60 | 1.62 | — |
| | | | | | | | | |
| 3 | 4.57 | | 100:0 | | 1.95 | 1.83 | 1.72 | 1.69 |
| | | | 75:25 | | 2.02 | 1.93 | 1.82 | 1.71 |
| | | | 50:50 | | 1.62 | 1.60 | 1.58 | 1.55 |
| | | | 35:65 | | 1.14 | 1.25 | 1.28 | 1.20 |
| | | | | | | | | |
| 5 | 2.10 | | 100:0 | | 1.07 | 1.015 | 0.95 | 0.920 |
| | | | 75:25 | | 1.12 | 1.085 | 1.02 | 0.925 |
| | | | 50:50 | | 0.92 | 0.904 | 0.90 | — |
| | | | 35:65 | | 0.69 | 0.720 | 0.75 | 0.672 |
| | | | | | | | | |

sidered as the first known examples of polymers with structural differences very similar to those between isotactic and syndiotactic polymer of the same monomer. However, in the case of a 35/65% nitromethane-methanol mixture as solvent, it was observed that for high molecular weight fractions, $[\eta]$ of the solution increased as the temperature increased from 35 to 50°C. and then suddenly decreased at 60°C. This is the only mixture which behaves contrary to the general behavior of other solvents. It may be due to the fact that it has least solvent power compared to the others used in the present investigation. A similar type of change has been observed even in the case of flexible polymers like polyisobutylene,¹³ where $[\eta]$ decreases with increase in temperature in a good solvent, while on decreasing the solvent power of a solvent $[\eta]$ increases with increase in temperature.

Table III gives a comparison of the values of $[\eta]$ observed by the authors and those reported by Cowie¹⁴ for amylose acetate of the same molecular weight. The values of $[\eta]$ observed in the present investigation are 1.7–2.0 times the values reported by Cowie¹⁴ for the same molecular weight fractions at the same temperature. Similar results were obtained by Burchard,¹⁵ who worked on amylose with dimethyl sulfoxide (DMSO) as solvent. A comparison of his results and those obtained by Cowie¹⁶ for amylose in DMSO are compiled in Table IV. Again the values of $[\eta]$ obtained by Burchard are higher, being 1.7–1.8 times those of Cowie.¹⁶

TABLE III
Intrinsic Viscosities $[\eta]$ of Amylose Acetate Fractions
in Chloroform and Nitromethane at 30°C.

| $\bar{M}_w \times 10^{-5}$ | $[\eta]$ in CHCl_3 | | | $[\eta]$ in CH_3NO_2 | | |
|----------------------------|-----------------------------|------------------------|-------|--------------------------------------|------------------------|-------|
| | (This work) | (Cowie ¹⁴) | a/A | (This work) | (Cowie ¹⁴) | b/B |
| | a | A | | b | B | |
| 10.30 | 6.30 | 3.31 | 1.90 | 3.65 | 1.77 | 2.05 |
| 6.31 | 4.05 | 2.20 | 1.77 | 2.54 | 1.23 | 2.07 |
| 4.57 | 3.12 | 1.85 | 1.70 | 1.95 | 0.97 | 2.00 |
| 2.10 | 1.62 | 0.89 | 1.82 | 1.07 | 0.52 | 2.08 |

TABLE IV
Intrinsic Viscosities $[\eta]$ of Amylose in DMSO at 30°C.

| $\bar{M}_w \times 10^{-5}$ | n | | Ratio a/b |
|----------------------------|---------------------------|------------------------|----------------|
| | (Burchard ¹⁵) | (Cowie ¹⁶) | |
| | a | b | |
| 10.00 | 3.31 | 1.95 | 1.70 |
| 6.31 | 2.26 | 1.32 | 1.71 |
| 3.16 | 1.29 | 0.74 | 1.75 |
| 1.58 | 0.72 | 0.41 | 1.78 |
| 1.28 | 0.60 | 0.33 | 1.81 |

There can be two main reasons for the higher viscosities obtained in the present work, the first being that the experimentally determined values of \bar{M}_w may be low and the second that the composition of the polymer may be different.

In the present work the values of \bar{M}_w determined by light scattering were confirmed by: (1) determining \bar{M}_w of the same fraction in another solvent (the values of \bar{M}_w were found to vary only by about 5%); (2) determining the number-average molecular weight \bar{M}_n of the same fractions in chloroform and nitromethane at different temperatures. The values of \bar{M}_n were found to be approximately the same, indicating that the fractions were homogeneous. (3) The light-scattering measurements were also checked with a standard polystyrene sample of known \bar{M}_w and τ .

It is, therefore, clear that there is little likelihood of error in the evaluation of the values of \bar{M}_w in the present investigation.

Hence, it may be conjectured that the lower values reported by Cowie¹⁴ may be due to the difference in the composition of amylose acetate. This may be due to: (1) a small amount of branching existing in amylose, (2) incomplete acetylation of amylose, or (3) the presence of amylopectin acetate in the amylose acetate.

It has been observed with other polymers that a small amount of branching and a small change in the degree of substitution do not alter the intrinsic viscosity to the extent observed in the case of Cowie.¹⁴ Thus the only possibility left for the low values of $[\eta]$ is the existence of amylopectin acetate in the sample. Amylopectin acetate, being a branched polymer, lowers the viscosity of amylose acetate considerably.

Burchard¹⁵ also attributes the low values of $[\eta]$ obtained by Cowie¹⁶ to the presence of amylopectin in the sample. Hence it is quite probable that the low values of $[\eta]$ reported by Cowie^{14,16} of amylose as well as amylose acetate may be due to the presence of amylopectin, which, due to its highly branched nature, has a lower extension for the same molecular weight, and hence, has a lower intrinsic viscosity.

COMPARISON OF EQUATIONS (1), (2), AND (3) WITH EXPERIMENT

Analysis of Flory's Relation

According to eq. (1) plots of $(\alpha^5 - \alpha^3)$ against $M^{1/2}$ are expected to give a straight line passing through the origin. Figures 1 and 2 show $(\alpha^5 - \alpha^3)$ plotted against $M^{1/2}$ for different solvent-nonsolvent mixture systems at different temperatures. Figure 1 represents such plots for chloroform-cyclohexane mixtures of different proportions at 30°C. and for 80/20%, chloroform-cyclohexane mixtures at 15, 30, 40, and 50°C. Figure 2 shows similar plots for nitromethane-methanol mixtures; the compositions of the mixtures studied at different temperatures are 35, 50, and 75% nitromethane and 100% nitromethane. The data for all six nitromethane

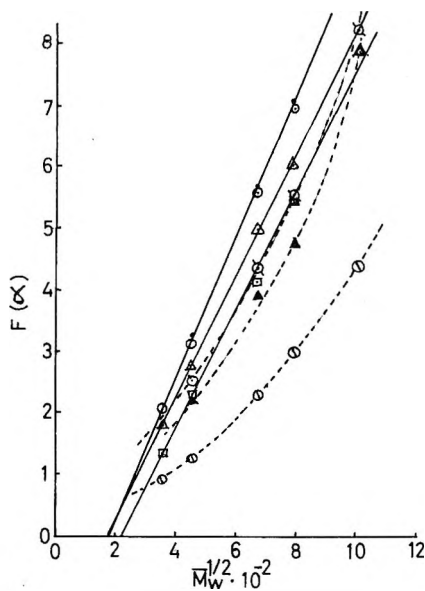


Fig. 1. $F(\alpha)$ vs. $\bar{M}_w^{1/2}$ for Flory equation: (●) 80% CHCl_3 , 15°C.; (○) 100% CHCl_3 , 30°C.; (△) 80% CHCl_3 , 30°C.; (□) 65% CHCl_3 , 30°C.; (◇) 80% CHCl_3 , 40°C.; (▲) 80% CHCl_3 , 50°C.; (⊕) 50% CHCl_3 , 30°C.

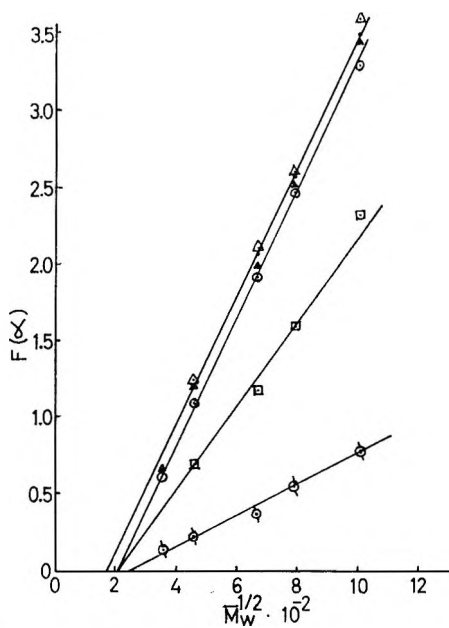


Fig. 2. $F(\alpha)$ vs. $\bar{M}_w^{1/2}$ for Flory equation: (△) 75% CH_3NO_2 , 30°C.; (●) 75% CH_3NO_2 , 40°C.; (▲) 75% CH_3NO_2 , 50°C.; (○) 100% CH_3NO_2 , 30°C.; (□) 50% CH_3NO_2 , 30°C.; (⊕) 35% CH_3NO_2 , 30°C.

systems fall reasonably well on straight lines. On the other hand, three of the seven chloroform systems show an upward curvature. The systems showing deviation from a straight line are those containing 80% chloroform at 40 and 50°C., and the 50% chloroform system at 30°C. It may be suggested that there are both temperature and solvent effects up to 30°C. The system containing 80% chloroform gives straight lines, while above this temperature (at 40 and 50°C.) marked curvature is observed. On the other hand, a study of the systems at 30°C. but at different compositions indicates that a deviation from a straight line is shown by the poor solvent. Thus the Flory equation as far as linearity is concerned is not obeyed above 30°C. for good solvents and for poor solvents at lower temperatures. However none of the linear plots of the thirteen systems studied passes through the origin but always give positive intercepts on the abscissa. The intercept is about 2×10^2 which corresponds to a molecular weight of 40,000. However, below this molecular weight the value of α should be unity and also independent of molecular weight. This is in contradiction to the Flory eq. (1), according to which α should approach unity as the molecular weight approaches zero. Similar behavior has been observed by Fujita et al.¹¹ for polystyrene in methyl ethyl ketone and toluene systems at 34.5°C. Even with toluene, which is a good solvent, plots showed a marked upward curvature, while the intercept for the methyl ethyl ketone system corresponded to 30,000 molecular weight. The value of molecular weight = 40,000, below which Flory theory is not applicable, appears to be too large to be accepted as a critical value. However there is a little possibility of attributing this deviation to experimental error as it is a common value for both the solvent-nonsolvent systems studied at different temperatures. It is also difficult to attribute it to certain specific interaction as this type of interaction would ordinarily show variation in the values of intercept with the variation of solvent and its solvent power and also with temperature. Hence one is tempted to suggest that Flory's equation, eq. (1), is not applicable to these systems.

Analysis of Ptitsyn's Relation

According to eq. (3) the plots of $[(4.68\alpha^2 - 3.68) - 1]$ against $M^{1/2}$ are expected to give straight lines passing through the origin. Figures 3 and 4 show such plots for the same systems studied for the Flory relationship, viz., chloroform-cyclohexane and nitromethane-methanol, at different temperatures. In contrast to the Flory relationship it is observed that all the solvent-nonsolvent mixture systems, irrespective of temperature and solvent give reasonably linear plots. It is also noted that five of the seven nitromethane systems studied pass through the origin as required. The remaining two systems give an intercept which corresponds to about 30,000 molecular weight. These systems consist of solvent having a composition near to the Θ solvent composition. In the case of the chloroform systems, almost all the linear plots do not pass through the origin but give positive intercept on abscissa. All the plots seem to have a common intercept

corresponding to about 3,000 molecular weight. This deviation can be regarded as comparatively negligible in the light of the great range of temperature as well as solvents of different solvent power. On the whole one can conclude that Ptitsyn equation is obeyed reasonably well except for

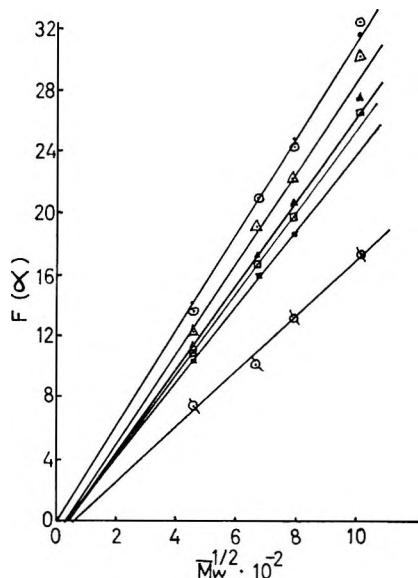


Fig. 3. $F(\alpha)$ vs. $\bar{M}_w^{1/2}$ for Ptitsyn equation: (○) 80% CHCl_3 , 15°C.; (●) 100% CHCl_3 , 30°C.; (Δ) 80% CHCl_3 , 30°C.; (▲) 80% CHCl_3 , 40°C.; (□) 65% CHCl_3 , 30°C.; (■) 80% CHCl_3 , 50°C.; (◻) 50% CHCl_3 , 30°C.

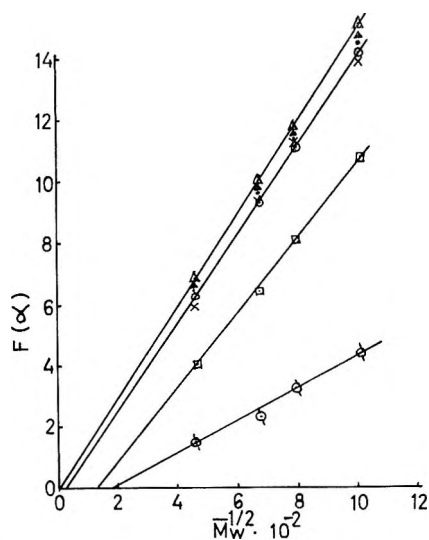


Fig. 4. $F(\alpha)$ vs. $\bar{M}_w^{1/2}$ for Ptitsyn equation: (Δ) 75% CH_2NO_2 , 30°C.; (▲) 75% CH_2NO_2 , 40°C.; (●) 75% CH_2NO_2 , 50°C.; (○) 75% CH_2NO_2 , 60°C.; (×) 100% CH_2NO_2 , 30°C.; (□) 50% CH_2NO_2 , 30°C.; (◻) 35% CH_2NO_2 , 30°C.

solvents for very poor solvent power. However it is definite that the data confirm to eq. (3) better than to eq. (1).

Analysis of Kurata's Relation

Figures 5 and 6 show the viscosity data plotted in the form convenient for testing the Kurata equation, eq. (2), viz., $(1 - \alpha^{-2})(\alpha^2 + 1/3)$ against $M^{1/2}$. All the plots for the chloroform systems at different temperatures

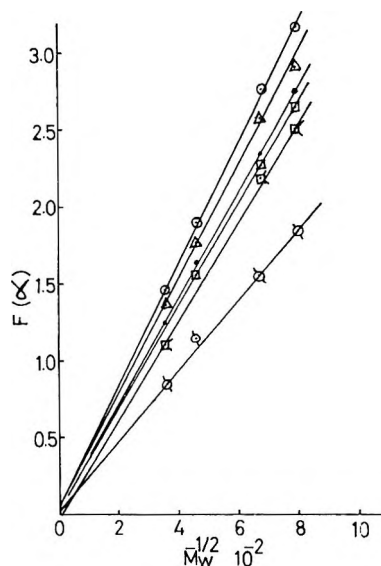


Fig. 5. $F(\alpha)$ vs. $\bar{M}_w^{1/2}$ for Kurata equation: (O) 100% or 80% CHCl_3 , 30°C.; (Δ) 80% CHCl_3 , 30°C.; (\bullet) 80% CHCl_3 , 40°C.; (\square) 65% CHCl_3 , 30°C.; (\blacksquare) 80% CHCl_3 , 50°C.; (\diamond) 50% CHCl_3 , 30°C.

are given in Figure 5 while those of nitromethane systems are given in Figure 6. According to equation (2) all the plots should be straight lines passing through the origin. All the data for chloroform fall on straight lines passing through the origin. In contrast to both the Flory and Ptitsyn relations, even for poor solvents the plots are found to pass almost through the origin, while the plots for nitromethane systems give both positive and negative intercepts, and two plots do pass through the origin. This type of negative intercept is also observed if the data of Fujita et al.¹¹ for polystyrene in cyclohexane at 45 and 50°C. are extrapolated without considering the points below 160,000 molecular weight as in the present study. The negative intercepts are shown by 75/25 nitromethane-methanol mixtures at 30, 40, and 50°C., while the positive intercept is exhibited as usual by the system containing poor solvents. Thus the nitromethane systems of poor solvent power do not obey any of the three relationships studied. It is also very difficult to decide whether the Kurata or Ptitsyn theory is in better agreement with the experimental results.

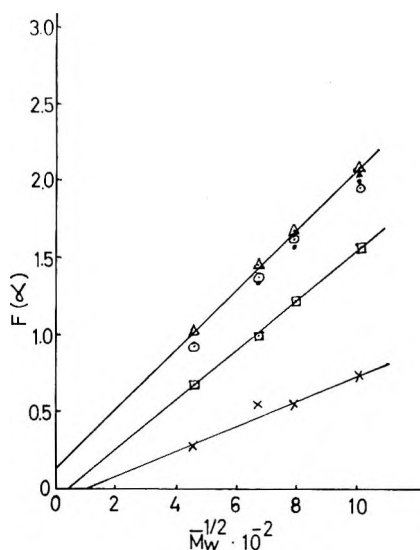


Fig. 6. $F(\alpha)$ vs. $\bar{M}_w^{-1/2}$ for Kurata equation: (Δ) 75% CH_3NO_2 , 30°C.; (\blacktriangle) 75% CH_3NO_2 , 40 or 50°C.; (\bullet) 75% CH_3NO_2 , 60°C.; (\circ) 100% CH_3NO_2 , 30°C.; (\square) 50% CH_3NO_2 , 30°C.; (\times) 35% CH_3NO_2 , 30°C.

The viscosity data of Fujita et al.¹¹ for polystyrene were utilized to test the Ptitsyn relation. It was observed that only one straight line was obtained with the toluene system, while the other systems showed a marked curvature as obtained in the case of Kurata's relation.

References

1. Flory, P. J., *J. Chem. Phys.*, **17**, 303 (1949).
2. Fixman, M., *J. Chem. Phys.*, **23**, 1656 (1955).
3. Ptitsyn, O. B., *Vysokomol. Soedin.*, **1**, 715 (1959).
4. Krigbaum, W. R., and D. K. Carpenter, *J. Phys. Chem.*, **59**, 1166 (1955).
5. Notely, N. and P. Debye, *J. Polymer Sci.*, **17**, 99 (1955).
6. Kurata, M., W. H. Stockmayer, and A. Roig, *J. Chem. Phys.*, **33**, 151 (1960).
7. Wall, F. T., and J. J. Erpenbeck, *J. Chem. Phys.*, **30**, 634 (1959).
8. Kurata, M., and W. H. Stockmayer, *Rept. Progr. Polymer Phys. Japan*, **5**, 23 (1962).
9. Tsvetkov, V. N., and S. Ya. Lyubina, *Vysokomol. Soedin.*, **2**, 75 (1960).
10. Ptitsyn, O. B., *Polymer Sci., U.S.S.R.*, **3**, 1061 (1962).
11. Fujita, H., R. Okada, and Y. Toyoshima, *Makromol. Chem.*, **59**, 137 (1963).
12. Potter, A. L., and W. Z. Hassid, *J. Am. Chem. Soc.*, **70**, 3774, 1948.
13. Patel, R. D., and C. E. H. Bawn, *Trans. Faraday Soc.*, **52**, 1669 (1956).
14. Cowie, J. M. G., *J. Polymer Sci.*, **49**, 455 (1961).
15. Burchard, W., *Makromol. Chem.*, **64**, 110 (1963).
16. Cowie, J. M. G., *Makromol. Chem.*, **42**, 230 (1961).
17. Kurata, M., and W. H. Stockmayer, paper presented at IUPAC Symposium on Macromolecular Chemistry, Montreal, 1961.
18. Patel, R. S., Ph.D. Thesis, Sardar Vallabhba; Vidyapeeth, Vallabh Vidyanagar, India.

Résumé

On a déterminé le facteur d'expansion linéaire α suivant la relation de Kurata, pour les fractions d'acétate d'amylose dans différents mélanges solvant-précipitant et à différentes températures. On a contrôlé la validité des théories de Flory, Kurata, et Ptitsyn du point de vue de la dépendance de α en fonction du poids moléculaire. On a trouvé que la théorie de Flory n'est pas applicable, tandis que les théories de Kurata et de Ptitsyn expliquent bien les résultats.

Zusammenfassung

Der lineare Expansionsfaktor α wurde mit der Beziehung von Kurata für Amylose-acetatfraktionen in verschiedenen Lösungsmittel- und Fällungsmittelgemischen bei verschiedenen Temperaturen bestimmt. Die Gültigkeit der Theorien von Flory, Kurata, und Ptitsyn wurde anhand der Abhängigkeit von α vom Molekulargewicht überprüft. Es zeigte sich, dass die Theorie von Flory nicht anwendbar ist, während die Theorien von Kurata und Ptitsyn gute Übereinstimmung liefern.

Received January 15, 1964

Revised December 9, 1964

(Prod. No. 4584A)

Interaction of Ethylaluminum Dichloride with Organic Nitrogen and Phosphorus Compounds in Three-Component Polyolefin Catalysts

RICHARD L. McCONNELL, MARVIN A. McCALL, G. O. CASH, JR.,
F. B. JOYNER, and H. W. COOVER, JR., *Research Laboratories,*
Tennessee Eastman Company, Division of Eastman
Kodak Company, Kingsport, Tennessee

Synopsis

The chemistry of three-component coordination catalysts for the polymerization of α -olefins is very complex. The present investigation was initiated to elucidate the chemistry involved in the interaction of third-component compounds such as hexamethylphosphoric triamide, tributylamine, triphenylphosphine, or dimethylformamide with ethylaluminum dichloride. The present chemical and spectral data demonstrate that ethylaluminum dichloride and third-component compounds form stable complexes even at temperatures up to 100°C. in the absence of solvents or in homogeneous solutions. These data are in agreement with the fact that organoaluminum compounds form stable complexes with a variety of electron-donor compounds. The ethylaluminum dichloride-third-component complexes in combination with titanium(III) chloride produce highly stereospecific catalysts for the polymerization of α -olefins.

INTRODUCTION

Certain organic compounds containing phosphorus and/or nitrogen, such as hexaalkylphosphoric triamides, tertiary phosphines, tertiary amines, and dialkylformamides, are important components of highly stereospecific coordination catalysts for the polymerization of α -olefins.¹⁻⁷ For example, alkylaluminum dihalides and also sesquihalides in combination with titanium or vanadium trichlorides are ineffective for the polymerization of propylene to solid polymers. However, by using a suitable amount of one of the previously identified nitrogen or phosphorus compounds in combination with an alkylaluminum dihalide or sesquihalide and a titanium or vanadium trichloride, catalysts yielding highly stereoregular polymers of propylene, 1-butene, and other α -olefins are obtained. In this paper the modifying nitrogen or phosphorus compound will be referred to as a third component and the combination of the organoaluminum halide and the third component will be called an adduct. For optimum rate of polymerization and optimum stereoregularity of the polyolefin produced, the mole ratio of alkylaluminum dihalide or sesquihalide to the third component usually lies in the range of 1/0.4 to 1/0.8. Larger amounts of the third component tend to deactivate the catalyst.

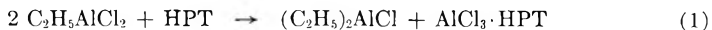
The chemistry of these three-component coordination catalysts is very complex, and the present investigation was initiated to elucidate the chemistry involved in the interaction of the third-component compounds with ethylaluminum dichloride. In this work, the organoaluminum compounds and the complexes derived from the organoaluminum and certain third-component compounds were studied in dry benzene solutions by far-infrared spectroscopy and by cryoscopic measurements. In addition, the catalytic behavior of these adducts in combination with α -TiCl₃ (hereafter referred to as TiCl₃) were studied and compared with those of the (C₂H₅)₂AlCl/TiCl₃ catalyst.

There are many references in the literature pertaining to the formation of stable complexes when an organoaluminum or organoaluminum halide compound is treated with electron-donor compounds such as ethers or trialkylamines.⁸⁻¹⁵ Jacober and Kraus observed a maximum conductivity when 0.5 mole of dimethyl ether was added to 1.0 mole of methylaluminum dibromide; they attributed this conductivity to the formation of a 2/1 complex, (CH₃AlBr₂)₂·O(CH₃)₂.⁹ Peters and co-workers isolated and characterized a number of organoaluminum·trimethylamine complexes including the ethylaluminum dichloride·trimethylamine and diethylaluminum chloride·trimethylamine complexes.¹³ These complexes are stable either as the isolated compound or in ether solution. In fact, these complexes are so stable that they can be reacted with lithium hydride to produce the corresponding alkylaluminum hydride·trimethylamine complexes in good yield.¹³

Complexes are also known to form between many organoaluminum compounds and certain alkali metal halides.^{10b, 16-18} The organoaluminum halide·alkali metal halide complexes are known to be extremely stable and tend to disproportionate only at high temperatures (>160°C.).^{17, 18}

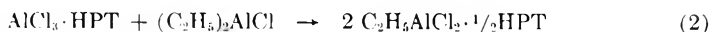
It is known that very rapid exchanges of substituents attached to the aluminum are possible if compounds of the types R₃Al, R₂AlX, RAlX₂, and AlX₃ are mixed.¹⁴ Although two adjacent members of this series, such as R₂AlX and RAlX₂ are stable in a mixture, nonadjacent members are not. For example, mixing R₂AlX with AlX₃ in equimolar quantities results in the formation of RAlX₂.

Recently, Zambelli and co-workers postulated that a dismutation reaction occurs even at room temperature when ethylaluminum dichloride is treated with a third-component compound such as hexamethylphosphoric triamide (HPT) according to the eq. (1):^{19, 20}



The present investigation demonstrates that a molecular complex is formed when ethylaluminum dichloride is treated with a third-component compound at or below 100°C. in the absence of a solvent or in a homogeneous solution and that a dismutation reaction does not occur under these conditions. Also, it was found that an equimolar mixture of AlCl₃·HPT

and $(C_2H_5)_2AlCl$ in a homogeneous solution produced $C_2H_5AlCl_2 \cdot 1/2 HPT$ as illustrated in the eq. (2):



EXPERIMENTAL

Equipment

A Perkin-Elmer Infracord spectrophotometer, Model 137, containing potassium bromide prisms was used to record the infrared spectra in the 12.5–25 μ region. The cells used were Press-lok cells with potassium bromide plates supplied by the Connecticut Instrument Corp. of Wilton, Connecticut.

Polymerizations were conducted in 300-ml. stainless steel microautoclaves.

Cryoscopic Apparatus

The apparatus used was designed for freezing point studies by the U. S. Bureau of Standards.²¹ A platinum resistance thermometer was used as the temperature-sensing device.

Materials

The diethylaluminum chloride and ethylaluminum dichloride were obtained from Ethyl Corp. The ethylaluminum dichloride was purified by three recrystallizations from its own melt and this material was used for all studies reported in this paper.

Heptane and tributylamine were Eastman-grade chemicals from Distillation Products Industries. The heptane was dried over clean sodium wire and the tributylamine was redistilled.

B and A reagent-grade benzene was obtained from the General Chemical Division of Allied Chemical Corp. and was dried over clean metallic sodium.

Dimethylformamide was obtained from E. I. du Pont de Nemours and Co., Inc., and redistilled prior to use.

The triphenylphosphine was obtained from Metal and Thermit Corp. and recrystallized from benzene.

Redistilled hexamethylphosphoric triamide from the Organic Chemicals Division of Tennessee Eastman Co. contained no impurities detectable by gas chromatography.

The propylene was obtained from Sun Oil Co. It was dried by passing it through a bed of molecular sieve 4A, and analysis showed it contained 98.7% propylene, 1.2% propane, <0.1% ethylene and carbon dioxide, and only a trace of oxygen.

Titanium(III) chloride was obtained from Stauffer Chemical Co. The types used included both hydrogen-reduced (H) grade and hydrogen-reduced activated (HA) grade of α - $TiCl_3$.

Infrared Studies

Solutions of the organoaluminum compounds in a suitable solvent were prepared in a nitrogen-filled dry box to prevent oxidation or hydrolysis of the organoaluminum compounds. Exactly 4.5 g. of dry solvent and 0.5 g.

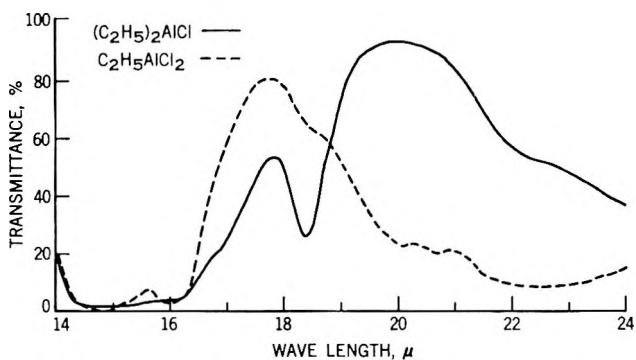


Fig. 1. Far-infrared spectra of diethylaluminum chloride and ethylaluminum dichloride in benzene.

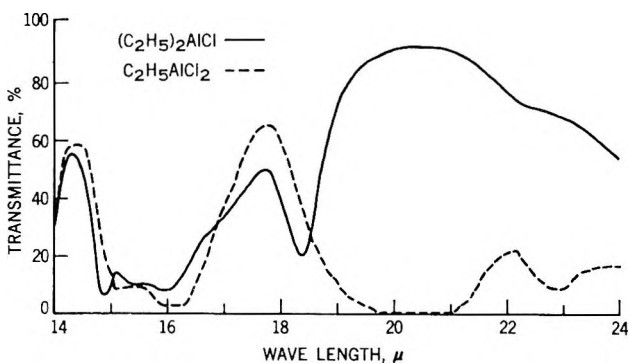


Fig. 2. Far-infrared spectra of diethylaluminum chloride and ethylaluminum dichloride in heptane.

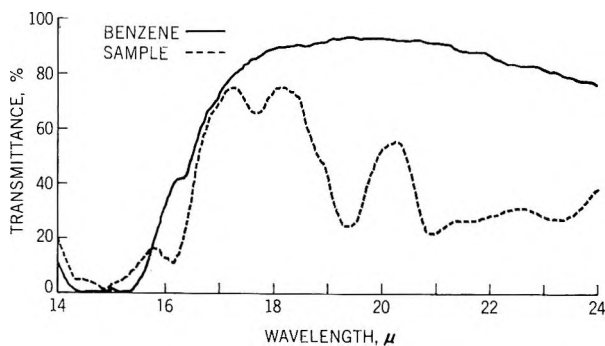


Fig. 3. Far-infrared spectra of benzene and ethylaluminum dichloride:HPT complex in benzene.

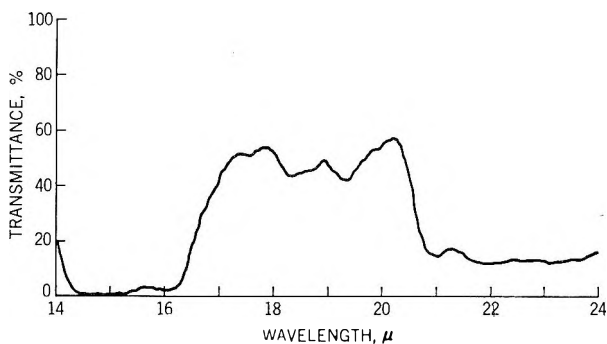


Fig. 4. Far-infrared spectrum of ethylaluminum dichloride-HPT complex plus added diethylaluminum chloride in benzene.

of the organoaluminum compound were weighed in glass vials in the dry box. In the nitrogen-filled dry box, samples were loaded into a Press-lok cell with potassium bromide plates (0.2 mm. thickness of solution) and the

TABLE I
Far-Infrared Study of Organoaluminum Compounds and
Ethylaluminum Dichloride-Third-Component Mixtures

| Sam- ple | Solution compositions ^a | Solvent | Infrared absorption band at 18.2- 18.4 μ |
|-------------|--|---------|--|
| 1 | (C ₂ H ₅) ₂ AlCl | Benzene | Present |
| 2 | (C ₂ H ₅) ₂ AlCl | Heptane | Present |
| 3 | C ₂ H ₅ AlCl ₂ | Benzene | Absent ^b |
| 4 | C ₂ H ₅ AlCl ₂ | Heptane | Absent |
| 5 | C ₂ H ₅ AlCl ₂ + added (C ₂ H ₅) ₂ AlCl ^c | Benzene | Present |
| 6 | (C ₂ H ₅) ₂ AlCl + 1/2[(CH ₃) ₂ N] ₃ P(O) | Benzene | Present |
| 7 | C ₂ H ₅ AlCl ₂ + 1/2[(CH ₃) ₂ N] ₃ P(O) ^d | Benzene | Absent |
| 8 | C ₂ H ₅ AlCl ₂ + 1/2[(CH ₃) ₂ N] ₃ P(O) | None | Absent |
| 9 | [C ₂ H ₅ AlCl ₂ + 1/2[(CH ₃) ₂ N] ₃ P(O)] + added (C ₂ H ₅) ₂ AlCl ^c | Benzene | Present |
| 10 | C ₂ H ₅ AlCl ₂ + 1/2(C ₆ H ₅) ₃ N ^d | Benzene | Absent |
| 11 | [C ₂ H ₅ AlCl ₂ + 1/2(C ₆ H ₅) ₃ N] + added (C ₂ H ₅) ₂ AlCl ^c | Benzene | Present |
| 12 | C ₂ H ₅ AlCl ₂ + 1/2(C ₆ H ₅) ₃ P ^d | Benzene | Absent |
| 13 | [C ₂ H ₅ AlCl ₂ + 1/2(C ₆ H ₅) ₃ P] + added (C ₂ H ₅) ₂ AlCl ^c | Benzene | Present |
| 14 | C ₂ H ₅ AlCl ₂ + 1/2 HCON(CH ₃) ₂ ^d | Benzene | Absent |
| 15 | [C ₂ H ₅ AlCl ₂ + 1/2 HCON(CH ₃) ₂] + added (C ₂ H ₅) ₂ AlCl ^c | Benzene | Present |
| 16 | (C ₂ H ₅) ₂ AlCl + AlCl ₃ ·HPT | Benzene | Absent |

^a Solutions contained 10% organoaluminum compound or complex except in the case where no solvent was used.

^b The shoulder which appears at about 18.3 μ in this benzene spectrum (Fig. 1) cannot be attributed to (C₂H₅)₂AlCl impurity since the spectrum of the same dichloride determined in heptane, in which (C₂H₅)₂AlCl is easily detectable (Fig. 2), has no shoulder.

^c Amount of (C₂H₅)₂AlCl added was equivalent (in moles) to the C₂H₅AlCl₂ present.

^d The mixture of C₂H₅AlCl₂ and third component was heated to 100°C. and allowed to cool before diluting with benzene.

spectrum was run immediately. The infrared spectra of 10% solutions of diethylaluminum chloride, ethylaluminum dichloride, the ethylaluminum dichloride·HPT complex, and the ethylaluminum dichloride·HPT complex to which diethylaluminum chloride had been added are included as Figures 1-4. These spectral data and similar data obtained on solutions containing tributylamine, triphenylphosphine, and dimethylformamide instead of HPT are summarized in Table I.

Diethylaluminum chloride was added in small increments to 10% solutions of ethylaluminum dichloride and also ethylaluminum dichloride·HPT adduct in order to determine the smallest amount of diethylaluminum chloride detectable in the presence of these organoaluminum compounds. The data obtained are summarized in Table II.

TABLE II
Limit of Detection of Diethylaluminum Chloride in Ethylaluminum Dichloride and Ethylaluminum Dichloride·HPT Adduct Solutions

| Sample | Solution compositions ^a | (C ₂ H ₅) ₂ AlCl added, % ^b | Infrared absorption band at 18.2-18.4 μ |
|--------|---|--|---|
| 1 | C ₂ H ₅ AlCl ₂ | None | Absent |
| 2 | C ₂ H ₅ AlCl ₂ | 0.1 | Absent |
| 3 | C ₂ H ₅ AlCl ₂ | 0.2 | Present |
| 4 | C ₂ H ₅ AlCl ₂ | 0.3 | Present |
| 5 | Adduct ^c | None | Absent |
| 6 | Adduct ^c | 0.1 | Absent |
| 7 | Adduct ^c | 0.2 | Present |
| 8 | Adduct ^c | 0.3 | Present |

^a Solutions contained 10% C₂H₅AlCl₂ in heptane or 10% C₂H₅AlCl₂·HPT adduct in benzene.

^b Amount of (C₂H₅)₂AlCl added was based on total solution.

^c Mole ratio of C₂H₅AlCl₂/HPT in adduct was 1/0.6.

Typical Polymerization of Propylene

In a nitrogen-filled dry box, 100 ml. of pure, sodium-dried solvent (benzene or heptane) was added to a clean, dry 300-ml. stainless steel microautoclave. The ethylaluminum dichloride·third-component adduct was added and then the TiCl₃. The total catalyst charge was 1.0 g. when 1/0.5/1 mole proportions of C₂H₅AlCl₂/HPT/TiCl₃ were used.

The autoclave was sealed with a neoprene stopper, removed from the dry box, and then capped with a clean, dry autoclave head assembly while being purged with dry nitrogen.

A total of 100 ml. of liquid propylene was charged to the autoclave by using a calibrated sight glass. The reaction was then conducted at a specified temperature usually for 4 hr. with rocking, and the mixture was then cooled and vented. Isobutyl alcohol was added to deactivate the catalyst and the reaction mixture was digested in isobutyl alcohol on a steam

bath to remove catalyst residues. The polymer slurry was cooled to 25°C., filtered, washed with methanol, and then the polymer was dried in air. Final drying was conducted in a circulating-air oven at 50°C.

Determination of Heptane Index

A carefully weighed sample (usually 10 g.) of the polypropylene was exhaustively extracted with heptane in a Soxhlet extractor (usually 24 hr.). The residue was dried to constant weight. The heptane index for the catalyst was then calculated as the percentage of the polypropylene insoluble in refluxing heptane.

DISCUSSION

The ethylaluminum dichloride-third-component adducts are generally readily soluble in aromatic solvents such as benzene but have only limited solubility in aliphatic solvents. The stereospecificity of the $C_2H_5AlCl_2/HPT/TiCl_3$ catalyst is identical, however, regardless of whether the polymerization is conducted in aromatic (benzene) or aliphatic (propylene or heptane) solvents (Table III).

TABLE III
Polymerization of Propylene With Some Three-Component Systems^a

| Organo-metallic compound | TiCl ₃ ^b | Third component (TC) | Solvent | Al/TC ratio | Al/Ti ratio | Polymerization temp., °C. | Polymer obtained | |
|--|--------------------------------|----------------------|---------|-------------|-------------|---------------------------|------------------|------------------------------|
| | | | | | | | Total yield, g. | Heptane-insoluble portion, % |
| (C ₂ H ₅) ₂ AlCl | Stauffer H | None | Heptane | — | 0.5 | 85 | 45.7 | 88.0 |
| (C ₂ H ₅) ₂ AlCl | Stauffer HA | None | Heptane | — | 1 | 70 | 46.5 | 90.0 |
| C ₂ H ₅ AlCl ₂ | Stauffer H | HPT | Heptane | 2 | 1 | 85 | 44.0 | 96.5 |
| C ₂ H ₅ AlCl ₂ | Stauffer H | HPT | Benzene | 2 | 1 | 85 | 47.7 | 97.2 |
| C ₂ H ₅ AlCl ₂ | Stauffer H | HPT | None | 1.67 | 1 | 25 ^c | 90.0 | 97.0 |
| C ₂ H ₅ AlCl ₂ | Stauffer HA | HPT | None | 1.67 | 1 | 85 | 99.0 | 96.0 |

^a Catalysts contained 0.4 g. TiCl₃ except in the run made with 1/1 (C₂H₅)₂AlCl/TiCl₃ where 0.2 g. of TiCl₃ was used. Polymerizations were conducted for 4 hr. using 100 ml. solvent and 100 ml. propylene except in those cases where no solvent was used. In these cases 200 ml. of liquid propylene was used.

^b H refers to hydrogen-reduced grade and HA refers to hydrogen-reduced activated grade.

^c Reaction conducted for 24 hr.

Benzene has an absorption band at 12.9μ and a broad band at $14\text{--}16 \mu$ in the far-infrared wavelengths, but the spectrum is clear in the $16\text{--}25 \mu$ region. The good solubility of the adducts in benzene and the limited number of absorption bands in the region to be studied made it an ideal solvent for our infrared studies. Heptane is a suitable solvent for determining the spectra of organoaluminum compounds which are soluble in it since its spectrum is clear in the $14.5\text{--}25 \mu$ region.

It was found that the far-infrared spectrum of diethylaluminum chloride showed a characteristic absorption band at 18.3μ . This 18.3μ band was not present in the spectrum of either ethylaluminum dichloride or the $\text{C}_2\text{H}_5\text{AlCl}_2 \cdot \frac{1}{2}\text{HPT}$ adduct but did appear in the infrared spectra of similar solutions to which diethylaluminum chloride had been purposely added. By the incremental addition of diethylaluminum chloride to solutions of ethylaluminum dichloride and ethylaluminum dichloride-HPT adduct in heptane and benzene, respectively, it was demonstrated that diethylaluminum chloride is detectable in the presence of these organoaluminum compounds at a concentration of 0.2% based on total solution or 2% based on the amount of organoaluminum compound present.

When 1 mole of $\text{AlCl}_3 \cdot \text{HPT}$ adduct was mixed with 1 mole of $(\text{C}_2\text{H}_5)_2\text{AlCl}$ in benzene at room temperature, the infrared spectrum of this solution did not show the 18.3μ band which is characteristic of $(\text{C}_2\text{H}_5)_2\text{AlCl}$ (sample 16, Table I). Instead, the spectrum was identical with that of the $\text{C}_2\text{H}_5\text{AlCl}_2 \cdot \frac{1}{2}\text{HPT}$ adduct in benzene. This demonstrates that $\text{AlCl}_3 \cdot \text{HPT}$ and $(\text{C}_2\text{H}_5)_2\text{AlCl}$ reacted to produce the dichloride adduct.

The 18.3μ band was also quite evident in a solution containing a $1/0.5$ mole ratio of diethylaluminum chloride and HPT. Similar results were obtained when tributylamine, triphenylphosphine, or dimethylformamide were used instead of HPT. As is usual in infrared spectroscopy, minor shifts were sometimes observed in the 18.3μ band, but the band characteristic of diethylaluminum chloride was generally observed in the $18.2\text{--}18.4 \mu$ region. Triphenylphosphine has an absorption band at 18.45μ , but the $(\text{C}_2\text{H}_5)_2\text{AlCl}$ band at 18.3μ is discernible in the presence of triphenylphosphine. The other third components studied (HPT, tributylamine, and dimethylformamide) are completely free of bands in the 18.3μ region. These data clearly indicate that when 1 mole of ethylaluminum dichloride is mixed with $\frac{1}{2}$ mole of third component and the mixture preheated to 100°C ., cooled, and dissolved in benzene, no diethylaluminum chloride is present.

Since polymerizations are initiated immediately after the catalyst components are mixed, the infrared curves were usually determined by using freshly prepared solutions. However, the results were the same when the $\text{C}_2\text{H}_5\text{AlCl}_2 \cdot \text{HPT}$ adduct which had aged for several months was used as they were when $\text{C}_2\text{H}_5\text{AlCl}_2$ and HPT were added separately to the benzene solvent and heated. Also, the adduct did not change when the benzene solution was aged, as demonstrated by the fact that the infrared spectra determined immediately after mixing and after 24 hr. were identical.

TABLE IV
 Cryoscopic Study of $C_2H_5AlCl_2$ Adducts With HPT and $(C_6H_5)_3P$

| Run | Compound, g. | Relative f.p., °C. ^a | ΔT found, °C. | Indicated mol. wt. | Avg. mol. wt. |
|-----|------------------|---------------------------------|-----------------------|--------------------|---------------|
| 1 | Benzene | 26.2389 | 2.325 | — | — |
| 2 | Benzene | 26.2805 | 2.325 | — | — |
| 3 | HPT | 0.6308 | 1.588 | 0.737 | 166.7 |
| | Benzene | 26.2996 | 2.325 | — | — |
| 4 | HPT | 0.6208 | 1.612 | 0.713 | 169.5 |
| | Benzene | 26.3011 | 2.235 | — | — |
| 5 | HPT | 0.5946 | 1.514 | 0.811 | 166.0 |
| | Benzene | 30.9014 | 2.325 | — | — |
| 6 | $C_2H_5AlCl_2$ | 1.1407 | 1.583 | 0.742 | 254.7 |
| | Benzene | 31.3356 | 2.325 | — | — |
| 7 | $C_2H_5AlCl_2$ | 0.9082 | 1.713 | 0.612 | 242.5 |
| | Benzene | 32.7399 | 2.325 | — | — |
| 8 | $C_2H_5AlCl_2$ | 0.8101 | 1.812 | 0.513 | 247.0 |
| | Benzene | 31.3356 | 2.325 | — | — |
| 9 | $C_2H_5AlCl_2^b$ | 0.9082 | — | — | — |
| | HPT | 0.64 | 1.903 | 0.422 | 599.4 |
| 10 | Benzene | 32.7399 | — | — | — |
| | $C_2H_5AlCl_2^b$ | 0.8101 | — | — | — |
| 11 | HPT | 0.57 | 1.967 | 0.358 | 602.9 |
| | Benzene | 32.8443 | 2.325 | — | — |
| 12 | $C_2H_5AlCl_2^c$ | 1.6105 | 1.909 | 0.416 | 603.5 |
| | HPT | — | — | — | — |
| 13 | Benzene | 32.7399 | — | — | — |
| | $C_2H_5AlCl_2$ | 0.8101 | — | — | — |
| 14 | HPT ^d | 1.14 | 1.700 | 0.625 | 487.9 |
| | Benzene | 31.6094 | 2.325 | — | — |
| 15 | $(C_6H_5)_3P^e$ | 0.5141 | 1.943 | 0.382 | 218.0 |
| | Benzene | 30.6426 | 2.325 | — | — |
| 16 | $(C_6H_5)_3P$ | 0.5272 | 1.888 | 0.437 | 201.6 |
| | Benzene | 33.2136 | 2.325 | — | — |
| 17 | $(C_6H_5)_3P$ | 0.5480 | 1.902 | 0.423 | 199.7 |
| | Benzene | 30.5462 | 2.325 | — | — |
| 18 | $C_2H_5AlCl_2^f$ | 0.6669 | — | — | — |
| | $(C_6H_5)_3P$ | 0.7229 | 1.692 | 0.633 | 371.9 |
| 19 | Benzene | 29.7384 | — | — | — |
| | $C_2H_5AlCl_2^f$ | 1.3945 | — | — | — |
| 20 | $(C_6H_5)_3P$ | 1.5489 | 1.017 | 1.308 | 387.4 |
| | Benzene | — | — | — | — |

^a Beckmann thermometer reading (not actual freezing point).

^b $C_2H_5AlCl_2$ added to benzene prior to the addition of HPT.

^c Mixture of $C_2H_5AlCl_2$ and HPT preheated to 100°C. and allowed to cool before adding to benzene.

^d An additional 0.57 g. HPT added to run 9.

^e Recrystallized from benzene: m.p. 79–80°C.; mol. wt. by boiling point elevation in benzene 288.

^f $C_2H_5AlCl_2$ added to benzene prior to the addition of $(C_6H_5)_3P$.

It is known that ethylaluminum dichloride exists as a dimer. During this study, the molecular weight of the dimer in benzene was determined by cryoscopic measurements (runs 5-7, Table IV). The average of the molecular weights (248.1) determined by this method was quite close to the theoretical value (253.9). The molecular weight determined for the HPT used was also quite close to the theoretical value. Cryoscopic measurements on benzene solutions containing both ethylaluminum dichloride and HPT in a mole ratio of 1/0.5 indicated that a highly associated complex was formed which actually caused a cryoscopic increase with respect to the freezing point of the benzene solution containing only the ethylaluminum dichloride (runs 5-9, Table IV). Thus, there were fewer particles in solution after the addition of HPT than before. The average molecular weight of the $C_2H_5AlCl_2 \cdot HPT$ complex was calculated to be 601.1 (runs 8 and 9, Table IV). As shown in Table IV, essentially the same results were obtained by adding HPT to the benzene solution of ethylaluminum dichloride (runs 8 and 9) or by adding the preheated (to 100°C.) complex derived from ethylaluminum dichloride (1 mole) and HPT ($1/2$ mole) to benzene (run 10). When equimolar quantities of ethylaluminum dichloride and HPT were present, the observed molecular weight of the complex was 487.9. That the molecular weights of these adducts are greater than the combined molecular weights of ethylaluminum dichloride and HPT is not surprising, since there are three nitrogen atoms in each HPT molecule available for complexing action.

Similar cryoscopic data obtained when 1 mole of $C_2H_5AlCl_2$ was mixed with $1/2$ mole of $(C_6H_5)_3P$ indicated an average molecular weight of 379.7, which is very close to that of the combined molecular weights of ethylaluminum dichloride and triphenylphosphine (389.2).

If triphenylphosphine cleaves $(C_2H_5AlCl_2)_2$ to $C_2H_5AlCl_2 \cdot (C_6H_5)_3P$ as expected, the solution should contain $C_2H_5AlCl_2 \cdot (C_6H_5)_3P$ and $(C_2H_5AlCl_2)_2$ in the mole ratio of 2/1 and have an average molecular weight of 344.1.

For some unexplained reason, the cryoscopic molecular weight determined on the triphenylphosphine alone in benzene was somewhat lower than the theoretical value. The purity of the triphenylphosphine was not in question, since the sample melted sharply at the expected melting point and the molecular weight as determined by boiling point elevation in benzene was quite close to the theoretical value.

These data, which show that the cryoscopic molecular weight of the complex formed from ethylaluminum dichloride with either HPT or triphenylphosphine is always equal to or greater than the theoretical molecular weight, clearly indicate that dismutation does not occur in these benzene solutions.

At Al/Ti ratios of 0.5/1 and 1/1, the $(C_2H_5)_2AlCl/TiCl_3$ catalyst produces polypropylene with a heptane index in the range of 88-90 (Table III). The $C_2H_5AlCl_2/HPT/TiCl_3$ catalyst consistently produces polypropylene with a heptane index of 96-97 using heptane, benzene, or liquid propylene as the reaction medium. Thus the stereospecificity of the $C_2H_5AlCl_2/$

HPT/TiCl₃ catalyst is higher than that observed for the (C₂H₅)₂AlCl/TiCl₃ catalyst.

As discussed earlier, the ethylaluminum dichloride·HPT adduct is not completely soluble in aliphatic hydrocarbons such as heptane. A solid phase (insoluble in heptane), when combined with TiCl₃, is inactive for the polymerization of propylene (Table V). The liquid phase (heptane-soluble portion), when combined with TiCl₃, does polymerize propylene, but the heptane index (80) is much lower than that observed for the total catalyst and is lower than that observed for the (C₂H₅)₂AlCl/TiCl₃ catalyst. When the heptane-soluble and -insoluble components were recombined and used in combination with TiCl₃, the heptane index was the typical 97 usually observed for this three-component catalyst. This demonstrates that all of the catalyst components must be present to produce highly stereoregular polypropylene.

It has been reported previously that the kinetics of the C₂H₅AlCl₂/HPT/TiCl₃ and (C₂H₅)₂AlCl/TiCl₃ catalyst are entirely different.⁷ The difference in kinetics referred to includes differences in rate of polymerization, number of active sites, and chain transfer. The difference in chain transfer leads to different levels of molecular weight and molecular weight distribution in polymers prepared with the two systems. Zambelli and co-workers suggested that the activity of the three-component catalysts based on C₂H₅AlCl₂ derives from the formation of (C₂H₅)₂AlCl by dismutation of the C₂H₅AlCl₂. This assumption is obviously unjustified since the kinetics and nature of the polymer produced indicate that there are significant differences in the chemistry of active site formation, in the nature of the active sites, and in the stereospecificity of the three-component catalyst system as compared with the binary system based on (C₂H₅)₂AlCl.

TABLE V
Polymerization Studies With Soluble and Insoluble Portions of C₂H₅AlCl₂·HPT Adduct^a

| Phase tested | TiCl ₃ ^b | Solvent | Polymerization temp., °C. | Reaction rate, g./g. TiCl ₃ /hr. | Polymer obtained | |
|---|--------------------------------|---------|---------------------------|---|------------------|------------------------------|
| | | | | | Total yield, g. | Heptane-insoluble portion, % |
| Solid phase (insoluble in heptane) | Stauffer H | Heptane | 85 | 0.31 | 0.5 | — |
| Liquid phase (soluble in heptane) | Stauffer H | Heptane | 85 | 27.5 | 44.0 | 80.0 |
| Solid phase + liquid phase (recombined) | Stauffer H | Heptane | 85 | 32.4 | 51.7 | 97.0 |

^a Polymerizations were conducted for 4 hr. using 1.0 g. total catalyst (1/0.5/1-C₂H₅AlCl₂/HPT/TiCl₃).

^b H refers to hydrogen-reduced grade.

In summary, a combination of $C_2H_5AlCl_2$ and $TiCl_3$ is an ineffective catalyst and third-component compounds such as HPT must be added to produce active, stereospecific catalysts for the polymerization of propylene. $C_2H_5AlCl_2$ produces stable complexes with the third components, such as HPT, amines, and phosphines, in the absence of solvents or in homogeneous solutions. Finally, it has been shown that the $C_2H_5AlCl_2$ /HPT/ $TiCl_3$ catalyst is different from the $(C_2H_5)_2AlCl$ / $TiCl_3$ catalyst chemically and in polymerization characteristics.

The authors appreciate the assistance of H. M. Beard, Jr., R. B. Blanton, C. A. Glover, A. L. Thompson, and D. A. Weemes in some of the experimental work reported in this paper.

References

1. Coover, H. W., Jr., and F. B. Joyner (to Eastman Kodak Co.), U. S. Pat. 2,956,991 (1960).
2. Coover, H. W., Jr., and F. B. Joyner (to Eastman Kodak Co.), U. S. Pat. 2,969,345 (1961).
3. Coover, H. W., Jr., and F. B. Joyner (to Eastman Kodak Co.), U. S. Pat. 2,958,688 (1960).
4. Coover, H. W., Jr., and F. B. Joyner (to Eastman Kodak Co.), U. S. Pat. 2,967,856 (1961).
5. Coover, H. W., Jr., and F. B. Joyner (to Eastman Kodak Co.), U. S. Pat. 2,969,346 (1961).
6. Coover, H. W., Jr., and F. B. Joyner (to Eastman Kodak Co.), U. S. Pat. 2,973,348 (1961).
7. Coover, H. W., Jr., and F. B. Joyner, paper presented at 145th Meeting, American Chemical Society, New York, N. Y., Sept. 1963.
8. Ziegler, K., *International Conference on Coordination Chemistry*, The Chemical Society, London, 1959, p. 1.
9. Jacober, G., and C. A. Kraus, *J. Am. Chem. Soc.*, **71**, 2409 (1949).
10. Coates, G. E., *Organo-Metallic Compounds*, Wiley, New York, 1960, (a) p. 141; (b) pp. 138-139.
11. Davidson, N., and H. C. Brown, *J. Am. Chem. Soc.*, **64**, 316 (1942).
12. Fetter, N. R., B. Bartocha, F. E. Brinckman, Jr., and D. W. Moore, *Can. J. Chem.*, **41**, 1359 (1963).
13. Peters, F. M., B. Bartocha, and A. J. Bilbo, *Can. J. Chem.*, **41**, 1051 (1963).
14. Zeiss, H., *Organometallic Chemistry*, Reinhold, New York, 1960, pp. 202-203.
15. Clemens, D. F., W. S. Brey, Jr., and H. S. Sisler, *Inorg. Chem.*, **2**, 1251 (1963).
16. Hall, F. C., and A. W. Nash, *J. Inst. Petrol. Technologists*, **23**, 679 (1937).
17. Ziegler, K., R. Köster, H. Lehmkuhl, and K. Reinert, *Ann. Chem.*, **629**, 33 (1960).
18. Köster, R., and W. R. Kroll, *Ann. Chem.*, **629**, 50 (1960).
19. Zambelli, A., J. di Pietro, and G. Gatti, *Chim. Ind. (Milan)*, **44**, 529 (1962).
20. Zambelli, A., J. di Pietro, and G. Gatti, *J. Polymer Sci.*, **A1**, 403 (1963).
21. Glasgow, A. R., Jr., A. J. Streiff, and F. D. Rossini, *J. Res. Natl. Bur. Std.*, **35**, 355 (1945).

Résumé

La chimie des catalyseurs de coordination ternaire pour la polymérisation des α oléfins est très complexe. On a entrepris l'étude présente en vue d'élucider la chimie de l'interaction de composés ternaires tels que le triamide hexaméthylphosphorique, la tributylamine, la triphénylphosphine, ou le diméthylformamide avec le dichlorure

d'éthylaluminium. Les résultats chimiques et spectraux actuels démontrent que le dichlorure d'éthylaluminium et les composés ternaires forment des complexes stables, même à des températures allant jusqu'à 100°C en absence de solvant ou en solutions homogènes. Ces résultats sont en accord avec le fait que les composés organoaluminiques forment des complexes stables avec une variété de composés électrodonneurs. Les complexes du dichlorure d'éthylaluminium avec les composés ternaires, en combinaison avec le chlorure de titane(III) produisent des catalyseurs fortement stéréospécifiques pour la polymérisation des α -oléfinés.

Zusammenfassung

Die Chemie der Dreikomponenten-Koordinationskatalysatoren zur Polymerisation von α -Olefinen ist sehr komplex. Die vorliegende Untersuchung wurde unternommen, um die Chemie der Wechselwirkung der als dritte Komponente verwendeten Verbindungen Hexamethylphosphortriamid, Tributylamin, Triphenylphosphin, oder Dimethylformamid mit Äthylaluminiumdichlorid aufzuklären. Die erhaltenen chemischen und spektralen Daten zeigen, dass Äthylaluminiumdichlorid und die Dritt-Komponentenverbindungen in Abwesenheit von Lösungsmitteln oder in homogener Lösung sogar bei Temperaturen bis zu 100°C stabile Komplexe bilden. Diese Ergebnisse stimmen mit der Tatsache überein, dass Organoaluminiumverbindungen mit einer Vielzahl von Elektronendonoren stabile Komplexe bilden. Die Äthylaluminiumdichlorid-Dritte-Komponenten-Komplexe liefern mit Titan(III)-Chlorid hochgradig stereospezifische Katalysatoren für die Polymerisation von α -Olefinen.

Received April 6, 1964

Revised December 10, 1964

(Prod. No. 4592A)

Kinetic Study of Cyclopolymerization

YUJI MINOURA and MOTONORI MITOH, *Department of Chemistry, Osaka City University, Minami-Ogimachi, Kita-ku, Osaka, Japan*

Synopsis

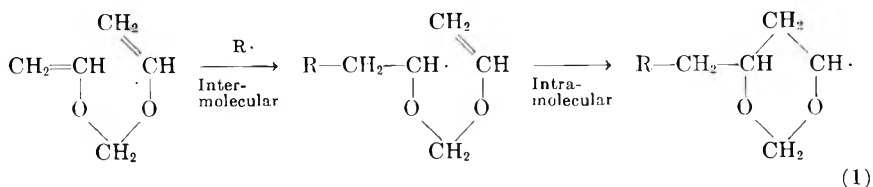
Kinetic studies of cyclopolymerization have been reported in several papers to date, but the overall kinetics is not yet established. Therefore, divinylformal was synthesized and polymerized as a difunctional monomer, and the overall rate equation, $R_p = k[I]^{3/4}[M]^{3/2-2}$, was obtained. To interpret this irregular rate equation, elementary reactions were considered and the theoretical rate equation, $R_p = k[I]^{1/2-1}[M]^{2-1}$, was obtained. The overall activation energy of polymerization was 27.7 kcal./mole, and this value, together with the result of the measurement of residual unsaturation in the polymer, yielded a value for the difference of activation energy between cyclization and propagation reaction of 2.6 kcal./mole. The results of measurements of intrinsic viscosities and residual unsaturation in the polymer at various conversions suggest that the branching reaction occurs to some extent during polymerization. The polydivinylformal was hydrolyzed to poly(vinyl alcohol) with hydroxylamine hydrochloride, and the 1,2-glycol structures in the poly(vinyl alcohol) were determined. The result showed a higher content of 1,2-glycol structures than that in commercial poly(vinyl alcohol).

INTRODUCTION

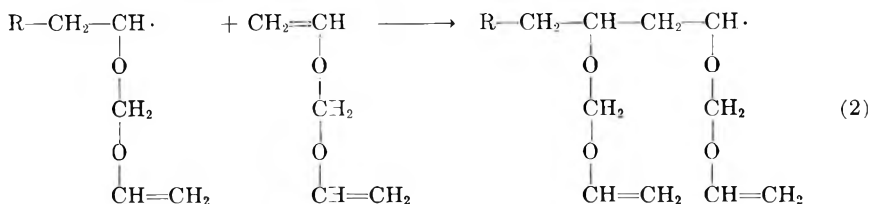
Since the discovery by Butler¹⁻³ that the polymerization of diallyl quaternary ammonium salts may proceed by a cyclopolymerization mechanism to produce linear soluble polymers, many investigators have reported the polymerization of bifunctional materials such as diolefins. Recently not only nonconjugated divinyl monomers, but also dialdehyde^{4,5} and diisocyanate⁶ were found to be polymerized by this mechanism producing cyclic units in the main chains. Although there are many reports describing the polymerization of such monomers, the overall kinetics is not yet established.

Divinylformal ($\text{CH}_2=\text{CHOCH}_2\text{OCH}=\text{CH}_2$) was polymerized with azobisisobutyronitrile. The time-conversion relationship, the residual vinyl groups in the polymer, intrinsic viscosities, and the structure of poly(vinyl alcohol) derived from the polymer by hydrolysis were investigated, and the overall kinetics was established.

Divinylformal was found to be polymerized with radical initiators by alternating inter-intramolecular propagation steps, forming dioxane rings in the chain as follows shown in eq. (1):^{7,8}



Here R· is an initiator radical or a polymer radical. A small amount of unsaturation always found in the polymer seems to be produced by the mechanism shown in eq. (2):

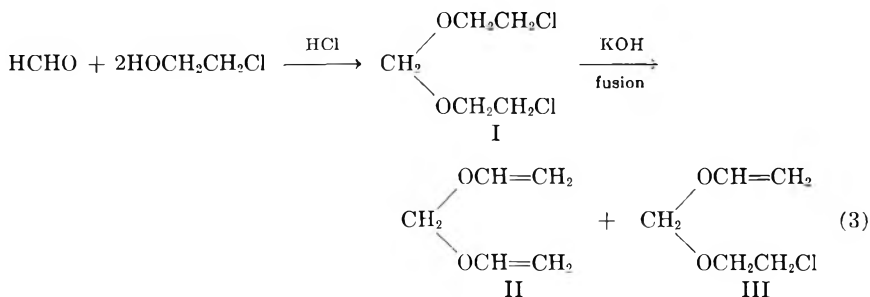


EXPERIMENTAL

Preparation of Monomer

The mixture of ethylenechlorohydrin, paraformaldehyde, and calcium chloride was heated at 95–100°C. for 2.5 hr. in a three-necked round-bottomed flask equipped with stirrer.⁷⁻⁹ During this period, dry hydrogen chloride was introduced slowly from the bottom of the flask with continuous stirring. The product was separated from the water layer, washed with water, dried over potassium carbonate, and then distilled under reduced pressure; b.p. 108°C./25 mm. Hg, n_D^{23} 1.4529 (literature:⁷ b.p. 94–96°C./10 mm. Hg, n_D^{20} 1.4550). The α, α' -dichlorodiethylformal (I) thus obtained was a colorless liquid with the stinging odor characteristic of acetals.

α, α' -Dichlorodiethylformal was then dehydrochlorinated by alkali fusion at 180–200°C.



Divinylformal(II) and water were distilled off spontaneously from the reaction mixture. To separate the product from the α -chloroethyl vinylformal(III) formed, a Vigreux column was attached to the outlet of the reaction flask. The product was then dried and redistilled through a

Vigreux column just before use; b.p. 89–90°C., n_D^{23} 1.4143 (literature:⁷ b.p. 87–89°C./680 mm. Hg, n_D^{20} 1.4215).

ANAL. Calc.: C, 60.03%; H, 8.06%. Found: C, 60.02%; H, 8.42%.

Polymerization Procedure

Divinylformal was polymerized in benzene at 50°C. with azobisisobutyronitrile as a radical initiator. The monomer, solvent, and initiator were charged in an ampule and, after degassing by the freeze-thaw method, the ampule was sealed under vacuum. The sealed tube was then set into a thermostated water bath and taken out after a proper time interval. The polymer was collected by pouring the contents of the ampule into methanol, filtering, and then drying *in vacuo*. The polymerization proceeded homogeneously under these experimental conditions. The polymer was a white solid which was quite soluble in common organic solvents such as benzene, acetone, and chloroform.

Characterization of Polymer

Intrinsic viscosity was measured with a modified Ubbelohde viscometer at 30°C. and benzene was used as solvent. The intrinsic viscosity of the polymer was in the range of 0.10–0.29, suggesting low degrees of polymerization.

Residual double bonds were calculated by means of the intensity of infrared absorption at 1640 cm.^{-1} which is the characteristic absorption band of the terminal ethylenic bond. This absorption band was not equally strong in all cases; therefore, some errors were inevitable for the calculation of residual unsaturation. Most polymers prepared under various conditions had only a few per cent unsaturation, indicating a predominant intermolecular propagation reaction.

Polydivinylformal was hydrolyzed to poly(vinyl alcohol) with hydroxylamine hydrochloride in *n*-butanol under reflux and reprecipitated from aqueous solution.^{7,10} The poly(vinyl alcohol) thus obtained was in some cases discolored and a small amount of water-insoluble material was found. The soluble material was identified as poly(vinyl alcohol) by comparison of the infrared absorption spectrum with that of commercial poly(vinyl alcohol). To determine the occurrence of head-to-head structures in the polymerization, the hydrolyzed polymer was oxidized with periodic acid and the 1,2-glycol structures in the poly(vinyl alcohol) were determined viscometrically as reported by Flory.¹¹ The infrared spectra of monomer, polymer, and poly(vinyl alcohol) thus obtained are shown in Figure 1.

RESULTS AND DISCUSSION

General Kinetics

To determine the rate dependence on monomer and initiator concentrations, polymerization was carried out under various conditions. The

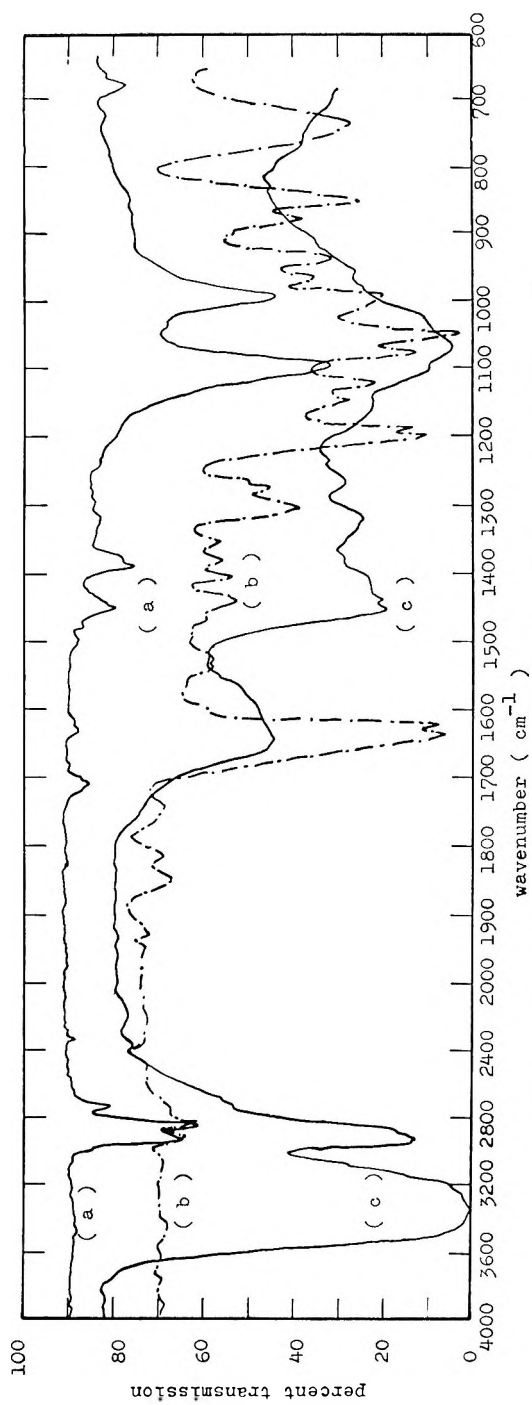


Fig. 1. Infrared spectra of (a) polydivinyldivinylformal; (b) divinylformal; (c) poly(vinyl alcohol).

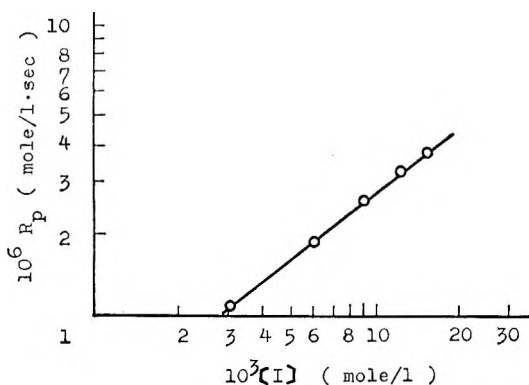


Fig. 2. Effect of initiator concentration on rate of polymerization; $[M] = 2.70$ mole/l., polymerization temperature 50°C .

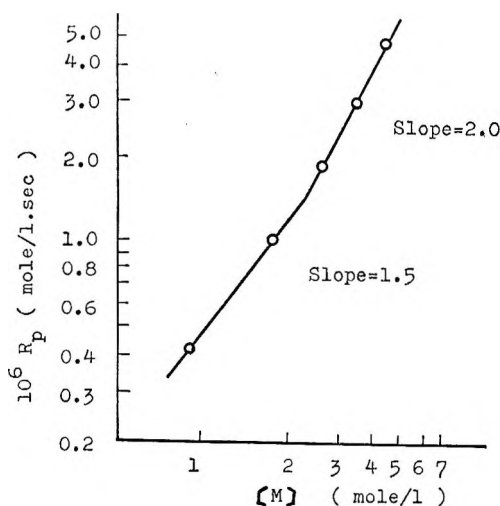


Fig. 3. Effect of monomer concentration on rate of polymerization; $[I] = 6.20 \times 10^{-3}$ mole/l., polymerization temperature 50°C .

polymerization rate was determined gravimetrically. The monomer and the initiator concentrations were in the range of 0.90–4.49 mole/l. and 0.31 – 1.55×10^{-2} mole/l., respectively.

Figure 2 shows the rate dependence on initiator concentration.

Apparently the order of the polymerization reaction was $3/4$ for the initiator concentration. Such irregular orders of reaction can be found in the literature: 0.67–1.0 for the polymerization of acrylic anhydride¹² and 0.58 in the case of vinyl *trans*-cinnamate.¹³

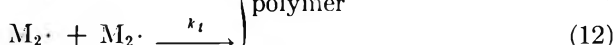
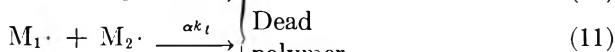
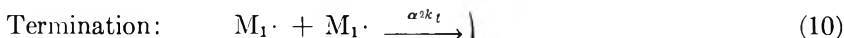
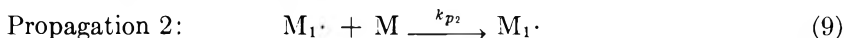
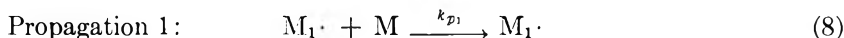
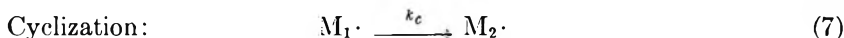
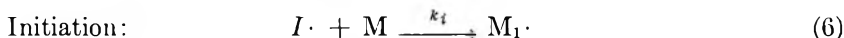
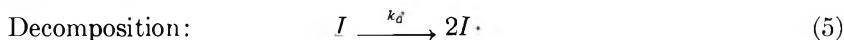
The variation of polymerization rate with monomer concentration is more complicated. The apparent order of reaction varied with respect to the monomer concentration: it was $3/2$ in the monomer concentration range between 0.9 and 2.7 mole/l. and 2 at higher concentration; this is illustrated

in Figure 3. Such a nodal point as found in Figure 3 has also been noted in other cases: the polymerizations of acrylic anhydride,¹² methacrylic anhydride,¹⁵ and vinyl *trans*-cinnamate.¹³ From these results, the overall polymerization rate R_p could be indicated as follows:

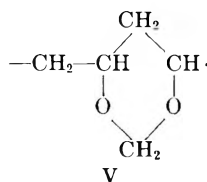
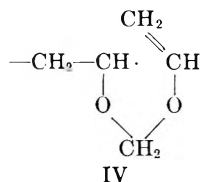
$$R_p = k[I]^{3/4}[M]^{3/2-1} \quad (4)$$

where k is overall polymerization rate constant, and $[I]$ and $[M]$ are the initiator and the monomer concentrations, respectively. Such an irregular rate equation seems to be inevitable for the cyclopolymerization.

To interpret this irregularity, the elementary reactions shown in eqs. (5)–(12) were presumed.



Here I is an initiator molecule, $I \cdot$ is an initiator radical, M is monomer, and $M_1 \cdot$ and $M_2 \cdot$ are radicals IV and V, respectively.



α is a certain constant introduced to simplify the following algebraic treatment, and the rate constants of the three termination reactions are of course decided by the value of α . If a stationary state is assumed, the eqs. (13)–(15) can be obtained.

$$d[I \cdot]/dt = fk_d[I] - k_i[I \cdot][M] = 0 \quad (13)$$

$$d[M_1 \cdot]/dt = k_i[I \cdot][M] - k_c[M_1 \cdot] + k_{p_2}[M_2 \cdot][M] - \alpha^2 k_t[M_1 \cdot]^2 - \alpha k_t[M_1 \cdot][M_2 \cdot] = 0 \quad (14)$$

$$d[M_2 \cdot]/dt = k_c[M_1 \cdot] - k_{p_2}[M_2 \cdot][M] - \alpha k_t[M_1 \cdot][M_2 \cdot] - k_t[M_2 \cdot]^2 = 0 \quad (15)$$

Here f denotes the efficiency of the initiator.

Addition of eqs. (13), (14), and (15) gives

$$\alpha[M_{1\cdot}] + [M_{2\cdot}] = (fk_d/k_t)^{1/2}[I]^{1/2} \quad (16)$$

On combining eqs. (14) and (16), we have

$$[M_{1\cdot}] = \frac{(fk_d/k_t)^{1/2}[I]^{1/2}\{k_{p2}[M] + (k_tfk_d)^{1/2}[I]^{1/2}\}}{k_c + \alpha\{k_{p2}[M] + (k_tfk_d)^{1/2}[I]^{1/2}\}} \quad (17)$$

and then

$$[M_{2\cdot}] = \frac{k_c(fk_d/k_t)^{1/2}[I]^{1/2}}{k_c + \alpha\{k_{p2}[M] + (k_tfk_d)^{1/2}[I]^{1/2}\}} \quad (18)$$

can be obtained. Hence the rate of polymerization is given by

$$R_p = -d[M]/dt = k_{p1}[M_{1\cdot}][M] + k_{p2}[M_{2\cdot}][M] \quad (19)$$

R_p is obtained as:

$$R_p = \frac{k_{p1}(fk_d/k_t)^{1/2}[I]^{1/2}\{k_{p2}[M] + (k_tfk_d)^{1/2}[I]^{1/2}\}[M]}{k_c + \alpha\{k_{p2}[M] + (k_tfk_d)^{1/2}[I]^{1/2}\}} + \frac{k_{p2}k_c(fk_d/k_t)^{1/2}[I]^{1/2}[M]}{k_c + \alpha\{k_{p2}[M] + (k_tfk_d)^{1/2}[I]^{1/2}\}} \quad (20)$$

which on rearrangement gives

$$R_p = k_{p2}(fk_d/k_t)^{1/2}[I]^{1/2}[M] \times \frac{1 + (k_{p1}/k_{p2})\{(k_{p2}/k_c)[M] + (1/k_c)(k_tfk_d)^{1/2}[I]^{1/2}\}}{1 + \alpha\{(k_{p2}/k_c)[M] + (1/k_c)(k_tfk_d)^{1/2}[I]^{1/2}\}} \quad (21)$$

Equation (21) can be developed as

$$R_p = R_0[1 + (a - b)x - b(a - b)x^2 + \dots] \quad (22)$$

where

$$R_0 = k_{p2}(fk_d/k_t)^{1/2}[I]^{1/2}[M]$$

$$a = k_{p1}/k_{p2}$$

$$b = \alpha$$

and

$$x = (k_{p2}/k_c)[M] + (k_tfk_d)^{1/2}(1/k_c)[I]^{1/2} \quad (23)$$

From the result of investigation of residual unsaturation, it was found that the rate of cyclization was far faster than that of propagation 1, namely,

$$k_c[M_{1\cdot}] \gg k_{p1}[M_{1\cdot}][M] \quad (24)$$

therefore,

$$k_c \gg k_{p1}[M] \quad (25)$$

Both k_{p_1} and k_{p_2} are the rate constants of propagation and may be boldly assumed to be of the same order.

Then eq. (25) is given by

$$k_c \gg k_{p_2}[M] \quad (26)$$

The second term of x in eq. (23) is rewritten as

$$(1/k_c)(k_t f k_d)^{1/2} [I]^{1/2} = (1/k_c) k_t^{1/2} R_i^{1/2} \quad (27)$$

where R_i is the rate of initiation.

Generally, R_i is of the order of about 10^{-8} and k_t is about 10^8 in the case of radical polymerization as described in this experiment. Therefore, the second term of x in eq. (27) is affected only by $1/k_c$.

The result of residual unsaturation measurement showed that the value of k_c was about 130 times larger than that of k_{p_1} . The rate constant of propagation reaction in radical polymerization is in the range of 10 – 10^3 , at least more than unity; therefore, the value of k_c becomes very large and $1/k_c$ is very small.

From this consideration and eq. (26), x is very small, and x^2 and x^3 or other higher terms in eq. (23) may become negligible.

Considering this approximation, R_p is indicated as:

$$\begin{aligned} R_p &= R_0 \{ 1 + (a - b)x \} \\ &= k_{p_2} (f k_d / k_t)^{1/2} [I]^{1/2} [M] + (k_{p_2} / k_c) (f k_d / k_t)^{1/2} (k_{p_1} - \alpha k_{p_2}) [I]^{1/2} [M]^2 \\ &\quad + (f k_d / k_c) (k_{p_1} - \alpha k_{p_2}) [I] [M] \end{aligned} \quad (28)$$

If the second and third terms are very small as compared with the first one in eq. (28), the overall rate equation is given by

$$R_p = k [I]^{1/2} [M]$$

which can be found in the ordinary radical polymerization.

When the second term contributes significantly together with the first one during the polymerization, the experimental overall rate equation must be:

$$R_p = k [I]^{1/2} [M]$$

Similarly, if the third term of eq. (28) makes a large contribution to R_p , the following rate equation can be obtained

$$R_p = k [I]^{1/2-1} [M]^{1-2}$$

Then the overall rate equation is generalized as follows:

$$R_p = k [I]^{1/2-1} [M]^{1-2} \quad (29)$$

Equation (29) represents the general rate equation of cyclopolymerization and this could explain the results obtained in this experiment and other experimental results described above.

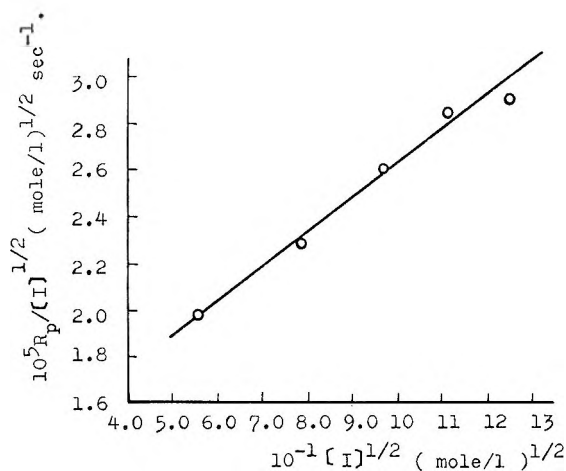


Fig. 4. Plot of $R_p/[I]^{1/2}$ vs. $[I]^{1/2}$; $[M] = 2.70$ mole/l., polymerization temperature 50°C .

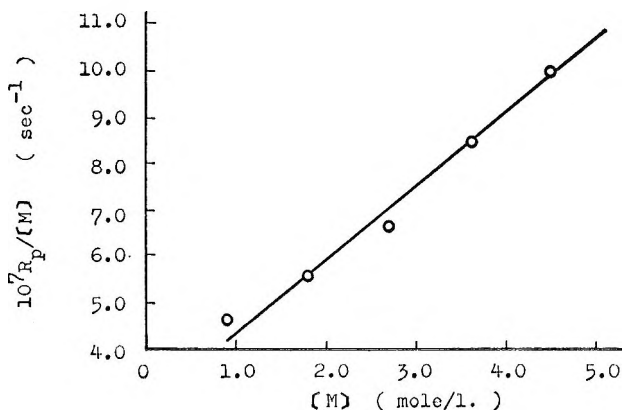


Fig. 5. Plot of $R_p/[M]$ vs. $[M]$; $[I] = 1.80 \times 10^{-2}$ mole/l., polymerization temperature 50°C .

Another explanation could be made by using eq. (28). If the initiator concentration is kept constant and the monomer concentration is varied, eq. (28) can be written as follows:

$$R_p/[M] = A + B[M] \quad (30)$$

where

$$A = k_{p_2}(fk_d k_i)^{1/2} + (fk_d/k_c)(k_{p_1} - \alpha k_{p_2})[I] = \text{const.}$$

$$B = (k_{p_2}/k_c)(fk_d/k_i)^{1/2}(k_{p_1} - \alpha k_{p_2})[I]^{1/2} = \text{const.}$$

Similarly, when the monomer concentration is kept constant and the initiator concentration is varied,

$$R_p/[I]^{1/2} = C + D[I]^{1/2} \quad (31)$$

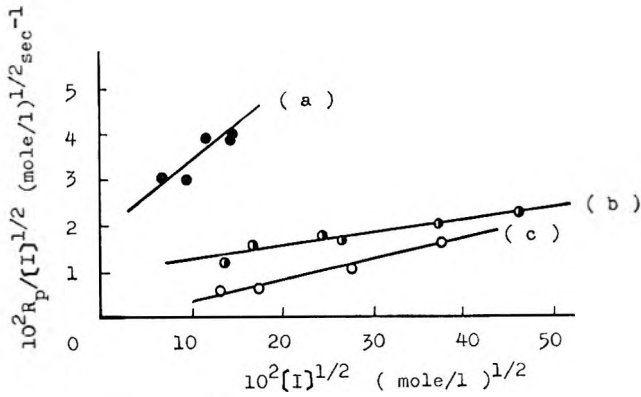


Fig. 6. Plot of $R_p/[I]^{1/2}$ vs. $[I]^{1/2}$ obtained in the polymerization of acrylic anhydride: (a) polymerization in cyclohexanone with AIBN, $[M] = 6.0$ mole/l.; (b) polymerization in cyclohexanone with AIBN, $[M] = 1.5$ mole/l.; (c) polymerization in DMF with AIBN, $[M] = 1.8$ mole/l.

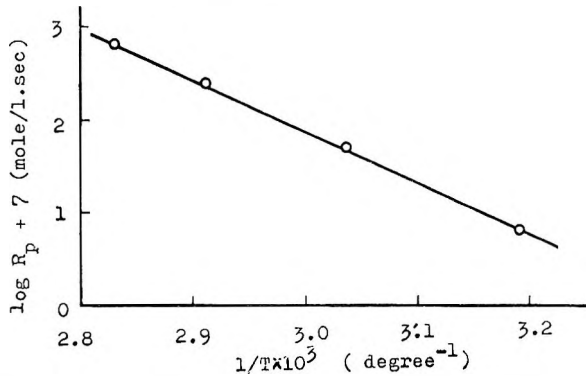


Fig. 7. Plot of $\log R_p$ vs. $1/T$; $[M] = 2.70$ mole/l., $[I] = 1.00 \times 10^{-2}$ mole/l.

can be obtained, where

$$C = k_{p_2}(fk_d/k_t)^{1/2}[M] + (k_{p_2}/k_c)(fk_d/k_t)^{1/2}(k_{p_1} - \alpha k_{p_2})[M]^2 = \text{const.}$$

$$D = (fk_d/k_c)(k_{p_1} - \alpha k_{p_2})[M] = \text{const.}$$

Equations (30) and (31) show that the plots of $R_p/[M]$ versus $[M]$, and $R_p/[I]^{1/2}$ versus $[I]^{1/2}$ must be straight lines. These plots are shown in Figures 4 and 5, respectively. Application of this technique for the polymerization of acrylic anhydride is shown in Figure 6 for data obtained from the paper Smets.¹² The plots were also linear. This treatment also suggests that the technique based on eq. (29) is justifiable.

Activation Energy

To determine the overall activation energy, the polymerization was carried out at 40, 55, 70, and 80°C. A plot of the logarithm of R_p versus

$1/T$ is shown in Figure 7. The E_a value calculated from the slope of the curve was 27.7 kcal./mole, slightly higher than that of methacrylic anhydride¹⁵ but reasonable for the radical polymerization.

Intrinsic Viscosity

The intrinsic viscosity of the polymer was measured at 30°C. in benzene solution. The results at various degrees of conversion are summarized in Table I. Apparently the intrinsic viscosity of the polymer increased with increasing conversion, which suggests the occurrence of some branching reaction during the polymerization. As the intrinsic viscosity changes with

TABLE I
Intrinsic Viscosities of Polymer Prepared at 50°C. under Various Conditions

| Run no. | [I], mole/l. | [M], mole/l. | Conversion, % | $[\eta]$, dl./g. |
|---------|-----------------------|--------------|---------------|-------------------|
| D-5 | 0.50×10^{-2} | 2.70 | 3.1 | 0.220 |
| D-6 | | | 5.6 | 0.221 |
| D-7 | | | 7.7 | 0.242 |
| D-8 | | | 10.4 | 0.244 |
| D-9 | 1.00×10^{-2} | 2.70 | 2.7 | 0.214 |
| D-10 | | | 5.4 | 0.209 |
| D-11 | | | 9.6 | 0.220 |
| D-12 | | | 13.7 | 0.242 |
| E-9 | 1.00×10^{-2} | 3.60 | 2.7 | 0.913 |
| E-10 | | | 6.1 | 0.250 |
| E-11 | | | 10.8 | 0.253 |
| E-12 | | | 13.9 | 0.286 |
| E-13 | 1.00×10^{-2} | 4.49 | 3.0 | 0.173 |
| E-14 | | | 6.0 | 0.249 |
| E-15 | | | 8.9 | 0.264 |

TABLE II
Residual Unsaturation of Polymer Prepared under Various Conditions

| Run no. | [I], mole/l. | [M], mole/l. | Temp., °C. | Conversion, % | F_d |
|---------|-----------------------|--------------|------------|---------------|--------|
| H-7 | 6.20×10^{-3} | 2.70 | 50 | 5.9 | 0.0344 |
| H-8 | | | | 7.8 | 0.0121 |
| H-18 | 1.55×10^{-2} | 2.70 | 50 | 5.5 | 0.0434 |
| H-19 | | | | 7.9 | 0.0354 |
| H-20 | | | | 9.8 | 0.0209 |
| I-10 | | | | 3.8 | 0.0290 |
| I-11 | 6.20×10^{-3} | 3.60 | 50 | 5.0 | 0.0291 |
| I-12 | | | | 7.1 | 0.0246 |
| I-13 | | | | 1.5 | 0.0509 |
| F-4 | 1.00×10^{-2} | 2.70 | 40 | 3.7 | 0.0267 |
| F-14 | | | 70 | 41.5 | 0.0353 |
| F-17 | | | 80 | 26.9 | 0.0406 |
| F-18 | | | 28.8 | 0.0434 | |

conversion, it is impossible to find a definite relationship between the monomer concentration or the initiator concentration and the intrinsic viscosity, but it is obvious that the degree of polymerization decreases with increasing initiator concentration and increases with increasing monomer concentration.

Residual Unsaturation

Residual unsaturation was calculated from the infrared absorption at 1640 cm.^{-1} . The results are shown in Table II. Residual unsaturation was also affected by conversion. It decreased with increasing conversion. This also suggests the occurrence of a branching reaction.

The pendant double bond in the polymer is formed by propagation 1 in the elementary reactions. The fraction of residual double bonds in the polymer F_d is given as

$$F_d = R_{p1}/(R_c + R_{p1}) \quad (32)$$

where R_{p1} is the rate of propagation 1 and R_c is the rate of cyclization.

$$\begin{aligned} 1/F_d &= 1 + (R_c/R_{p1}) \\ &= 1 + (k_c[M_1\cdot]/k_{p1}[M_1\cdot][M]) \\ &= 1 + (k_c/k_{p1})(1/[M]) \end{aligned} \quad (33)$$

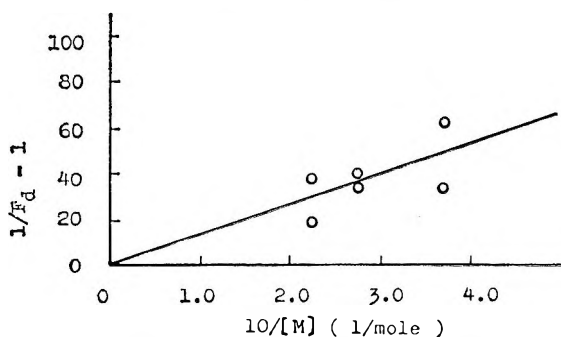


Fig. 8. Plot of $[(1/F_d) - 1]$ vs. $1/[M]$; $[I] = 6.20 \times 10^{-3}$ mole/l.

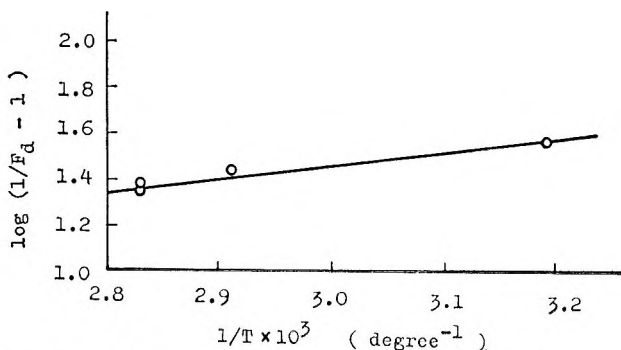


Fig. 9. Plot of $[(1/F_d) - 1]$ vs. $1/T$; $[I] = 6.20 \times 10^{-3}$ mole/l.

From eq. (33), the slope of the plot of $(1/F_d) - 1$ vs. $1/[M]$ gives the value of k_c/k_{p1} . Figure 8 shows such a plot; k_c/k_{p1} was calculated as about 130. This was almost the same as that ratio previously reported, namely 1000/75 for the polymerization of vinyl *trans*-cinnamate.¹³

From eq. (33),

$$(1/F_d) - 1 = k_c/k_{p1}[M] = A_c e^{-E_c/RT} / A_{p1} e^{-E_{p1}/RT} \quad (34)$$

so that,

$$\ln [(1/F_d) - 1] = \ln (1/[M])(A_c/A_{p1}) + (E_{p1} - E_c)/RT \quad (35)$$

The Arrhenius plot of eq. (35) gives the difference of activation energy between propagation 1 and cyclization reaction. Figure 9 shows this plot; the difference of the activation energy was calculated to be about 2.6 kcal./mole, which was about the same as that for vinyl *trans*-cinnamate (2.4 kcal./mole).¹³

Hydrolysis of Polymer

Polydivinylformal was hydrolyzed with hydroxylamine hydrochloride as described previously. The poly(vinyl alcohol) derived from the polymer was a somewhat discolored water-soluble resin; it was purified by reprecipitation from aqueous solution to acetone. This poly(vinyl alcohol) was treated with periodic acid as described by Flory.¹¹ As periodic acid reacts on 1,2-glycol structures in the polymer and the polymer chain is broken at this point, the increase of the number of molecules per gram-mole structural unit (44 g.), Δ , is given as follows:

$$\Delta = 44[(1/\bar{M}_n) - (1/\bar{M}_{n0})] \quad (36)$$

where \bar{M}_{n0} is the initial number-average molecular weight of PVA and \bar{M}_n is the number-average molecular weight of PVA after treating with periodic acid.

To evaluate the \bar{M}_n and \bar{M}_{n0} , the following intrinsic viscosity-molecular weight relationship (for aqueous solution at 30°C.) was used:¹⁴

$$[\eta] = 6.67 \times 10^{-4} \bar{M}_n^{0.64} \quad (37)$$

Results are shown in Table III.

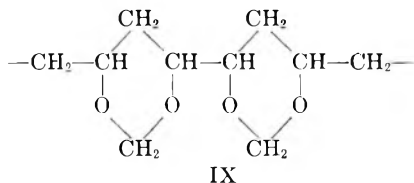
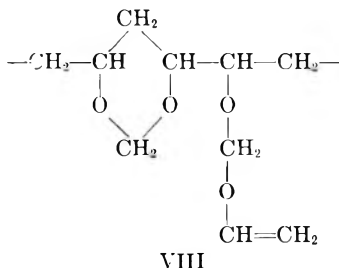
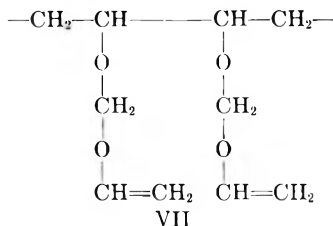
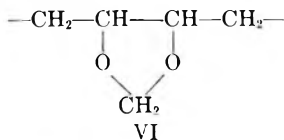
TABLE III
Amount of 1,2-Glycol Structures in Poly(vinyl Alcohol)
Derived from Polydivinylformal

| Polymer | $[\eta]_0$ | $[\eta]$ | \bar{M}_{n0} | \bar{M}_n | $\Delta \times 100$ |
|----------------|------------|----------|--------------------|--------------------|---------------------|
| A ^a | 0.250 | 0.0225 | 1.05×10^4 | 2.44×10^2 | 17.6 |
| B ^b | 0.299 | 0.024 | 9.16×10^3 | 2.70×10^2 | 15.8 |

^a Polymerized at 50°C., 47 hr., $[I] = 1.47 \times 10^{-4}$ mole/l., $[M] = 4.49$ mole/l.

^b Polymerized at 50°C., 8 hr., $[I] = 8.80 \times 10^{-3}$ mole/l., $[M] = 6.22$ mole/l.

Values for $\Delta \times 100$ were very high as compared with commercial poly-(vinyl alcohol). 1,2-Glycol structures seem to be formed by the structural units VI-IX.



It was impossible to determine which structural unit contributed most to the formation of 1,2-glycol structures, but as structures VII, VIII, IX are formed by intermolecular head-to-head combination, while the structure VI is formed by the intramolecular combination it seems that the structure VI is the one most likely to be formed.

References

1. Butler, G. B., and R. L. Ingley, *J. Am. Chem. Soc.*, **73**, 895 (1951).
2. Butler, G. B., and R. J. Angelo, *J. Am. Chem. Soc.*, **79**, 3128 (1957).
3. Butler, G. B., A. Crawshaw, and W. L. Miller, *J. Am. Chem. Soc.*, **80**, 3615 (1958).
4. Aso, C., and Y. Aito, *Makromol. Chem.*, **58**, 195 (1962).
5. Mayersen, K., R. C. Shultz, and W. Kern, *Makromol. Chem.*, **58**, 204 (1962).
6. Miller, W. L., and W. B. Black, paper presented at 142nd American Chemical Society Meeting, Atlantic City, September 1962.
7. Matsoyan, S. G., *J. Polymer Sci.*, **52**, 189 (1961).
8. Miyake, T., *Kogyo Kagaku Zasshi*, **64**, 1272 (1961).
9. Koffman, D. D., U. S. Pat. 2,374,078.

10. *A.S.T.M. Standards*, Am. Soc. Testing Materials, Philadelphia, 1958, D1396-58.
11. Flory, P. J., and F. S. Leutner, *J. Polymer Sci.*, **3**, 880 (1948).
12. Mayersen, J., and G. Smets, *J. Polymer Sci.*, **57**, 763 (1962).
13. Roovers, J., and G. Smets, *Makromol. Chem.*, **60**, 89 (1963).
14. Nakajima, A., and K. Furudate, *Kobunshi Kagaku*, **6**, 460 (1949).
15. Gibbs, W. E., and J. T. Murray, *J. Polymer Sci.*, **58**, 1211 (1962).

Résumé

Jusqu'à ce jour l'étude cinétique de la cyclopolymérisation a été décrite dans plusieurs articles, mais les cinétiques globales n'ont pas encore été établies. Ainsi le divinylformal a été synthétisé et polymérisé comme un monomère bifonctionnel et on a obtenu l'équation globale de vitesse, $R_p = k[I]^{3/4}[M]^{3/2-2}$. Pour interpréter cette équation de vitesse irrégulière, des réactions élémentaires ont été considérées et on a obtenu l'équation de vitesse théorique, $R_p = k[I]^{1/2-1}[M]^{1-2}$. L'énergie globale d'activation pour la polymérisation est de 27.7 kcal/mole, et conjointement avec les résultats de la mesure de l'insaturation résiduelle dans le polymère, on a trouvé pour la différence d'énergie d'activation entre la réaction de cyclisation et de propagation, 2.6 kcal/mole. Les résultats des mesures des viscosités intrinsèques et de l'insaturation résiduelle dans le polymère à différents taux de conversion suggèrent que certaines réactions de ramification ont lieu pendant la polymérisation. Le polydivinylformal a été hydrolysé en alcool polyvinylique au moyen de chlorhydrate d'hydroxylamine, et on a détecté des structures 1,2-glycol dans l'alcool polyvinylique. Les résultats indiquent une teneur plus élevée en structures 1,2-glycol que celle de l'alcool polyvinylique commercial.

Zusammenfassung

Über die kinetische Untersuchung der Cyklopolymerisation wurde bis jetzt in einigen Arbeiten berichtet, es wurde jedoch noch kein vollständiges kinetisches Schema aufgestellt. Daher wurde Divinylformal synthetisiert und als difunktionelles Monomeres polymerisiert; für die Bruttogeschwindigkeit wurde die Gleichung $R_p = k[I]^{3/4}[M]^{3/2-2}$ erhalten. Zur Interpretation dieser ungewöhnlichen Geschwindigkeitsgleichung wurden gewisse Elementarreaktionen in Betracht gezogen und so die theoretische Geschwindigkeitsgleichung $R_p = k[I]^{1/2-1}[M]^{1-2}$ erhalten. Die Bruttoaktivierungsenergie der Polymerisation betrug 27,7 kcal/Mol und durch Messung der restlichen Doppelbindungen im Polymeren wurde der Unterschied in der Aktivierungsenergie zwischen der Zyklisierungs- und der Wachstumsreaktion zu 2,6 kcal/Mol gefunden. Die Messergebnisse für die Viskositätszahl und die restlichen Doppelbindungen im Polymeren bei verschiedenen Umsätzen zeigen, dass während der Polymerisation in gewissem Ausmaß eine Verzweigungsreaktion stattfindet. Polydivinylformal wurde mit Hydroxylaminhydrochlorid zu Polyvinylalkohol hydrolysiert und die 1,2-Glycolstruktur im Polyvinylalkohol bestimmt. Der Gehalt an 1,2-Glycolstruktur ist höher als bei handelsüblichem Polyvinylalkohol.

Received September 21, 1964

Revised December 22, 1964

(Prod. No. 4594A)

Copolymer Composition and Microstructure

KOICHI ITO and YUYA YAMASHITA, *Department of Synthetic Chemistry, Faculty of Engineering, Nagoya University, Furo-cho, Chikusa-ku, Nagoya, Japan*

Synopsis

A simple theory and treatment to characterize copolymer composition and microstructure was developed by applying the statistical stationary process given by Coleman and Fox to the three models in binary copolymerization in which the last one, two, and three monomer units in the growing polymer chain affect the probability of monomer addition. A simple method to distinguish the three models from each other is also presented. The theory was applied to a cationically obtained β -propiolactone-3,3-bis-chloromethyloxetane copolymer reported by Tada et al., to indicate how the penultimate units affect the copolymer composition and microstructure. The significance of the monomer reactivity ratios from the standpoint of copolymer microstructure is discussed briefly.

INTRODUCTION

Most types of copolymerization have been successfully treated by the Mayo-Lewis equation,¹ which postulates that only the terminal unit of a growing polymer chain affects the probability of monomer addition. However, such studies include no experimentally independent evidence to support this assumption, the failure of which would apparently lead to erroneous conclusions about the microstructures of copolymers as well as the monomer reactivity indices. Several cases of radical copolymerization were reported to fail to obey the assumption, particularly with monomers of high polarity such as acrylonitrile and fumaronitrile.²⁻⁴

Recently, Szwarc showed that the nature of the penultimate unit has a significant effect upon the absolute rate constant in anionic copolymerization of styrene derivatives.⁵ On the characterization of stereoregular polymers, the microtacticity of poly(methyl methacrylate) prepared with anionic initiators was shown not to obey Bovey's σ -treatment but to depend upon the configuration of the penultimate unit also.⁶⁻⁸ Very recently, there has arisen evidence that some cationically obtained copolymers have mean sequence lengths longer than expected from the apparent monomer reactivity ratios.^{9,10} These facts tempted us to reexamine copolymerization from the standpoint of copolymer microstructure and to test whether the assumption does hold or not, particularly in ionic copolymerization. This paper presents a simple theory and treatment to characterize the copolymer microstructure in the cases including the

terminal, penultimate, and pen-penultimate effects, based on the general theory of statistical stationary process developed by Coleman and Fox.¹¹ Application of the present theory to a cationically obtained copolymer of β -propiolactone and 3,3-bischloromethyloxetane is included to show the importance of the penultimate effect in determining the copolymer microstructure.

THEORY

Definitions and Postulates

Consider a binary copolymerization between monomers A and B with the assumption of statistical stationarity.¹¹ Thus, endgroup effects are neglected. Based on the general theory of Coleman and Fox,¹¹ the following definitions are sufficient for the present purpose.

Definition 1. $P_n\{X_1X_2\cdots X_n\}$ is a probability or a number fraction of finding a particular sequence $X_1X_2\cdots X_n$ among all the sequences with length n , where X is A or B.

It follows that, for example,

$$P_1\{A\} + P_1\{B\} = 1 \quad (1.1)$$

$$P_2\{AA\} + P_2\{AB\} + P_2\{BA\} + P_2\{BB\} = 1 \quad (1.2)$$

and so on, to P_n .

From the assumption of statistical stationarity, any sequence has a successor or a predecessor unit which is either A or B. As a consequence,

$$\begin{aligned} P_n\{X_1 X_2 \dots X_n\} &= P_{n+1}\{X_1 X_2 \dots X_n A\} + P_{n+1}\{X_1 X_2 \dots X_n B\} \\ &= P_{n+1}\{A X_1 X_2 \dots X_n\} + P_{n+1}\{B X_1 X_2 \dots X_n\} \end{aligned} \quad (2)$$

For example,

$$P_1\{A\} = P_2\{AA\} + P_2\{AB\} = P_2\{AA\} + P_2\{BA\} \quad (2.1)$$

$$P_1\{B\} = P_2\{BA\} + P_2\{BB\} = P_2\{AB\} + P_2\{BB\}$$

$$P_2\{AA\} = P_3\{AAA\} + P_3\{AAB\} = P_3\{AAA\} + P_3\{BAA\} \quad (2.2)$$

$$P_2\{BB\} = P_3\{BBA\} + P_3\{BBB\} = P_3\{ABB\} + P_3\{BBB\} \quad (2.3)$$

$$P_3\{AAA\} = P_4\{AAAA\} + P_4\{AAAB\} = P_4\{AAAA\} + P_4\{BAAA\} \quad (2.4)$$

$$P_3\{BBB\} = P_4\{BBBA\} + P_4\{BBBB\} = P_4\{ABBB\} + P_4\{BBBB\} \quad (2.5)$$

$$P_3\{BAA\} = P_4\{BAAA\} + P_4\{BAAB\} = P_4\{ABAA\} + P_4\{BBAA\} \quad (2.6)$$

$$P_3\{ABB\} = P_4\{ABBA\} + P_4\{ABBB\} = P_4\{AABB\} + P_4\{BABB\} \quad (2.7)$$

From eqs. (2),

$$P_2\{AB\} = P_2\{BA\} \quad (3.1)$$

$$P_3\{AAB\} = P_3\{BAA\} \quad (3.2)$$

$$P_3\{BBA\} = P_3\{ABB\} \tag{3.3}$$

$$P_4\{AAAB\} = P_4\{BAAA\} \tag{3.4}$$

$$P_4\{BBBA\} = P_4\{ABBB\} \tag{3.5}$$

Definition 2. $P_{x_1x_2 \dots x_nx_{n+1}}$ defines the conditional probability with which the growing polymer chain with the terminal sequence $X_1 X_2 \dots X_n$ adds the particular monomer X_{n+1} ;

$$P_{x_1x_2 \dots x_nx_{n+1}} = P_{n+1}\{X_1X_2 \dots X_nX_{n+1}\} / P_n\{X_1X_2 \dots X_n\} \tag{4}$$

For example,

$$\begin{aligned} P_{ab} &= P_2\{AB\} / P_1\{A\} \\ P_{aab} &= P_3\{AAB\} / P_2\{AA\} \\ P_{aaab} &= P_4\{AAAB\} / P_3\{AAA\} \end{aligned}$$

From eqs. (2) and (4), it is obvious for any particular sequence $X_1X_2 \dots X_n$ that

$$P_{x_1x_2 \dots x_na} + P_{x_1x_2 \dots x_nb} = 1 \tag{5}$$

Combining the definitions 1 and 2, any particular sequence probability $P_n\{X_1X_2 \dots X_n\}$ can be described as a product of $P_1\{A\}$ or $P_1\{B\}$ and appropriate conditional probabilities.

$$\begin{aligned} P_n\{X_1X_2 \dots X_n\} &= P_{n-1}\{X_1X_2 \dots X_{n-1}\} P_{x_1x_2 \dots x_n} \\ &= P_{n-2}\{X_1X_2 \dots X_{n-2}\} P_{x_1x_2 \dots x_{n-1}} P_{x_1x_2 \dots x_n} \\ &\quad \vdots \\ &= P_1\{X_1\} P_{x_1x_2} P_{x_1x_2x_3} P_{x_1x_2x_3x_4} \dots P_{x_1x_2 \dots x_n} \end{aligned} \tag{6}$$

For example,

$$\begin{aligned} P_2\{AB\} &= P_1\{A\} P_{ab} \\ P_3\{AAB\} &= P_2\{AA\} P_{aab} = P_1\{A\} P_{aa}P_{aab} \\ P_4\{AAAB\} &= P_3\{AAA\} P_{aaab} = P_2\{AA\} P_{aaa}P_{aaab} = P_1\{A\} P_{aa}P_{aaa}P_{aaab} \end{aligned}$$

Since $P_1\{A\}$ and $P_1\{B\}$ can be expressed as functions of conditional probabilities, as shown later in eqs. (28), any sequence probability can be described as a function of conditional probabilities. The next purpose is, therefore, to derive these conditional probabilities corresponding to each model as functions of monomer reactivity indices. This can be done with use of definitions 1 and 2, as shown in the next section.

To simplify the following treatments, it is assumed that we are concerned with a copolymer from a very low conversion and hence the monomer feed ratio does not change in the course of polymerization.

Derivation of Copolymer Composition Equation

The above definitions simplify the derivations of copolymer composition equations in the cases where the last one, two, and three monomer units in the growing chain affect the probability of monomer addition, confirming the utility and validity of the treatment. The distributions of monomer units A and B in the resulting copolymers are said to obey Markoffian statistics of order 1, 2, and 3, respectively, and will be denoted in the following as the terminal, penultimate, and pen-penultimate models.

Terminal Model. There are two independent conditional probabilities, which can be written kinetically as following.

$$P_{ab} = 1/(1 + r_A x), P_{aa} = 1 - P_{ab} \quad (7.1)$$

$$P_{ba} = 1/(1 + r_B/x), P_{bb} = 1 - P_{ba} \quad (7.2)$$

with $r_A = k_{aa}/k_{ab}$, $r_B = k_{bb}/k_{ba}$, and $x = [A]/[B]$, where k_{aa} , for example, is the rate constant of the growing polymer chain ending in A monomer unit to add monomer A and [A] and [B] are the molar concentrations of monomers A and B in feed.

Since eqs. (3.1) and (6) yield

$$P_1\{A\} P_{ab} = P_1\{B\} P_{ba} \quad (8)$$

hence,

$$P_1\{A\}/P_1\{B\} = P_{ba}/P_{ab} \quad (9)$$

Combining this with eqs. (7) gives the usual Mayo-Lewis equation:¹

$$P_1\{A\}/P_1\{B\} = (1 + r_A x)/(1 + r_B/x) \quad (10)$$

Penultimate Model. Four independent conditional probabilities can be written with four monomer reactivity ratios, as in the terminal model.

$$P_{aab} = 1/(1 + r_A x), P_{aaa} = 1 - P_{aab} \quad (11.1)$$

$$P_{baa} = r_A' x/(1 + r_A' x), P_{bab} = 1 - P_{baa} \quad (11.2)$$

$$P_{abb} = (r_B'/x)/(1 + r_B'/x), P_{aba} = 1 - P_{abb} \quad (11.3)$$

$$P_{bba} = 1/(1 + r_B/x), P_{bbb} = 1 - P_{bba} \quad (11.4)$$

where $r_A = k_{aaa}/k_{aab}$, $r_A' = k_{baa}/k_{bab}$, $r_B' = k_{abb}/k_{aba}$, and $r_B = k_{bbb}/k_{bba}$.

From eqs. (3.2) and (6) combined with eq. (3.1),

$$P_1\{A\} P_{aa} P_{aab} = P_2\{BA\} P_{baa} = P_2\{AB\} P_{baa} = P_1\{A\} P_{ab} P_{baa} \quad (12)$$

Since $P_{aa} = 1 - P_{ab}$,

$$(1 - P_{ab})P_{aab} = P_{ab}P_{baa}$$

Therefore,

$$P_{ab} = P_{aab}/(P_{aab} + P_{baa}) \quad (13.1)$$

Similarly from eq. (3.3),

$$P_{ba} = P_{bba}/(P_{abb} + P_{bba}) \tag{13.2}$$

Consequently, eq. (9) gives

$$\frac{P_1\{A\}}{P_1\{B\}} = \frac{P_{bba}(P_{aab} + P_{baa})}{P_{aab}(P_{abb} + P_{bba})} = \frac{1 + P_{baa}/P_{aab}}{1 + P_{abb}/P_{bba}} \tag{14}$$

Substituting the relations (11) yields the equation of Merz, Alfrey, and Goldfinger:¹²

$$\frac{P_1\{A\}}{P_1\{B\}} = \frac{1 + r_A'x(1 + r_Ax)/(1 + r_A'x)}{1 + (r_B'/x)(1 + r_Bx)/(1 + r_B'/x)} \tag{15}$$

Pen-penultimate Model. Eight independent conditional probabilities can be written with eight monomer reactivity ratios, as in the case of the terminal model.

$$P_{aaab} = 1/(1 + r_Ax), P_{aaaa} = 1 - P_{aaab} \tag{16.1}$$

$$P_{baaa} = r_A'x/(1 + r_A'x), P_{baab} = 1 - P_{baaa} \tag{16.2}$$

$$P_{abaa} = r_A''x/(1 + r_A''x), P_{abab} = 1 - P_{abaa} \tag{16.3}$$

$$P_{bbab} = 1/(1 + r_A'''x), P_{bbaa} = 1 - P_{bbab} \tag{16.4}$$

$$P_{aaba} = 1/(1 + r_B'''/x), P_{aabb} = 1 - P_{aaba} \tag{16.5}$$

$$P_{babb} = (r_B''/x)/(1 + r_B''/x), P_{baba} = 1 - P_{babb} \tag{16.6}$$

$$P_{abbb} = (r_B'/x)/(1 + r_B'/x), P_{abba} = 1 - P_{abbb} \tag{16.7}$$

$$P_{bbba} = 1/(1 + r_B/x), P_{bbbb} = 1 - P_{bbba} \tag{16.8}$$

where $r_A = k_{aaaa}/k_{aaab}$, $r_A' = k_{baaa}/k_{baab}$, $r_A'' = k_{abaa}/k_{abab}$, $r_A''' = k_{bbaa}/k_{bbab}$, $r_B = k_{bbaa}/k_{bbaa}$, $r_B' = k_{abbb}/k_{abba}$, $r_B'' = k_{babb}/k_{baba}$ and $r_B''' = k_{aabb}/k_{aaba}$.

From eqs. (3.4) and (6) combined with eq. (3.2),

$$\begin{aligned} P_2\{AA\} P_{aaa}P_{aaab} &= P_3\{BAA\} P_{baaa} \\ &= P_3\{AAB\} P_{baaa} \\ &= P_2\{AA\} P_{aab}P_{baaa} \end{aligned} \tag{17}$$

Since $P_{aaa} = 1 - P_{aab}$ after dividing by $P_2\{AA\}$,

$$(1 - P_{aab}) P_{aaab} = P_{aab}P_{baaa}$$

Therefore,

$$P_{aab} = P_{aaab}/(P_{aaab} + P_{baaa}) \tag{18.1}$$

Similarly from eq. (3.5),

$$P_{bba} = P_{bbba}/(P_{abbb} + P_{bbba}) \tag{18.2}$$

It is also necessary to formulate P_{abb} and P_{baa} similarly, but these cannot be derived from the relations (3.4) and (3.5) alone. However, eqs. (2.6) and (2.7) may be useful for this purpose. From eq. (2.6),

$$P_3\{BAA\} = P_4\{ABAA\} + P_4\{BBAA\}$$

Applying eq. (6),

$$P_2\{BA\}P_{baa} = P_2\{AB\}P_{aba}P_{abaa} + P_3\{BBA\}P_{bbaa}$$

Since $P_{aba} = 1 - P_{abb}$, $P_3\{BBA\} = P_3\{ABB\} = P_2\{AB\}P_{abb}$ and $P_2\{BA\} = P_2\{AB\}$, this reduces to

$$P_{baa} = (1 - P_{abb})P_{abaa} + P_{abb}P_{bbaa}$$

Therefore,

$$P_{abb}(P_{bbaa} - P_{abaa}) - P_{baa} = -P_{abaa}$$

Similarly, it follows from eq. (2.7) that

$$P_{abb} - P_{baa}(P_{aabb} - P_{babb}) = P_{babb}$$

Solving the last two simultaneous equations with $P_{bbaa} = 1 - P_{bbab}$ and $P_{aabb} = 1 - P_{aaba}$, we obtain

$$P_{abb} = \frac{[P_{babb}(1 - P_{abaa}) + P_{abaa}(1 - P_{aaba})]}{[P_{babb}(1 - P_{abaa}) + P_{abaa}(1 - P_{aaba}) + P_{aaba}(1 - P_{bbab}) + P_{bbab}(1 - P_{babb})]} \tag{18.3}$$

$$P_{baa} = \frac{[P_{abaa}(1 - P_{babb}) + P_{babb}(1 - P_{bbab})]}{[P_{abaa}(1 - P_{babb}) + P_{babb}(1 - P_{bbab}) + P_{bbab}(1 - P_{aaba}) + P_{aaba}(1 - P_{abaa})]} \tag{18.4}$$

P_{ab} and P_{ba} for this model are readily obtained by substituting eqs. (18) into eqs. (13).

$$P_{ab} = \frac{1}{1 + \frac{P_{baaa}}{P_{aaab}}} \tag{19.1}$$

$$1 + \frac{P_{aaba} \left(\frac{1 - P_{abaa}}{P_{abaa}} + \frac{1 - P_{aaba}}{P_{aaba}} \frac{P_{bbab}}{P_{abaa}} \right)}{1 + \frac{P_{babb} \left(\frac{1 - P_{babb}}{P_{babb}} + \frac{1 - P_{bbab}}{P_{abaa}} \right)}$$

$$P_{ba} = \frac{1}{1 + \frac{P_{abbb}}{P_{bbba}}} \left[1 + \frac{P_{bbab} \left(\frac{1 - P_{bbab}}{P_{bbab}} + \frac{1 - P_{babb}}{P_{aaba}} \right)}{P_{abaa} \left(\frac{1 - P_{aaba}}{P_{aaba}} + \frac{1 - P_{abaa} P_{babb}}{P_{abaa} P_{aaba}} \right)} \right] \tag{19.2}$$

Substituting eqs. (19) into eq. (9) yields the same equation as that derived by Price.¹³

$$\frac{P_1\{A\}}{P_1\{B\}} = \frac{1 + \frac{P_{baaa}}{P_{aaab}}}{1 + \frac{P_{aaba} \left(\frac{1 - P_{abaa}}{P_{abaa}} + \frac{1 - P_{aaba} P_{bbab}}{P_{aaba} P_{abaa}} \right)}{P_{babb} \left(\frac{1 - P_{babb}}{P_{babb}} + \frac{1 - P_{bbab}}{P_{abaa}} \right)}}{1 + \frac{P_{abbb}}{P_{bbba}}} \left[1 + \frac{P_{bbab} \left(\frac{1 - P_{bbab}}{P_{bbab}} + \frac{1 - P_{babb}}{P_{aaba}} \right)}{P_{abaa} \left(\frac{1 - P_{aaba}}{P_{aaba}} + \frac{1 - P_{abaa} P_{babb}}{P_{abaa} P_{aaba}} \right)} \right] \tag{20}$$

Substituting the relations (16), we have

$$\frac{P_1\{A\}}{P_1\{B\}} = \frac{1 + r_A'x \frac{1 + r_Ax}{1 + r_A'x}}{1 + \frac{1}{r_A''x} \left[1 + \frac{r_B''(1 + r_A''x)}{x(1 + r_A''x)} \right]} \left[\frac{r_B'''(r_B''' + x)}{x(r_B'' + x)} \left[\frac{x}{r_B''} + \frac{r_A''(1 + r_A''x)}{r_A''(1 + r_A''x)} \right] \right] \tag{21}$$

$$1 + \frac{1}{r_A''x} \frac{r_B' r_B + x}{x r_B' + x} \left[\frac{1}{r_A''x} \frac{(1 + r_A''x) \left[r_A'''x + \frac{r_B''' + x}{r_B'' + x} \right]}{(1 + r_A''x) \left[r_A'''x + \frac{r_B''' + x}{r_B'' + x} \right]} \right]$$

$$1 + \frac{1}{x} \left[r_B''' + \frac{r_B''}{r_A''x} (r_B''' + x) \right]$$

Equation (21) does not agree with Ham's equation for the same model in its general form,⁴ which was derived with the assumption that the equation in the pen-penultimate model might be obtained from the penultimate model with the similar substitutions as done in the progression from

the terminal model to the penultimate model. It seems that Ham's simple postulate $P_{baa} = P_{bbaa}/(P_{bbaa} + P_{abab})$, for example, may be inappropriate for the general case, as shown in eq. (18.4). For the case of B not adding to B, however, the present treatment or eq. (20) can be reduced to Ham's recent novel equation¹⁴ [eq. (20) in ref. 14], since it follows from eqs. (18) that $P_{aab} = P_{aaab}/(P_{aaab} + P_{baaa})$, $P_{bba} = 1 - P_{bbb} = 1$, $P_{abb} = 0$, and $P_{baa} = P_{abaa}$ to produce, from eqs. (9), (13), (14),

$$P_1\{A\}/P_1\{B\} = P_{ba}/P_{ab} \\ = 1/P_{ab} \quad (\text{Terminal}) \quad (20.1)$$

$$= 1 + (P_{baa}/P_{aab}) \quad (\text{Penultimate}) \quad (20.2)$$

$$= 1 + [P_{abaa}(P_{aaab} + P_{baaa})/P_{aaab}] \quad (\text{Pen-penultimate}) \quad (20.3)$$

Equations (20.1), (20.2), and (20.3) are the same as those to be derived from Ham's equation¹⁴ for these models.

As a matter of course, letting $r_A = r_A'$, $r_A'' = r_A'''$, $r_B = r_B'$, and $r_B'' = r_B'''$ in eq. (21) yields the Merz-Alfrey-Goldfinger equation, eq. (15), and $r_A = r_A' = r_A'' = r_A''' = r_A'''$ with $r_B = r_B' = r_B'' = r_B'''$ yields the Mayo-Lewis equation, eq. (10).

It must be mentioned also that the basic equations, eqs. (3) can be readily obtained by employing Ham's recent concept on the equality of probabilities for reversed sequences.¹⁵

Copolymer Microstructure and Its Experimental Treatment

The purpose of this section is to characterize the copolymer microstructure and to present a method for distinguishing between the terminal model and the penultimate or pen-penultimate model. It is convenient for the purpose to define run fraction (R_f), block character (η), mean run length (number-average, l_A and l_B), and bond fraction (α_A and α_B). Since the number fractions of A and B runs of length n can be written as $P_{n+2}\{BA^nB\}$ and $P_{n+2}\{AB^nA\}$, respectively, and since¹¹

$$\sum_{n=1}^{\infty} P_{n+2}\{BA_nB\} = P_2\{AB\}$$

and

$$\sum_{n=1}^{\infty} P_{n+2}\{AB_nA\} = P_2\{BA\}$$

hence, $P_2\{AB\}$ or $P_2\{BA\}$ is equal to fraction of the sum of all A or B runs. Bearing this in mind, we can define and formulate the above quantities as following.

$$R_f = \text{Sum of fractions of all A and B runs} \\ = P_2\{AB_nBA\} = P_2\{AB\} + P_2\{BA\} = 2P_2\{AB\} = 2P_2\{BA\} \quad (22)$$

R_f is equivalent to run number (R) of Harwood¹⁶ which is defined as the sum of the numbers of A and B runs per 100 monomer units along the chain, and obviously $R = 100R_f$.

Also we define

$$\begin{aligned} \eta &= \text{Measure of departure from random statistics}^{7,11} = R_f/R_{f, \text{random}} \\ &= P_2\{AB_uBA\}/2P_1\{A\} P_1\{B\} = P_2\{AB\}/P_1\{A\} P_1\{B\} \\ &= P_2\{BA\}/P_1\{A\} P_1\{B\} \quad (23) \end{aligned}$$

where $R_{f, \text{random}} (= 2P_1\{A\} P_1\{B\})$ is a run fraction of a copolymer with random distribution of A and B, which is realized when the two monomers add to a growing chain with their own reactivities, not depending upon the nature of the growing chain. $\eta > 1$ means the more alternating tendency and $\eta < 1$ means the more block character of the copolymer than expected from random statistics. $\eta = 2$ means a completely alternating copolymer and $\eta = 0$ means a completely block copolymer or a mixture of homopolymers.

We further define

$$l_A = \text{Number-average length of A runs} = P_1\{A\}/P_2\{AB\} \quad (24.1)$$

$$l_B = \text{Number-average length of B runs} = P_1\{B\}/P_2\{BA\} \quad (24.2)$$

$$\alpha_A = \text{Fraction of A-A bonds in A-X bonds} = P_2\{AA\}/P_1\{A\} \quad (25.1)$$

$$\alpha_B = \text{Fraction of B-B bonds in B-X bonds} = P_2\{BB\}/P_1\{B\} \quad (25.2)$$

where X = A and B.

Statistical stationarity assumption demands the following relations between these quantities¹¹ [see eqs. (1), (2.1), and (3.1)].

$$P_2\{AB\} = P_2\{BA\} = R_f/2 \quad (26.1)$$

$$P_2\{AA\} = P_1\{A\} - (R_f/2) \quad (26.2)$$

$$P_2\{BB\} = P_1\{B\} - (R_f/2) \quad (26.3)$$

$$P_1\{A\} = 1/2 [1 + P_2\{AA\} - P_2\{BB\}] \quad (26.4)$$

$$P_1\{A\} = 1 - (R_f/2) - P_2\{BB\} \quad (26.5)$$

$$P_1\{B\} = 1/2 [1 + P_2\{BB\} - P_2\{AA\}] \quad (26.6)$$

$$P_1\{B\} = 1 - (R_f/2) - P_2\{AA\} \quad (26.7)$$

and

$$l_A = 1/(1 - \alpha_A) \quad (27.1)$$

$$l_B = 1/(1 - \alpha_B) \quad (27.2)$$

These are the basic relations of statistical stationary process and they hold regardless of the number of the last monomer units of the growing chain which affects the probability of the monomer addition. The statisti-

cal stationarity assumption can be checked by fitting the experimentally independent quantities into any one of the above relations.

From eqs. (1.1) and (8), it follows that

$$P_1\{A\} = P_{ab}/(P_{ab} + P_{ba}) \quad (28.1)$$

$$P_1\{B\} = P_{ab}/(P_{ab} + P_{ba}) \quad (28.2)$$

Hence, from the definitions,

$$\begin{aligned} R_f &= 2P_1\{A\} P_{ab} = 2P_1\{B\} P_{ba} \\ &= 2P_{ab}P_{ba}/(P_{ab} + P_{ba}) \\ &= 2/[(1/P_{ba}) + (1/P_{ab})] \end{aligned} \quad (29)$$

$$\eta = P_{ba}/P_1\{A\} = P_{ab}/P_1\{B\} = P_{ab} + P_{ba} \quad (30)$$

$$l_A = P_1\{A\}/P_2\{AB\} = 1/P_{ab} \quad (31.1)$$

$$l_B = P_1\{B\}/P_2\{BA\} = 1/P_{ba} \quad (31.2)$$

$$\alpha_A = P_2\{AA\}/P_1\{A\} = P_{aa} = 1 - P_{ab} \quad (32.1)$$

$$\alpha_B = P_2\{BB\}/P_1\{B\} = P_{bb} = 1 - P_{ba} \quad (32.2)$$

Substituting the appropriate probabilities into eqs. (29)–(32) gives the above quantities, now including the knowledge of the microstructure corresponding to each model.

Terminal Model. Substituting eqs. (7) yields

$$R_f = 2/(r_A x + 2 + r_B/x) \quad (33)$$

$$\eta = (r_A x + 2 + r_B/x)/(r_A x + 1 + r_A r_B + r_B/x) \quad (34)$$

$$l_A = 1 + r_A x \quad (35.1)$$

$$l_B = 1 + r_B/x \quad (35.2)$$

$$1/\alpha_A = 1 + 1/r_A x \quad (36.1)$$

$$1/\alpha_B = 1 + x/r_B \quad (36.2)$$

In this model, only the value of the $r_A r_B$ product determines whether the copolymer is of more alternating character ($\eta > 1$) or of more block character ($\eta < 1$) as compared with that obtained from random statistics. Thus, from eq. (34), if $r_A r_B < 1$, then $\eta > 1$; if $r_A r_B = 1$, then $\eta = 1$; if $r_A r_B > 1$, then $\eta < 1$.

Since a copolymer with sufficiently high degree of polymerization obeys the relations (26) and (27), measurements of copolymer composition and any one of bond or diad concentrations would permit evaluation of all the above quantities. If these are significantly different from those calculated from eqs. (33)–(36) with monomer reactivity ratios and feed ratio, the Mayo-Lewis equation does not hold, apparently. It is more straightforward, however, to use the relations (35) or (36) over a certain range of x , as will be shown in the following.

Penultimate Model. Substituting eqs. (11) and (13) into eqs. (29)–(32) yields

$$\begin{aligned}
 R_f &= 2/(P_{baa}/P_{aab} + 2 + P_{abb}/P_{bba}) \\
 &= 2/[r_A'x(1 + r_Ax)/(1 + r_A'x) + 2 \\
 &\quad + (r_B'/x)(r_B + x)/(r_B' + x)] \quad (37)
 \end{aligned}$$

$$\begin{aligned}
 \eta &= \frac{P_{baa}/P_{aab} + 2 + P_{abb}/P_{bba}}{P_{baa}/P_{aab} + 1 + (P_{baa}/P_{aab})(P_{abb}/P_{bba}) + P_{abb}/P_{bba}} \\
 &= \frac{r_A'x \left(\frac{1 + r_Ax}{1 + r_A'x} \right) + 2 + \frac{r_B'}{x} \left(\frac{r_B + x}{r_B' + x} \right)}{r_A'x \left(\frac{1 + r_Ax}{1 + r_A'x} \right) + 1 + r_A'r_B' \left(\frac{1 + r_Ax}{1 + r_A'x} \right) \left(\frac{r_B + x}{r_B' + x} \right) + \frac{r_B'}{x} \left(\frac{r_B + x}{r_B' + x} \right)} \quad (38)
 \end{aligned}$$

$$l_A = 1 + \frac{P_{baa}}{P_{aab}} = 1 + \left[r_A'x \left(\frac{1 + r_Ax}{1 + r_A'x} \right) \right] x \quad (39.1)$$

$$l_B = 1 + \frac{P_{abb}}{P_{bba}} = 1 + \left[r_B' \left(\frac{r_B + x}{r_B' + x} \right) \right] / x \quad (39.2)$$

$$1/\alpha_A = 1 + \frac{P_{aab}}{P_{baa}} = 1 + 1/\left[r_A' \left(\frac{1 + r_Ax}{1 + r_A'x} \right) \right] x \quad (40.1)$$

$$1/\alpha_B = 1 + \frac{P_{bba}}{P_{abb}} = 1 + x/\left[r_B' \left(\frac{r_B + x}{r_B' + x} \right) \right] \quad (40.2)$$

As a consequence, whether $\eta > 1$ or $\eta < 1$ generally depends not only upon the monomer reactivity ratios but also upon the monomer feed ratio.

Comparing eqs. (39) or (40) with eqs. (35) or (36) permits us to distinguish between the terminal and the penultimate models. Suppose, for example, l_A plotted against x as to give the intercept of unity. Then, a straight line should be obtained with a slope r_A in the case of the terminal model, while a concave or a convex curve should be obtained in the penultimate model, depending upon whether $r_A > r_A'$ or $r_A < r_A'$, because it follows from eq. (39.1) that

$$dl_A/dx = r_A - (r_A - r_A')/(1 + r_A'x)^2$$

$$d^2l_A/dx^2 = 2r_A'(r_A - r_A')/(1 + r_A'x)^3$$

Thus, in the case of the penultimate model, the slope as $x \rightarrow \infty$ will be r_A and the slope at $x \rightarrow 0$ will be r_A' (Fig. 1). Quite analogously, the following relations will be obtained; plots of l_B versus $1/x$ will give slopes r_B as $1/x \rightarrow \infty$ and r_B' at $1/x \rightarrow 0$, plots of $1/\alpha_A$ versus $1/x$ will give slopes

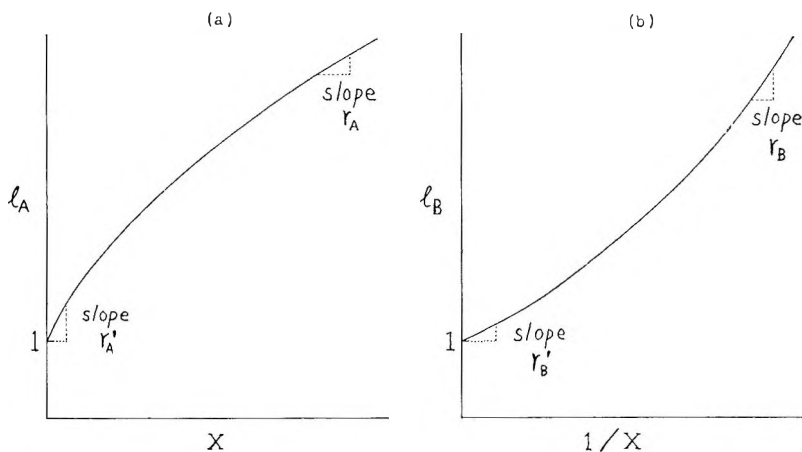


Fig. 1. Plots of mean run length vs. monomer feed ratio in the penultimate model: (a) l_A ; (b) l_B .

$1/r_B'$ as $1/x \rightarrow \infty$ and $1/r_B$ at $1/x \rightarrow 0$, and plots of $1/\alpha_B$ versus x will give slopes $1/r_B'$ as $x \rightarrow \infty$ and $1/r_B$ as $x \rightarrow 0$.

Consequently, determination of copolymer composition and any one kind of bond or diad concentrations over a certain range of x would permit the evaluation of the four monomer reactivity ratios from the appropriate two of the four relations above, under the statistical stationarity assumption.

More exact determination of r 's can be done by using eqs. (41), which can be derived from eqs. (39).

$$(l_A - 2)/x = r_A - (1/r_A')(l_A - 1)/x^2 \quad (41.1)$$

$$(l_B - 2)x = r_B - (1/r_B')(l_B - 1)x^2 \quad (41.2)$$

Since each experiment gives the values of $(l_A - 2)/x$, $(l_A - 1)/x^2$, $(l_B - 2)x$, and $(l_B - 1)x^2$, direct plots according to eqs. (41) or line intersection methods of r_A versus $1/r_A'$ or of r_B versus $1/r_B'$ plots should determine the four monomer reactivity ratios.

In principle, an alternative method to distinguish the penultimate model from the terminal model by using only the copolymer composition could be developed. The copolymer composition equations, eqs. (10) and (15), in the two models can be rewritten as

$$\frac{P_1\{A\}}{P_1\{B\}} = \frac{1 + (r_A)x}{1 + (r_B)/x} \quad (42)$$

In the terminal model, (r_A) and (r_B) are constant and equal to the true monomer reactivity ratios r_A and r_B , but in the case of the penultimate model, they are functions of x ;

$$(r_A) = r_A' (1 + r_A x)/(1 + r_A' x) \quad (43.1)$$

$$(r_B) = r_B' (1 + r_B/x)/(1 + r_B'/x) \quad (43.2)$$

and vary from r_A' to r_A and from r_B to r_B' , respectively, as x varies from zero to infinity. Therefore, eq. (42) tends to

$$P_1\{A\}/P_1\{B\} = (1 + r_A'x)/(1 + r_B/x) = x/r_B \quad \text{As } x \rightarrow 0 \quad (44.1)$$

$$P_1\{A\}/P_1\{B\} = (1 + r_Ax)/(1 + r_B'/x) = r_Ax \quad \text{As } x \rightarrow \infty \quad (44.2)$$

Thus, r_A and r_B in either model can be readily estimated from the slopes of the $P_1\{A\}/P_1\{B\}$ versus x plot at $x \rightarrow \infty$ and $x \rightarrow 0$. Then, it will be possible to test whether r_A and r_B thus estimated can describe the copolymer compositions over a whole range of x employed (terminal model) or not (penultimate model). In the latter case (penultimate model), the other two reactivity ratios r_A' and r_B' might be roughly estimated by the curve-fitting method. However, this method seems very difficult to apply at the present, because it requires very precise determination of the copolymer composition, particularly at low and high x , and moreover, the copolymer composition itself is not so sensitive to small changes in r and to the penultimate effect (see discussion).

Once the four monomer reactivity ratios in the penultimate model have been estimated, it is possible to calculate the mean monomer reactivity ratios, (\bar{r}_A) , and (\bar{r}_B) averaged over a range of x employed (from x_1 to x_2) according to the following equations.¹⁷

$$(\bar{r}_A) = \frac{\int_{x_1}^{x_2} (r_A) dx}{\int_{x_1}^{x_2} dx} = \frac{r_A (x_2 - x_1) + \left(1 - \frac{r_A}{r_A'}\right) \ln \left(\frac{1 + r_A'x_2}{1 + r_A'x_1}\right)}{x_2 - x_1} \quad (45.1)$$

$$(\bar{r}_B) = \frac{\int_{x_1}^{x_2} (r_B) d(1/x)}{\int_{x_1}^{x_2} d(1/x)} = \frac{r_B \left(\frac{1}{x_1} - \frac{1}{x_2}\right) + \left(1 - \frac{r_B}{r_B'}\right) \ln \left(\frac{1 + r_B'/x_1}{1 + r_B'/x_2}\right)}{\frac{1}{x_1} - \frac{1}{x_2}} \quad (45.2)$$

Importantly, it must be emphasized that (\bar{r}_A) and (\bar{r}_B) thus estimated are the apparent but mean monomer reactivity ratios which involves the knowledge how the nature of the penultimate unit affects the monomer addition and they are, generally, not identical with those obtained with the usual Mayo-Lewis equation. In other words, applying the Mayo-Lewis equation to the penultimate model, even if it were possible, would not produce (\bar{r}_A) and (\bar{r}_B) generally, but produce only the apparent monomer reactivity ratios with no reflection of the penultimate effect or of the copolymer microstructure (see discussion).

Pen-penultimate Model. Substituting eqs. (16) and (19) into eqs. (29)–(32) yields similar equations as above. For example,

$$\begin{aligned}
 l_A &= 1 + \frac{1 + \frac{P_{baaa}}{P_{aaab}}}{1 + \frac{P_{aaba} \left(1 - \frac{P_{abaa}}{P_{abaa}} + \frac{1 - P_{aaba} P_{bbaa}}{P_{aaba} P_{abaa}} \right)}{P_{baab} \left(1 - \frac{P_{babb}}{P_{babb}} + \frac{1 - P_{bbaa}}{P_{abaa}} \right)}} \\
 &= 1 + \frac{1 + r_A' x \left(\frac{1 + r_A x}{1 + r_A' x} \right)}{1 + \frac{\frac{1}{r_A'' x} \left[1 + \frac{r_B''}{x} \left(\frac{1 + r_A'' x}{1 + r_A'' x} \right) \right]}{r_B'' \left(\frac{r_B''' + x}{r_B'' + x} \right) \left[\frac{x}{r_B''} + \frac{r_A'''}{r_A''} \left(\frac{1 + r_A'' x}{1 + r_A'' x} \right) \right]} \quad (46)
 \end{aligned}$$

However, the relations obtained are too complex to apply to the experiment and to distinguish from the penultimate model and to estimate the eight monomer reactivity ratios, except for a special case ($r_B = r_B' = r_B'' = r_B''' = 0$, for example). Determination of the triad concentration would simplify the treatments in this model (see the following).

Further Relations

The following relations, which are convenient to use for getting more detailed information about microstructure, can be readily obtained in similar ways as above from definitions 1 and 2.

Copolymer Composition

Terminal Model.

$$\begin{aligned}
 P_1\{A\} &= \frac{P_{ba}}{P_{ab} + P_{ba}} = \frac{1 + r_A x}{r_A x + 2 + r_B/x} \\
 P_1\{B\} &= 1 - P_1\{A\} \quad (47)
 \end{aligned}$$

Penultimate Model.

$$\begin{aligned}
 P_1\{A\} &= \frac{1 + \frac{P_{baa}}{P_{aab}}}{\frac{P_{baa}}{P_{aab}} + 2 + \frac{P_{abb}}{P_{bba}}} = \frac{1 + r_A' x \frac{1 + r_A x}{1 + r_A' x}}{r_A' x \frac{1 + r_A x}{1 + r_A' x} + 2 + \frac{r_B' r_B + x}{x r_B' + x}} \\
 P_1\{B\} &= 1 - P_1\{A\} \quad (48)
 \end{aligned}$$

Equations for the pen-penultimate model are obtained by substituting eqs. (18) and (16) into the above eq. (48).

Bond or Diad Concentration

Terminal Model.

$$\begin{aligned}
 P_2\{AA\} &= \frac{P_{ba}(1 - P_{ab})}{P_{ab} + P_{ba}} = \frac{r_A x}{r_A x + 2 + r_B/x} \\
 P_2\{AB\} &= P_2\{BA\} = \frac{P_{ba}P_{ab}}{P_{ab} + P_{ba}} = \frac{1}{r_A x + 2 + r_B/x} \\
 P_2\{BB\} &= 1 - 2P_2\{AB\} - P_2\{AA\} \tag{49}
 \end{aligned}$$

Penultimate Model.

$$\begin{aligned}
 P_2\{AA\} &= \frac{\frac{P_{baa}}{P_{aab}}}{\frac{P_{baa}}{P_{aab}} + 2 + \frac{P_{abb}}{P_{bba}}} = \frac{r_A' x \left(\frac{1 + r_A x}{1 + r_A' x} \right)}{r_A' x \left(\frac{1 + r_A x}{1 + r_A' x} \right) + 2 + \frac{r_B' (r_B + x)}{x (r_B' + x)}} \\
 P_2\{AB\} &= P_2\{BA\} = \frac{1}{\frac{P_{baa}}{P_{aab}} + 2 + \frac{P_{abb}}{P_{bba}}} = \frac{1}{r_A' x \left(\frac{1 + r_A x}{1 + r_A' x} \right) + 2 + \frac{r_B' (r_B + x)}{x (r_B' + x)}} \\
 P_2\{BB\} &= 1 - 2P_2\{AB\} - P_2\{AA\} \tag{50}
 \end{aligned}$$

Equations for the pen-penultimate model are obtained by substituting eqs. (18) and (16) into the above eq. (50).

Triad Fraction

Let F_{AAA} , F_{BAB} , F_{BAA} , and F_{AAB} represent the fractions of monomer unit A in the centers of the triads AAA, BAB, BAA, and AAB, respectively. Then,

$$\begin{aligned}
 F_{AAA} + F_{BAB} + F_{BAA} + F_{AAB} &= 1 \tag{51} \\
 F_{AAA} &= P_3\{AAA\}/P_1\{A\} = P_{aa}P_{aaa} = (1 - P_{ab})(1 - P_{aab}) \\
 F_{BAB} &= P_3\{BAB\}/P_1\{A\} = P_1\{B\} P_{ba}P_{bab}/P_1\{A\} = P_{ab}(1 - P_{baa}) \\
 F_{BAA} &= F_{AAB} = P_3\{AAB\}/P_1\{A\} = P_{aa}P_{aab} = (1 - P_{ab})P_{aab} \tag{52}
 \end{aligned}$$

Substituting appropriate probabilities gives these as functions of r and x .

Terminal Model.

$$\begin{aligned}
 F_{AAA} &= (1 - P_{ab})^2 = (r_A x)^2 / (1 + r_A x)^2 \\
 F_{BAB} &= P_{ab}^2 = 1 / (1 + r_A x)^2 \\
 F_{BAA} &= F_{AAB} = P_{ab}(1 - P_{ab}) = r_A x / (1 + r_A x)^2 \tag{53}
 \end{aligned}$$

In this model, $P_{aa} = P_{aaa} = P_{baa}$, hence, it follows¹⁶ that

$$\begin{aligned} F_{AAA} &= (P_2\{AA\})^2 / (P_1\{A\})^2 = (P_1\{A\} - R_f/2)^2 / (P_1\{A\})^2 \\ F_{BAB} &= (P_2\{AB\})^2 / (P_1\{A\})^2 = R_f^2 / (2P\{A\})^2 \\ F_{BAA} &= F_{AAB} = P_2\{AA\} P_2\{AB\} / (P_1\{A\})^2 = \\ &\quad (R_f/2) (P_1\{A\} - R_f/2) / (P_1\{A\})^2 \quad (54) \end{aligned}$$

Penultimate Model.

$$\begin{aligned} F_{AAA} &= \frac{P_{baa} (1 - P_{aab})}{P_{baa} + P_{aab}} = \frac{r_A x r_A' x \left(\frac{1 + r_A x}{1 + r_A' x} \right)}{(1 + r_A x) \left[1 + r_A' x \left(\frac{1 + r_A x}{1 + r_A' x} \right) \right]} \\ F_{BAB} &= \frac{P_{aab} (1 - P_{baa})}{P_{baa} + P_{aab}} = \frac{1}{(1 + r_A' x) \left[1 + r_A' x \left(\frac{1 + r_A x}{1 + r_A' x} \right) \right]} \\ F_{BAA} &= F_{AAB} = \frac{P_{baa} P_{aab}}{P_{baa} + P_{aab}} = \frac{r_A' x \left(\frac{1 + r_A x}{1 + r_A' x} \right)}{(1 + r_A x) \left[1 + r_A' x \left(\frac{1 + r_A x}{1 + r_A' x} \right) \right]} \quad (55) \end{aligned}$$

Triad fractions can be used for confirmation of the penultimate model by comparing the observed triad fractions with the values calculated from the above equations. The distinction between the penultimate model and the pen-penultimate model can be done more straightforwardly utilizing the ratios of diad to triad concentrations; for example, $P_2\{AA\} / P_3\{AAA\} = 1 / P_{aaa} = 1 + (1/r_A x)$ for terminal and penultimate models, and $P_2\{AA\} / P_3\{AAA\} = (P_{baa} + P_{aab}) / P_{baa} = 1 + (1/r_A' x) [(1 + r_A' x) / (1 + r_A x)]$ for the pen-penultimate model.

Run Length Distribution

Let $N_A(n)$ and $W_A(n)$ represent the number and weight fractions of A runs with length n , respectively; then, from the definition,

$$N_A(n) = P_{n+2}\{BA^n B\} / \sum_{n=1}^{\infty} P_{n+2}\{BA^n B\} = P_{n+2}\{BA^n B\} / P_2\{BA\} \quad (56)$$

$$W_A(n) = nN_A(n) / \sum_{n=1}^{\infty} nN_A(n) \quad (57)$$

Number-average and weight-average lengths of A runs, denoted by l_A and l_{WA} , are, then,

$$l_A = \sum_{n=1}^{\infty} nN_A(n) / \sum_{n=1}^{\infty} N_A(n) = \sum_{n=1}^{\infty} nN_A(n) \quad (58)$$

$$\begin{aligned} l_{WA} &= \sum_{n=1}^{\infty} nW_A(n) / \sum_{n=1}^{\infty} W_A(n) = \sum_{n=1}^{\infty} nW_A(n) = \\ &\quad \sum_{n=1}^{\infty} n^2 N_A(n) / \sum_{n=1}^{\infty} nN_A(n) \quad (59) \end{aligned}$$

Terminal Model.

$$\begin{aligned}
 N_A(n) &= P_{aa}^{n-1} P_{ob} \\
 W_A(n) &= nP_{ab}^2 P_{aa}^{n-1} \\
 l_A &= 1/P_{ab} \\
 l_{WA} &= 1 + 2(1 - P_{ab})P_{ab}
 \end{aligned} \tag{60}$$

Penultimate Model.

$$\begin{aligned}
 N_A(n) &= P_{baa}P_{aab}P_{aaa}^{n-2} & (n \geq 2) \\
 N_A(1) &= P_{bab} = 1 - P_{baa} & (n = 1) \\
 W_A(n) &= nN_A(n) P_{aab}/(P_{aab} + P_{baa}) \\
 l_A &= 1 + P_{baa}/P_{aab} \\
 l_{WA} &= 1 + 2P_{baa}/(P_{aab}^2 + P_{baa}P_{aab})
 \end{aligned} \tag{61}$$

Pen-penultimate Model.

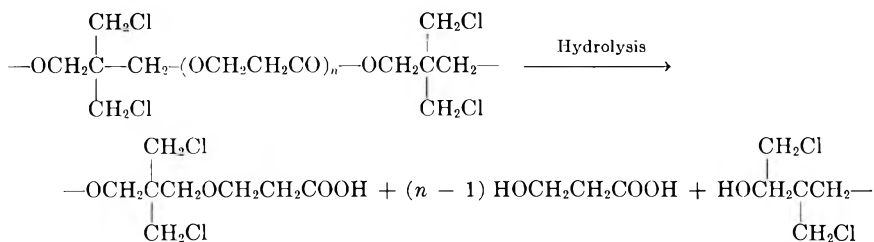
$$\begin{aligned}
 N_A(n) &= P_{baa}P_{baaa}P_{aaab}P_{aaaa}^{n-3} & (n \geq 3) \\
 N_A(2) &= P_{baa}P_{baab} = P_{baa}(1 - P_{baaa}) & (n = 2) \\
 N_A(1) &= P_{bab} = 1 - P_{baa} & (n = 1) \\
 W_A(n) &= nN_A(n)P_{aaab}/(P_{aaab} + P_{baa}P_{aaab} + P_{baa}P_{baaa}) \\
 l_A &= 1 + P_{baa}(1 + P_{baaa}/P_{aaab}) \\
 l_{WA} &= 1 + 2P_{baa}/[P_{aaab}^2/(P_{aaab} + P_{baaa})^2 + \\
 & \qquad \qquad \qquad P_{baa}P_{aaab}/(P_{aaab} + P_{baaa})] \tag{62}
 \end{aligned}$$

where P_{baa} is given in eq. (18.4).

Substituting the appropriate probabilities will give these as functions of r and x . Equations for B runs can be obtained by replacing A with B and a with b in the above equation.

APPLICATION

Cationic copolymerization between β -propiolactone (denoted by A) and 3,3-bischloromethyloxetane (denoted by B) with $BF_3 \cdot Et_2O$ at $-50^\circ C.$, recently reported by Tada, Saegusa, and Furukawa,⁹ can be easily treated by the present theory. They obtained $r_A = 0.05 \pm 0.05$ and $r_B = 16 \pm 3$ from the copolymer compositions (determined by chlorine analyses) with the usual Mayo-Lewis equation (by combination of intersection and curve-fitting methods). They also determined the amounts of β -hydroxypropionic acid which is to be formed by hydrolysis of the ester bonds in the copolymer.



Since the amount of β -hydroxypropionic acid produced corresponds to the number of AA bonds, we can calculate various quantities under the assumption of statistical stationarity, with the results given in Table I.

TABLE I
Data on Copolymer Composition and Microstructure

| No. | x | $P_1\{A\}$ | $P_1\{B\}$ | $P_2\{AA\}$ | R_f | l_A | l_B | $R_{f,\text{calc.}}^a$ |
|-----|-----|------------|------------|-------------|-------|-------|-------|------------------------|
| 1 | 3 | 0.168 | 0.832 | 0.0643 | 0.208 | 1.62 | 8.00 | 0.268 |
| 2 | 4 | 0.189 | 0.811 | 0.0563 | 0.266 | 1.42 | 6.10 | 0.322 |
| 3 | 9 | 0.388 | 0.612 | 0.225 | 0.326 | 2.38 | 3.76 | 0.472 |
| 4 | 19 | 0.592 | 0.408 | 0.425 | 0.334 | 3.54 | 2.44 | 0.528 |

^a Calculated from eq. (33) with $r_A = 0.05$ and $r_B = 16$.

Run fraction $R_{f,\text{calc.}}$, calculated from eq. (34) with $r_A = 0.05$ and $r_B = 16$, is always considerably greater than observed R_f , indicating that the Mayo-Lewis equation does not fit to microstructure of this copolymer and that the distribution of the two monomers in this copolymer is of more block character than expected from the Markoffian statistics of first order (Mayo-Lewis equation). Plots of l_A and l_B according to eqs. (39), in Figure 2,

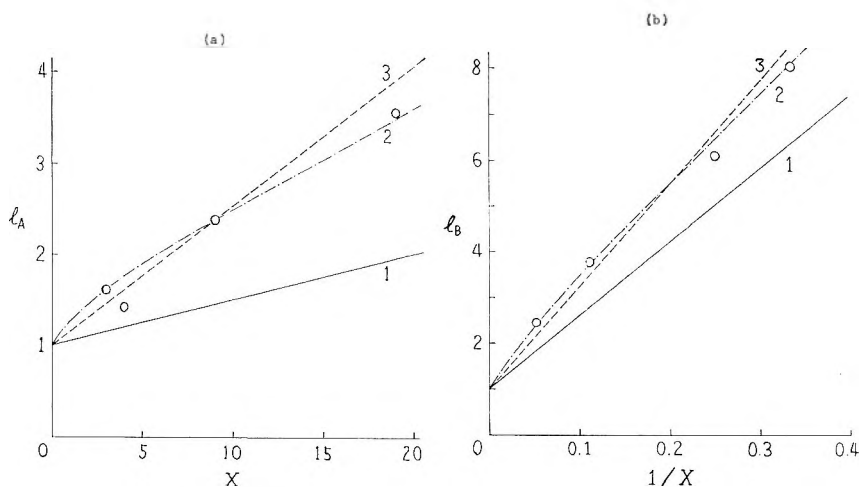


Fig. 2. Plots of mean run length vs. monomer feed ratio for (a) l_A and (b) l_B : (O) experimental; (—) calculated, with (1) $r_A = 0.05$, $r_B = 16$; (2) $r_A = 0.10$, $r_A' = 0.30$, $r_B = 20$, $r_B' = 45$; (3) $(\bar{r}_A) = 0.152$, $(\bar{r}_B) = 22.5$.

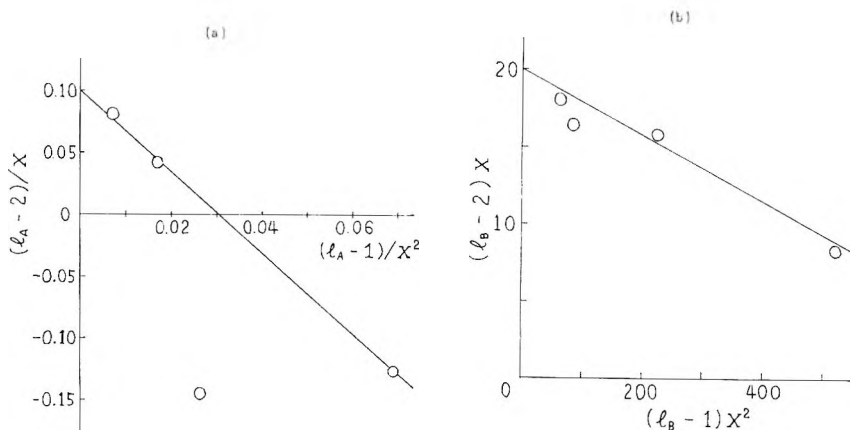


Fig. 3. Plots according to eqs. (41) to determine the four monomer reactivity ratios; (a) r_A and r_A' ; (b) r_B and r_B' .

seem to show that the penultimate effects exist and curves 1, calculated from the above monomer reactivity ratios, lie considerably below the observed points. Plots according to eqs. (41) give fairly good straight lines except the data for No. 2 (Fig. 3), from which we can readily estimate the four monomer reactivity ratios; $r_A = 0.10$, $r_A' = 0.30$, $r_B = 20$, and $r_B' = 45$. The mean monomer reactivity ratios calculated from eqs. (45) are $(\bar{r}_A) = 0.152$ and $(\bar{r}_B) = 22.5$, averaged over $x = 3-19$. The calculated mean run lengths with r_A , r_A' , r_B , and r_B' (curves 2 in Fig. 2) are in good accord with the experiments.

The copolymer composition $P_1\{A\}$ and bond or diad concentration $P_2\{AA\}$ were calculated with these three sets of monomer reactivity ratios with the results given in Table II. It is worthy of note that the difference in r values is not so much reflected on the copolymer compositions $P_1\{A\}$, and deviations from observed $P_1\{A\}$ values are not so large, but that the

TABLE II
Experimental and Theoretical
Copolymer Composition and Diad Concentration

| No. | x | $P_1\{A\}$ | | | | $P_2\{AA\}$ | | | |
|-----|-----|------------|----------------|----------------|----------------|-------------|----------------|----------------|----------------|
| | | Obs. | Calc. | | | Obs. | Calc. | | |
| | | | 1 ^a | 2 ^b | 3 ^c | | 1 ^a | 2 ^b | 3 ^c |
| 1 | 3 | 0.168 | 0.154 | 0.165 | 0.146 | 0.0643 | 0.0201 | 0.0627 | 0.0459 |
| 2 | 4 | 0.189 | 0.194 | 0.213 | 0.195 | 0.0563 | 0.0323 | 0.0923 | 0.0738 |
| 3 | 9 | 0.388 | 0.343 | 0.393 | 0.404 | 0.225 | 0.107 | 0.225 | 0.233 |
| 4 | 19 | 0.592 | 0.514 | 0.591 | 0.640 | 0.425 | 0.250 | 0.425 | 0.475 |

^a Calculated from eqs. (47), (49) (terminal) with $r_A = 0.05$, $r_B = 16$.

^b Calculated from eqs. (48), (50) (penultimate) with $r_A = 0.10$, $r_A' = 0.30$, $r_B = 20$, $r_B' = 45$.

^c Calculated from eqs. (47), (49) (terminal) with $(\bar{r}_A) = 0.152$, $(\bar{r}_B) = 22.5$.

bond or diad concentrations $P_2\{AA\}$ are sensitive enough to reflect these differences in r values.

DISCUSSION

It is obvious from the above application that the present treatment simplifies the distinction between the terminal model and the penultimate model and the determination of the four monomer reactivity ratios, if we can measure bond or diad concentrations.

On the other hand, copolymer-monomer composition curves calculated from the above three sets of reactivity ratios (1) $r_A = 0.05$, $r_B = 16$; (2) $r_A = 0.10$, $r_A' = 0.30$, $r_B = 20$, $r_B' = 45$; and (3) $(\bar{r}_A) = 0.152$, $(\bar{r}_B) = 22.5$ are shown in Figure 4. These calculated lines lie very close to each other, and experimental points appear to fit to any one of these lines. Hence, as Berger and Kuntz have pointed out,¹⁷ application of an alternative method to distinguish between the terminal and the penultimate models seems to be very difficult, until the very precise determination of composition, particularly at low and high x , is developed. According to the Fineman-Ross equation,¹⁸ which is derived from eq. (42),

$$(y - 1)/x = (r_A) - (r_B) \cdot (y/x^2) \quad (63)$$

where $y = P_1\{A\}/P_1\{B\}$, $(y - 1)/x$ versus (y/x^2) plots were calculated with the above r 's and are shown in Figure 5. Calculated curve 2 with the penultimate effect hardly deviates from the straight line except at considerably low and high region of x ($x < 2$ and $x > 30$). In the interval

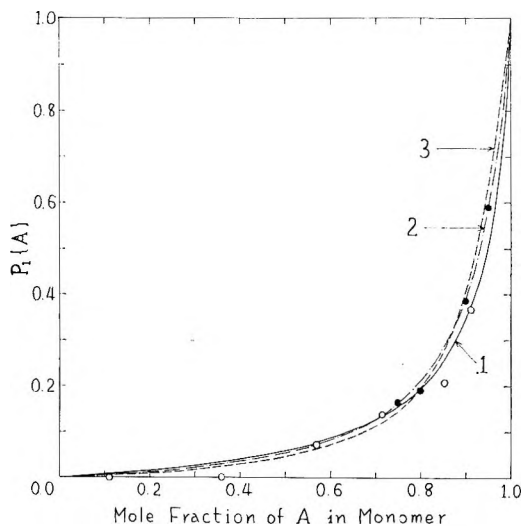


Fig. 4. Copolymer-monomer composition curves according to (1) terminal model with $r_A = 0.05$, $r_B = 16$; (2) penultimate model with $r_A = 0.10$, $r_A' = 0.30$, $r_B = 20$, $r_B' = 45$; (3) terminal model with $(\bar{r}_A) = 0.152$, $(\bar{r}_B) = 22.5$; (O) experimental points determined from Cl analyses; (●) experimental points from titration of carboxyl groups after hydrolysis of the copolymer.

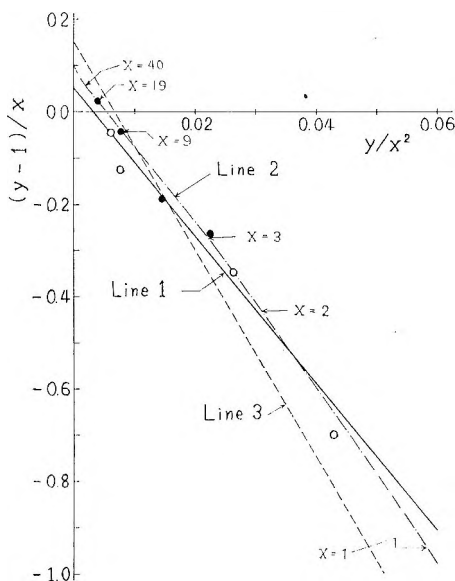


Fig. 5. Fineman-Ross plots. Curves and points are the same as given for Figure 4. Actual values of x are shown in curve 2 with arrows for the sake of convenience.

region of x , i.e., for example, $x = 3-19$, the line is almost perfectly straight, and yields values of $r_A = 0.09$ and $r_B = 16$ by extrapolation; it thus appears as if the Mayo-Lewis equation could be applied and as if the penultimate effect were absent. Although the experimental points would be scattered near the true line, it is hoped to determine the copolymer compositions as precisely as possible over as wide a range of x as possible and to test a complete fitting of the Mayo-Lewis equation over the whole range of x employed. Particularly, ionic copolymerization seems to be likely to produce a copolymer of more or less block character, apart from the origin of the phenomena.

The effect of involving the penultimate effect is reflected more markedly, the greater the length of the sequence considered. This is evident from the run length distributions (Fig. 6) calculated with the above monomer reactivity ratios from eqs. (60) and (61).

The pen-penultimate model can be treated easily with the determination of the triad concentrations but, in the authors' opinion, the nature of the pen-penultimate or more remote monomer units could hardly control the probability of the monomer addition, for they are separated so far from the reaction centers.

The above theory and discussions were made under the assumption of statistical stationarity or of sufficiently high degree of polymerization to permit the end effects to be neglected. This assumption can be checked by use of eqs. (26) and (27) as described, but it requires the measurement of at least two kinds of bond or diad concentrations. The effects of involving the probability of the monomer selection in the initiation step

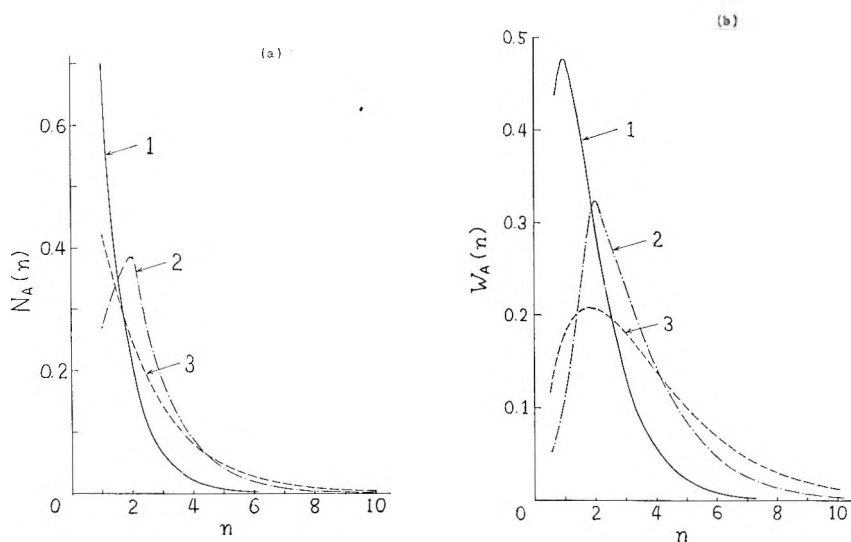


Fig. 6. Run length distribution at monomer feed ratio $x = 9$: (a) number fraction; (b) weight fraction. Curves are for same r values as in Figure 4.

upon the copolymer composition, as discussed very recently by Fueno and Furukawa,¹⁹ show that the stationary state is reached at a degree of polymerization of about 50, usually, after which only the probabilities in the propagation step determine the copolymer composition. When the difference between the probabilities in the initiation step and those in the propagation step is small, the stationary state should be reached at a lower degree of polymerization (probably about 10). It is safely said, therefore, that a copolymer with a higher degree of polymerization than 50 or so could be treated by the present method. From the concept that any sequence cannot be, usually in vinyl copolymerization, distinguished from its reversed sequence,¹⁵ however, the problem of the degree of polymerization of the copolymer seems to be of minor importance, until we know which end of the polymer chain is initially formed. The more special case in which one monomer reacts only in the initial stage to produce a completely block copolymer was treated by O'Driscoll,²⁰ and some applications and discussions were recently presented.²¹

At any rate, the development of analytical procedures to determine copolymer compositions and particularly microstructures would present more precise and complete information on propagation mechanisms. High resolution NMR spectroscopy appears to be a most convenient and precise means for these purposes.^{16,22,23} Whether the penultimate effect truly operates or not to determine the copolymer microstructure should be then clarified. At present, the data of microstructure seem to be too poor to permit a decisive conclusion to be reached. However, it will be of use to apply the present theory, when the Mayo-Lewis equation appears to be inappropriate to describe copolymerization behavior.

References

1. Mayo, F. R., and F. M. Lewis, *J. Am. Chem. Soc.*, **66**, 1594 (1944).
2. Barb, W. G., *J. Polymer Sci.*, **11**, 117 (1953).
3. Ham, G. E., *J. Polymer Sci.*, **11**, 87 (1954).
4. Ham, G. E., *J. Polymer Sci.*, **45**, 169, 177 (1960); *ibid.*, **61**, 9 (1962).
5. Szwarc, M., *J. Am. Chem. Soc.*, **85**, 533 (1963); *J. Polymer Sci.*, **61**, 31 (1962).
6. Bovey, F. A., and G. V. D. Tiers, *J. Polymer Sci.*, **44**, 173 (1960).
7. Miller, R. L., and L. E. Nielsen, *J. Polymer Sci.*, **56**, 375 (1962); *ibid.*, **46**, 303 (1960).
8. Johnsen, J., *Kolloid Z.*, **178**, 161 (1961).
9. Tada, K., T. Saegusa, and J. Furukawa, *Makromol. Chem.*, **71**, 71 (1964).
10. Okada, M., M. Hayashi, Y. Yamashita, and Y. Ishii, paper presented at the 13th Polymer Symposium, Tokyo, Japan, 1964.
11. Coleman, B. D., and T. G. Fox, *J. Polymer Sci.*, **A1**, 3183 (1963).
12. Merz, E., T. Alfrey, and G. Goldfinger, *J. Polymer Sci.*, **1**, 75 (1946).
13. Price, F. P., *J. Chem. Phys.*, **36**, 209 (1962).
14. Ham, G. E., *J. Polymer Sci.*, **A2**, 3633 (1964).
15. Ham, G. E., *J. Polymer Sci.*, **A2**, 2735 (1964).
16. Harwood, H. J., and W. M. Ritchey, *J. Polymer Sci.*, **B2**, 601 (1964).
17. Berger, M., and I. Kuntz, *J. Polymer Sci.*, **A2**, 1687 (1964).
18. Fineman, M., and S. D. Ross, *J. Polymer Sci.*, **5**, 259 (1950).
19. Fueno, T., and J. Furukawa, *J. Polymer Sci.*, **A2**, 3681 (1964).
20. O'Driscoll, K. F., *J. Polymer Sci.*, **57**, 721 (1962).
21. Dawans, F., and G. Smets, *Makromol. Chem.*, **59**, 163 (1963).
22. Nishioka, A., *J. Polymer Sci.*, **62**, S10 (1962).
23. Bovey, F. A., *J. Polymer Sci.*, **62**, 197 (1962).

Résumé

Pour caractériser la composition d'un copolymère et déterminer sa microstructure, on a développé une théorie simple en appliquant le processus de stationnarité statistique de Coleman et Fox aux trois modèles de copolymérisation binaire dans laquelle les trois dernières unités monomériques de la chaîne polymérique en croissance affectent la probabilité d'addition de monomère. On présente également une méthode simple pour distinguer les trois modèles à partir de chaque autre. La théorie a été appliquée à un copolymère obtenu cationiquement, le β -propiolactone-3,3-bischlorométhylloxétane, décrit par Tada et al., en vue de montrer comment les unités pénultièmes affectent la composition et la microstructure du copolymère. On fournit certaines discussions au sujet de la signification des rapports de réactivité des monomères du point de vue de la microstructure du copolymère.

Zusammenfassung

Eine einfache theoretische Behandlung zur Charakterisierung der Polymerzusammensetzung und Mikrostruktur wurde durch Anwendung des statistischen Stationären Prozesses von Coleman und Fox auf die drei binären Copolymerisationsmodelle entwickelt, bei welchem derletzte, die letzten zwei und die letzten drei Monomerbausteine der wachsenden Polymerkette die Wahrscheinlichkeit der Monomeraddition beeinflussen. Weiters wurde eine einfache Methode zur Unterscheidung der drei Modelle voneinander angegeben. Die Theorie wurde auf ein kationisch erhaltenes β -Propiolacton-3,3-bis-chlormethylloxétanocopolymeres nach Tada u.a. angewendet, um zu zeigen, wie die vorletzten Bausteine die Copolymer zusammensetzung und-Mikrostruktur beeinflussen. Die Bedeutung der Monomerreaktivitätsverhältnisse wurde vom Standpunkt der Copolymermikrostruktur aus diskutiert.

Received September 21, 1964

Revised December 15, 1964

(Prod. No. 4598A)

Block Copolymers Based on 2,2-Bis(4-hydroxyphenyl)propane Polycarbonate. II. Effect of Block Length and Composition on Physical Properties

STEWART H. MERRILL and S. E. PETRIE, *Research Laboratories, Eastman Kodak Co., Rochester, New York*

Synopsis

Block copolymers of 2,2-bis(4-hydroxyphenyl)propane (BPA) polycarbonate and poly(ethylene oxide) (PEG) were used in a study of the influence of composition and block size on the thermal and mechanical properties of block copolymers. By copolymerizing polycarbonates of controlled molecular weight with similarly characterized poly(ethylene oxide) glycols, it was found feasible to alter the size of each type of block independently of the other. To complement this investigation, the effect of varying the concentration of a compatible plasticizer on the physical properties of the BPA polycarbonate was also studied. The BPA polycarbonate was rendered thermally crystallizable and flexible either by the copolymerization with PEG or by the addition of low molecular weight plasticizer. Degradation of tensile modulus and strength was observed with increased PEG content but was less for the copolymers with the longer blocks.

INTRODUCTION

Block copolymers with sufficiently long blocks offer the possibility of combining the desirable properties of two different homopolymers rather than averaging them out, as is frequently the case for random copolymers.¹⁻⁴ Both the size of each type of block and the overall composition greatly influence the properties of a particular block copolymer.

Some work has been reported in the literature on the properties of block copolymers as a function of block size, in which the size of each block type was varied independently of the other. Schlick and Levy,⁵ who prepared styrene-isoprene block copolymers of controlled size, reported only solution properties. Coleman⁶ made a study of block copolymers consisting of poly(ethylene terephthalate) in which a few blocks of poly(ethylene oxide) of known molecular weight were incorporated in the polyester molecule. There appeared to be little alteration of the crystallites, and the melting point was relatively unaffected by the limited quantities of polyether. The glass transition temperature, however, decreased linearly with increasing weight per cent of poly(ethylene oxide). Similar observations were made by Iwakura et al.⁷ on polyester-urethane block copolymers having sufficiently long blocks, and by Grieveson⁸ on aliphatic polyesters.

Goldberg³ introduced poly(ethylene oxide) (PEG) into 2,2-bis(4-hydroxyphenyl)propane (BPA) polycarbonate chains and studied the effect on mechanical properties of variations of the size of the PEG in the range 1000–20,000 at 50 wt.-%. With a PEG of molecular weight 4000 in the polycarbonate, he showed the effect of various PEG–BPA ratios on thermal and mechanical properties.

Because block copolymers often are unusual, further studies were made of the effect of block size and composition on the mechanical and thermal properties of the copolymers. Of the series of block copolymers prepared from BPA polycarbonate and various hydroxy-terminated homopolymers described in the previous paper,⁴ the block copolymer of BPA polycarbonate and PEG seemed to be a suitable choice for a general study of this nature. It combined the highly flexible chains of the polyether, which is crystalline and low-melting, with the rigid chains of the polycarbonate, which, at high molecular weight, is normally amorphous. The two homopolymers are not miscible.⁴

Several molecular weight grades of PEG ranging from 200 to 3000 were copolymerized via their bischloroformates in an interfacial condensation reaction with BPA polycarbonates of three different average molecular weights—2000, 3000, and 4700. Each of the resulting three series of block copolymers consisted of a particular size of polycarbonate block, the polyether blocks varying in size within the series. Previously, it was concluded that the two types of blocks, joined by carbonate groups, alternated along the chain, each block retaining its original size and structure. These series, therefore, permitted the effect of the size of each type of block to be evaluated separately. The thermal and mechanical properties were measured on cast films, which were also examined for crystallinity by x-ray diffraction.

In order to compare the properties of the BPA polycarbonate with blocks of PEG incorporated in the chains with those of BPA polycarbonate modified with a compatible plasticizer, data have been obtained for high molecular weight BPA polycarbonate plasticized with various amounts of Aroclor 1254, a mixture of chlorinated biphenyls.

EXPERIMENTAL

Materials

The preparations and molecular weight determinations of the low molecular weight BPA polycarbonate and PEG employed as blocks, as well as the copolymerization technique, have been described previously.⁴ Since that work was reported, the vapor-pressure method¹⁰ has been found to be more accurate for the determination of the molecular weight of the polycarbonate. The revised values were used in this work. Also, for the block copolymers containing PEG blocks of molecular weight 3000, a mixture of ethyl ether and methanol rather than pure methanol was used to precipitate the block copolymer from the final solution, because the

latter produced small, highly swollen particles of the copolymer. BPA polycarbonates of high molecular weight were prepared by an interfacial condensation. The inherent viscosities were measured in chloroform at 25°C. at a concentration of 0.25 g./100 ml. of solution.

Aroclor 1254 was obtained from the Monsanto Chemical Company.

Preparation of Films

The copolymer films, 0.3–0.5 mil thick, were prepared by casting on glass from a 20–30%, by weight, solution in methylene chloride. After being dried in air, the films were heated at 75°C. for a period of approximately 16 hr. The mechanical properties were measured at 24°C. and 50% R. H. on samples that had been equilibrated under these conditions for 24 hr.

The plasticized BPA polycarbonate films were also cast from methylene chloride solution to an average thickness of about 5 mil. Measurements of the properties of these films were made under conditions comparable to those used for the block copolymer films.

Testing Procedure

Tensile properties were measured with an Instron tester having a cross-head speed of 5 in./min. on film specimens 1.5 cm. wide. Tear strength was determined with a Thwing-Albert tear tester.

Heat distortion was defined as the temperature at which elongation was 2% with a load of 50 psi. Glass transition temperatures and fusion and crystallization data were obtained by the differential thermal method¹² on 1 g. samples at a heating rate of 2.5°C./min. and a sensitivity of 5 μ v./in.

RESULTS AND DISCUSSION

Elemental analyses of the block copolymers of BPA polycarbonate and PEG are listed in Table I. The values of weight per cent of PEG given were calculated on the basis of the assumption of equimolar combination of blocks.

Since equimolar amounts of the constituent blocks were used in the copolymerization, little homopolymer should have remained. Furthermore, the extraction of the polymer solution with three or four portions of water, followed by precipitation in methanol, would have been expected to remove any PEG homopolymer. Because of its low molecular weight, any unreacted polycarbonate homopolymer would have dispersed in the precipitant and would not have been collected with the precipitated block copolymer. The elemental analyses, in general, supported such reasoning.

On the basis of the inherent viscosity values given in Table I, the block copolymers were considered to be high molecular weight materials.

Thermal and mechanical data collected on films of the various block copolymers of BPA polycarbonate and PEG are recorded in Table II. The copolymers are arranged in three series based on the size of the polycarbonate block, the size of the PEG block varying within each series.

TABLE I
Composition Data for BPA Polycarbonate-PEG Block Copolymers

| Polycarbonate MW | PEG MW | PEG concn., wt.-% | Inherent viscosity | Elemental analysis | | | |
|---------------------|-----------|-------------------------|-----------------------|--------------------|------|-------|------|
| | | | | Calculated | | Found | |
| | | | | C, % | H, % | C, % | H, % |
| 2000 | | | 0.12 | | | | |
| 3000 | | | 0.18 | | | | |
| 4700 | | | 0.29 | | | | |
| High-A | | | 0.78 | 75.5 | 5.6 | | |
| High-B | | | 0.81 | | | | |
| 2000 | 200 | 9 | 0.65 | 71.7 | 5.7 | 71.6 | 5.8 |
| 2000 | 400 | 17 | 0.69 | 70.8 | 6.0 | 70.7 | 6.1 |
| 2000 | 620 | 24 | 0.60 | 69.4 | 6.2 | 69.5 | 5.8 |
| 2000 | 1050 | 34 | 0.78 | 67.4 | 6.6 | 66.7 | 7.4 |
| 2000 | 1340 | 40 | 0.82 | 66.5 | 6.8 | 65.8 | 7.0 |
| 2000 | 3000 | 60 | 0.72 | 62.9 | 7.6 | 62.6 | 7.9 |
| 3000 | 620 | 17 | 0.52 | 70.9 | 6.1 | 71.5 | 6.0 |
| 3000 | 1050 | 26 | 0.46 | 69.7 | 6.4 | 69.5 | 6.3 |
| 3000 | 1340 | 31 | 0.54 | 68.9 | 6.6 | 67.8 | 6.2 |
| 3000 | 3000 | 50 | 0.43 | 65.1 | 7.3 | 65.5 | 7.1 |
| 4700 | 1050 | 18 | 0.59 | 71.2 | 6.1 | 71.5 | 6.4 |
| 4700 | 1340 | 22 | 0.59 | 71.1 | 6.3 | 70.4 | 6.6 |
| 4700 | 3000 | 39 | 0.53 | 67.8 | 6.9 | 69.1 | 6.6 |

For comparison, data for the thermal behavior of the parent homopolymer blocks are included, along with data for the mechanical and thermal behavior of high molecular weight BPA polycarbonate.

BPA Homopolymers

The thermal properties observed for the BPA polycarbonate homopolymers of low molecular weight were similar to those reported by Kozlov et al.¹¹ Low molecular weight BPA polycarbonate crystallized fairly readily, although the high molecular weight material was generally amorphous. This effect of chain length on the rate of crystallization was apparent in the differential thermal analysis¹² (DTA) traces illustrated in Figure 1 for initially amorphous samples. In the trace for the high molecular weight material, the only thermal effect observed was the endothermic baseline shift at the glass transition at 154°C., similar to the results of O'Reilly et al.¹⁶ for heat capacity measurements. The DTA trace for the low molecular weight polymer, BPA 4700, was typical of those obtained for crystallizable polymers that have been quenched to their glassy states prior to thermogramming and crystallize spontaneously during the programmed heating cycle.¹² Following the glass transition was the exotherm resulting from the crystallization of the polymer and an endotherm from subsequent fusion. The broadness of the exotherm was indicative of a rather slow rate of crystallization. DTA traces of the two lower molecular weight homopolymers were similar to that of BPA 4700, except

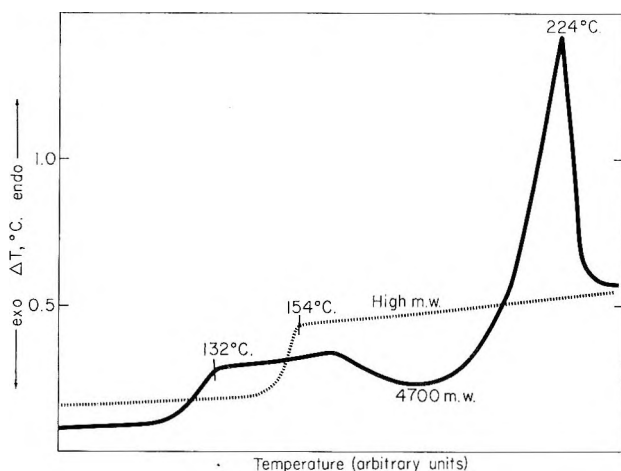


Fig. 1. Differential thermographs of BPA polycarbonate, reduced from experimental traces.

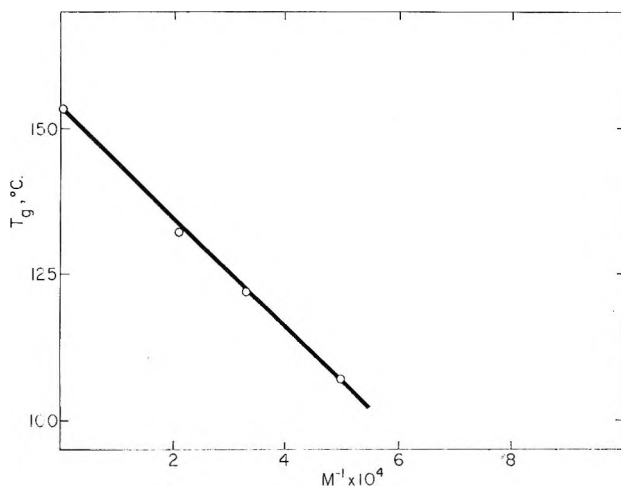


Fig. 2. Dependence of a glass transition temperature of BPA polycarbonate homopolymer on molecular weight.

that the spontaneous crystallization appeared to proceed at a little faster rate.

In the range of molecular weights of the BPA polycarbonate homopolymers, the glass transition was dependent on molecular weight, varying from 107°C. for amorphous BPA 2000 to 154°C. for the high molecular weight polymer. This dependence is illustrated by the plot of glass transition temperature versus reciprocal molecular weight in Figure 2.¹³

The melting point of BPA polycarbonate homopolymer having a molecular weight of about 3000 or more was approximately 225°C. This value is in good agreement with that reported by Schnell.¹⁴

PEG Homopolymers

The fusion data for the crystalline PEG homopolymers are plotted as a function of reciprocal molecular weight in Figure 3. Extrapolation of the data yields a value of about 65°C. for the melting point of high molecular weight PEG. Such a value is in good agreement with that reported in the literature.¹⁵

Glass transition temperature data were not obtained for the PEG homopolymers because the polymers could not be quenched. Read¹⁹ reported a value of -67°C. for the glass transition temperature of high molecular weight PEG. The glass transition temperatures for the low molecular weight PEG's reported here are probably considerably lower.

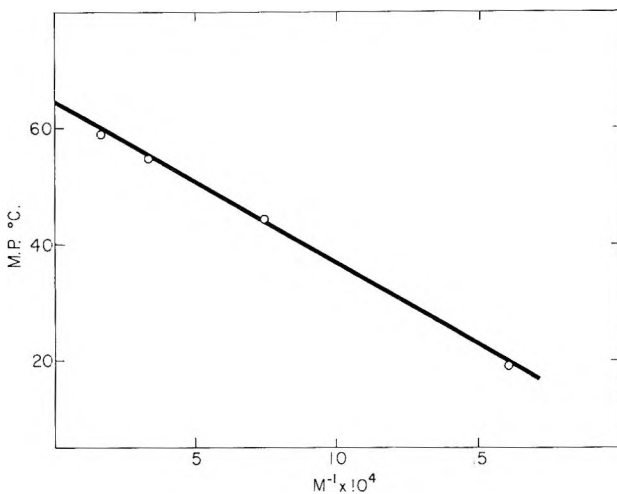


Fig. 3. Dependence of melting point of PEG homopolymer on molecular weight.

BPA Polycarbonate-PEG Block Copolymers

The glass transition temperature data for the BPA polycarbonate-PEG block copolymers given in Table II and plotted in Figure 4 were obtained on amorphous material. As discussed previously, the incorporation of PEG blocks in the BPA polycarbonate chains resulted in a lowering of the glass transition. The extent of the lowering was dependent on the overall composition of the copolymer and not on the number or size of the blocks. This was to be expected if the block copolymers were homogeneous. Crystallization of either component would have affected the glass transition greatly, because it would then have been determined essentially by the composition of the material remaining in the amorphous phase.

Except for the block copolymers with lowest quantities of PEG, the presence of PEG blocks in the BPA polycarbonate chains did enhance the ability of the polycarbonate to crystallize. From x-ray diffraction data it was concluded that the crystalline phase was BPA polycarbonate,

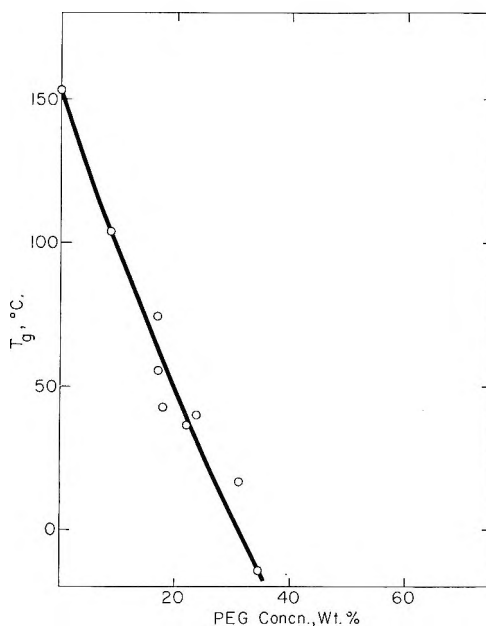


Fig. 4. Dependence of glass transition temperature of BPA polycarbonate-PEG block copolymers on composition.

with slight modification in some cases. In the copolymers with the longer PEG blocks, two crystalline phases were detected, the second phase being PEG.

An estimation of the relative extent of crystallinity in the films was made by comparing the intensities of the x-ray diffraction patterns.

Fusion data were obtained on solvent-cast films of the block copolymers. Although the melting point of the BPA polycarbonate crystalline phase was dependent on the length of the polycarbonate blocks, the length of the PEG block had relatively little effect on this melting point. Such was also the case for the PEG crystalline phase in the copolymers. Both components crystallized independently of the other, with very little modification. This result is not surprising since the homopolymers are incompatible.

The data for the mechanical properties are given in Table II. In general, as the PEG content increased, the Young's modulus and tensile strength dropped, while elongation and flexibility increased. Tear resistance maintained a rather high level throughout the series. The heat distortion data that were available were erratic. Although increasing PEG content did lower the heat distortion temperature, in general, it also enhanced the crystallinity of the polycarbonate. Increased crystallinity tended to raise the heat distortion temperature. Consequently, in some cases the presence of PEG actually resulted in a higher heat distortion temperature than that observed for pure amorphous BPA polycarbonate.

It is rather difficult to remove the last traces of solvent from solvent-cast BPA polycarbonate films. Frequently, the removal of residual solvent

TABLE II
Thermal and Mechanical Properties of BPA Polycarbonate-PEG Block Copolymers

| Poly- carbonate MW | PEG MW | Crystallinity | Young's modulus, kg. cm. ² × 10 ⁻⁴ | Tensile strength, kg. cm. ² % | Elonga- tion, % | Tear strength, g. | MIT folds | Heat distor- tion temp., °C. | <i>T_g</i> , C. ^a | DTA data | |
|--------------------------|-----------|---------------|---|---|-----------------------|-------------------------|--------------|---------------------------------------|---|--|--------------------------|
| | | | | | | | | | | Spontaneous crystal- lization, °C. ^b | Melting point, °C. |
| | 620 | | | | | | | | | | 19 |
| | 1340 | | | | | | | | | | 45 |
| | 3000 | | | | | | | | | | 55 |
| | 6000 | | | | | | | | | | 59 |
| 2000 | | High-medium | | | | | | | 107 | 173 | 205 |
| 3000 | | High-medium | | | | | | | 122 | 174 | 226 |
| 4700 | | High-medium | | | | | | | 132 | 187 | 224 |
| High-A ^c | | Amorphous | 2.24 | 575 | 6 | 160 | 270 | | | | |
| High-B ^d | | Amorphous | 3.06 | 1020 | | | | | | | 154 |

| | | | | | | | | | |
|------|------|------------------------|------|-----|--------|-----|-------|-----|---------|
| 2000 | 200 | Amorphous | 2.91 | 620 | 3 | 150 | 280 | 105 | |
| 2000 | 400 | Amorphous | 2.80 | 615 | 4 | 180 | 1350 | 75 | |
| 2000 | 620 | Slight BPA | 1.59 | 388 | 6 | 170 | >2000 | 40 | 190 |
| 2000 | 1050 | Medium BPA | 0.07 | 103 | >200 | 180 | >2000 | -15 | 188 |
| 2000 | 1340 | Medium BPA | 0.07 | 90 | >200 | 160 | >2000 | | 186 |
| 2000 | 3000 | Two crystalline phases | 0.05 | 47 | >200 | 90 | >2000 | | 36; 176 |
| 3000 | 620 | { High-medium BPA | 2.30 | 460 | 3 | 140 | 380 | 125 | 225 |
| | | { Very slight PEG | | | | | | | |
| 3000 | 1050 | { High-medium BPA | 0.72 | 220 | 17-29 | 90 | 350 | 87 | |
| | | { Slight PEG | | | | | | | |
| 3000 | 1340 | { High-medium BPA | 0.37 | 150 | | 145 | >2500 | 108 | 17 |
| | | { Slight PEG | | | | | | | |
| 3000 | 3000 | { High-medium BPA | 0.33 | 32 | 10 | 8 | 0 | 60 | 103 |
| | | { Medium-slight PEG | | | | | | | 41; 220 |
| 4700 | 1050 | { High-medium BPA | 1.90 | 420 | 6-58 | 170 | 2500 | 166 | 101 |
| | | { Very slight PEG | | | | | | | 227 |
| 4700 | 1340 | { High-medium BPA | 0.97 | 300 | 18-147 | 170 | >5000 | 133 | 36 |
| | | { Slight PEG | | | | | | | 88 |
| 4700 | 3000 | { High-medium BPA | 0.97 | 240 | 67-95 | 150 | 1850 | 176 | 4 |
| | | { Slight PEG | | | | | | | 36; 230 |

^a Glass transition temperatures were taken on amorphous material.

^b Heated at 2.5°C./min.

^c Solvent-cast film, inherent viscosity 0.78.

^d Melt-extruded fiber, inherent viscosity 0.81.

is enhanced in the presence of a plasticizer. Therefore, it is possible that the modulus of the high molecular weight homopolymer was low because of the presence of residual solvent, rather than the moduli of block copolymers, with small PEG contents, having been raised above that of the homopolymer. The fact that the modulus of a melt-extruded polycarbonate fiber was found to be 3.06×10^4 kg./cm². supports the former supposition.

Goldberg⁹ found, however, that the flexural modulus of molded bars increased as small amounts of PEG were introduced into the polycarbonate molecule. He attributed this to the onset of crystallization. Although neither x-ray nor DTA gave any evidence of crystallinity in our samples with the short PEG blocks. (MW 200 and 400), a very low order of crystallinity would not be detected by either of these methods. The crystallinity explanation cannot be ruled out.

Of the block copolymers having similar compositions but different block lengths, the longer PEG blocks imparted more flexibility. Also, the corresponding longer BPA polycarbonate blocks were able to retain higher tensile properties at the higher PEG compositions. With the short BPA polycarbonate blocks, no appreciable gain in elongation was achieved until enough of the flexible element had been added to convert the copolymer to an elastomer.

The mechanical properties of the BPA polycarbonate 3000-PEG 3000 film appeared at first sight to be anomalous in that their values were low. The x-ray diffraction data, however, indicated that the PEG constituent had crystallized to the greatest extent in this block copolymer. Furthermore, the inherent viscosity of 0.43 for this block copolymer was the lowest. Probably the high level of PEG crystallinity contributed most to the degradation of mechanical properties.

BPA Polycarbonate-Aroclor 1254

There is some discussion in the literature¹⁷ on the effect of the presence of various amounts of plasticizer on the thermal and mechanical properties of BPA polycarbonate. Nevertheless, a study was made of the system BPA polycarbonate-Aroclor 1254 in order to make a direct comparison between the thermal and mechanical behavior of the plasticized polymer and that of the BPA polycarbonate-PEG block copolymer having a plasticizing component incorporated in the polymer chain. In Table III are given the thermal and mechanical data for solvent-cast films of the BPA polycarbonate containing quantities of Aroclor 1254 ranging from 0 to 30% by weight.

As noted previously, the modulus of solvent-cast, unmodified BPA polycarbonate film is frequently low because of the presence of residual solvent. Such was the case in this series. Not only was the glass transition temperature some 10°C. below that normally observed for BPA polycarbonate, but there was definite evidence of the presence of residual solvent in the DTA trace.

TABLE III
Thermal and Mechanical Properties of BPA Polycarbonate-Aroclor 1254^a

| Aroclor concn., wt.-% | Crystal- linity | Young's modulus, kg./cm. ² × 10 ⁻⁴ | Tensile strength, kg./cm. ² | Elonga- tion, % | Tear strength, g. | MIT folds | Heat distor- tion temp., °C. | DTA data | | |
|-----------------------------|--------------------|---|--|-----------------------|-------------------------|--------------|--|----------------------|--------|--------------------------|
| | | | | | | | | T _g , °C. | | Melting point, °C. |
| | | | | | | | | First | Second | |
| 0 | | 2.4 | 613 | 39 | 92 | 265 | 150 | 145 ^b | 151 | |
| 5 | | 2.9 | 755 | 14 | 93 | 76 | 135 | 124 | 133 | |
| 10 | | 3.1 | 937 | 4 | 135 | 48 | 111 | 105 | 115 | |
| 20 | Slight | 3.4 | 964 | 3 | 134 | 26 | 96 | 78 | 92 | 190-195 |
| 30 | Medium | 3.6 | 896 | 3 | 94 | 22 | 123 | 53 | 81 | 194 ^c |

^a BPA polycarbonate inherent viscosity 0.83.

^b Residual solvent detected.

^c Spontaneously crystallized at 160°C.; heating rate 2.5°C./min.

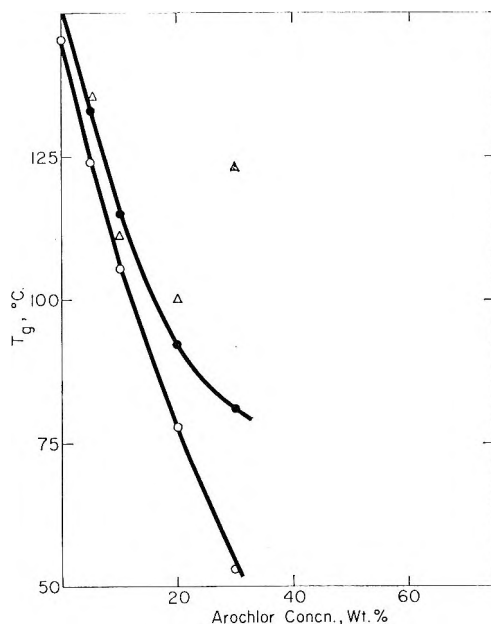


Fig. 5. Depression of glass transition temperature of BPA polycarbonate with increasing Arochlor concentration: (O) coatings run as received; (●) rerun; (Δ) heat distortion temperature.

In the presence of sufficient quantities of plasticizer, the BPA polycarbonate crystallized. On the basis of the relative areas of the fusion peaks in the DTA thermographs, it is apparent that the level of crystallinity was fairly high in the polycarbonate film containing 30% Arochlor, whereas that in the film containing 20% Arochlor was much lower. Although no fusion was observed in the films in this series containing lower quantities of Arochlor, it is possible that the level of crystallinity was too low to be detected in this way.

Of course, with the increase in plasticizer content, there was a lowering of the glass transition temperature. Since the crystallization of the BPA polycarbonate would have resulted in the concentration of the plasticizer in the amorphous regions, the glass transition temperatures of the most highly plasticized films may have been lower than those for amorphous films of the same composition. After fusion, the plasticized films were quenched and checked again for their thermal behavior. The glass transition temperature of the unplasticized film was substantially increased because of the removal of some of the residual solvent. An increase in the glass transition temperatures of all the plasticized films over the initial values was observed. Probably this increase was mainly the result of loss of Arochlor during the previous heating cycle, although the possibility exists that the level of crystallinity in the most highly plasticized film was altered. As the plots in Figure 5 indicate, these latter values were, in general, in fairly good agreement with the heat distortion temperatures

except for the most highly plasticized film. A loss of plasticizer would also have been anticipated in these measurements.

For the BPA polycarbonate film with 30% Aroclor, the heat distortion temperature was elevated considerably above those of films with lower plasticizer contents. It appears that the substantial level of crystallinity in this film was sufficient to offset the plasticizing influence of Aroclor.

With the increase in the level of crystallinity in these films, there was a corresponding increase in the modulus, which attained a level of 3.6×10^4 kg./cm.² for the film with the highest level of crystallinity. On the other hand, an increase in flexibility, which might have been expected with plasticization, was offset by the advent of crystallinity. Similar observations have been noted by others^{9,17,18} when no crystallinity was detected. Both the elongation and folds dropped to rather low values.

CONCLUSIONS

Because of the lack of flexibility in the polymer chain, high molecular weight BPA polycarbonate does not crystallize easily and is, therefore, generally amorphous. Low molecular weight BPA polycarbonate, however, crystallizes fairly readily, the fusion temperature being dependent on the molecular weight.

Crystallization of BPA polycarbonate is also promoted by the presence of a flexible element added either in the form of a plasticizer or in the form of flexible blocks in the polymer chain. For BPA polycarbonate copolymerized with blocks of PEG or plasticized with Aroclor 1254, about 20–30%, by weight, of the flexible component is necessary to render the polycarbonate readily crystallizable thermally. In the case of the block copolymer, longer blocks are more effective at the same composition level than the short ones.

The melting point of the BPA polycarbonate is not affected greatly by the presence of the flexible component. In the case of the block copolymers it is dependent on the block size rather than on composition. The glass transition temperature, however, is lowered, the extent of the lowering being dependent on the overall composition expressed in weight per cent. This dependence applies only to the amorphous polymers. Since the glass transition temperature is a property of the amorphous regions of the polymer system, it would be altered accordingly if there were any change in the concentration of flexible components in the amorphous regions as a result of crystallization of the BPA polycarbonate or the PEG.

Some of Goldberg's⁹ data indicate that the glass transition temperature is largely dependent on the length of the polycarbonate block. Our results do not confirm this. The glass transition temperature of the copolymers of constant polycarbonate block length rapidly decrease with increased PEG block length.

Although it is necessary to employ copolymers with long polycarbonate blocks in order to maintain the modulus level, the block copolymers have

some advantages over the plasticized film. Long PEG blocks impart flexibility to the polymer, provided the PEG does not crystallize extensively. Since the longer blocks do tend to crystallize, the PEG block size is limited to about 1000. The plasticized films, on the other hand, are brittle at the plasticizer level which permits thermal crystallization. Also, since the flexible unit is permanently incorporated in the chain, the unit is not subject to migration and loss.

The authors are indebted to L. E. Contois, R. J. Rauscher, B. W. Straube, and S. S. Sweet, for the preparation of the films and the measurement of the mechanical properties, and to O. E. Schupp, III, for the molecular weight determinations.

References

1. Mandelkern, L., *Rubber Chem. Technol.*, **32**, 1392 (1959).
2. Coffey, D. H., and T. J. Meyrick, *Proc. 3rd Rubber Technol. Conf., London, 1954*, p. 170.
3. Charch, W. H., and J. C. Shivers, *Textile Res. J.*, **29**, 536 (1959).
4. Merrill, S. H., *J. Polymer Sci.*, **55**, 343 (1961).
5. Schlick, S., and M. Levy, *J. Phys. Chem.*, **64**, 883 (1960).
6. Coleman, D., *J. Polymer Sci.*, **14**, 15 (1954).
7. Iwakura, Y., Y. Taneda, and S. Uchida, *J. Appl. Polymer Sci.*, **5**, 108 (1961).
8. Grieveson, B. M., *Polymer*, **1**, 499 (1960).
9. Goldberg, E. P., *J. Polymer Sci.*, **C4**, 707 (1964).
10. Neumayer, J. J., *Anal. Chem. Acta*, **20**, 519 (1959).
11. Kozlov, P. V., L. Makaruk, V. N. Fomin, and V. I. Olkhovskii, *Vysokomol. Soedin.*, **2**, 770 (1960).
12. Coste, J., *Ind. Plastiques Moderns*, **9**, No. 4, 37 (1957); B. Ke, in *Organic Analysis*, Vol. 4, J. Mitchell, Jr., I. M. Kolthoff, E. S. Proskauer, and A. Weissberger, Eds., Interscience, New York-London, 1960.
13. Fox, T. G., and P. J. Flory, *J. Appl. Phys.*, **21**, 581 (1950).
14. Schnell, H., *Angew. Chem.*, **68B**, 633 (1956).
15. Mandelkern, L., F. A. Quinn, and P. J. Flory, *J. Appl. Phys.*, **25**, 830 (1954).
16. O'Reilly, J. M., F. E. Karasz, and H. E. Bair, *J. Polymer Sci.*, **C6**, 109 (1964).
17. Sears, J. K., and J. R. Darby, *SPEJ.*, **19**, 623 (1963).
18. Jackson, W. J., Jr., and J. R. Caldwell, paper presented at 147th National Meeting, American Chemical Society, Philadelphia, April 1964; reported in *Chem. Eng. News*, **42**, 78 (April 20, 1964).
19. Read, B. E., *Polymer*, **3**, 529 (1962).

Résumé

On a utilisé des copolymères à blocs du polycarbonate de 2,2-bis(4-hydroxyphényl)propane (BPA) et de l'oxyde de polyéthylène (PEG) pour étudier l'influence de la composition et de la dimension du bloc sur les propriétés thermiques et mécaniques des copolymères à blocs. En copolymérisant des polycarbonates de poids moléculaire contrôlé avec des poly(éthylène oxyde)glycols également bien définis, on a trouvé qu'il était possible de changer la dimension de chaque type de bloc indépendamment de l'autre. Pour compléter cette étude, on a également étudié l'influence sur les propriétés physiques du polycarbonate BPA de différentes concentrations d'un plastifiant compatible. Le polycarbonate BPA a été rendu thermiquement cristallisable et flexible soit par copolymérisation avec le PEG, soit par addition d'un plastifiant de bas poids moléculaire. On a observé une diminution du module de tension et de la force lorsqu'on augmentait la teneur en PEG, mais d'une façon moindre pour les copolymères à blocs plus longs.

Zusammenfassung

Blockkopolymere von 2,2-Bis(4-hydroxyphenyl)propan-(BPA)-polycarbonat und Poly(äthylenoxyd) (PEG) wurden zur Untersuchung des Einflusses der Zusammensetzung und der Blockgrösse auf die thermischen und mechanischen Eigenschaften von Blockkopolymeren verwendet. Durch Kopolymerisation von Polycarbonaten mit kontrolliertem Molekulargewicht mit in ähnlicher Weise charakterisierten Poly(äthylenoxyd)glycolen war eine Änderung der Grösse jedes Blocktyps unabhängig vom anderen möglich. Zur Vervollständigung dieser Untersuchung wurde auch der Einfluss einer Variation der Konzentration eines mit dem Polymeren verträglichen Weichmachers auf die physikalischen Eigenschaften des BPA-Polycarbonats bestimmt. Das BPA-Polycarbonat erhielt durch die Kopolymerisation mit PEG oder durch den Zusatz eines niedermolekularen Weichmachers eine thermische Kristallisationsfähigkeit und Biegsamkeit. Mit zunehmendem PEG-Gehalt wurde eine Abnahme des Zugmoduls und der Festigkeit beobachtet; diese war bei den Kopolymeren mit längeren Blöcken geringer.

Received September 17, 1964

Revised December 12, 1964

(Prod. No. 4599A)

Effect of Atomic Oxygen on Polymers

R. H. HANSEN, J. V. PASCALE, T. DE BENEDICTIS, and P. M. RENTZEPIS. *Bell Telephone Laboratories, Incorporated, Murray Hill, New Jersey*

Synopsis

A stream of atomic oxygen, produced by passing oxygen at low pressure through a radio-frequency coil, was allowed to impinge on films prepared from several dozen different polymers. The flow of oxygen radicals was regulated so that the reaction temperatures were between 40 and 70°C. The rapid reactions which occurred at the polymer film-oxygen radical interface were essentially unaffected by the presence of phenolic antioxidants over a wide range of concentrations but rate of reaction was greatly affected by the structure of the polymer. Bulk properties of the polymers were unchanged because the attack by atomic oxygen is limited to the surface of the polymer. In many instances a simple ablation of the surface was observed, but in some cases, especially polyethylene and polypropylene, a highly oxidized surface layer was created. These oxidized surface layers had remarkably low contact angles with water and should be of great interest in improving adhesion and other surface-dependent properties of polymers.

Introduction

A stream of atomic oxygen, produced by passing oxygen at low pressure through a radio-frequency coil, was allowed to impinge on molded and cast films prepared from many different polymers. The rapid reactions which occurred at the polymer film-oxygen radical interface were greatly affected by the structure of the polymer. All polymers reacted but highly branched polymers such as polypropylene and polymers having ether linkages such as polymers of formaldehyde were most readily attacked. Those polymers which were most resistant to oxidation by atomic oxygen were the perfluorinated polymers, sulfur-vulcanized rubbers, and highly aromatic polymers (Fig. 1).

EXPERIMENTAL

Rates of reaction were observed to be constant over relatively long periods of time and were found to be independent of sample thickness, for the amount of polymer which reacted was directly related to the surface area exposed to the stream of atomic oxygen. For this reason, no special effort was made to maintain uniform sample thickness from polymer to polymer. Instead, uniform $1/2$ in. by $1 1/2$ in. strips of molded or cast samples of commercial and experimental polymers and modified or blended polymers were used in all cases. Polymer samples were weighed periodically to determine oxidation rates, and the results obtained by this technique are summarized in Table I.

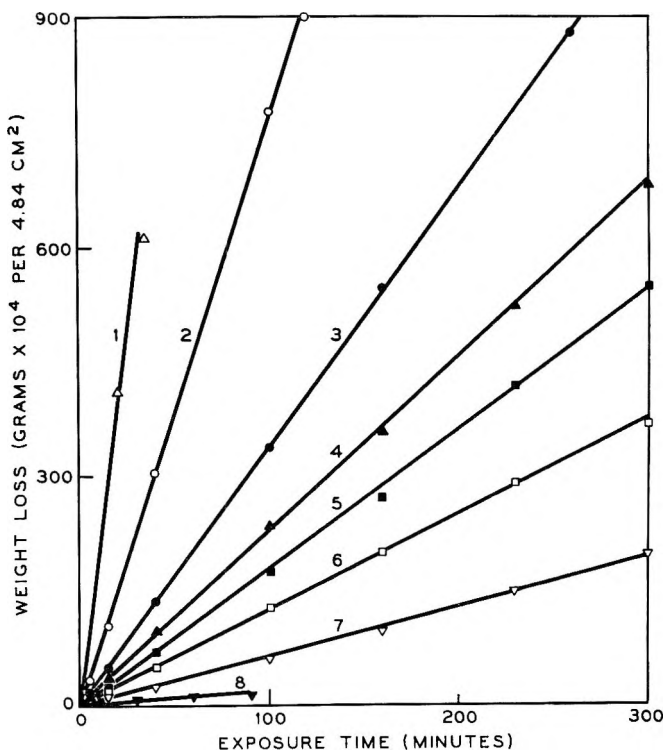


Fig. 1. Relative effect of atomic oxygen on a variety of polymers: (1) polysulfide polymer; (2) formaldehyde polymer; (3) polypropylene; (4) low-density polyethylene; (5) poly(ethylene glycol terephthalate); (6) polystyrene; (7) polytetrafluoroethylene; (8) sulfur-vulcanized natural rubber.

Oxidation reactions were carried out by placing polymer specimens on glass slides in the sample chambers of a Tracerlab low temperature asher Model 500A.¹ This equipment essentially consists of a radio-frequency coil which produces oxygen atoms and ions from oxygen by an electrodeless discharge process. The metastable oxygen species produced from Linde U.S.P. oxygen were allowed to impinge on the polymer films at a pressure of about 1 mm., and the flow of these active gases was so controlled that the temperature of the polymer was less than 70°C. except when the polymer contained metallic copper. In the latter case, temperature frequently exceeded 100°C. Sample temperatures of about 40°C. or less were usually observed when the low temperature asher was operated at low power. The presence of copper and the higher specimen temperature observed when metals are present had little effect on the oxidation of polypropylene and no significant effect on the rate of oxidation of other polymers.

The oxygen atom concentration was of the order of 10^{14} – 10^{15} atoms/cc. at a pressure of 1 mm., and the flow of oxygen was about 4 cc. (STP)/min. There was very little light emitted by the excited oxygen species in empty reaction chambers but a blue light having intensities which varied directly with rates of reaction of atomic oxygen with the polymers appeared when

samples were inserted into the stream of gases. The spectra of the emitting gases indicated the presence of excited O₂ and O and showed other bands which varied with the polymer under investigation. For example, CO₂

TABLE I

| Type of polymer | Rate of weight loss, g. × 10 ⁴ /4.84 cm. ² /min. ^a |
|---|---|
| Low-density polyethylene | 2.48 |
| Irradiated low-density polyethylene (1 Mrad) | 2.77 |
| Irradiated low-density polyethylene (10 Mrad) | 3.41 |
| Irradiated low-density polyethylene (105 Mrad) | 4.12 |
| Chemically crosslinked low-density polyethylene | 3.31 |
| Low molecular weight highly branched polyethylene | 3.26 |
| High-density ethylene-butene copolymer | 3.09 |
| Polypropylene | 3.45 |
| Polybutene-1 | 3.56 |
| Chlorinated high-density polyethylene | 5.00 |
| Chlorinated polyethylene plus 10% polysulfide polymer | 2.90 |
| Natural rubber | 3.39 |
| Natural rubber-sulfur raw stock | 1.20 |
| Natural rubber-sulfur vulcanizate | 0.16 |
| Natural rubber-peroxide raw stock | 2.99 |
| Natural rubber-peroxide cured | 1.67 |
| Commercial hard rubber | 2.71 |
| Vulcanized ethylene-propylene rubber | 0.20 |
| Polystyrene | 1.26 |
| Poly-3-phenyl-1-propene | 1.43 |
| Poly-4-phenyl-1-butene | 1.67 |
| Polyvinylcyclohexane | 2.28 |
| ABS polymers, several types | 2.68 |
| Unplasticized poly(vinyl chloride) copolymer | 4.71 |
| Poly(vinyl fluoride) | 2.54 |
| Polytetrafluoroethylene | 0.62 |
| Perfluorinated ethylene-propylene copolymer | 0.44 |
| Poly(methyl methacrylate) | 2.14 |
| Polyimide | 1.19 |
| Polycarbonate | 2.59 |
| Poly(ethylene terephthalate) | 1.82 |
| Nylon 6 | 2.77 |
| Nylon 610 | 3.24 |
| Formaldehyde polymers | 5.77-7.85 |
| Polysulfide (chloroethyl formal disulfide) | 19.45 |
| Cellulose acetate | 5.00 |

^a Low power, Tracerlab LTA-500A.

bands and (O,O; OH) bands were emitted strongly with hydrocarbon polymers such as polyethylene; these same bands and SO bands were emitted during the oxidation of sulfur-containing polymers. No CO band was observed, but since this is not usually emitted the formation of CO cannot be ruled out. In some cases a band emitted by CN was detected which indicated the presence of nitrogen as an impurity.

Results and Discussion

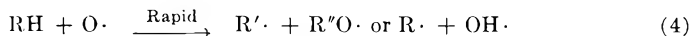
Highly branched saturated hydrocarbon polymers such as polypropylene and polybutene-1 are not readily attacked by molecular oxygen or by ozone at the temperature used in these studies but their rate of oxidation by atomic oxygen was found to be considerably higher than that of relatively unbranched hydrocarbon polymers such as polyethylene or highly branched but sterically hindered hydrocarbon polymers such as polyvinylcyclohexane. Thus, even though the bond energies in these polymers are alike, atomic oxygen can distinguish between sites which are more readily attacked by molecular oxygen and those which are less readily attacked. Atomic oxygen was not able to discriminate between the presence or absence of a good conventional thermal antioxidant, however, for polypropylene specimens containing 0, 0.5, and 1% of 4,4'-butylidenebis-(3-methyl-6-*tert*-butylphenol) were all oxidized at the same rate, and a sample containing 10% of the same antioxidant was oxidized slightly more rapidly than the others. For every polymer studied, oxidation by atomic oxygen began immediately without evidence of induction periods or autocatalysis.

A mixture of active oxygen species is produced in the electrodeless discharge chamber. Some of the reactions which are believed to occur include those shown in eqs. (1)–(3).



Oxygen ions may also be produced but ozone is not formed under the experimental conditions used.

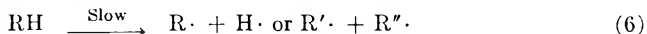
The mechanism by which a hydrocarbon polymer is attacked by the mixture of oxygen atoms, oxygen ions, electronically and vibrationally excited oxygen molecules, and ground state molecular oxygen is somewhat different than that suggested for simple thermal oxidation of hydrocarbons. The initiation stage during oxidation by atomic oxygen is a direct and rapid attack on the polymer and accounts for a much greater proportion of the overall oxidation of the polymer than do the corresponding initiation reactions which occur during simple thermal oxidation. Oxidation is initiated by oxygen radicals by the rapid reaction shown in eq. (4):

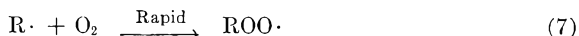


Accessible alkyl radicals such as those formed during the reaction described in equation (4) probably react rapidly with oxygen radicals as shown in eq. (5).

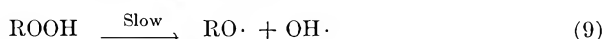
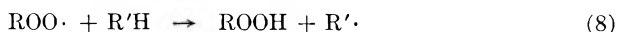


Initiation of simple thermal oxidation begins with the relatively slow formation of hydrocarbon radicals as shown in eq. (6), followed by the rapid reaction of these radicals with molecular oxygen as shown in eq. (7).

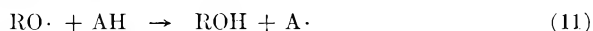
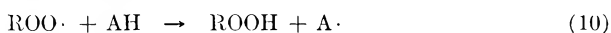




Propagation of simple thermal oxidation depends on the interaction of peroxy radicals, formed by the reaction shown in eq. (7), with the polymer to form new alkyl radicals and hydroperoxides, as shown in eq. (8), and the subsequent slow and rate-determining decomposition of these hydroperoxides, as is shown in eq. (9).



Oxidation of polymers by atomic oxygen occurs rapidly at the surface because the hydrocarbon radicals formed together with alkoxy or hydroxy radicals during the initiation stage [eq. (4)] react rapidly with oxygen atoms or with molecular oxygen by the reactions shown in eqs. (5) and (7). Subsequent reactions which are common to both thermal oxidation and attack by oxygen radicals, such as those shown in eqs. (8) and (9) are much slower and considerably less important in attack by atomic oxygen as is evidenced by the absence of autocatalysis or induction periods. For this reason, polymer beneath the surface is unaffected, while the surface is rapidly oxidized. The unimportance of the reactions shown in eqs. (8) and (9) during oxidation of polymers by atomic oxygen is also demonstrated by the ineffectiveness of antioxidants as protectants in this reaction. By contrast, during simple thermal oxidation, antioxidants normally decrease the chain length of the autocatalytic reaction by competing successfully with the hydrocarbon for peroxy radicals by the termination reactions shown in eq. (10)–(12).



Hydroxy radicals produced during oxidation of hydrocarbon polymers by atomic oxygen by reactions such as those shown in eqs. (4) and (9) were detected spectroscopically, but their contribution and the contribution of alkoxy radicals formed in the same reactions are certainly less important factors in the overall oxidation of the polymer than the reactions described by eqs. (4) and (5) or (7).

The remarkable resistance of sulfur-vulcanized rubbers toward attack by atomic oxygen was rather unexpected, particularly in view of the susceptibility of a polysulfide polymer (Fig. 1 and Table I). Unvulcanized natural rubber was oxidized at about the same rate as polypropylene and polybutene-1, but the addition of sulfur and typical vulcanization accelerators caused a decrease in the rate of oxidation (Fig. 2). The effect of vulcanization of this composition was even more beneficial in increasing the resistance of the composition toward attack by atomic oxygen, for the vulcanized composition was less affected by oxygen radicals than polymers such as polytetrafluoroethylene. Vulcanized ethylene-propylene terpolymers also were quite resistant to oxidation by atomic oxygen. Peroxide-cured

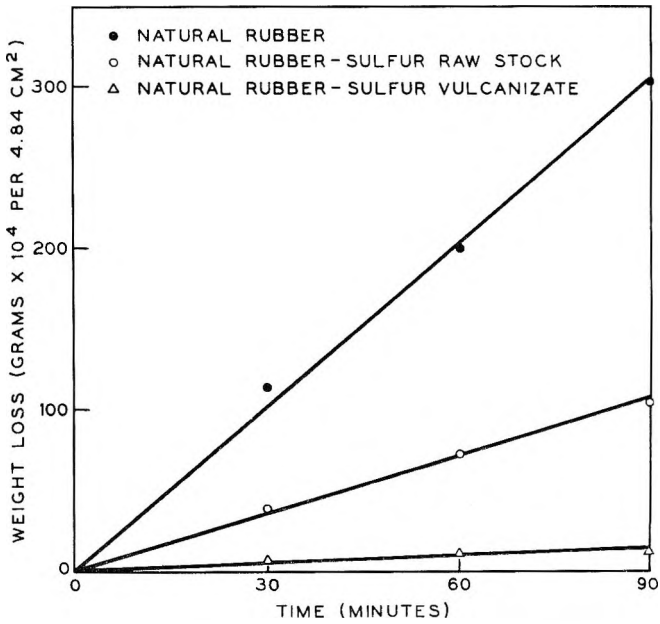


Fig. 2. Effect of vulcanization on the resistance of natural rubber toward attack by atomic oxygen.

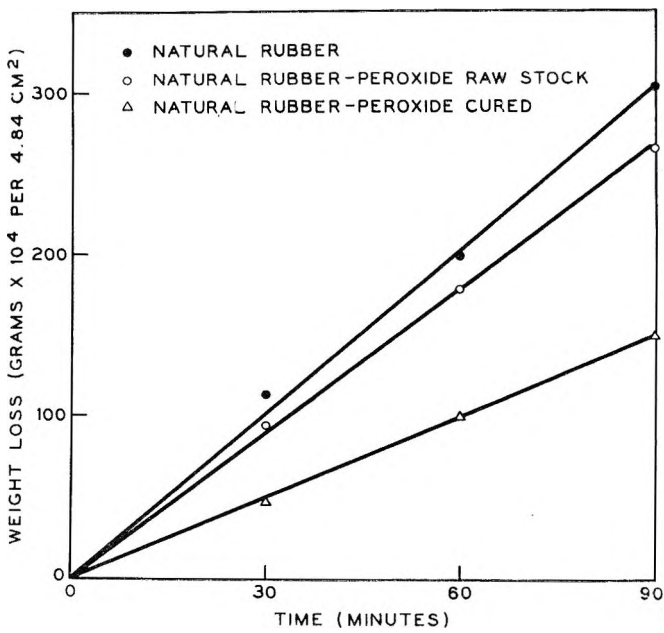


Fig. 3. Effect of peroxide curing on the resistance of natural rubber toward attack by atomic oxygen.

natural rubber showed an improvement in stability toward attack by oxygen radicals (Fig. 3), but polyethylene which had been chemically crosslinked in about the same way was oxidized more rapidly than untreated polyethylene (Table I). Crosslinking of polyethylene by electron bombardment also increased the susceptibility of the polymer to oxidation by atomic oxygen (Fig. 4). Apparently, then, crosslinking is not a general

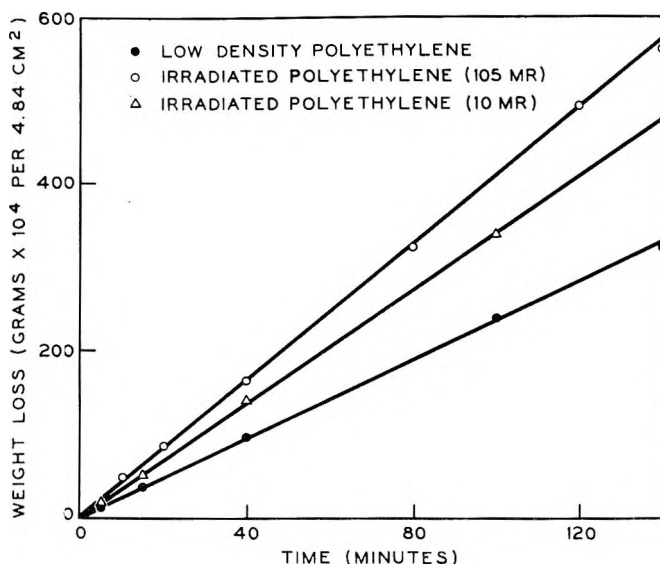


Fig. 4. Effect of electron bombardment on the subsequent resistance of polyethylene toward attack by atomic oxygen.

method for improving resistance of a polymer to attack by atomic oxygen. Since addition of a polysulfide rubber to chlorinated polyethylene was beneficial, there may be an optimum concentration of disulfide linkages which results in improved resistance to attack by atomic oxygen. We will report elsewhere further studies along these lines because we believe that the relative order of stabilities of polymers obtained by studying their rates of reaction with atomic oxygen can be correlated with the expected stabilities of these materials in regions between the upper atmosphere and outer space where an abundance of atomic gases prevails, for retention of desirable physical and dielectric properties of materials exposed in these regions is mainly a function of their radiation resistance and their resistance to attack by gaseous radicals.

Sulfur-vulcanized rubber under stress was attacked rapidly enough to break the specimen within a few minutes, although only a comparatively slight oxidation of the surface occurs in this short interval. The appearance of the oxidized composition resembled that of a similar specimen which was exposed to ozone under stress. This effect was not unique to rubber, for polyethylene under stress also cracked severely within a few minutes during exposure to atomic oxygen. In one set of experiments, polyethylene stress-crack samples (ASTM D-1693 test specimens) were

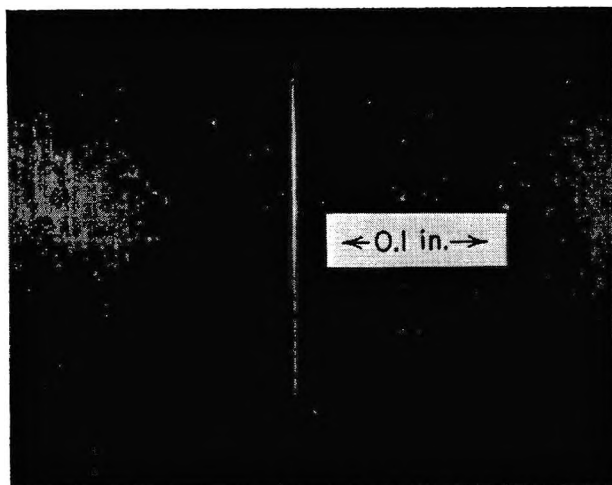


Fig. 5. Polyethylene stress crack specimen (ASTM D-1993) under stress before being exposed to atomic oxygen.

placed in the discharge chamber. The surface of a stressed but unoxidized sample is shown in Figure 5. The surface of the same sample after exposure to atomic oxygen while under the same stress is shown in Figure 6 and at higher magnification in Figure 7. Samples of polypropylene under stress failed in much the same way, the surface of the specimen in each case resembling the surface of rubber which has been attacked by ozone. Oriented polypropylene films which were no longer under stress were unaffected, except that they developed the usual highly oxidized surface layer. Polyethylene stress-crack specimens which were exposed to atomic oxygen before stressing them and testing them in solutions of wetting agents showed a slightly increased resistance to stress-cracking as compared with unoxidized specimens, possibly because unintentional surface imperfections were removed during oxidation.

Bulk properties of unstressed polymers were unchanged because attack by atomic oxygen is limited to the surface of the polymer. Surface-sensitive properties, however, were affected. For example, the elongation and tensile strength of polyethylene specimens were somewhat lower after exposure to atomic oxygen. In many instances a simple ablation of the polymer surface was observed during oxidation by atomic oxygen because the polymer surface was simply oxidized and volatilized. Polytetrafluoroethylene and other fluorinated polymers behaved in this manner. They were attacked quite slowly by atomic oxygen, and apparently the primary oxidation products were attacked more rapidly than the polymers themselves, for little or no change in contact angle with water was observed. In other polymers, especially polyethylene and propylene, a hazy and highly oxidized surface layer was created by exposure to atomic oxygen. These oxidized surfaces exhibited remarkably low contact angles with water and should be of great interest in improving adhesion and other surface-dependent

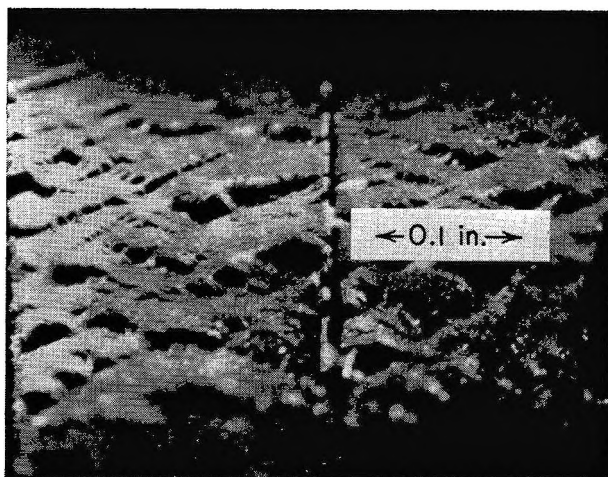


Fig. 6. Polyethylene stress-crack specimen (ASTM D-1693) after exposure to atomic oxygen while under stress. Much of the stress has been relieved by the development of many surface cracks. The cracks began to appear after ablation of about 10^{-4} g. of polymer and reached the extent shown here when the specimen had lost about 5×10^{-4} g. of its original weight of 1.25 g.

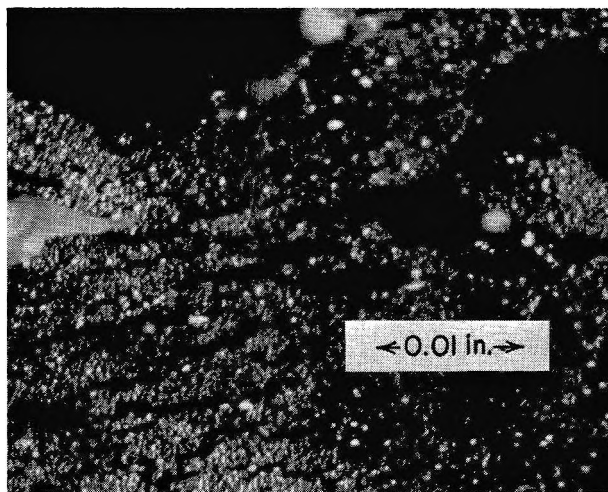


Fig. 7. Same as Figure 6 but at $10\times$ higher magnification. Even the cracks appear to have cracks.

properties of the polymers. For example, an oxidized polypropylene specimen had a contact angle with water of nearly zero degrees. If the surface of the polymer had simply been roughened, a contact angle with water of over 90° would have been produced.² When two pieces of this oxidized polymer were joined by an epoxy adhesive prepared from 100 parts of the diglycidyl ether of bisphenol A cured with 7 parts of diethylaminopropylamine, good joint strength was observed because failure occurred in the polymer rather than at the surface. The usefulness of atomic oxygen in improving properties such as adhesion and printability of polypropylene has also been studied by others.³ In the present study it was found that the following polymers showed the greatest change (decrease) in contact angle with water after treatment with atomic oxygen: polycarbonate,

polyimide, various types of nylon, chlorinated polyethylene containing 10 wt.-% of a polysulfide polymer, polyethylene, polypropylene, and unvulcanized natural rubber.

The authors wish to thank Tracerlab for the use of the low temperature asher and want to thank Dr. Harold Schonhorn for his help and advice on the contact angle and adhesion portion of this work and Messrs. Malcolm P. Schard, Harold M. Gilroy, and William M. Martin for their interest and help in relating reactions of polymers with atomic oxygen to changes in stability, physical properties, and stress cracking.

References

1. Gleit, C. E., and W. D. Holland, *Anal. Chem.*, **34**, 1454 (1962); see also C. E. Gleit, *Am. J. Med. Electronics*, **1963**, 112 (April-June, 1963).
2. Schonhorn, H., private communication.
3. Mantell, R. M., and W. L. Ormand, *Ind. Eng. Chem. Product Res. Dev.*, **3**, 300-303 (1964).

Résumé

Un courant d'oxygène atomique produit par passage d'oxygène sous faible pression à travers une spire émettant des radio fréquences heurte des films préparés à partir de plusieurs douzaines de polymères différents. Le courant de radicaux oxygène a été réglé de façon à maintenir la température de réaction entre 40 et 70°C. Les réactions rapides, qui ont lieu à l'interface entre le film de polymère et l'oxygène radicalaire, ne sont pas affectées par la présence d'antioxydants phénoliques dans un large domaine de concentrations, mais la vitesse de réaction est fortement influencée par la structure du polymère. Les propriétés principales des polymères sont inchangées parce que l'attaque par l'oxygène atomique est limitée à la surface du polymère. Dans plusieurs cas, on a observé un simple enlèvement de la surface mais dans certains cas, spécialement dans celui du polyéthylène et du polypropylène, on provoque en surface une couche fortement oxydée. Ces couches superficielles oxydées possèdent de faibles angles de contact avec l'eau et pourraient être d'un grand intérêt dans le cas de l'adhésion et d'autres propriétés dépendantes de la surface des polymères.

Zusammenfassung

Einen Strom von Sauerstoffatomen, der durch Durchgang von Sauerstoff bei niedrigem Druck durch eine Radiofrequenzspule erzeugt worden war, liess man auf Filme aus einigen Dutzend verschiedenen Polymeren auftreffen. Der Fluss der Sauerstoffradikale wurde so reguliert dass die Reaktionstemperaturen zwischen 40 und 70°C lagen. Die raschen Reaktionen, welche an der Polymerfilm-Sauerstoffgrenzfläche auftraten, wurden über einen weiten Konzentrationsbereich durch die Gegenwart phenolischer Antioxydantien im wesentlichen nicht beeinflusst, es bestand jedoch ein grosser Einfluss des Polymeren auf die Reaktionsgeschwindigkeit. Die Eigenschaften der Polymermasse blieb unverändert, da der Angriff der Sauerstoffatome auf die Oberfläche des Polymeren beschränkt ist. In vielen Fällen wurde eine einfache Abhebung der Oberfläche beobachtet, in manchen Fällen, besonders bei Polyäthylen und Polypropylen entstand jedoch eine hochgradig oxydierte Oberflächenschicht. Diese oxydierten Oberflächenschichten besaßen bemerkenswert niedrige Kontakwinkeln mit Wasser und sollten für die Verbesserung der Adhäsion und anderer oberflächenabhängiger Eigenschaften von Polymeren von grossem Interesse sein.

Received September 17, 1964

Revised December 24, 1964

(Prod. No. 4600A)

Solvent Effects in Anionic Copolymerization. II. Molecular Orbital Treatment for the Pair: Styrene—Methylstyrene

K. F. O'DRISCOLL,* T. YONEZAWA, and T. HIGASHIMURA, *Departments of Polymer Chemistry and Fuel Chemistry, Kyoto University, Kyoto, Japan*

Synopsis

A model is proposed for the transition state of the anionic copolymerization of styrene and *p*-methylstyrene in hydrocarbon solvent with lithium counterion. An LCAO-MO treatment which considers the effect of the positive counterion on the negative chain end is used to calculate the electrostatic and the π electron resonance contributions to the activation energies of the four propagation reactions. The electron contributions to the activation energies are also calculated for the propagation reactions of free ions, i.e., in the absence of a counterion. The previously determined rate constants in benzene and tetrahydrofuran are then compared with the results of these calculations.

Introduction

In the previous paper¹ the monomer pair consisting of styrene (M_1) and *p*-methylstyrene (M_2) were anionically copolymerized with a lithium counterion in benzene and in benzene containing tetrahydrofuran (THF). It was reported that r_1 and r_2 had values of 2.5 and 0.4 in benzene and that $k_{11} = k_{21}$ and $k_{22} = k_{12}$ in that solvent. In the presence of THF, however, the r_1 , r_2 values were essentially unchanged, but $k_{11} \neq k_{21}$ and $k_{22} \neq k_{12}$. To give a consistent explanation of these and other data in the literature it was suggested that anionic polymerization proceeds through π complex formation by the monomer with the positive counterion in hydrocarbon solvents such as benzene or heptane. In the presence of strongly solvating solvents such as THF it was suggested that the monomer could not compete easily with the solvent to form a π complex and propagation would take place by direct addition to the ion pair consisting of chain end and THF-solvated Li^+ .

In this paper we consider two admittedly extreme models for the transition state of the anionic propagation reaction: one approximating the reaction where the monomer complexes the positive counterion and then rearranges to become the terminal unit; the other representing the reaction where the counterion, being highly solvated by THF, does not influence the

* On leave of absence from Villanova University, Villanova, Pa.

terminal unit to which monomer directly adds. We have attempted to evaluate the electrostatic and resonance contributions to the activation energies of the four propagation reactions for the monomer pair styrene and *p*-methylstyrene. We do not suggest that the model transition states are exact, but only that they enable us to make a rough evaluation of the relative magnitudes of the various energies involved. We will show that this evaluation, and therefore the qualitative nature of the transition states, is consistent with the experimental data.

Complex Formation

It has previously been demonstrated² that the equilibrium constant for complex formation between silver ions and aromatic hydrocarbons correlates very well with the π electronic stabilization energy, E_{rs}^π , calculated by the equation

$$E_{rs}^\pi = (-2\gamma_{rs}^2\beta) \sum_j^{\text{occ}} (C_r^j + C_s^j)^2/(\lambda_j - h) \quad (1)$$

where in a Hückel treatment of the aromatic molecule, C_r^j is the coefficient of the r th atomic orbital in the j th molecular orbital, the energy of which is given by $(\alpha + \lambda_j\beta)$. The quantities $\alpha + h\beta$ and $\gamma_{rs}\beta$ represent the Coulomb integral of the cation and the resonance integral between the cation and the adjacent atoms r and s . This equation is here applied to complex formation between the lithium cation (where h is taken as -2.0 based on the ionization potential of lithium atom) and either a benzyl anion (representing the chain end) or styrene monomer, both with and without *p*-methyl substitution. The simple Hückel LCAO-MO treatment neglecting overlap was first used. The benzyl carbanion was assumed to have sp^2 hybridization. The results of these calculations indicated that the counterion would be located over the vinyl bond in the monomer and between the benzyl carbon and the ring in the benzyl anions. The position of maximum overlap, based on Mulliken's tables,³ would be 1.9 Å. above the axis of the C—C bond, equidistant from the two carbons. Further calculations showed that this position is favored over one where the cation is localized directly over the benzyl carbanion.

Model for Transition State with Complex Formation

On the basis of the above considerations, the polymerization propagation reaction in hydrocarbons was assumed to proceed as shown in Figure 1. The geometry of the complex transition state is shown in Figure 2. It is presumed that the cation is interacting with carbon atoms 1 and 2 in the ground state, and with carbon atoms 1, 2, α , and β in the transition state. It is further assumed that resonance stabilization of the transition state occurs due to interaction between carbon atoms 1 and β . The distances shown in Figure 2 are somewhat arbitrary, and it is felt that they represent an extreme version of a tightly complexed monomer. The symmetry of the transition state geometry was assigned only to simplify the calculations.

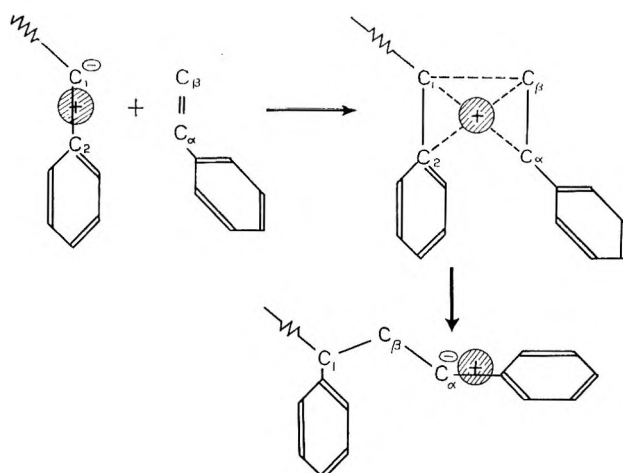


Fig. 1. Assumed mechanism for anionic propagation via complex formation.

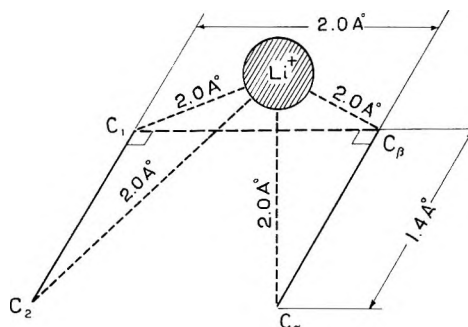


Fig. 2. Assumed geometry of complex transition state. Carbon atoms 1, 2, α , and β are coplanar; Li^+ is 1.8 Å. above center of rectangle formed by four C atoms.

Calculation of Contributions to Activation Energy

Before the various energy terms could be calculated, it was felt that the simple MO for the negatively charged chain end should be modified, both in the ground and transition states, to account for the proximity of the lithium counterion. The mode of perturbation due to the counterion is determined from the configurations of the ground and transition states (cf. Fig. 1). Accordingly, the coulomb integrals of the chain end benzyl anion were changed from α to $\alpha + \delta[(Q_r'e^2/R_r)]\beta$, where e is the charge of an electron, Q_r' is the net charge on the r th carbon in the nonperturbed molecule as calculated in the simple Hückel approximation, and R_r is the distance from the r th carbon atom to the positive counterion. This procedure is based upon the idea of a semiempirical SCF treatment, combining the net charge on the r th atom with the static interaction between that charge and the counterion. The parameter δ was calculated to be 0.2 e.v.⁻¹ from

$$\delta/0.6 = (I_{\text{Li}} - I_{\text{C}})/(I_{\text{N}} - I_{\text{C}})$$

where I is the ionization potential and 0.6 corresponds (in units of β) to the difference between the coulomb integrals of nitrogen and carbon.⁴

The results from the calculations considering the perturbation of the positive counterion on the chain end were then used in the equations below. Since monomers are uncharged, perturbation was not considered for them and simple MO's were used.

Inspection of Figure 1 shows that the electrostatic interaction between the negative chain end and the positive counterion will be changed on going from the ground state to the transition state. The interaction in each state was calculated as E_Q in units of electron volts, assuming a dielectric constant ϵ of unity.

$$E_Q = \sum_r Q_r e^2 / \epsilon R_r \quad (2)$$

In eq. (2), Q_r is the net charge on the r th carbon atom in the perturbed system as calculated by the LCAO method.

The resonance interactions,² in both the ground and transition states, were evaluated as E_{12}^π for the chain end-counterion and as $E_{\alpha\beta}^\pi$ for the monomer-counterion by using eq. (1). In the case of E_{12}^π the perturbed molecular orbitals were used.

The resonance stabilization of the transition state due to bond formation between C_1 and C_β was calculated from the equation:⁵

$$E_{1\beta} = \left(\sum_m^{\text{occ}} \sum_n^{\text{unocc}} - \sum_m^{\text{unocc}} \sum_n^{\text{occ}} \right) [(C_\beta^m)^2 (C_1^n)^2 (-\gamma_{1\beta}^2 \beta)] / (\lambda_n - \lambda_m) \quad (3)$$

where m, n are the molecular orbital numbers for the monomer and perturbed chain end, respectively, and $\gamma_{1\beta}^2 \beta$ is the overlap integral for the incipient bond between C_1 and C_β .

Table I shows the results of calculations by use of eqs. (1)–(3) on the molecular orbitals for styrene (M_1) and *p*-methylstyrene (M_2) and the perturbed molecular orbitals of their derived anions. Also included in

TABLE I
Calculated Contribution to the Activation Energies $E_{a(i,j)}$

| Energy ^a | <i>ij</i> | | | |
|-----------------------------|-----------|--------|--------|--------|
| | 11 | 12 | 22 | 21 |
| E_Q (ground state), e.v. | -6.532 | -6.532 | -7.012 | -7.012 |
| E_Q (trans. state), e.v. | -6.057 | -6.057 | -6.393 | -6.393 |
| E_{12}^π (ground state) | 1.014 | 1.014 | 0.995 | 0.995 |
| E_{12}^π (trans. state) | 1.044 | 1.044 | 1.074 | 1.074 |
| ΔE_Q , e.v. | 0.475 | 0.475 | 0.619 | 0.619 |
| ΔE_{12}^π | 0.030 | 0.030 | 0.079 | 0.079 |
| $E_{\alpha\beta}^\pi$ | 1.260 | 1.272 | 1.260 | 1.272 |
| $E_{1\beta}$ | 0.564 | 0.560 | 0.559 | 0.589 |
| $E_{1\beta}'$ | 0.901 | 0.859 | 0.909 | 0.970 |

^a E_Q and ΔE_Q values are in electron volts; all others are in units of β times their respective γ^2 values.

TABLE II
Experimental Rate Constants for Styrene (M_1)-*p*-Methylstyrene
(M_2) with Lithium Counterion

| Solvent | k_{11} | k_{12} | k_{22} | k_{21} |
|----------------------|----------|----------|----------|----------|
| THF ^a | 950 | 180 | 210 | 1150 |
| Benzene ^b | 0.0155 | 0.0062 | 0.0062 | 0.0155 |

^a Data of Shima et al.⁶

^b The absolute value⁷ of k_{11} was used with relative k_{ij} values.¹

Table I, on the last line, are the values for $E_{1\beta}'$ which was calculated by use of eq. (3) with the unperturbed anion MO's. $E_{1\beta}'$ is considered to be an approximation to the behavior which would be encountered in the presence of a strong solvating agent such as THF.

Table II shows previously determined polymerization rate constants.

Discussion of Results

Since the chain ends are so similar, differences in the observed experimental reaction rate constants, seen in Table II, can be attributed to differences in activation energies. Using the models described above, the activation energy $E_{a(i,j)}$ for reaction between chain end i and monomer j ($i, j = 1$ or 2) will be given by eq. (4) in the absence of a strong solvating agent:

$$E_{a(i,j)} = (\text{constant}) + (\Delta E_Q - \Delta E_{12}^\pi - E_{\alpha\beta}^\pi - E_{1\beta})_{i,j} \quad (4)$$

where ΔE_Q and ΔE_{12}^π are defined by eqs. (5) and (6):

$$\Delta E_Q = E_Q(\text{transition state}) - E_Q(\text{ground state}) \quad (5)$$

$$\Delta E_{12}^\pi = E_{12}^\pi(\text{transition state}) - E_{12}^\pi(\text{ground state}) \quad (6)$$

In the presence of a strong solvating agent, the monomer might not interact so strongly with the counterion in the transition state, and, in addition, the counterion would exist at a considerably further distance from the chain end. In that case, the activation energy might be better described as:

$$E_{a(i,j)} = (\text{constant})' - E_{1\beta}' \quad (7)$$

where $E_{1\beta}'$ is the resonance stabilization energy due to π conjugation between the unperturbed polymer anion and the monomer.

In eqs. (4) and (7) the constant terms represent sigma electron contributions and such other effects which are not here considered. These effects are believed to be either small compared to the π contributions or common to all four ij combinations.

Unfortunately, eqs. (4) and (7) cannot yet be quantitatively employed in comparing activation energies for the various propagation steps. This is because it is impossible to precisely evaluate the various γ values. However for the sake of discussion we may note that if γ were to have a value of 0.3, this would make $-\gamma^2\beta$ equal to approximately 0.1 e.v.

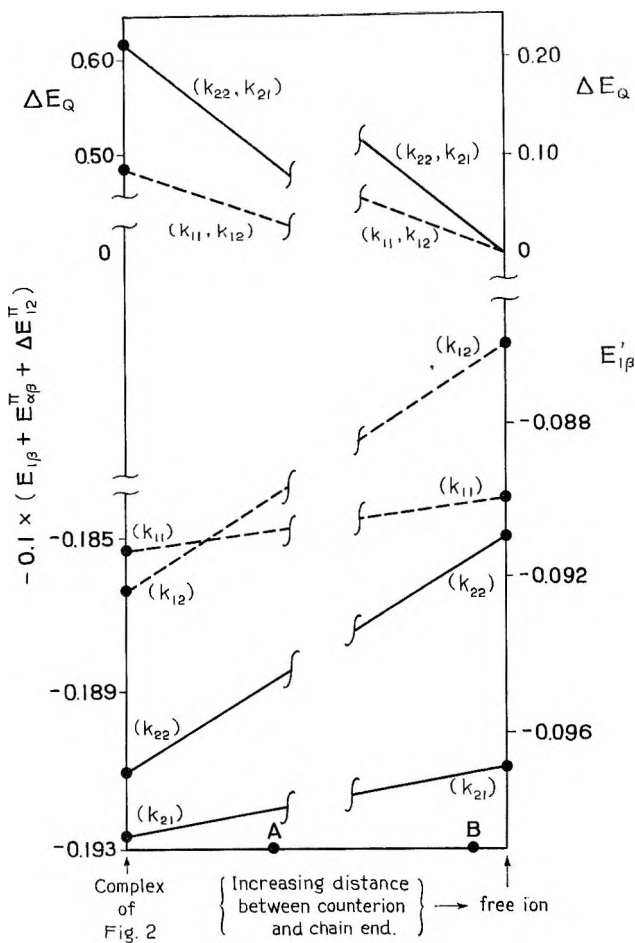


Fig. 3. Schematic presentation of data in Table I.

(Before making comparisons it must again be emphasized that the transition states chosen for calculation are arbitrary with respect to the exact physical parameters they contain. As a consequence the results of the calculations must be regarded as establishing trends, useful for qualitative comparisons. It is important to understand the direction of such trends, since Tobolsky and co-workers have shown^{8,9} that a continuous scale of "ionic character" exists in anionic polymerization with lithium in hydrocarbons such as benzene at one end of the scale and THF solvent at the other end.)

In benzene the experimental order of the rate constants is $k_{21} = k_{11} > k_{22} = k_{12}$; in THF the order is $k_{21} > k_{11} > k_{22} > k_{12}$. We shall interpret these two sequences in terms of the results of Table I by presenting those results in graphical form. Because of the difficulty mentioned above concerning γ values, this presentation has been done in an unorthodox fashion in Figure 3 and deserves some explanation. The abscissa of Figure 3 represents in going from left to right a continuous change from the transi-

tion state geometry of Figure 2 to a transition state which is essentially a free anion adding a monomer. The abscissa might then be regarded as a continuous scale of increasing "ionic character." The ordinate of Figure 3 is energy and represents in the upper portion the term ΔE_Q in electron volts. On the lower right-hand ordinate $0.1 \times E_{1\beta}'$ is plotted for each of the four propagation reactions. On a different scale we have plotted on the lower left ordinate $-0.1 \times (\Delta E_{12}^\pi + E_{\alpha\beta}^\pi + E_{1\beta})$. The use of the factor 0.1 is equivalent to assuming that all γ values are equal to 0.3. This is certainly quantitatively invalid, but it does serve to show roughly the differences in the transition states' activation energies.

Referring to the left-hand side of Figure 3, one can see that the large magnitude of the ΔE_Q term dominates the relative activation energies for the transition state geometry shown in Figure 2. But this would mean that the order of the reactivity would be $k_{12} > k_{11} > k_{21} > k_{22}$ in hydrocarbons, in contradiction to the experimental order mentioned above. However, if we consider a transition state described by a point such as A on the abscissa, where the complex would not be so tight, we can recognize that the differences in ΔE_Q would not be so large, the contributions of the resonance energies would be relatively more important, and, therefore, the relative order would be shifted to that observed experimentally. In a similar fashion we can see at the right-hand side of Figure 3 that the incorrect order $k_{21} > k_{22} > k_{11} > k_{12}$ given by the calculated values of $E_{1\beta}'$ would be corrected by considering the transition state in THF to exist at a point such as B on the abscissa. At point B, the value of $E_{1\beta}'$ would have changed little from that of the free ion, but small contributions from ΔE_Q would significantly affect the differences between the four activation energies and therefore the order of rate constants. It can be seen that all such changes would be in the proper direction.

Conclusions

Our assumed transition states were too extreme, but they do shed some light on the problem. In the absence of a solvating agent the complex may resemble Figure 2 but the distances between monomer, chain end, and counterion would be larger. On the other hand, the presence of THF should not be considered to free the transition state from the influence of the counter-ion. It is quite probable that the differences in physical dimensions of the transition state in the presence and absence of THF may be quite small.

In spite of its present limitations this method shows much promise as an aid in interpreting the results of ionic copolymerization. Most importantly, it shows that complex formation contributes significantly to lowering the activation energy in anionic polymerization. In this particular case, there was little difference between the $E_{\alpha\beta}^\pi$ values for the two monomers being considered, but this need not always be so. The calculation method also shows that movement of the positive counterion, which is essentially an ionization process is a very large factor in determining the activation energy. This has previously been suggested for

both anionic⁸ and cationic¹⁰ polymerizations. Extension of these calculations to cationic copolymerizations will have to recognize the larger size and more complicated nature of their negative counterions. In this work only the 2s orbital of lithium counterion was used. To consider stereoregular, anionic diene polymerizations it may be necessary to hybridize s and p orbitals as Kennedy and Langer have suggested.¹¹

Support of K. F. O'D. by a grant from the Petroleum Research Fund administered by the American Chemical Society is greatly appreciated.

References

1. O'Driscoll, K. F., and R. Patsiga, *J. Polymer Sci.*, **A3**, 1037 (1965).
2. Fukui, K., A. Imamura, T. Yonezawa, and C. Nagata, *Bull. Chem. Soc. Japan*, **34**, 1076 (1961).
3. Mulliken, R., C. Rieke, D. Orloff, and H. Orloff, *J. Chem. Phys.*, **17**, 1248 (1959).
4. Brown, R. D., and R. D. Harcourt, *J. Chem. Soc.*, **1959**, 3451.
5. Yonezawa, T., T. Higashimura, K. Katagiri, K. Hayashi, S. Okamura, and K. Fukui, *J. Polymer Sci.*, **26**, 311 (1951).
6. Shima, M., D. Bhattacharyys, J. Smid, and M. Szwarc, *J. Am. Chem. Soc.*, **85**, 1306 (1963).
7. Worsfold, D. J., and S. Bywater, *Can J. Chem.*, **38**, 1891 (1950).
8. Tobolsky, A. V., D. J. Kelley, K. F. O'Driscoll, and C. E. Rogers, *J. Polymer Sci.*, **28**, 425 (1958).
9. Tobolsky, A. V., and C. E. Rogers, *J. Polymer Sci.*, **38**, 205 (1959).
10. Kanoh, N., A. Gotoh, T. Higashimura, and S. Okamura, *Makromol. Chem.*, **63**, 115 (1963).
11. Kennedy, J., and A. Langer, *Fortschr. Hochpolymer. Forsch.*, **3**, 508 (1964).

Résumé

On propose un modèle pour l'état de transition de la copolymérisation anionique du styrène et du *p*-méthylstyrène dans les solvants hydrocarbonés en présence de lithium comme contre-ion. On applique un traitement LCAO-MO qui considère l'influence du contre-ion positif sur la fin de chaîne négative pour calculer les contributions électrostatiques et de la résonance de l'électron π aux énergies d'activation de quatre réactions de propagation. On a également calculé les contributions de l'électron aux énergies d'activation pour les réactions de propagation des ions libres, c'est-à-dire en l'absence d'un contre-ion. Les constantes de vitesse déterminées antérieurement dans le benzène et le tétrahydrofurane sont alors comparées avec les résultats de ces calculs.

Zusammenfassung

Für den Übergangszustand bei der anionischen Kopolymerisation von Styrol und *p*-Methylstyrol in Kohlenwasserstofflösung mit Lithium als Gegenion wird ein Modell vorgeschlagen. Eine LCAO-MO-Behandlung unter Berücksichtigung des positiven Gegenions am negativen Kettenende wird zur Berechnung des elektrostatischen und des π -Elektronenresonanzbeitrags zur Aktivierungsenergie der vier Wachstumsreaktionen verwendet. Der Elektronenbeitrag zur Aktivierungsenergie wird auch für die Wachstumsreaktionen der freien Ionen, d.h. in -Abwesenheit eines Gegenions, berechnet. Die früher in Benzol und Tetrahydrofuran bestimmten Geschwindigkeitskonstanten werden dann mit dem Ergebnis der Berechnung verglichen.

Received October 21, 1964

Revised December 31, 1964

(Prod. No. 4601A)

Solvent Effects in Anionic Copolymerization. III. Reactivity of Dienes

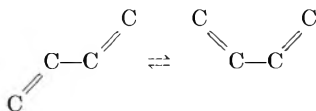
K. F. O'DRISCOLL,* *Department of Polymer Chemistry,
Kyoto University, Kyoto, Japan*

Synopsis

The effect of monomer configurations (*s-cis* or *s-trans*) on the observed rate of propagation of butadiene, isoprene and 2,3-dimethylbutadiene is considered. It is shown that this effect can be separated from the electronic effect of methyl substitution. Equations and numerical values are derived which can serve as a basis for quantitative treatment of the effect of solvent on diene reactivity and microstructure.

In a recent publication Szwarc et al.¹ have presented some very important data on the rate constants for the addition of butadiene (B), isoprene (I), and 2,3-dimethylbutadiene (D) monomers to polystyryl chain ends in tetrahydrofuran (THF). They gave a qualitative interpretation of these data in terms of the electronic effects of methyl substituents on butadiene and contrasted these with the effects in *p*-methylstyrene and α -methylstyrene. In view of the tremendous correlation between isoprene-styrene copolymerization behavior and polyisoprene structure that was demonstrated by Tobolsky and Rogers,² I believe that the data of Szwarc can be more quantitatively interpreted. In particular, I will show in this paper that the observed rate effects are a sum of electronic effects on the reaction system plus configurational effects on the free energy of the monomers, both of which are caused by methyl substitution on butadiene.

It has long been recognized that a butadiene can exist in the *s-cis* or *s-trans* configuration with rotation about the central carbon-carbon bond:



where the equilibrium would be described by the constant

$$K = [M_c]/[M_t] = \exp\{- (F_{M_c} - F_{M_t})/RT\} \quad (1)$$

The subscripts *c* and *t* refer to *cis* and *trans* forms of the monomer M with absolute free energy *F*. In polymerization, the monomer is incorporated

* On leave of absence from Villanova University, Villanova, Pa.

into the polymer chain in a given configuration, x , with a rate constant k_{tx} or k_{cx} . The concentration of propagating chain ends is $[P^*]$.

$$d[x]/dt = [P^*](k_{tx}[M_t] + k_{cx}[M_c]) \quad (2)$$

The term x refers to additions which result in a polymer microstructure which may be 1,2 or 3,4 or *cis*- or *trans*-1,4. If we write the rate constant in terms of the free energies of the reactants, F_P and F_M , and the transition state, F^\ddagger , we can obtain:

$$k_{tx}/k_{cx} = \exp\{- (F_{tx}^\ddagger - F_P - F_{M_t})/RT\} / \exp\{- (F_{cx}^\ddagger - F_P - F_{M_c})/RT\} \quad (3)$$

Using eq. (1) gives

$$k_{tx}/k_{cx} = ([M_c]/[M_t]) \exp(F_{cx}^\ddagger - F_{tx}^\ddagger) \quad (4)$$

Szwarc³ has shown that addition of dienes to a chain end in THF probably occurs only with the monomer being in a *trans* configuration. However in Diels-Alder reactions, additions are always *cis*,⁴ as is true for iron carbonyl complex formation with dienes.⁵ It is reasonable to assume from these and similar considerations that, whatever the configuration of a diene in a transition state for a particular reaction, there is only one transition state having a single absolute free energy. In terms of the symbols above, we can write then

$$F_{tx}^\ddagger \equiv F_{cx}^\ddagger \quad (5)$$

which gives [from eq. (4)]

$$k_{tx}[M_t] = k_{cx}[M_c] \quad (6)$$

The total rate of formation of all possible configurations, x , must correspond to the overall rate of polymerization:

$$\sum_x d[x]/dt = - d([M_c] + [M_t])/dt = k_p[P^*]([M_c] + [M_t]) \quad (7)$$

$$\sum_x (k_{tx}[M_t] + k_{cx}[M_c])[P^*] = k_p[P^*]([M_c] + [M_t]) \quad (8)$$

where k_p is the observed rate constant.

Using eqs. (6) and (8) and defining f_c as the fraction of monomer molecules in the *cis* configuration, ($f_c + f_t = 1$) we obtain:

$$k_p = 2f_c \sum_x k_{cx} \quad (9)$$

This can be further simplified by recognizing that

$$\sum_x k_{cx} = k_{cx} [1 + \sum_{x' \neq x} (k_{cx'}/k_{cx})] = k_{cx}/dx \quad (10)$$

where dx is the mole fraction of configuration x in the chain.

$$k_p = 2f_c k_{cx}/dx \quad (11)$$

It is now necessary to consider the values of f_c for different monomers. For butadiene, f_c^B has been established as between 0.03 and 0.07 based on chemical behavior⁶ and as 0.04 from thermodynamic and spectroscopic evidence.⁷ There is a barrier of 4.9 kcal. of free energy to rotation. No such clearcut evaluation is possible for isoprene or 2,3-dimethylbutadiene. Several workers have argued for a predominantly *trans* configuration, based on spectroscopic observation of near coincident Raman and infrared absorptions.^{4,3} Other work, the only quantitative estimate, gives⁹ f_c^I as 0.85 at 50°C. with ΔS of 7 e.u., and ΔH of 900 cal./mole. No estimate of the rotational barrier is made. Hannay and Smythe measured¹⁰ a considerable dipole moment of 0.5 D. for 2,3-dimethylbutadiene. Since the *trans* form of this monomer would be symmetric, we can conclude that, like isoprene, it would be mostly *cis*. The contrary spectroscopic evidence must be regarded as speculative, especially since such evidence was once offered to show that butadiene is mostly *cis*.¹¹

TABLE I
Polymer Microstructure (dx) in Anionic Polymerization

| Monomer | Configuration (x) | | | | Solvent |
|------------------------|-----------------------|------|-----------------|-------------------|-------------|
| | 1,2 | 3,4 | <i>cis</i> -1,4 | <i>trans</i> -1,4 | |
| Isoprene ^a | 0.16 | 0.54 | 0 | 0.30 | THF |
| Butadiene ^b | 0.51 ^c | — | 0.25 | 0.24 | THF |
| Isoprene ^a | 0 | 0.06 | 0.94 | 0 | Hydrocarbon |
| Butadiene ^b | 0.10 ^c | — | 0.46 | 0.44 | Hydrocarbon |

^a Data from Bawn and Ledwith.¹³

^b Data of Kuntz and Gerber.¹²

^c These numbers were divided by 2 in all calculations to account for the symmetry of butadiene.

In Table I are shown the previously established values of dx for butadiene¹² and isoprene¹³ when anionically polymerized in THF or hydrocarbons. Table II gives relative polymerization rate constants in the same solvents.^{1,14}

TABLE II
Relative Anionic Propagation Rate Constants

| Monomer | Relative rate constants | |
|-----------------------|-------------------------|-----------------------------|
| | In THF ^a | In hydrocarbon ^b |
| Butadiene | 1 | 1 |
| Isoprene | 1/2 | 1/3 |
| 2,3-Dimethylbutadiene | 1/69 | — |

^a Data of Shima et al.¹

^b Data of O'Driscoll and Kuntz.¹⁴

For two monomers, isoprene (I) and butadiene (B), we now have enough information to calculate the ratio

$$\frac{k_{cx}^I}{k_{cx}^B} = \frac{k_p^I}{k_p^B} \left(\frac{dx^I}{dx^B} / \frac{f_c^I}{f_c^B} \right) \quad (12)$$

This ratio is the combined effect of monomer configuration and electronic substituent effect on the reaction site for the addition resulting in any configuration x . If we can isolate electronic effect by itself, it would be of interest for purposes of fundamental calculations as in the previous paper.¹⁵ I suggest that the electronic effect can be separated from the combined effects by writing

$$k_{px}^I/k_{px}^B = (f_t^I k_{tx}^I + f_c^I k_{cx}^I) / (f_t^B k_{tx}^B + f_c^B k_{cx}^B) \quad (13)$$

where the ratio k_{px}^I/k_{px}^B represents the electronic effect only. This is so since each of the rate constants k_{tx} and k_{cx} have been corrected for the corresponding free energy level of the monomer by multiplying by f_t and f_c , respectively. Such correction is possible if no f values are unity. By means of eq. (6), eq. (13) becomes:

$$k_{px}^I/k_{px}^B = f_t^I k_{tx}^I / f_t^B k_{tx}^B = f_c^I k_{cx}^I / f_c^B k_{cx}^B \quad (14)$$

TABLE III
Calculated Electronic Effect (k_{px}^I/k_{px}^B) on Reaction which yields Microstructure x

| Solvent | k_{px}^I/k_{px}^B | | | |
|-------------|---------------------|------|-----------------|-------------------|
| | 1,2 | 3,4 | <i>cis</i> -1,4 | <i>trans</i> -1,4 |
| THF | 0.31 | 0.97 | ^a | 0.31 |
| Hydrocarbon | ^a | 0.40 | 0.31 | ^a |

^a Because the corresponding dx was zero for isoprene, these values are incalculable, but not necessarily zero.

Table III gives the results of using eq. (14) on the data of Table I and II, considering $f_c^B = 0.04$ and $f_c^I = 0.85$. In making these calculations, it was assumed that the allylic carbanion from butadiene, like the allyl radical,¹⁶ cannot retain its configuration during propagation. Therefore the sum of the observed *cis*- and *trans*-1,4 values of dx were used for the butadiene *cis*-1,4 dx in hydrocarbon and for the butadiene *trans*-1,4 dx in THF. In addition, as noted at the bottom of Table I, dx values for butadiene 1,2 addition were divided by 2 to account for symmetry.

Unfortunately, the *cis/trans* ratio for the monomer 2,3-dimethylbutadiene has not been experimentally determined. However, we can test the above suggested separation of electronic and monomer configuration effects on k_p by means of a calculation as follows:

Since eq. (14) represents electronic effects and eq. (12) represents a combination of electronic effects and monomer configuration, dividing eq. (12) by eq. (14) gives the effect of monomer configuration as $(f_c^B/f_c^I) = 0.047$.

This can be written as the equilibrium constant for the hypothetical interchange of a methyl group between *s-cis* isoprene and *s-cis* butadiene

$$f_c^B/f_c^I = \exp\{-(F_{Bc} - F_{Ic})/RT\} \quad (15)$$

and can be seen to represent the difference in free energy levels between *s-cis* butadiene and *s-cis* isoprene caused by the addition of a methyl group to the 2 position. If we assume, as a first approximation, that the difference in free energy between butadiene and 2,3-dimethylbutadiene is just twice the difference between butadiene and isoprene, then the monomer configuration effect for 2,3-dimethylbutadiene relative to butadiene would be given by the square of (f_c^B/f_c^I) , which would be 2.2×10^{-3} . This quantity indicates that 2,3-dimethylbutadiene would be totally *cis*; it can be used to calculate the overall relative rate of propagation of dimethylbutadiene and butadiene.

The electronic effect of 2-methyl substitution can be seen from Table III to be 0.31 for 1,2 addition, but 3,4 addition is unaffected by the 2-methyl substitution. This suggests, as Szwarc et al. had noted,¹ that the electronic effect of 2-methyl substitution is not felt at the 3,4 reaction site. Similarly, we may assume that the addition of a second methyl at the 3 position will cause an electronic effect of 0.31 on the 3,4 addition but will not affect the 1,2 reaction site electronically. As pointed out in the preceding paragraph, it will affect the monomer configuration. So the total effect at the 1,2 or 3,4 reaction sites (which are stereochemically indistinguishable in butadiene and 2,3-dimethylbutadiene) will be the product of the electronic effect, 0.31 and the monomer configuration effect, estimated above as 2.2×10^{-3} :

$$k_{cx}^D/k_{cx}^B = 6.9 \times 10^{-4} \quad (16)$$

where x refers to 1,2 or 3,4 addition. For want of more information I will consider x also refers to 1,4 addition. Then it is possible to write for the relative rates of propagation:

$$k_p^D/k_p^B = \sum_x (f_c^D k_{cx}^D + f_t^D k_{tx}^D) / \sum_x (f_c^B k_{cx}^B + f_t^B k_{tx}^B) \quad (17)$$

which can be simplified, since both f_c^B and f_t^D are virtually zero, to

$$k_p^D/k_p^B \cong \sum_x k_{cx}^D / \sum_x k_{tx}^B \quad (18)$$

We can then invoke eq. (6) and the numerical result of eq. (16):

$$\begin{aligned} k_p^D/k_p^B &= k_{cx}^D / [k_{cx}^B (f_c^B/f_t^B)] \\ &= \frac{6.9 \times 10^{-4}}{0.04/0.96} = 1/60 \end{aligned} \quad (19)$$

The observed ratio was 1/69, as given in Table II. The excellent agreement strengthens the hypothesis that eq. (14) and the calculated data in Table III represent the true electronic contributions of the methyl group,

isolated from the effect of monomer configuration. An explanation of these effects as well as the data in Table I, based on LCAO-MO calculations, is possible. Such calculations are presently being done in this laboratory, and will be published in the near future.

Support of this work by an International Award of the Petroleum Research Fund administered by the American Chemical Society is greatly appreciated.

References

1. Shima, M., J. Smid, and M. Szwarc, *J. Polymer Sci.*, **B2**, 735 (1964).
2. Tobolsky, A. V., and C. E. Rogers, *J. Polymer Sci.*, **38**, 205 (1959).
3. Szwarc, M., *J. Polymer Sci.*, **40**, 583 (1959).
4. Craig, D., J. Shipman, and R. Fowler, *J. Am. Chem. Soc.*, **83**, 2885 (1961).
5. Hallam, B., and P. Pauson, *J. Chem. Soc.*, **1958**, 642.
6. Smith, W., and J. Massingill, *J. Am. Chem. Soc.*, **83**, 4301 (1961).
7. Aston, J., G. Szacz, H. Wooley, and F. Brickwedde, *J. Chem. Phys.*, **14**, 67 (1946).
8. Szacz, G., and N. Sheppard, *Trans. Faraday Soc.*, **49**, 358 (1953).
9. Nikitin, V., and T. Yakovleva, *Zh. Fiz. Khim.*, **28**, 697 (1954).
10. Hannay, N., and C. P. Smythe, *J. Am. Chem. Soc.*, **64**, 1931 (1943).
11. Rasmussen, R., D. Tunnicliff, and R. Brattain, *J. Chem. Phys.*, **11**, 432 (1943).
12. Kuntz, I., and A. Gerber, *J. Polymer Sci.*, **42**, 299 (1960).
13. Bawn, C. E. H., and A. Ledwith, *Quart. Rev.*, **16**, 388 (1962).
14. O'Driscoll, K. F., and I. Kuntz, *J. Polymer Sci.*, **61**, 19 (1962).
15. O'Driscoll, K. F., T. Yonezawa, and T. Higashimura, *J. Polymer Sci.*, **A3**, 2215 (1965).
16. Walling, C., *Free Radicals in Solution*, Wiley, New York, 1957, p. 230.

Résumé

On considère l'influence des configurations du monomère (*s-cis* ou *s-trans*) sur les vitesses de propagation observées dans le cas du butadiène, de l'isoprène, et du 2,3-diméthylbutadiène. On a montré que cette influence peut être séparée de l'influence électronique due à la substitution par le méthyle. On a déduit des équations et des valeurs numériques qui peuvent servir de base pour une étude quantitative de l'influence du solvant sur la réactivité diénique et sur la microstructure.

Zusammenfassung

Der Einfluss der Monomerkonfiguration (*s-cis* oder *s-trans*) auf die beobachtete Wachstumsgeschwindigkeit von Butadien, Isopren, und 2,3-Dimethylbutadien wird untersucht. Es wird gezeigt, dass dieser Einfluss vom elektronischen Einfluss des Methylsubstituenten getrennt werden kann. Gleichungen und numerische Werte werden als Basis für eine quantitative Behandlung des Einflusses des Lösungsmittels auf die Dienreaktivität und die Mikrostruktur abgeleitet.

Received October 21, 1964

Revised December 31, 1964

(Prod. No. 4602A)

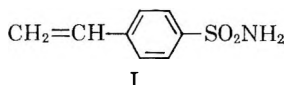
Base-Catalyzed Polymerization of Aromatic Sulfonamides with an Activated Double Bond. I

NAOYA YODA*,† and C. S. MARVEL, *Department of Chemistry, University of Arizona, Tucson, Arizona*

Synopsis

The base-catalyzed polymerization of *p*-styrenesulfonamide has given a product with mixed recurring units, some produced by anionic-initiated vinyl polymerization and some by proton-transfer polymerization. The products are high softening but yield brittle films. Some preliminary results have been obtained for the polymerization of *p*-acrylamidobenzenesulfonamide and the related crotonyl and cinnamoyl derivatives. Synthetic methods for the monomers are described.

Since polysulfonamides have proved to be difficult to obtain in high molecular weight by condensation,¹⁻⁶ it was thought that the proton-transfer type of polymerization described by Breslow, Hulse, and Matlack⁷ might be developed with an aromatic sulfonamide such as *p*-styrenesulfonamide (I).



This monomer has been polymerized in a variety of solvents with a range of basic initiators to yield white products that melt above 276°C. In the preliminary experiments reported in Table I, the inherent viscosities of the polymers varied from 0.09 to 0.75. After a more complete investigation of the reaction variables and the kinetics of the polymerization a preferred set of conditions for the polymerization in dry dimethylformamide with the use of potassium butoxide as initiator was determined; the details are recorded in the experimental part. Under these conditions polymers with inherent viscosities of 1.6 (0.5% in dimethyl sulfoxide) have been obtained. However, usually the polymers had viscosities of about 0.8-0.9. When the reaction conditions were such as to produce higher molecular weight polymers, gelation often set in due to a crosslinking or branching re-

* Postdoctoral Research Associate supported by Textile Fibers Department of E. I. du Pont de Nemours and Company, 1962-63.

† Present address: Toyo Rayon Co., Ltd., Basic Research Laboratories, Kamakura, Japan.

TABLE I

| Expt. no. | Monomer g. (mole) | Catalyst, g. | Inhibitor, g. | Solvent, ml. | Temp., °C. | Time, hr. | Yield of polymer, % | η_{inh} at 30°C. (0.5% DMF) |
|-----------|-------------------------|---|-----------------------------|---------------------------|---------------|--------------|---------------------------|---|
| PSTA-1 | 5.0 (0.027) | <i>t</i> -BuONa (0.02) | PBNA ^a (0.01) | DMF ^b (50) | 100 | 16 | 77.5 | 0.21 (0.5% H ₂ SO ₄ /0.25) |
| PSTA-2 | 5.0 (0.027) | <i>t</i> -BuONa (0.02) | PBNA (0.01) | DMAc ^c (50) | 140 | 20 | 65.1 | 0.31 (0.5% H ₂ SO ₄ /0.41) |
| PSTA-3 | 5.0 (0.027) | Na (0.02) | PBNA (0.01) | DMF (50) | 120 | 20 | 76.5 | 0.36 (0.5% H ₂ SO ₄ /0.45) |
| PSTA-4 | 5.0 (0.027) | K (0.02) | PBNA (0.01) | DMF (50) | 120 | 20 | 81.2 | 0.58 (0.5% H ₂ SO ₄ /0.85) |
| PSTA-5 | 5.0 (0.027) | Mesityl- magnesium bromide (0.170) | PBNA (0.01) | DMAc (50) | 120 | 20 | 78.1 | 0.42 (0.5% H ₂ SO ₄ /0.55) |
| PSTA-6 | 5.0 (0.027) | <i>t</i> -BuONa (0.02) | PBNA (0.01) | Pyridine (50) | 120 | 20 | 58.0 | 0.32 (0.5% H ₂ SO ₄ /0.44) |
| PSTA-7 | 5.0 (0.027) | Mesityl- magnesium bromide (0.17) | PBNA (0.01) | Pyridine (50) | 120 | 20 | 62.0 | 0.25 (0.5% H ₂ SO ₄ /0.28) |
| PSTA-8 | 5.0 (0.027) | <i>t</i> -BuONa (0.02) | PBNA (0.01) | DMSO ^d (50) | 160 | 20 | 76.5 | 0.56 (0.5% H ₂ SO ₄ /0.61) |
| PSTA-9 | 5.0 (0.027) | Mesityl- magnesium bromide (0.17) | PBNA (0.01) | DMSO (50) | 160 | 20 | 68.0 | 0.43 (0.5% H ₂ SO ₄ /0.49) |

| | | | | | | | | |
|---------|----------------|--------------------------|----------------|---------------------------|-----|----|------|-------------------|
| PSTA-10 | 5.0 (0.027) | Na (0.02) | PBNA (0.01) | Pyridine (50) | 100 | 20 | 38.5 | 0.31 |
| PSTA-11 | 5.0 (0.027) | <i>n</i> -BuLi | PBNA (0.01) | DMAc | 60 | 20 | 26.4 | 0.26 |
| PSTA-12 | 5.0 (0.027) | <i>t</i> -BuONa | PBNA (0.01) | THF ^e | 100 | 20 | 95.0 | 0.09 |
| PSTA-13 | 5.0 (0.027) | <i>t</i> -BuONa | PBNA (0.01) | Chloro- benzene | 120 | 20 | 40.4 | 0.21 |
| PSTA-14 | 5.0 (0.027) | <i>t</i> -BuONa | PBNA (0.01) | <i>p</i> -Dioxane (50) | 100 | 20 | 9.6 | 0.35 |
| PSTA-15 | 5.0 (0.027) | NaNH ₂ | PBNA (0.01) | DMF | 120 | 12 | 45.5 | 0.06 ^f |
| PSTA-16 | 5.0 (0.027) | NaNH ₂ | PBNA (0.01) | THF | 70 | 12 | 28.3 | 0.08 ^f |
| PSTA-17 | 5.0 (0.027) | <i>t</i> -BuOK (0.02) | PBNA (0.01) | DMF | 135 | 20 | 97.2 | 0.86 |
| PSTA-18 | 5.0 (0.027) | <i>t</i> -BuOK | PBNA | Diglyme (50) | 150 | 20 | 8.6 | 0.34 |
| PSTA-19 | 5.0 (0.027) | <i>t</i> -BuOK | PBNA | DMF (50) | 170 | 20 | 75.6 | 0.75 |

^a PBNa = phenyl- β -naphthylamine.

^b DMF = dimethylformamide.

^c DMAc = dimethylacetamide.

^d DMSO = dimethyl sulfoxide.

^e THF = tetrahydrofuran

^f Light brown polymer was obtained.

action. Gelation occurred readily when the concentration of the monomer in the polymerization mixture was higher than 60 g./100 ml.

The gelation reaction appeared to be centered at the —NH— bond and was a proton-transfer type of reaction since it was accompanied by a de-

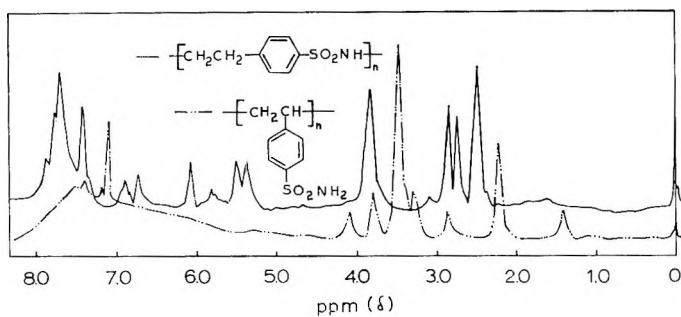


Fig. 1. Room temperature 60 Mcycle/sec. high resolution NMR spectra of 60% solution of poly-*p*-styrenesulfonamide in dimethyl-*d*₆ sulfoxide: (—) base-catalyzed polymer; (---) radical-induced polymer. Tetramethylsilane (TMS) internal references.

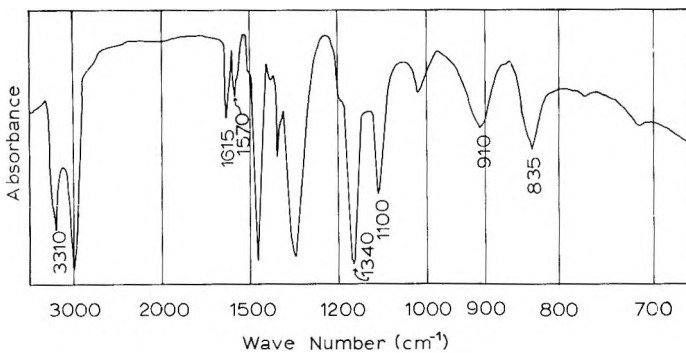


Fig. 2. Infrared spectrum of poly-*p*-styrenesulfonamide obtained by base-catalyzed polymerization (Nujol).

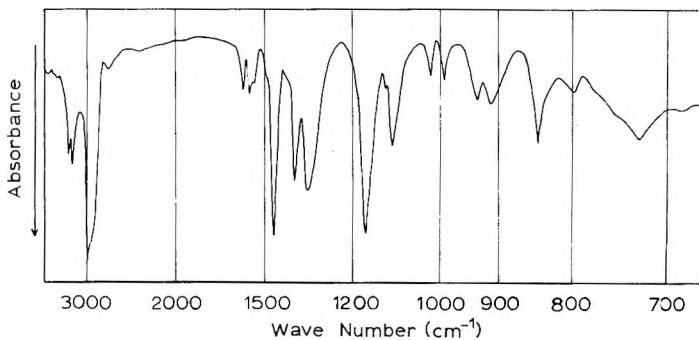


Fig. 3. Infrared spectrum of poly-*p*-styrenesulfonamide obtained by radical-induced polymerization (Nujol).

crease in the —NH— stretching band at 3310 and 1615 cm.^{-1} in the spectra of gelled polymers.

The polymer was soluble in methanol, dimethylacetamide, dimethylformamide, dimethyl sulfoxide, sulfuric acid, and 10% aqueous sodium hydroxide solution. Polymers with inherent viscosities of 1 or more gave

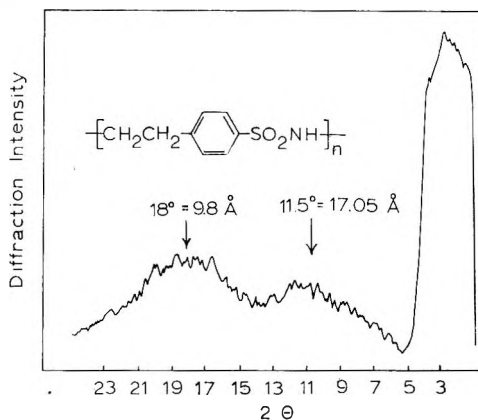


Fig. 4. X-Ray diffraction pattern of a base-catalyzed polymer of *p*-styrenesulfonamide.

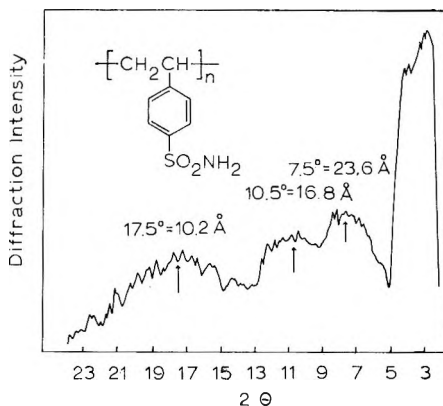


Fig. 5. X-ray diffraction pattern of a free radical-initiated polymer of *p*-styrene-sulfonamide.

clear bright films when cast from solution but the unoriented films were very brittle.

Polymers were also prepared by radical initiation to yield a product melting at $285\text{--}288^\circ\text{C.}$, soluble in dimethylformamide and having an inherent viscosity of 0.16 (0.5% solution in dimethylformamide) at 30°C. This polymer resembles the base-catalyzed polymer in many respects and differs in others. The NMR spectra of the two polymers were determined in dimethyl *d* sulfoxide (Merck, Sharp and Dohme of Canada) at 60%

concentration at room temperature in a Varian A-60 spectrometer. These are shown in Figure 1.

The infrared spectra of the two polymers taken with Nujol mulls are recorded in Figures 2 and 3. They show marked similarities in some regions but distinct differences in others. X-ray diffraction patterns were taken on the two polymers with a Phillips x-ray diffraction instrument using filtered copper $K\alpha$ radiation. These are recorded in Figures 4 and 5. These measurements do not help determine the exact ratio of the two recurring units in the polymers.

Some preliminary studies in the base-catalyzed polymerization of *p*-acrylamidobenzenesulfonamide (which had been studied before by Breslow, Hulse, and Matlack⁷), *p*-crotylamidobenzenesulfonamide, and *p*-cinnamoylamidobenzenesulfonamide have been made. The polymers are low molecular weight and have not been extensively investigated.

EXPERIMENTAL

The melting points were measured by a Bausch and Lomb polarizing microscope and are corrected.

Preparation of Monomers

***p*-Sodium Styrenesulfonate.** A sample of this salt obtained from du Pont Company assayed 90.5%; a sample obtained from Dow Chemical Company assayed 90% with approximately 10% of the *ortho* isomer present.

***p*-Styrenesulfonyl Chloride.** A 20.8-g. (0.10 mole) portion of phosphorus pentachloride was placed in a 500-ml. round-bottomed flask and 17.4 g. (0.084 mole) of pulverized *p*-sodium styrenesulfonate was added slowly with ice bath cooling. The mixture was stirred cautiously with a magnetic stirrer. After 30 min. it was heated under reflux at 50–60°C. for 2 hr. The product was cooled and poured into 100 g. of crushed ice and extracted with 100 ml. of chloroform. The organic layer was separated, washed several times with distilled water, and dried over magnesium sulfate. The chloroform solution (100 ml.) of the sulfonyl chloride was used directly for the reaction with ammonium hydroxide.

***p*-Styrenesulfonamide.** The chloroform solution (100 ml.) containing 17 g. of *p*-styrenesulfonyl chloride was added with mechanical stirring into 340 ml. of 30% ammonium hydroxide (specific gravity 0.90) under ice cooling over a period of about 30 minutes. The mixture was heated to 50°C. for 10 hr. under a reflux condenser and then cooled to room temperature. The solid was removed by filtration, washed three times with 500 ml. of distilled water and then dried under vacuum. The yield of the product was 10 g. (65%). The crude product was recrystallized four times from aqueous ethanol in the presence of traces of phenyl β -naphthylamine at 60°C. The more soluble *ortho* isomer was separated from *para* isomer by recrystallization from aqueous ethanol. The *p*-styrenesulfonamide was obtained as colorless prisms, melting at 136–137°C.

Wiley and Ketterer⁸ have prepared this amide by dehydrobromination of β -*p*-sulfonamidophenylmethylformamide with a reported melting point of pure material as 138–139°C. In order to obtain soluble base-catalyzed polymer free of gel it is important that no radical-induced polymer of the styrenesulfonamide be present in the monomer. This is prevented by recrystallizing from aqueous ethanol at temperatures below 60°C. The product was thoroughly dried at low temperature under reduced pressure.

ANAL. Calcd. for $C_8H_9O_2NS$: C, 52.30%; H, 4.95%; N, 7.65%; S, 17.40%. Found: C, 52.17%; H, 4.93%; N, 7.69%; S, 17.62%.

The infrared spectrum shows N—H stretching vibration bands at 3390, and 1549, cm^{-1} and SO_2 absorption bands at 1300 and 1160 cm^{-1} . The presence of the *p*-phenylene group was confirmed by two C—H absorption bands at 882 cm^{-1} .

The formation of the acid chloride was also carried out by treating *p*-sodium styrenesulfonate with an excess of thionyl chloride at 80–90°C. The yield of *p*-styrenesulfonyl chloride was 40–45%. The product was found to be easily hydrolyzed during the separation and purification process.

***p*-Acrylamidobenzenesulfonamide.** Acrylic acid (B. F. Goodrich Chemical Company, m.p. 13°C.) was converted to acrylyl chloride by treatment with phthaloyl chloride.¹⁰ *p*-Acrylamidobenzenesulfonamide was prepared by reaction of *p*-sulfanilamide (Eastman Organic Chemicals, m.p. 163–165°C.) with acrylyl chloride in acetone at room temperature.

Into a solution of 34.4 g. of *p*-sulfanilamide in 180 ml. of dry acetone containing 0.1 g. of phenyl β -naphthylamine was added 18 g. of acrylyl chloride in 40 ml. of acetone at room temperature and the mixture heated at 50°C. for 2 hr. The white precipitate was removed by filtration and washed with acetone and ether successively. After the product was dissolved in water, it was neutralized with 17 g. of sodium bicarbonate in 20 ml. of water. The solution was filtered and the precipitate recrystallized three times from aqueous ethanol, m.p. 219–220°C. The yield was 80%.

The reaction of *p*-sulfanilamide and acrylyl chloride in the presence of pyridine in dimethylacetamide was unsatisfactory because *p*-acrylamidobenzenesulfonamide is unstable in basic media above 50°C., even in the presence of phenyl β -naphthylamine, and is easily polymerized to form insoluble material.

The infrared spectrum (Nujolmull) shows N—H stretching bands at 3450, 3320, and 1660 cm^{-1} , and amide-carbonyl stretching bands at 1695 and 1660 cm^{-1} . The absorption bands due to an olefinic double bond fall at 1620 and 979 cm^{-1} , and S=O stretching bands of the sulfone group are at 1318 and 1175 cm^{-1} .

ANAL. Calcd. for $C_9H_{10}N_2SO_3$: C, 47.77%; H, 4.46%; N, 12.39%. Found: C, 47.94%; H, 4.71%; N, 11.69%.

***p*-Crotonylamidobenzenesulfonamide.** To 17.2 g. (0.1 mole) of *p*-sulfanilamide (Eastman Organic Chemicals, m.p. 164–65°C.) dissolved in 100 ml. of acetone (containing about 0.01 g. of phenyl β -naphthylamine) was added 10.5 g. (0.1 mole) of crotonyl chloride (Eastman Organic Chemicals) in 20 ml. of dry acetone at room temperature with mechanical stirring. The addition required 20 min. After the addition the mixture was heated at 50°C. for 3 hr. After cooling to room temperature, the resultant white precipitate was removed by filtration, washed with distilled water and hot ethanol, and recrystallized from aqueous dimethylformamide. The yield was 83%, m.p. 262–263°C.

ANAL. Calcd. for $C_{10}H_{12}O_3N_2S$: C, 49.49%; H, 5.04%; N, 11.40%; S, 13.35%. Found: C, 49.85%; H, 5.06%; N, 11.44%; S, 13.38%.

The infrared spectrum has amide carbonyl bands at 1698 and 1659 cm^{-1} . Sulfone bands were found at 1318 and 1195 cm^{-1} .

***p*-Cinnamoylamidobenzenesulfonamide.** A solution of 17.2 g. (0.1 mole) of *p*-sulfanilamide (Eastman Organic Chemicals) in 100 ml. of acetone (containing 0.01 g. of phenyl β -naphthylamine) was heated at 40°C. with mechanical stirring. Into the solution was added dropwise a solution of 16.7 g. (0.1 mole) of cinnamoyl chloride (Eastman Organic Chemicals) in 20 ml. of dry acetone during a period of 20 min. The solution was stirred at 50°C. for 3 hr. The solution was cooled to room temperature, filtered and the residue washed with distilled water.

Recrystallization from aqueous ethanol afforded crystals melting at 275–276°C. The yield was 89%.

ANAL. Calcd. for $C_{15}H_{14}O_3N_2S$: C, 59.58%; H, 4.67%; N, 9.27%; S, 10.61%. Found: C, 59.63%; H, 4.65%; N, 9.19%; S, 10.48%.

The infrared spectrum shows amide carbonyl absorption bands at 1695 and 1660 cm^{-1} . Sulfone bands appear at 1318 and 1175 cm^{-1} .

Preparation of Catalysts

Mesitylmagnesium Bromide. An ethereal solution of mesitylmagnesium bromide prepared from 2.4 g. of magnesium, 20 g. of bromomesitylene, and 25 ml. of ether was used directly as the polymerization catalyst.

Sodium *tert*-Butoxide. A 25-g. portion of sodium was added to 74.1 g. of redistilled dry *tert*-butyl alcohol and the mixture refluxed for 15 hr. The excess *tert*-butyl alcohol was distilled under reduced pressure, and the product was obtained as a white powder free from the alcohol.

Potassium *tert*-Butoxide. To 74.1 g. of redistilled dry *tert*-butyl alcohol was added 39 g. of freshly cut potassium and the mixture refluxed for 15 hr. After the reaction, the excess *tert*-butyl alcohol was distilled under reduced pressure; the product was obtained as a white powder free from the alcohol.

Sodium Amide. Sodium amide was prepared in liquid ammonia solution by the procedure of Rabjohn.¹¹ For the preparation of a tetrahydrofuran solution of sodium amide, 50 g. of tetrahydrofuran was added to 42.8 g.

of sodium amide in liquid ammonia. A dimethylformamide solution of sodium amide was prepared by adding 50 g. of dimethylformamide to 34.5 g. of sodium amide in liquid ammonia.

***n*-Butyllithium.** *n*-Butyllithium in *n*-heptane (concentration 0.07 mole-%) was obtained from Beacon Chemical Industries, Inc.

Polymerization

Base-Catalyzed Polymerization of *p*-Styrenesulfonamide. The following basic catalysts were studied for polymerization of *p*-styrenesulfonamides at 10% monomer concentration in an argon atmosphere: sodium, lithium, potassium, sodium *tert*-butoxide, potassium *tert*-butoxide, *n*-butyllithium, sodium amide, and mesitylmagnesium bromide. Solvents drastically altered the rate and products of polymerization. Therefore the effects of a number of solvents were studied. Each solvent was dried over calcium hydride and redistilled immediately before use.

The general procedure used to obtain the polymers recorded in Table I was as follows. A solution of 5.0 g. of *p*-styrenesulfonamide (0.027 mole) and 0.01 g. of phenyl β -naphthylamine in 50 ml. of solvent was prepared in a 100-ml., round-bottomed flask which was protected from the atmosphere by an argon inlet tube attached to a mercury bubbler to vent argon when the vessel was closed. The solution was stirred with a magnetic stirrer and heated at the reflux temperature in a silicone bath for 3 hr. when the catalyst was added to the solution. Polymerization started in 10–15 min. After stirring for the time noted in Table I the reaction mixture was poured into distilled water containing 10% ethanol and a trace of hydrochloric acid. The polymer was removed by filtration and dried at 70°C. for 24 hr. in vacuum. The experimental results obtained with various basic catalysts and solvents are summarized in Table I.

The polymer melt temperature was above 276°C. The infrared spectrum (Fig. 2) shows N—H stretching bands at 3310, 1615, 1570, and 1555 (sh) cm.^{-1} , and SO_2 absorption bands appear at 1340 and 1160 cm.^{-1} .

Preferred Method of Base-Catalyzed Polymerization of *p*-Styrenesulfonamide. A solution of 12.05 g. of *p*-styrenesulfonamide in 20 ml. of dimethylformamide in a 100-ml., round-bottomed flask with a reflux condenser and a calcium chloride tube was protected from the atmosphere by an argon gas flow when the vessel was closed. A 0.008-g. portion of phenyl β -naphthylamine was added and the solution stirred with a magnetic stirrer at 135°C. in a silicone bath for 1 hr. Then 0.088 g. of potassium *tert*-butoxide was quickly added to the solution. After stirring for 8 hr. the reaction mixture became very viscous. The reaction product was quenched in distilled water containing 10% ethanol and a trace of hydrochloric acid. The polymer was washed thoroughly with ethanol and water and dried at 70°C. for 24 hr. The yield of polymer was 97.5%, $\eta_{\text{inh}} = 2.26$ (in dimethylformamide at 30°C., 0.5%).

Radical-Induced Polymerization of *p*-Styrenesulfonamide. A 10.0-g. sample of *p*-styrenesulfonamide was dissolved in 100 ml. of tetrahydrofuran

TABLE II

| Expt. no. | Monomer, g. (mole) | Catalyst, g. | Inhibitor, g. | Solvent, ml. | Temp., °C. | Time, hr. | Conversion of polymer | | | Water-insoluble polymer η_{rel} 0.5% (in DMF at 30°C.) | Color |
|-----------|--------------------|-----------------------------------|--------------------------|-------------------------------|------------|-----------|----------------------------|--------------------------|------------------|---|-----------|
| | | | | | | | Water-insoluble polymer, % | Water-soluble polymer, % | Total polymer, % | | |
| PSA-1 | 5.00 (0.22) | Mesityl-magnesium bromide (0.170) | PBNA ^a (0.05) | DMAc ^b (50) | 100 | 6 | 30 | 50 | 80 | 0.05 | Yellow |
| PSA-2 | 5.00 (0.22) | <i>t</i> -BuONa (0.025) | PBNA (0.05) | DMAc (25) | 100 | 16 | 50 | 25 | 75 | 0.08 | Yellow |
| PSA-3 | 2.50 (0.11) | <i>t</i> -BuONa (0.015) | PBNA (0.02) | Pyridine (25) | 100 | 16 | 35 | 40 | 75 | 0.07 | Colorless |
| PSA-4 | 2.50 (0.11) | Na (0.02) | PBNA (0.02) | Pyridine (25) | 120 | 20 | 55 | 30 | 85 | 0.08 | Colorless |
| PSA-5 | 2.50 (0.11) | Li (0.02) | PBNA (0.02) | Pyridine (25) | 120 | 20 | 45 | 30 | 75 | 0.11 | Colorless |
| PSA-6 | 2.50 (0.11) | Na (0.02) | PBNA (0.02) | DMF ^c (25) | 120 | 20 | 30 | 45 | 75 | 0.06 | Colorless |
| PSA-7 | 2.50 (0.11) | Na (0.02) | PBNA (0.02) | Aniline (25) | 120 | 20 | Trace | 75 | ca. 75 | 0.14 | Yellow |
| PSA-8 | 2.50 (0.11) | Na (0.02) | PBNA (0.02) | DMF/chloro-benzene (1:1) (25) | 120 | 20 | Trace | 60 | ca. 60 | 0.09 | Colorless |

| | | | | | | | | | | | |
|--------|----------------|--|----------------|---------------------------|-----|----|-------|----|--------|------|-----------|
| PSA-9 | 2.50 (0.11) | Na ^a (0.02) | PBNA (0.02) | DMAc (25) | 120 | 20 | 55 | 20 | 75 | 0.15 | Colorless |
| PSA-11 | 2.50 (0.11) | Na ^a (0.02) | PBNA (0.02) | DMF (25) | 50 | 16 | Trace | 35 | ca. 35 | 0.01 | Yellow |
| PSA-12 | 2.50 (0.11) | Na ^a (0.02) | PBNA (0.02) | DMF (25) | 75 | 16 | 15 | 20 | 35 | 0.04 | Yellow |
| PSA-13 | 2.50 (0.11) | Na ^a (0.02) | PBNA (0.02) | DMF (25) | 100 | 16 | 35 | 18 | 53 | 0.06 | Colorless |
| PSA-14 | 2.50 (0.11) | Na ^a (0.02) | PBNA (0.02) | DMF (25) | 115 | 16 | 56 | 6 | 62 | 0.16 | Colorless |
| PSA-15 | 2.50 (0.11) | Na ^a (0.02) | PBNA (0.02) | DMF (25) | 140 | 16 | 45 | 11 | 56 | 0.21 | Colorless |
| PSA-16 | 2.50 (0.11) | <i>t</i> -BuONa ^a (0.02) | PBNA (0.02) | DMSO ^d (25) | 115 | 20 | 65 | 21 | 86 | 0.05 | Colorless |
| PSA-17 | 2.50 (0.11) | <i>t</i> -BuONa ^a (0.02) | PBNA (0.02) | DMAc (25) | 115 | 20 | 60 | 25 | 85 | 0.18 | Colorless |

^a PBNA = phenyl β -naphthylamine.

^b DMac = dimethylacetamide.

^c DMF = dimethylformamide.

^d DMSO = dimethyl sulfoxide.

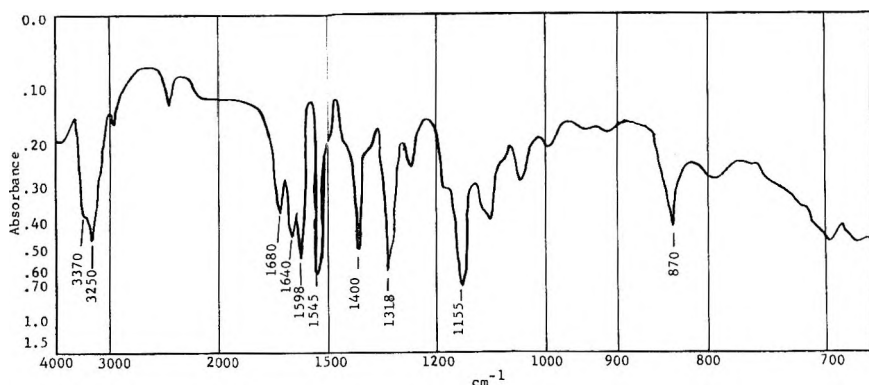


Fig. 6. Infrared spectrum of poly-*p*-acrylamidobenzenesulfonamide obtained by base-catalyzed polymerization (KBr disk).

in a nitrogen atmosphere and 0.50 g. of α, α' -azobisisobutyronitrile was added. The solution was heated at 100°C. for 24 hr. with magnetic stirring. The resulting polymer was collected on a filter and washed several times with acetone. The conversion to polymer was 78%, m.p. 285–288°C. The inherent viscosity measured in dimethylformamide (0.5% concentration) at 30°C. was 0.16. The infrared spectrum is shown in Figure 3.

Polymerization of *p*-Acrylamidobenzenesulfonamide. The polymerization of carefully purified *p*-acrylamidobenzenesulfonamide with basic catalysts such as potassium, lithium, or sodium *tert*-butoxide in dimethylacetamide, pyridine, dimethylformamide, aniline, or chlorobenzene–dimethylformamide (1:1) afforded white polymers with inherent viscosities of 0.03–0.15 (0.5% in dimethylacetamide at 30°C.). The polymers had melting points above 350°C. Under similar conditions in the presence of mesitylmagnesium bromide a lower molecular weight polymer with an inherent viscosity of 0.05 was obtained (0.5% in dimethylacetamide at 30°C.).

In a typical polymerization, a solution of 2.50 g. (0.11 mole) of the sulfonamide in 25 ml. dimethylacetamide was prepared in a 100-ml., round-bottomed flask which was protected from the atmosphere by a nitrogen inlet tube attached to a mercury bubbler to vent nitrogen when the vessel was closed. The solution was heated to 120°C. in a silicone bath with a magnetic stirrer and 0.08 g. (0.03 mole/mole) of sodium was added. Polymerization was completed in 16–20 hr. The reaction mixture was poured in 20 ml. of water, the polymer collected by filtration and washed with water several times in a blender. The polymer, dried at 70°C. for 24 hr. in a vacuum, weighed 1.5–1.8 g. (60–75%), had a polymer melt temperature above 350°C., and an inherent viscosity of 0.15 in dimethylformamide (0.5% concentration at 30°C.) (Expt. PSA-9, Table II).

The experimental results under various polymerization conditions are summarized in Table II.

Some of the polymers recorded in Table II had inherent viscosities slightly higher than those reported previously.⁷

The infrared spectrum of the polymer (Fig. 6) shows a typical amide carbonyl band at 1680 cm.^{-1} , NH bands at 1640 and 1599 cm.^{-1} , and SO_2 bands fall at 1318 and 1155 cm.^{-1} .

Base-Catalyzed Polymerization of *p*-Crotonylamidobenzenesulfonamide and *p*-Cinnamoylbenzenesulfonamide. The polymerizations of these sulfonamides were carried out under the following conditions. To 50 ml. of freshly distilled solvent was added 5 g. of monomer. Then 0.04 mole/ratio of catalyst and 0.02 g. of phenyl β -naphthylamine were added to the reaction flask under flushing argon at 100 – 120°C . After 20 hr., the product was filtered, washed with ethanol and dried.

In dimethylformamide at 120°C . *p*-crotonylamidobenzenesulfonamide gave 7% conversion to a polymer with an inherent viscosity of 0.03 (0.5% concentration in dimethylformamide at 30°C .) which melted at 263 – 266°C . In pyridine at 100°C . the conversion was 65.5%, the inherent viscosity was 0.14, and the melting point 262 – 264°C . In dimethylformamide at 120°C ., *p*-cinnamoylamidobenzenesulfonamide gave 90% conversion and the polymer had an inherent viscosity of only 0.02 and melted at 266 – 268°C . In pyridine at 100°C . the conversion was 71.2%, inherent viscosity 0.13, and m.p. 265 – 267°C .

We are indebted to Professor M. L. Corrin for x-ray measurements and to Dr. James H. Griffith for the nuclear magnetic resonance measurements. We also wish to thank Dr. W. K. Wilkinson of du Pont Company and Dr. G. D. Jones of Dow Chemical Company for the generous gifts of samples of sodium styrenesulfonate. One of us (N. Y.) gratefully acknowledges the permission of Toyo Rayon Company, Ltd., for postdoctoral study in the United States.

The financial support of the Textile Fibers Department of E. I. du Pont de Nemours and Company is gratefully acknowledged.

References

1. Berchet, G. J., U. S. Pat. 2,321,891 (1943).
2. Murahashi, S., and T. Takizawa, *Kogyo Kagaku Zasshi*, **47**, 794 (1944).
3. Helferich, B., and A. Giltges, Ger. Application H6599 (1950).
4. Raghavar, M., B. H. Iyer, and P. C. Guha, *J. Indiana Inst. Sci.*, **34**, 87 (1952).
5. Sundet, S. A., W. A. Murphey, and S. P. Speck, *J. Polymer Sci.*, **40**, 389 (1959).
6. Jones, W. D., and S. B. McFarlane, U. S. Pat. 2,667,469 (1954).
7. Breslow, D. S., G. E. Hulse, and A. S. Matlack, *J. Am. Chem. Soc.*, **79**, 3760 (1957); A. S. Matlack, U. S. Pat. 2,672,980 (1954); D. S. Breslow, Brit. Pat. 736,461 (1955); U. S. Pat. 2,749,331 (1956).
8. Wiley, R. H., and C. C. Ketterer, *J. Am. Chem. Soc.*, **75**, 4518 (1953).
9. Shepherd, R. C., *J. Org. Chem.*, **12**, 275 (1947).
10. Mouvean, *Ann. Chim.* [7], **2**, 161; *Bull. Soc. Chim.* [3], **9**, 424 (1893); E. P. Kohler, *Am. Chem. J.*, **42**, 380.
11. Rabjohn, N., *Organic Syntheses*, Coll. Vol. IV, Wiley, New York, 1963, p. 763.

Résumé

La polymérisation, catalysée par les bases, du *p*-styrènesulfonamide, a donné un produit possédant des unités périodiques mélangées, certaines produites par polymérisation vinylique initiée anioniquement et certaines par polymérisation par transfert de proton. Les produits sont formoux mais fournissent des films cassants. Certains résultats préliminaires ont été obtenus pour la polymérisation du *p*-acrylamidobenzènesulfonamide

et de ses dérivés crotonyle et cinnamoyle. On décrit les méthodes de synthèse de ces monomères.

Zusammenfassung

Die basenkatalysierte Polymerisation von *p*-Styrolsulfonamid lieferte ein Produkt mit einer Mischung von Bausteinen, bei denen die einen durch eine anionisch gestartete Vinylpolymerisation und die anderen durch eine Protonenübertragungsreaktion gebildet wurden. Die Produkte besitzen einen hohen Erweichungspunkt, liefern aber spröde Filme. Für die Polymerisation vom *p*-Acrylamidobenzolsulfonamid und die verwandten Crotonyl- und Cinnamoylderivate wurden einige vorläufige Ergebnisse erhalten. Synthetische Methoden für die Gewinnung der Monomeren werden beschrieben.

Received January 6, 1965

(Prod. No. 4604A)

Alkyl-Free Cobalt Catalyst for the Stereospecific Polymerization of Butadiene*

J. G. BALAS, H. E. DE LA MARE, and D. O. SCHISLER,
*Emeryville Research Center, Shell Development Company, Emeryville,
California*

Synopsis

The stereoselective polymerization of butadiene to a predominantly *cis* polymer has been carried out with complex cobaltous halide catalysts, e.g., $\text{CoCl}_2 \cdot \text{AlCl}_3$. The unique features of such polymerizations are the homogeneous nature of the catalysis and the activity of such catalysts in the absence of any added reducing agent. The composition and spectroscopy of some of these catalyst solutions have been studied and possible structures proposed. The present status of the work does not permit a conclusive report on the mechanism of this polymerization, but some results of termination with tritiated methanol (CH_3OH^3) are described. Unfortunately, these experiments do not define the nature of the propagating end of the polymer chain.

INTRODUCTION

Several reports describing the polymerization of butadiene to a high-*cis* polymer by soluble cobalt salts and alkylaluminum catalysts prompted us to report the results of our work first disclosed in the patent literature several years ago.¹

Reported polymerizations of diolefins by transition metal salts and organometallic reducing agents are legion. With specific regard to solution polymerization of butadiene, it has been shown that a large number of cobalt salts are equally effective; it is only necessary that these salts be treated with an appropriate alkylaluminum in large molar excess.²⁻⁴ Useful as they are for the preparation of high-*cis* polybutadiene, these systems may be unduly complicated because of the presence of large quantities of apparently unnecessary catalyst components.

The simple catalyst systems which constitute the basis for this report are prepared by dissolving cobaltous halide-aluminum halide mixtures in benzene or cyclohexane. We have unequivocally demonstrated that such catalysts will polymerize butadiene to a high-*cis*-1,4 product in the absence of any added reducing agent. While this manuscript was in preparation, papers by Scott et al.⁵ and O'Reilly et al.⁶ appeared in this journal describing the study of a similar system. However, these workers reported: (1)

* Paper presented at Northern California American Chemical Society Meeting-in-Miniature, December 1963.

thiophene was a necessary third component of the catalyst system, and polymerizations carried out in the absence of thiophene yielded low molecular weight polymers whose unsaturation was far below theoretical; (2) even in the presence of thiophene, polymerization failed in the absence of an aromatic solvent. Neither one of these restrictions actually applies, and hence, the rather complicated mechanism proposed to account for the effect of thiophene is, in general, unnecessary.

We have not attempted to repeat Scott's work with thiophene. However, we believe the effect of thiophene can most easily be explained by assuming it simply inhibits cationic polymerization. Overberger, as cited by Scott,⁵ has observed an 8-fold reduction in polymerization rate of styrene catalyzed by SnCl_4 upon the addition of only 0.17 mole-% of thiophene. Since Scott et al. used ≈ 3.5 mole-% based on butadiene, the retardation of cationic polymerization of butadiene should be considerable here also. Furthermore, Scott et al. actually suggest an acid-scavenging role for the metallic aluminum used to treat catalyst solutions subsequently employed for the preparation of *cis*-polybutadiene in thiophene-free systems. Little attention seems to be paid to this important fact in the subsequent discussion of a mechanism.

We have found that great care is necessary, particularly in experimental manipulation. In our preliminary work low molecular weight polymers of low unsaturation were frequently obtained. More rigorous techniques however, resulted in the work we report here.

COMPOSITION AND STRUCTURE OF THE CATALYST

The polymerization catalyst used for the major part of this investigation was a homogeneous solution of $\text{CoCl}_2 \cdot \text{AlCl}_3$ in cyclohexane or benzene. However, catalyst solutions in cyclohexane were also prepared and investigated using $\text{CoCl}_2 \cdot \text{AlBr}_3$, $\text{CoBr}_2 \cdot \text{AlBr}_3$, and $\text{CoI}_2 \cdot \text{AlI}_3$. The composition of the catalyst solution can be influenced by the relative amounts and purity of the respective components used in the preparation; therefore, reproducibility of catalyst composition is not precisely achieved.

Data representative of catalyst preparations used in this study are summarized in Table I. For comparative purposes, the solubility of anhydrous aluminum chloride and bromide in cyclohexane are recorded in the footnotes to Table I. As seen in Table I, soluble chloride catalyst containing as much as 420 ppm of Co in cyclohexane was made; however, this solution was diluted to 220 ppm Co where it could be stored for several weeks without significant decrease in Co concentration. In benzene it is possible to obtain much higher concentrations of Co (800-2000 ppm). Gradual changes in cobalt and aluminum concentrations occurred during long storage, and therefore periodic analyses were performed to determine cobalt or aluminum content accurately. It should be noted that anion exchange occurred during the preparation of a catalyst from cobaltous chloride and aluminum bromide, and the resulting soluble catalyst contained principally chloride anions (Prep. 93, Table I).

TABLE I
 Cobaltous Halide-Aluminum Halide Catalysts

| Prep. | Solvent | Catalyst | Co | | Al ^a | | Al/Co mole ratio |
|-------|------------------|--------------------------------------|------|----------|-----------------|----------|------------------------|
| | | | ppm | mmole/l. | ppm | mmole/l. | |
| 107 | Cyclo- hexane | CoCl ₂ ·AlCl ₃ | 420 | 5.55 | 1860 | 53.8 | 9.7 |
| 107-1 | | CoCl ₂ ·AlCl ₃ | 212 | 2.80 | — | — | ^b |
| 107-2 | | CoCl ₂ ·AlCl ₃ | 190 | 2.51 | 694 | 20.3 | 8.0 |
| 107-3 | | CoCl ₂ ·AlCl ₃ | 135 | 1.79 | 459 | 13.4 | 7.5 ^c |
| 93 | | CoCl ₂ ·AlBr ₃ | 79 | 1.05 | 471 | 13.6 | 13.1 ^d |
| 106 | | CoBr ₂ ·AlBr ₃ | 69 | 0.91 | 2320 | 66.8 | 73 |
| 151C | | CoI ₂ ·AlI ₃ | 176 | 2.33 | 2565 | 74.1 | 32 |
| 200B | | CoCl ₂ ·AlCl ₃ | 90 | 1.19 | 511 | 14.8 | 12.5 |
| 1001B | Benzene | CoCl ₂ ·AlCl ₃ | 883 | 13.2 | 1000 | 32.6 | 2.5 |
| 166 | | CoCl ₂ ·AlCl ₃ | 2000 | 30.0 | 2200 | 71.6 | 2.4 |
| 196A | | CoBr ₂ ·AlBr ₃ | 69 | 1.01 | 850 | 27.7 | 27.3 |

^a Solubility of aluminum chloride in cyclohexane (our determination): Al = 12.7 mmole/l. (439 ppm); Cl = 30.8 mmole/l.; Cl/Al ~2.5. Solubility of aluminum bromide in cyclohexane (26.4°C.) = 45.1 g. AlBr₃/100 g. sat'd. soln. = 0.169 mole AlBr₃/100 g. sat'd. soln. ≈ 1.7 mole/l.⁷

^b Estimated to be ≥8.0 on the basis of succeeding analyses on stocks 107-2 and 107-3. Stocks 107-1, 107-2, and 107-3 were made by dilution of 107.

^c Original composition ≈ that of 107-1. This analysis was made after 7 months storage.

^d Chlorine/bromine ratio = 8.2.

Cobaltous chloride is virtually insoluble in benzene. A recent and reliable determination places the solubility in the region of about 1 part of cobalt per billion parts of benzene. The mere fact that one can obtain benzene solutions as high as $3 \times 10^{-2}M$ in cobalt (2000 ppm) with the aid of AlCl₃ indicates a profound interaction between these components. Repeated analyses of chloride catalyst solutions indicate approximately 2-4 moles AlCl₃/mole of CoCl₂ in benzene solution and 7-12 moles/mole in cyclohexane solution. The observed ratio in benzene or cyclohexane is roughly independent of the starting amounts provided that sufficient quantities of both reactants are present.

Preliminary powder x-ray diagrams of a solid material made by melting together anhydrous AlCl₃ and CoCl₂ demonstrated the formation of a new compound.* The melt-formed solid dissolves in cold benzene with the immediate formation of a green solution, unlike a mixture of AlCl₃ and CoCl₂ which requires some time for color formation unless heated. Deep purple crystals isolated from an actual catalyst preparation also formed a green solution immediately upon mixing with benzene. However, the most striking indication of a new compound formation was the observation that the blue melt-formed solid could be distilled at 200°C. in an atmosphere of aluminum chloride. This temperature is far below the boiling point (or melting point) of CoCl₂. It is now clear that the pure solid (blue) is

* We are indebted to our colleague, A. E. Smith, for the x-ray work.

$\text{Co}(\text{AlCl}_4)_2$, and the structure has been conclusively established as one consisting of infinite chains of $\text{Co}(\text{AlCl}_4)_2$ containing octahedrally-coordinated cobalt.⁸ Identical blue crystalline solids have been isolated from benzene solution, although on occasion the solid crystallizes in a purple form. It is possible that two crystalline forms exist, one containing benzene of crystallization; however, it is also possible that the crystals become purple because of contamination. At present this question remains unresolved.

Information concerning the geometry of the catalyst complex in solution was obtained by examination of the electronic absorption spectra of the anhydrous catalyst solutions in cells protected from the atmosphere. The benzene solution of $\text{CoCl}_2 \cdot \text{AlCl}_3$ is a deep green and is characterized by two bands in the long wavelength visible and near ultraviolet regions, respectively (Table II). The spectrum of the $\text{CoBr}_2 \cdot \text{AlBr}_3$ is remarkably similar to the chloride catalyst and both complexes appear to have substantially the same structure in benzene. The bands at $\sim 3500 \text{ \AA}$. are believed to be due to charge transfer absorption, indicating that one or more benzene molecules serve as ligands to each cobalt atom. The long-wavelength absorption bands arise from $d-d$ transitions. The relatively high absorptivities of these bands suggested an unsymmetrical arrangement of ligands

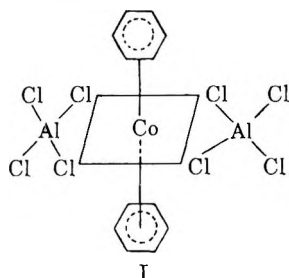


TABLE II
Spectroscopy in Benzene

| Catalyst | λ_{max} , A. | a_{max} , l./mole-cm. |
|-------------------------------------|--------------------------------|-----------------------------------|
| $\text{CoCl}_2 \cdot \text{AlCl}_3$ | 6380 | 136 |
| | 3500 | 1470 |
| $\text{CoBr}_2 \cdot \text{AlBr}_3$ | 6800 | 178 |
| | 3600 | 1840 |

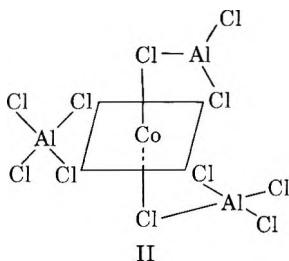
TABLE III
Spectroscopy in Cyclohexane

| Catalyst | Molar ratio Al/Co | λ_{max} , A. | a_{max} , l./mole-cm. |
|-------------------------------------|-------------------------|--------------------------------|-----------------------------------|
| $\text{CoCl}_2 \cdot \text{AlCl}_3$ | 8 | 6000 | 18.6 |
| $\text{CoBr}_2 \cdot \text{AlBr}_3$ | 73 | ~ 6250 | ~ 40 |

since complexes possessing an inversion center usually have low absorptivities, e.g., $\text{Co}(\text{H}_2\text{O})_6^{++}$ has $a = 10$ l./mole-cm. The most probable structure for the chloride and bromide complexes in benzene is that shown in structure I above.

The recent crystal structure analysis⁹ of the cuprous ion-benzene complex ($\text{C}_6\text{H}_6 \cdot \text{CuAlCl}_4$) reveals that a benzene molecule occupies one of four, nearly tetrahedral coordination sites around the cuprous ion. Similarly, it is reasonable to expect that the $\text{CoCl}_2 \cdot 2\text{AlCl}_3$ complex, with a square planar configuration of chloride ligands, will accept benzene or other unsaturated molecule(s) to complete the approximately octahedral coordination sphere of the cobaltous ion. This type of interaction is necessary to explain the differences in the absorption spectra of solutions of the complex in aromatic solvents as contrasted to the spectrum of the solid and its solution in cyclohexane described below.

In contrast, the cyclohexane solutions (Table III) show no charge transfer absorption band at 3500 Å., and the chloride catalyst gives a blue solution in cyclohexane. Spectroscopically, the chloride and bromide catalysts are very similar in cyclohexane, and apparently have essentially the same structural features in solution despite the large excess of AlBr_3 in the bromide catalyst. At present, the most acceptable structure for these catalysts in cyclohexane is that of an octahedral distribution of halide ligands shown as II for the chloride complex.



It is significant that the cyclohexane solution has the same blue color and the same visible ($d \rightarrow d$ transition) absorption band as the solid $\text{CoCl}_2 \cdot 2\text{AlCl}_3$ wherein the environment of the cobalt atom is known to be six chlorine atoms in a nearly perfect octahedral arrangement.^{5,6,8} However, in benzene solution, the color is green, the cobalt $d \rightarrow d$ transition band is at shorter wavelength and more intense, and a charge transfer absorption band is observed, the intensity of which is proportional to cobalt concentration. Moreover, when benzene is added to a cyclohexane solution, the color and absorption spectrum change to those characteristic of benzene solutions. These facts indicate that in cyclohexane solution the cobalt atom has only chloride ligands, and that benzene can displace a molecule of AlCl_3 as a ligand. Butadiene, when added to either solution, can be expected to displace either AlCl_3 or benzene as a ligand to cobalt.

Surprisingly, spectroscopic investigation of the $\text{CoI}_2 \cdot \text{AlI}_3$ catalyst ($\text{Al/Co} \sim 32$) showed the same principal band (7730 Å., $a \sim 990$ l./mole-cm.) in either benzene or cyclohexane. The strong absorptivity of the iodide

complex, the shift of the principal absorband (a *d-d* transition) to 7730 Å. and the lack of any charge transfer band in benzene indicate that the iodide catalyst is a different species. The spectroscopic data suggest a tetrahedral distribution of iodide ligands about cobalt, and an absence of any intimate association of solvent with the complex. The spectrum of $(\text{CoI}_4)^-$ in nitromethane solution has been reported by Gill and Nyholm¹⁰ to have its principal *d-d* absorption band centered at ~ 7500 Å. with a peak absorptivity of 1126 l./mole-cm. The similar spectrum of the iodide catalyst in benzene solution is evidence for the presence of tetrahedral $(\text{CoI}_4)^-$, probably as the undissociated complex $\text{Co}(\text{AlI}_4)_2$.

POLYMERIZATION STUDIES

Butadiene

Repeated experiments have demonstrated that $\text{CoCl}_2 \cdot \text{AlCl}_3$ complexes free of alkylaluminum or other added reducing agents are capable of polymerizing butadiene to a relatively high *cis*-1,4 polymer in either benzene or cyclohexane. These results are in direct contrast to those of Scott et al., who did not describe the extent of their attempts in, e.g., cyclohexane, but state that successful polymerization would not take place except in benzene containing thiophene. Our cyclohexane was known to be free of benzene and both solvents were free of thiophene. Although either solvent is satisfactory, cyclohexane proves to be somewhat superior as far as *cis* selectivity is concerned (Table IV). Since this difference does not persist in the coagulated polymer, it appears that polymerization in benzene leads to a small fraction of lower molecular weight polymer of very low *cis* content.

TABLE IV
Effect of Solvent on Polymerizations with $\text{CoCl}_2 \cdot \text{AlCl}_3$

| Polymerization solvent ^a | [η] (25°C., toluene), dl./g. | Whole polymer structure, % ^b | | | Isopropanol coagulated polymer, % | | |
|-------------------------------------|--|---|-------------------|-----|-----------------------------------|-------------------|-----|
| | | <i>cis</i> -1,4 | <i>trans</i> -1,4 | 1,2 | <i>cis</i> -1,4 | <i>trans</i> -1,4 | 1,2 |
| Cyclohexane | 3.6 | 95.5 | 2.5 | 2.0 | — | — | — |
| Benzene | 6.8 | 92.3 | 6.3 | 1.4 | — | — | — |
| Cyclohexane | 4.5 | 96.2 | 2.6 | 1.2 | 97.3 | 1.6 | 1.1 |
| Benzene | 6.6 | 92.9 | 5.8 | 1.3 | 97.7 | 1.3 | 1.0 |

^a Solvent, 50 cc., saturated with Phillips Special Purity butadiene. Catalyst: 4 ppm Co as $\text{CoCl}_2 \cdot \text{AlCl}_3$ in cyclohexane. Polymerization time ~ 15 min. to limiting viscosity, $T \sim 25^\circ\text{C}$.

^b Infrared analyses were made on films cast directly from reaction mixture.

In general, the chloride system gave $\sim 95\%$ *cis*-1,4 polybutadiene consistently with essentially theoretical unsaturation ($\geq 96\%$). The system is very sensitive to contamination and reproducibility in rate was difficult to achieve.

Polymerizations in cyclohexane were carried out conveniently at $\sim 1M$ in butadiene with catalyst levels ranging from 5 to 15 ppm of cobalt. As shown in Table V, there is only slight variation of *cis* content in this catalyst range. Periodically we have had catalyst stocks which gave

TABLE V
Polymerization of Butadiene (BD) in Cyclohexane.
Effect of Initial Cobalt Concentration ($\text{CoCl}_2 \cdot \text{AlCl}_3$)^a

| Expt. ^b | [Co], ppm | [η], dl./g. ^c | Conver- sion, % | Structure, % ^d | | |
|--------------------|--------------|------------------------------------|--------------------|---------------------------|--------------|-----|
| | | | | <i>cis</i> | <i>trans</i> | 1,2 |
| 113-C | 5 | 1.32 | 5 | 94.6 | 3.6 | 1.8 |
| 114-A ^e | 10 | 1.31 | 27 ^e | 92.3 | 4.3 | 3.4 |
| 114-B | 15 | 2.85 | 45 | 96 | 2.2 | 1.6 |

^a $[\text{BD}]_0 = 8 \text{ wt.-%}$; $T = 25^\circ\text{C}$.; $t = 33 \text{ min}$.

^b Butadiene was added to 50 cc. of cyclohexane to give $[\text{BD}]_0 = 8 \text{ wt.-%}$ ($\sim 1M$), and stock catalyst was then added to give stated [Co]. With butadiene at saturation level ($\sim 17 \text{ wt.-%}$), a limiting viscosity with the same catalyst stock was attained in 9–13 min. at [Co] = 5 ppm; 17% conversion; [η] of polymer = 3.42 dl./g.

^c Intrinsic viscosities (25°C . in toluene) were determined on isopropanol-coagulated polymers.

^d Structures were determined on the isopropanol-coagulated polymers dissolved in CS_2 ; % *cis*-1,4 was assigned by difference after determining the 1,2 and *trans* contents (see Experimental).

^e Since the viscosity was not limiting here, this polymerization was allowed to proceed overnight ($t \sim 16.5 \text{ hr.}$), but apparently the polymerization ceased after 27% conversion. Structure may be somewhat poorer because of the long reaction time.

TABLE VI
Polymerization of Butadiene in an Alkyl-Free System (Cyclohexane)^a

| Time, min. | [Butadiene], moles/l. | |
|---------------|-----------------------|-----------------|
| | Analytical run | Control run |
| 0 | 1.04 | 1.10 |
| 15 | 1.00 (Sample 1) | — |
| 30 | 0.98 | — |
| 60 | 0.98 | — |
| 160 | — | 0.77 (Sample 1) |
| 190 | — | 0.76 |
| 250 | — | 0.75 |

^a $[\text{Co}]_0 = 0.066 \text{ mmole/l.}$ ($\sim 5 \text{ ppm}$); $T = 25.0^\circ\text{C}$.

cis contents in the 80–90% range. This may reflect deterioration of the catalyst or adventitious introduction of impurities in the system. (Originally, considerable effort was expended to achieve the high-*cis* contents herein reported.) The marked sensitivity of the system to contamination is seen in expt. 114-A, where the polymerization ceased after $\sim 27\%$ conversion.

Most attempts to remove samples by careful hypodermic techniques terminated the polymerization. Typical of the sensitivity to sampling of this system are the data shown in Table VI.

Any withdrawal of sample by hypodermic syringe was sufficient to terminate the polymerization; therefore, further attempts to obtain quantitative rate data were not made. In addition to being sensitive to sampling, the chloride system was also quite prone to undergo gelation. However, careful techniques permitted the isolation of essentially gel-free polymers in most experiments. The factors responsible for gelation in this system are not clearly understood. Since the catalyst contains aluminum chloride, gelation may occur upon termination of the polymerization with methanol or isopropanol (potential Friedel-Crafts cocatalysts).

A typical alkyl-free polymerization with a bromide catalyst resulted in a polybutadiene ($\sim 30\%$ conversion in 74 min.; $[\text{BD}]_0 \sim$ saturated in cyclohexane; $25^\circ\text{C}.$) having a relatively high *cis*-1,4 content (*cis*, 80%; *trans*, 12%; 1,2, 8%). However, polymerizations with the bromide catalysts usually produced some gel. The increased gel content may be attributed to the high aluminum bromide content of the catalyst stock used ($\text{Al/Co} = 35/1$ with $[\text{Co}]_0 \sim 5$ ppm). Catalysts at lower aluminum/cobalt ratios have not yet been examined in an alkyl-free system. The presence of the larger bromide anion appears to lead to higher *trans* and 1,2 contents than does the chloride anion, but the extent to which this difference can be traced solely to the anion is not known.

Other Monomers

The $\text{CoCl}_2 \cdot \text{AlCl}_3$ catalyst was examined for the polymerization of 2,3-dimethylbutadiene and isoprene under the same conditions described above for butadiene. In both cases, the selectivity was poorer and the rate of polymerization slower than with butadiene.

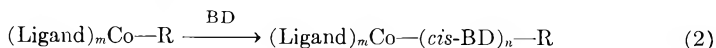
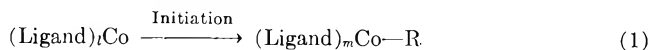
In the case of dimethylbutadiene, x-ray examination* of the annealed solid polymer from some experiments indicates that the product is largely a *cis-trans* mixture with the *trans*-1,4 structure predominating. However, other experiments (different catalyst stocks) indicate a nearly 50-50 distribution of *cis-trans* microstructure. In all cases, the 1,2 structure and cyclized segments appear to be minor contaminants. The cyclic structure is confirmed by the less than theoretical unsaturation found when the polymer is titrated with perbenzoic acid. Unpublished NMR work from this laboratory has also indicated the presence of cyclized structures.

In the case of polyisoprene a mixed microstructure was obtained, and this undoubtedly varies somewhat with conditions. A representative microstructure was estimated by NMR analysis¹² to be 67% *cis*, 23% *trans* + 3,4, and 10% 1,2.

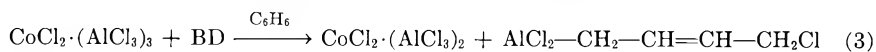
* We are indebted to T. C. Yao for the x-ray work. We used the data of Yen.¹¹

MECHANISM

The stereospecific polymerization of butadiene may be rationalized by assuming a controlled propagation within the cobalt complex in the following greatly simplified manner:



In an "alkyl" system the Co—R bond is probably established by the added alkylaluminum or other reducing agent; however, this cannot be the case here. We have made several attempts using equimolar ratios of butadiene and $\text{CoCl}_2\text{-AlCl}_3$ in benzene solution to demonstrate the possible *in situ* formation of an alkylaluminum by a reaction such as (3).



Our failure to identify (by gas-liquid chromatography) crotyl chloride as one of the reaction products following hydrolysis is unfortunate but does not rule out this or similar modes of initiation. It is most likely that the actual course of initiation, whatever it may be, was obscured by the great Friedel-Crafts activity of the catalyst under these conditions of high concentration.

In any event, it is obvious from the results of the present work that thiophene is not a necessary catalyst component. Furthermore, unlike Scott et al., we find no compelling reasons to postulate polymer growth off aluminum. Our data are most consistent with the coordination of butadiene to cobalt in the active complex, and chain growth off cobalt in subsequent propagation steps. A forthcoming publication¹³ from this laboratory will describe the photochemical polymerization of butadiene to a high-*cis* polymer utilizing solid cobaltous chloride as the only catalyst. A previous publication from this laboratory¹⁴ has also reported the polymerization of butadiene to a high-*cis* polymer by use of only CoSiF_6 in water.* Although these latter systems differ markedly from the one under discussion here, they present compelling arguments for maintaining cobalt as the primary site for polymerization.

In order to determine the second facet of the mechanism, i.e., the nature of the chain growth (anionic, cationic, etc.) on cobalt, several polymerizations were carried out and terminated with tritiated methanol. Independently, several workers¹⁶⁻¹⁸ have recently reported on such isotopic tracer experiments in cobalt systems containing alkylaluminums as cocatalysts. In summary, Childers¹⁶ has proposed a coordinated cationic growth, Cooper¹⁷ a coordinated anionic growth, and Natta et al.¹⁸ have supported Cooper with important reservations. The reservations of Natta are (a) that preformed polymer incorporates tritium in the presence of the

* Other workers¹⁵ have contradicted this observation, but we think future publications will fully support the finding that this system is productive of high-*cis*-polybutadiene.

TABLE VII
 Tritium Termination of Butadiene Polymers^a

| Run | Type ^b | Conversion, ~% | Time, min. | Solvent | Structure ^c | | Activity of duplicates, dpm/g. ^d | \bar{M}_n (osmotic) | M_H^e (one H ³ /chain) ^e |
|-----------------------------|-----------------------------------|-------------------|-----------------|-------------------------------|------------------------|--------------|--|--------------------------|---|
| | | | | | <i>cis</i> | <i>trans</i> | | | |
| Propagating Polymerizations | | | | | | | | | |
| 181A ^f | | 10 | 1 ^g | C ₆ H ₆ | 92.1 | 5.7 | 26,845 25,292 | 40,800 | 470,750 |
| 182A | | 9 | 3 ^g | C ₆ H ₆ | 94.2 | 3.9 | 16,470 17,209 | 65,700 | 723,650 |
| 182B | | 9 | 4 ^g | Cyclohexane | 92.2 | 4.8 | 83,199 80,130 | 60,300 | 149,200 |
| Preformed Polymers | | | | | | | | | |
| 181D | Soluble | | 30 ^h | C ₆ H ₆ | 96.6 | 1.8 | 23,278 24,581 | 94,000 | 509,350 |
| 181D-2 | (Second purification of 181-D) | | | | — | — | 23,731 23,210 | — | — |
| 181D | Gel | | 30 ^h | C ₆ H ₆ | — | — | 55,634 60,606 | — | — |

| | | | | | | | | | |
|------|---------------------------------|-----------------|-------------------------------|------|-----|-----|-------------------------|--------|-----------|
| 181E | Soluble + gel | 31 ^b | Cyclohexane | 96.3 | 1.7 | 2.0 | 184,896 185,849 | — | 65,705 |
| 176 | Control Soluble ^c | 0 ^b | C ₆ H ₆ | 25 | 34 | 40 | 1,785 2,018 2,043 | 76,500 | 6,282,333 |

^a Conditions: $T = 25^\circ\text{C}$.; $[\text{Co}] = 0.1$ mmole/l.; $[\text{BD}] = \text{saturated solution}$. All reactions terminated with CH_3OH^3 . All mixtures (propagating and preformed) were treated with 5 ml. of 20 vol.-% CH_3OH^3 (1.218×10^{10} dpm/mole) in benzene for 110 ± 25 ml. of the polymerization mixture. A 10% conversion is equivalent to 2.3% solids in benzene.

^b This indicates the condition of the polymer after aging with catalysts and reacting with CH_3OH^3 . The poly-BD was a cobalt-catalyzed polymer (181D and E) having originally 96.5% *cis*, 1.8% *trans*, 1.7% 1,2. Some gel was precipitated in 181D, and was separated and counted separately. In 181E some gel developed in storage.

^c All structures were determined by an infrared method of analysis on films of once-coagulated polymers. The second value for 182A represents that obtained on polymer after removal of $\sim 6.5\%$ of low molecular weight material ($[\eta] = 0.1$ dl./g., 25°C . in toluene). The \bar{M}_n was determined on the remaining 95.5% of the polymer.

^d Disintegrations per minute per gram.

^e \bar{M}_{H^3} is based on the assumption of 1 H³/chain, and an isotope factor of 1.

^f $[\text{Co}] = 0.16$ mmole/l. Perbenzoate unsaturation = 100%, iodine number (IC1) = 96%.

^g Polymerization time.

^h Time of aging for ~ 2 wt.-% polymer solutions with $\text{CoCl}_2 \cdot \text{AlCl}_3$ catalyst prior to addition of the CH_3OH^3 solution.

ⁱ This was an alkali metal-catalyzed polybutadiene which was dissolved in benzene, treated by the CH_3OH^3 termination method and purified for counting. The residual activity indicated that all the tritium was not removed by two freeze dryings. However, this tritium level represents $\leq 10\%$ of the counts with most of the live or preformed polymers.

catalyst, and (b) the reaction of tritiated methanol with the cobalt-carbon bond is probably not quantitative. Representative results of our tritium work in the alkyl-free system are summarized in Table VII. Clearly, the termination of an active polymerization with tritiated methanol in either benzene or cyclohexane leads to significant tritium incorporation in the polymer. Unfortunately, the results are quite inconclusive because preformed and redissolved polybutadiene when treated with CH_3OH^3 in the presence of the same catalyst ($\text{CoCl}_2 \cdot \text{AlCl}_3$) undergoes substantial tritium incorporation in both benzene and cyclohexane (see expts. 181D and 181E). Tritium incorporation is greater in cyclohexane than in benzene in both cases. Our results are, therefore, similar to those of Natta et al.,¹⁸ except that there is not even qualitative evidence for anionic chain growth in our alkyl-free system, since the tritium counts are higher in some cases with the preformed polymer than with the propagating polymers.

The mechanism of these polymerizations is still not established. It is possible, in light of Pettit's¹⁹ recent work on the formation of carbonium ion complexes of Fe, that HCl or HAlCl_4 (formed *in situ*) play a role in initiating the cobalt chloride-aluminum chloride-catalyzed polymerization of conjugated dienes. A thorough, but infrequent, examination of very carefully prepared catalyst solutions disclosed the presence of small but variable amounts of HCl. Further work is needed to establish the role, if any, of very low HCl concentrations in these polymerizations.

In summary, the cobaltous halide-aluminum halide complexes represent an interesting class of homogeneous catalysts for the polymerization of dienes in hydrocarbon media. In particular, the $\text{CoCl}_2 \cdot \text{AlCl}_3$ complex can be employed to give a highly sensitive but stereospecific *cis* polymerization of butadiene in either benzene or cyclohexane without any added reducing metal alkyl. The behavior of this complex with other dienes has not been fully explored, but cursory examination with isoprene and 2,3-dimethylbutadiene has shown much less selectivity for a given stereoisomer. The exact nature of chain growth could not be defined by tritiated methanol termination, and therefore, elucidation of the mechanism of polymerization will require further study.

EXPERIMENTAL

Materials

The following materials were used in this study. They were dried or purified as described below: benzene, J. T. Baker (reagent grade, thiophene-free); cyclohexane, Shell Chemical Company; butadiene, Phillips (special purity); aluminum chloride, anhydrous, B and A reagent grade (Allied Chemical).

Reagent grade chemicals were otherwise employed with the exception of cobaltous iodide, which was prepared by the reaction of cobaltous carbonate with hydriodic acid.

Purification of Materials

Cyclohexane was purified by washing with concentrated sulfuric acid followed by chromatography on silica gel. It was then distilled from sodium and/or calcium hydride in a nitrogen atmosphere. The distilled cyclohexane was collected over calcium hydride. Alternatively, distillation from lithium aluminum hydride-calcium hydride gave satisfactory material. Reproducible "dryness" could be attained by stirring the distilled solvent overnight in the presence of solid calcium hydride and in a nitrogen atmosphere.

Benzene was purified in a similar manner to cyclohexane except it was not subjected to the acid-wash step.

Butadiene was purified by passage through a delivery train consisting of industrial glass tubes packed with calcium hydride, Drierite, and Ascarite, and 3-A molecular sieves (2 tubes), in the order stated. Following the hydride tube, an Engelhard catalytic Deoxo unit was placed in the purification train to help scavenge oxygen. After flushing the line, a butadiene pressure of ~ 22 psig was maintained in the delivery train. A typical analysis of butadiene from this train for oxygen content showed 7 ppm (on a volume basis).

Nitrogen (Air Reduction Co. High Purity) and argon (Linde high purity, dry) were delivered through successive columns of indicating Drierite and 3-A or 4-A molecular sieves.

Anhydrous cobalt salts were usually prepared by dehydration of the hydrated salts at ~ 120 – 150°C . *in vacuo*.

Catalyst Preparation

The solid components were transferred into the catalyst flask in a suitable dry box. Solvent was added in an inert atmosphere and the mixture refluxed under nitrogen for ~ 24 hr. The suspension was allowed to settle (usually overnight) and the clear supernatant solution was carefully pressured (under Ar or N_2) through U-shaped hypodermic tubing into an appropriate storage bottle. These supernatant solutions appeared to be true solutions, i.e., devoid of Tyndall effects.

Polymerization Procedure

The polymerization experiments were carried out in small cylindrical reactors (~ 120 ml. volume) equipped with a standard taper 45/50 ground glass joint bearing three entry ports closed by stopcocks. One of the side ports was attached to a 8-mm. dip tube extending to within 2 cm. of the bottom of the reactor. This latter side port was used to introduce argon and/or nitrogen or butadiene. The central port was used for introduction of catalyst, solvent, etc., and withdrawal of samples by hypodermic needle. The central port was closed by a serum cap on the external side of the stopcock and equipped with inlet and outlet arms for maintaining an inert atmosphere at all times between the stopcock and the serum cap.

All glass equipment was thoroughly cleaned in a chromic acid bath, rinsed with water and oven-dried (125°C.) prior to use. Likewise, all hypodermic syringes and needles were oven-dried prior to use. The standard procedure consisted of: (a) assembling the reactor while still hot from the oven (120°C.) using a minimum of Apiezon grease on the joints; (b) alternately flushing with argon and evacuating the reactor three times prior to introduction of solvent; (c) normally introducing the reactants in the order: solvent, butadiene to desired level, catalyst solution; (d) terminating with a dilute solution (10 vol.-%) of isopropanol in benzene or cyclohexane; (e) coagulating by pouring the polymerization mixture into a large excess of methanol or isopropanol. The poly-BD was normally inhibited with *N,N'*-diphenylphenylenediamine.

Analytical Methods

Cobalt, aluminum, and chlorine were determined by standard analytical methods. In some cases, aluminum and chlorine were determined by neutron activation analysis.

The structures of the butadiene polymers produced were determined from their infrared absorption spectra. In different phases of the work, different spectroscopic methods based on spectra of both solid films and carbon disulfide solutions were used. Because all of the polymers were of high *cis*-1,4 content and the direct spectroscopic measurement of this structure is subject to large errors, our methods were designed to determine as accurately as possible the concentrations of *trans*-1,4 and 1,2 double bonds. These latter values were obtained from the absorbances at 10.34 and 10.98 μ respectively, and the *cis*-1,4 concentration was obtained by difference. Our methods gave results which would not be significantly different from those obtained by various published methods.^{20,21}

Tritium Termination Experiments

The polymers from the tritium (CH_3OH^3)-terminated polymerizations were purified by precipitation from methanol. The precipitated polymer was then redissolved in benzene, centrifuged to remove any insoluble particles if necessary, and freeze-dried *in vacuo*. A second freeze-drying from benzene completed the purification.

The polymers were counted for tritium by standard scintillation counting methods. The analysis employed an internal standard and quenching corrections were applied.*

The authors wish to acknowledge the excellent technical assistance of R. M. Ross in much of this work.

References

1. Union of South Africa Pat. 59/2287 (October 1959); U. S. Pat. 3,066,125 (November 27, 1963).
2. Gippin, M., *Ind. Eng. Chem. Prod. Res. Develop.*, **1**, 32 (1962).

* The authors are indebted to B. E. Gordon for assistance in this phase of the work.

3. Longiave, C., R. Castelli, and G. F. Croce, *Chim. Ind. (Milan)*, **43**, 625 (1961).
4. Natta, G., L. Porri, and A. Carbonaro, *Atti Accad. Naz. Lincei, Rend. Classe Sci. Fis. Mat. Nat.*, **29**, 491 (1960).
5. Scott, H., R. E. Frost, R. F. Belt, and D. E. O'Reilly, *J. Polymer Sci.*, **A2**, 323 (1964).
6. O'Reilly, D. E., C. P. Poole, Jr., R. F. Belt, and H. Scott, *J. Polymer Sci.*, **A2**, 3257 (1964).
7. Seidell, A., and W. F. Linke, *Solubilities of Inorganic and Organic Compounds*, Van Nostrand, New York, 1952, Suppl. to 3rd Ed., p. 29.
8. Ibers, J., *Acta Cryst.*, **15**, 967 (1962).
9. Turner, R., and E. Amma, *J. Am. Chem. Soc.*, **85**, 4047 (1963).
10. Gill, N. S., and R. S. Nyholm, *J. Chem. Soc.*, **1959**, 4000.
11. Yen, T. F., *J. Polymer Sci.*, **38**, 272 (1959).
12. Chen, H.-Yu., *Anal. Chem.*, **34**, 1792 (1962).
13. Anderson, W. S., Shell Development Company.
14. Canale, A. J., W. A. Hewett, T. M. Shryne, and E. A. Youngman, *Chem. Ind. (London)*, **1962**, 1054.
15. Giannini, U., E. Ciampelli, and G. Bruckner, *Makromol. Chem.*, **66**, 209 (1963).
16. Childers, C., *J. Am. Chem. Soc.*, **85**, 229 (1963).
17. Cooper, W., D. E. Eaves, and G. Vaughan, *Makromol. Chem.*, **67**, 229 (1963).
18. Natta, G., L. Porri, A. Carbonaro, and A. Greco, *Makromol. Chem.*, **72**, 207 (1964).
19. Pettit, R., and G. Emerson, *J. Am. Chem. Soc.*, **84**, 4591 (1962).
20. Binder, J. L., *Anal. Chem.*, **26**, 1877 (1954).
21. Silas, R. S., J. Yates, and U. Thornton, *Anal. Chem.*, **31**, 529 (1959).

Résumé

La polymérisation stéréosélective du butadiène en polymère-*cis* a été effectuée au moyen de catalyseurs complexes formés d'halogénure de cobalt, par exemple $\text{CoCl}_2 \cdot \text{AlCl}_3$. Les caractéristiques uniques de telles polymérisations sont la nature homogène de la catalyse et l'activité de ces catalyseurs en absence d'agent réducteur additionnel. On a étudié la composition et la spectroscopie de certaines de ces solutions de catalyseur et on a proposé des structures possibles. L'état d'avancement actuel des travaux ne permet pas de décrire le mécanisme de cette polymérisation, mais on décrit certains résultats de terminaison au moyen de méthanol marqué au tritium (CH_3OH^3). Malheureusement, ces expériences ne définissent pas la nature de la fin de propagation de la chaîne polymérique.

Zusammenfassung

Die stereoselektive Polymerisation von Butadien zu einem vorwiegend *cis*-Polymeren wurde mit komplexen Kobalthalogenidkatalysatoren, z.B. $\text{CoCl}_2 \cdot \text{AlCl}_3$ durchgeführt. Die besonderen Merkmale dieser Polymerisationen sind die homogene Natur der Katalyse und die Aktivität solcher Katalysatoren in Abwesenheit eines Reduktionsmittels. Zusammensetzung und Absorptionsspektren einiger dieser Katalysatorlösungen wurden untersucht und mögliche Strukturen vorgeschlagen. Der gegenwärtige Stand der Arbeit erlaubt keine zwingenden Schlüsse auf den Mechanismus dieser Polymerisation; es werden aber einige Ergebnisse für den Abbruch mit tritiiertem Methanol (CH_3OH^3) beschrieben. Unglücklicherweise liefern diese Versuche keinen Aufschluss über die Natur des wachsenden Endes der Polymerkette.

Received September 20, 1964

Revised November 20, 1964

(Prod. No. 4305A)

Study of the Effects of Additives in Homogeneous Anionic Polymerization of α -Methylstyrene by *n*-Butyllithium (To Prepare Polymers Having Narrow Molecular Weight Distribution)

TERUO FUJIMOTO, NORIYOSHI OZAKI, and MITSURU NAGASAWA, *Department of Synthetic Chemistry, Nagoya University, Chikusa-ku, Nagoya, Japan*

Synopsis

Polymerization of α -methylstyrene with *n*-butyllithium was carried out in the presence of some additives such as LiBr, LiOH, LiOBu, and LiN(Et)₂ in THF. The change in the color of the α -methylstyryl anion with amount of the additives, the activity of *n*-BuLi, the average molecular weights, and the molecular weight distributions of polymers obtained were observed to clarify the interaction of *n*-BuLi (or of α -methylstyryl anion) with these additives. It was concluded that LiBr and LiOH deactivate the initiator in the mole ratio of 1:1 and only the remaining part of *n*-BuLi participates in polymerization, while LiOBu and LiN(Et)₂ do not. The order of the additives in the capacity to form deactivating centers (possibly by complex formation) follows the order of nucleophilicity and is opposite to the order of activity for initiating the polymerization. The molecular weight distribution of the polymer obtained with pure *n*-BuLi in the absence of additives was extremely sharp.

INTRODUCTION

Homogeneous anionic polymerization has attracted a great interest of not only organic chemists but also of many physical chemists, since it gives polymers having very narrow molecular weight distribution or samples of well defined molecular structures. From the papers so far published on homogeneous anionic polymerization, the following may be summarized on the standpoint of making monodisperse polymers.

(1) Initiators such as sodium naphthalene or α -methylstyrene tetramer, which give dianionic chains, lead to double-peaked molecular weight distributions,¹⁻³ while alkylolithiums, which are monofunctional compounds, lead to single-peaked molecular weight distribution.^{4,5} Therefore, the latter initiators are more suitable for preparing samples of narrow molecular weight distribution than the former.

(2) It is believed that an association exists between active anions in hydrocarbon solutions, and hence, the velocity of initiation may not be very much faster than that of propagation, hence leading to broad molecular weight distribution. On the other hand, as no such association occurs in

tetrahydrofuran solutions, samples of very narrow molecular weight distribution may be obtained in THF if the polymerization temperature is low enough to avoid the reaction between alkyllithium (or styryl anion) and THF.⁶

(3) Impurities in the monomer, such as H_2O , O_2 , cause termination, resulting in broad molecular weight distribution. However, as α -methylstyrene can be mixed with initiators above the ceiling temperature⁷⁻⁹ the impurities may be consumed before initiating polymerization, and the molecular weight distribution of poly- α -methylstyrene may be narrower than that of polystyrene, to which such a polymerization method cannot be applied.^{5,10} It is true that the molecular weight distribution of "living" poly- α -methylstyrene is not narrow if the polymerization-depolymerization equilibrium is attained.⁷ However, the polymerization is usually stopped very much before the equilibrium is attained, so that the molecular weight distribution may become very narrow.⁹

(4) *n*-Butyl bromide, remaining unreactive in *n*-butyl-lithium, may also cause termination, resulting in broad molecular weight distribution.¹¹

(5) Some impurities, such as amines may form a complex with an anionic active end,¹² and this may lead to a broad molecular weight distribution.

(6) There is some controversy among researchers on the stereoregularity of polystyrene polymerized with *n*-butyllithium. Worsfold and Bywater¹³ stated that the presence of water in the solution may be a reason for stereoregularity of polystyrene, while Kern¹⁴ and Braun, Betz, and Kern¹⁵ reported that *n*-butyl-lithium-catalyzed polystyrene has a crystalline fraction if ether and lithium halide are not present in the solution.

Although it thus seems to us that the experimental conditions for preparing samples of narrow molecular weight distribution have been quite well defined, there still remain some problems which should be clarified. If *n*-alkyllithium is made by Ziegler's method,^{16,17} the initiator solution may include lithium halide as well as alkyl halide, which remain unreactive. It is possible that these substances affect either the initiation process or the propagation process or both, because these substances may form a sort of "complex" with anionic active ends or because the presence of those electrolytes may depress the ion-pair dissociation.

The reaction of lithium alkyls or growing chain ends with those additives has not yet been studied fully. Therefore, it seems meaningful from the standpoint of organic chemistry, too, to clarify the interaction between these compounds and particularly to clarify what kinds of electrolytes would form complexes with lithium alkyls. In the present experiments, α -methylstyrene was polymerized by *n*-butyllithium in THF in the presence of LiBr, LiOH, LiOBu, (lithium butoxide), and LiN(Et)₂ (lithium diethylamide). Those electrolytes were chosen because of their different degrees of nucleophilicity. The change in the color of the α -methylstyryl anion, the reactivity of *n*-BuLi in the presence of the additives, and the molecular weights and the molecular weight distributions of the polymers obtained were observed to clarify the interaction of *n*-BuLi (or α -methylstyryl anion) with these additives. The results obtained show that the order of these additives in their ability to form "complexes" with

active end (or in their ability to deactivate the active ends) follows in the order of their nucleophilicity which is opposite to the order of these compounds in the ability of initiating polymerization of double bond: LiBr deactivates *n*-BuLi almost completely in THF, probably because it forms a complex with *n*-BuLi. The lithium diethylamide has the least tendency to form a "complex" but instead it has the ability of initiating polymerization of styrene in THF. Others are in between these two compounds. The molecular weight distribution of polymer is broadened by the presence of these compounds.

The molecular weight distribution of poly- α -methylstyrene obtained in the absence of such additives is found to be very sharp but still broader than the theoretical limit.

PREPARATIONS

Purification of THF and Monomers

The general apparatus and technique were similar to those used by various researchers, particularly to that of Morton et al.⁴ The main vacuum line was pumped to 10^{-6} mm. Hg pressure. The THF (Katayama Chemical Co.), was preliminarily fractionally distilled by ordinary purification techniques and then refluxed over sodium metal for several hours and distilled into a flask containing a few pieces of sodium and anthracene. The liquid was repeatedly degassed at a low temperature and refluxed until a permanent dark color was observed. The method of purification of α -methylstyrene was the same as that of THF except that α -methylstyrene tetramer was used in place of sodium anthracene. The liquids thus purified were distilled into a graduated flask and then into ampules with breakable seals.

Although it is likely that traces of impurities which might deactivate the initiator still remain in THF and monomers so purified, the presence of such impurities is not serious for the purpose of the present research, because they can be completely consumed before the polymerization starts. All solvents and monomers used for a series of experiments were sealed into ampules at the same time and stored under refrigeration.

The styrene monomer (Katayama Chemical Co.) was purified by fractional distillation and dried with calcium hydride.

Preparation of *n*-Butyllithium

The method of preparing pure *n*-butyllithium free of LiBr and LiOH used in the present experiments was different from the ordinary method in which dialkyl mercury is used.^{4,15} *n*-BuLi was prepared from the reaction between *n*-butyl bromide and metallic lithium. The reaction was carried out in the apparatus shown in Figure 1. First the metallic lithium was placed in the flask R and the pressure in the system was reduced to 10^{-5} mm. Hg. Next, the ether (in flask S) which was purified by the same method as THF, and *n*-BuBr (in flask B), which was purified by distillation with calcium hydride, were added to the reactor R. The reaction was carried out at 0–10°C. for several hours. The LiBr produced by the reaction is

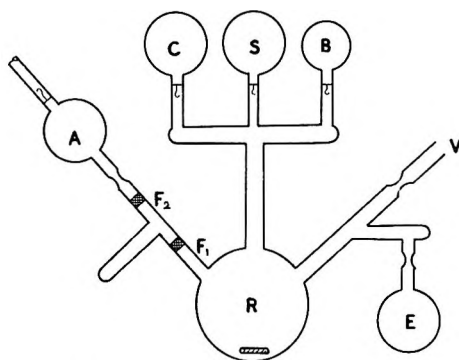


Fig. 1. Apparatus for preparing *n*-butyllithium.

completely soluble in ether.¹⁹ Therefore, benzene (in C), which was distilled after refluxing with sodium metal until the surface of the metal showed a metallic luster, was added to precipitate LiBr. If all ether was removed by distillation into the flask E, no trace of Br⁻ could be detected with AgNO₃ in the final initiator solution (indicator K₂CrO₄). The solubility of LiBr in benzene is negligible. The precipitates were filtered through sintered glass filters F₁ and F₂, and the final initiator solution was sealed in A. The concentration of *n*-BuLi was determined by titration with a standard acid solution. It was confirmed from the same titration that all *n*-BuBr had reacted with Li metal.

Preparation of *n*-BuLi Containing Additives

(1) *n*-BuLi Containing LiBr. The original ether solution of *n*-BuLi which contains an equal amount of LiBr was used without removing LiBr. That the solution contains *n*-BuLi and LiBr in the mole ratio of 1:1 was confirmed by titrating the solution with standard acid and AgNO₃ solutions (though the possible error was almost 10%).

(2) *n*-BuLi Containing LiOH, LiOBu, and LiN(Et)₂. If H₂O, BuOH, and HN(Et)₂ are added to a mixture of *n*-BuLi and α -methylstyrene, they immediately react with active centers to produce LiOH, LiOBu, and LiN(Et)₂, respectively. Therefore, the effects of LiOH, LiOBu, LiN(Et)₂ in the polymerization with *n*-BuLi can be observed if the amounts of H₂O, BuOH, HN(Et)₂ are less than the amount of *n*-BuLi. If the amounts of those compounds are greater than the amount of *n*-BuLi, naturally all active centers are killed and no polymerization can occur when the solution is cooled down to -78°C., except for the case of LiN(Et)₂ which itself has the ability of initiating polymerization. H₂O, BuOH, and HN(Et)₂ were purified by methods similar to that applied to other liquids. After purification they were diluted with THF and sealed in ampules. The amounts of liquids taken were determined by the volumes in ampules which were measured by using mercury after experiment. The estimated accuracy was generally better than $\pm 1\%$.

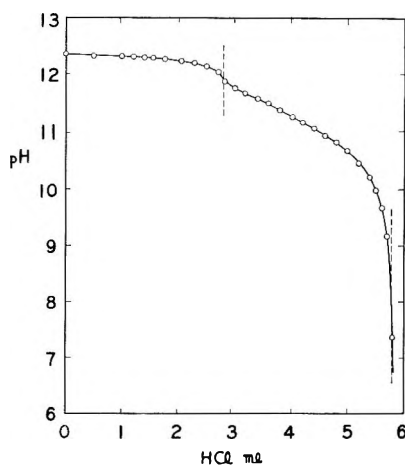


Fig. 2. Potentiometric titration curve of lithium diethylamide ($\text{LiN}(\text{Et})_2$) with standard HCl.

Preparation of $\text{LiN}(\text{Et})_2$ Initiator

$\text{LiN}(\text{Et})_2$, which was precipitated from the reaction mixture of n -BuLi and $\text{HN}(\text{Et})_2$ in benzene, was filtered through sintered glass filters, washed with benzene several times, and dried in vacuum. The purified sample was dissolved in ether. The aqueous solution of $\text{LiN}(\text{Et})_2$ was titrated with standard HCl to determine the concentration. The potentiometric titration curve showed two breaking points at the equivalent points of LiOH and $\text{LiOH} + \text{LiN}(\text{Et})_2$, as shown in Figure 2.

Polymerization

Polymerization was carried out in the apparatus shown in Figure 3. THF, α -methylstyrene, and methanol are placed in ampules S, M, and A, respectively. The n -BuLi solution and the additives (H_2O , BuOH, $\text{HN}(\text{Et})_2$, 1:1 mixture of n -BuLi and LiBr) were placed in ampules I and Cl. After the reaction vessel R was evacuated, flamed, and the pressure reduced to 10^{-6} mm. Hg, the whole apparatus was sealed off. Then, the initiator and additive were introduced into the reaction vessel (R) by breaking the seals. As explained above, the mixture must contain a reactive product (LiOH , LiOBu , $\text{LiN}(\text{Et})_2$, or LiBr) and the remaining part of n -BuLi. Next, α -methylstyrene and then THF were introduced into the vessel R. The mixture was kept at 40°C . for about 30 min., so that all impurities were consumed by reaction of the active centers. Therefore, if the apparatus is cooled as quickly as possible in a Dry Ice-acetone bath, the polymerization starts from all initiators at the same time and no termination can occur. The reaction was continued for a few hours. Finally, methanol in ampule A was added to kill the active end.

The product was precipitated from the solution and washed repeatedly with methanol. The sample used in the measurement of the solution

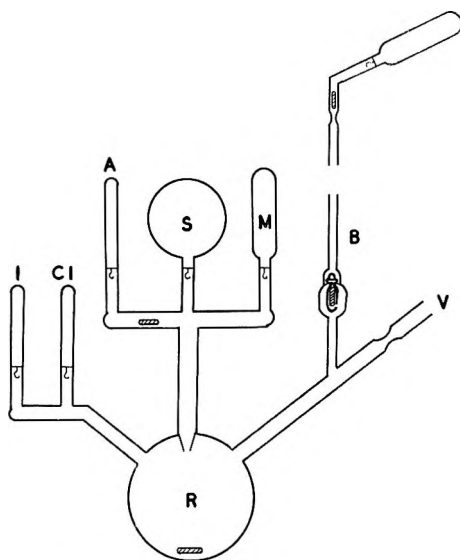


Fig. 3. Apparatus for polymerization.

properties was purified by repeated dissolution and precipitation with THF and methanol, respectively, and then lyophilized. Conversion to polymer was about 90%.

The polymerization of styrene with $\text{LiN}(\text{Et})_2$ in THF was carried out in a similar way. However, the monomer was mixed with the initiator at Dry Ice-ether temperature, where no polymerization occurred, and then gradually warmed to polymerize. The temperature of the mixture was measured with a thermocouple.

The concentration of the active end was determined by titration with butanol THF solution using a vacuum buret B shown in Figure 3 (made by Ando Glass Co., Tokyo Institute of Technology, Meguro, Tokyo) after completion of polymerization. This has a spherical ground glass joint with a pin-hole which can be opened and closed by a magnet. A leak through the glass joint was observed but the leak could be calibrated easily.

MEASUREMENTS

Light Scattering

The weight-average molecular weights were determined from light-scattering measurements, with the use of an instrument of the Brice type manufactured by Shimadzu Instruments Co. The cell used was a cylindrical cell with a ground glass back to permit the back-refraction correction to be neglected. The calibration of the instrument was carried out by using benzene as a standard (R_{90} of benzene = 4.85×10^{-5}). The cell had a slight angular dependence when it was checked by measuring the angular envelope of fluorescein solution, and, hence, a correction was given to observed values. However, the correction has little effect on the molecular weight obtained. All original solutions were cleaned by centri-

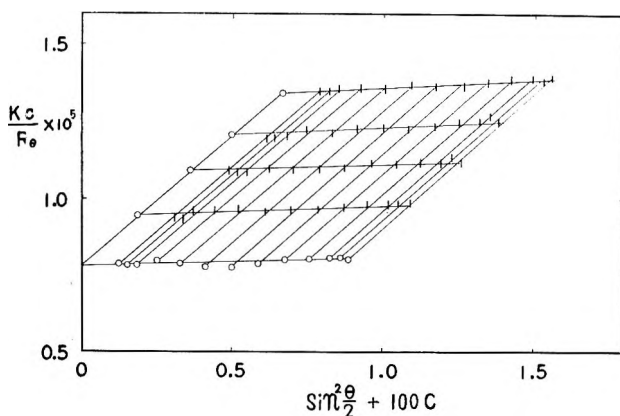


Fig. 4. Example of the Zimm plot of poly- α -methylstyrene in toluene solution. Sample No. 3-1; 25°C.

fugation with a Sakuma preparative centrifuge at 2×10^4g for 1 hr. at 25°C. The dilution of the original solution was carried out in the cell. The refractive index increment (dn/dC) was found to be 1.31×10^{-1} with the use of a differential refractometer of the Debye type manufactured by Shimadzu Instrument Co. The solvent used was toluene, and the measurement temperature was $25 \pm 1^\circ\text{C}$. A typical Zimm plot obtained is shown in Figure 4.

Osmotic Pressure Measurements

The number-average molecular weight was determined in an osmometer of the Zimm-Myerson type made by Shibata Glass Co. The membrane used was No. 600 gel-cellophane (Fuji Cellophane Co.), and the conditioning of the membrane was carried out by the method of Pinner.¹⁹ The measurements were carried out by the static method in toluene solution at $25 \pm 0.005^\circ\text{C}$. An example of the measurements of equilibrium pressure is shown in Figure 5. The change in pressure observed when the solvent is renewed was less than 1%. In Figure 6, examples of π/C versus C plots are shown.

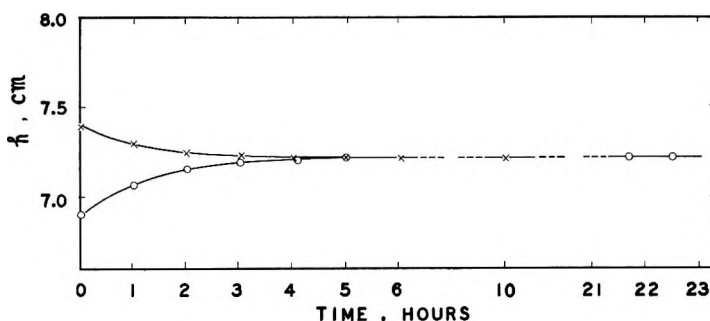


Fig. 5. Example of obtaining the equilibrium osmotic pressure of poly- α -methylstyrene. Sample No. 2-1; 0.951 g./100 ml. toluene; 25°C.

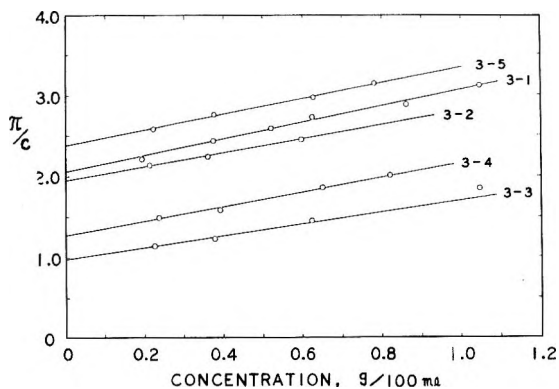


Fig. 6. Relationship between π/C and C of poly- α -methylstyrene in toluene solution at 25°C.

Viscosity Measurements

Intrinsic viscosities of the samples in toluene solution were determined with a capillary viscometer of the modified Ubbelohde type. The efflux time of toluene at $25 \pm 0.01^\circ\text{C}$. was 120.5 sec., and the kinetic energy correction was less than 1%. The viscosity-average molecular weight of poly- α -methylstyrene and polystyrene were computed from the intrinsic viscosity by using eqs. (1) and (2), respectively.^{1,20}

$$[\eta] = 7.81 \times 10^{-5} M_w^{0.73} \quad (1)$$

$$[\eta] = 17 \times 10^{-5} M_w^{0.69} \quad (2)$$

Equation (1) was confirmed by the present experiments.

Determination of Molecular Weight Distribution from Sedimentation Velocity Experiments

A Spinco Model E ultracentrifuge was used for sedimentation experiments. All measurements were made at a speed of 59,780 rpm and at $35 \pm 0.1^\circ\text{C}$. in cyclohexane, which is the theta point for polystyrene and must be very close to the theta point of poly- α -methylstyrene.¹ As shown in Figure 7, it was confirmed that the sedimentation velocity of poly- α -

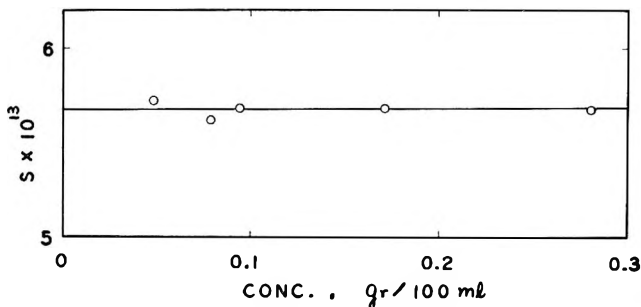


Fig. 7. Concentration dependence of the sedimentation constant of poly- α -methylstyrene in cyclohexane at 35°C. Sample No. 3-1.

methylstyrene is practically independent of the concentration of polymer for samples of such a molecular weight as used here.²¹ Therefore, the molecular weight distribution was calculated from experiments at one concentration between 0.1 and 0.15 g./100 ml. A correction for diffusion was obtained by extrapolating the results obtained at different times to infinite time, but no correction was given for the pressure effect. The actual calculation procedure of molecular weight distribution from sedimentation patterns followed the method of Cantow.²²

The relationships between sedimentation constant and molecular weight of poly- α -methylstyrene and polystyrene at 35°C. in cyclohexane are given by eqs. (3) and (4), respectively.^{1,23}

$$S = 1.72 \times 10^{-2} M_w^{0.49} \quad (3)$$

$$S = 1.69 \times 10^{-2} M_w^{0.48} \quad (4)$$

Equation (3) was confirmed by the present experiments.

RESULTS AND DISCUSSION

As the THF solution of *n*-BuLi and α -methylstyrene has a red color of α -methylstyryl anion and the polymerization does not occur at room temperature, the effect of additives in the anionic polymerization can be observed easily. When there is no additive, *n*-BuLi initiates the polymerization of α -methylstyrene as soon as the mixture is cooled down to Dry Ice-acetone temperature (-78°C .). However, if an ether solution of *n*-BuLi containing LiBr in the mole ratio 1:1 is used, neither red color nor polymerization can be observed for an indefinite period, even if the mixture is put in a bath of Dry Ice-acetone. If there is a slight amount of *n*-BuLi in excess in the solution, the red color of α -methylstyryl anion appears and polymerization occurs. The same phenomena are observed for LiOH, too. If H₂O is added to a red solution of α -methylstyryl anion at room temperature, there is an immediate reaction to produce LiOH. The colorless endpoint is observed when the quantity of H₂O added is half as much as the equivalence of active centers, i.e., when the amount of LiOH becomes equal to the amount of α -methylstyryl anion remaining (see Table I). The colorless solution has no ability to initiate polymerization when the solution is cooled down to -78°C .

The α -methylstyryl anion is also reacted with butanol to produce LiOBu. In this case, the red color does not disappear when the amount of

TABLE I
Titration of α -Methylstyryl Anion with Butanol and Water^a

| | α -MeSt $\times 10^3, M$ | <i>n</i> -BuLi $\times 10^3, M (A)$ | Amount <i>n</i> -BuLi consumed $\times 10^3, M (B)$ | A/B |
|------------------|------------------------------------|--|--|------------------|
| BuOH | 3.41 | 0.47 | 0.47 | 1.0 |
| H ₂ O | 3.43 | 0.82 | 0.40 | 2.0 ₅ |

^a Solvent: THF (14 ml.); temp.: room temperature.

TABLE II
 Polymerization of α -Methylstyrene (α -MeSt) with n -BuLi in the Presence of Additives^a

| Sample no. | α -MeSt, M | n -BuLi $\times 10^3, M$ | Additives $\times 10^3, M$ | Active ends $\times 10^3, M^b$ | Loss of n -BuLi, % ^c | $M_k \times 10^{-4}$ | $M_w \times 10^{-4}$ | $\bar{M}_n \times 10^{-4}$ | Effective active end $(M_w/M_n), \%$ |
|------------|---------------------|----------------------------|-----------------------------|--------------------------------|-----------------------------------|----------------------|----------------------|----------------------------|--------------------------------------|
| 2-1 | 0.137 | 0.46 | — | 0.44 | 4 | 3.3 | 6.4 | 6.4 | 52 |
| 2-2 | 0.151 | 0.48 | LiOH, 0.20 | 0.26 | 7 | 6.1 | 11.2 | — | 54 |
| 2-3 | 0.130 | 0.66 | LiBr, 0.29 | 0.34 | 8 | 4.0 | 7.7 | — | 52 |
| 2-4 | 0.114 | 0.32 | LiOBu, 0.13 | 0.30 | 6 | 4.1 | 7.2 | — | 57 |
| 2-5 | 0.138 | 0.27 | LiN(Et) ₂ , 0.16 | ca. 0.44 | — | 5.5 | 8.3 | — | 66 |

^a Solvent: THF (ca. 200 ml.); temp.: -78°C .

^b Titrated with butanol.

^c Calculated assuming that LiOH and LiBr form complexes with the active center in 1:1, but others do not.

^d Number-average molecular weight calculated from the amount of active centers, and α -methylstyrene. (Conversion to polymer was taken to be 90% for all experiments.)

 TABLE III
 Molecular Weight of Poly- α -methylstyrene Determined by Various Methods

| Sample no. | α -MeSt, M | n -BuLi $\times 10^3, M$ | Additives $\times 10^3, M$ | $M_n \times 10^{-4}$ | $\bar{M}_n \times 10^{-4}$ | $\bar{M}_w \times 10^{-4}$ | \bar{M}_w/\bar{M}_n | From molecular weight distribution | |
|------------|---------------------|----------------------------|----------------------------|----------------------|----------------------------|----------------------------|-----------------------|------------------------------------|------------------------|
| | | | | | | | | \bar{M}_w/\bar{M}_n | $\Delta M/\bar{M}_n^a$ |
| 3-1 | 0.847 | 1.3 | — | 12.8 | 12.6 | 12.7 | 1.01 | 1.00 ₃ | 0.09 ₃ |
| 3-2 | 0.668 | 2.0 | LiOH, 0.5 | 13.6 | 13.0 | 13.5 | 1.04 | 1.00 ₈ | 0.11 ₈ |
| 3-3 | 0.512 | 1.0 | LiBr, 0.6 | 27.2 | 25.9 | 27.8 | 1.07 | 1.00 ₆ | 0.09 ₂ |
| 3-4 | 0.714 | 0.6 | LiOBu, 3.0 | 20.8 | 19.8 | 20.3 | 1.03 | 1.00 ₄ | 0.08 ₇ |
| 3-5 | 0.663 | 1.5 | LiNEt ₂ , 1.3 | 12.7 | 10.8 | 11.4 | 1.06 | 1.01 ₂ | 0.17 ₄ |

^a $\Delta M/\bar{M}_n = [(M - M_n)^2]^{1/2}/\bar{M}_n$.

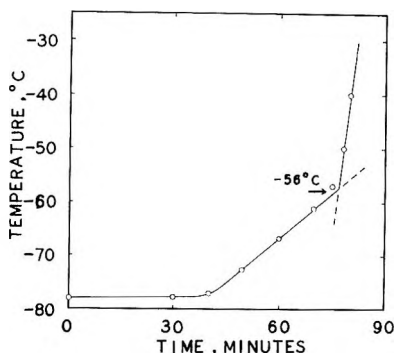


Fig. 8. Temperature change in the polymerization of styrene with $\text{LiN}(\text{Et})_2$. Styrene, 24.5 ml.; THF, 200 ml.; initiator concn.: $2.5 \times 10^{-2} M$.

LiOBu becomes equal to that of α -methylstyryl anion but does disappear when all active ends are destroyed (see Table I).

Table II shows more precise titration data of α -methylstyryl anion with butanol (THF solution) when there are additives in the solution. It is seen that the amount of active ends determined by titration is equal to the difference between the amount of n -BuLi and that of additive for LiBr and LiOH, while it is equal to the amount of n -BuLi itself for LiOBu.

The effect of $\text{LiN}(\text{Et})_2$ is complicated. If $\text{HN}(\text{Et})_2$ is added to the red mixture of n -BuLi and α -methylstyrene, it reacts with the active centers to produce $\text{LiN}(\text{Et})_2$. In this case, the endpoint is not so clear, but it is certain that the endpoint is beyond the equivalent point of n -BuLi. Therefore, $\text{LiN}(\text{Et})_2$ does not seem to deactivate the active centers. Moreover, it is interesting to see that $\text{LiN}(\text{Et})_2$ itself has a faint yellow color and is capable to some extent of initiating polymerization. When an amount of purified $\text{LiN}(\text{Et})_2$ is added to styrene in THF at Dry Ice-ether temperature, the solution is colorless and no polymerization occurs at first. However, if the solution is warmed gradually, the solution shows abrupt yellow coloring and very fast polymerization at about -56°C . The polymerization is completed almost instantaneously. The temperature change in the solution is shown in Figure 8. Therefore, it is clear that $\text{LiN}(\text{Et})_2$ has the capability of initiating polymerization of styrene, though it may be in an associated form even in THF at low temperature, just as n -BuLi is associated in hydrocarbon solvents.

The molecular weights (M_η) of poly- α -methylstyrene obtained were calculated from intrinsic viscosity by using eq. (1) for comparison with the values (M_k) predicted from the weight of polymer and the concentration of active ends, as shown in Table II. Although M_η is always higher than M_k , it is seen that the same ratio ($M_k/M_\eta = 0.54$) is obtained for all experiments.

From these observations, it may be concluded that both LiBr and LiOH form a kind of complex with α -methylstyryl anion in the mole ratio of 1:1 in THF and that this complex has no ability to initiate polymerization,

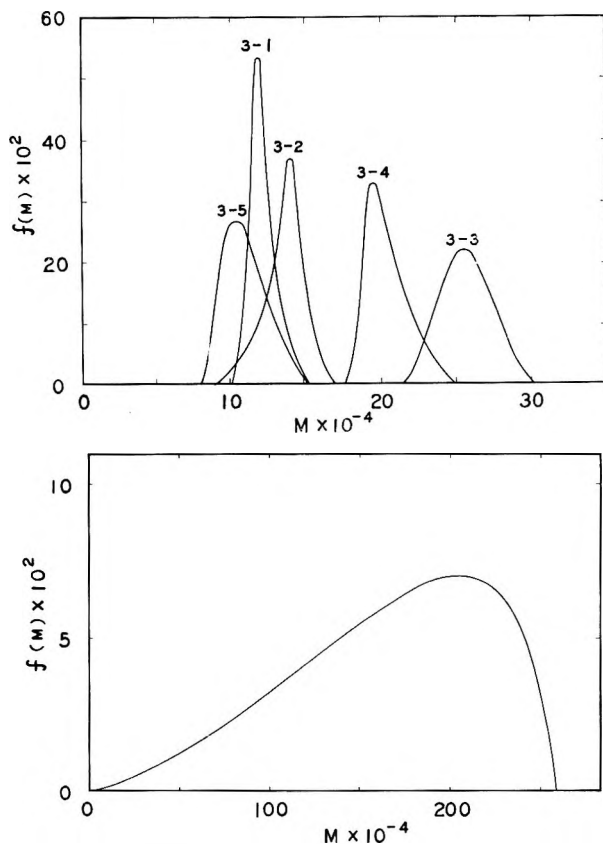


Fig. 9. Molecular weight distributions of (a) poly- α -methylstyrene and (b) polystyrene polymerized with $\text{LiN}(\text{Et})_2$ under conditions given in Figure 8.

while LiOBu and $\text{LiN}(\text{Et})_2$ do not form such complexes. As the change of color is so critical, it is unlikely that the effect of additives is to suppress the dissociation of ion-pair. Here, it is to be noted that polystyrene polymerized with $n\text{-BuLi}$ in the presence of LiOH had no fraction insoluble in methyl ethyl ketone, and the infrared spectrum of the polystyrene showed no stereoregularity.

The fact that M_n is almost twice as large as M_k is in conflict with the experimental results of Morton et al.⁴ There may be two reasons for the disagreement. One is that α -methylstyryl anion may attack THF at room temperature. The product may consume BuOH but does not participate in polymerization. However, it is unlikely that this is the main reason, considering the slow reaction rate between styryl anion and THF.²⁴ The other reason is that the dielectric constant of solvent (THF) is changed by addition of α -methylstyrene monomer and, hence, some of the α -methylstyryl anion may be associated in mixed solutions of THF and α -methylstyrene monomer. Only dissociated molecules should participate in polymerization. According to Morton et al.,²⁵ such association is ob-

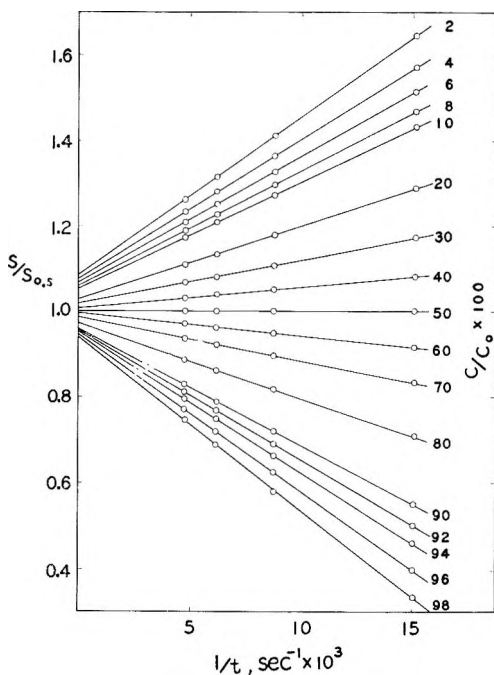


Fig. 10. Sedimentation velocity of poly- α -methylstyrene at various concentration points in its sedimentation pattern. Sample No. 3-1; solvent, cyclohexane; temp., 35°C.; initial concentration; 0.15%.

served in pure hydrocarbon solvents but is easily destroyed by addition of small amounts of THF at room temperature. However, the association might exist at -78°C ., as it is observed in the data of Morton et al.²⁵ that the degree of association increases with decreasing temperature. This is simply a speculation, but we can not find any other reason at present. The result was confirmed by repeated experiments and has no direct bearing on the remaining parts of this paper.

The interaction between the additives and the active centers may have an effect not only on the average molecular weight but also on the molecular weight distribution, because there must be an association-dissociation equilibrium between them. If free anions are liberated from the complex during polymerization or if growing chain ends are stopped by the additives from time to time, both must lead to broad molecular weight distribution. The weight-average (\bar{M}_w) and number-average (\bar{M}_n) molecular weights determined by light scattering and osmotic pressure measurements are listed in Table III, together with the ratio \bar{M}_w/\bar{M}_n . The molecular weight distributions of the polymers calculated from sedimentation experiments are shown in Figure 9, and the standard deviations of the distribution curves as well as the values of \bar{M}_w/\bar{M}_n calculated from the distribution curves are also listed in Table II. The ratio \bar{M}_w/\bar{M}_n determined from light scattering and osmotic pressure, which is usually used

to express the degree of polydispersity, is not accurate enough to express the polydispersity of a polymer having such a sharp molecular weight distribution. The values of \bar{M}_w/\bar{M}_n determined from the molecular weight distribution curves are more reliable. The molecular weight distribution of the polymer obtained in the presence of pure *n*-BuLi is found to be sharper than those of all other polymers prepared in the presence of additives. Its \bar{M}_w/\bar{M}_n is closer to unity than the values of all other polymers. Therefore, it may be concluded that there is an association-dissociation equilibrium between the additives and the active centers. Since the rate of depolymerization is very slow,^{8,9} it is not likely that this difference is caused by the influence of the equilibrium molecular weight distribution of "living" polymers which has $\bar{M}_w/\bar{M}_n = 2$.⁷ It was preliminarily confirmed that the molecular weight distribution of the product is not changed with polymerization time.

Combining these results, it may be concluded that the ability of additives to deactivate α -methylstyryl anion (probably by making a sort of complex) decreases in the order of $\text{LiBr} \approx \text{LiOH} > \text{LiOBu} > \text{LiN}(\text{Et})_2$ ($> n\text{-BuLi}$) which is the same as the order of nucleophilicity and opposite to the order of the ability to initiate polymerization of double bonds. In the present paper, however, we do not intend to explain the relationship between the abilities of complex formation and of initiating polymerization or to discuss the mechanism of complex formation.

The molecular weight distribution of poly- α -methylstyrene polymerized in the absence of additives is found to be extremely sharp compared with those of polymers so far published. To show the reliability of such sharp molecular weight distribution, the sedimentation velocity of molecules at various concentration points in the sedimentation pattern are shown in Figure 10, in relation to that at the half concentration point. S and $S_{0.5}$ are the sedimentation constants of molecules which are at the positions of concentration C and $0.5C_0$, respectively, (where C_0 denotes initial concentration). When $S/S_{0.5}$ is plotted against reciprocal time, all experimental points at the same C/C_0 are on straight lines. If the polymer were a monodisperse polymer, all straight lines at different C/C_0 should converge to unity at $1/t = 0$. The deviation from unity, as observed in Figure 10, is due to the deviation from monodispersity. $S/S_{0.5}$ is proportional to the ratio of the square roots of molecular weights, $\sqrt{\bar{M}}/\sqrt{\bar{M}_{0.5}}$.

The theoretical limit of the molecular weight distribution of polymer as polymerized by this way can be estimated as follows. If it is assumed that all α -methylstyryl anion initiates the polymerization of monomers at the same time when the solution is put in a Dry Ice-acetone bath and also that the deviation from monodispersity has only a statistical source, the distribution of polymerization degree must follow the Poisson distribution:⁷

$$f(n) = e^{-N}(N^n/n!) \quad (5)$$

where n is the degree of polymerization and N is the number-average de-

gree of polymerization. Then, the number-average and weight-average degrees of polymerization are as given in eqs. (6) and (7):

$$\sum_0^{\infty} nf(n) / \sum_0^{\infty} f(n) = N \quad (6)$$

$$\sum_0^{\infty} n^2 f(n) / \sum_0^{\infty} nf(n) = N + 1 \quad (7)$$

Thus, the ratio of weight-average and number-average molecular weights is given by

$$\bar{M}_w / \bar{M}_n = 1 + (1/N) \quad (8)$$

and the standard deviation is

$$\Delta M / M_n = [\sum_0^{\infty} (n-N)^2 f(n)]^{1/2} / N = 1/\sqrt{N} \quad (9)$$

Therefore, the theoretical limit for the present sample having $\bar{M}_n = 1.26 \times 10^4$ is $\bar{M}_w / \bar{M}_n = 1.001$ and, $\Delta M / M_n = 0.03$. The values obtained ($\bar{M}_w / \bar{M}_n = 1.003$ and $\Delta M / M_n = 0.09$) are very close to the limit, though still larger than the limit. We have, at present, no explanation for the deviation from the theoretical limits. Heterogeneity of temperature in the polymerization cell may be a reason and the association of α -methylstyryl anions in the mixture of THF and monomer may be another reason, if there is really association present.

After preparing the manuscript for the present study we found a paper by Waak and Daran on a similar subject.²⁶ The conclusions they obtained for phenyllithium and styrene in THF are analogous to our conclusions for *n*-BuLi and α -methylstyrene. However, there is a very distinct difference between the two papers. We found very strong interaction between *n*-BuLi and LiBr in THF, whereas they stated that there is no effect of LiBr to the reactivity of *n*-BuLi. We can not understand the difference since we confirmed by repeated experiments that *n*-BuLi containing LiBr in the mole ratio of 1:1 can polymerize not only α -methylstyrene but also styrene.

The present work was carried out with constant advice from Professor Ryuzo Asami of Nagoya Institute of Technology and Professor Yuya Yamashita of Nagoya University. The work would have been immeasurably more difficult without their advice. We wish to express our deepest thanks to both professors. We are also indebted to Dr. A. Takahashi and Mr. N. Kato for their aid in measuring light scattering and osmotic pressure.

References

1. McCormick, H. W., *J. Polymer Sci.*, **16**, 327 (1959).
2. Wenger, F., *Makromol. Chem.*, **64**, 151 (1963).
3. Hostalka, H., R. V. Figini, and G. V. Schulz, *Makromol. Chem.*, **71**, 198 (1964).
4. Morton, M., A. A. Rembaum, and J. L. Hall, *J. Polymer Sci.*, **A1**, 461 (1963).
5. Wenger, F., and S. P. S. Yen, *Makromol. Chem.*, **43**, 1 (1961).
6. Morton, M., E. E. Bostick, and R. Livigni, *Rubber Plastics Age*, **42**, 397 (1961).
7. Brown, W. B., and M. Szwarc, *Trans. Faraday Soc.*, **54**, 416 (1958).
8. McCormick, H. W., *J. Polymer Sci.*, **25**, 488 (1957).
9. Worsfold, D. J., and S. Bywater, *J. Polymer Sci.*, **26**, 299 (1957).

10. Wenger, F., *Makromol. Chem.*, **37**, 143 (1960).
11. O'Driscoll, K. F., and A. V. Tobolsky, *J. Polymer Sci.*, **35**, 259 (1959).
12. Welch, F. J., *J. Am. Chem. Soc.*, **82**, 6000 (1960).
13. Worsfold, D. J., and S. Bywater, *Makromol. Chem.*, **65**, 245 (1963).
14. Kern, R. J., *Nature*, **187**, 410 (1960).
15. Braun, D., W. Betz, and W. Kern, *Makromol. Chem.*, **42**, 89 (1960).
16. Ziegler, K., and H. Colonius, *Ann.*, **479**, 135 (1930).
17. Gilman, H., E. A. Zoellner, and W. M. Selby, *J. Am. Chem. Soc.*, **54**, 1957 (1932); *ibid.*, **55**, 1252 (1933); *ibid.*, **57**, 1061 (1935); *ibid.*, **63**, 2479 (1941).
18. *Kagaku-benran*, Chemical Society of Japan, ed. by S. Nagai, Maruzen, Tokyo, 1958, p. 121.
19. Pinner, S. H., *A Practical Course in Polymer Chemistry*, Pergamon Press, London, 1961, p. 90.
20. Outer, P., C. I. Carr, and B. H. Zimm, *J. Chem. Phys.*, **18**, 830 (1950).
21. Homma, T., K. Kawahara, H. Fujita, and M. Ueda, *Makromol. Chem.*, **67**, 132 (1963).
22. Cantow, H. J., *Makromol. Chem.*, **30**, 169 (1959).
23. McCormick, H. W., *J. Polymer Sci.*, **36**, 34¹ (1959).
24. Fetters, L. J., *J. Polymer Sci.*, **B2**, 425 (1964).
25. Morton, M., and L. J. Fetters, *J. Polymer Sci.*, **A2**, 3311 (1964).
26. Waak, R., and M. A. Daran, *Chem. Ind. (London)*, **1964**, 496.

Résumé

La polymérisation de l' α -méthyl-styrène avec du *n*-butyle-lithium a été effectuée dans le THF en présence de certains additifs tels que LiBr, LiOH, LiOBu, et LiN(Et)₂. On a observé le changement de couleur de l'anion α -méthyle styryle avec la teneur en additifs, l'activité du *n*-BuLi, les poids moléculaires moyens et les distributions des poids moléculaires des polymères obtenus en vue d'éclaircir l'interaction du *n*-BuLi (ou de l'anion α -méthyle styryle) avec ces additifs. On est arrivé à la conclusion que LiBr et LiOH désactivent l'initiateur dans le rapport molaire 1:1 et que uniquement la partie restante de *n*-BuLi participe à la polymérisation, tandis que LiOBu et LiN(Et)₂ ne le font pas. L'ordre des additifs quant au pouvoir de désactivation des centres actifs (peut-être par formation de complexe) suit l'ordre de nucléophilie et est inverse de l'ordre du pouvoir initiateur de polymérisation. La distribution du poids moléculaire du polymère obtenu au moyen de *n*-BuLi pur en absence d'additifs est extrêmement étroite.

Zusammenfassung

Die Polymerisation von α -Methylstyrol mit *n*-Butyllithium wurde in Gegenwart einiger Zusätze wie LiBr, LiOH, LiOBu, und LiN(Et)₂ in THF ausgeführt. Die Farbänderung des α -Methylstyrylanions mit der Menge der zugesetzten Stoffe, die Reaktivität des *n*-BuLi, das mittlere Molekulargewicht und die Molekulargewichtsverteilung der erhaltenen Polymeren wurden bestimmt, um Aufklärung über die Wechselwirkung von *n*-BuLi (oder des α -Methylstyrylanions) mit diesen Zusätzen zu erhalten. Man kam zu dem Schluss, dass LiBr und LiOH den Initiator im Molverhältnis 1:1 desaktivieren und dass nur der restliche Teil des *n*-BuLi an der Polymerisation teilnimmt, während LiOBu und LiN(Et)₂ nicht teilnehmen. Die Reihenfolge der Zusätze in der Fähigkeit, aktive Zentren zu desaktivieren (vielleicht durch Komplexbildung) entspricht der nukleophilen Reihenfolge und ist der Reihenfolge für die Startfähigkeit der Polymerisation entgegengesetzt. Die Molekulargewichtsverteilung des mit reinem *n*-BuLi in Abwesenheit von Zusätzen erhaltenen Polymeren war extrem scharf.

Received September 29, 1964

Revised December 7, 1964

(Prod. No. 4606A)

Raman Spectra of Polyethers*

YOSHIKI MATSUI and TANEKAZU KUBOTA, *Shionogi Research Laboratory, Shionogi & Co., Ltd., Fukushima-ku, Osaka, Japan*, and HIROYUKI TADOKORO and TOSHIO YOSHIHARA,† *Department of Polymer Science, Faculty of Science, Osaka University, Nakanoshima, Osaka, Japan*

Synopsis

Experimental techniques for the measurements of the Raman spectra of crystalline high polymers have been developed. The preparation of samples and a procedure for the measurements are described in some detail. The Raman spectra of polyoxymethylene ($-\text{CH}_2\text{O}-$)_n, deuterated polyoxymethylene ($-\text{CD}_2\text{O}-$)_n, poly(ethylene oxide) ($-\text{CH}_2\text{CH}_2\text{O}-$)_n, and polytetrahydrofuran ($-\text{CH}_2\text{CH}_2\text{CH}_2\text{CH}_2\text{O}-$)_n have been obtained. These results as well as the infrared data are interpreted on the basis of the factor group analyses and the normal coordinate treatments. The experimental results are in fairly good agreement with the results of the theoretical treatments for these polyethers.

INTRODUCTION

The first Raman spectrum of a high polymer, i.e., polystyrene, was observed by Signer and Weiler¹ in 1932, four years after the discovery of the Raman effect by Raman. It was not until twenty years later that the second spectrum, that of poly(methyl methacrylate)^{2,3} was observed. Recently, it has become possible to treat the vibrations of high polymers theoretically, so that the Raman spectra of the polymers have become much desirable. However, the Raman data on high polymers reported so far have been limited to the following polymers: polystyrene,^{1,4-6} poly(methyl methacrylate),^{2,3,6,7} polyethylene,⁸⁻¹⁰ polypropylene,^{6,9,11,12} poly-3-methyl-1-butene,⁶ poly(vinyl acetate),⁵ poly(acrylic acid ethyl ester),⁵ poly(acrylic acid).⁵

We have studied the structures of polyethers, expressed by the general formula, $[-(\text{CH}_2)_m-\text{O}-]$ _n. Of these the structure of polyoxymethylene (POM) has been determined by x-ray analysis,¹³ and the vibrational spectra of POM have been analyzed by the normal coordinate treatment.¹⁴ Poly(ethylene oxide) (PEO) and polytetrahydrofuran (PTHF) have also been extensively investigated in order to elucidate the relationships between the

* This paper was presented at the International Symposium on Molecular Structure and Spectroscopy (A-115), Tokyo, Japan, Sept. 1962.

† Present address: Research Laboratory, Mitsubishi Rayon Co., Ltd., Otake, Hiroshima, Japan.

structure and physical properties.¹⁵⁻¹⁷ As a part of these studies, we have developed sampling techniques for the measurement of the Raman spectra of crystalline high polymers and obtained good Raman spectra of these polymers.

In this paper we should like to report the experimental procedures for measuring Raman spectra of these polyethers and the interpretation of the spectra obtained. Parts of the results of the present work have already been reported, together with the infrared data.^{18,19}

EXPERIMENTAL

The Raman spectra were photographed with a model RL-II Raman spectrograph constructed by the Yuki-Gosei-Yakuhin Co., Ltd. The reciprocal linear dispersion is 15 Å./mm. at 4358 Å. A part of the apparatus is shown in Figure 1. The main improvement of the apparatus used for the measurement on solid samples is a means of eliminating the undesired light (shown by the dotted lines in Figure 1) reflections on the surfaces of the right-angled prism; this arrangement will be reported elsewhere in detail.²⁰

The conditions of the measurements are as follows. The exciting light used was from a mercury lamp (4358 Å.). The mercury lamp was used

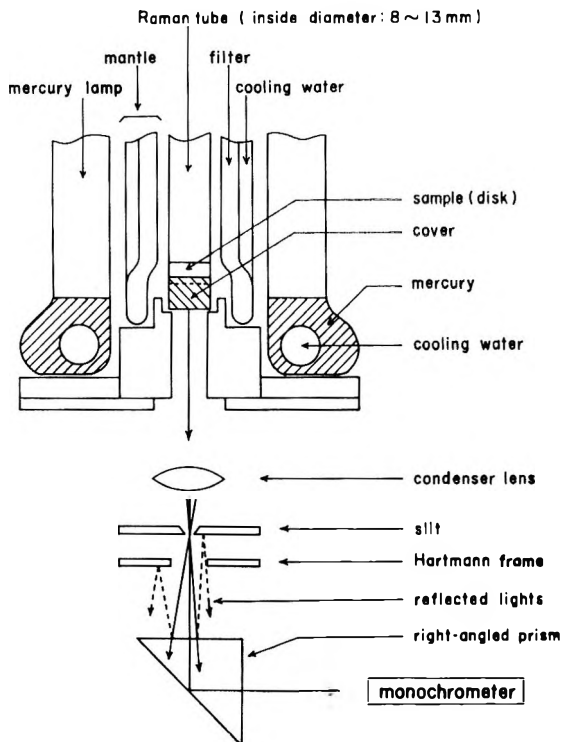


Fig. 1. Apparatus.

with an electric current of 15–20 amp. in order to reduce the other mercury lines, although the maximum current of this lamp is 30 amp. The exposure time was 2–6 hr. Neopan SSS film and Pandol (a fine grading developer), both manufactured by the Fuji Photo Film Co., Ltd., were used at a development time of 7 min. at 20°C. As a filter, a saturated solution of potassium nitrite was always used. In some cases, the Raman tube was coated with Rhodamine 5GDN in order to reduce unwanted mercury lines in the region of 4800–5700 Å.

SPECIMENS AND OBSERVED RESULTS

Polyoxymethylene

Delrin acetal resin (du Pont), a high molecular weight POM, and paraformaldehyde, a low molecular weight POM, were examined. In the case of Delrin acetal resin, no Raman line was observed because of heavy background, probably due to some fluorescent impurities, while in the case of paraformaldehyde several Raman lines were observed. In the latter case, the spectra measured on the powder form of the polymer were compared with those obtained on pressed disks, and it was found that a better spectrum can be obtained in the case of the disk form than the powder form. The disk was prepared by the pressing disk technique for the in-

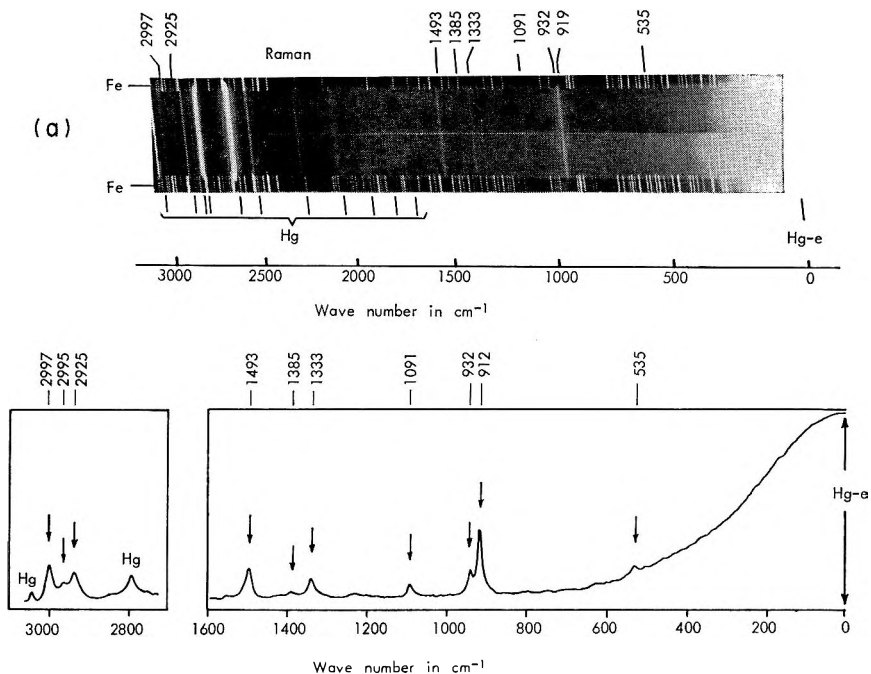


Fig. 2. Raman spectra of polyoxymethylene (paraformaldehyde): (a) photograph and (b) microphotometer curve.

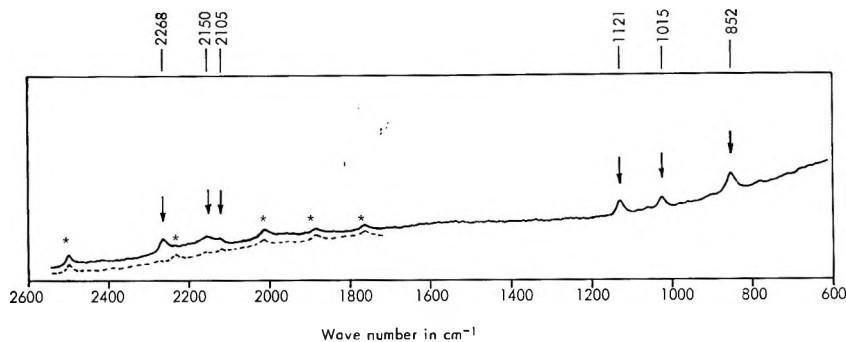


Fig. 3. Raman spectrum (microphotometer curve) of polyoxymethylene- d_2 (paraformaldehyde- d_2). A part of the spectrum of paraformaldehyde is reproduced with dotted line for comparison. The asterisk (*) denotes the lines of the mercury lamp.

frated measurements. A disk 11 mm. in diameter and about 3 mm. in thickness (about 0.5 g.) was found to give the best spectrum.

In Figure 2 the Raman spectra, both as a photograph and in the form of a microphotometer curve of POM (paraformaldehyde) are shown. The spectrum of paraformaldehyde- d_2 (Merck & Company, Inc.) was also measured by this method, and several bands were observed, as shown in Figure 3.

Poly(ethylene Oxide)

Carbowax 4000, Carbowax 6000, and Carbowax 20-M (Carbide & Carbon Chemicals Corp.) were examined. Considerable background appeared in all these spectra, especially in the case of Carbowax 20-M. This background may be due to some fluorescent impurities. All of these specimens were purified by repeated reprecipitation by cooling concentrated acetone solutions prepared at about 50°C. down to 0°C. These attempts were partly successful for Carbowax 4000 and Carbowax 6000, but not for Carbowax 20-M. Of these specimens, Carbowax 6000 gave the best spectrum and Carbowax 20-M gave only two lines because of heavy background. The spectra were measured on the disk form samples of 13 mm. in diameter and 8 mm. in thickness (about 1 g.). The Raman spectrum is shown in Figure 4. The low frequency Raman lines were not so clear as the high frequency lines (solid line in Fig. 4), but they were confirmed thereafter more clearly by using a Cary 81 spectrophotometer (dotted line in Fig. 4a).*

Polytetrahydrofuran

Low molecular weight ($[\eta] = 1.6$) and high molecular weight ($[\eta] = 3.0$) specimens¹⁷ were examined. The low molecular weight specimen gave better spectra than the high molecular weight one, just as in the case of the

* By courtesy of Miss M. Matsushima, Government Chemical Industrial Research Institute of Tokyo.

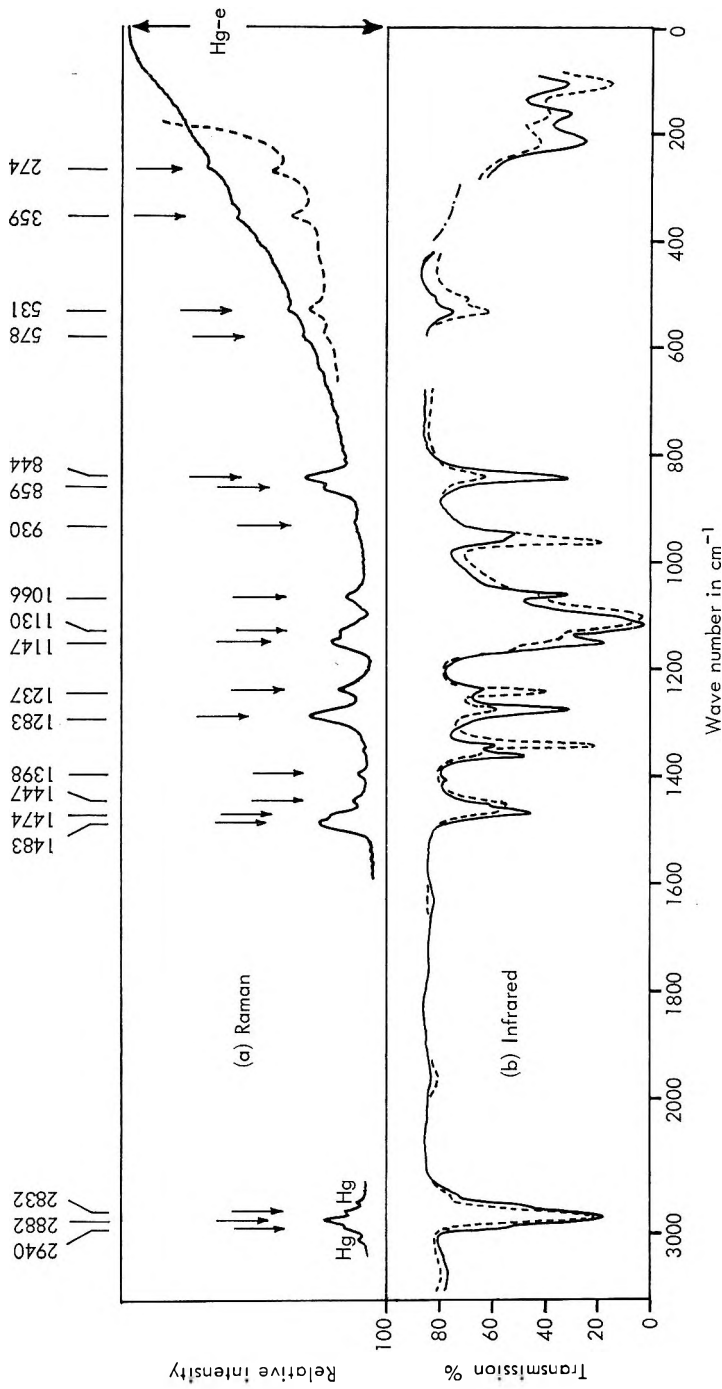


Fig. 4. (a) Raman spectra of poly(ethylene oxide) (Carbowax 6000): (—) microphotometer curve; (---) the curve measured by a Cary 81 spectrophotometer. (b) Polarized infrared spectra of poly(ethylene oxide): (—) electric vector perpendicular to elongation; (---) electric vector parallel to elongation.

other polyethers. The low molecular weight specimen was measured in the form of a disk, 11 mm. in diameter and about 6 mm. in thickness (about 1 g.). Several Raman lines were observed, as shown in Table VI, although they were obscured by a background of medium intensity.

DISCUSSION

Polyoxymethylene

The POM molecule in the crystalline state has a helical conformation which contains nine chemical units ($-\text{CH}_2\text{O}-$) and five turns in a fiber identity period of 17.3 Å,¹³ as shown in Figure 5a. The fundamental

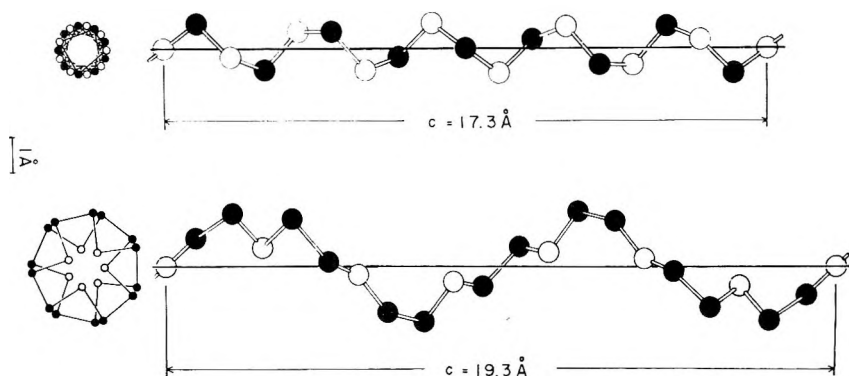


Fig. 5. Skeletal models of (a) polyoxymethylene^{13,16} and (b) poly(ethylene oxide):¹⁶ (O) oxygen atom; (●) methylene group.

TABLE I
Number of Normal Frequencies and Selection Rules for Polyoxymethylene under the Factor Group $D(10\pi/9)$

| Species | N^a | Infrared ^b | Raman ^b |
|---------|-------------------------------------|-----------------------|--------------------|
| A_1 | 5 | F | A |
| A_2 | $7-2(T_{\parallel}, R_{\parallel})$ | A (\parallel) | F |
| E_1 | $12-1(T_{\perp})$ | A (\perp) | A |
| E_2 | 12 | F | A |
| E_3 | 12 | F | F |
| E_4 | 12 | F | F |

^a N : number of normal frequencies under each symmetry species. T_{\parallel} and T_{\perp} : pure translations parallel and perpendicular to the helix axis, respectively. R_{\parallel} : pure rotation about the axis.

^b A: active, F: forbidden. \parallel or \perp indicates that the oscillating electric vector is parallel or perpendicular, respectively, to the helix axis.

vibrational modes of an infinitely extended helical molecule of POM may be treated by the factor group $D(10\pi/9)$.^{*} The number of normal frequencies and selection rules for this molecule are given in Table I. The

* For the notations of factor groups used here, see the paper by Liang and Krimm.²¹

Raman spectra are quite important for the analyses of the A_1 and E_2 species, since the vibrations of these species are active only in Raman spectra. For the A_1 species, five bands are expected and were observed, as shown in Figure 2 and Table II. The Raman bands at 919, 1333, and

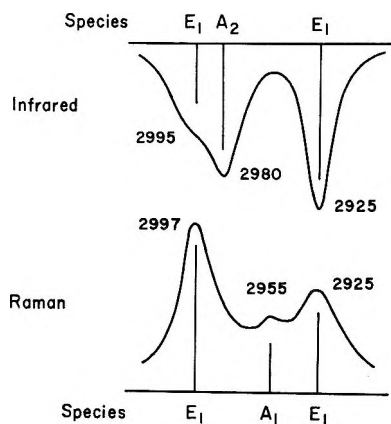


Fig. 6. Infrared and Raman spectra of polyoxymethylene (paraformaldehyde) in the region of 2900–3000 cm^{-1} .

TABLE II
Infrared and Raman Spectra of Polyoxymethylene

| Species | Observed, cm^{-1} | | Calcd. cm^{-1} | Assignment ^a |
|---------|----------------------------|----------|----------------------------|---|
| | Infrared | Raman | | |
| A_1 | | 535 w | 587 | $\delta(\text{COC}), \delta(\text{OCO})$ |
| | | 919 s | 916 | $\nu_s(\text{COC}), \delta(\text{OCC})$ |
| | Inactive | 1333 m | 1330 | $t(\text{CH}_2)$ |
| | | 1493 m | 1508 | $\delta(\text{CH}_2)$ |
| | | 2955 w | 2924 | $\nu_s(\text{CH}_2)$ |
| A_2 | 235(∥)w | | 237 | τ_n |
| | 903(∥)vvs | | 922 | $r(\text{CH}_2), \nu_s(\text{COC})$ |
| | 1097(∥)vvs | Inactive | 1118 | $\nu_a(\text{COC}), r(\text{CH}_2)$ |
| | 1381(∥)m | | 1425 | $w(\text{CH}_2)$ |
| | 2978(∥)s | | 2977 | $\nu_s(\text{CH}_2)$ |
| E_1 | — | | 22 | τ_{s1}, τ_n |
| | 455(⊥)m | | 483 | $\delta(\text{COC}), r(\text{CH}_2)$ |
| | 630(⊥)s | | 634 | $\delta(\text{COC}), \nu_a(\text{COC})$ |
| | 932(⊥)vvs | 932 w | 930 | $\nu_s(\text{COC}), r(\text{CH}_2)$ |
| | 1091(⊥)vvs | 1091 w | 1072 | $\nu_a(\text{COC}), \delta(\text{OCO})$ |
| | 1235(⊥)vs | | 1169 | $r(\text{CH}_2), \delta(\text{COC}), \nu_s(\text{COC})$ |
| | 1286(⊥)vw | | 1318 | $t(\text{CH}_2)$ |
| | 1434(⊥)w | | 1407 | $w(\text{CH}_2)$ |
| | 1471(⊥)m | | 1506 | $\delta(\text{CH}_2)$ |
| | 2924(⊥)s | 2925 m | 2926 | $\nu_s(\text{CH}_2)$ |
| | 2980(⊥)s | 2997 s | 2982 | $\nu_s(\text{CH}_2)$ |

^a ν : stretching, ν_a : antisymmetric stretching, ν_s : symmetric stretching, δ : bending, w : wagging, t : twisting, r : rocking, τ : torsion.

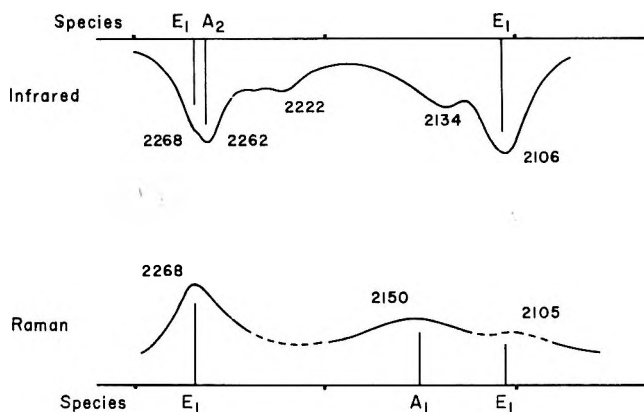


Fig. 7. Infrared and Raman spectra of polyoxymethylene- d_2 (paraformaldehyde- d_2) in the region of 2100–2300 cm^{-1} .

1493 cm^{-1} have been reported already.^{14,18} The Raman band at 535 cm^{-1} was predicted to appear below 600 cm^{-1} by the calculations.^{14,18} The weak band at 2955 cm^{-1} was recently confirmed by the microphotometer curve and assigned to the A_1 species, so that the infrared and Raman bands in the region of 2900–3000 cm^{-1} are reasonably explained as shown in Figure 6. Similar assignments are also held for the bands of paraformaldehyde- d_2 in the region of 2100–2300 cm^{-1} as shown in Figure 7, although the Raman band at 2105 cm^{-1} is not so clear.*

Poly(ethylene Oxide)

It was found by x-ray analysis that the PEO molecule in the crystalline state has a helical conformation which contains seven chemical units ($-\text{CH}_2\text{CH}_2-\text{O}-$) and two or five turns in a fiber identity period of 19.3 Å.¹⁶ However, it was difficult to obtain a more detailed structure analysis by x-ray methods alone, since each unit cell contains four molecular chains. Here the vibrational analysis of this molecule played an important role in the determination of the molecular structure.†

The fundamental modes of infinitely extended helical molecule of PEO may be treated by the cyclic factor group $C(4\pi/7)$ or $C(10\pi/7)$ or the dihedral factor group $D(4\pi/7)$ or $D(10\pi/7)$, according to whether the helical chain possesses two kinds of twofold axes or not: one passing through the oxygen atom and the other bisecting the C—C bond. The determination of whether the molecule comes under the cyclic or the dihedral groups, is to be made by the vibrational analysis.

* The band frequencies of POM, 2979 (\perp) and 2919 (\perp), and those of POM- d_2 , 2235 (\parallel), 2235 (\perp), and 2105 (\perp) reported in a previous paper¹⁴ should be corrected as 2980 (\perp), 2924 (\perp), 2263 (\parallel), 2263 (\perp), and 2106 (\perp), respectively, according to the more accurate measurement.

† Detailed descriptions of the structure determination and the vibrational analysis of PEO are given in refs. 16 and 22, respectively.

TABLE III
Number of Normal Frequencies and Selection Rules for Poly(ethylene Oxide) under the
Factor Group $C(4\pi/7)$ or $D(4\pi/7)$

| Groups | Species | N | Infrared | Raman |
|-------------|---------|--|-------------------|-------|
| $C(4\pi/7)$ | A | 21-2($T_{\parallel}, R_{\parallel}$) | A (\parallel) | A |
| | E_1 | 21-1(T_{\perp}) | A (\perp) | A |
| | E_2 | 21 | F | F |
| | E_3 | 21 | F | F |
| $D(4\pi/7)$ | A_1 | 10 | F | A |
| | A_2 | 11-2($T_{\parallel}, R_{\parallel}$) | A (\parallel) | F |
| | E_1 | 21-1(T_{\perp}) | A (\perp) | A |
| | E_2 | 21 | F | A |
| | E_3 | 21 | F | F |

Table III shows the numbers of the normal frequencies and the selection rules for a PEO molecule under the factor groups $C(4\pi/7)$ and $D(4\pi/7)$. The result of the factor group analysis for $C(10\pi/7)$ is the same as that for $C(4\pi/7)$, because these two factor groups are isomorphous to each other. The same holds for the factor groups $D(10\pi/7)$ and $D(4\pi/7)$. In the case of the cyclic group, the species of parallel infrared bands is A , and 19 infrared bands should be observed. In the case of the dihedral group, the species of parallel infrared bands is A_2 , and only 9 bands should be observed. Furthermore, in this case it is expected that 10 modes are only Raman active and no Raman bands should be observed at the same frequencies of the parallel infrared bands.

According to the view of the group frequencies, the 9 A_2 vibrational modes allowed for the factor group $D(4\pi/7)$ or $D(10\pi/7)$, may consist of two CH_2 stretching, and one each for CH_2 bending, CH_2 wagging, CH_2 twisting, CH_2 rocking, COC stretching, COC bending vibrations and one for torsional vibration of the skeleton. In fact, 9 parallel infrared bands which are reasonable for the fundamental modes, appear in the range from 3000 to 100 cm^{-1} as shown in Figure 4 and Table IV. Furthermore, no Raman lines are found at the same frequencies as those of the parallel infrared bands. In this way, it was established that the PEO molecule has dihedral symmetry. In other words, the helical chain possesses two types of twofold axis mentioned above.

By assuming the bond length $\text{C—O} = 1.43 \text{ \AA}$, $\text{C—C} = 1.54 \text{ \AA}$, and the bond angles $\angle \text{OCC} = \angle \text{COC} = 109^\circ 28'$ (tetrahedral angle), two types of models with $D(4\pi/7)$ symmetry were found as follows: model I [internal rotation angle $\tau(\text{CCOC}) = 188^\circ 15'$ and $\tau(\text{OCCO}) = 64^\circ 58'$] and model II [$\tau(\text{CCOC}) = 111^\circ$, $\tau(\text{OCCO}) = 202^\circ 26'$]. As for the factor group $D(10\pi/7)$, none was obtained under these restrictions for the bond lengths and bond angles.

Thereafter it has been established by the results of the normal coordinate treatments based on the infrared and Raman data of PEO and PEO- d_4 that model I is the most reasonable for the PEO molecule.^{16,22} This was

TABLE IV
 Infrared and Raman Spectra of Poly(ethylene Oxide) and Assignments and Calculated Frequencies

| Observed, cm. ⁻¹ | | Calcd., cm. ⁻¹ | Species | Assignment ^a |
|-----------------------------|---------|------------------------------|-----------------------|--|
| Infrared | Raman | | | |
| | | 92 | <i>E</i> ₁ | $\tau(\text{CO})_i$ |
| 106 m () | | 108 | <i>A</i> ₂ | $\tau(\text{CO})_o$ |
| 165 w (⊥) | | 162 | <i>E</i> ₁ | $\tau(\text{CC}), \tau(\text{CO})_o$ |
| 215 w (⊥) | | 211 | <i>E</i> ₁ | $\delta(\text{OCC})_i, \delta(\text{OCC})_o, \delta(\text{COC})$ |
| | | | | $\tau(\text{CC})$ |
| | | 212 | <i>A</i> ₁ | $\delta(\text{COC}), \tau(\text{CO})_i$ |
| | 274 w | 270 | <i>A</i> ₁ | $\delta(\text{OCC})_i, \delta(\text{COC})$ |
| | 359 w | 366 | <i>E</i> ₁ | $\delta(\text{COC}), \delta(\text{OCC})_i$ |
| 508 w | | | | |
| 530 w () | | 544 | <i>A</i> ₂ | $\delta(\text{OCC})_o$ |
| 532 w (⊥) | 531 w | 501 | <i>E</i> ₁ | $\delta(\text{OCC})_o$ |
| | 578 vw | | | |
| 844 s (⊥) | 844 s | 856 | <i>E</i> ₁ | $\tau(\text{CH}_2)_o$ |
| | 859 m | 876 | <i>A</i> ₁ | $\tau(\text{CH}_2)_i, \nu(\text{CO})_i$ |
| 947 m (⊥) | 930 vw | 924 | <i>E</i> ₁ | $\tau(\text{CH}_2)_i, \nu(\text{CO})_i$ |
| 958 s () | | 884 | <i>A</i> ₂ | $\tau(\text{CH}_2)_o$ |
| 1060 m (⊥) | | 1033 | <i>E</i> ₁ | $\tau(\text{CH}_2)_i, \nu(\text{CO})_i, \nu(\text{CO})_o$ |
| | 1066 m | 1093 | <i>A</i> ₁ | $\nu(\text{CO})_i, \tau(\text{CH}_2)_i$ |
| 1103 vs () | | 1061 | <i>A</i> ₂ | $\nu(\text{CO})_o$ |
| 1116 s (⊥) | | 1110 | <i>E</i> ₁ | $\nu(\text{CC}), \nu(\text{CO})_i$ |
| | 1130 m | 1138 | <i>A</i> ₁ | $\nu(\text{CC}), w(\text{CH}_2)_i$ |
| 1147 s (⊥) | 1147 s | 1161 | <i>A</i> ₂ | $\nu(\text{CO})_o$ |
| | | 1243 | <i>A</i> ₁ | $t(\text{CH}_2)_i$ |
| 1234 w (⊥) | 1237 m | 1250 | <i>E</i> ₁ | $t(\text{CH}_2)_i, t(\text{CH}_2)_o$ |
| 1240 m () | | 1280 | <i>A</i> ₂ | $t(\text{CH}_2)_o$ |
| 1278 m (⊥) | 1283 s | 1282 | <i>E</i> ₁ | $t(\text{CH}_2)_o, t(\text{CH}_2)_i$ |
| 1342 s () | | 1386 | <i>A</i> ₂ | $w(\text{CH}_2)_o$ |
| 1358 m (⊥) | | 1354 | <i>E</i> ₁ | $w(\text{CH}_2)_i, \nu(\text{CC})$ |
| | 1398 w | 1381 | <i>A</i> ₁ | $w(\text{CH}_2)_i, \nu(\text{CC})$ |
| 1411 w (⊥) | | 1396 | <i>E</i> ₁ | $w(\text{CH}_2)_o$ |
| 1448 sh (⊥) | 1447 w | 1470 | <i>E</i> ₁ | $\delta(\text{CH}_2)_i$ |
| 1457 m () | | 1471 | <i>A</i> ₂ | $\delta(\text{CH}_2)_o$ |
| 1466 m (⊥) | 1474 sh | 1474 | <i>E</i> ₁ | $\delta(\text{CH}_2)_o$ |
| | 1483 s | 1473 | <i>A</i> ₁ | $\delta(\text{CH}_2)_i$ |
| 2805 w | | | | |
| 2825 w | 2832 m | | | |
| 2862 sh | | | | |
| 2885 s | 2882 s | | | |
| 2950 w | 2940 w | | | |

^a The subscripts *i* and *o* denote the in-phase and out-of-phase modes in the structural unit O—CH₂—CH₂—O. The other symbols are the same as those in Table II.

also supported by the x-ray diffraction study.¹⁶ Figure 5*b* shows the skeletal model of PEO (model I) drawn in the same scale as the model of POM in Figure 5*a*. The structure of model I is the succession of the nearly *trans*, *trans*, and *gauche* conformations.

It may be mentioned here that, although the calculation of the normal vibrations was carried out without the low frequency Raman data, the results of the calculation for model I agreed with the observed Raman band at 274, 359, and 531 cm^{-1} , which was observed after the calculation had been made (Fig. 4 and Table IV).

Polytetrahydrofuran

The molecular and crystal structure of PTHF has been analyzed and reported already.^{15,17} According to these results, the PTHF molecule has an essentially planar zigzag conformation, as shown in Figure 8. Consequently, the fundamental vibrational modes of the PTHF molecule may be treated under the factor group D_{2h} .¹⁷ Because of the existence of the center of symmetry, the rule of mutual exclusion is expected for this

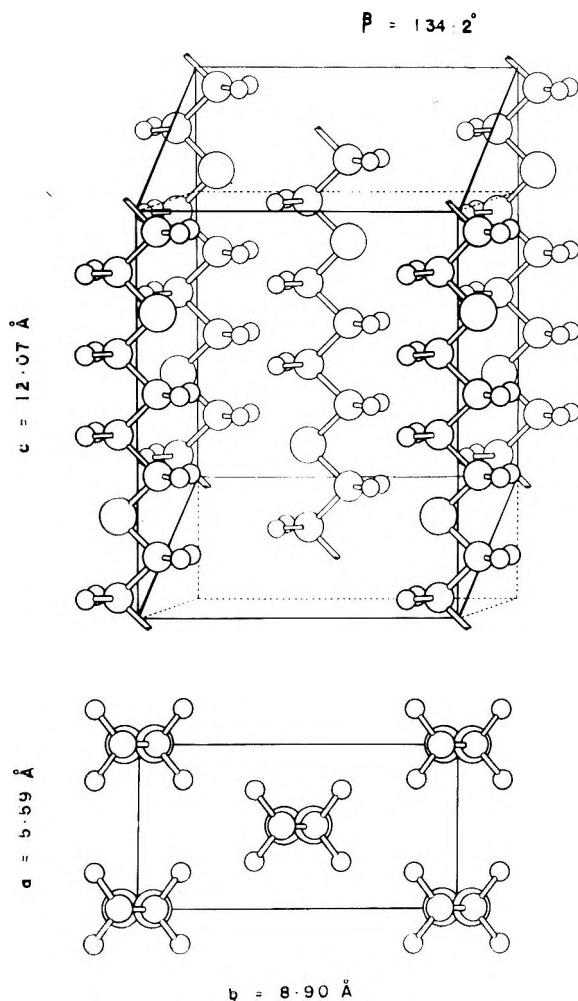


Fig. 8. Crystal structure of polytetrahydrofuran.^{15,17}

molecule as shown in Table V. In fact, this rule may be considered to hold for the Raman and infrared spectra (Table VI).

TABLE V
Number of Normal Frequencies and Selection Rule for Polytetrahydrofuran under the Factor Group D_{2h}

| Species | N^a | Infrared | Raman |
|----------|----------------|----------|-------|
| A_g | 11 | F | A |
| B_{1g} | 11 | F | A |
| B_{2g} | 8 | F | A |
| B_{3g} | 9-1 (R_z) | F | A |
| A_u | 8 | F | F |
| B_{1u} | 9-1 (T_z) | A | F |
| B_{2u} | 11-1 (T_y) | A | F |
| B_{3u} | 11-1 (T_x) | A | F |

^a The directions of the x , y , and z axes were assumed as follows: x : parallel to the molecular chain axis; y : parallel to the molecular plain, and perpendicular to the molecular axis; z : perpendicular to the molecular plane.

TABLE VI
Infrared and Raman Spectra of Polytetrahydrofuran

| Infrared, cm. ⁻¹ | Raman, cm. ⁻¹ | Assignment ^a |
|--------------------------------|-----------------------------|-------------------------|
| 565 m | | Skeletal deformation |
| 744 w | | $r(\text{CH}_2)$ |
| 995 s | | $\nu_s(\text{COC})$ |
| 1009 m | | Skeletal stretching |
| 1106 vvs | | $\nu_a(\text{COC})$ |
| | 1149 m | Skeletal stretching |
| 1207 s | | $t(\text{CH}_2)$ |
| 1230 w | | $w(\text{CH}_2)_2$ |
| 1250 m | | $w(\text{CH}_2)_2$ |
| | 1295 m | $w(\text{CH}_2)$ |
| 1370 s | | $w(\text{CH}_2)_1$ |
| | 1455 m | $\delta(\text{CH}_2)$ |
| 1460 w | | $\delta(\text{CH}_2)_2$ |
| 1476 w | | $\delta(\text{CH}_2)_1$ |
| | 1492 m | $\delta(\text{CH}_2)$ |
| 1495 m | | $\delta(\text{CH}_2)_1$ |
| 2804 m | | $\nu_s(\text{CH}_2)_1$ |
| | 2810 w | |
| 2863 w | | $\nu_s(\text{CH}_2)_2$ |
| | 2870 m | $\nu_s(\text{CH}_2)_2$ |
| 2920 sh | | |
| | 2930 w | $\nu_a(\text{CH}_2)$ |
| 2946 s | | $\nu_a(\text{CH}_2)$ |
| | 2955 vw | |

^a The $(\text{CH}_2)_1$ and $(\text{CH}_2)_2$ indicate the α and β methylenes, respectively ($\text{O}-\overset{\alpha}{\text{CH}_2}-\overset{\beta}{\text{CH}_2}$). The other symbols are the same as those in Table II.

The authors wish to express their gratitude to Professor S. Murahashi of Osaka University and Dr. T. Nakagawa of Shionogi Research Laboratory for the valuable discussions and to Mr. K. Iwatani of this laboratory for assisting in the experiments.

We (Y. M. and T. K.) also thank Dr. K. Takeda, Director of Shionogi Laboratory, for permission to publish this work.

References

1. Signer, R., and J. Weiler, *Helv. Chim. Acta*, **15**, 649 (1932).
2. Hibben, J. H., *J. Chem. Phys.*, **5**, 706 (1937).
3. Palel, M. M., *Current Sci. (India)*, **18**, 436 (1949).
4. Palm, A., *J. Phys. Chem.*, **55**, 1320 (1951).
5. Simon, A., M. Mücklich, D. Kunath, and G. Heintz, *J. Polymer Sci.*, **30**, 201 (1958).
6. Ferraro, J. R., J. S. Ziomek, and G. Mack, *Spectro Chim. Acta*, **17**, 802 (1961).
7. Sirkar, S. C., and N. K. Roy, *J. Chem. Phys.*, **21**, 938 (1953).
8. Nielsen, J. R., and A. H. Woollett, *J. Chem. Phys.*, **26**, 1391 (1957).
9. Tobin, C. M., *J. Phys. Chem.*, **64**, 216 (1960).
10. Brown, R. G., *J. Chem. Phys.*, **38**, 221 (1963).
11. Tobin, C. M., *J. Opt. Soc. Am.*, **49**, 850 (1959).
12. Nikitin, V. N., and L. I. Maklakov, *Opt. Spectry. (USSR)*, **13**, 343 (1962).
13. Tadokoro, H., T. Yasumoto, S. Murahashi, and I. Nitta, *J. Polymer Sci.*, **44**, 266 (1960).
14. Tadokoro, H., M. Kobayashi, Y. Kawaguchi, A. Kobayashi, and S. Murahashi, *J. Chem. Phys.*, **38**, 703 (1963).
15. Tadokoro, H., Y. Chatani, M. Kobayashi, T. Yoshihara, S. Murahashi, and K. Imada, *Repts. on Progr. Polymer Phys. Japan*, **6**, 303 (1963).
16. Tadokoro, H., Y. Chatani, T. Yoshihara, and S. Murahashi, *Makromol. Chem.*, **73**, 109 (1964).
17. Imada, K., T. Miyakawa, Y. Chatani, H. Tadokoro, and S. Murahashi, *Makromol. Chem.*, in press.
18. Tadokoro, H., A. Kobayashi, Y. Kawaguchi, S. Sobajima, S. Murahashi, and Y. Matsui, *J. Chem. Phys.*, **35**, 369 (1961).
19. Matsui, Y., T. Kubota, and H. Tadokoro, *Bunko Kenkyū*, **10**, 107 (1962).
20. Matsui, Y., and K. Iwatani, *Bull. Chem. Soc. Japan*, to be published.
21. Liang, C. Y., and S. Krimm, *J. Chem. Phys.*, **25**, 563 (1956).
22. Yoshihara, T., H. Tadokoro, and S. Murahashi, *J. Chem. Phys.*, **41**, 2902 (1964).

Résumé

On a mis au point des techniques expérimentales pour mesurer les spectres Raman des polymères cristallins. La préparation des échantillons, ainsi que le procédé de mesure sont décrits en détails. On a obtenu les spectres Raman du polyoxyméthylène ($-\text{CH}_2\text{O}-$)_n, du polyoxyméthylène deutéré ($-\text{CD}_2\text{O}-$)_n, du polyoxyéthylène ($-\text{CH}_2\text{CH}_2\text{O}-$)_n et du polytétrahydrofuranne ($-\text{CH}_2\text{CH}_2\text{CH}_2\text{CH}_2\text{O}-$)_n. Ces résultats ainsi que ceux obtenus par analyse infra-rouge sont interprétés sur la base des analyses de groupe de facteurs et des calculs en coordonnées normales. Les résultats expérimentaux sont en très bon accord avec les résultats théoriques obtenus pour ces polyéthers.

Zusammenfassung

Versuchsmethoden zur Messung des Raman-Spektrums kristalliner Hochpolymerer wurde entwickelt. Die Darstellung der Proben sowie das Messverfahren werden im einzelnen beschrieben. Die Raman-Spektren von Polyoxymethylen ($-\text{CH}_2\text{O}-$)_n, deuteriertem Polyoxymethylen ($-\text{CD}_2\text{O}-$)_n, Polyäthylenoxyd ($-\text{CH}_2\text{CH}_2\text{O}-$)_n und Polytetrahydrofuran ($-\text{CH}_2\text{CH}_2\text{CH}_2\text{CH}_2\text{O}-$)_n wurden erhalten. Diese Ergebnisse

sowie die Infrarotdaten werden auf Grundlage der Faktorgruppenanalyse und des Normalkoordinatenverfahrens interpretiert. Die Versuchsergebnisse stehen mit dem Ergebnis der theoretischen Behandlung bei diesen Polyäthern in ziemlich guter Übereinstimmung.

Received October 14, 1964
(Prod. No. 4608A)

Electron Spin Resonance Studies on Oriented Polyoxymethylene

HIROSHI YOSHIDA and BENGT RÅNBY, *Department of Polymer
Technology, Royal Institute of Technology, Stockholm, Sweden*

Synopsis

Electron spin resonance spectra of stretched polyoxymethylene irradiated with γ -rays from a Co^{60} source were studied. With suitable treatment three kinds of spectra were selectively observed: doublet with irradiation and measurement at room temperature; singlet with irradiation and measurement at about -180°C .; triplet with the irradiation at about -180°C . and the measurement at -102°C . The doublet and the triplet spectra showed anisotropy, while the singlet did not. These observations confirm the assignment of the spectra so far reported with unoriented polyoxymethylene, i.e., $-\dot{\text{C}}\text{H}_2-\text{O}$, $-\text{O}-\dot{\text{C}}\text{H}-\text{O}-$, $-\text{O}-\dot{\text{C}}\text{H}_2$ for the singlet, doublet, and triplet, respectively. The doublet spectrum is treated as related to the anisotropic hyperfine coupling tensor, the anisotropic g value and the chain conformation in crystalline polyoxymethylene. A rather small value, $\rho \approx 0.45$, was obtained for the spin density at the central carbon atom.

Introduction

Electron spin resonance (ESR) spectra of irradiated polyoxymethylene (POM) have been reported by several authors.¹⁻⁵ Among them, extensive studies were made on singlet and triplet spectra of POM irradiated at -196°C . by Marx and Chachaty,² on doublet spectra with the polymer irradiated at room temperature by Lenk,⁴ who studied mainly the effect of irradiation dose on spectral shape, and on the same doublet spectra by Neiman et al.,⁵ who studied mainly the kinetics of radical recombinations. In previous work, three kinds of ESR spectra were observed from irradiated POM: singlet, doublet, and triplet spectra, and these were attributed to the radical structures, $-\text{CH}_2-\dot{\text{O}}$, $-\text{O}-\dot{\text{C}}\text{H}-\text{O}-$, and $-\text{O}-\dot{\text{C}}\text{H}_2$, respectively.

In general, irradiated polymers give ESR spectra with less well resolved structures because of anisotropic hyperfine splittings. Since the first successful observations by Kiselev et al. of well resolved ESR spectra of oriented polyethylene,⁶ however, many ESR studies have been made with oriented polymers to derive more detailed and reliable information of free radicals in irradiated polymers, e.g., with polyethylene,⁷⁻¹⁰ polypropylene,^{11,12} and polyamides.¹³

In the present investigation, the anisotropy of ESR spectra was studied with stretched POM in order to clarify the assignments of the ESR spectra

in previous studies where unoriented POM was used. In all POM spectra studied, anisotropy was observed. Especially, the doublet spectrum which is stable at room temperature showed a marked anisotropy. The hyperfine structure of the doublet spectrum is treated as determined by the anisotropic hyperfine coupling tensor the anisotropy of the g values, and the chain conformation in crystalline POM.

Experimental

Celcon polyoxymethylene (Celanese Corp.) was used. The Celcon granules were pressed at 180°C. into a 1-mm. thick sheet. A strip of the sheet was stretched at 150°C. to 6-7 times the original length. An x-ray diffraction study of the stretched sheet showed a good orientation of the polymer chain lattice in the stretching direction. Delrin POM (E. I. du Pont de Nemours Co.) was also examined. The Delrin sheets received a sixfold elongation at 175°C. After irradiation, Celcon and Delrin gave similar ESR spectra, except for some slight differences which are discussed later. Most of the present investigation was done with Celcon, which seems to be a purer POM sample than Delrin and more suitable for our work.

Irradiation was carried out in a Co^{60} γ -cell at a dose rate of 0.3 mrad/hr. under a vacuum better than 10^{-4} mm. Hg. ESR measurements were made with an x-band spectrometer model JES-3B from Japan Electron Optics Laboratory Co. High frequency field modulation (100 kcycles) was used with the modulation width of 2 gauss. The g values were measured with reference to the spectrum of diphenylpicrylhydrazyl (DPPH) powder ($g = -2.0036$) as a standard with an experimental accuracy of ± 0.0001 . ESR spectra were recorded with different angles (ϑ) between the stretching direction of the polymer samples and the applied magnetic field. The angles were varied by rotation of the samples in a rectangular TE_{102} sample cavity.

Observed Spectra

Free radicals with a short lifetime in irradiated POM disappeared completely within about 1 day after irradiation at room temperature. The stable ESR spectra of POM irradiated and measured at room temperature were doublets (cf. Fig. 1) which were attributed to radicals of the structure $-\text{O}-\dot{\text{C}}\text{H}-\text{O}-$.^{1,3-5} As expected from the radical structure having a σ -proton directly bonded to an unsaturated carbon,¹⁴ the doublet spectra showed a remarkably anisotropic hyperfine structure. A doublet separation of 15.6 gauss was observed with the applied magnetic field parallel to the stretching direction of the sample ($\vartheta = 0^\circ$), and 11.5 gauss with the magnetic field perpendicular to the stretching direction ($\vartheta = 90^\circ$). These data correspond to the separation of ~ 13 gauss reported by Lenk⁴ for the unoriented polymer. The g values also showed marked anisotropy, giving -2.0039 for $\vartheta = 90^\circ$ as the smallest and -2.0054 for $\vartheta = 0^\circ$ as the largest

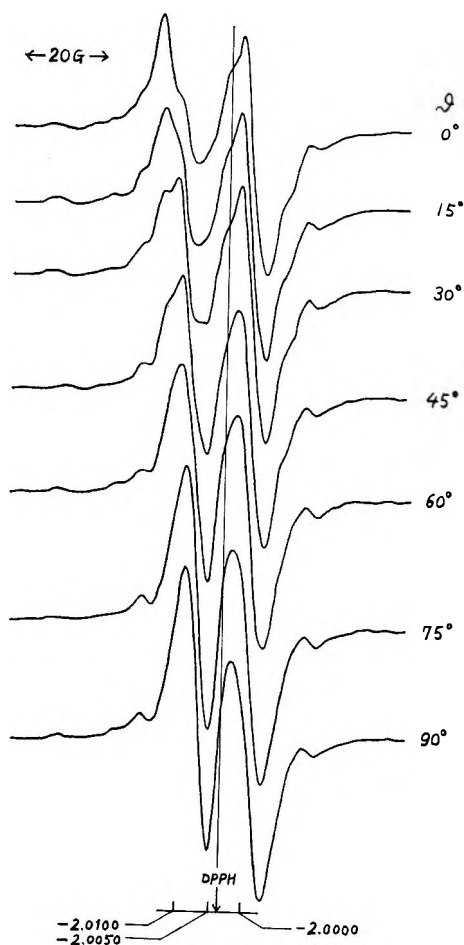


Fig. 1. ESR spectra of POM (Celcon) irradiated at room temperature with 12 Mrad γ -rays from Co^{60} and observed at 22°C.

value. Moreover, asymmetry was observed with the magnetic field applied around $\vartheta = 0^\circ$.

The doublet spectra were also examined at different temperatures ranging from -196°C . to 22°C . Some examples of observed spectra for $\vartheta = 0^\circ$ and $\vartheta = 90^\circ$ are shown in Figure 2. The hyperfine splitting became somewhat smaller with decreasing temperature for $\vartheta = 90^\circ$, but it remained unchanged for $\vartheta = 0^\circ$. Moreover, the asymmetry of the spectra increased at lower temperatures e.g., for $\vartheta = 0^\circ$ the spectrum showed considerable asymmetry at -196°C . Such a temperature dependence of spectral shape may, of course, be due to freezing of some molecular motions in POM, but it cannot be interpreted from the experimental results obtained so far. Neiman et al. reported that the width of each hyperfine component increased with decreasing temperature,⁵ but such effects were not observed in the present investigation of stretched polymer.

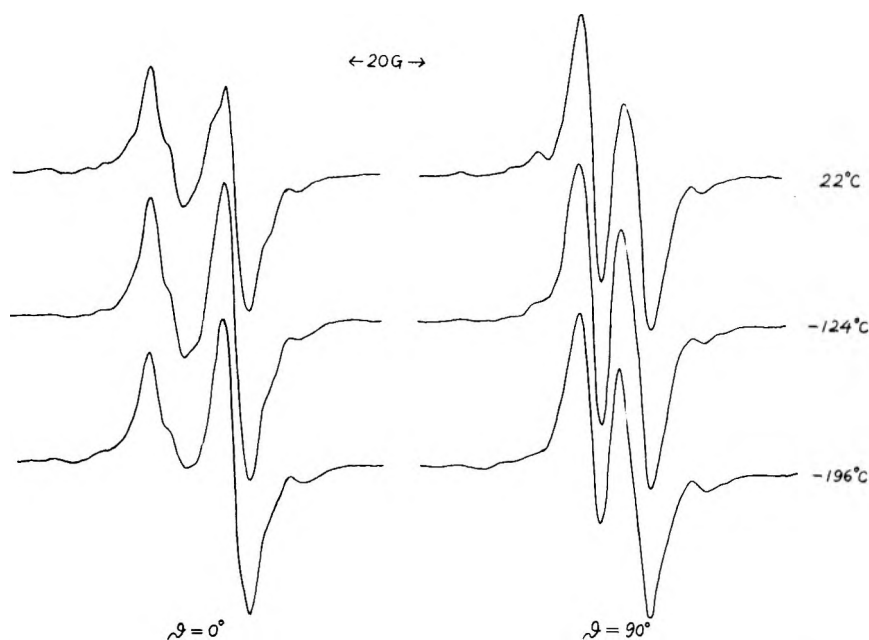


Fig. 2. ESR spectra of POM (Celcon) irradiated at room temperature with 12 Mrad and observed at different temperatures with two orientations, $\vartheta = 0^\circ$ and $\vartheta = 90^\circ$.

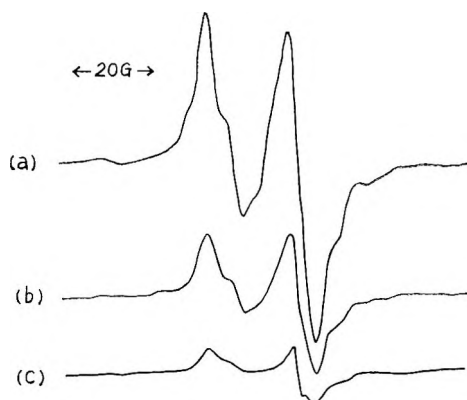


Fig. 3. Change of ESR spectra of POM (Celcon) irradiated at room temperature with 12 Mrad and observed at 22°C . for $\vartheta = 0^\circ$: (a) original spectra, (b) after heating to 80°C . for 10 min., and (c) to 105°C . for 7 min.

The intensity of the doublet spectra decreased with heating of the irradiated POM sample to higher temperature, as shown in Figure 3. Although less than 20% of original free radicals survived after heating to 105°C . for 7 min., the observed spectral shape was very similar to that of the original doublet spectrum. This observation suggests that most free radicals in POM, irradiated and measured at room temperature, are of the same molecular structure, presumably $-\text{O}-\dot{\text{C}}\text{H}-\text{O}-$.

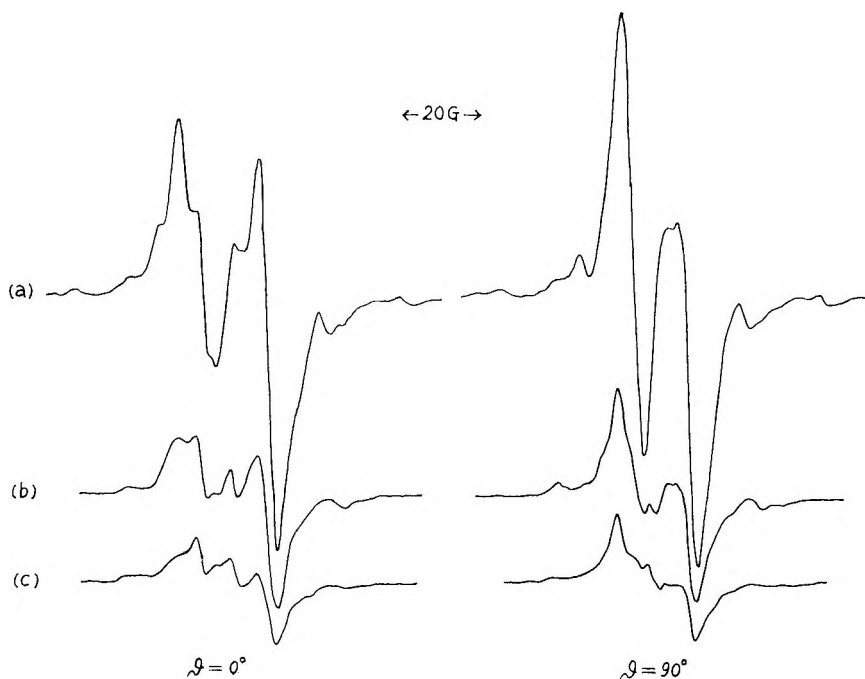


Fig. 4. Change of ESR spectra of POM (Delrin) irradiated at room temperature with 12 Mrad and observed at 22°C.; (a) original spectrum; (b) after heating to 100°C. for 15 min.; and (c) after heating to 110°C. for 10 min., with two orientations, $\vartheta = 0^\circ$ and $\vartheta = 90^\circ$.

For comparison, a Delrin sample was also examined in the same way as Celcon. Delrin irradiated at room temperature gave ESR spectra, shown in Figure 4a, which are similar to those of Celcon except some indications of other structures. Irradiated Delrin, after heating to high temperature, gave a trace of another spectrum which seemed to be an anisotropic triplet as shown in Figure 4c. The trace spectrum, probably due to a minor amount of polyamide (nylon) added to the polyoxymethylene in Delrin, is superimposed on the main spectrum, causing a slight difference in the original doublet spectra of Celcon and Delrin, respectively.

POM irradiated at about -180°C . (liquid air temperature) gave, at the same temperature, a singlet spectrum with somewhat less well resolved structures. The structures showed anisotropy, especially at the central part of the spectrum, as shown in Figure 5. The main singlet was, however, isotropic, with a line width between maximum slope points of 17 gauss. The isotropic singlet spectrum can be attributed to the radical structure $-\text{CH}_2-\text{O}\cdot$ having no σ -proton. This spectrum seems to correspond to the asymmetric singlet spectrum observed by Marx and Chachaty² and also to the one more vaguely reported by Sasakura et al.³

POM samples irradiated at about -180°C . gave complicated spectra at the measuring temperature of -102°C ., as recorded in Figure 6. The

spectra showed a remarkable anisotropy and consisted mainly of a triplet. The spectrum around $\vartheta = 90^\circ$ seems to be similar to those obtained for unoriented polymer as reported in earlier papers.^{2,3,5} Our data indicate (Fig. 6) that the triplet separation has a largest value ≤ 19 gauss and that each hyperfine component has the narrowest line width for $\vartheta = 0^\circ$, while the separation becomes smaller and the width of each component becomes broader with larger values of ϑ . The above mentioned value (≤ 19 gauss) is not in contradiction to that previously reported (17–18 gauss).²

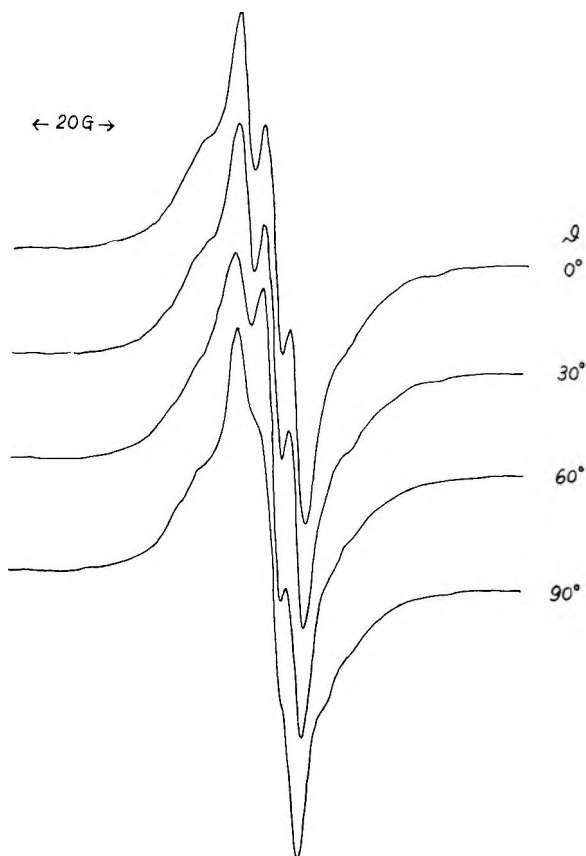


Fig. 5. ESR spectra of POM (Celcon) irradiated with 2 Mrad and observed at about -180°C . (liquid air temperature).

Considering the conformation of the molecular chains in stretched POM (later discussed in detail), it seems reasonable to assume that the free radicals in POM giving doublet spectra orient more preferentially than those giving singlets and triplets, and that σ -protons give a larger hyperfine separation with the magnetic field nearer to $\vartheta = 0^\circ$. Accordingly, the assignment of the triplet spectra as being due to the radical structure $-\text{O}-\dot{\text{C}}\text{H}_2$ is well in line with the observed change of the spectra.

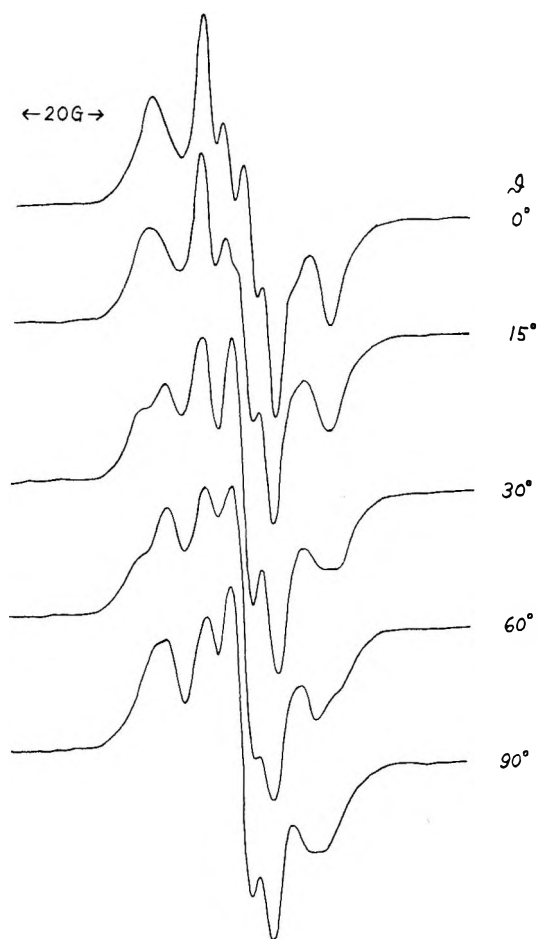


Fig. 6. ESR spectra of POM (Celcon) irradiated at about -180°C . (liquid air temperature) with 2 Mrad, and observed at -102°C .

With further warming of POM irradiated at about -180°C ., ESR spectra became weaker and more asymmetric. This observation is interpreted to mean that the free radicals $-\text{O}-\dot{\text{C}}\text{H}-\text{O}-$ become relatively more predominant because of the disappearance of $-\text{O}-\dot{\text{C}}\text{H}_2$, e.g., by hydrogen extraction or combination.

In conclusion, at least three kinds of ESR spectra, doublet, singlet, and triplet, respectively, were selectively observed in irradiated POM with suitable treatment. Based mainly on the anisotropy, these three spectra were assigned to the radical structures, $-\text{O}-\dot{\text{C}}\text{H}-\text{O}-$, $-\dot{\text{C}}\text{H}_2-\text{O}$, and $-\text{O}-\dot{\text{C}}\text{H}_2$, respectively. Although the assignments of the three spectra in the present investigation are in accordance with those of Sasakura et al.³ the triplet spectra were, contrary to their observations but in agreement with those of Marx and Chachaty,² more stable than the singlet spectra.

Discussion

As the observed anisotropy of the singlet and the triplet spectra are too complex to be analyzed, the discussion in this section will be limited mainly to the anisotropic doublet spectra of irradiated POM.

In studies of radiation damage in organic single crystals, several authors have observed anisotropic ESR spectra of organic free radicals. Especially, McConnell et al.¹⁵ gave a generalized theory of anisotropic hyperfine splitting due to the σ -proton of the $\text{HOOC}-\dot{\text{C}}\text{H}-\text{COOH}$ radicals in irradiated malonic acid. Considering the hydrogen involved, the free radicals studied by McConnell et al. resemble the free radicals $-\text{O}-\dot{\text{C}}\text{H}-\text{O}-$ in irradiated POM.

According to their theory,¹⁵ the anisotropic hyperfine splitting due to the σ -protons is expressed in terms of a hyperfine coupling tensor. One σ -proton splits an ESR line into two sets of doublets with a separation expressed as follows:

For an outer doublet:

$$D_+ = \left[\left(\nu_p - \rho \frac{A}{2} \right)^2 \alpha^2 + \left(\nu_p - \rho \frac{B}{2} \right)^2 \beta^2 + \left(\nu_p - \rho \frac{C}{2} \right)^2 \gamma^2 \right]^{1/2} \\ + \left[\left(\nu_p + \rho \frac{A}{2} \right)^2 \alpha^2 + \left(\nu_p + \rho \frac{B}{2} \right)^2 \beta^2 + \left(\nu_p + \rho \frac{C}{2} \right)^2 \gamma^2 \right]^{1/2} \quad (1)$$

For an inner doublet:

$$D_- = \left[\left(\nu_p - \rho \frac{A}{2} \right)^2 \alpha^2 + \left(\nu_p - \rho \frac{B}{2} \right)^2 \beta^2 + \left(\nu_p - \rho \frac{C}{2} \right)^2 \gamma^2 \right]^{1/2} \\ - \left[\left(\nu_p + \rho \frac{A}{2} \right)^2 \alpha^2 + \left(\nu_p + \rho \frac{B}{2} \right)^2 \beta^2 + \left(\nu_p + \rho \frac{C}{2} \right)^2 \gamma^2 \right]^{1/2} \quad (2)$$

In eqs. (1) and (2), α , β , and γ are direction cosines of the applied magnetic field with respect to the axes fixed to the free radicals as shown in Figure 7, and A , B , and C are the principal values of the hyperfine coupling tensor along the axes, a , b , and c , respectively. ν_p is the magnetic field strength corresponding to the proton magnetic resonance frequency with the applied

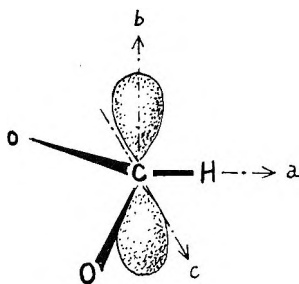


Fig. 7. The abc -coordinate system fixed on the free radical having one σ -proton in irradiated POM.

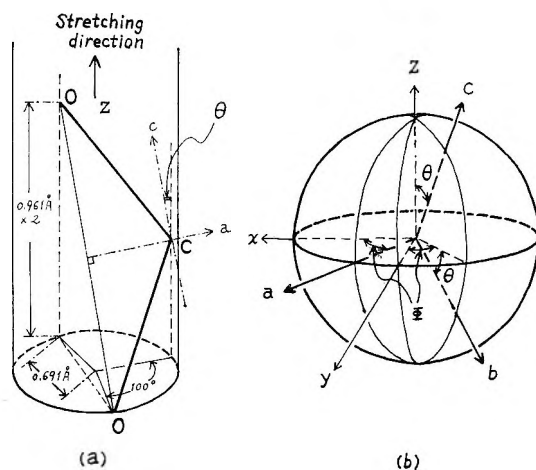


Fig. 8. Orientation of the $-\dot{\text{C}}\text{H}-$ free radical in POM; (a) polymer chain conformation in the stretched sample, and (b) the relation between abc -coordinate system fixed to the free radical and xyz -coordinate system fixed to the stretched sample.

magnetic field, and it is equal to 5.3 gauss in the x-band used in the present ESR investigation. ρ is the spin density of radical electrons on the central carbon atom.

It is derived from the theory that, when $D_+ \gg 2\nu_p$, the outer doublet is much stronger than the inner and, accordingly, the latter is negligible (this is the usual case with the ESR in x-band). Conversely, when $D_- \ll 2\nu_p$, the outer doublet is negligible. But, when $D_+ \approx D_- \approx 2\nu_p$, two sets of doublets have a comparable intensity.

Following the above-mentioned theory, the anisotropic hyperfine splitting due to a σ -proton was calculated by Kashiwagi¹³ for the free radicals in a uniaxially stretched polymer with planar zigzag polymer chains, with the assumption that the g value of the spectra (the center position of the spectra) is isotropic. The calculations were referred to an ESR study of irradiated polyamides. The chain conformation of POM in the crystalline state is more complicated. No principal axis of the hyperfine coupling tensor coincides with the stretching direction, because the chains are in a spiral form (9_5 -type spiral).

It is assumed, as in previous papers,^{13,15} that (1) the crystallization and the orientation of the polymer chains are complete, (2) each atom in the chain (except the σ -proton) has the same position as before the formation of the free radicals, and (3) that the σ -proton is coplanar with the O—C—O segment and that C—H bond bisects the O—C—O angle of the original chain. Using the knowledge of chain conformation for POM obtained by x-ray studies,¹⁶ the orientation of the free radical is as shown in Figure 8a. The a axis fixed on a free radical, which is the C—H bond direction, is always in a plane perpendicular to the stretching direction. The c axis is always inclined at $35^\circ 19'$ from the stretching direction. Taking an

xyz -coordinate system fixed on a sample with the stretching direction in the z axis, the relation between the abc and the xyz systems is defined in terms of the angles Θ and Φ , as in Figure 8*b*. The angle Θ is constant ($35^\circ 19'$ for POM) and the Φ values are distributed uniformly from 0° to 360° .

Taking the direction cosines of the applied magnetic field with respect to the xyz coordinate system as $(\sin \vartheta \cos \zeta, \sin \vartheta \sin \zeta, \cos \vartheta)$, where ϑ is the angle between the magnetic field and the stretching direction of the sample (the value depends on the experimental conditions) and ζ is distributed uniformly from 0° to 360° , the direction cosines (α, β, γ) are expressed as follows:

$$\begin{aligned}\alpha &= \sin \vartheta (\cos \zeta \cos \Phi + \sin \zeta \sin \Phi) \\ \beta &= \sin \vartheta (\sin \zeta \cos \Phi - \cos \zeta \sin \Phi) \cos \Theta - \cos \vartheta \sin \Theta \\ \gamma &= \sin \vartheta (\sin \zeta \cos \Phi - \cos \zeta \sin \Phi) \sin \Theta + \cos \vartheta \cos \Theta\end{aligned}\quad (3)$$

For $\vartheta = 0^\circ$, D_+ and D_- are independent of ζ and Φ , and the following relations are obtained:

$$\begin{aligned}D_{\pm} &= \left[\left(\nu_p - \rho \frac{B}{2} \right)^2 \sin^2 \Theta + \left(\nu_p - \rho \frac{C}{2} \right)^2 \cos^2 \Theta \right]^{1/2} \\ &\pm \left[\left(\nu_p + \rho \frac{B}{2} \right)^2 \sin^2 \Theta + \left(\nu_p + \rho \frac{C}{2} \right)^2 \cos^2 \Theta \right]^{1/2}\end{aligned}\quad (4)$$

For $\vartheta = 90^\circ$, D_+ and D_- are functions of ζ and Φ :

$$\begin{aligned}D_{\pm} &= \left[\left(\nu_p - \rho \frac{A}{2} \right)^2 (\cos \zeta \cos \Phi + \sin \zeta \sin \Phi)^2 + \left\{ \left(\nu_p - \rho \frac{B}{2} \right)^2 \cos^2 \Theta \right. \right. \\ &\quad \left. \left. + \left(\nu_p - \rho \frac{C}{2} \right)^2 \sin^2 \Theta \right\} (\sin \zeta \cos \Phi - \cos \zeta \sin \Phi)^2 \right]^{1/2} \\ &\pm \left[\left(\nu_p + \rho \frac{A}{2} \right)^2 (\cos \zeta \cos \Phi + \sin \zeta \sin \Phi)^2 + \left\{ \left(\nu_p + \rho \frac{B}{2} \right)^2 \cos^2 \Theta \right. \right. \\ &\quad \left. \left. + \left(\nu_p + \rho \frac{C}{2} \right)^2 \sin^2 \Theta \right\} (\sin \zeta \cos \Phi - \cos \zeta \sin \Phi)^2 \right]^{1/2}\end{aligned}\quad (5)$$

McConnell and Strathdee¹⁷ calculated the values of A , B , and C theoretically and obtained -7.5 , -24.6 , and -36.8 gauss respectively. Using these values and $\Theta = 35^\circ 19'$, the expected D_+ and D_- values were calculated as a function of ζ from eq. (4) for the doublet splitting due to the σ -protons (cf. Fig. 9). The observed value of the splitting is 15.6 gauss for $\vartheta = 0^\circ$ at 22°C ., from which a spin density (ρ) of about 0.45 is derived.

The recorded spectra for $\vartheta = 90^\circ$ are the sum of the component spectra of all possible orientations with respect to ζ and Φ . An apparent splitting of the doublet spectrum can be estimated with some assumption about the shape of the component spectra, the D values of which are distributed as eq. (5). When resonance curves are synthesized from eq. (5) by use of the

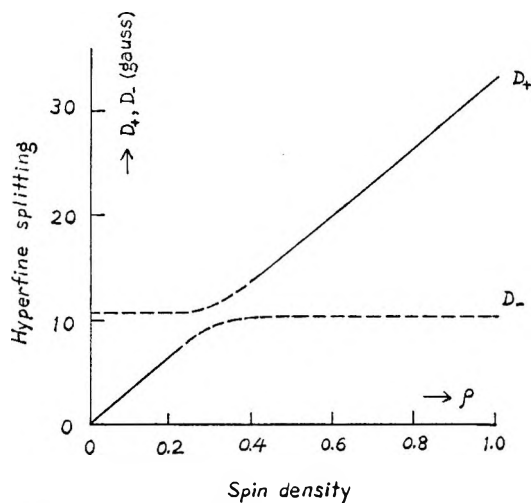


Fig. 9. Hyperfine doublet splitting due to a σ -proton in stretched POM vs. the spin density ρ on the central carbon atom for $\vartheta = 0^\circ$. The solid curves represent the doublet which is more intense than the other.

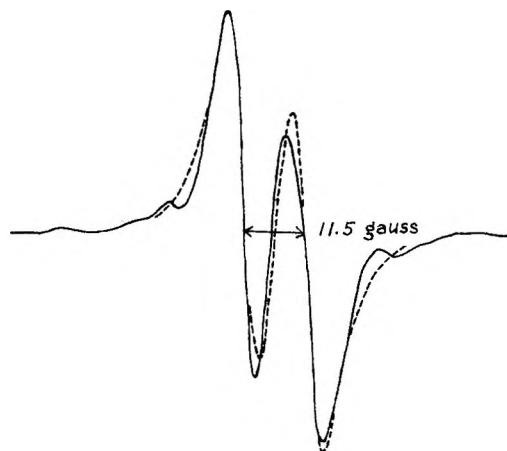


Fig. 10. ESR spectrum observed for $\vartheta = 90^\circ$ and spectrum calculated from eq. (5) with the assumption that each component spectrum has Lorentzian shape with the width between the maximum slope points 7 gauss: (—) observed; (--) calculated.

value $\rho = 0.45$ and with the assumption of Lorentzian shape and the width 7 gauss between the maximum slope points for the component spectra, good fitting with the observed doublet spectrum is obtained at 22°C . (cf. Fig. 10). The assumption of Gaussian shape does not give good fitting. With the assumed width of 7 gauss for the component spectra, the apparent doublet splitting for $\vartheta = 0^\circ$ is only 0.3 gauss smaller than the D value obtained from eq. (4), the difference being due to overlapping of the doublet lines. Accordingly, the interpretation of the spectrum for $\vartheta = 90^\circ$ is consistent with the value $\rho \approx 0.45$ obtained from the spectrum for $\vartheta = 0^\circ$.

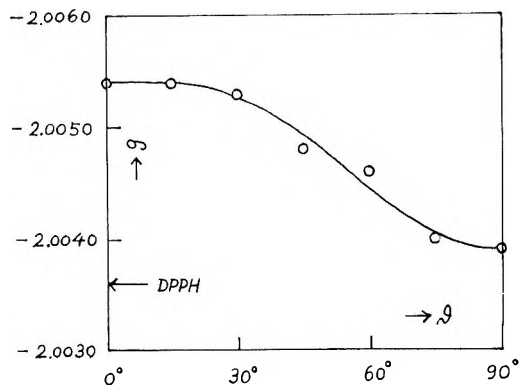


Fig. 11. Dependence of g factor on ϑ for the doublet spectra of irradiated POM.

The doublet spectra always showed a significant asymmetry for small values of ϑ . The asymmetry is, in general, caused by (1) other spectra superimposed on the doublet spectra, (2) distortion of the spectral shape due to microwave power saturation, and (3) anisotropic g factor. The asymmetry of the doublet spectra, reported by Lenk,⁴ which disappeared gradually at room temperature, seems to be caused by superposition of other spectra, presumably the triplet spectrum mentioned in the preceding section. The asymmetry observed in the present investigation is not the same as that observed by Lenk, since it was observed only with small values of ϑ and it was, showing no decrease with time, inherent to the doublet spectra. The effect of microwave power was examined within the range of about 1–10 mw., at -196°C ., but no change of the spectral shape was observed. This means that the asymmetry cannot be attributed to distortion of spectra due to microwave power saturation.

A possible cause of the asymmetry is the anisotropic g factor. Based on the observed spectra in Figure 1, the g factor is plotted in Figure 11 as a function of ϑ . Although the g factors observed for the uniaxially oriented free radicals in POM were averaged in a complicated way, the variation of the g factor was more pronounced than that observed for $-\dot{\text{C}}\text{H}-$ type free radicals by McConnell et al.¹⁵ and Atherton and Whiffen.¹⁸ Because of this anisotropic g factor as well as the anisotropic hyperfine splitting, the observed spectra were asymmetric at small ϑ values for the stretched polymer. As a result, the positions of the hyperfine component at lower magnetic fields were widely distributed corresponding to each possible orientation of the free radicals. The positions of the higher field component on the other hand were distributed over a narrow region because the anisotropic effects of both g factor and hyperfine coupling accidentally cancelled each other.

According to the theoretical treatment of the g factor in aromatic radicals, it is suggested that g factors with the magnetic field along b and c axes, (g_b and g_c in Fig. 7) are larger than those along the a axis (g_a).^{14,19} It is

difficult to analyze in detail the observed anisotropic g factor of uniaxially oriented free radicals because of the fact that the a , b , c axes do not agree with the principal axes of the g tensor.¹⁸ Considering the molecular chain conformation in POM as in Figure 8a, however, it is true that the observed g factor with $\vartheta = 0^\circ$ depends mainly on g_c and the g factor with $\vartheta = 90^\circ$ mainly on g_a and g_b . The observed dependence of the g factor on ϑ is, therefore, in agreement with the theoretical predictions. According to the same treatment, the remarkable anisotropy of the g factor may be attributed to the adjacent oxygen atoms, of which the spin-orbit coupling is much stronger than that of carbon atoms.

In conclusion, free radicals of the $-\text{O}-\dot{\text{C}}\text{H}-\text{O}-$ type in stretched POM with doublet spectra gave pronounced anisotropy. Although the observed hyperfine splitting constant was less reliable because of the complicated conformation of the molecular chains in POM, the remarkably anisotropic g factor, and probably the overlapping of the weaker doublet due to forbidden transitions, the spin density on the central carbon atom of the free radical, which was obtained from McConnell's theory of hyperfine interaction between π -electron and σ -proton, was rather low ($\rho \approx 0.45$) compared to the spin densities obtained for $\text{HOOC}-\dot{\text{C}}\text{H}-\text{COOH}$ in irradiated malonic acid ($\rho \approx 1.0$),¹⁵ $-\text{CH}_2-\dot{\text{C}}\text{H}-\text{CH}_2-$ in irradiated polyethylene ($\rho \approx 1.0$)^{10,20} and $-\text{NH}-\dot{\text{C}}\text{H}-\text{CH}_2-$ in irradiated polyamides ($\rho \approx 0.7$).¹³ Such a low spin density leaves still interesting problems in connection with the effect of heteroatoms in free radicals and the effect of the distortion in molecular conformation (the internal rotation angle of the POM molecular chain deviates from 60° , the value for undistorted configuration, to $77^\circ 23'$)¹⁶ on hyperfine interaction.

It is more complicated to discuss the anisotropy of the triplet spectra due to the free radical, $-\text{O}-\dot{\text{C}}\text{H}_2$. The two C—H bonds are more randomly oriented than the C—H bond in the free radical, $-\text{O}-\dot{\text{C}}\text{H}-\text{C}-$, contributing to the sp^2 configuration of the carbon atom at the chain end. Moreover, the crystalline structure may be more or less destroyed in the vicinity of main chain fractures. Although the orientation of the free radicals, $-\text{O}-\dot{\text{C}}\text{H}_2$, in stretched POM may be less regular than $-\text{O}-\dot{\text{C}}\text{H}-\text{O}-$, the axis along which the hyperfine coupling constant is largest (c axis in Fig. 8a, 2 axes per one free radical $-\text{O}-\dot{\text{C}}\text{H}_2$) lies on the average, preferentially along the stretching direction of the polymer. This prediction is in agreement, qualitatively, with the observed spectra.

The authors wish to express their thanks to Prof. L. Ehrenberg and his co-workers for making available their Co⁶⁰ irradiation facilities. This investigation was supported by Malmfonden (Swedish Foundation for Scientific and Industrial Development).

References

1. Tsvetkov, Yu. D., Yu. N. Molin, and V. V. Voevodskii, *Vysokomol. Soedin.*, **1**, 1805 (1959).
2. Marx, R., and M. C. Chachaty, *J. Chem. Phys.*, **58**, 527 (1961).
3. Sasakura, H., N. Takeuchi, and T. Mizuno, *J. Phys. Soc. Japan*, **17**, 572 (1962).
4. Lenk, R., *Czech. J. Phys.*, **12**, 833 (1962).

5. Neiman, M., T. S. Fedoseeva, G. V. Chubarova, A. L. Buchachenko and Ya. S. Lebedev, *Vysokomol. Soedin.*, **5**, 1339 (1963).
6. Kiselev, A. G., M. A. Mokul'sky, and Yu. S. Lazulkin, *Vysokomol. Soedin.*, **2**, 1678 (1960).
7. Libby, D., and M. G. Ormerod, *Phys. Chem. Solids*, **18**, 316 (1961).
8. Kashiwagi, M., *J. Chem. Phys.*, **36**, 575 (1962).
9. Ohnishi, S., S. Sugimoto, and I. Nitta, *J. Chem. Phys.*, **37**, 1283 (1962).
10. Solovey, R., and W. A. Yager, *J. Polymer Sci.*, **A2**, 219 (1964).
11. Fischer, H., and K.-H. Hellwege, *J. Polymer Sci.*, **56**, 33 (1962).
12. Fischer, H., K.-H. Hellwege, and P. Neudörfel, *J. Polymer Sci.*, **A1**, 2109 (1963).
13. Kashiwagi, M., *J. Polymer Sci.*, **A1**, 189 (1963).
14. Heller, C., and H. M. McConnell, *J. Chem. Phys.*, **32**, 1535 (1960).
15. McConnell, H. M., C. Heller, T. Cole, and R. W. Fessenden, *J. Am. Chem. Soc.*, **82**, 766 (1960).
16. Tadokoro, H., T. Yasumoto, S. Murahashi, and I. Nitta, *J. Polymer Sci.*, **44**, 266 (1960).
17. McConnell, H. M., and J. Strathdee, *Mol. Phys.*, **2**, 129 (1959).
18. Atherton, N. M., and D. H. Whiffen, *Mol. Phys.*, **3**, 1 (1960).
19. McConnell, H. M., and R. E. Robertson, *J. Phys. Chem.*, **61**, 1018 (1957).
20. Higuchi, J., *J. Chem. Phys.*, **39**, 2366 (1963).

Résumé

On a étudié les spectres de résonance de spin électronique du polyoxy-méthylène étiré et irradié par des rayons gamma provenant d'une source de Co^{60} . Moyennant des traitements appropriés, il est possible d'observer sélectivement trois types de spectres: le doublet par irradiation avec mesure à température de chambre, le singulet par irradiation avec mesure à environ -180°C et le triplet par irradiation à -180°C et la mesure opérée à -102°C . Le doublet et le triplet révélaient de l'anisotropie tandis que le singulet n'en montrait pas. Ces observations confirment les interprétations spectrales données à ce jour concernant le polyoxyméthylène désorienté, à savoir que $-\text{CH}_2-\text{O}^\cdot$, $-\text{O}-\dot{\text{C}}\text{H}-\text{O}-$ et $-\text{O}-\dot{\text{C}}\text{H}_2$ correspondant respectivement au singulet, au doublet et au triplet. Le traitement du doublet spectral est obtenu en rapportant au tenseur de copulation anisotropique hyperfine, la valeur du g -anisotropique et la conformation caténaire du polyoxyméthylène cristallin. On a obtenu une valeur assez petite de ρ ($\cong 0.45$) pour la densité de spin au niveau de l'atome de carbone central.

Zusammenfassung

Elektronenspinresonanzspektren von gestrecktem, mit $\text{Co-60-}\gamma$ -Strahlen bestrahltem Polyoxymethylen wurden untersucht. Bei entsprechender Behandlung waren drei verschiedene Spektren zu beobachten. Ein Dublett bei Bestrahlung und Messung bei Raumtemperatur, ein Singulett bei Bestrahlung und Messung bei -180°C und ein Triplett bei Bestrahlung bei -180°C und Messung bei -102°C . Die Dublett- und Triplett-spektren zeigen Anisotropie, das des Singulett's hingegen nicht. Diese Beobachtungen bilden eine Stütze für die Interpretation der bisher mit unorientiertem Polyoxymethylen erhaltenen Spektren, d.h. $-\text{CH}_2-\text{O}^\cdot$, $-\text{O}-\dot{\text{C}}\text{H}-\text{O}-$ bzw. $-\text{O}-\dot{\text{C}}\text{H}_2$ für das Singulett, Dublett bzw. Triplett. Das Dublettspektrum wird als vom anisotropen Hyperfein-Kopplungstensor, von den anisotropen g -Werten und der Kettenkonformation im kristallinen Polyoxymethylen abhängig behandelt. Für die spindichte am zentralen Kohlenstoffatom des $-\text{O}-\dot{\text{C}}\text{H}-\text{O}-$ Radikals wurde ein recht kleiner Wert $\rho \cong 0,45$ beobachtet.

Received October 19, 1964

Revised November 3, 1964

(Prod. No. 4610A)

Photodegradation of Poly(α -methylstyrene) in Solution

R. B. FOX and T. R. PRICE, *U. S. Naval Research Laboratory, Washington, D. C.*

Synopsis

Apparent quantum yields for the random scission of poly(α -methylstyrene) in solution by 2537 Å. radiation were shown to be solvent-dependent, indicating that processes other than the direct photolysis of the polymer are taking place. Quantum yields on the order of 10^{-3} scissions per quantum absorbed by the polymer were found in benzene, dioxane, cyclohexane, and methylene chloride and about 0.2 in chloroform and carbon tetrachloride; the quantum yields were unaffected by oxygen. In carbon tetrachloride, the quantum yields decreased slightly with increasing polymer concentration. Ethanol and cyclohexane were inhibitors for the photolysis in carbon tetrachloride, while the latter solvent acted as a sensitizer in cyclohexane. By comparison with model compounds irradiated in carbon tetrachloride, it was shown that an early step in the photolysis of poly(α -methylstyrene) in this solvent involves reaction with a main-chain methylene group and eventual substitution with a trichloromethyl group.

INTRODUCTION

For practical reasons, most polymer photodegradation work has involved the study of the effects of ultraviolet radiation on solid materials. The interpretation of results from this type of investigation is complicated by the lack of information concerning chain mobility and diffusion phenomena and by the lack of control over the composition of the system being irradiated. Some of the difficulties can be circumvented by the use of solutions. In particular, the study of photolysis of polymers in solution should afford an insight into both the mechanism of degradation and the interaction between the polymer and other molecules which may act as inhibitors or sensitizers.

The degradation of polymers in solution by ultraviolet¹ and ionizing² radiation has shown that many analogies can be drawn between the effects of the two types of radiation. In most of the photolytic work, the solvent has been relatively transparent to the incident radiation, and the effect of the solvent other than as a diluent was usually not considered. Baxendale and Thomas³ have studied the photolysis of poly(methacrylic acid) in aqueous solutions containing hydrogen peroxide, and Mönig and co-workers⁴ have shown the photodegradation of poly(methyl methacrylate) to be markedly affected by solvents (benzene, chloroform, and dioxane)

and by photosensitizers such as 3, 4-benzpyrene in the presence of oxygen in benzene solutions.

To supplement our earlier investigation of the photodegradation of poly (α -methylstyrene) (PMS) films,⁵ we are reporting the photolysis of the same polymer in solution. This polymer is not readily crosslinked in the solid state and would not be expected to crosslink in solution. It is a strong absorber at 2537 Å. and therefore is, in many solvents, the major absorbing species of the system when a low-pressure mercury radiation source is used. The chemical structure of PMS makes it amenable to comparison with its homolog polystyrene and with poly(methyl methacrylate).

EXPERIMENTAL

Materials

The same broad-distribution PMS used in the earlier film studies⁵ was employed in this work. After purification, the PMS was exhaustively extracted with methanol until no material absorbing at wavelengths above 2300 Å. was found in the extracts. On the basis of its sedimentation pattern, the PMS was assumed to have a "most probable" molecular weight distribution; the intrinsic viscosity of the polymer in benzene indicated a number-average molecular weight of 1.07×10^5 . Spectroscopic grade or freshly distilled solvents were used throughout. Changes in the ultraviolet spectra of the solvents during irradiation were negligible except where noted.

Source, Actinometry, and Irradiation Cell

All exposures were made with the radiation emitted by a U-shaped Hanovia 84A-1 low-pressure mercury lamp. With PMS, the only photo-

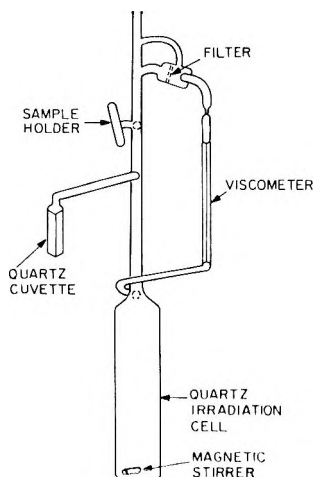


Fig. 1. Irradiation apparatus.

lytically active radiation from this lamp is at 2537 Å., since shorter wavelengths (primarily 1849 Å.) are absorbed by the irradiation cell, and longer wavelengths are not absorbed by the solutions used. Ferrioxalate actinometry⁶ was employed, and the lamp output was continuously monitored with a photocell.

The irradiation apparatus, shown in Figure 1, consisted of a 2.5-cm. diameter quartz cell of about 30 ml. volume, containing a glass-enclosed stirring bar. This cell was surmounted by a capillary viscometer, a cuvet for spectroscopic measurements, and a side-arm for the polymer sample.

Viscosity Measurements

Intrinsic viscosities determined by dilution were run in Ubbelohde-type dilution viscometers having a running time of about 170 sec. for benzene at 30°C., the temperature at which all viscosity measurements were made. Single-point viscosities measured in the irradiation apparatus were converted to intrinsic viscosities through a modification⁷ of the Huggins equation,

$$[\eta] = (2^{1/2}/C)(\eta_{sp} - \ln \eta_r)^{1/2}$$

where C is concentration in grams per deciliter.

Procedure

All irradiations were made at room temperature, 22–25°C., with solution volumes of approximately 20 ml. For exposures in air either pre-prepared polymer solutions were used, or air-equilibrated solvent was added to the polymer sample in the cell and the concentration determined by weighing. For exposures in the absence of air, degassed solvent was distilled into the cell. After sealing off the entire apparatus, the spectrum of the solvent and its running time in the viscometer were measured. The polymer sample, previously sealed in the side-arm, was then mixed with solvent and the spectrum and viscometer time again measured before beginning an exposure series. Mixed solvents were added directly to the cell and degassed by three freeze-thaw cycles. Each system was degassed to a pressure of 10^{-3} Torr. After each exposure, spectra and relative viscosities were determined.

Evaluation of Quantum Yields

Since random scission was found to be the major photodegradation process in PMS films in vacuum at room temperature,⁵ it is reasonable to assume the same process in solution. The quantum yield for random scission, ϕ_s^i , is given in scissions per quantum absorbed by the species i at a rate I^i in time t . In terms of measured quantities, ϕ_s^i can be calculated from the equation

$$\phi_s^i = (CA/\bar{M}_n) \{ ([\eta_0]/[\eta])^{1/\alpha} - 1 \} / I^i t$$

where C is concentration, A is Avogadro's number, and \bar{M}_{n_0} is the initial number-average molecular weight. The number of scissions per polymer molecule, $(\bar{M}_{n_0}/\bar{M}_n) - 1$, has been equated to $([\eta_0]/[\eta])^{1/\alpha} - 1$, where α is the exponent in the relation $[\eta] = KM^\alpha$. Plots of the number of scissions against the quanta absorbed per unit volume, I^2t , were generally linear, although at low polymer concentrations or where total absorption increased significantly, ϕ_s^i tended to decrease with increasing dose. In such cases, initial slopes were used to evaluate the quantum yields. Since PMS is a strong absorber at 2537 Å., I^2 was normally equal to the incident intensity. The quantum yield based on energy absorbed by the polymer only, ϕ_s^P , differs from that based on energy absorbed by the entire solution, ϕ_s^{soln} , where the solvent is itself a strong absorber.

Most of the exponents α for the various solvents used were not available. They were estimated by the method of Meyerhoff⁸ from a plot of α against the $[\eta]$ found for our PMS in cyclohexane and in benzene, for which the exponents are known. Some of the values so obtained are included in Table I.

TABLE I
Quantum Yields for Scission of PMS in Solution ($C = 1$ g./dl.)

| Solvent | α | $\phi_s^P \times 10^4$ | | $\phi_s^{\text{soln}} \times 10^4$ | |
|---------------------------|----------|------------------------|----------|------------------------------------|----------|
| | | Air | Degassed | Air | Degassed |
| Benzene | 0.71 | 95 | — | 0.53 | — |
| Dioxane | 0.68 | 4 | 5 | 4 | 5 |
| Cyclohexane | 0.5 | — | 6 | — | 6 |
| Methylene chloride | 0.72 | 50 | 50 | 50 | 50 |
| Chloroform (alcohol-free) | 0.76 | 1600 | — | 1570 | — |
| Carbon tetrachloride | 0.76 | 2110 | 1850 | 1680 | 1460 |

RESULTS AND DISCUSSION

A summary of the quantum yields for random chain scission for PMS at one concentration in a number of solvents is given in Table I. These data indicate that there is no correlation between the quantum yields and the polymer-solvent interaction parameters, α , of the solvents or their ultraviolet cut-offs. The similarity of the results obtained in the presence and absence of air may be fortuitous, since there is no reason to suppose that the mechanisms under the two conditions are the same. Oxygen does not affect the photolysis of poly(methyl vinyl ketone) in dioxane⁹ but does markedly increase the apparent rate of degradation of polystyrene in solution.¹⁰

Some of these solvents act as "inner" optical filters. In benzene solutions, for example, most of the incident energy is absorbed by the solvent; if the filter effect is eliminated by calculating the quantum yield on the basis of energy absorbed by the polymer only, the resulting ϕ_s^P is about the same magnitude as that found in many other solvents. In the presence

of such a filter, the rate of absorption of radiation by the polymer will be greatly reduced. This effect has not been assessed, but with films of PMS no intensity effect was found.⁵

The very fact that ϕ_s^P is solvent-dependent shows that more than direct photolysis of a polymer dispersed in an inert medium is involved. In PMS films, ϕ_s^P is about 1×10^{-3} at room temperature in the absence of air.⁵ The low values of ϕ_s^P for cyclohexane, dioxane, methylene chloride, and benzene solutions make these solvents appear to be relatively inert compared to chloroform and carbon tetrachloride under these conditions. No changes in ϕ_s^P other than those produced by dilution were observed in mixtures of dioxane or methylene chloride with cyclohexane. It is of further interest that in cyclohexane, a theta solvent for PMS, no insoluble material was formed during irradiation, giving added evidence to the idea that crosslinking did not occur.

In all solvents, irradiation of PMS produced a general increase in the absorbance at wavelengths below 350 m μ . A shoulder in the 290–300 m μ region of the spectrum was also observed after irradiation of PMS in cyclohexane, dioxane, and methylene chloride in the absence of air, and in chloroform in air. A possible source of this absorption may be in the formation of a β -substituted styrene grouping in the polymer chain, since β -alkylstyrenes do exhibit maxima at 293 m μ .

Chloroform and carbon tetrachloride are solvents in which the photolysis of PMS is relatively rapid in either the presence or absence of air. The rates in both solvents were quite sensitive to traces of ethanol, which is normally found as a preservative in commercial chloroform. In freshly distilled Spectrograde chloroform, the ϕ_s^P for PMS is 0.091, while in the same solvent washed ten times with water, the ϕ_s^P is 0.16 in the presence of air. Similarly, addition of 2% by volume of ethanol to carbon tetrachloride reduces the ϕ_s^P in this solvent from 0.21 to 0.015. These findings are qualitatively similar to those observed by Durup¹¹ in his investigation of the radiolysis of polystyrene.

Because of the high rate of photolysis of PMS in carbon tetrachloride, this solute-solvent combination received somewhat greater attention than the other systems. The rate of scission decreased somewhat with increasing PMS concentration: at 0.46, 0.98, and 5.64 g./dl., ϕ_s^{soln} was 0.17, 0.15, and 0.13 scissions per quantum absorbed by the solutions, respectively. This result probably reflects the decreasing mobility of polymer molecules in a more viscous medium.

In degassed mixtures of carbon tetrachloride and cyclohexane, PMS undergoes photodegradation at rates which are not proportional to the carbon tetrachloride concentration. The results are shown in Figure 2. At very low concentrations of carbon tetrachloride, there appears to be sensitization, and the rate of degradation is greater than that predicted from simple mixing of the two solvents. The results could be explained either on the basis of energy transfer from the carbon tetrachloride to the PMS or on attack on the PMS by free radicals formed from the solvent. Complex

formation among the reactants may well facilitate such interactions. The inhibition of the photolysis by small amounts of cyclohexane is difficult to explain except on the basis of competition for radicals from the carbon tetrachloride.

Hydrogen chloride was formed in all photolyses in carbon tetrachloride. At this point little can be said regarding the mechanism of hydrogen chloride formation: the choice appears to be (a) homolysis of carbon tetrachloride to yield atomic chlorine followed by abstraction of a hydrogen atom from the polymer, or (b) elimination of a hydrogen atom from the

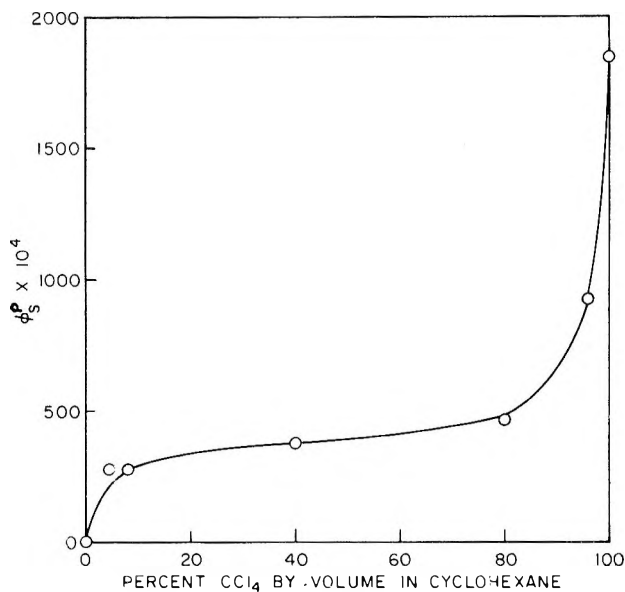


Fig. 2. Photolysis of PMS in mixtures of cyclohexane and carbon tetrachloride in the absence of air.

polymer after the absorption of a photon, followed by reaction of the hydrogen atom with carbon tetrachloride. The usual formulation in photochlorinations is (a). In carbon tetrachloride containing chlorine in the absence of air PMS was found to be rapidly degraded and the chlorine consumed even upon irradiation by a tungsten lamp. Under the same conditions, polystyrene underwent almost no chain breaking under 2537 Å. irradiation, although the chlorine was rapidly consumed.¹⁰ The stability of the polymer radical formed during photochlorination obviously determines the rate of degradation under these conditions.

While the initiation step in photochlorination and in photodegradation in carbon tetrachloride not containing dissolved chlorine may well be the same, the final products are not identical. This was demonstrated by minor differences in the infrared spectra of the products and the fact

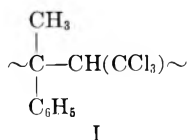
that in the absence of air, the photolysis of PMS in carbon tetrachloride resulted in a well-defined band at 326 $m\mu$ in the ultraviolet spectrum of the mixture. Chlorine solutions absorb at the same wavelength; the disappearance of this band was used to measure chlorine consumption, and no absorption at 326 $m\mu$ was observed after completion of the reaction with chlorine.

The 326 $m\mu$ absorption, formed in the absence of air, did not increase after the cell was opened to the atmosphere; further irradiation in air resulted in a decrease in absorption in this region. The absorption at 326 $m\mu$ was not eliminated by reprecipitating the polymer, and it did not form in the absence of carbon tetrachloride. Polystyrene solutions undergo a similar sequence of spectral changes at the same wavelength.

In carbon tetrachloride solution in the absence of air, the irradiation of α -methylstyrene gave rise to a spectrum similar to those of the two polymers, while styrene did not. Although *tert*-butylbenzene does not undergo spectral changes in the 300–350 $m\mu$ region, ethyl-, isopropyl-, and (1,1-dimethylpropyl)benzene do develop new absorption bands in this region, generally at slightly shorter wavelengths than that of the band formed by PMS. Of these model compounds, only with (1,1-dimethylpropyl)benzene was the additional feature of band loss encountered after further irradiation in air. This suggests that it is the backbone methylene group in PMS which is involved in reactions with carbon tetrachloride under ultraviolet irradiation; the analogous methylene group in polystyrene may also be involved in similar reactions with this polymer, even though the benzylic carbon atom would be the choice on the basis of other radical reactions.

A somewhat tenuous identification of the substituting group in the carbon tetrachloride reactions as being the trichloromethyl radical was made by examination of the infrared spectrum of the mixture resulting from the irradiation of (1,1-dimethylpropyl)benzene in carbon tetrachloride. In the unirradiated solution in a 1-mm. cell, there were no bands having greater than 1% absorption in the 1650–1950 cm.^{-1} region. After irradiation of the solution in the absence of air, followed by irradiation in the presence of air, its spectrum contained a sharp band of medium intensity at 1812 cm.^{-1} and a very weak band at 1690 cm.^{-1} . Under the same conditions, carbon tetrachloride alone gave a lower intensity band at 1817 cm.^{-1} (phosgene) and no new absorption in the 1690 cm.^{-1} region. The 1812 cm.^{-1} absorption is reasonable for the carbonyl band in an acid chloride or possibly an anhydride. After irradiation, the hydrocarbon solution was stirred with hot water several hours. The spectrum of the dried organic phase had negligible absorption at 1812 cm.^{-1} and slightly increased absorption at 1690 cm.^{-1} as well as a general increase in absorption in the 3300–3600 cm.^{-1} region. Again, this is reasonable for bands to be expected from a carboxyl derivative.

On this basis, it might be inferred that the initial substitution product, giving rise to the 326 $m\mu$ ultraviolet absorption band in the PMS solution in the absence of air, is a trichloromethyl derivative (I) of the polymer.



Further irradiation in the presence of atmospheric moisture and oxygen results in conversion of this derivative to an acid chloride or an anhydride, for which the longest wavelength band is likely to be below 240 m μ .

Some explanation can now be offered for the great differences in stability of PMS and polystyrene. In the absence of oxygen, both polymers undergo random scission, which in the case of polystyrene is concomitant with crosslinking. Both polymers are resonance-stabilized to about the same extent. If the relative ease of homolysis, C—H > C—CH₃ > C—C₆H₅, observed in alkylbenzenes in rigid media¹² holds in liquids as well, then a C—H bond is likely to be the first to undergo scission. In PMS, a secondary free radical will result from elimination of a hydrogen atom from the methylene group, while from polystyrene, a less reactive tertiary radical will probably result. The relatively rapid yellowing of polystyrene films in vacuum¹³ indicates that formation of double bonds competes with chain-breaking for subsequent processes involving this radical. Photodegradation by chlorine may involve some of these same steps. In the presence of oxygen, it is suggested that the oxygen-headed radicals which would result may be of more nearly the same stability, and therefore the rates of degradation of the two polymers in air would be similar.

References

1. Jellinek, H. H. G., *Pure Appl. Chem.*, **4**, 419 (1962).
2. Chapiro, A., *Radiation Chemistry of Polymeric Systems*, Interscience, New York, 1962.
3. Baxendale, J. H., and J. K. Thomas, *Trans. Faraday Soc.*, **54**, 1515 (1958).
4. Mönig, H., *Naturwiss.*, **45**, 12 (1958); H. Mönig and H. Kriegel, *Z. Naturforsch.*, **15b**, 333 (1960).
5. Stokes, S., and R. B. Fox, *J. Polymer Sci.*, **56**, 507 (1962).
6. Hatchard, C. G., and C. A. Parker, *Proc. Roy. Soc. (London)*, **A235**, 518 (1956).
7. Catsiff, E. H., *J. Appl. Polymer Sci.*, **7**, S37 (1963).
8. Meyerhoff, G., *Makromol. Chem.*, **37**, 97 (1960).
9. Guillet, J. E., and R. G. W. Norrish, *Proc. Roy. Soc. (London)*, **A233**, 153 (1955).
10. Price, T. R., unpublished work.
11. Durup, J., *J. Chim. Phys.*, **54**, 739, 746 (1957); *ibid.*, **56**, 873 (1959).
12. Porter, G., and E. Strachan, *Trans. Faraday Soc.*, **54**, 1595 (1958).
13. Isaacs, L. G., M. V. McDowell, F. E. Saalfeld, and R. B. Fox, paper presented to Organic Coatings and Plastics Division, American Chemical Society, 145th Meeting, New York, Sept. 1963.

Résumé

On montre que les rendements quantiques apparents pour la scission statistique du poly(α -méthylstyrène) en solution, par un rayonnement de 2537 Å, dépendent du solvant, ce qui indique qu'il y a d'autres processus que la photolyse directe du polymère. On a trouvé des rendements quantiques de l'ordre de 10⁻³ scissions par quantum absorbé par le polymère dans le benzène, le dioxane, le cyclohexane et le chlorure de

méthylène et d'environ 0.2 dans le chloroforme et le tétrachlorure de carbone. Les rendements quantiques ne sont pas modifiés par l'oxygène. Dans le tétrachlorure de carbone, les rendements quantiques diminuent légèrement lorsque la concentration en polymère augmente. L'éthanol et le cyclohexane sont des inhibiteurs de la photolyse dans le tétrachlorure de carbone, tandis que ce dernier solvant agit comme sensibilisateur dans le cyclohexane. Par comparaison avec des composés modèles irradiés dans le tétrachlorure de carbone, on montre qu'une première étape de la photolyse du poly(α -méthylstyrène) dans ce solvant implique une réaction avec un groupe méthylène de la chaîne principale et une substitution éventuelle par un groupe trichlorométhyle.

Zusammenfassung

Scheinbare Quantenausbeuten für die statistische Spaltung von Poly(α -methylstyrol) in Lösung durch 2537-A.-Strahlung erwies sich als lösungs-mittelabhängig, was zeigt, dass andere Prozesse als die direkte Photolyse des Polymeren stattfinden. Quantenausbeuten in der Größenordnung von 10^{-3} Spaltungen pro vom Polymeren absorbierten Quant wurden in Benzol, Dioxan, Cyklohexan und Methylenchlorid und von etwa 0,2 in Chloroform und Tetrachlorkohlenstoff gefunden; die Quantenausbeute wurde durch Sauerstoff nicht beeinflusst. In Tetrachlorkohlenstoff nahm die Quantenausbeute mit steigender Polymerkonzentration etwas ab. Äthanol und Cyklohexan wirkten für die Photolyse in Tetrachlorkohlenstoff als Inhibitoren, während letzteres Lösungsmittel in Cyklohexan einen Sensibilisator bildet. Durch Vergleich mit der Bestrahlung von Modellverbindungen in Tetrachlorkohlenstoff wurde gezeigt, dass am Beginn der Photolyse von Poly(α -methylstyrol) in diesem Lösungsmittel ein Schritt unter Beteiligung einer Reaktion mit einer Hauptkettenmethylengruppe und eventueller Substitution durch eine Trichlormethylgruppe auftritt.

Received October 19, 1964
(Prod. No. 4612A)

Effect of Film Thickness on the Dynamic Elastic Modulus of Cellophane*

EDWARD GIPSTEIN, LEON MARKER,† ERIC WELLISCH,
and ORVILLE J. SWEETING,‡ *Olin Mathieson Chemical
Corporation, New Haven, Connecticut*

Synopsis

The effect of film thickness on the dynamic modulus of cellophane has been investigated to inquire into structural differences that may exist in cellophane, resulting from different conditions of regeneration. Modulus measurements on different types of plate-cast and commercial films at first indicated a decrease in modulus with an increase in film thickness. For all films a limiting stiffness was approached with increasing thickness which appeared to be independent of the type of film. This result, however, was proved to be an artifact introduced by an instrumental effect; the dynamic modulus apparatus was found to behave as a spring in series with the film. The moduli of all films were corrected for this effect and the mean values of the moduli in the machine and transverse directions were averaged for all films separately by types and by thicknesses. The values were found to be independent of film thickness, for all types of cellophane. Cellophane by this method of study shows no indication of a point-to-point variation in structure in the thickness dimension. Differences in modulus do exist among different types of cellophanes, however, and are undoubtedly the result of structural differences that arise during different methods of preparation.

INTRODUCTION

A knowledge of the fine structure of cellulose film is essential in relating processing conditions to film properties such as toughness, durability, and dimensional stability. The lack of suitable experimental techniques which permit reliable quantitative measurements of small film specimens has made it difficult in the past to establish meaningful relationships between film structure and properties.

The degree of lateral order in regenerated cellulose has been reported to have a pronounced effect on the physical properties of the film.¹ Films with a very low degree of lateral order exhibited unusual toughness and extensibility. Also, a study of the molecular orientation in cellophane by examining cross sections of film as a function of time during the coagulation

* Taken from the thesis submitted by E. Gipstein in partial fulfillment of the requirements for the Master of Arts Degree at St. Joseph College, West Hartford, Connecticut.

† Present address: Central Research Laboratories, The General Tire and Rubber Co., Akron, Ohio.

‡ Present address: Yale University, New Haven, Connecticut.

and regeneration of viscose² has revealed variations in the degree of uniaxial orientation across the sheet, but no significant differences between the surface and center layers were observed. Variations in the degree of order and orientation of regenerated cellulose films in cross section have been observed with an interference microscope.³

Structural studies of regenerated cellulose films prepared in different ways have been made in these laboratories by x-ray and dye staining methods,⁴ which indicate significant structural differences among films. For films cast on glass plates, the side in contact with the plate during casting and regeneration is porous and picks up dye readily, whereas the side away from the glass plate is not dyed at all. Machine-cast commercial films, which have dense structures on both sides, could not be dyed readily. In the case of hydroxyethylcellulose films, both surfaces were accessible to dye. Evidently, hydroxyethylcellulose films have a more open structure and are less affected by contact with the regenerating bath than are viscose films.

During the investigation of the mechanical properties of films regenerated from hydroxyethylcellulose and viscose mixtures in our laboratories, it was observed that the dynamic elastic modulus of these films appeared to be dependent on the gauge or thickness of the film: the thicker the film, the smaller the modulus. Since the dynamic mechanical properties of films are quite sensitive to changes in structure, it was considered possible that the molecular order of these films varies with the thickness of the film. Variations in the structure of regenerated cellulose could occur as a function of the regeneration process, particularly in the thickness dimension, since material at points away from the surface of the film may not be regenerated in the same manner as that nearer the surface. Therefore, it seemed logical to investigate the effect of film thickness on the mechanical properties of regenerated cellulose films prepared in different ways. A study of the modulus of such films might permit us to measure structural differences in regenerated cellulose by a single reliable technique and thereby relate the structure, method of preparation, and the mechanical properties of cellophane.

EXPERIMENTAL

Preparation of Film Samples

Many of the modulus measurements reported in this study were carried out on unsoftened cellophane films prepared in this laboratory. These films, approximately 8×11 in., were cast by pouring solutions of viscose on glass plates and spreading the mixture with a stainless steel casting bar. The settings on the bar were previously adjusted by micrometer screws at both ends to obtain the desired thickness of film. The uniformity of gap between bar and plate throughout the length of the bar was checked with a feeler gage. Films were cast with bar settings to give film thicknesses of 0.75–2.5 mils. The films were then regenerated at room temperature from standard regenerating baths containing 12.5% sulfuric acid and 20%

sodium sulfate. After 3 min. regeneration time, the films were washed in running tap water at room temperature for several hours. The wet films were allowed to dry on glass plates after securing the edges of the film with tape to prevent shrinkage and curling. Measurements were also carried out on commercial cellophane films from which the softeners had been removed by washing in hot water for several hours. All of the films in this study were preconditioned at 35% R.H. and 75°F. for 24 hr. before measurement at these conditions.

Determination of the Modulus

The modulus measurements were carried out in the conditioning room, by use of the dynamic tensile modulus apparatus described previously.⁵

In these experiments, two modifications in the measurement procedure were introduced. In all experiments to find the modulus of films, a constant fixed weight of 86.05 g. was hung on the lower clamp holding the film specimen. The resonant frequencies were then adjusted to obtain the maximum amplitudes at a fixed voltage of 3 v. for the longitudinal frequency and 8 v. for the transverse frequency.

Specimen Preparation

Two samples in the machine direction, and two in the transverse direction, were cut from 8 × 8 in. sheets as described.⁶

Measurements

Operation of the apparatus (including adjustments and measurement of resonant frequencies) and determination of sample length were done as before.⁵ Thickness of the samples was determined by use of an Ames hand gauge and checked by calculation from the relationship between transverse frequency f_t and density ρ . Thus, by use of eq. (2) of Hansen et al.⁵ $A = mg./4\rho(f_t l)^2$, and the corresponding gauge is $A/2.00$ mm.

Determination of the Density

The density specimens were placed in bottles which had been conditioned at the same relative humidity as the films. The density was determined by a sink-float method. The specimen was placed in a mixture of *s*-tetrachloroethane and *o*-dichlorobenzene. The concentration of the mixture was adjusted until the specimen was just suspended. The density of the mixture was then determined by using a hydrometer. When the proper mixture had been obtained, the density of a duplicate specimen was generally determined as a check against changes in the density of the first specimen during the determination.⁷

Determination of Moisture

All analyses for moisture were done by the Karl Fischer method. After conditioning, two specimens of about 0.5 g. each were put into tared

TABLE I
Description of Film Samples: Density and Moisture Content
at 75°F. and 35% R. H.

| Film | ρ , g./cc. | Water, % |
|---|-----------------|----------|
| Commercial PT films ^a | | |
| PT-30 | 1.508 | 8.27 |
| PT-35 | 1.504 | 8.44 |
| PT-40 | 1.509 | 8.52 |
| PT-50 | 1.501 | 8.41 |
| PT-60 | 1.509 | 8.50 |
| PT-80 | 1.505 | 8.40 |
| Commercial PUT films ^b | | |
| 183 PUT | 1.502 | 8.67 |
| 140 PUT | 1.509 | 8.77 |
| 128 PUT | 1.509 | 8.41 |
| Plate-cast laboratory films | | |
| Salt index <1 ^c | | |
| X-33-1 | 1.496 | 9.27 |
| X-39-1 | 1.509 | 9.93 |
| X-41-2B | 1.504 | 9.18 |
| X-19-1 | 1.506 | 9.28 |
| Salt index 8.8 | | |
| X-57-1 | 1.509 | 8.25 |
| X-55-1 | 1.509 | 8.06 |
| X-58-1 | 1.515 | 8.34 |
| Plate-cast laboratory films, heated dielectrically ^d | | |
| 30 Sec., salt index <1 | | |
| X-33-2 | 1.500 | 10.21 |
| X-39-2 | 1.508 | 10.32 |
| X-41-3 | 1.508 | 9.75 |
| X-19-2 | 1.507 | 9.79 |
| 30 Sec., salt index 8.8 | | |
| X-57-3 | 1.510 | 8.62 |
| X-55-3 | 1.510 | 8.74 |
| X-58-3 | 1.512 | 8.52 |
| 90 Sec., salt index 8.8 | | |
| X-57-5 | 1.512 | 8.88 |
| X-55-5 | 1.516 | 8.46 |
| X-58-4 | 1.509 | 8.16 |

^a PT films are unsoftened. The following number indicates the unit weight, expressed as grams/square meter; e.g., PT-30 designates a regenerated cellulose sheet weighing approximately 30 g./m².

^b PUT films used here have had the glycerol softener washed out. The preceding number expresses the approximate coverage in square inches/pound $\times 10^{-2}$; e.g., 182 PUT designates a regenerated cellulose film softened with glycerol (here removed) of approximately 18,200 in.²/lb.

^c Salt index is a measure of the degree of xanthation related empirically to the rate of coagulation of the film in a given sodium chloride solution.

^d This series of films was heated dielectrically for the time stated at 22 kv. and 700 ma. before regeneration. The apparatus used was a Model 1000 Thermal (15 kw.) manufactured by W. T. Larose Inc., Troy, New York.

weighing bottles, and 25 ml. of methanol was added to minimize changes in moisture content after conditioning and before the determination.

Table I summarizes the samples on which measurements were determined, together with density and moisture content.

RESULTS

Measurements were made on all films and related to gauge. The apparent moduli, E , were calculated according to the equation developed previously,⁵ where ρ is the volumetric density, l is the length of the specimen, g is the gravitational constant, and f_l and f_{tr} are the lengthwise and transverse frequencies, respectively.

$$\begin{aligned} E &= (4\pi^2/g) \rho l^3 (f_l f_{tr})^2 \\ &= 0.1611 \rho l^3 (f_l f_{tr})^2 \end{aligned} \quad (1)$$

The data and calculations are presented in Table II. It should be noted that this table is a summary of a large number of measurements in both the machine and transverse directions of the film samples (MD and TD respectively); after the first example in each group of films, only the MD data and the average E values are listed. (The experimental films designated X- . . . have no machine and transverse direction; for these the data given are typical values, usually one of four, and averages.)

For each set of films, the modulus thus calculated appears to decrease with increase in gauge, with only small differences among the films.

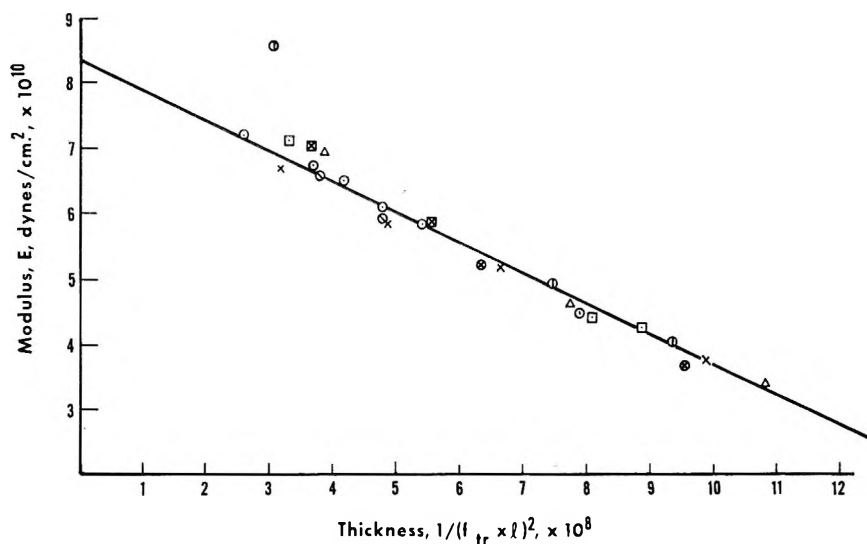


Fig. 1. Effect of film thickness on the dynamic elastic modulus of cellophane films: (○) commercial PT films; (⊠) commercial PUT films; (×) control films, plate-cast, salt index <1; (⊕) dielectrically treated films (30 sec.), salt index <1; (Δ) control films, plate-cast, salt index 8.8; (◻) dielectrically treated films (30 sec.), salt index 8.8; (⊙) dielectrically treated films (90 sec.), salt index 8.8.

TABLE II
Dynamic Elastic Modulus Data for Cellophane Films

| Film | Nominal gauge, mils | f_{tr} | f_t | Length, l , cm. | E , dynes/cm. ² $\times 10^{10}$ | Average E , dynes/cm. ² $\times 10^{10}$ | $\frac{E}{(f_{tr}l)^2} \times 10^3$ | $\left\langle \frac{E}{(f_{tr}l)^2} \right\rangle \times 10^3$ ^a |
|---------|---------------------|--------------------|-------|-------------------|---|---|-------------------------------------|---|
| PT-30 | 0.72-0.80 | 939.3 ^b | 41.20 | 6.1176 | 8.329 | 7.227 | 2.5224 | 2.2164 |
| | | 919.6 ^b | 41.60 | 6.1198 | 8.148 | | 2.5726 | |
| | | 940.1 ^c | 36.03 | 6.1323 | 6.427 | | 1.9338 | |
| PT-35 | 1.0-1.2 | 939.6 ^e | 36.00 | 6.0717 | 6.257 | | 1.9225 | 2.5405 |
| | | 839.7 | 43.75 | 6.0820 | 7.356 | 6.755 | 2.8204 | |
| | | 796.0 | 44.80 | 6.0800 | 6.947 | 6.483 | 2.9615 | |
| PT-40 | 1.1-1.25 | | | | | | | |
| PT-50 | 1.40-1.45 | | | | | | | |
| PT-60 | 1.50 | | | | | | | |
| PT-80 | 2.1-2.2 | 679.7 | 45.06 | 6.0783 | 6.358 | 5.413 | 3.4027 | 3.1623 |
| | | 599.3 | 50.04 | 6.1101 | 4.788 | 4.481 | 3.5707 | |
| 182 PUT | 0.9-1.0 | 851.8 ^b | 45.09 | 6.1269 | 7.916 | 7.023 | 2.9063 | 2.574 |
| | | 861.0 ^b | 44.05 | 6.0698 | 8.070 | | 2.9547 | |
| | | 843.6 ^c | 38.98 | 6.1488 | 6.083 | 2.2608 | | |
| 140 PUT | 1.1 | 858.3 ^e | 39.06 | 6.1257 | 6.260 | 6.260 | 2.2645 | 2.927 |
| | | 847.6 | 47.87 | 6.1376 | 9.253 | 7.847 | 3.4192 | |

| | | | | | | | | |
|---------|-----------|-------|-------|--------|-------|-------|--------|--------|
| 128 PUT | 1.4-1.5 | 682.0 | 49.50 | 6.1668 | 6.459 | 5.872 | 3.6515 | 3.249 |
| X-33-1 | 0.72-0.96 | 959.3 | 36.10 | 6.1124 | 7.468 | 6.678 | 2.1718 | 1.979 |
| X-39-1 | 1.22-1.40 | 740.0 | 42.90 | 6.1226 | 5.915 | 5.846 | 2.8816 | 2.841 |
| X-41-2B | 1.65-1.85 | 619.5 | 48.20 | 6.1538 | 5.034 | 5.170 | 3.4636 | 3.427 |
| X-19-1 | 2.45-2.90 | 517.3 | 49.50 | 6.1051 | 3.797 | 3.759 | 3.8069 | 3.724 |
| X-57-1 | 0.70-0.75 | 850.6 | 43.00 | 6.0753 | 6.941 | 6.960 | 2.6025 | 2.6882 |
| X-55-1 | 1.65-1.75 | 601.1 | 49.90 | 6.0830 | 4.618 | 4.618 | 3.4555 | 3.5869 |
| X-58-1 | 2.30-2.50 | 503.7 | 50.40 | 6.0487 | 3.432 | 3.422 | 3.6375 | 3.7155 |
| X-33-2 | 0.75-0.80 | 869.4 | 40.21 | 6.0872 | 6.657 | 6.592 | 2.378 | 2.309 |
| X-39-2 | 1.20-1.25 | 768.7 | 44.30 | 6.1030 | 6.001 | 5.938 | 2.730 | 2.722 |
| X-41-3 | 1.75-1.90 | 636.9 | 48.00 | 6.1137 | 5.188 | 5.105 | 3.423 | 3.491 |
| X-19-2 | 2.3-2.5 | 530.9 | 51.00 | 6.1114 | 3.889 | 3.666 | 3.695 | 3.632 |
| X-57-3 | 0.7-0.9 | 899.4 | 40.00 | 6.0888 | 7.286 | 7.111 | 2.4298 | 2.3535 |
| X-55-3 | 2.1-2.2 | 553.4 | 49.20 | 6.0717 | 4.486 | 4.462 | 3.5754 | 3.6057 |
| X-58-3 | 2.5-2.9 | 558.3 | 49.90 | 6.0900 | 4.270 | 4.253 | 3.6938 | 3.7160 |
| X-57-5 | 0.70-0.85 | 929.2 | 41.88 | 6.1069 | 8.425 | 8.566 | 2.6163 | 2.6193 |
| X-55-5 | 1.9-2.2 | 607.2 | 49.06 | 6.1311 | 4.995 | 4.914 | 3.6042 | 3.6596 |
| X-58-4 | 2.4-2.6 | 539.8 | 50.30 | 6.0900 | 4.066 | 4.041 | 3.7513 | 3.7880 |

^a The average of geometric means of the value for machine and transverse directions for each film.

^b Values in the machine direction.

^c Values in the transverse direction.

TABLE III
Effect of Mass on the Longitudinal and Transverse Frequencies

| Film type | Tension w , g. | f_{tr} | f_l | $f_l l/w^{1/2}$ | Length l cm. | $flw^{1/2}$ | Modulus E , dynes/ cm. ² $\times 10^{10}$ |
|-----------|---------------------|----------|-------|-----------------|-------------------|-------------|--|
| 182 PUT | 23.62 | 453.0 | 61.81 | 569.2 | 6.107 | 300.4 | 4.32 |
| | 36.40 | 583.8 | 59.88 | 590.9 | 6.107 | 358.2 | 6.62 |
| | 49.64 | 642.2 | 57.82 | 556.7 | 6.108 | 407.4 | 7.60 |
| | 63.09 | 728.5 | 51.98 | 560.2 | 6.109 | 412.9 | 7.91 |
| | 76.44 | 804.0 | 48.29 | 561.8 | 6.109 | 422.2 | 8.31 |
| | 86.09 | 857.3 | 45.09 | 564.5 | 6.109 | 418.4 | 8.27 |
| 140 PUT | 23.62 | 555.9 | 64.10 | 696.2 | 6.086 | 311.5 | 6.96 |
| | 36.40 | 634.2 | 62.40 | 640.3 | 6.089 | 376.5 | 8.59 |
| | 49.64 | 708.6 | 58.58 | 612.3 | 6.090 | 412.8 | 9.46 |
| | 63.09 | 764.8 | 54.35 | 588.0 | 6.097 | 431.7 | 9.52 |
| | 76.44 | 845.6 | 50.06 | 589.8 | 6.097 | 437.7 | 9.87 |
| | 86.09 | 863.0 | 47.50 | 565.4 | 6.099 | 444.4 | 9.43 |
| 128 PUT | 23.62 | 367.7 | 68.41 | 465.9 | 6.158 | 332.5 | 3.59 |
| | 36.40 | 450.4 | 64.94 | 459.7 | 6.158 | 391.8 | 4.86 |
| | 49.64 | 524.2 | 59.96 | 458.2 | 6.159 | 422.5 | 5.61 |
| | 63.09 | 592.9 | 55.82 | 460.0 | 6.163 | 433.4 | 6.23 |
| | 76.44 | 645.1 | 51.94 | 454.8 | 6.165 | 454.1 | 6.39 |
| | 86.09 | 682.0 | 49.50 | 453.3 | 6.167 | 459.3 | 6.50 |
| PT-80 | 36.40 | 396.8 | 63.97 | 400.6 | 6.091 | 385.9 | 2.10 |
| | 49.65 | 466.4 | 58.10 | 402.9 | 6.091 | 409.6 | 2.66 |
| | 63.10 | 516.4 | 55.46 | 395.9 | 6.091 | 444.5 | 3.17 |
| | 76.44 | 561.0 | 51.50 | 391.0 | 6.091 | 445.3 | 3.39 |
| | 86.09 | 583.6 | 50.90 | 383.2 | 6.095 | 472.5 | 3.60 |

The data of Table II were plotted in three ways to determine the significance of this apparent trend in the data.

(1) Since all films were of the same width, and the weight was suspended from the lower clamp, $(f_{tr}l)^2$ is proportional to the reciprocal of thickness and can be used as a measure of thickness. Figure 1 shows the modulus data plotted as a function of the reciprocal of $(f_{tr}l)^2$, from which it can be seen that the differences among films seem to be small; within the range studied, they lie close to a straight line.

(2) An analogous plot of a function of the total stiffness as a function of the same thickness function, i.e., $E/(f_{tr}l)^2$ as a function of $1/(f_{tr}l)^2$, showed very small differences among films. The curve rose rapidly and asymptotically toward a limiting value of about 4×10^3 for $E/(f_{tr}l)^2$.

(3) Finally, a plot of the compliance, i.e., $1/E$, as a function of stiffness showed small differences among films, save at low values of stiffness.

It was necessary to determine whether this small apparent variation of modulus with gage is an artifact introduced by the instrument, or whether the differences in modulus result from real differences in structure through the thickness dimension. The latter is possible, since under the conditions

of regeneration of cellophane, the outside layers may have a higher modulus than the inner layers. The thicker the film, the greater would be the contribution of the less dense inner layers to the average modulus of the sheet, since presumably the outside denser layers of constant thickness would have the same constitution, regardless of gauge.

The effects of tension (mass) and film width (cross-sectional area) on the longitudinal and transverse frequencies of film specimens of different gauge were investigated. Any large change in either frequency should have a correspondingly greater effect on the modulus which depends on both frequencies [eq. (1)].

The effect of tension was measured on both the longitudinal and transverse frequencies with applied weights between 23 and 86 g. The data obtained in these experiments and the modulus calculated from these experiments are given in Table III. In column 5 of this table, we have calculated $f_{tr}l/w^{1/2}$ values for each film. In all cases this value decreases slightly with increasing weight. In column 7, we have calculated $flw^{1/2}$ values which increase with increasing weight. This increase is approximately proportional to the increase in modulus and may be thus considered the chief cause of the variation in modulus.

In the derivation of the equations for the Vibroscope it was shown that fibers or films of high stiffness do not vibrate as perfectly flexible strings, but have an additional restoring force caused by the elastic deformation of the fiber or film.^{7,8} Therefore a correction is needed for determination of linear density. The equation for a fiber can be put into the equivalent form for films:

$$f_{tr}l/w^{1/2} = 1/2(\rho A)^{1/2} + (E/w)^{1/2}(t/2l\rho^{1/2}) \quad (2)$$

where w is the tension in grams; ρ is the density of the specimen; t is the thickness; and A is the cross-sectional area of the specimen.

Only at very high gauge and high modulus would an appreciable variation of the transverse frequency with tension be expected. In all cases the data of Table III have the form given by eq. (2) with a very low slope. For tensions greater than 50 g., the variation of the transverse frequency with tension was negligible.

If the tension is insufficient and the amplitude of vibration too large, the film specimen will not be in compression throughout the entire cycle and the longitudinal frequency will be larger than would be predicted from the equation. This effect becomes less important as the applied stress is increased. Plots of the variation of f_l with tension showed that the 86-g. tension which was used in measuring the modulus of the film specimens as given in Table II is sufficient for keeping all films in compression.

It is possible that the instrument itself distorts in some way during the application of stress. In this case, the behavior will be as if there is a spring, which may be nonlinear, in series with the film. If this were so, then the apparent modulus should vary with the cross-sectional area rather than

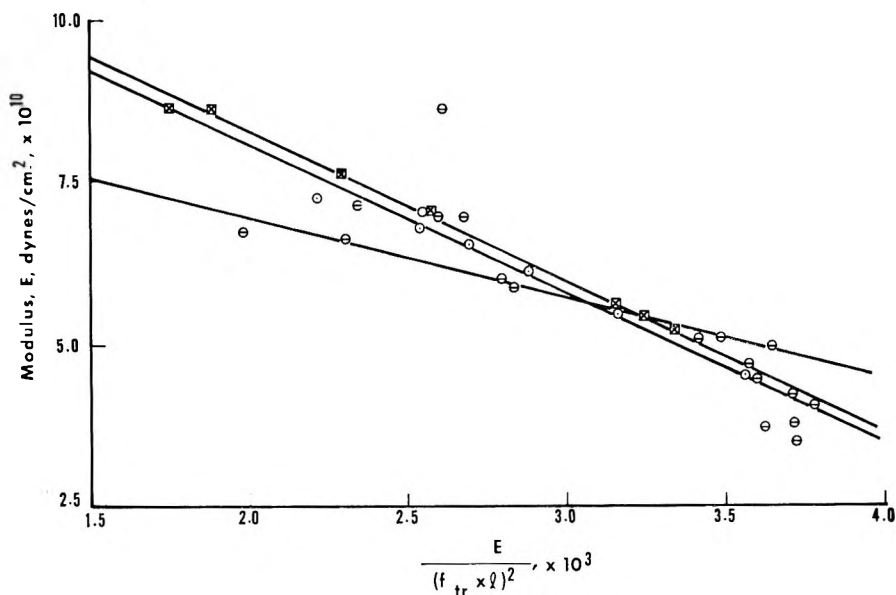


Fig. 2. Apparent modulus as a function of stiffness of cellophane films: (○) commercial PT films; (⊠) commercial PUT films; (⊖) plate-cast films.

with the thickness alone, and the modulus would appear to increase with increasing specimen width.

In order to explore this possibility, specimens from each of several commercial PUT films were cut in the machine and transverse directions at average widths of 1.31, 2.33, and 2.84 mm. The longitudinal and transverse frequencies of these specimens were measured as before at tensions from 23 to 86 g. These data were treated in the same way as those of Table III; they were also adjusted for differences in width in order to obtain equivalent tensions per cross-sectional area.

Horizontal straight lines were obtained in a plot of $f_{tr}l/(wr)^{1/2}$ as a function of $1/(wr)^{1/2}$, thus showing that the transverse frequency is unaffected by changes in film width. On the other hand, three nonsuperimposable curves were obtained for each of the films, 128, 140, and 182 PUT, indicating an appreciably large effect of width on the longitudinal frequency.

The data were therefore fit into a spring equation in which the instrument behaves as a spring in series with the film. The final form of this equation which is developed in the Appendix is

$$E_0 = E - \frac{E_0 mg E}{4G_I \rho l (f_{tr} l)^2} \quad (3)$$

where E_0 is the true modulus, E is the measured modulus, G_I is an instrumental constant, m is the mass or tension, g is the acceleration due to gravity; ρ is the specimen density, l is the length, and f_{tr} is the transverse frequency.

By use of this equation, all of the previous data of Table II were plotted with the modulus as a function of stiffness as shown in Figure 2. An average instrument constant of 10.66×10^6 dynes/cm. was calculated from the slopes and intercepts of the straight lines by the equation:

$$G_I = (\text{intercept/slope}) (mg/4\pi l) \quad (4)$$

Experiments were carried out to confirm the spring constant of the apparatus.⁹ Weights were hung directly from the end of a clamp mounted in the recording head instead of the end of the specimen. The resonant frequency of the system was then determined by using a series of weights ranging from 7.5716 to 107.6606 g. The frequencies obtained in each experiment are given in Table IV. The spring constant of the recording head

TABLE IV
Confirmation of the Spring Constant

| f_i | Mass m , g. | $1/m \times 10^2$, g. ⁻¹ | Instrument constant k , dynes/cm. $\times 10^6$ |
|--------|---------------|--------------------------------------|--|
| 134.74 | 7.5716 | 13.21 | 5.43 |
| 125.10 | 9.2972 | 10.75 | 5.74 |
| 126.35 | 12.8071 | 7.81 | 8.07 |
| 122.90 | 13.6964 | 7.30 | 8.17 |
| 117.46 | 15.9405 | 6.29 | 8.68 |
| 110.19 | 18.3876 | 5.46 | 8.81 |
| 109.05 | 20.3092 | 4.93 | 9.54 |
| 105.00 | 23.4893 | 4.26 | 10.22 |
| 93.99 | 33.5461 | 2.99 | 11.70 |
| 84.55 | 46.2727 | 2.16 | 13.06 |
| 75.92 | 60.9800 | 1.64 | 13.88 |
| 70.08 | 76.0168 | 1.32 | 14.74 |
| 66.05 | 86.0428 | 1.16 | 14.82 |
| 64.94 | 91.5725 | 1.09 | 15.25 |
| 59.93 | 107.6606 | 0.94 | 15.27 |

was found to vary linearly with the reciprocal of the mass (Fig. 3) according to equation:

$$k \times 10^{-6} \text{ dynes/cm.} = 16.691 - 15.826/m \quad (5)$$

where k is the spring constant of the recording head and m is the mass in grams. Below 23 g., the spring constant falls off asymptotically as expected for small tensions.

The value of the instrument constant k for a mass of 86 g. is 14.82×10^6 dynes/cm. This value was used to correct the apparent modulus values of Table II obtained previously when using that mass to apply tension to the film specimen. This was done by the application of the equation:*

$$E_0 = E(1 - 4\pi^2 f_i^2 m/k)^{-1} \quad (6)$$

* Equation 6 is the correct form; the note on p. 1599 of ref. 5 is in error.

where E_0 is the true modulus and E is the measured modulus [one form of eq. (3) developed in the appendix].

The corrected modulus values for all films are given in Table V. These values are summarized in Table VI. The new values appear to be independent of film thickness for all films and similar in magnitude to values previously reported for cellophane.¹⁰ Therefore, cellophanes by this method

TABLE V
Corrected Modulus Values for Cellophane Films

| Film | f_l | $1 - (f_l/k)^2$ | E , dynes/cm. ² $\times 10^{10}$ | | Average, corrected |
|---------|-------|-----------------|---|-----------|--------------------|
| | | | Measured | Corrected | |
| PT-30 | 41.20 | 0.6110 | 8.33 | 13.63 | 11.23 |
| | 41.60 | 0.6096 | 8.15 | 13.20 | |
| | 36.03 | 0.7025 | 6.43 | 9.15 | |
| | 36.10 | 0.7014 | 6.26 | 8.92 | |
| PT-35 | 43.75 | 0.5613 | 7.36 | 13.11 | 11.43 |
| PT-40 | 44.80 | 0.5400 | 6.95 | 12.87 | 11.47 |
| PT-50 | 45.13 | 0.5332 | 6.36 | 11.92 | 11.14 |
| PT-60 | 45.06 | 0.5347 | 5.15 | 9.63 | 10.82 |
| PT-80 | 50.04 | 0.4261 | 4.54 | 10.60 | 10.44 |
| 182 PUT | 45.09 | 0.5341 | 8.27 | 15.48 | 13.62 |
| | 44.05 | 0.5554 | 9.14 | 16.45 | |
| | 38.98 | 0.6517 | 6.08 | 9.33 | |
| | 39.06 | 0.6503 | 6.26 | 9.63 | |
| 140 PUT | 47.87 | 0.4747 | 9.25 | 19.49 | 17.69 |
| 128 PUT | 49.50 | 0.4384 | 6.50 | 14.82 | 12.27 |
| X-33-1 | 36.10 | 0.7014 | 6.92 | 9.86 | 9.64 |
| X-39-1 | 42.90 | 0.5783 | 6.10 | 10.39 | 10.14 |
| X-41-2B | 48.20 | 0.4676 | 5.03 | 10.77 | 10.43 |
| X-19-1 | 49.50 | 0.4385 | 3.72 | 8.49 | 8.87 |
| X-57-1 | 43.00 | 0.5763 | 6.78 | 11.76 | 11.90 |
| X-55-1 | 49.90 | 0.4293 | 4.55 | 10.60 | 10.42 |
| X-58-1 | 50.40 | 0.4179 | 3.41 | 8.16 | 8.37 |
| X-33-2 | 40.21 | 0.6297 | 6.66 | 10.58 | 10.47 |
| X-39-2 | 44.30 | 0.5502 | 7.38 | 13.41 | 12.15 |
| X-41-3 | 48.00 | 0.4720 | 5.19 | 11.00 | 11.13 |
| X-19-2 | 50.10 | 0.4248 | 3.71 | 8.73 | 8.86 |
| X-57-3 | 40.00 | 0.6333 | 7.28 | 11.50 | 11.46 |
| X-55-3 | 49.20 | 0.4421 | 4.49 | 10.16 | 10.12 |
| X-58-3 | 49.90 | 0.4292 | 4.27 | 9.95 | 9.98 |
| X-57-5 | 41.88 | 0.5980 | 8.27 | 13.83 | 13.79 |
| X-55-5 | 49.06 | 0.4484 | 5.00 | 11.15 | 11.13 |
| X-58-5 | 50.30 | 0.4202 | 4.07 | 9.69 | 9.72 |

of study show no indication of a point-to-point variation in structure in the thickness direction and appear to be homogeneous materials. Differences in modulus do exist among different types of cellophanes, however, and are undoubtedly the result of structural differences that arise during different methods of preparation.

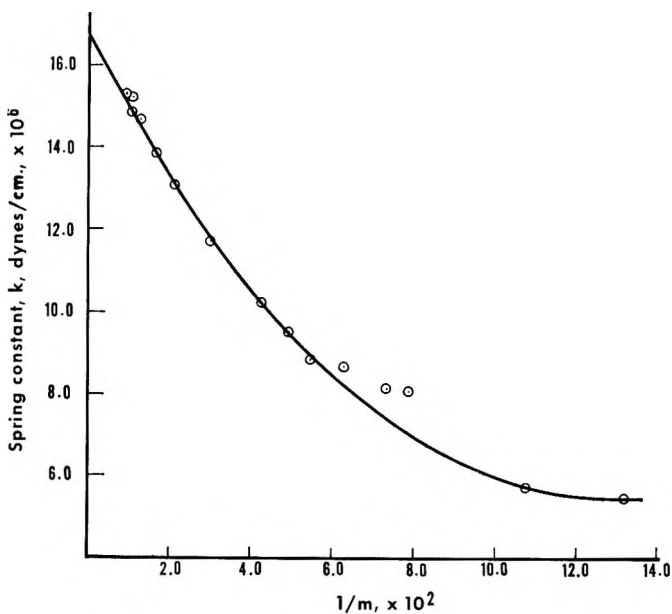


Fig. 3. Confirmation of instrument constant.

TABLE VI
Corrected Mean Values for the Modulus for Cellophane Films

| Film type | Average modulus, dynes/cm. ² $\times 10^{10}$ |
|-----------------------------|--|
| Commercial PT films | 11.02 |
| Commercial PUT films | 14.53 |
| Plate-cast laboratory films | |
| Salt index <1 | |
| Control | 9.73 |
| Heated 30 sec. | 10.64 |
| Salt index 8.8 | |
| Control | 10.23 |
| Heated 30 sec. | 10.52 |
| Heated 90 sec. | 11.52 |

APPENDIX

Derivation of an Equation for Elastic Modulus Corrected for a Spring in Series with the Film

Spring Equation. The compliance of the recording head may be combined to act as a spring with spring constant G_I in series with the film which has a spring constant G_F . The resultant measured spring constant G will be given by:

$$1/G = 1/G_I + 1/G_F$$

Since $G = EA/l$ and $G_F = E_0A/l$, where E is the measured value of the modulus, E_0 is the true value of the modulus, A is the cross-sectional area of the film, and l is the length of the specimen,

$$G = G_F - G(G_F/G_I)$$

On dividing through by A/l we obtain

$$E = E_0 - E_0(AE/G_I l)$$

and since $A = mg/4l^2\rho f_{tr}^2$,

$$E_0 = E - \frac{E_0 mg E}{4G_I \rho l (f_{tr} l)^2} \quad (3)$$

Correction Equation. Equation (3) can be transformed into another form to correct the modulus values by using k to replace G :

$$\begin{aligned} 1/k &= 1/k_I + 1/k_F \\ k_F &= k_I k_F / (k_F - k_I) \\ &= k_F / [1 - (k_F/k_I)] \end{aligned}$$

Since⁵ $f_l = 1/2 \pi (EA/m)^{1/2}$ and $k = EA/l$, $f_l = 1/2 \pi (k/m)^{1/2}$, and $k = 4\pi^2 f_l^2 m$.

Wherefore

$$E_0 = E(1 - 4\pi^2 f_l^2 m/k)^{-1} \quad (6)$$

References

1. Price, C. R., and V. C. Haskell, *J. Appl. Polymer Sci.*, **18**, 635 (1961).
2. Haskell, V. C., and D. K. Owens, *J. Appl. Polymer Sci.*, **4**, 225 (1960).
3. Pearse, H. A., D. J. Priest, R. J. Shimell, and A. G. White, *Tappi*, **46**, 622 (1963).
4. Gupta, M. K., L. Marker, E. Wellisch, and O. J. Sweeting, *J. Appl. Polymer Sci.*, to be published.
5. Hansen, O. C., Jr., T. L. Fabry, L. Marker, and O. J. Sweeting, *J. Polymer Sci.*, **A1**, 1585 (1963).
6. Hansen, O. C., Jr., L. Marker, K. W. Ninnemann, and O. J. Sweeting, *J. Appl. Polymer Sci.*, **7**, 817 (1963).
7. Gonsalves, V. E., *Textile Res. J.*, **17**, 369 (1947).
8. Dart, S. L., and L. E. Peterson, *Textile Res. J.*, **22**, 819 (1952).
9. Hansen, O. C., Jr., E. Gipstein, L. Marker, and O. J. Sweeting, *J. Polymer Sci.*, **A3**, 409 (1965).
10. Treloar, L., *Polymer*, **1**, 95, 279 (1960).

Résumé

On a étudié l'influence de l'épaisseur de film sur le module dynamique de la cellophane en vue de rechercher les différences de structure qui peuvent exister dans la cellophane, différences qui résultent des conditions différentes de régénération. Des mesures du module, effectuées sur différents types de films coulés et commerciaux, montrent une diminution du module avec une augmentation de l'épaisseur du film. Pour tous les films la rigidité est indépendante du type de film. Cependant on a prouvé que ce résultat était un artefact introduit par une cause instrumentale; on a trouvé que l'appareil de mesure du module dynamique se comportait comme un ressort en série avec

le film. Les modules de tous les films ont été corrigés pour cet effet et on a pris la moyenne des valeurs moyennes des modules dans la machine ainsi que des directions transverses pour tous les films séparément par types et par épaisseurs. On a trouvé que les valeurs étaient indépendantes de l'épaisseur du film pour tous les types de cellophane. Par cette méthode d'étude, la cellophane ne donne pas d'indication d'une variation point-par-point de la structure dans l'épaisseur du film. Cependant il n'existe pas de différences dans le module des différents types de cellophanes, et celles observées sont indubitablement le résultat des différences de structure qui proviennent des différentes méthodes de préparation.

Zusammenfassung

Der Einfluss der Filmdicke auf den dynamischen Modul von Zellophan wurde zur Aufklärung struktureller Unterschiede, welche in Zellophan als Ergebnis verschiedener Regenerationsbedingungen vorhanden sein können, untersucht. Modulmessungen an verschiedenen Typen von in Platten gegossenen und kommerziellen Filmen liessen zuerst eine Abnahme des Moduls mit steigender Filmdicke erkennen. Bei allen Filmen näherte man sich mit steigender Dicke einer Grenzsteifigkeit, welche vom Filmtyp unabhängig zu sein schien. Dieses Ergebnis erwies sich jedoch als ein durch einen Instrumenteneffekt bedingtes Artefakt; der Apparat zur Bestimmung des dynamischen Moduls verhielt sich wie eine mit dem Film in Serie geschaltete Feder. Die Moduln aller Filme wurden für diesen Effekt korrigiert und die Mittelwerte des Moduls in der Bewegungs- und der dazu normalen Richtung wurden für Filme getrennt nach Typen und Dicken gemittelt. Die Werte erwiesen sich bei allen Zellophantypen als unabhängig von der Filmdicke. Nach dieser Untersuchungsmethode zeigt Zellophan keine Anzeichen für eine Variation der Struktur von Punkt zu Punkt in der Dickendimension. Es bestehen jedoch Unterschiede in Modul zwischen verschiedenen Zellophantypen, und diese sind unzweifelhaft das Ergebnis struktureller Unterschiede, welche während verschiedener Darstellungsmethoden auftreten.

Received October 28, 1964
(Prod. No. 4614A)

1-Fluorovinyl Methyl Ketone: Preparation and Polymerization

JOHN A. SEDLAK and KEN MATSUDA, *Central Research Division,
American Cyanamid Company, Stamford, Connecticut*

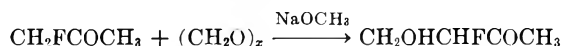
Synopsis

1-Fluorovinyl methyl ketone, a new vinyl monomer, was prepared by dehydration of 1-fluoro-2-hydroxyethyl methyl ketone with phosphoric acid or boric anhydride. The monomer was stabilized with anhydrous ammonia during preparation and storage. Homopolymers of 1-fluorovinyl methyl ketone were prepared with free-radical initiators in bulk, in solution, and in buffered emulsions.

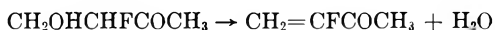
INTRODUCTION

1-Fluorovinyl methyl ketone has never been reported in the literature, although the chloro and bromo analogs have long been known.¹⁻⁴ Our interest in the effect of fluorine substituents on the properties of vinyl polymers⁵ led us to investigate the preparation and polymerization of this novel monomer.

A convenient starting material for the synthesis of 1-fluorovinyl methyl ketone was 1-fluoro-2-hydroxyethyl methyl ketone, which has been prepared by the base-catalyzed condensation of fluoroacetone and formaldehyde:⁶



We have developed an efficient method for dehydrating this compound to produce 1-fluorovinyl methyl ketone:



The dehydration was readily accomplished with phosphoric acid at 150-155°C. or with boric anhydride^{7,8} at 170-175°C., but special precautions were necessary to suppress the great tendency of the monomer to polymerize.

EXPERIMENTAL

Analytical Methods

Boiling points are uncorrected. Gas chromatographic analyses were performed with helium carrier gas on a Wilkens A-90-C chromatograph equipped with a 10-ft. column of 20% dinonyl phthalate on firebrick or 20%

polypropylene glycol on firebrick. Infrared spectra were recorded on a Perkin-Elmer Model 137B spectrophotometer. The NMR spectra were obtained with a Varian V4300B spectrometer operating at 56.4 Mcycles; the samples were dissolved in approximately 10% concentration in carbon tetrachloride containing a small amount of tetramethylsilane or in trichlorofluoromethane.

Materials

Fluoroacetone was prepared from chloroacetone (Eastman Organic Chemicals, practical) and potassium bifluoride;⁹ the potassium bifluoride (Baker and Adamson, crystal, technical) was prepared for reaction by heating at 150°C., ball-milling with intermittent heating to produce a fine powder, and finally drying at 150°C. The fluoroacetone was condensed with paraformaldehyde (Eastman Organic Chemicals) to prepare 1-fluoro-2-hydroxyethyl methyl ketone in 37% yield.⁶ The buffer solution was prepared with Beckman dry reagents and boiled deionized water. Triton X-305 poly(ethylene oxide) type emulsifying agent was obtained from Rohm and Haas.

Preparation of 1-Fluorovinyl Methyl Ketone

Phosphoric Acid Dehydrating Agent. A 50-ml., round-bottomed, three-necked, Pyrex glass flask was equipped with a sealed stirrer, a pressure-equalizing dropping funnel, and a distillation head leading to a take-off condenser. The distillation head was provided with an inlet just above the neck of the flask to allow the passage of anhydrous ammonia gas through the head and out the condenser and receiver. The dropping funnel was equipped with an inlet for a stream of nitrogen gas passing in over the reaction mixture and out through the distillation head. By regulating the velocities of the two gas streams, it was possible to keep ammonia in contact with the distillate while avoiding contact of ammonia with the bulk of the reaction mixture.

In the flask was placed 8 ml. of 85–87% phosphoric acid and in the dropping funnel was placed 25.5 g. (0.240 mole) of 1-fluoro-2-hydroxyethyl methyl ketone. Small amounts of hydroquinone were added to the phosphoric acid, fluorohydroxyketone, and receiver. The apparatus was swept with nitrogen and the ammonia stream was started. During 55 min., the 1-fluoro-2-hydroxyethyl methyl ketone was added dropwise to the reaction mixture stirred in an oil bath held at 150–155°C. The product distilled as formed. After an additional 15 min., distillation ceased. The distillate consisted of 4.4 g. of an aqueous phase and 13.2 g. of an organic phase; the mixture was alkaline, due to dissolved ammonia. Gas chromatography (dinonyl phthalate, 110°C.) showed that the organic material was 95% 1-fluorovinyl methyl ketone, amounting to a yield of 12.5 g. (0.14 mole) or 58% based on 0.240 mole of 1-fluoro-2-hydroxyethyl methyl ketone.

To the distillate was added 15 ml. of tetralin and 5 ml. of saturated aqueous sodium chloride. The organic layer was separated and washed with two 5-ml. portions of saturated aqueous sodium chloride. After the washings, the organic solution still contained some ammonia. A small amount of hydroquinone was added and the solution was dried at -20°C . over anhydrous magnesium sulfate. The product was distilled at atmospheric pressure under nitrogen on a 1.2-cm. \times 10-cm. Vigreux column. The receivers were cooled in Dry Ice-acetone and the distillate was stored at Dry Ice temperature until used for polymerization. Distillation gave three fractions: (1) 2.4 g., b.p. $66.8\text{--}71.3^{\circ}\text{C}$.; (2) 4.4 g., b.p. 71.3°C .; (3) 0.5 g., b.p. $71.3\text{--}71.5^{\circ}\text{C}$. The pot temperature during the distillation was $94\text{--}180^{\circ}\text{C}$.; these high temperatures caused considerable polymerization in the pot which probably could have been lessened by lowering the distilling pressure. The distillate was alkaline, due to ammonia, and colorless. Gas chromatography (dinonyl phthalate, 110°C .) showed that fraction 2 was pure 1-fluorovinyl methyl ketone while fractions 1 and 3 contained very small amounts of impurities. The infrared spectrum of 1-fluorovinyl methyl ketone shows absorptions at 1715 cm.^{-1} for $\text{C}=\text{O}$, 1650 cm.^{-1} for $\text{C}=\text{C}$, and 1136 cm.^{-1} for $\text{C}-\text{F}$. The mass spectrum was consistent with the assigned structure. The NMR spectrum shows F^{19} resonance centered at $116.2\ \phi$ which is the expected quartet doubled twice. H^1 resonances; hydrogen *cis* to fluorine, $4.88\ \tau$; hydrogen *trans* to fluorine, $4.55\ \tau$; methyl, $77.4\ \tau$. Couplings; $J_{\text{F-H}}$ (*cis*), 14.1 cycles/sec.: $J_{\text{F-H}}$ (*trans*), 47.9 cycles/sec.: $J_{\text{F-CH}_3}$, 2.8 cycles/sec.

ANAL. Calcd. for $\text{C}_4\text{H}_5\text{FO}$: C, 54.54% ; H, 5.72% ; F, 21.57% . Found: C, 54.19% ; H, 5.47% ; F, 21.37% .

Boric Anhydride Dehydrating Agent. A 50-ml. round-bottomed Pyrex flask was equipped with a sealed stirrer and a distillation head leading to a take-off condenser. In the flask were placed 20.0 g. (0.189 mole) of 1-fluoro-2-hydroxyethyl methyl ketone and 7.5 g. (0.108 mole) of powdered boric anhydride. The stirred mixture was heated in an oil bath. As the temperature exceeded 100°C ., the mixture began to darken, and, when the temperature reached 170°C ., foaming and charring became evident and distillation started. Distillation proceeded during 10 min. while the bath temperature was held at $170\text{--}175^{\circ}\text{C}$. The condenser became plugged with an off-white solid after only 4.5 g. of organic product, together with some water, was collected. Gas chromatography (polypropylene glycol, 115°C .) showed that the product was largely 1-fluorovinyl methyl ketone.

Polymerization of 1-Fluorovinyl Methyl Ketone

Benzene Solvent. Under a nitrogen atmosphere, a Pyrex glass tube was charged with 1.4 g. of freshly-distilled 1-fluorovinyl methyl ketone (containing a small amount of ammonia but no other inhibitor), 0.0014 g. of azobisisobutyronitrile, and 7 ml. of benzene. The mixture was purged

with a stream of nitrogen and the tube was sealed. The tube was immersed in an oil bath at 65°C. for 17 hr., during which an off-white polymer precipitated from the solution. The mixture tested neutral on moist Alkacid paper. The benzene was decanted and the polymer was dissolved in chloroform. The solution was slowly poured into stirred methanol to form fibrous particles of off-white polymer. The polymer was dried, redissolved, reprecipitated, and finally dried in the open and then under vacuum at 50°C. for 6 hr. The dry polymer weighed 0.9 g.

The infrared spectrum of poly(1-fluorovinyl methyl ketone) shows absorptions at 1740 cm.^{-1} for C=O, 1360 cm.^{-1} for $-\text{CH}_3$ next to C=O, and 1145 cm.^{-1} for C—F; there was no absorption in the C=C region.

ANAL. Calcd. for $\text{C}_4\text{H}_5\text{FO}$: C, 54.54%; H, 5.72%; F, 21.57%. Found: C, 54.43%; H, 5.81%; F, 21.73%.

Chloroform Solvent. The preceding experiment was repeated, except that 7 ml. of chloroform was used in place of the benzene. The polymer remained in solution (neutral) which was treated as above to give 0.7 g. of off-white polymer.

Bulk. The same experiment was repeated, except that no solvent was used. A hard, clear, solid polymer was formed. Portions of the polymer were faintly yellow and portions were colorless. The polymer was dissolved in chloroform or nitromethane by intermittent agitation and heating for a few minutes followed by standing for several hours at room temperature.

Neutral Emulsion. In a 100-ml. three-necked creased flask equipped with a nitrogen inlet tube, stirrer, reflux condenser, and gas exit through a bubbler, were placed 20 ml. of an aqueous buffer at pH 6.86 and 0.11 g. of Triton X-305 emulsifying agent. The stirred solution was purged with prepurified nitrogen for 20 min. Freshly distilled 1-fluorovinyl methyl ketone (2.1 g.), containing a small amount of ammonia but no other inhibitor, was added, and a milky white emulsion formed immediately. Ammonium persulfate (0.035 g.) and triethanolamine (0.022 g.) were added and the nitrogen purge was continued for 10 min. The mixture was stirred at 35°C. for 24 hr. The emulsion was poured into 200 ml. of stirred methanol to precipitate the polymer, which was separated by centrifuging. Drying under vacuum for 8 hr. at 50°C. gave 1.2 g. of polymer as a nearly white fine powder which was partially soluble in chloroform.

Basic Emulsion. The emulsion polymerization was repeated, except that a buffer at pH 9 was used. The nearly white powdery polymer weighed 1.4 g. and was insoluble in chloroform.

RESULTS AND DISCUSSION

Preparation of 1-Fluorovinyl Methyl Ketone

Polymerization of 1-fluorovinyl methyl ketone in the dehydration mixture was minimized by distilling the monomer as it formed. Poly-

merization which occurred on condensation was inhibited by passing a stream of ammonia gas through the distilling apparatus in quantity sufficient to leave free ammonia dissolved in the product. By means of this procedure, a 58% yield of the monomer was isolated. Little inhibition resulted when nitric oxide, a free-radical scavenger,¹⁰ was substituted for the ammonia, leading to the conclusion that a free-radical process was not the primary cause of polymerization of the distillate. It therefore seemed likely that the polymerization was catalyzed by small amounts of acid entrained with the monomer. Ethylene oxide was also tried as an inhibitor, but with little success.

A different route to 1-fluorovinyl methyl ketone utilizing the Mannich reaction was evaluated. Equimolar quantities of fluoroacetone, paraformaldehyde, and dimethylamine hydrochloride were refluxed in ethanol to form the Mannich base, which was decomposed¹¹ by heating in Dowtherm-A heat transfer medium. However, 60% of the fluoroacetone was recovered unchanged, and only very small quantities of 1-fluorovinyl methyl ketone and vinyl fluoromethyl ketone, identified by mass spectrometry, were produced.

1-Fluorovinyl methyl ketone is a colorless, volatile liquid with an odor typical of ketones. The boiling point is 71°C. Elemental analysis, infrared absorption, nuclear magnetic resonance, and mass spectrum were used to substantiate the assigned structure. Stringent safety precautions were observed against personnel exposure to 1-fluorovinyl methyl ketone and 1-fluoro-2-hydroxyethyl methyl ketone because many monofluorinated compounds are extremely toxic;¹² no toxicity tests were performed.

Anhydrous ammonia, which is known to inhibit polymerization of unsaturated ketones,¹³ acted as an inhibitor during storage of 1-fluorovinyl methyl ketone; at -20°C. no polymerization was noted after several weeks. Monomer samples containing free ammonia were also stable for several hours at room temperature, but acidification with a small amount of 85-87% phosphoric acid or glacial acetic acid caused polymerization. This polymerization occurred even when oxygen was excluded, indicating that it was not initiated by autoxidation. Because polymerization was often very rapid and exothermic, only small quantities of monomer were stored in any one container.

Polymerization of 1-Fluorovinyl Methyl Ketone

The infrared spectrum of the poly(1-fluorovinyl methyl ketone) prepared in benzene exhibited no olefinic absorption, and elemental analysis showed the theoretical content of fluorine. Furthermore, no free acid was detected in the polymerization mixtures. These results demonstrated that no more than trace quantities of hydrogen fluoride could have been evolved during polymerization, contrasting with the autocatalytic evolution of hydrogen fluoride previously observed in the polymerization of α -fluorostyrene.⁵ With α -fluorostyrene, hydrogen fluoride elimination and accompanying color formation was suppressed only by employing

buffered neutral or basic emulsion polymerization systems. Similar emulsion systems produced 1-fluorovinyl methyl ketone polymers of even lighter color than those obtained from the solution systems.

The molecular weights of the polymers prepared in benzene and in chloroform were quite high, as shown by intrinsic viscosities of 3.1 and 1.4 dl./g., respectively, measured in chloroform solution at 30°C. The polymer prepared in bulk was probably still higher in molecular weight and was therefore less readily dissolved in chloroform. The complete solubility of these polymers in organic solvents indicated that they were not crosslinked. Polymer solutions were suitable for casting films which were clear, hard, and flexible after drying. The polymers prepared in emulsion systems were not completely soluble in chloroform, indicating that, as expected, they were of much higher molecular weight than the polymers prepared in solution.

The glass transition temperature of the poly(1-fluorovinyl methyl ketone) prepared in benzene was 142°C., as measured by differential thermal analysis. This value is probably higher than that of poly(vinyl methyl ketone), for which a glass transition temperature has not been reported but which softens¹⁴ at about 40°C. Thermogravimetric analysis, with the polymer contained in a porcelain crucible subjected to a programmed heating at 10°C./min., showed T_i 280°C., T_{10} 316°C. in air, and T_i 280°C., T_{10} 325°C. in nitrogen. The thermogravimetric curve did not show the abrupt quantitative evolution of hydrogen fluoride that was observed on heating poly- α -fluorostyrene.⁵

The authors thank Mr. N. B. Colthup for assistance in interpreting the infrared spectra, Dr. J. E. Lancaster for the NMR spectra, Mrs. R. H. Barritt for the mass spectrometric analysis, Miss E. C. Eberlin for the thermogravimetric and differential thermal analyses, and the Microanalytical Department for elemental analyses. The emulsion polymerizations were based on general procedures developed by Mr. E. R. Kolodny of these laboratories.

References

1. Metzger, L. W. and O. Bayer, U. S. Pat. 2,173,066 (1939).
2. Metzger, L. W. and O. Bayer, German Pat. 708,371 (1941).
3. Nield, C. H., *J. Am. Chem. Soc.*, **67**, 1145 (1945).
4. Kosower, E. M., and G.-S. Wu, *J. Org. Chem.*, **28**, 633 (1963).
5. Matsuda, K., J. A. Sedlak, J. S. Noland, and G. C. Gleckler, *J. Org. Chem.*, **27**, 4015 (1962).
6. Bergmann, E. D., and S. Cohen, *J. Chem. Soc.*, **1961**, 3457.
7. Brandenburg, W., and A. Galat, *J. Am. Chem. Soc.*, **72**, 3275 (1950).
8. Walborsky, H. M., and M. Schwarz, *J. Am. Chem. Soc.*, **75**, 3241 (1953).
9. Cherbuliez, E., A. de Picciotto, and J. Rabinowitz, *Helv. Chim. Acta*, **43**, 1143 (1960).
10. Dreher, E., and H. Pasedach, German Pat. 892,455 (1953).
11. Hagemeyer, H. J., Jr., *J. Am. Chem. Soc.*, **71**, 1119 (1949).
12. Pattison, F. L. M., *Toxic Aliphatic Fluorine Compounds*, Elsevier, New York, 1959.
13. Dannenberg, H., and D. E. Adelson, U. S. Pat. 2,294,286 (1942).
14. Schildknecht, C. E., *Vinyl and Related Polymers*, Wiley, New York, 1952, pp. 687-688.

Résumé

Un nouveau monomère vinylique, la 1-fluorovinyle-méthyle-cétone, a été préparé par déshydratation de la 1-fluoro-2-hydroxyéthyle-méthyle-cétone par l'acide phosphorique ou l'anhydride borique. Le monomère a été stabilisé au moyen d'ammoniac anhydre pendant sa préparation et sa conservation. Des homopolymères de la 1-fluorovinyle-méthyle-cétone ont été préparés, au moyen d'initiateurs radicalaires, en bloc, en solution et en émulsions tamponnées.

Zusammenfassung

1-Fluorvinylmethylketon, ein neues Vinylmonomeres, wurde durch Dehydratisierung von 1-Fluor-2-hydroxyäthylmethylketon mit Phosphorsäure oder Borsäureanhydrid dargestellt. Das Monomere wurde während der Darstellung und Lagerung mit wasserfreiem Ammoniak stabilisiert. Homopolymere von 1-Fluorvinylmethylketon wurden mit Radikalstartern in Substanz, in Lösung und in gepufferten Emulsionen dargestellt.

Received October 28, 1964

Revised December 29, 1964

(Prod. No. 4616A)

Synthesis and Structure of Polyglyoxal*

WILLIAM T. BRADY and HUBERT R. O'NEAL, *Chemistry Department, North Texas State University, Denton, Texas*

Synopsis

The polymerization of glyoxal has been carried out in the presence of sodium naphthalene in THF at -78°C . The polyglyoxal decomposed at 150°C . and was slightly soluble in water and alcohol. The polymer was readily acetylated with acetic anhydride to yield a material that decomposed at about 290°C . Structure elucidation of the glyoxal polymer indicated that it had a polyacetal type of structure containing pendant enol groups and also a cyclic chelated structure involving hydrogen bonding between an enolic hydroxy group and a pendant carbonyl group.

INTRODUCTION

Relatively little work has been published on the controlled polymerization of dialdehydes. Glyoxal, the simplest dialdehyde, has been reportedly polymerized by Okamura and his co-workers¹ and Morimoto and his co-workers² by irradiation to an insoluble white solid. The infrared data reportedly showed acetal absorption and the absence of carbonyl absorption, but no structure was proposed for the polymer.^{1,2} Bevington recently made a review of the developments in the field of aldehyde polymerization and predicted that the aldehyde units of glyoxal would probably react independently, giving a crosslinked polymer.³ This paper is concerned with the controlled polymerization of glyoxal and the structure elucidation of the polymer. A preliminary report of this work has appeared.⁴

EXPERIMENTAL

Monomeric Glyoxal

A commercially available 30% aqueous solution of glyoxal was distilled under reduced pressure (1-2 cm.) until water ceased to be removed. The hard and brittle residue was pulverized and dried in a vacuum oven at 60°C . for 120 hr. Upon pyrolysis of this residue, which is believed to be a trimeric form of glyoxal, the characteristic green vapor of monomeric glyoxal was obtained.⁵ This vapor was passed with nitrogen through a 14-in. drying column containing 8 mesh anhydrous CaCl_2 . The vapor was then passed directly into the polymerization flask containing the solvent and catalyst at -78°C .

* Paper was presented at the 20th Southwest Regional Meeting of the American Chemical Society, Shreveport, Louisiana, December 5, 1964.

Solvent

Tetrahydrofuran (THF) was purified by refluxing over sodium wire and then distilling under an inert atmosphere on a 30-plate Oldershaw column.

Catalyst

Sodium naphthalene was prepared according to the method described by Scott and co-workers.⁶

Polymerization of Glyoxal

To a 300-ml. three-necked flask equipped with a stirrer and nitrogen inlet and outlet was added 170 ml. of THF under a nitrogen atmosphere. This solvent was cooled to -78°C . by immersing the flask in an acetone-Dry Ice mixture. The solvent was saturated with dry monomeric glyoxal and then 5 ml. (0.29 g.; 0.0018 mole) of sodium naphthalene in THF was added by means of a hypodermic syringe. Polymerization occurred within 5–10 min. as evidenced by an increase in viscosity and eventual gelation. Stirring in the cold was continued for 30 min. and the polymer isolated by filtration. The polymer was washed with THF, acetone, acetone-water, and finally acetone. The solid was dried at 60°C . in a vacuum oven for 24 hr. The polymer was quite stable at room temperature but decomposed upon heating to 150°C . A thermogram obtained from a Perkin-Elmer differential calorimeter indicated a melting transition at 144°C . and an immediate exothermic transition corresponding to thermal degradation.

The polymer was soluble to the extent of about 1% in hot water. Polyglyoxal isolated from an aqueous solution had the same physical properties and infrared spectrum as the original polymer. The polymer was also sparingly soluble in ethanol (0.5%) and very soluble in dilute sodium hydroxide solution. Some of the polymer could be recovered from the basic solution by acidification, but extensive degradation occurred, as the

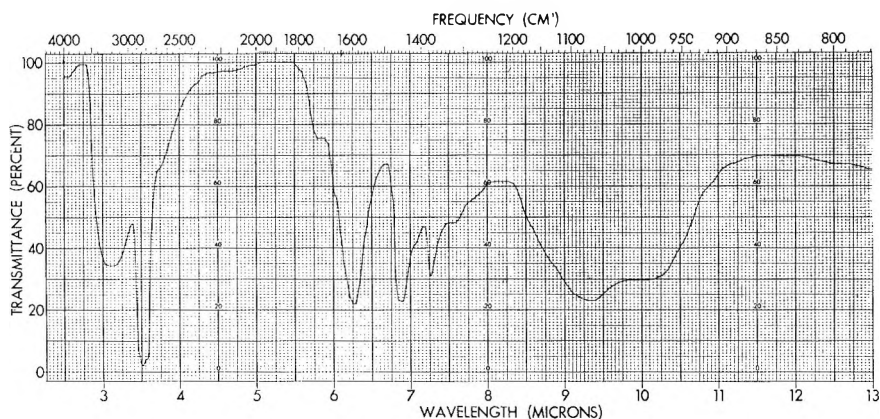


Fig. 1. Infrared spectrum of polyglyoxal.

polymer was very unstable in the presence of acid. A positive enol test was obtained when an aqueous solution of polyglyoxal was treated with bromine and KI.⁷ Inherent viscosities of 0.2–0.3 (0.2 g./100 ml. ethanol, 25°C.) have been obtained.

An infrared spectrum of this polymer is shown in Figure 1. Attempts to obtain a useful NMR spectrum were unsuccessful due to the limited solubility of the polymer. An x-Ray diffraction pattern indicated the polymer was amorphous.

Acetylation of Polyglyoxal

A 2.0-g. sample of polyglyoxal was placed in a flask containing a few milligrams of sodium acetate. A 75-ml. portion of acetic anhydride was added to the flask and the mixture was heated at reflux for 3 hr. with agitation. After cooling to room temperature and filtering, 1.13 g. of material was isolated. This material was washed repeatedly with acetone, water, acetone, and finally anhydrous ether. The solid was then dried in a vacuum oven at 60°C. for several hours. This polymer decomposed upon heating to 290°C. A thermogram obtained from a Perkin-Elmer differential calorimeter showed a melting transition at 280°C. with an exothermic transition occurring thereafter.

The infrared spectrum of this acetylated polyglyoxal is shown in Figure 2. The acetylated polymer was slightly soluble in dilute sodium hydroxide solution but insoluble in water.

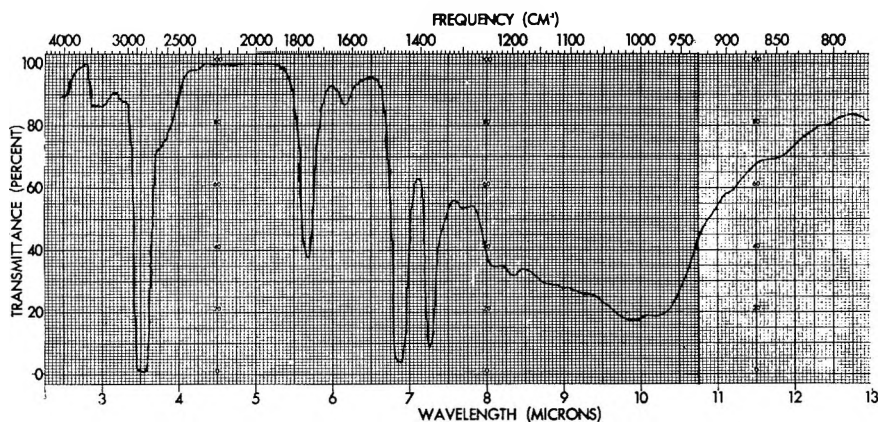


Fig. 2. Infrared spectrum of acetylated polyglyoxal.

DISCUSSION

The preparation of anhydrous monomeric glyoxal was an extremely critical step in the synthesis of polyglyoxal. The method selected has been very successful. However, if the solid isolated from the vacuum distillation was not finely pulverized and carefully dried, the polymerization would not occur due to residual water.

The solubility of glyoxal was found to be a limiting factor in the selection of a suitable solvent for the polymerization. Glyoxal is only sparingly soluble in hydrocarbon solvents at the low temperature necessary for polymerization. THF is a good solvent for this monomer at -78°C . but must be rigorously purified prior to use as the polymerization solvent.

Sodium naphthalene was found to be an active catalyst for the polymerization of glyoxal in THF at -78°C . Triethylaluminum forms an etherate with THF, but this etherate was not an active catalyst for this polymerization. However, triethyl aluminum in hexane was found to be effective for the polymerization of glyoxal at -78°C . Due to the limited solubility of the monomer in this solvent, only a small amount of polymer was obtained.

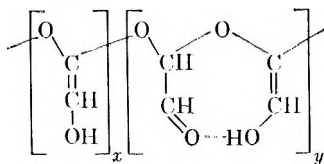
The infrared spectrum of polyglyoxal shows strong hydroxyl absorption at 3200 cm.^{-1} , a strong absorption at 1595 cm.^{-1} , strong acetal absorption in the $1100\text{--}950\text{ cm.}^{-1}$ region, and the absence of carbonyl absorption at the usual 1725 cm.^{-1} . The data obtained from this spectrum do not agree with the predicted structure.³

It was observed that if glyoxal polymerized as Bevington predicted, an α hydrogen would be available for enolization. An enolic structure would thus account for the strong hydroxyl absorption at 3200 cm.^{-1} , the acetal absorption, and the absence of carbonyl absorption. However, the strong absorption at 1595 cm.^{-1} would remain unassigned. The presence of an enolic structure was confirmed by an enol spot test.⁷ Also, the polymer was very soluble in dilute sodium hydroxide solution and slightly soluble in water, which further substantiates the enolic structure.

The strong absorption at 1595 cm.^{-1} cannot be assigned to a carbon-carbon double bond because vinyl ethers absorb at $1610\text{--}1640\text{ cm.}^{-1}$. Also, carbon-carbon double bond absorption is usually not very intense in the infrared.

Acetylacetone, known to exist in an enolic form, was selected as a model compound for study in the structure of polyglyoxal. A strong absorption at 1595 cm.^{-1} has been reported for acetyl-acetone and is attributed to hydrogen bonding between an enolic hydroxyl group and a carbonyl oxygen. This results in a shift of the carbonyl absorption from the usual 1725 to 1595 cm.^{-1} . The absorption is an extremely strong absorption and is reportedly about 100 times stronger than the normal carbonyl absorption.⁸ Since there is a strong absorption at 1595 cm.^{-1} for polyglyoxal, it has been proposed that there is hydrogen bonding between an enolic hydroxyl group and a carbonyl oxygen.⁴

Consequently, on the basis of the infrared data, the solubility data, and the positive enol test, structure I was proposed for polyglyoxal:



I

A molecular model of the chelated structure does not appear to involve any straining whatsoever. The relative intensities of the infrared spectrum indicate that x is considerably larger than y .

The infrared spectrum of the acetylated polyglyoxal indicates a large decrease in hydroxyl absorption. The spectrum also indicates an ester carbonyl absorption and strong acetal absorption. The 1625 cm.^{-1} absorption is assigned to carbon-carbon unsaturation which was masked by the strong 1595 cm.^{-1} absorption in the polyglyoxal spectrum. The position and intensity of the band further substantiates the chelated structure of polyglyoxal. The results of this spectrum are exactly as would be expected for the acetylation of a polymer with the proposed enolic structure. The slight solubility of this polymer in sodium hydroxide solution is apparently due to the residual hydroxyl groups present in the material as evidenced by the infrared spectrum.

References

1. Okamura, S., K. Hayashi, and K. Mori, paper presented at 10th Annual Meeting of the High Polymer Society, Japan, Tokyo, May 1961; cited by J. Furakawa and T. Saegusa, *Polymerization of Aldehydes and Oxides*, Wiley, New York, 1963.
2. Morimoto, G., H. Kawazura, and Y. Yoshie, *Nippon Kagaku Zasshi*, **82**, 1464 (1961).
3. Bevington, J. C., *Brit. Plastics*, **35**, 75 (1962).
4. Brady, W. T., and H. R. O'Neal, *J. Polymer Sci.*, **B2**, 647 (1964).
5. Harries, C., and P. Femme, *Ber.*, **40**, 165 (1907).
6. Scott, N. D., J. F. Walker, and V. L. Hansley, *J. Am. Chem. Soc.*, **68**, 2442 (1936).
7. Feigl, F., *Spot Tests in Organic Analysis*, Elsevier, Amsterdam-New York, 1960, 6th edition, p. 213.
8. Rasmussen, R. B., D. D. Tunnicliff, and R. R. Brattain, *J. Am. Chem. Soc.*, **71**, 1068 (1949).

Résumé

On a effectué la polymérisation du glyoxal en présence de sodium naphthalène dans le THF à -78°C . Le polyglyoxal se décompose à 150°C et est faiblement soluble dans l'eau et dans l'alcool. Le polymère est facilement acétylé au moyen de l'anhydride acétique pour fournir un produit qui se décompose aux environs de 290°C . L'élucidation de la structure du polyglyoxal indique qu'il y a un type de structure polyacétal contenant des groupements enol latéraux ainsi qu'une structure cyclique chélatée impliquant une liaison hydrogène entre un groupe hydroxy-énolique et un groupe carboxylique latéral.

Zusammenfassung

Die Polymerisation von Glyoxal wurde in Gegenwart von Natriumnaphthalin in THF bei -78°C ausgeführt. Das Polyglyoxal zersetzte sich bei 150°C und war in Wasser und Alkohol etwas löslich. Das Polymere konnte mit Essigsäureanhydrid leicht unter Bildung eines bei etwa 290°C zersetzlichen Materials acetyliert werden. Die Strukturaufklärung des Glyoxalpolymeren zeigte, dass es eine Polyacetalstruktur mit anhängenden Enolgruppen und auch eine zyklische Chelatstruktur mit Wasserstoffbindungen zwischen einer enolischen Hydrozylgruppe und einer anhängenden Carbonylgruppe besitzt.

Received June 30, 1964

Revised January 12, 1965

(Prod. No. 4620A)

Redox Kinetics of the Peroxydisulfate-Iron-Sulfoxylate System

H. M. ANDERSEN and S. I. PROCTOR, JR., *Monsanto Company,
Central Research Department, St. Louis, Missouri*

Synopsis

Inhibition kinetics were used to study the peroxydisulfate-iron-sulfoxylate redox initiation system. Onset of polymerization was detected by a thermometric technique permitting accurate measurement of short inhibition periods. Rate constants were derived from the inhibition periods by using an analog simulation. A good fit of calculated to observed results was obtained, based on a simple model, for experiments in ammonia buffer (pH ca 10). In bicarbonate buffer (pH ca 8.5), however, the same simple model was inadequate; additional involvement of iron is indicated. Evidence was found that the reduction of ferric versenate by sulfoxylate yields a free radical, tentatively $(\text{HCHO})\text{SO}_2\cdot$. Absolute rates of radical generation were calculated.

INTRODUCTION

The redox systems used as emulsion polymerization initiators have been the object of many studies^{1,2} and justifiably so, because their behavior is a major factor in determining the rate, yield, and molecular parameters of the product polymer.

Two of the methods most commonly used to study these redox systems are to follow the disappearance of one of the reagents by a suitable analytical method, or to follow the conversion of monomer to polymer. In the present work, inhibition kinetics were employed. Thereby the rate of radical generation, which is the quantity of primary interest, can be measured directly rather than indirectly, and independently of the polymerization process *per se*. Although a series of both consecutive and simultaneous reactions are involved, rate constants for individual reactions can be determined by using an analog computer to fit the experimental data to the kinetic model proposed.

The system reported on here is the peroxydisulfate-iron-sulfoxylate system, of which no detailed study appears to have been published. The primary cycle comprises the reaction of peroxydisulfate with ferrous ion to yield sulfate radicalion, followed by reduction of the ferric ion to ferrous by the sulfoxylate, thus allowing the iron to cycle. Actually, radicals from reactions other than the peroxydisulfate-ferrous reaction are also involved.

In using inhibition kinetics to study the rate of radical generation, an inhibitor capable of successfully competing with monomer for the radicals was present in the system, so that polymerization was prevented until the

inhibitor was consumed. Thus, the inhibition period, t_i , from the start of the reaction to the onset of polymerization is an inverse function of the rate of radical generation.

The exotherm caused by polymerization was used to detect the end of the inhibition period, which was generally from 2 to 60 min. long.

By using this technique, the effect of reagent concentrations, temperature, and other factors on the system can be determined in the total milieu of emulsion polymerization, including emulsifier and monomer. The existence of any significant side reactions may be detected by testing the kinetic model based on the postulated reactions against experimental data. If a reasonable fit cannot be found, the existence of additional significant reactions is indicated. Further, the role, if any, of the emulsifier, monomer, and electrolyte can be determined.

Despite the apparent attractiveness of inhibition kinetics⁴ as a means of measuring this process, relatively little application of the method to emulsion polymerization appears to have been reported;^{1,5-11} only one of these papers¹⁰ deals with redox emulsion polymerization. The approach has been used extensively, however, in studying the related problem of autooxidation of various substrates.¹²⁻¹⁹ The papers by George, Rideal, and Robertson¹³ include a thorough mathematical treatment relating inhibition periods to rate constants.

It is emphasized that the present work was concerned solely with measuring the rate of generation of free radicals, and not with the subsequent polymerization rate. With this restriction, the monomer functions only as an "indicator," the onset of its polymerization signaling the consumption of the inhibitor. Styrene was used in all the experiments reported here.

The oxygen or peroxide present in commercial styrene was used as the inhibitor. No other reagent was found to function as well for this purpose.^{1,8-11,20-24}

In this work, as noted above, the polymerization exotherm has been used to detect the end of the inhibition period, rather than the usual dilatometric or gravimetric procedures. We believe this offers substantial advantages in sensitivity and speed.

In addition to the inhibition experiments, the rates of one of the reactions was measured independently, in the absence of monomer and emulsifier, to help simplify the kinetic analysis.

A procedure employing exotherms to measure polymerization rates has recently appeared in the literature.²⁵

In three very recent papers,^{2,26,27} Kolthoff, Meehan, and co-workers have studied related redox systems; in their work, the disappearance of the oxidant is followed polarigraphically.

EXPERIMENTAL

Apparatus

The reactor consisted of a 200-ml. jacketed glass vessel, equipped with a stirrer, thermistor probe, and ports for the admission of reagents; a bottom

draw-off permitted dumping of the contents and flushing after each run, without disassembly. Water from a thermostat was pumped through the jacket, so that the temperature of the reactor contents was constant to $\pm 0.01^\circ\text{C}$.

The thermistor comprised one leg of a simple Wheatstone bridge. The bridge output fed a 10-mv. recorder; values were so chosen that full-scale deflection on the recorder equaled 2.00°C ., readable to 0.01°C . The recorder was equipped with a control switch operating a timer, and an event-marker on the chart paper.

Recipe

The recipes used were as follows: water, 100 ml.; D-94 (sodium dodecylbenzenesulfonate), 2 g.; buffer, NH_4OH , NaHCO_3 , or phosphate, as indicated (most runs in $0.06M$ NH_4OH or $0.10M$ NaHCO_3); SFS (sodium formaldehyde sulfoxylate), varied $(6-104) \times 10^{-4}M$, Fe, varied $(0-70) \times 10^{-3}M$; EDTA (ethylenediaminetetraacetate), $2 \times [\text{Fe}]$ in each case; KPS (potassium peroxydisulfate), varied $(0-300) \times 10^{-4}M$; styrene, 100 ml.

Procedure

The reactor was flushed with lamp-grade nitrogen, and the water, emulsifier, buffer, and sulfoxylate were charged (final total aqueous volume = 100 ml.). The solution was thoroughly purged with nitrogen through the bottom port, and a slight positive nitrogen pressure maintained on the system. Monomer (100 ml.) containing inhibitor (oxygen) was added, and the system allowed to come to thermal equilibrium as indicated by a straight line on the recorder (about 10 min.). The iron and peroxydisulfate were then added from a stock solution containing both reagents (having been thermostatted at the same temperature) and the timer started. As an auxiliary timing method, an event marker on the recorder simultaneously marked the beginning of the run. Control runs (with no inhibitor) started polymerization in 15-30 sec.; this is believed to represent the mixing and response time of the system. Any inhibiting impurities in the system would have their effect included in these 15-30 sec. In inhibited runs, values were generally chosen so as to give periods of 2-60 min.; no attempt to apply blank corrections was made.

The onset and initial rate of polymerization were clearly recorded by the slope of the resultant exotherm. The recorder control switch having been set at $0.01-0.02^\circ\text{C}$. above the equilibrium temperature, the timer was automatically turned off just at the beginning of the exotherm, which usually reached $0.5-1.0^\circ\text{C}$.; the event marker also permitted reading the time directly from the chart. In addition to obtaining the inhibition period, the slope, amplitude, and duration of the exotherm provided at least a qualitative, and perhaps quantitative, indication of the rate and yield of the polymerization; as noted above, no attempt has been made to measure the latter in this work.

In this report, 30°C. was considered the "standard" temperature. Runs at 10, 20, 40, and 50°C. were also made to permit estimation of the temperature effect.

Reagents

Water. Deionized water having a specific resistance of 1-2 megohms was used.

Sodium Dodecylbenzenesulfonate (D-94). Commercial Monsanto DDBSA-94 slurry, made up in stock solutions containing 10-14% solids, was used.

Sodium Formaldehyde Sulfoxylate (SFS). Rohm and Haas Formopon assaying 98-100% was used. Fresh stock solutions were prepared frequently and were standardized daily.

Iron Ethylenediaminetetraacetate (FeY). Stock solutions containing 2 mole EDTA/mole iron were prepared from reagent ferric ammonium sulfate and tetrasodium EDTA; all runs in this report used this ratio of EDTA to iron. Daily, an appropriate volume of this FeY solution was mixed with the potassium peroxydisulfate to provide a "starter solution" of desired concentration. In this way, it was assured that all the iron was in the ferric condition at the start of each run.

Styrene. Either Monsanto or Matheson, Coleman, and Bell styrene was used; no significant difference was observed. For blank runs, styrene was purified by distillation under nitrogen at about 55°C./35 mm. As reported below, for inhibited runs the styrene was used in an "as is" or "raw" condition.

All other reagents were of reagent grade, used as stock solutions of appropriate concentration. Potassium peroxydisulfate stock solution was prepared fresh daily.

RESULTS

Conditions for Consistent Results

In order to get consistent results in measuring the relatively short inhibition periods encountered here, three experimental conditions were vital.

(1) There must be thorough exclusion of adventitious oxygen. As little as 0.1 ml. may produce a measurable inhibition period.

(2) Oxygen must be used as the inhibitor. A dozen or so other reagents tested, including galvinoxyl and diphenylpicrylhydrazyl, either were inert, erratic, or produced retardation (i.e., reduced the rate of polymerization so that the onset of polymerization was too gradual to give a well defined inhibition period). Oxygen gave consistent, well-defined inhibition periods. It was probably present or effective as styrene peroxide, but this is a moot question for the present.

(3) Starting of the reaction must be adding the iron and peroxydisulfate simultaneously, as the last reagent (the "starter solution"). If the

opposite order were used, i.e., the sulfoxylate added last, the inhibition times were erratic. This is presumably due to a slow decomposition of the peroxydisulfate during the thermal equilibration period (about 10 min.), thus destroying a part of the inhibitor present. Further, if the iron is added prior to the peroxydisulfate, it will be partially reduced prior to starting, thereby affecting the observed inhibition period, and greatly complicating the data analysis. When these conditions are observed, a precision of about 15 sec. can be realized.

Originally, purified styrene was used, and air or oxygen was added to the emulsion via a gas buret or a syringe. It was subsequently found, however, that the oxygen or peroxide content of styrene in the "as is" or raw condition was remarkably constant, and that the inhibitor present in the commercial product was inert under our conditions. Samples from different manufacturers gave the same results over a period of several weeks. Use of such raw styrene eliminated the difficulties of adding air or oxygen under conditions assuring quantitative uptake and permitted a major time saving. A series of runs was always completed from the same bottle of styrene, and reference runs at suitable intervals were made to assure a constant baseline. The results given are all normalized to the same inhibitor concentration, $11.2 \times 10^{-6}M$, to permit direct comparisons. Most runs were actually made at inhibitor concentration of $(20-30) \times 10^{-6}M$, and with correspondingly longer inhibition periods. The system was investigated with the use of two buffers, ammonium hydroxide (pH ca. 10) and sodium bicarbonate (pH ca. 8.5), with considerably different results. For this reason, the two series are considered separately in the following. Results for a limited series with phosphate buffers are also presented.

Results in Ammonium Hydroxide Buffer

Figures 1-7 present the results in terms of t_i versus the concentration and temperature variables studied in the ammonia series. In Figures 2, 3, 4, and 6 the points are experimental values, while the lines are theoretical, calculated from the rate constants as described later.

Inhibitor Concentration $[I]_0$. Figure 1 shows that t_i , the inhibition period, is a linear function of $[I]_0$ for the recipe used. This indicates that the rate of radical generation, $dR\cdot/dt$,* is constant during each inhibition period for this recipe and value of $[I]_0$. $[I]_0$ was originally expressed as the fraction of raw styrene in the mixture of raw and purified styrene used in each run. As described under Discussion, the initial effective inhibitor concentration was later calculated on an analog computer.

Sodium Formaldehyde Sulfoxylate Concentration $[SFS]_0$. Figure 2 shows the effect of $[SFS]_0$ on t_i over the range $(6-70) \times 10^{-4}M$. The curve is steep at low $[SFS]_0$, flattening out at higher levels.

* Here and later, the symbol R, is used to signify all radicals capable of initiating polymerization.

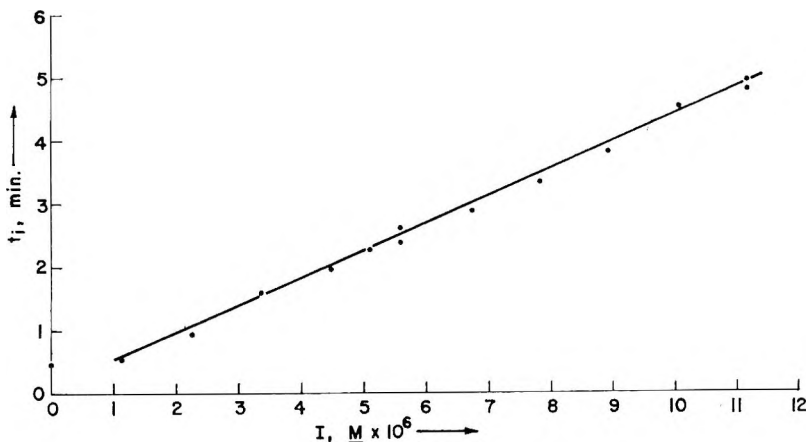


Fig. 1. Plot of t_i vs. $[I]$. NH_4OH buffer; $[\text{SFS}] = 0.002M$, $[\text{Fe}] = 0.0002M$, $[\text{KPS}] = 0.010M$, $T = 30^\circ\text{C}$.

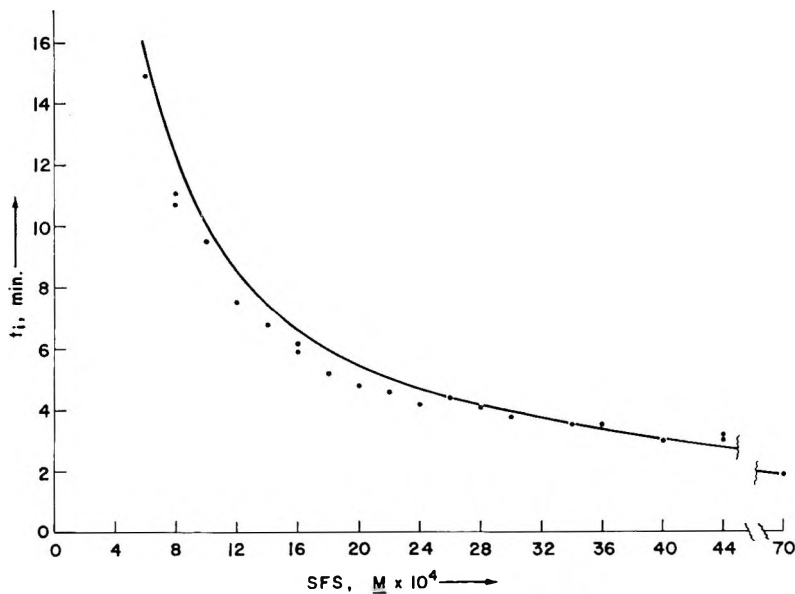


Fig. 2. Plot of t_i vs. $[\text{SFS}]$. NH_4OH buffer; $[I] = 11.2 \times 10^{-6}M$, $[\text{Fe}] = 0.0002N$, $[\text{KPS}] = 0.01M$, $T = 30^\circ\text{C}$. Points are experimental; line is calculated.

Potassium Peroxydisulfate Concentration $[\text{KPS}]_0$. Figure 3 shows the effect of $[\text{KPS}]_0$ on t_i over the range $(0-300) \times 10^{-4}M$. The curve shows much less slope than the corresponding SFS curves. Note that polymerization "starts" were obtained even with zero $[\text{KPS}]_0$ due to radicals from the reduction of Fe(III)EDTA by SFS. These starts, however, were much weaker and of much shorter duration than normal starts obtained with KPS present, corresponding presumably to a single reduction of the

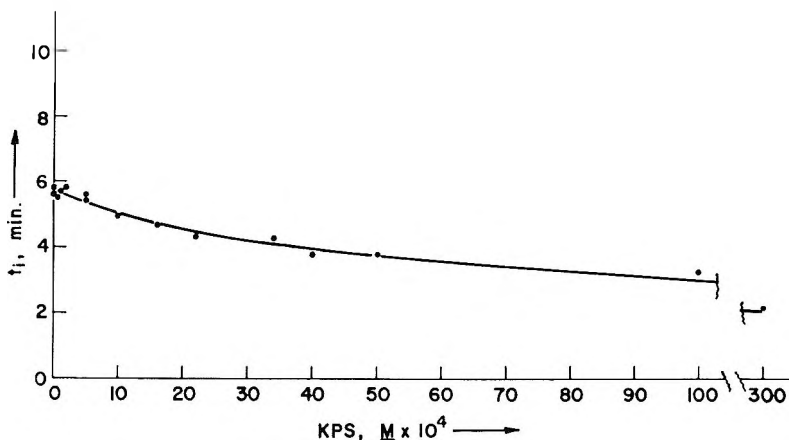


Fig. 3. Plot of t_i vs. [KPS]. NH_4OH buffer; $[\text{I}] = 11.2 \times 10^{-4}M$, $[\text{Fe}] = 0.0002M$, $[\text{SFS}] = 0.004M$, $T = 30^\circ\text{C}$. Points are experimental; line is calculated

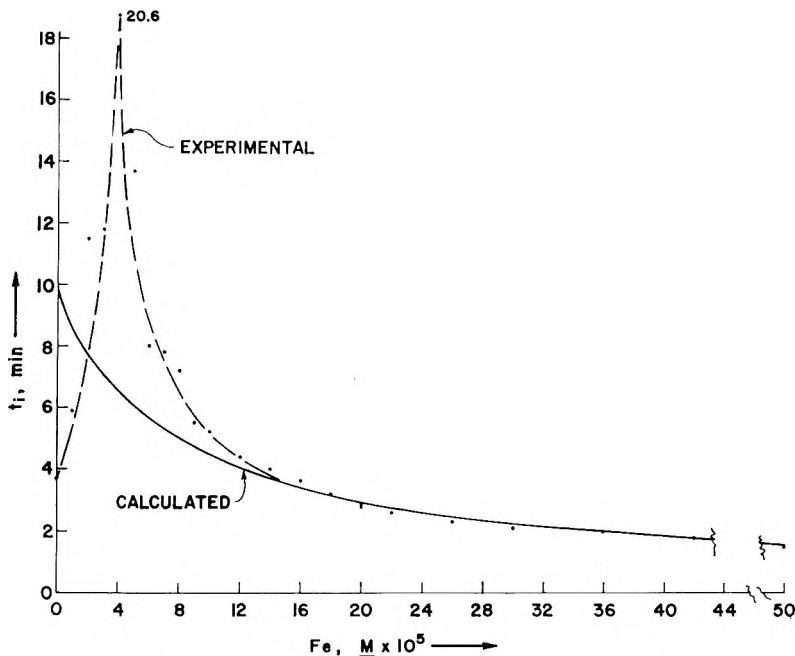


Fig. 4. Plot of t_i vs. $[\text{Fe}]$. NH_4OH buffer; $[\text{I}] = 11.2 \times 10^{-6}M$, $[\text{SFS}] = 0.004M$, $[\text{KPS}] = 0.010M$, $T = 30^\circ\text{C}$. Points are experimental; solid line is calculated.

iron. The usual concentration of KPS used in polymerization was about $0.01M$.

Iron. Figure 4 shows the effect of $[\text{Fe}]$ on t_i over the range $(0-50) \times 10^{-5}M$. The steep cusp at about $4 \times 10^{-5}M$ was confirmed repeatedly. The cusp is absent in the bicarbonate buffer. Note that the curve shows only the effect of total Fe , rather than Fe(II) , or Fe(III) .

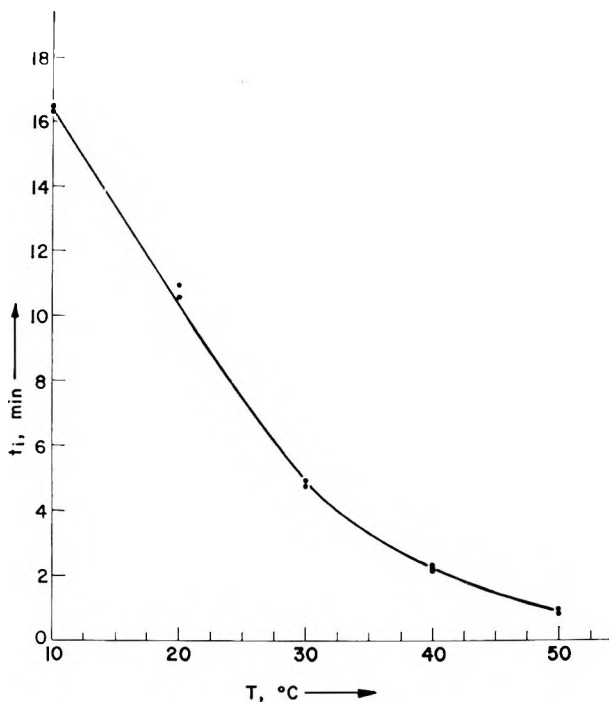


Fig. 5. Plot of t_i vs. temperature. NH_4OH buffer; $[\text{I}] = 11.2 \times 10^{-6}M$, $[\text{SFS}] = 0.002M$, $[\text{Fe}] = 0.0002M$, $[\text{KPS}] = 0.010M$.

The normal Fe level used in synthesis is about $(5-10) \times 10^{-4}M$, far distant from the cusp.

The possible significance of the apparent inhibitory activity of iron at low levels is considered later.

The exotherms marking t_i in the area to the left of the cusp were much weaker than "normal" ones, as observed at higher iron levels. The steepness of the curve makes it difficult to get good precision here; a more detailed examination of this area has not yet been attempted.

Temperature. Figure 5 shows the effect of temperature on t_i at 10, 20, 30, 40, and 50°C. for single recipe.

Stirring Speed. The effect of stirring speed was determined because both heat and mass transfer might be expected to influence the results. It was established that at 700–900 rpm, in the present apparatus, stirring speed had no effect. The runs in this report were all at 800 rpm.

Zero Peroxydisulfate. Since polymerization starts could be obtained with no KPS in the system, this afforded an opportunity to measure the isolated ferric-sulfoxylate reaction via radical generation. Figure 6 gives the results. The inhibition times are continuous, nonlinear functions of both SFS and of Fe.

These data assisted in separating the rate constants of the several reactions involved.

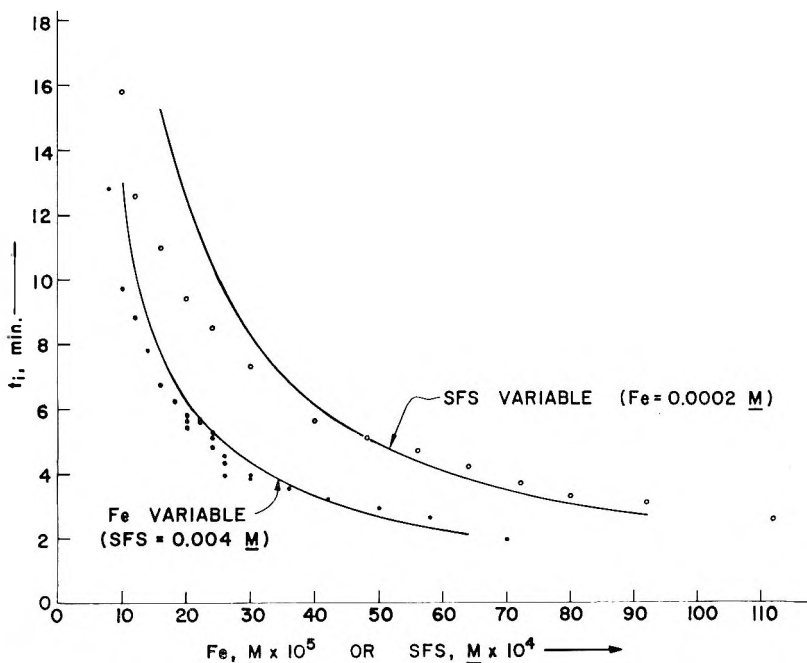


Fig. 6. Plots of t_i vs. [SFS] and t_i vs. [Fe]. NH_4OH buffer; no KPS, $[\text{I}] = 11.2 \times 10^{-6}M$, $T = 30^\circ\text{C}$. Points are experimental; lines are calculated.

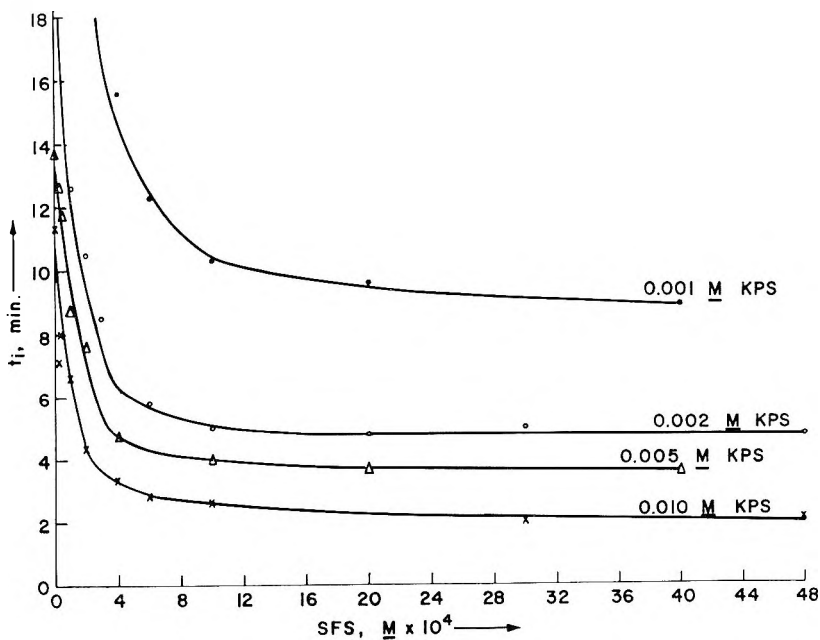


Fig. 7. Plots of t_i vs. [SFS]. NH_4OH buffer; no Fe, KPS varied, $[\text{I}] = 11.2 \times 10^{-6}M$, $T = 30^\circ\text{C}$.

“Zero” Iron. Figure 7 presents data for a series of runs with no added iron. The curves are steep below ca. $0.001M$ SFS, and become quite flat at higher concentrations. If iron were truly absent, this should afford a measurement of the “direct” KPS + SFS reaction. It cannot be taken as such, however, because adventitious traces of iron were known to be present, introduced principally via the commercial emulsifier used. Presumably for this reason, these data were not useful in the kinetic analysis. Rigorous exclusion of metallic traces, or their masking by EDTA, would make the data valid.

EDTA/Fe Ratio. The effect of the EDTA/Fe ratio in the ammonia system was also determined. At a mole ratio of 2–20, the effect is slight, but at EDTA/Fe = 1, the inhibition times were completely erratic. We ascribe this to the variable precipitation of iron at the lower ratio (visible in the absence of monomer), while at the higher ratios the EDTA–iron equilibria are shifted sufficiently to prevent precipitation of the hydroxides. An EDTA/Fe ratio of 2 was used in all other runs.

Results in Phosphate Buffer

pH. The initial series of runs was in ammonia buffer ($0.06M$) giving a pH of about 10.0. To determine the effect of pH, two series of runs were made using phosphate buffer at $0.03M$ and at $0.06M$. By adding appropriate volumes of sodium hydroxide to potassium dihydrogen phosphate, the pH was varied from 5.8 to 10.8. The results are shown in Figure 8; there is a definite minimum in t_i at a pH of about 7.8–8.5. The results were not much different in either 0.03 or $0.06M$ phosphate, showing little

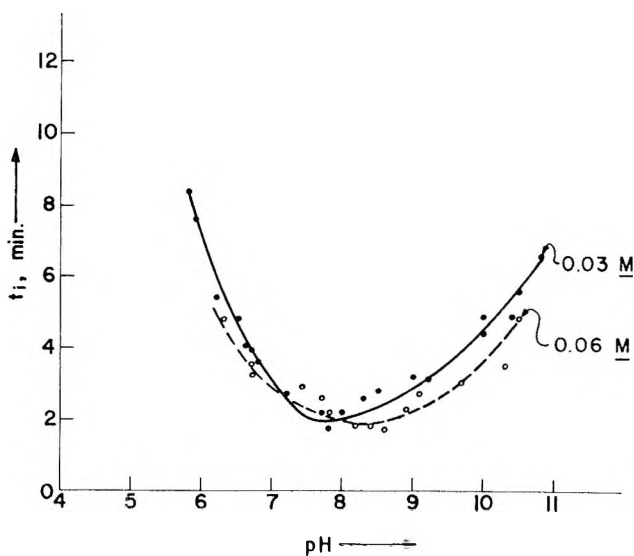


Fig. 8. Plots of t_i vs. pH. Phosphate buffer, 0.03 and $0.06M$; NaOH varied, $[I] = 11.2 \times 10^{-6}$; $[SFS] = 0.002M$, $[Fe] = 0.0002M$, $[KPS] = 0.010M$, $T = 30^\circ C$.

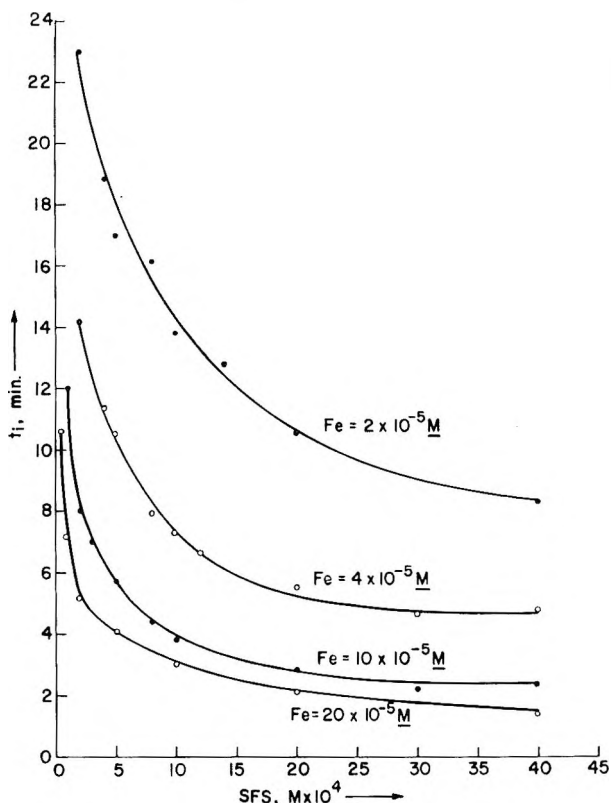


Fig. 9. Plots of t_i vs. [SFS]. NaHCO_3 buffer; $[I] = 11.2 \times 10^{-6} M$, $[\text{KPS}] = 0.010 M$, $T = 30^\circ \text{C}$.

dependence on ionic strength. To take advantage of this greater rate of radical production, the pH of the "standard" recipe was shifted to ca. 8.5 by using sodium bicarbonate instead of ammonia for the buffer. Essentially the same t_i was obtained in bicarbonate as in phosphate at the same pH. Phosphate was not considered as good a buffer at this pH, this being at or near a "knee" on the pH-NaOH curve for this substance. The concentration of ammonia or of bicarbonate had no major effect on t_i (at their respective pH's) over a range of 0.02–0.2M.

At pH's below about 6, and above about 11, results became erratic. At the low pH's, an acid decomposition of sulfoxylate is suspected. At the high pH's, iron is no longer effectively complexed by EDTA, so that precipitation of iron hydroxide occurs.

Results in Sodium Bicarbonate Buffer

In view of the increased rate of radical generation at pH 8 compared to pH 10, an essentially similar study was made of the system using bicarbonate buffer (pH 8.5) instead of ammonia. Results are given in Figures 9–12, including the effect of temperature at 20, 30, and 40°C. They are similar

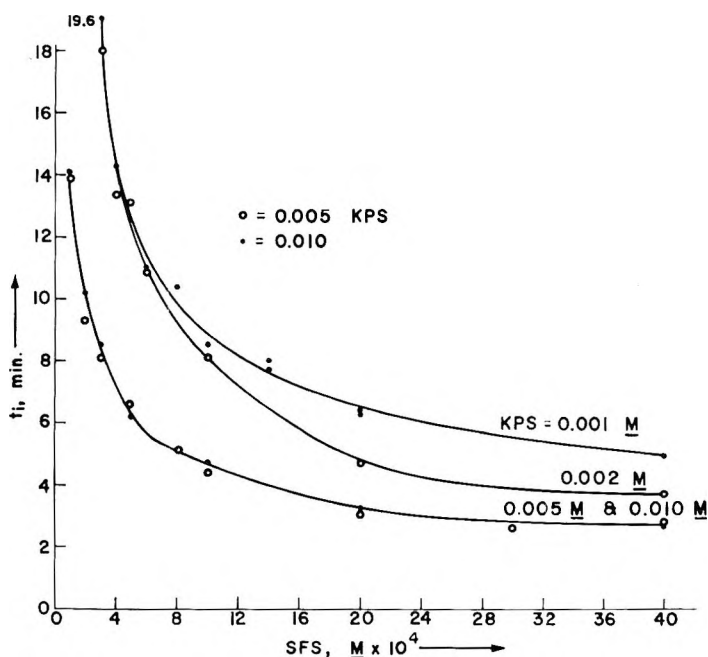


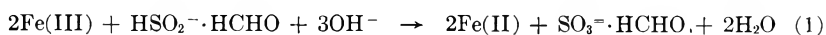
Fig. 10. Plots of t_i vs. [SFS] at four KPS levels. NaHCO_3 buffer, $0.10M$; $[\text{FeY}] = 10^{-4}M$, $[\text{I}] = 11.2 \times 10^{-6}M$, $T = 30^\circ\text{C}$.

to those for the ammonia system except for the shorter inhibition times and the fact that no cusp in the iron curve was found.

Reduction of Fe(III) by SFS

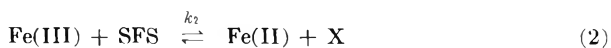
The reduction of Fe(III)Y by SFS is not straight-forward. It was followed by rapidly titrating with iodine aliquots of a mixture of the two reagents buffered with NH_4OH and H_2SO_4 so as to give a pH ca. 10.0. Oxygen was excluded by a nitrogen purge. Under these conditions, the iron-iodine reaction does not interfere,²⁸ and the SFS concentration is determined directly.

The stoichiometry of this reaction is uncertain. A reasonable stoichiometry would be:



However, it was found that the reaction stops well before the required amount of SFS [$1/2$ mole per mole of Fe(III)] is consumed. In fact, less than one mole of Fe(III) appears to be reduced per mole of SFS.

A formal and tentative solution may be had if the reaction is formulated as:



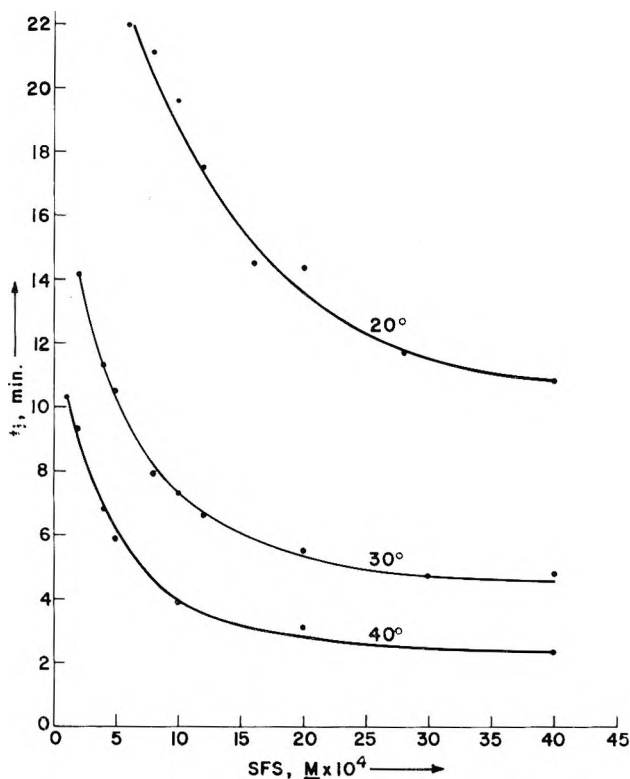


Fig. 11. Plots of t_i vs. [SFS]. NaHCO_3 buffer; $[\text{Fe}] = 4 \times 10^{-5}M$, $[\text{I}] = 11.2 \times 10^{-6}M$, $[\text{KPS}] = 0.010M$.

where X represents an unknown oxidation product of SFS. Using this expression, both a formal "equilibrium constant" and a second-order rate constant can be calculated as shown by the data of Table I.

TABLE I^a

| $[\text{Fe}^{+3}]_i$ | $[\text{SFS}]_i$ | $[\text{Fe}^{+3}]_f$ | $[\text{Fe}^{+2}]_f$ | $[\text{SFS}]_f$ | $[\text{X}]_f$ | K_{eq} |
|----------------------|------------------|----------------------|----------------------|------------------|----------------|----------|
| 2.00 | 4.00 | 1.33 | 0.67 | 3.33 | 0.67 | 0.10 |
| 4.00 | 4.00 | 3.00 | 1.00 | 3.00 | 1.00 | 0.11 |
| 4.00 | 2.07 | 3.33 | 0.67 | 1.40 | 0.67 | 0.10 |

^a Concentrations given are $M \times 10^3$.

$[\text{X}]_f$ was calculated by assuming one mole to appear per mole of SFS disappearing. K_{eq} is defined as:

$$K_{eq} = [\text{Fe}^{+2}]_f [\text{X}]_f / [\text{Fe}^{+3}]_f [\text{SFS}]_f$$

Note that K_{eq} calculated for three different combinations on initial concentrations are essentially the same. There is no direct evidence, of course, that the reaction is actually reversible, and this is not implied.

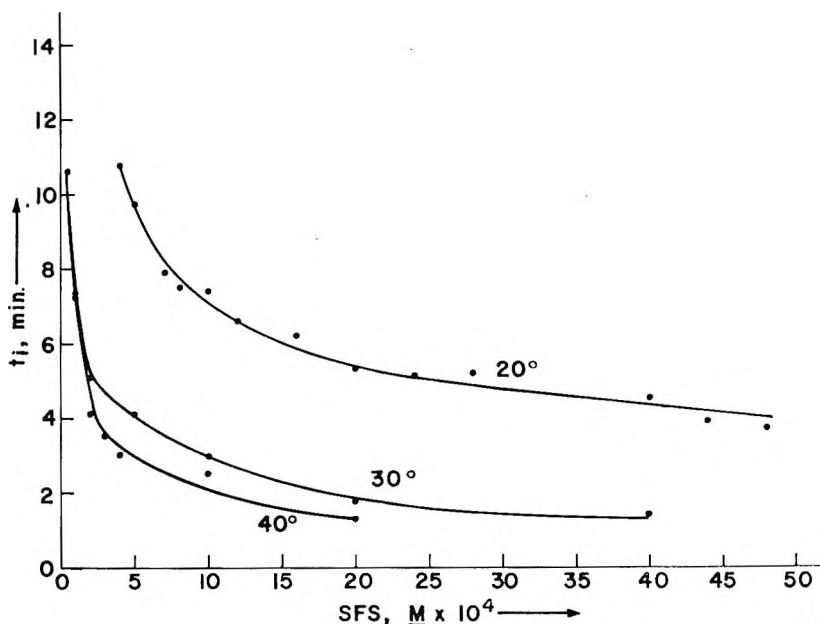


Fig. 12. Plots of t_i vs. [SFS]. NaHCO_3 buffer; $[\text{Fe}] = 20 \times 10^{-6}M$, $[\text{I}] = 11.2 \times 10^{-6}M$, $[\text{KPS}] = 0.010M$.

The concentrations of Fe(III) , Fe(II) , and X in Table I are calculated on the assumption that one mole of SFS reduces one mole of Fe(III) . If the stoichiometry of the first reaction above is assumed [two moles Fe(III) per mole SFS], the K_{eq} varies widely as the initial concentrations are changed.

Assuming a stoichiometry of 1:1 and assuming that it is first-order in both reactants, the rate constant calculated for the reaction is essentially the same for three different combinations of initial concentrations, as shown in Table II.

TABLE II^a

| $[\text{SFS}]i \times 10^3$ | $[\text{Fe}^{+3}]i \times 10^3$ | $k_2, M^{-1} \text{ min.}^{-1}$ |
|-----------------------------|---------------------------------|---------------------------------|
| 4.0 | 2.0 | 2.7 |
| 4.0 | 4.0 | 2.5 |
| 2.0 | 4.0 | 2.4 |

^a Concentrations given are $M \times 10^3$.

As seen, the agreement is only fair, but does extend to 70% or 80% of completion. If the rate constants are calculated assuming the stoichiometry of the eq. (1) above [two moles Fe(III) per mole SFS], they differ widely. Therefore, at least for formal kinetic purposes, the reaction may be treated as if it involved one mole of Fe(III) per mole of SFS, and as if it were first-order in each reagent, having a rate constant of about $2.5M^{-1} \text{ min.}^{-1}$.

These determinations obviously do not yield a precise value of k_2 , but the approximation obtained was of great help in subsequent solution of the kinetic model on the analog computer. It provided an initial and tentative value for k_2 , which could later be adjusted for a better fit.

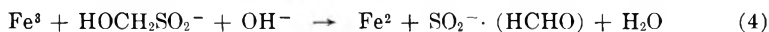
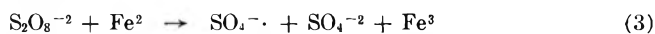
The significance of the polymerization starts obtained by the reaction between Fe(III)Y and SFS is discussed below.

DISCUSSION

General

The observed inhibition periods *per se* suffice to show the overall effect of the variables on the rate of radical generation, and also the relationship of practical synthesis recipes to any critical part of the t_i curves. Further, since t_i has a much greater dependence on SFS than on KPS, it is evident that the reduction of Fe(III) by SFS is by far the main rate-determining step, rather than the reaction of KPS with Fe(II). This is in agreement with the findings of other workers on related systems.^{29,30}

On the basis of the data presented, we assumed reactions (3)–(5) as the simplest possible model to describe the main features of the system:



Reaction (3) is well known,^{31–33} but measurement of its rate under these conditions is of interest.

That radicals are generated in the reduction of Fe(III)–EDTA by SFS [reaction (4)] is evident from the data shown in Figure 6. Radicals from the reduction of Fe(III) by sulfite and dithionite have long been known or proposed,^{3,29,32} but only recently have Kerber and Gregory³⁴ proposed $\text{HOCH}_2\text{SO}_2^{\cdot-}$ radicals from the corresponding SFS reaction (in acid media). Additional recent evidence for $\text{SO}_2^{\cdot-}$ radicals is in the work of Kolker and Waters,³⁵ Rinker et al.,^{36,37} and Wasmuth, Edwards, and Hutcherson.³⁸ The evidence is that a relatively small, single "burst" of radicals is generated by the Fe(III)+SFS reaction as would be expected from the low iron concentration used here. The exotherms observed were of distinctly lesser slope, amplitude, and duration than those observed with KPS present, e.g., about 0.1 to 0.25°C. for 6–8 min. total duration versus 0.5–1.0°C. for over 60 min. This presumably corresponds to a "single" reduction of the Fe(III) present, which in the absence of an oxidant could not cycle as it does in the normal system.

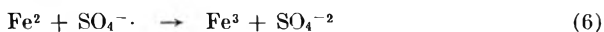
Radicals are most probably also generated in the "direct" reaction of KPS and SFS [reaction (5)], as they are considered to be in the KPS + HSO_3^- reaction.^{3,32} We obtained good polymerization "starts" with styrene in recipes containing no added iron (Fig. 7), but the data are clouded by the fact that no attempt was made to rigorously exclude traces of iron or other metals. Unless extreme care is taken to exclude metallic traces,

detailed analyses of such reactions as the "direct" KPS + SFS reaction are suspect.

Both reactions (4) and (5) were included in the kinetic model to get a good fit of the calculated to the experimental values.

Although all the three kinds of radicals from reactions (3), (4), and (5) will initiate styrene polymerization, this was not true of other monomers tried, notably certain ethylene copolymer systems. The latter were initiated only by the $\text{SO}_4^{\cdot-}$ radicals from reaction (3). It is believed that this affords a qualitative and quantitative differentiation between kinds of radicals. Use of a monomer which would be initiated only by the sulfate radicals, or at least not by those from the reduction of ferric versenate by SFS would considerably simplify the analysis.

Reactions (3)–(5) cannot explain the sharp maximum in t_i observed in the ammonia system at iron levels of about $4 \times 10^{-3}M$. Reaction (6) might account for this effect:



This apparent inhibitory effect of iron occurs only at very low levels, where the ratio SFS/Fe is very high, so that the Fe(II)/Fe(III) ratio might also be higher than otherwise. Since the "iron cusp" was absent in the bicarbonate system, the phenomenon may be related to the effectiveness of iron complexation by the EDTA. In the ammonia system, the pH (ca. 10) is at about the maximum allowed before ferric hydroxide precipitates, and some iron may actually be precipitated. In the bicarbonate system (pH ca. 8.3), the iron is easily complexed by the EDTA.

According to reactions (4) and (5), the radical generation rate should be increased at higher pH's by hydroxyl ion participation, but this is complicated by the pH dependence of the iron–EDTA equilibria. The result observed is an optimum pH of about 8.0–8.5. The pH effect as well as the effect of the EDTA–Fe ratio could probably be better expressed in terms of the redox potential of the system. Campbell,³⁹ Novoselov et al.,⁴⁰ and Bond and Hobson⁴¹ have recently published pertinent work in this area.

Determination of Rate Constants

In this work, the rate of radical generation was observed directly, and the pertinent rate constants derived therefrom, rather than vice versa. For this reason, it might be more appropriate to refer to the derived values as apparent or effective rate constants. The inherent tacit assumption is made that the simplest model permitting a fit of experimental to calculated values is the correct model. This is not necessarily true, of course, but the constants so derived do describe the system, *ipso facto*.

In order to determine the specific rate constants of the kinetic mechanism recourse was made to an analog computer simulation by using an Electronic Associate's PACE 131-R computer. A mathematical model was developed for the system and an analog computer wiring diagram representing the model was constructed.

The differential equations (7)–(14) were used as a model for reactions considered to be operative in the system:

$$d[\text{S}_2\text{O}_8^{-2}]/dt = -k_1[\text{S}_2\text{O}_8^{-2}][\text{Fe}^{+2}] - k_3[\text{S}_2\text{O}_8^{-2}][\text{HSO}_2^-] \quad (7)$$

$$d[\text{HSO}_2^-]/dt = -k_2[\text{HSO}_2^-][\text{Fe}^{+3}] + k_2'[\text{SO}_2^{\cdot-}][\text{Fe}^{+2}] - k_3[\text{S}_2\text{O}_8^{-2}][\text{HSO}_2^-] \quad (8)$$

$$d[\text{Fe}^{+2}]/dt = -k_1[\text{S}_2\text{O}_8^{-2}][\text{Fe}^{+2}] + k_2[\text{HSO}_2^-][\text{Fe}^{+3}] - k_2'[\text{SO}_2^{\cdot-}][\text{Fe}^{+2}] \quad (9)$$

$$d[\text{Fe}^{+3}]/dt = k_1[\text{S}_2\text{O}_8^{-2}][\text{Fe}^{+2}] - k_2[\text{HSO}_2^-][\text{Fe}^{+3}] + k_2'[\text{SO}_2^{\cdot-}][\text{Fe}^{+2}] \quad (10)$$

$$d[\text{SO}_2^{\cdot-}]/dt = k_2[\text{HSO}_2^-][\text{Fe}^{+3}] - k_2'[\text{SO}_2^{\cdot-}][\text{Fe}^{+2}] - k_1[\text{I}][\text{SO}_2^{\cdot-}] \quad (11)$$

$$d[\text{SO}_3^{\cdot-}]/dt = 2k_3[\text{S}_2\text{O}_8^{-2}][\text{HSO}_2^-] - k_i[\text{I}][\text{SO}_3^{\cdot-}] \quad (12)$$

$$d[\text{SO}_4^{\cdot-}]/dt = k_1[\text{S}_2\text{O}_8^{-2}][\text{Fe}^{+2}] - k_i[\text{I}][\text{SO}_4^{\cdot-}] \quad (13)$$

$$d[\text{I}]/dt = -k_i[\text{I}][\text{SO}_2^{\cdot-} + \text{SO}_3^{\cdot-} + \text{SO}_4^{\cdot-}] \quad (14)$$

It was assumed that because of the sharply defined inhibition times polymerization did not occur to any significant extent during the inhibition period.¹³ That is, a reaction of the type, $\text{M} + \text{SO}_4^{\cdot-} \rightarrow \text{R}\cdot$ (M = monomer), was negligible with respect to the competing reaction $\text{I} + \text{SO}_4^{\cdot-} \rightarrow$ nonpropagating species. For computational purposes, the inhibition period t_i was defined as that time at which the inhibitor concentration $[\text{I}]$ equals the active initiating radical concentration, $[\text{R}\cdot] = [\text{SO}_2^{\cdot-}] + \text{SO}_3^{\cdot-} + \text{SO}_4^{\cdot-}$. That is, it was assumed that polymerization would begin as soon as the radical concentration exceeded the inhibitor concentration. Although somewhat arbitrary, this convention appears reasonable, and has allowed consistent solutions to the above equations. By inhibitor concentration $[\text{I}]$ is meant, of course, the actual concentration times an efficiency factor, or the effective concentration. This approach enables one to determine the rate constants without knowing or making any assumptions regarding the inhibitor concentration or efficiency. Indeed, the effective initial inhibitor concentration, $[\text{I}]_0$ is constant for a given series of runs; this is readily established by reference runs at suitable intervals.

NH₄OH System. The procedure used in determining the rate constants for the NH₄OH buffered system was as follows.

(1) It was assumed that the reaction between inhibitor and radicals was so fast that the radicals were destroyed as soon as they were generated. It was also assumed that reactivity of each radical specie with the inhibitor was the same. Therefore, k_i was arbitrarily set at a very large value, $k_i = 10^7 \text{ M}^{-1}\text{-min.}^{-1}$.

(2) k_2 and k_2' were set at the values determined independently. $[\text{I}]_0$ was adjusted to get a fit of the data for t_i versus $[\text{Fe}^{+3}]_0$ and $[\text{SFS}]_0$ with no

KPS. A knowledge of k_1 and k_3 was not necessary at this time since, in the absence of KPS, reactions (3) and (5) were inoperative.

(3) By using the values of $[I]_0$ obtained above (2), k_1 and k_3 were adjusted to yield a fit of the t_i versus $[SFS]_0$ curve with all reactants present.

(4) These values were tested by comparing the model with the data for t_i versus $[KPS]_0$, $[Fe^{+3}]$, and $[I]_0$, all reactants present. A satisfactory comparison was obtained.

As a result of this procedure, the following values were obtained for the NH_4OH buffered system:

$$\begin{aligned} [I]_0 &= 11.24 \times 10^{-6} M \\ k_1 &= 14.2 M^{-1} \text{ min.}^{-1} \\ k_2 &= 2.5 M^{-1} \text{ min.}^{-1} \\ k_2' &= 25.0 \text{ min.}^{-1} \\ k_3 &= 0.014 M^{-1} \text{ min.}^{-1} \\ k_9 &= 1 \times 10^7 M^{-1} \text{ min.}^{-1} \end{aligned}$$

Using these values, the change with time of the component concentrations in typical runs were obtained directly from the analog computer simulation by using an X - Y recorder. Figures 2, 3, and 4 compare the calculated and experimental values of t_i as functions of $[SFS]_0$, $[KPS]_0$, and $[Fe^{+3}]_0$. Good agreement was achieved except for low $[Fe^{+3}]_0$ levels on the t_i versus $[Fe^{+3}]$ curve as discussed earlier. k_4 was set equal to zero and no attempts were made to find a value for it which would not affect the previous fit of the data.

Since good fits of the experimental to the calculated values were found in the ammonia series, the simple model comprising reactions (3)–(5) appears to represent the dominant reactions at pH 10.

The values of $k_1 = 14.1 M^{-1} \text{ min.}^{-1}$ compares with values of ca. 6–400 $M^{-1} \text{ min.}^{-1}$ found using various other iron complexes under a variety of conditions, and independent methods.^{42,43} Clearly, additional work in this area would be fruitful; Wilmarth and Haim⁴³ have reviewed the problem recently.

The value of $k_2 = 2.5 M^{-1} \text{ min.}^{-1}$ is nearly the same as that for the reduction of ferric versenate by hydrazine ($2.3 M^{-1} \text{ min.}^{-1}$) at 25°C. found by Mechan et al.²

$NaHCO_3$ System. In order to find the rate constants for the $NaHCO_3$ system the following procedure was used.

(1) Since $[I]_0$ had previously been determined in the NH_4OH system simulation this value was fixed. k_1 was also maintained at $10^7 M^{-1} \text{ min.}^{-1}$.

(2) The t_i versus $[SFS]_0$ data, no KPS, was used to determine k_2 and k_2' in the manner described previously. It was found that the value of k_2' was not at all critical and it was arbitrarily set equal to ten times k_2 , thus giving the same value of the equilibrium constant for reaction (4) as was used in the NH_4OH system.

(3) Finally, k_1 and k_3 were adjusted to give a fit of the data for $[SFS]_0$ versus t_i , all reactants present. Here also it was found that the results were

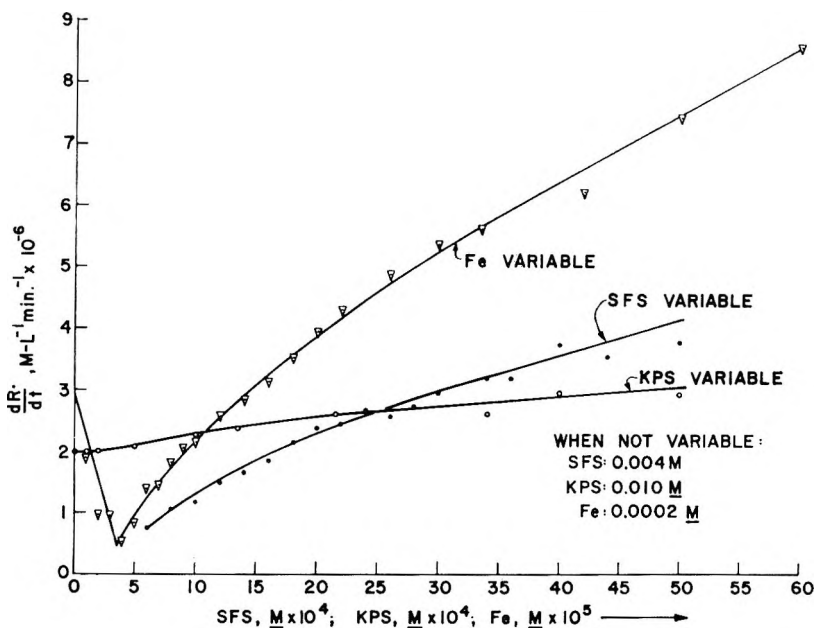


Fig. 13. Plots of dR/dt vs. [SFS], [KPS], and [Fe]. NH_4OH buffer; $T = 30^\circ\text{C}$.
When not variable, [SFS] = $0.004M$, [KPS] = $0.010M$, [Fe] = $0.0002M$.

quite insensitive to the value of k_1 . It was therefore maintained at the value determined for the NH_4OH system. The following values were the best obtained for the NaHCO_3 system:

$$\begin{aligned} [I]_0 &= 11.24 \times 10^{-6} M \\ k_1 &= 14.1 M^{-1} \text{min}^{-1} \\ k_2 &= 8.2 M^{-1} \text{min}^{-1} \\ k_2' &= 82.0 M^{-1} \text{min}^{-1} \\ k_3 &= 0.064 M^{-1} \text{min}^{-1} \\ k_I &= 1 \times 10^7 M^{-1} \text{min}^{-1} \end{aligned}$$

The experimental and calculated results for the NaHCO_3 -buffered system were not in good agreement. Failure to get a better fit in the bicarbonate series indicates that some additional reactions are involved. In particular, additional involvement of iron is indicated by the failure of the model to predict the observed dependence on iron and SFS concentrations. We suggest that either iron is really involved in the "direct" reaction of peroxydisulfate with sulfoxylate, or that the dependence of the iron-EDTA equilibria on pH changes the system's redox potential so as to account for the results.

As stated earlier, simplification of the system by use of a monomer sensitive, preferably, only to sulfate radicals might permit a better description of the mechanism. Meanwhile, additional attempts are being made, using more complicated models, to get a better fit on the analog simulation.

Determination of Rate of Radical Generation

The primary objective of this work was to determine the rate of radical generation by redox systems. This quantity, \overline{dR}/dt , is presented as a function of reagent concentrations and of temperature in Figures 13–16.

The average rate of radical generation, \overline{dR}/dt , may be readily calculated from the inhibition time t_i and the initial effective inhibitor concentration, $[I]_0$, by eq. (15):

$$\overline{dR}/dt = [I]_0/t_i \quad (15)$$

The instantaneous rate (\overline{dR}/dt) will differ from the average rate only to the extent that steady-state conditions do not apply, particularly with respect to the $[Fe(II)]/[Fe(III)]$ ratio. The steady-state assumption probably applies fairly well to most of these experiments, as shown by the linearity of t_i versus $[I]_0$ (Fig. 1). Also, [KPS] and [SFS] undergo only minor changes during a typical run; the change in $[Fe(II)]$ may be appreciable, depending on the recipe.

Therefore, it is necessary to know only the effective initial inhibitor concentration $[I]_0$ to calculate dR/dt from a given t_i , and this will in many cases be a fair approximation to \overline{dR}/dt .

The original determination of $[I]_0$ requires, as seen, solution of the kinetic model. But once the corresponding values of t_i and $[I]_0$ for a "standard recipe" are known, $[I]_0$ can be easily determined for a given monomer-inhibitor mixture by measuring t_i with the "standard recipe." Hence,

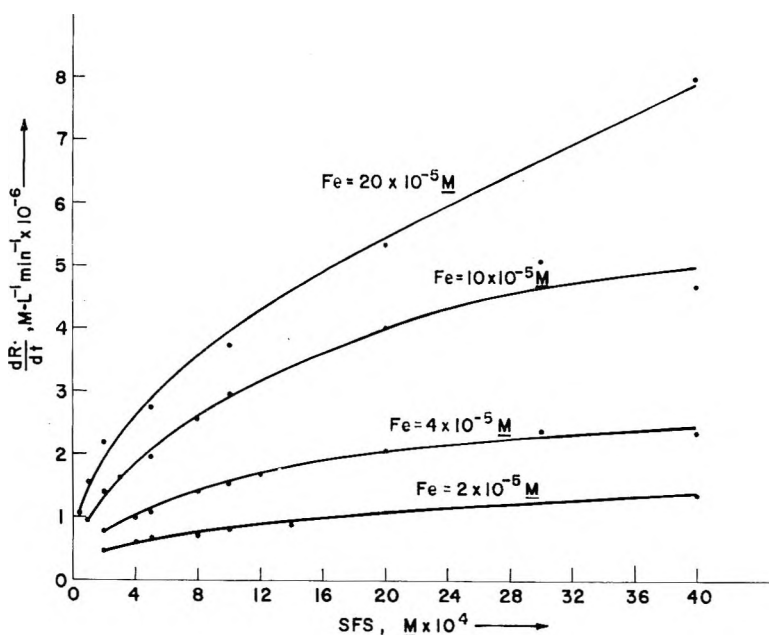


Fig. 14. Plots of dR/dt vs. SFS. $NaHCO_3$ buffer; $[KPS] = 0.010M$, $T = 30^\circ C$.

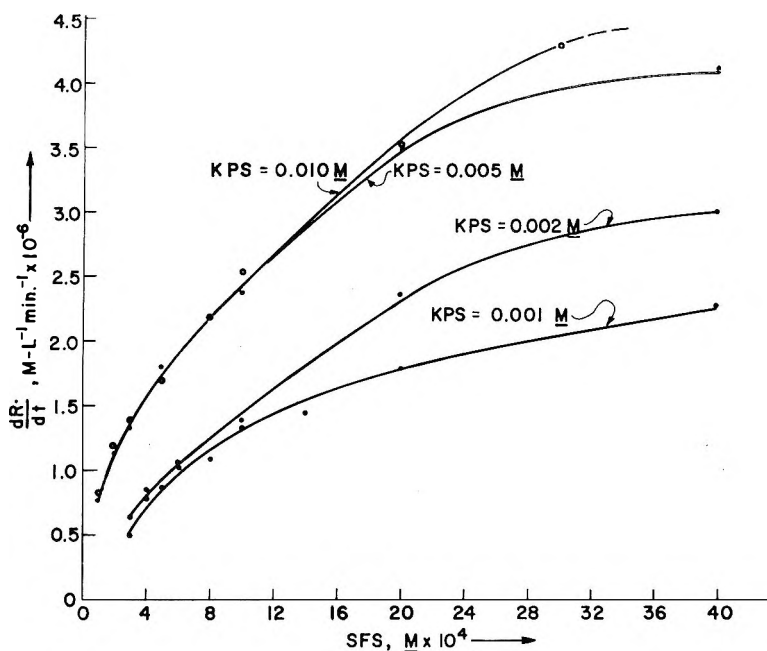


Fig. 15. Plots of $dR \cdot /dt$ vs. [SFS]. NaHCO_3 buffer; $[\text{Fe}] = 10^{-4}M$, $T = 30^\circ\text{C}$.

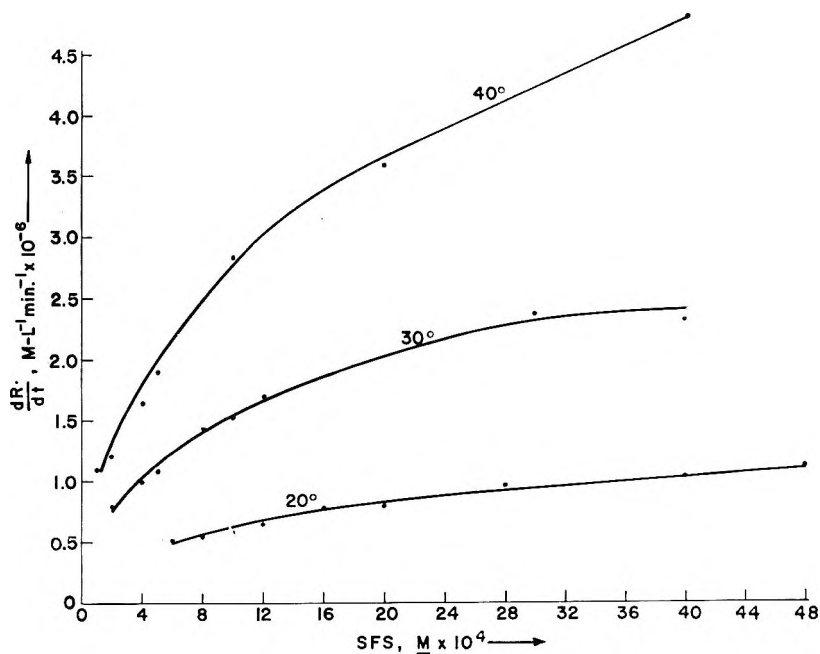


Fig. 16. Plots of $dR \cdot /dt$ vs. [SFS]. NaHCO_3 buffer; $[\text{Fe}] = 4 \times 10^{-5}M$, $[\text{KPS}] = 0.010M$.

\overline{dR}/dt is readily available. Even if $[I]_0$ is not known, relative values of \overline{dR}/dt can be determined directly, of course.

The effect of temperature on dR/dt has been presented in the curves. When calculation of the rate constants for temperatures other than 30°C. are complete, it should be possible to estimate the activation energies from the Arrhenius plots.

If it is assumed that: (1) steady-state conditions exist, (2) \overline{dR}/dt depends only on reaction (5), and (3) $[Fe(III)]$ is much larger than $[Fe(II)]$; then it can be shown that:

$$k_2 = (dR/dt)/[SFS]_0[Fe]$$

But, k_2 calculated in this way did not give a linear Arrhenius plot [$\log k_2$ vs. $1/T(^{\circ}K.)$] over the temperature range studied (10, 20, 30, 40, and 50°C.). This is probably due to the error of the second assumption above.

CONCLUSIONS

(1) Thermometry is a sensitive and convenient technique to measure polymerization inhibition periods.

(2) The kinetic model proposed adequately describes the peroxydisulfate-iron-sulfoxylate redox system in the NH_4OH buffer over most of the ranges studied. The model requires modification to fit the bicarbonate buffered system.

(3) The main rate-determining step in both buffers is the reduction of ferric EDTA by sulfoxylate.

(4) Absolute rates of radical generation up to ca. $10^{-5}M^{-1}\text{-min.}^{-1}$ have been measured in this system.

(5) The kinetic model proposed must be modified to account for discrepancies at low iron levels. Evidence was found for the generation of radicals by the ferric-sulfoxylate reaction and for an apparent inhibitory effect of iron at low concentrations.

(6) Temperature, in the range of 10-50°C., has a large effect on the rate of radical generation.

We are indebted to Professor Raymond M. Fuoss of Yale University who made major contributions in general discussions, and specifically in the mathematical approach.

Mr. Anthony Sotta performed many of the experiments reported here.

References

1. Kolthoff, I. M., and W. J. Dale, *J. Am. Chem. Soc.*, **69**, 441 (1947).
2. Meehan, E. J., I. M. Kolthoff, C. Auerbach, and H. Minoto, *J. Am. Chem. Soc.*, **83**, 2232 (1961).
3. Bevington, J. C., *Radical Polymerization*, Academic Press, New York, 1961, p. 35.
4. Bovey, F. A., and Kolthoff, I. M., *J. Polymer Sci.*, **5**, 569 (1950).
5. Hohenstein, W. P., and Mark, H., *J. Polymer Sci.*, **1**, 549 (1946).
6. Harkins, W. D., and N. Beeman, *J. Am. Chem. Soc.*, **51**, 1674 (1929).
7. Bovey, F. A., and I. M. Kolthoff, *J. Am. Chem. Soc.*, **69**, 2143 (1947).
8. Smeltz, K. C., and E. Dyer, *J. Am. Chem. Soc.*, **74**, 623 (1952).
9. Hobson, R. W., and J. D. D'Ianni, *Ind. Eng. Chem.*, **42**, 1572 (1950).

11. Bovey, F. A., and I. M. Kolthoff, *Chem. Rev.*, **42**, 491 (1948).
12. Blanchard, H. S., *J. Am. Chem. Soc.*, **82**, 2014 (1960).
13. George, P., E. K. Rideal, and A. Robertson, *Proc. Roy. Soc. (London)*, **A185**, 288 (1946); *ibid.*, **A185**, 309 (1946).
14. Kennerly, G. W., and W. L. Patterson, Jr., paper presented at 128th Meeting, American Chemical Society, Minneapolis, Minn., September 1955.
15. Lippincott, W. T., and W. G. Lloyd, *J. Am. Chem. Soc.*, **79**, 4811 (1957).
16. Blaven, G. H., R. Irving, and C. N. Thompson, *J. Inst. Petrol.*, **37**, 25 (1951).
17. Rosenwald, R. W., and J. R. Hoatson, *Ind. Eng. Chem.*, **41**, 914 (1949).
18. Boozer, C. E., G. S. Hammond, C. E. Hamilton, and J. N. Sen, *J. Am. Chem. Soc.*, **77**, 3233 (1955).
19. Kruegen, D. J. W., *J. Inst. Petrol.*, **38**, 449 (1952).
20. Bovey, F. A., I. M. Kolthoff, A. I. Medalia, and E. J. Meehan, *Emulsion Polymerization*, Interscience, New York, 1955, p. 228.
21. Kolthoff, I. M., P. R. O'Conner, and J. L. Hansen, *J. Polymer Sci.*, **15**, 459 (1955).
22. Meehan, E. J., I. M. Kolthoff, N. Tamberg, and C. L. Segal, *J. Polymer Sci.*, **24**, 215 (1957).
23. Tudos, F., I. Kende, and M. Azori, *J. Polymer Sci.*, **A1**, 1353 (1963).
24. Tudos, F., I. Kende, and M. Azori, *J. Polymer Sci.*, **A1**, 1369 (1963).
25. Manyasek, Z., and A. Rezabek, *J. Polymer Sci.*, **56**, 47 (1962).
26. Woods, R., I. M. Kolthoff, and E. J. Meehan, *J. Am. Chem. Soc.*, **85**, 2385 (1963).
27. Woods, R., I. M. Kolthoff, and E. J. Meehan, *J. Am. Chem. Soc.*, **85**, 3334 (1963).
28. Kolthoff, I. M., and R. Belcher, *Volumetric Analysis*, Vol. III, Interscience, New York, 1957, p. 342 ff.
29. Kolthoff, I. M., and E. J. Meehan, *J. Appl. Polymer Sci.*, **1**, 200 (1959).
30. Orr, R. J., and H. L. Williams, *J. Am. Chem. Soc.*, **77**, 3715 (1955).
31. Fordham, J. W. L., and H. L. Williams, *J. Am. Chem. Soc.*, **73**, 4855 (1951).
32. Ulbricht, J., and P. Fritzsche, *Faserforsch. Textiltech.*, **14**, 320 (1963).
33. Kolthoff, I. M., A. I. Medalia, and H. P. Raaen, *J. Am. Chem. Soc.*, **73**, 1733 (1951).
34. Kerber, R. V., and X. Gregory, *Makromol. Chem.*, **68**, 100 (1963).
35. Kolker, P. L., and W. A. Waters, *Proc. Chem. Soc.*, **1963**, 55.
36. Rinker, R. G., et al., *J. Phys. Chem.*, **64**, 573 (1960).
37. Rinker, R. G., et al., *Inorg. Chem.*, **3**, 1467 (1964).
38. Wasmuth, C. R., C. Edwards, and R. Hutcherson, *J. Phys. Chem.*, **68**, 423 (1964).
39. Campbell, C. H., *J. Polymer Sci.*, **32**, 413 (1958).
40. Novoselov, R. I., et al., *Russ. J. Inorg. Chem.*, **8**, 69 (1963).
41. Bond, J., and D. B. Hobson, *J. Polymer Sci.*, **A1**, 2179 (1963).
42. Fordham, J. W. L., and H. L. Williams, *J. Am. Chem. Soc.*, **73**, 1634 (1951).
43. Wilmarth, W. K., and A. Haim, in *Peroxide Reaction Mechanisms*, J. O. Edwards, Ed., Interscience, New York, 1962, p. 187.

Résumé

Les cinétiques d'inhibition ont été employées pour étudier le système d'initiation redox peroxydisulfate-fer-sulfoxylate. Le commencement de la polymérisation a été détecté par une méthode thermométrique permettant de mesurer avec précision de courtes périodes d'inhibition. Les constantes de vitesse ont été déduites à partir des périodes d'inhibition. Pour des expériences effectuées dans un tampon ammoniacal (pH d'environ 10) on a obtenu un bon accord entre les résultats calculés et observés en se basant sur un modèle simple. Dans un tampon bicarbonate (pH d'environ 8.5), cependant, le même modèle simple était inadéquat; l'intervention supplémentaire du fer est indiquée. On a mis en évidence que la réduction du versénate ferrique par le sulfoxylate produisait un radical libre, que l'on suppose être $(\text{HCHO})\text{SO}_2\cdot$. On a calculé les vitesses absolues de la formation de radicaux.

Zusammenfassung

Das Peroxydisulfat-Eisensulfoxylat-Redoxstartersystem wurde mit Hilfe der Inhibitionskinetik untersucht. Der Eintritt der Polymerisation wurde durch ein thermometrisches Verfahren festgestellt, welches eine genaue Messung kurzer Inhibitionsperioden erlaubte. Aus den Inhibitionsperioden wurden mit einer Analogsimulation Geschwindigkeitskonstanten berechnet. Auf Grundlage eines einfachen Modells wurde für Versuche in Ammoniakpuffer (pH etwa 10) eine gute Übereinstimmung zwischen berechneten und gemessenen Grössen erhalten. Im Bicarbonatpuffer (pH etwa 8,5) war jedoch dieses einfache Modell nicht anwendbar, was auf eine zusätzliche Beteiligung von Eisen schliessen lässt. Bei der Reduktion von Ferriversenat durch Sulfoxylat entsteht ein freies Radikal, für welches vorläufig $(\text{HCHO})\text{SO}_2\cdot$ vorgeschlagen wird. Die Absolutgeschwindigkeit der Radikalbildung wird berechnet.

Received December 16, 1964

(Prod. No. 4625A)

A Generalization of the Debye Light-Scattering Equation

WILFRIED HELLER, *Chemistry Department, Wayne State University, Detroit, Michigan*

Synopsis

The Debye light-scattering equation is generalized by making allowance for the variation of (dn/dc) —and therefore of H —with the concentration of the solute. This should allow one to use it with more concentrated solutions provided light scattering is weak enough (oligomer solutions) so that multiple scattering does not exclude such a procedure.

The well known Debye light-scattering equation

$$Hc/\tau = (1/M) + 2Bc \quad (1)$$

is derived in its simple form on the assumption that the refractive index of the solution, n_{12} , does not differ appreciably from that of the solvent, n_1 and that (dn/dc) is a constant. Since M is obtained from the intercept of the Hc/τ versus c plot and the second virial coefficient from the limiting slope, this assumption is of no consequence for the conventional use of the equation in connection with experimental work on dilute solutions. With low molecular solutes weight (e.g., oligomers), one may have to carry out light-scattering experiments at higher concentrations in order to obtain scattering values significantly above the threshold of experimental errors. (This is permissible as long as the excess of angular scattering relative to the scattering at $\theta = 90^\circ$ varies in direct proportion to $\cos^2 \theta$, i.e., as long as multiple scattering does not complicate matters as yet measurably.) If such data are combined with (dn/dc) data, intercept and slope are likely to be in error, unless one is certain that (dn/dc) , and therefore H , do not vary over the entire range of concentrations.

In cases where this is doubtful, a generalized form of eq. (1) should be used which takes into account the possible variation of H with c . Such a generalization is relatively easy. As shown many years ago,¹ the Debye and the Rayleigh equations are connected and interconvertible by means of the relation

$$dn/dc = (3/2) \bar{V}n_1 [(m^2 - 1)/(m^2 + 2)] \quad (2)$$

where \bar{V} is the partial specific volume of the solute and $m = (n_2/n_1)$, n_2 being the refractive index of the solute. Recently it could be shown² that eq. (2) is the limiting form, for $n_{12} \rightarrow n_1$, of a general equation given in 1910 by Wiener.³ Consequently, on bringing the Rayleigh equation, by means of the Wiener equation, into a form comparable to eq. (1), one will

have obtained in the simplest possible manner a generalized form of eq. (1). It is

$$H'(c)c/\tau = (1/M) + 2Bc + Cc^2 + \dots \quad (3)$$

where

$$H'(c) = [24\pi^3 n_1^4 / N_A \lambda_0^4] (dn/dc)^2 [(n_{12} + n_1)/(n_{12}^2 + 2n_1^2)]^2$$

Here, N_A is Avogadro's constant and λ_0 is the wavelength *in vacuo*. The very simple relation between $H'(c)$ and the constant H is

$$H'(c) = (9/4) n_1^2 [(n_{12} + n_1)/(n_{12}^2 + 2n_1^2)]^2 H. \quad (4)$$

It is seen that H' is a function of concentration. It reduces to H if $n_{12} \rightarrow n_1$.

Instead of the Wicner equation, one could use the generally somewhat better Lorentz-Lorenz equation to which it is intimately related. The $(dn/dc)(c)$ expression derived from the latter equation² is very cumbersome, however. Therefore, the relatively small gain in accuracy of the end result does not seem to warrant the greatly increased calculating work involved in using such an alternate $H'(c)$ function.

It is clear that the range of concentrations, over which the slope $2B$ is practically constant, will be reduced on operating with $H'(c)$ rather than H . Consequently, discrepancies between the concentration ranges for which the limiting slope of π/c versus c plots (where π is osmotic pressure) and that of Hc/τ versus c plots remains practically constant, will disappear on using eq. (3) instead of eq. (1).

In conclusion, attention may be drawn to the possibility offered by eq. (3) to evaluate the numerical value of the coefficient C . Its value, which in the case of random coils should reflect the optical consequences of mutual molecular entanglement, has thus far found no consideration.

This work was supported by the Office of Naval Research.

References

1. Heller, W., *Phys. Revs.*, **68**, 5 (1945).
2. Heller, W., *J. Phys. Chem.*, **69**, 1123 (1965).
3. Wiener, O., *Leipziger Ber.*, **62**, 256 (1910).

Résumé

On généralise l'équation de Debye, relative à la diffusion lumineuse, en tenant compte de la variation de (dn/dc) —et par conséquent de H —avec la concentration du soluté. Cela permet d'employer cette équation avec des solutions plus concentrées lorsque la lumière diffusée est assez faible (solutions d'oligomères) de telle sorte qu'une diffusion multiple n'exclut pas un tel procédé.

Zusammenfassung

Die Lichtstreuungsgleichung von Debye wird unter Berücksichtigung der Abhängigkeit von (dn/dc) , und daher von H , von der Konzentration des gelösten Stoffes verallgemeinert. Dadurch sollte eine Verwendung konzentrierterer Lösungen ermöglicht werden, vorausgesetzt, dass die Lichtstreuung schwach genug ist (Oligomerlösungen), sodass das Verfahren nicht durch Mehrfachstreuung unmöglich gemacht wird.

Received December 15, 1964
(Prod. No. 4631A)

Radiation Polymerization of Crystalline Trithiane*

J. B. LANDO and V. STANNETT, *Camille Dreyfus Laboratory,
Research Triangle Institute, Durham, North Carolina*

Synopsis

The polymerization of single crystals and finely powdered samples of trithiane (m.p. 215–216°C.) was accomplished by irradiation of the samples at room temperature with Co^{60} γ -radiation to doses of 1–10 Mrad. Polymerization occurred during subsequent heating of the samples at 180°C. The conversion to polythiomethylene after a given time of heating at 180°C. is dependent on radiation dose, the G values for conversion being higher at lower doses. Purified polymer samples were studied by means of differential thermal analysis. Polymerized single crystals of trithiane were found to retain their orientation in three dimensions, although the polymer samples were systematically twinned. The directions of greatest chain growth were along the diagonals in the (ab) plane of the monomer. This reaction can be classified as topotactic; that is, the molecular orientations of the product are correlated with the molecular orientation in the reactant crystal. The relationship between the polymer structure and that of the monomer is evaluated.

INTRODUCTION

The successful radiation polymerization of single crystals of trioxane reported by Hayashi et al.,¹ giving systematically twinned crystals of polyoxymethylene,^{2–4} has greatly stimulated interest in the solid-state polymerization of other ring compounds. The solid-state polymerization of trioxane can be classified as a topotactic reaction; that is, the molecular orientation of the product is correlated with the molecular orientation in the reactant crystal. Since the polymerization of symmetric ring compounds involves the breaking and formation of the same bond in each step of the reaction, the entire process must be almost thermoneutral. In the case of the post-polymerization of preirradiated crystalline trioxane, Nauta⁵ has reported a small exothermic heat of reaction of 1.88 ± 0.10 kcal./mole of trioxane at approximately 50°C. This situation should favor a topotactic reaction. However, a knowledge of other crystalline monomers which polymerize in this manner is necessary before any generalization can be made as to the relationship between the monomer and polymer crystal structures and the reactivity of the monomer in the solid state. Therefore, a study of the sulfur analog of trioxane, trithiane, is of considerable interest.

* Presented before the Division of Polymer Chemistry at the 148th Meeting of the American Chemical Society, Chicago, Illinois, August 31, 1964.

The radiation polymerization of crystalline trithiane has been reported by this laboratory, single crystals of trithiane yielding highly oriented polythiomethylene.⁶ Recently Carazzolo and Mammi⁷ have reported a hexagonal space group for polythiomethylene having 17 ($-\text{CH}_2-$) groups and 9 turns of the helix in the 36.52 Å. identity period along the hexagonal axis. They have reported that the x-ray data presented earlier⁶ are consistent with this polymer structure and have suggested that the polymer chains grow along the *b* axis of the orthorhombic trithiane crystal. The work discussed herein is an attempt to evaluate this polymerization reaction in greater detail.

EXPERIMENTAL

Polymerization

Finely ground samples of trithiane, m.p. 215–216°C., were sealed in Pyrex tubes under a pressure of 1 atm. nitrogen at -196°C . These samples received Co^{60} γ -radiation doses of up to 10 Mrad at room temperature and were subsequently polymerized at $180 \pm 2^\circ\text{C}$. for 185 hr. The extent of conversion to polythiomethylene was determined by extracting the remaining monomer in boiling chloroform solution and weighing the polymer residue. This product was identified by comparing its Debye-Scherrer x-ray pattern with that of polythiomethylene, chemically prepared in solution,⁸ and additionally by comparison of the *d* spacings with those reported for polythiomethylene by Lal.⁹ Melting points of polymer samples, prepared by irradiation of the solid monomer and by chemical methods in solution, were obtained by observing the disappearance of birefringence during melting on a heating stage under a polarizing microscope. Differential thermal analysis and thermal gravimetric analysis determinations were also made on 100 mg. of each of these samples.

Nuclear Magnetic Resonance

The hydrogen resonance at 60 Mcycles of polycrystalline trithiane was observed in the temperature range 25–180°C. by use of a Varian dual-purpose NMR spectrometer.

X-Ray Diffraction Studies

Needle single crystals of trithiane were sealed in air in thin-walled 0.5 mm. capillaries and given Co^{60} γ -radiation doses of 10 Mrad at room temperature. Changes in the trithiane crystals polymerizing at $180 \pm 2^\circ\text{C}$. were examined at various conversions by means of oscillation and equi-inclination Weissenberg x-ray photography, using $\text{CuK } \alpha$ x-rays. These pictures were used to establish the unit cell dimensions of the polymer and the orientations of the polythiomethylene chains with respect to crystallographic directions in the monomer crystal.

RESULTS

Polymerization

The observations that no polymerization of crystalline trithiane occurs during heating at 180°C. without prior γ -irradiation or during irradiation at room temperature enable one to study the propagation of the radiation-initiated polymerization of the solid monomer independent of initiation. An important consequence of this type of "post-polymerization" is that the polymer produced is not degraded by γ -radiation during the polymerization process. It should be noted that no polymerization is observed if post-irradiation heating is carried out at 150°C.

The dependence on irradiation dose of conversion of trithiane powder to polythiomethylene after heating for 185 hr. at 180°C. is shown in Table I. Also shown are the melting points of the polymer produced as compared to that of polythiomethylene prepared by chemical means in solution. It can be seen that there is a saturation effect on conversion; that is, the G - (conversion) values for trithiane, listed in Table I, decrease with increasing radiation dose. Assuming no chain transfer during the polymerization, it would be expected that the molecular weight of the polymer would also decrease with increasing radiation dose. Because considerable degradation occurs above 225°C. even under nitrogen, and no solvents are presently known that dissolve the polymer below this temperature, meaningful viscosity measurements on polythiomethylene could not be obtained.⁸ However, the increase in the temperature at which melting begins with decreasing radiation dose apparently supports the argument that the molecular weight of the polymer is higher for lower radiation doses. The lower temperature range of melting for the solution polymerized polythiomethylene may indicate that the molecular weight of this material is lower than that of polymer prepared in the solid state, although this could also be attributed to larger crystallite size in the latter samples. It should be noted that the melting points of all polythiomethylene samples decrease considerably upon recrystallization from the melt and subsequent re-melting.

TABLE I
Polymerization of Crystalline Trithiane During Heating
for 185 hr. at 180°C. after Various Radiation Doses

| Dose, Mrads | Conversion to polymer, % | G (conversion) | Melting temperature, °C. |
|----------------|--------------------------------|-------------------|--------------------------------|
| 1 | 16 | 1.1×10^3 | 253-260 |
| 4 | 21 | 3.7×10^2 | 252-259 |
| 7 | 37 | 3.7×10^2 | 247-258 |
| 10 | 42 | 2.9×10^2 | 243-258 |
| | | | 240-250 ^a |

^a Polymer prepared by chemical methods in solution.

DTA and TGA

To obtain more information concerning the possibilities discussed above, differential thermal analyses ($2.5^{\circ}\text{C./min.}$) of all samples listed in Table I were obtained. The variation of ΔT with temperature of these samples is shown in Figure 1. A striking difference between the samples produced in the solid state and the chemically initiated solution-polymerized sample was observed. The former samples gave two strong endotherms in the melting range, one at 240°C. and the other between 260 and 265°C. , while the polymer produced in solution gave one strong endotherm in this range at 255°C.

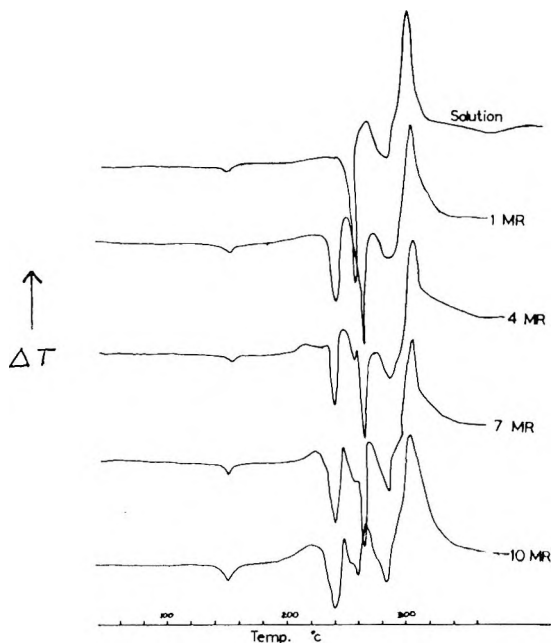


Fig. 1. Differential thermal analysis of polythiomethylene samples.

It should be noted that the size of the endotherm at 260 – 265°C. in relation to the 240°C. endotherm increases with decreasing radiation dose for the samples polymerized in the solid state. It was also observed that, after heating these samples to 245°C. and then cooling to 100°C. , both the endotherms at 240 and 260 – 265°C. occur upon reheating. However, if these polymer samples are heated to 265°C. before cooling to 100°C. , only one endotherm appears upon reheating, and that occurs below 240°C. Apparently there are two melting points for the polythiomethylene prepared in the solid state, the higher one attributable to polymer of larger crystallite size, greater crystalline order, and perhaps higher molecular weight; or, in other words, polymer originating from larger, better ordered monomer crystallites. This difference is destroyed after melting and degradation at 265°C. The increasing relative size of the higher endotherm

with decreasing initial monomer radiation dose is consistent with this interpretation.

The endotherms, attributable to melting, of all samples, including the polymer prepared in solution, occur at lower temperatures after each successive melting and recrystallization. This agrees with the results of the melting point determinations under the polarizing microscope and can be attributed to degradation. Thermal gravimetric analyses (2.5°C./min.) indicates that degradation is observable above 200°C.

It should be noted from Figure 1 that all polymer samples exhibit a small irreversible endotherm at 150°C. It is significant that the size of this endotherm decreases with decreasing monomer irradiation dose, and is smallest in the case of solution prepared polythiomethylene. It can be seen that the exothermic premelting crystallization hump at approximately 220°C. varies with dose in the same manner as the endotherm at 150°C.

Nuclear Magnetic Resonance

A study of hydrogen NMR spectra of polycrystalline trithiane (m.p. 215–216°C.) observed in the temperature range 25–180°C. indicated negligible line width change and the appearance of no narrow line component. This is in marked contrast to similar work performed on trioxane (m.p. 62°C.), in which the line width decreases markedly with increasing temperature (–48° to 54°C.) and a narrow line component is observable.¹¹

X-Ray Crystallography

The three-dimensional orientation of polythiomethylene, prepared by the radiation polymerization of single crystals of trithiane, was studied by means of x-ray diffraction techniques. The unit cell of trithiane has been shown to be orthorhombic, space group $Pmn2_1$ (no. 31), having lattice constants $a = 7.63$ Å., $b = 7.00$ Å., and $c = 5.25$ Å.¹⁰ All x-ray pictures of trithiane, trithiane–polymer mixtures, and polythiomethylene, shown in Figures 2–6, were taken with the original c (needle) axis of the monomer as the rotation axis. Figure 2 is a 180° oscillation picture of an unirradiated trithiane crystal, and Figures 3 and 4 are a 180° oscillation picture and a zero layer ($hk0$) Weissenberg picture, respectively, taken after the crystal had received a radiation dose of 10 Mrad and was heated at 180°C. for 66 hr. Figures 5 and 6 are identical to Figures 3 and 4, respectively, but taken after heating for 163 hr. and after the remaining monomer was removed by sublimation.

Figures 2, 3, and 5 show the orientation along the original c axis of the monomer, while Figures 4 and 6 give the distribution of intensities of x-ray reflections perpendicular to that axis. It can be seen that the polymer product is oriented in three dimensions, although the degree of disordering is apparently greater perpendicular to the original c axis than along it. From the pictures in Figures 5 and 6 and other upper layer Weissenberg

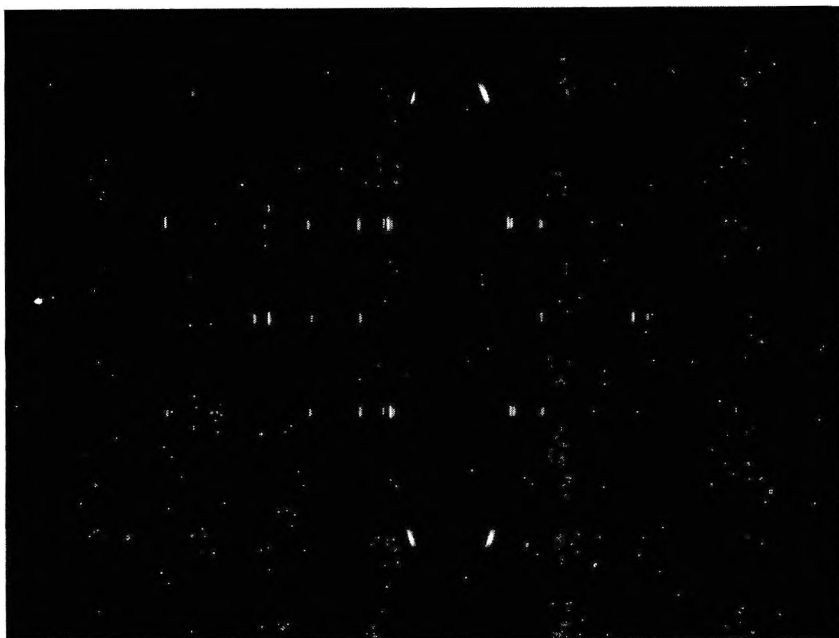


Fig. 2. 180° Oscillation picture of trithiane single crystal, exposure 30 min.; rotation axis, *c* trithiane.

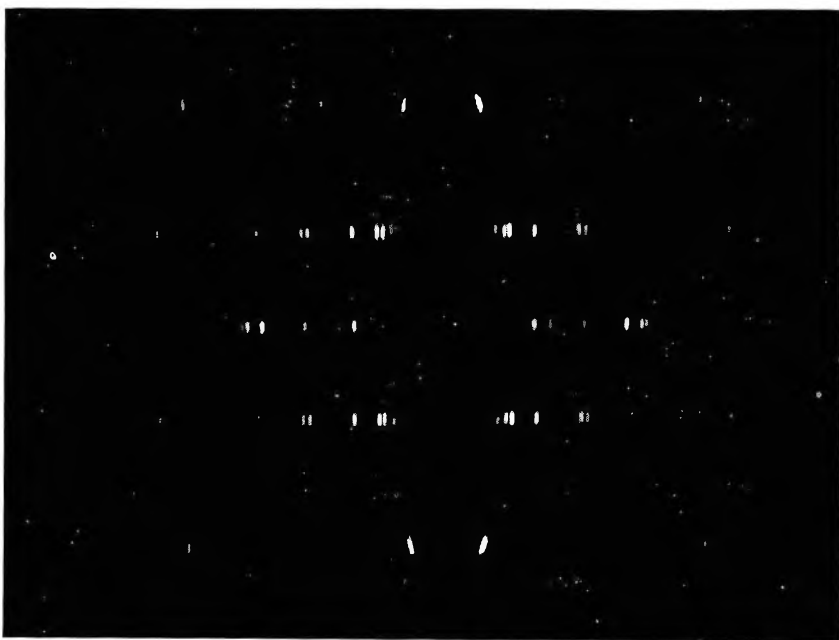


Fig. 3. 180° Oscillation picture of trithiane single crystal after irradiation (10 Mrad) and heating at 180°C. for 66 hr., exposure 30 min.; rotation axis, *c* trithiane.

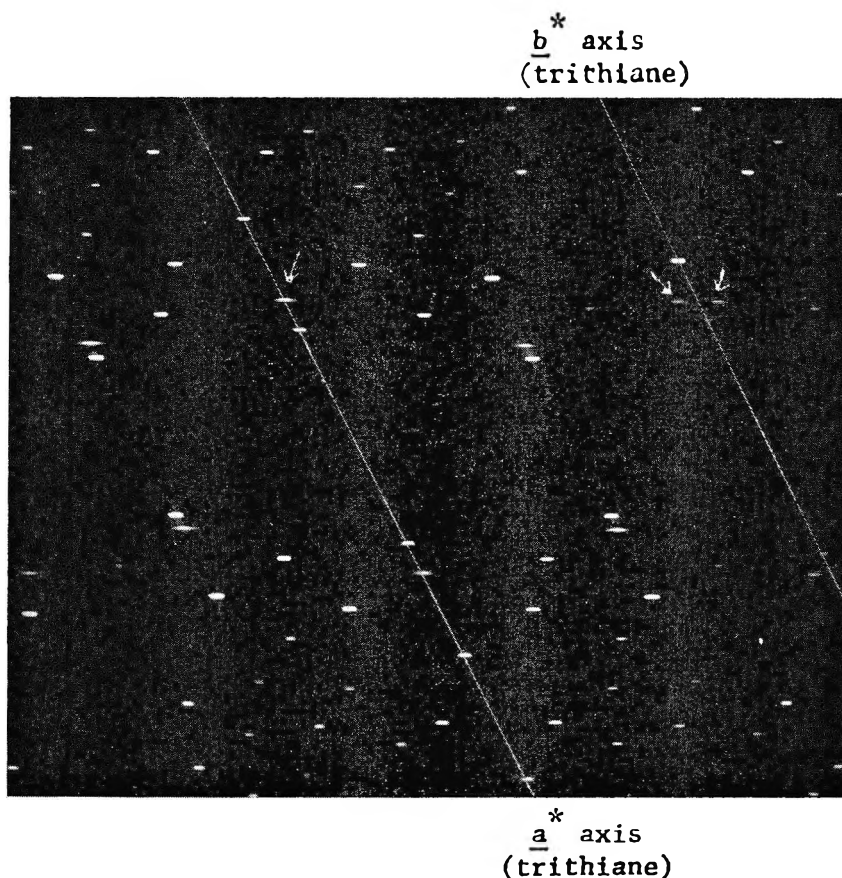


Fig. 4. ($hk0$) Weissenberg picture of trithiane single crystal after irradiation (10 Mrad) and heating at 180°C. for 66 hr., exposure 12 hr.; rotation axis, c trithiane.

photographs, it was found that most of the polymer reflections, including all of the intense ones, can be indexed in an orthorhombic unit cell with dimensions $a = 12.0$ A., $b = 12.7$ A., and $c = 5.10$ A. Figures 3 and 4, which are pictures taken after partial conversion to polymer, show that the a , b , and c axes of the apparent orthorhombic polythiomethylene unit cell are coaxial with the a , b , and c axes of trithiane, respectively. It can also be deduced from Figures 4 and 6, assuming the orthorhombic unit cell, that there are two reflections of equal intensity, 87° and 93° from each reflection in the orientation described above. The sum of the intensities of these two reflections is equal to the intensity of the reflection in the original orientation. The two reflections are attributable to twinning about the $d_{(110)}$ and $d_{(\bar{1}10)}$ directions of the monomer. The polymer reflection, designated (400) in the orthorhombic unit cell and its two twin reflections are indicated by the arrows in Figure 4. Notwithstanding the above analysis, the fact that some of the observed polymer reflections

cannot be indexed without postulating a fourfold increase in the length of the a and b axes makes the proposed orthorhombic unit cell unlikely.

As mentioned above, Carazzolo and Mammi⁷ have reported a hexagonal unit cell for polythiomethylene with $a = 5.07$ Å. and $c = 36.52$ Å., having the helical axis of the polymer parallel to c . They indicate that there are 17 ($-\text{CH}_2\text{S}-$) groups and 9 turns of the polymer helix in the identity period of 36.52 Å. They also reported that the new reflections in the 180° oscillation x-ray photograph of a partially polymerized single crystal of trithiane published by this laboratory⁶ (similar to Figure 3) was consistent with their hexagonal polymer unit cell if one assumes that an a axis of the

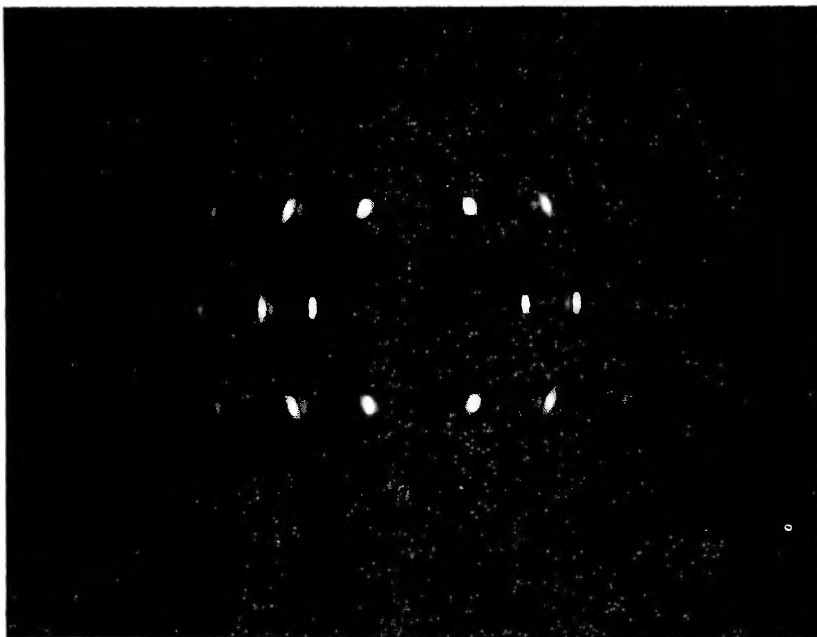


Fig. 5. 180° Oscillation picture of trithiane single crystal after irradiation (10 Mrad) and heating at 180°C . for 163 hr., exposure 30 min.; rotation axis, c trithiane (remaining trithiane removed by sublimation).

polymer is coaxial with the c axis of trithiane (the rotation axis). They have also suggested that the polymer helix grows along the b axis of the trithiane crystal.

An analysis of the polymer reciprocal lattice by using Weissenberg photographs, such as those shown in Figures 4 and 6, is consistent with the hexagonal unit cell proposed by Carazzolo and Mammi, an a axis of the polymer being coaxial with the c axis of the monomer. However, the polymer resulting from the polymerization of trithiane single crystals, although oriented in three dimensions, is systematically twinned as described below. Also, the direction of chain propagation is definitely not along the b axis of the monomer as suggested by Carazzolo and Mammi.

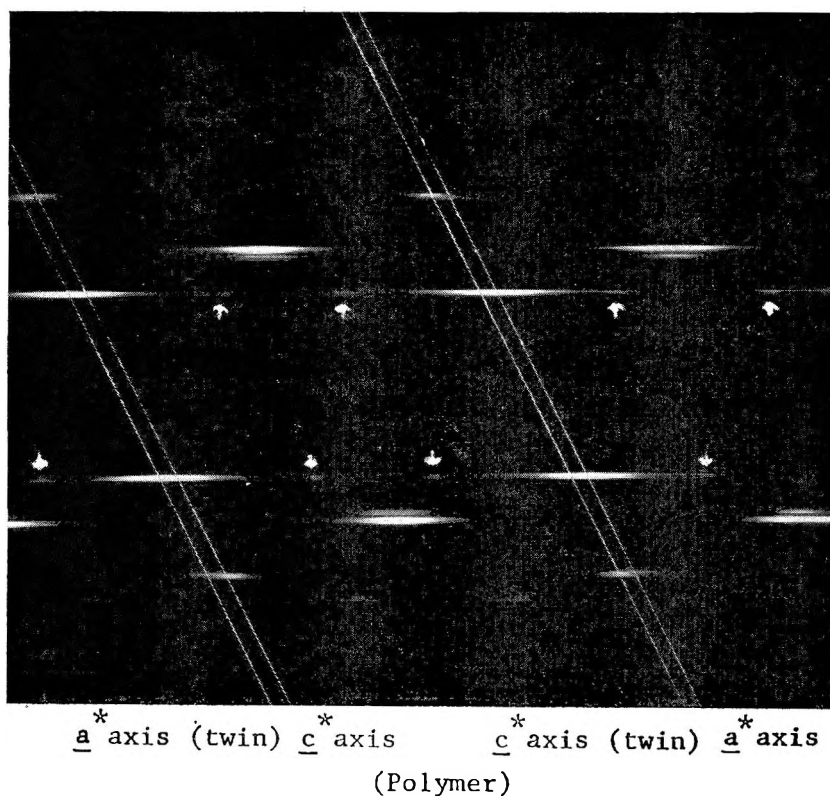


Fig. 6. ($hk0$) Weissenberg picture of trithiane single crystal after irradiation (10 Mrad) and heating at 180°C . for 163 hr., exposure 12 hr.; rotation axis, c trithiane (remaining trithiane removed by sublimation).

Since the c axis of trithiane is coaxial with an a axis of polythiomethylene, it is apparent that Figure 4, a ($hk0$) Weissenberg of a partially polymerized trithiane single crystal, has superimposed on it ($h0l$) polymer reflections. Thus, Figure 6 contains only ($h0l$) polymer reflections. From these pictures the polymer is seen to be twinned so that the a^* axis of the polymer is along both the $d^*_{(110)}$ and $d^*_{(\bar{1}10)}$ directions of the monomer, which are 87° and 93° apart. Thus the c axis of the polymer in each orientation, being 90° from a^* , will be 3° from either the $d^*_{(110)}$ or the $d^*_{(\bar{1}10)}$ directions in the monomer. Since in the monomer the $d^*_{(110)}$ and $d^*_{(\bar{1}10)}$ directions make an angle of 3° with the base diagonals of the (ab) plane, it can be seen that the polymer helix (c axis) grows along the diagonals in the (ab) plane of the monomer. Intensity measurements confirm that an equal amount of polymer grows in each direction. The reciprocal lattice axes of the monomer (coaxial with those of the apparent orthorhombic polymer cell) and the reciprocal lattice axes of the true hexagonal unit cell of the polymer are labeled in Figures 4 and 6, respectively. The (400) reflection of the apparent orthorhombic polymer unit cell and its

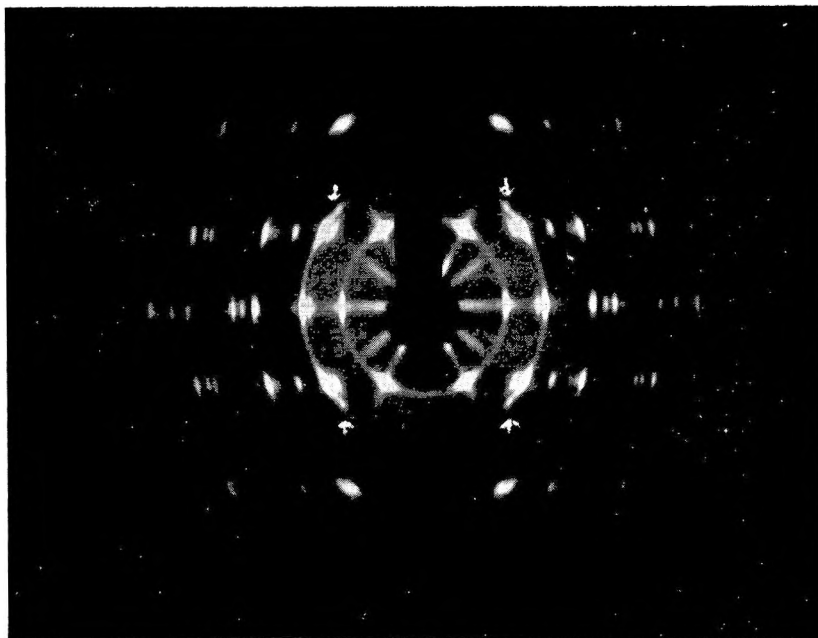


Fig. 7. 180° Oscillation picture of trithiane single crystal after irradiation (10 Mrad) and heating at 180°C. for 163 hr., exposure 6 hr.; rotation axis, c trithiane (remaining trithiane removed by sublimation).

twin reflections (indicated by the arrows in Figure 4) are in reality the (109) and $(\bar{1}09)$ reflections of the actual hexagonal cell with their twin reflections. Fortuitously, the (109) reflection and the $(\bar{1}09)$ twin superimpose on each other, giving a reflection of twice the intensity of the $(\bar{1}09)$ and (109) twin measured separately.

It should be noted that the above explanation does not account for the extra reflections, indicated by the arrows in Figure 6, and for the reflections just above the (109) and $(\bar{1}09)$ reflections on the first layer line and just below the $(\bar{1}09)$ and (109) reflections on the minus first layer line, indicated by the arrows in Figure 7. Figure 7 is an x-ray photograph of the same crystal as in Figure 5 but taken with a longer exposure time. The presence of these reflections can be explained with the help of Figure 8, which shows one orientation of the hexagonal unit cell of the polymer with respect to its reciprocal lattice. The spots represent reciprocal lattice points along the a^* axes. The c and c^* axes of the polymer, which are coaxial, are perpendicular to the plane of the paper at the origin. It should be noted that a rotation of the reciprocal lattice of 93° or 87° (a_2^* towards c^*) will give rise to the second orientation of the polymer previously explained. A similar rotation of a_1^* and a_3^* in both the a_2^* orientations will give rise to four new c^* directions and will explain the extra reflections labeled in Figures 6 and 7. In Figure 6 the extra reflections are the tails of the (100) reflections from a_1^* and a_3^* after a rotation of 87° or 93°. They occur, as

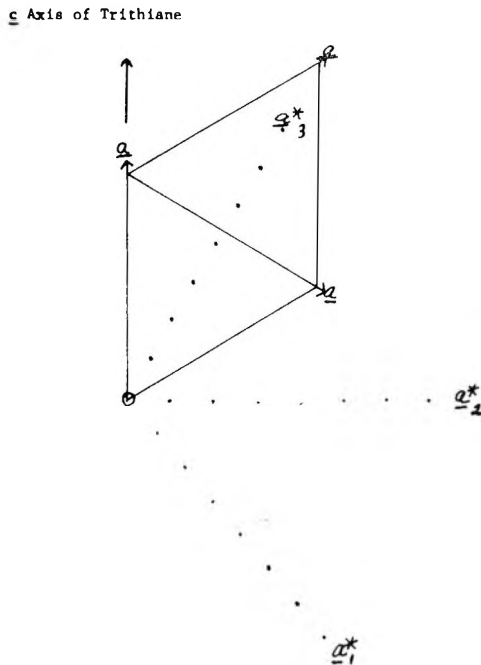


Fig. 8. Representation of the hexagonal polythiomethylene unit cell with respect to its reciprocal lattice and the trithiane unit cell, c and c^* of polymer perpendicular to plane of paper.

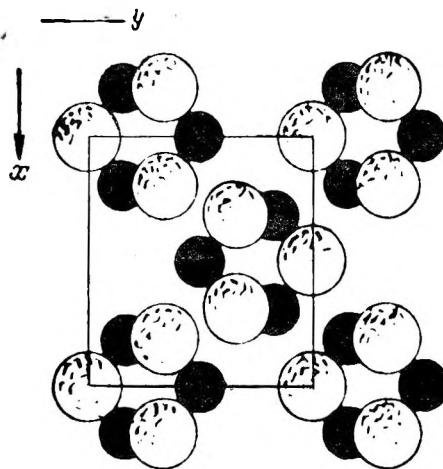


Fig. 9. Projection onto (ab) plane of trithiane unit cell (after Moerman¹⁰).

they should, either 60° away from the (100) reflection of a_2^* or its twin. In a like manner the unexplained reflections in Figure 7 are caused by the $(\pm 1,0,9)$ reflections after rotation.

Polythiomethylene chains grow, therefore, not only along the (ab) diagonals of the trithiane unit cell but also in four orientations at an angle of

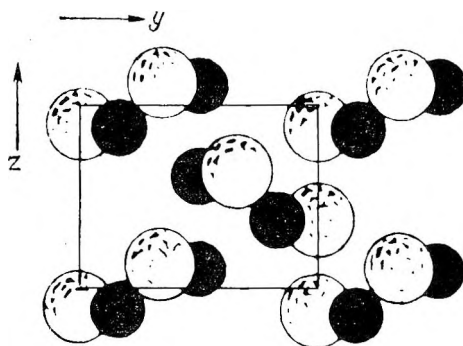


Fig. 10. Projection onto (bc) plane of trithiane unit cell (after Moerman¹⁰).

about 60 degrees from the (ab) diagonals of the monomer towards the trithiane c axis. From the intensities of the x-ray reflections it appears that the bulk of the polymer grows along the (ab) diagonals of trithiane. Figures 9 and 10 are the (ab) and (bc) projections of the trithiane unit cell reported by Moerman,¹⁰ from which these growth directions can be correlated with the molecular positions in the trithiane unit cell.

DISCUSSION

The polymerization of crystalline trithiane is seen to be a good example of a topotactic process. This polymerization is especially favorable to this type of process since the densities of the monomer and polymer are similar, being 1.62 and 1.60 g./cc., respectively. This compares with 1.41 and 1.49 g./cc. for trioxane and polyoxymethylene, respectively. As previously mentioned, the fact that the post-polymerization should be almost thermoneutral also is favorable to topotaxy. With reference to the latter statement it is interesting to note that Nauta,⁵ who found a small exothermic heat of reaction of 1.88 ± 0.10 kcal./mole in the similar polymerization of trioxane, estimates that this heat of reaction is caused by decreased molecular motion in going from the crystalline monomer just below its melting point ($62^\circ\text{C}.$) to a crystalline polymer far below its melting point ($198^\circ\text{C}.$). He proposes that this greater molecular motion within the trioxane crystal is necessary to overcome the hindrance to polymerization inherent in a rigid crystal. That the degree of molecular motion in trioxane does increase markedly in the temperature range where polymerization is appreciable has been confirmed by nuclear magnetic resonance.¹¹ In the polymerization of trithiane crystals at $180^\circ\text{C}.$ the relative proximity of the melting points of the monomer (215 – $216^\circ\text{C}.$) and the polymer ($\sim 260^\circ\text{C}.$), and the fact that our nuclear magnetic resonance measurements show little change in the molecular motion of trithiane (25 – $180^\circ\text{C}.$) indicates an even lower heat of reaction than that observed for trioxane.

We have attributed the two endotherms observed by differential thermal analysis in the melting range of the polythiomethylene samples prepared

from crystalline trithiane to polymer originating in large and small monomer crystallites, the larger monomer crystallites yielding larger polymer crystallites and perhaps higher molecular weight polymer. However, it is possible that the endotherm observed at the higher temperature is not only related to crystallite size and molecular weight, but also to the retention in a portion of the sample of the systematically twinned structure of the polymer observed in the polymerization of single crystals of trithiane. The meaning of the small irreversible endotherm at 150°C. observed in all polymer samples is obscure. It occurs in the solution-prepared polythiomethylene as well as in that prepared in the solid state, and thus it is difficult to relate it to the twinned structure of the latter samples. Also, in a predominantly crystalline polymer it is difficult to attribute this endotherm to the glass transition, even of a very rigid glass. In addition, a glass transition should be reversible if no crystallization is observed below the maximum temperature (170°C. in one case) to which the sample is heated.

In conclusion, it should be noted that along the directions of growth of the bulk of the polymer, i.e., the (*ab*) diagonals of the trithiane unit cell, there are two monomer molecules in the projection onto the (*ab*) plane in a distance of 10.4 Å. This distance is 2.5 Å. less than necessary to accommodate this number of atoms along the polymer helix. It is quite likely that growth occurs in the other directions to relieve the strain imposed by this difference. The possibility that the various orientations of the polymer chain are caused by "kinking" of individual chains or groups of chains as opposed to separate crystallites in different orientations should not be ignored. This "kinking" might also apply to the case of the polymerization of trioxane which also has a systematically twinned structure.⁴ Lastly, it should be pointed out that it is this twinning of the polythiomethylene prepared from single crystals of trithiane and its relation to the trithiane structure that gives rise to the apparent orthorhombic unit cell first proposed for the polymer.

We would like to acknowledge the support of this investigation by the Division of Isotopes Development, U. S. Atomic Energy Commission. We would also like to thank Mr. H. Olf for help with the nuclear magnetic resonance experiments and Mr. T. Tarim of the North Carolina State College School of Textiles for help with the differential thermal analysis and the thermal gravimetric analysis.

References

1. Hayashi, K., Y. Kitanishi, M. Nishii, and S. Okamura, *Makromol. Chem.*, **47**, 230 (1961).
2. Okamura, S., K. Hayashi, and M. Nishii, *J. Polymer Sci.*, **60**, S26 (1962).
3. Lando, J. B., N. Morosoff, H. Morawetz, and B. Post, *J. Polymer Sci.*, **60**, S24 (1962).
4. Carazzolo, G., S. Leghissa, and M. Mammi, *Makromol. Chem.*, **60**, 171 (1963).
5. Nauta, H., paper presented at 5th International Symposium on the Reactivity of Solids, Munich, Germany August 1964.
6. Lando, J. B., and V. Stannett, *J. Polymer Sci.*, **B2**, 375 (1964).
7. Carazzolo, G., and M. Mammi, *J. Polymer Sci.*, **B2**, 1057 (1964).
8. Wenger, F., private communication.

9. Lal, J., *J. Org. Chem.*, **26**, 971 (1961).
10. Moerman, N. F., and E. H. Wiebenga, *Z. Krist.*, **97**, 323 (1937).
11. Komaki, A., and T. Matsumoto, *J. Polymer Sci.*, **B1**, 671 (1963).

Résumé

La polymérisation de mono-cristaux de trithiane (F: 215–216°C) et d'échantillons réduits finement en poudre a été effectuée par irradiation des échantillons à température de chambre au moyen de rayonnement γ du Co⁶⁰ à des doses allant de 1 à 10 Mrads. La polymérisation s'effectue pendant le chauffage subséquent des échantillons à 180°C. La conversion en polythiométhylène après un temps de chauffage donné à 180°C dépend de la dose de rayonnement, les valeurs de G pour la conversion étant plus élevées à des doses plus faibles. Les échantillons de polymère purifiés ont été étudiés par analyse thermique différentielle. On a trouvé que les cristaux uniques de trithiane polymérisé conservaient leur orientation dans les trois dimensions, bien que les échantillons de polymère aient été systématiquement entremêlés. Les directions de la plus grande croissance de chaîne se font suivant les diagonales dans le plan (ab) du monomère. Cette réaction peut être classée comme étant une réaction topotactique, c'est-à-dire que les orientations moléculaires du produit sont reliées à l'orientation moléculaire du cristal en réaction. On évalue la relation entre la structure du polymère et celle du monomère.

Zusammenfassung

Die Polymerisation von Einkristallen und feingepulverten Proben von Trithian (F.P. 215–216°C) wurde durch Bestrahlung der Proben bei Raumtemperatur mit Co-60-Gammastrahlung bei Dosen von 1 bis 10 Mrad erreicht. Während des darauffolgenden Erhitzens der Proben auf 180°C trat Polymerisation ein. Der Umsatz zu Polythiomethylen nach einer gegebenen Erhitzungsdauer bei 180°C hängt von der Bestrahlungsdosis ab und zwar sind die G -Werte für den Umsatz bei niedrigeren Dosen höher. Gereinigte Polymerproben wurden differentialthermoanalytisch untersucht. Polymerisierte Trithianeinkristalle behielten ihre dreidimensionale Orientierung bei, obwohl die Polymerproben systematisch verdrillt wurden. Die Richtung des grössten Kettenwachstums lag längs der Diagonale in der (ab)-Ebene des Monomeren. Diese Reaktion kann als topotaktisch bezeichnet werden; d.h. die Molekülorientierung im Produkt steht in Korrelation zur Molekülorientierung im reagierenden Kristall. Die Beziehung zwischen der Polymerstruktur und derjenigen des Monomeren wird ermittelt.

Received November 24, 1964

Revised December 10, 1964

Prod. No. 4624A

BOOK REVIEWS

N. G. GAYLORD, Editor

Methoden der organischen Chemie (Houben-Weyl) Vol. XII, Part I. Organische Phosphorverbindungen, K. SASSE, E. MULLER, Editors, Georg Thieme Verlag, Stuttgart, 1963. Lxxii 683 pp., DM 166; DM 149.40 for subscribers.

Parts I and II of Volume XII of Houben-Weyl series *Methoden der organischen Chemie* treat the methods of synthesis and reactions of organophosphorus chemistry in a comprehensive manner. In addition to the discussion of the types of reactions, the book contains many tables of compounds with some physical properties such as melting points, boiling points, and yields, as well as literature references. The information is divided according to the major classes of organophosphorus compounds, not according to general methods of reaction. In this respect, Volume XII differs from other books of the Houben-Weyl series. Selection of this arrangement was obviously the right decision. Because of the great complexity of the classes of organophosphorus compounds, a single method such as the reaction of phosphorus halides, oxyhalides, or haloesters with the Grignard reagents can be used to prepare various types of phosphines, phosphine oxides, esters of several acids, and so forth. The uninitiated reader would be confused if all these products were listed in a single section. Furthermore, many types of reactions are specific for the class of compounds prepared by them; therefore they naturally fit this classification.

A beginner, e.g. a graduate student would not use this volume as a reference book for a specific problem as one would use *Chemical Abstracts*, but rather would read all of it for a broad survey of organophosphorus chemistry. It is recommended that he first become thoroughly familiar with the detailed classification of compounds. For this kind of systematic study, the book appears to be eminently suitable. It does not, however, eliminate the necessity of independent literature search for research chemists, since even a book of this size is too limited to list all compounds of at least one carbon-phosphorus bond which have been prepared. To this class belong phosphines, quaternary phosphonium compounds, phosphoranes, phosphine oxides, biphosphines and cyclophosphines, phosphinous acids, phosphinic acids, phosphonous acids, phosphonic acids, as well as the halides, esters, and other derivatives of these acids. Part II of the same volume discusses the methods of synthesis of the organic derivatives of hypophosphorous, hypodiphosphorous, hypophosphoric, phosphorous, and phosphoric acids. Thus in its division of material, Part I does not differ much from the organization of information in the first seven chapters of G. M. Kosolapoff's book *Organophosphorus Compounds* (Wiley, New York, 1950). However, the Houben-Weyl book by Dr. K. Sasse contains more information, and the literature is covered to the end of 1961.

The problem of the complex nomenclature of organophosphorus compounds is successfully tackled in the introduction to Part I. The logical derivation of the structures of some lower acids of phosphorus such as the enol forms of the primary and secondary phosphine oxides which are the corresponding keto forms, is shown. Although it is mentioned that free phosphinous acids do not have the properties of true acids, it might have been helpful to emphasize at this point Arbuzov's rule that a true hydroxyl cannot exist on a trivalent phosphorus atom. Concerning the strongly displaced keto-enol equilibrium, Van Wazer's well-known book of organophosphorus chemistry is

more explicit, since it shows numerically the extreme prevalence of the keto form. In general, Van Wazer's book offers a more comprehensive treatment of the theoretical and physico-chemical aspects of phosphorus chemistry. Part I of Volume XII of the Houben-Weyl series is closer in nature to Kosolapoff's book; these both describe in detail the methods of preparation. The Houben-Weyl book by Sasse also offers procedures of preparation of representative compounds, with amounts of materials and other data as in *Beilstein's Handbuch*.

From the experience in several organic research laboratories, it can be said that Kosolapoff's book has become an indispensable research tool for people working with organophosphorus compounds. Although not quite exhaustive in its treatment of the subject material, it provides a firm foundation to which a specific literature search of more recent publications can be added. For the same purpose, Volume XII of the Houben-Weyl series should be available in each laboratory where organophosphorus compounds are of some importance. In the absence of a more complete edition of Kosolapoff's book, the volume of Houben-Weyl comes closest to filling this gap. For a synthetic chemist, the numerous and detailed tables of compounds and the emphasis on yields is very important; in this respect, the book being reviewed is superior to some older books. For the industrial chemist, the easy accessibility of information concerning the yields is helpful in order to estimate the prospects of practical applications.

A large folded table at the end of Part I lists the types of compounds systematized by the number of P-C and P-P bonds and by the formal valency of phosphorus. The nomenclature of compounds with at least one P-C bond, the topic of Part I, is explained in somewhat greater detail in the introduction. Representative names of subclasses such as imides, amides, halides, cyano derivatives, thio analogs of phosphorus acids, and combinations of these and others are given. Nevertheless, it would be desirable to have a longer table of classes and subclasses of organophosphorus compounds, at least a hundred or more types with their general structural formulas, German, and English names. After all, the book is going to have perhaps a comparable number of English-speaking readers as German, and the English language is understood by chemists in almost all countries. In practice, I have observed that an average research worker in an American industrial laboratory can read the German text but he is compelled to seek help or a dictionary when he is not certain of the English equivalent of a type of compound such as one of the numerous acids or esters of phosphorus. Such a bilingual table would certainly increase the popularity of the book and would help to dispel the confusion brought about by several past changes of the nomenclature of phosphorus compounds.

The first general class discussed in Part I of Volume XII is the phosphines. The extent of the increase of information from the older literature summarized in Kosolapoff's book is remarkable. A reader of the older literature often obtains the impression that the available methods of synthesis of phosphines are either too expensive for the industry (such as those employing the Grignard reagents), hazardous for large scale operations (such as the Würtz reaction using metallic sodium), or form a spectrum of products and therefore are impractical. The reviewed book lists many new routes to phosphines and thus may provide a stimulus for practical applications which have been rather neglected in this area. On many pages, all references are more recent than 1950. It seems fitting that a German book describe the progress in this field, since many important research workers who have recently advanced the knowledge of the chemistry of phosphines are Germans: Professor L. Horner and his co-workers; K. Issleib, W. Kuchen, just to mention a few. Dr. Gerhard Schrader, one of the most eminent authorities on organophosphorus poisons, has made several contributions of experimental procedures and practical advice. The publication of the book was supported by the Farbenfabriken Bayer A. G., Leverkusen; the author, Dr. K. Sasse, is a staff member of this industrial concern. However, the book is not an industrial monograph emphasizing patents of practical utility, markets, and applications. The information is directed more toward the classification of methods and synthesis of representative pure, monomeric compounds.

The book will serve as a useful reference for research workers in the agricultural chemistry of insecticides, pesticides, herbicides, as well as for biochemists and polymer chemists who study or employ organophosphorus compounds. Nevertheless, there is still need for a more comprehensive treatment of the use of organophosphorus compounds for fireproofing plastics and other industrial applications. Geffer's book of organophosphorus monomers and polymers is more closely orientated toward this goal but it does not completely cover the field either.

Part I of Volume XII of the Houben-Weyl series attempts to unify several subtypes of reactions into a single method of broader scope. This treatment facilitates the survey and memorization of the principal synthetic approaches. For example, about a dozen related types of reactions of haloalkanes with phosphine, primary and secondary phosphines, with or without additional reagents, are discussed here together, and at the end of this section a table lists the principal raw materials, names of the phosphines prepared, yields, and references. This is an improvement over some older books in which the subtypes of reactions were discussed separately and a somewhat confused picture of the whole method was created.

For a quick scanning of references, it is convenient to have them listed at the bottom of each page as is done in the book being reviewed. However, this necessitates the listing of one and the same reference in several places of the book and thus increases the bulk of the volume. To facilitate the survey of the contribution of a particular author, their names are listed alphabetically at the end of the volume, with references to the pages in the book.

The Houben-Weyl book by Dr. K. Sasse is lucid, easily readable, remarkably free of errors, and amply illustrated by equations with structural formulas in the discussion of syntheses. The book is another example of the excellent quality, persevering industry, and accuracy of the work of German scientists. For a synthetic organophosphorus chemist, it is a milestone of systematized knowledge on the road of progress initiated by the book of V. M. Plets (*Organic Compounds of Phosphorus*, Moscow, 1938) and by Professor Kosolapoff's book in the United States. Part I of Volume XII of Houben-Weyl is warmly recommended for all academic institutions and industrial laboratories interested in the chemistry of phosphorus.

Nicodemus E. Boyer

Marlon Chemical Division
Borg-Warner Corporation
Washington, West Virginia

Determination of Molecular Weights and Polydispersity of High Polymers, S. R. RAFIKOV, S. A. PAVLOVA, and I. I. TVERDOKHLEBOVA, Trans. by J. ELIASSAF, Daniel Davey, New York, 1964. 357 pp., \$12.50.

A few months ago in this *Journal*, this reviewer stated that "practitioners of the molecular characterization of polymers badly need a good up-to-date book on this subject." The book being reviewed at that time, *Determination of Molecular Weights of High Polymers* by Ch'ien Jeu-yüan, was not the answer to this need, but it may have inspired Dr. Rafikov (who translated it from Chinese into Russian) to produce a better volume.

The present book, prepared under Dr. Rafikov's editorship, is still far from the ideal monograph on molecular weight measurement from the American standpoint, but it compares quite favorably with other volumes on this subject. Coverage is good, the only major techniques not covered being those which have been developed since the Russian version was written (most chapters contain few references as late as 1961). In general, the discussions are sound but terribly noncritical and nonselective; this is the

book's major disadvantage, and it is enough to warrant a warning that it *not* be used by the student or neophyte. There is no index, and there are many typographical errors, fortunately most of them minor. There are over 900 references, only 150 of them to Russian literature.

An introductory chapter is well written except for some crude concepts of how "tightly" or "loosely" packed structures affected solubility. Chapter II (fractionation) covers basic concepts well, but is noncritical when applications are discussed. Column fractionation is not well covered. Chapter III (light scattering) is sound but prosaic. Discussion of instruments is noncritical, but a section on estimating polydispersity from the $P(\theta)$ function presents (if a bit overenthusiastically) useful tables of data.

The Chapters on diffusion (IV) and ultracentrifugation (V) do not clarify the difference between thermodynamic equilibrium methods and semi-empirical transport techniques. Pitfalls in applying the latter to random-coil polymers are not discussed.

Chapters VI (osmometry) and VII (other colligative methods) are only fair, being badly outdated on instrumentation and nonselective elsewhere. Except for the latter defect, the section on osmotic membranes is one of the best available.

Endgroup analysis is discussed from the conventional chemical standpoint in Chapter VIII, and viscometry in Chapter IX. The latter is good in general, except for a preoccupation with low-concentration anomalies which overlooks the definitive work of Claesson. Chapter X, on methods based on physical properties, is virtually useless. A table of Mark Holiwink constants as an Appendix completes the work.

Determination of Molecular Weights and Polydispersity of High Polymers, by Rafikov et al., comes close to being a good book. It will serve the already knowledgeable reader well as a reference source until a modern American monograph or textbook on the subject appears.

Fred W. Billmeyer, Jr.

Rensselaer Polytechnic Institute
Troy, New York

NOTES

Decomposition of Azobisisobutyronitrile in Dioxane-Water Mixture and its Dependence on pH

The thermal decomposition of azobisisobutyronitrile (ABIN) is known to proceed via a first order reaction^{1,2} with no evidence of induced side reactions. Previous studies also showed that the rate of decomposition in organic solvents is independent of the dielectric constant of the medium in the range of 2-26. The decomposition of ABIN in aqueous media, however, has not been investigated in detail. We would like to report a study of the thermal decomposition of ABIN in water-dioxane mixtures. The dependence of the rate of decomposition on pH (apparent values) was examined. The dielectric constant of the medium reached 50 in a water-dioxane mixture containing 25% dioxane.

A 50 ml. two-necked round bottom flask was connected to a jacketed gas buret through a condenser and a capillary glass tube. A mixture of 10 ml. dioxane and 30 ml. water (with buffer solution) was added to the flask and the contents of the flask were flushed with nitrogen. The flask was then placed in a constant temperature bath ($\pm 0.1^\circ\text{C}.$) for 30 min. after which 0.1500 g. (9.14×10^{-4} mole) of recrystallized ABIN was added with stirring. The volume of nitrogen evolution over mercury was recorded every 10 min. The total volume of nitrogen evolution at complete decomposition was in excellent agreement with the theoretical value; the theoretical value was used as V_∞ in all our calculations.

The results of nitrogen evolution from ABIN decomposition in dioxane-water mixture were plotted as $\ln V_\infty/(V_\infty - V_t)$ vs. time. For experiments with pH greater than 10.67, there was a rapid evolution of gas during the first few minutes after which gas evolution proceeded at a smooth rate. As will be seen in the results of the hydrolysis of ABIN at pH greater than 10.67, ammonia and carbon dioxide were liberated in small amounts. This discontinuity in the curve of volume-time plot for nitrogen evolution was therefore ascribed to the liberation of ammonia and carbon dioxide in this early period, which is usually 3 to 7 min. In our calculation of the kinetic data (pH > 10.67), therefore, we have taken the end of this initial, rapid gas evolution as the zero time and zero volume. The corrected zero time may be discerned easily from a volume-time plot. The time correction is small as compared with the duration of the experiment, namely, about four to five hours. The zero volume so chosen afforded a good agreement (better than 2%) between the total gas evolution and the theoretical nitrogen content. It was, therefore, felt that the correction procedure was justified. The first order kinetic plots, after the correction, yielded good straight lines. The slopes of the linear plots were used for the calculation of the rate constants k .

Although the dielectric constant of dioxane-water mixture was high, the observed rates of decomposition of ABIN in this medium without buffer were essentially the same as the reported values^{4,6} obtained in a variety of organic solvents with dielectric constants ranging from 2-26. The dielectric constant of the dioxane-water (1:3) mixture used in the present study is around 50.⁵ For comparison, the decomposition rates of ABIN in various organic solvents are listed in Table I. The rate constants for ABIN decomposition in the dioxane-water mixture are 1.62×10^{-4} sec.⁻¹ at $80^\circ\text{C}.$, 3.20×10^{-5} sec.⁻¹ at $70^\circ\text{C}.$, and 2.53×10^{-5} sec.⁻¹ at $65.3^\circ\text{C}.$ as compared with literature values of $1.55-1.98 \times 10^{-4}$ sec.⁻¹ at $80^\circ\text{C}.$, 3.75×10^{-5} sec.⁻¹ at $70^\circ\text{C}.$, and 2.0×10^{-5} sec.⁻¹ at $65.3^\circ\text{C}.$ in organic solvents. Allowing for a possible minor solvent effect⁷ of

TABLE I
The Decomposition Rates^{1,4} of ABIN in Various Solvents

| | Dielectric constants | $k \times 10^4$ (sec. ⁻¹) at 80°C. | $k \times 10^5$ (sec. ⁻¹) at 70°C. | $k \times 10^5$ (sec. ⁻¹) at 65.3°C. |
|---|----------------------|--|--|--|
| Toluene | 2.4 (20°C.) | 1.55 | 3.75 | 2.00 |
| Xylene | 2.4 (20°C.) | 1.53 | | |
| Dimethylaniline | 4.5 (20°C.) | 1.83 | | |
| <i>n</i> -BuOH | 7.8 (19°C.) | 1.55 | | |
| Acetic Acid | 7.1 (17°C.) | 1.52 | | |
| iso-BuOH | 18.7 (20°C.) | 1.72 | | |
| Nitrobenzene | 26.3 (80°C.) | 1.98 | | |
| 20% Dioxane-H ₂ O ⁶ | 50.8 (60°C.) | | | 2.53 (pH = 7) |
| 20% Dioxane-H ₂ O ⁶ | 48.2 (70°C.) | | 3.20 (pH = 7) | |
| 20% Dioxane-H ₂ O ⁶ | 45.8 (80°C.) | 1.62 (pH = 7) | | |

dioxane on the rate of reaction, it may be concluded that the decomposition rates of ABIN are independent of the dielectric constants of the media ranging from 2-50.

The dependence of the rate constants of ABIN decomposition at 75°C. on pH (apparent) is shown in Figure 1. The rate constant k was 8.42×10^{-5} sec.⁻¹ at pH 7.0 and remained essentially the same between pH 7 and 9. A small increase in k was noticed between pH 9 and 10. At pH 10, k increased sharply to reach a maximum at pH 10.67 and then dropped off rapidly to 8.50×10^{-5} sec.⁻¹ as at pH 7.0 in more alkaline media. The maximum rate of decomposition at pH 10.67 was 17.2×10^{-5} sec.⁻¹, about twice the value at pH 7. This increase in the rate of decomposition, although small, was reproducible.

The activation energy of decomposition at pH 7.0 was 33.7 kcal./mole, the same as that obtained in organic solvents.⁴ Between pH 7 and 9 and also above pH 11.52, the $\log k$ vs. $1/T$ plot almost superimposes upon the data of Overberger (Fig. 2).

In a previous paper,⁸ the polymerization of *n*-vinylpyrrolidone with ABIN as initiator in aqueous solution at 50°C. was studied. The rate of polymerization was found to be

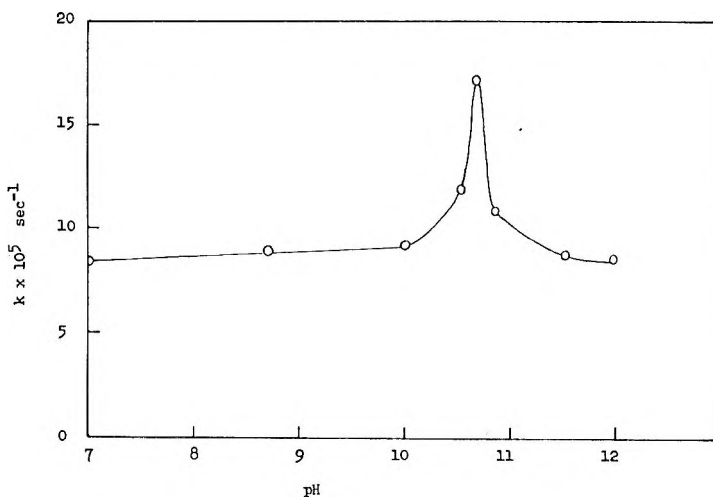


Fig. 1. Effect of pH on the rate of decomposition of ABIN in dioxane-water mixture at 75°C.

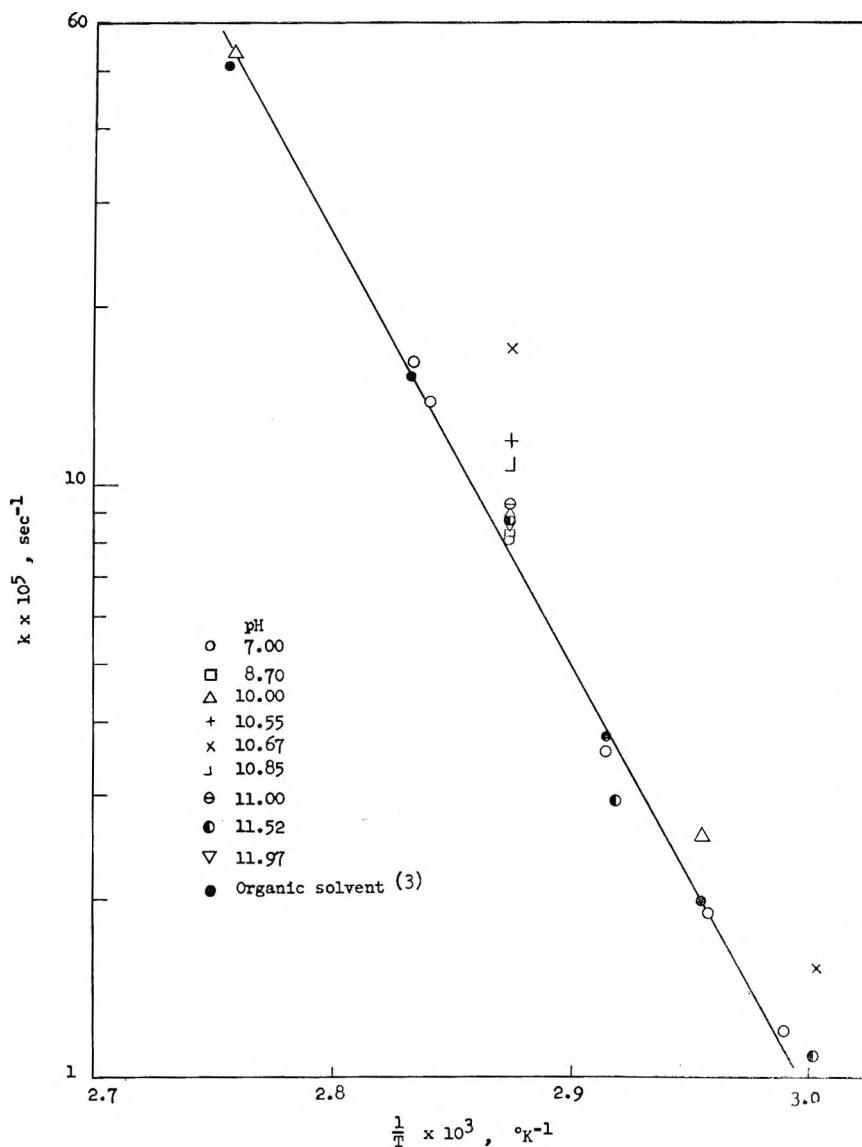


Fig. 2. Rates of decomposition of ABIN.

a function of pH between 7 and 12 with a maximum rate at pH 9.5 (Fig. 3). The maximum rate was approximately twice the rate at pH 7.0. In the polymerization of methacrylic acid initiated by ABIN in aqueous solution, Blauer⁹ reported that the rate of polymerization passed through a small maximum in the region between pH 6 and 12. The two monomers, one ionizable and the other non-ionizable, are sufficiently different that it is difficult to rationalize the occurrence of a rate maximum in each case by ascribing it to some properties common to both monomers. The present investigation seems to suggest that the dependence to the polymerization rates of these two monomers on pH (in alkaline solution) is perhaps related to the rates of ABIN decomposition in aqueous mixtures.

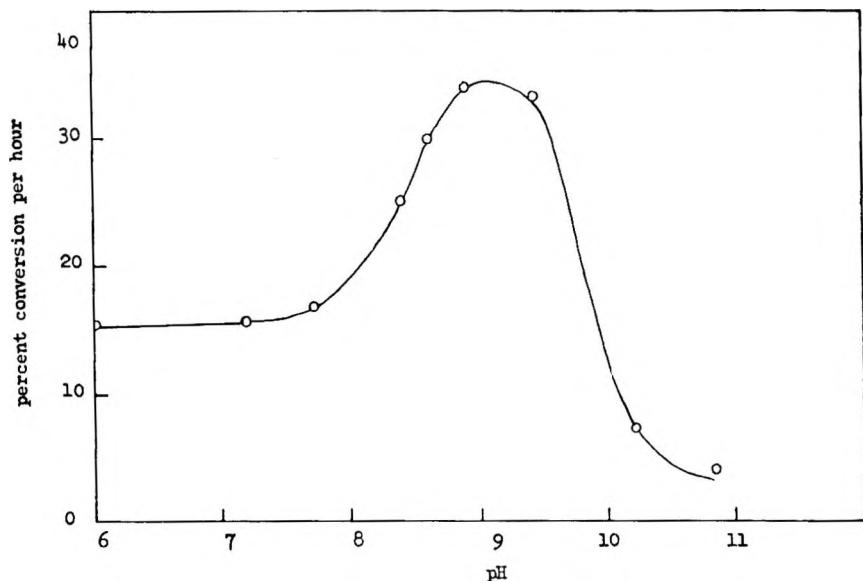


Fig. 3. Effect of pH on the rate of polymerization of vinylpyrrolidone with ABIN catalyst at 50°C.

A tentative explanation for the above observation is proposed as follows. In the alkaline medium, the hydrolysis of the nitrile groups¹⁰ in ABIN may result in the formation of a salt with the liberation of ammonia. The presence of an ionizable group, i.e., COO^- on the hydrolyzed ABIN molecule, may possibly enhance the rate of decomposition of ABIN. In the recent work by Hammond and Neuman,¹¹ the protonated azobisamidines were found to decompose at a considerably faster rate than the free base. Hammond concluded that the acceleration was mainly due to the stabilization of the ion radical and only slightly to the electrostatic repulsion of the ions. The observed rate increase between pH 9 and 10.7 in our study can probably be explained also as the stabilization of the ion radicals by the COO^- groups on the hydrolyzed ABIN molecules.

Above pH 10.67, the decomposition of ABIN slowed down sharply. We had found from the hydrolysis of ABIN in the alkaline media (see below) that decarboxylation had occurred in a negligible amount between pH 9 and 10.7, but to a larger extent above 10.7. Some partial or complete decarboxylation of COO^- groups¹² on the converted compound from ABIN may have occurred prior to nitrogen evolution to yield an azo-hydrocarbon which may decompose at a slower rate.¹³

The hydrolysis of ABIN is likely to occur prior to the nitrogen evolution because the activation energy for the hydrolysis and decarboxylation should be much smaller than that for the decomposition. If so, the gases such as ammonia and carbon dioxide would evolve at an early stage of the decomposition reaction. At pH 11, although the decomposition of ABIN did yield an appreciable amount of carbon dioxide (see below), the rate of nitrogen evolution could still be obtained from a smooth curve of volume-time plot after the correction for the initial gas liberation as described earlier. The corrected total gas evolution agreed well with the theoretical nitrogen content. Furthermore, the previous experiments in the polymerization of vinyl pyrrolidone initiated by ABIN⁸ also showed that the rate of polymerization or the rate of consumption of radicals decreased at a high pH level. We are, therefore, inclined to conclude that the effect of pH between 9–12 on the rate of decomposition of ABIN is to convert it to other compounds which decompose at different rates.

Some preliminary hydrolysis experiments of ABIN were carried out. In alcoholic potassium hydroxide at 50°C., ABIN was hydrolyzed overnight to the potassium salt of azobisisobutyric acid, m.p. 250°C.³ The salt seemed to decompose at a faster rate than ABIN at neutral pH. In buffered methanol-water solutions, the ABIN was completely hydrolyzed at low temperature for one week, i.e., 35°C., to give the amide of azobisisobutyric acid, m.p. 104°C.³ as a major product in 60% yield. The infrared¹⁴ and ultraviolet spectroscopy were used to identify these products. No carboxylic acid salts were found in this case. When ABIN was hydrolyzed at 75°C. for a few hours in buffered solutions, decomposition products were found to be largely of tetramethyl-succinamide and a small amount of an unidentified secondary amide. The inorganic salts and some of the unhydrolyzed ABIN were recovered, but no carboxylic acid salts were obtained. The gaseous products of the buffered hydrolysis reactions were analyzed quantitatively by mass spectrometry in the Gollob Laboratory, Berkeley Heights, New Jersey. Carbon dioxide was obtained appreciably only when the decomposition reactions of ABIN in methanol-water solutions were carried out at both high temperature and high pH level; e.g., 28% CO₂ at 79°C. and pH 11. At 75°C. and pH 10.7, only 1.4% CO₂ was obtained; at 35°C. and pH 10.70, less than 0.5% CO₂ was obtained. Therefore, decarboxylation was negligible at pH < 10.7.

Any definite explanation for the variations of the decomposition rates of ABIN in alkaline media is difficult at this stage. Some further work is necessary to clarify the situation.

The author wishes to acknowledge the assistance for this work from the Research Foundation of Newark College of Engineering. He also wishes to thank Dr. C. C. Overberger for his helpful discussions.

References

1. Walling, C., *Free Radicals in Solution*, Wiley, New York, 1957, p. 512.
2. Bevington, J. C., and H. G. Troth, *Trans. Faraday Soc.*, **58**, 186 (1962).
3. Thiele, J., and K. Heuser, *Justus Liebig's Annalen der Chemie*, **290**, 36 (1896).
4. Overberger, C. G., M. T. O'Shaughnessy, and H. Shalit, *J. Am. Chem. Soc.*, **71**, 2661 (1949).
5. Arnett, L. M., *J. Am. Chem. Soc.*, **74**, 2027 (1952).
6. Timmermans, J., *Physico-Chemical Constants of Binary Systems*, Vol. 4, Interscience, New York, 1960, p. 16.
7. Petersen, R. C., J. H. Markgraf, and S. D. Ross, *J. Am. Chem. Soc.*, **83**, 3819 (1961).
8. Kwei, Kwei-ping Shen, *J. Polymer Sci.*, **B1**, 379 (1963).
9. Blauer, G., *J. Polymer Sci.*, **11**, 189 (1953).
10. (a) Hickinbottom, W. J., *Reactions of Organic Compounds*, Longmans, Green & Co., London, 1957, p. 381; (b) Marvel, C. S., and R. Adams, *J. Am. Chem. Soc.*, **42**, 312 (1920).
11. Hammond, G. S., and R. C. Newman, Jr., *J. Am. Chem. Soc.*, **85**, 1501 (1963).
12. (a) *Organic Reactions*, Vol. 11, Wiley, New York, 1957, p. 206; (b) Vaughan, W. R. and R. Q. Little, *J. Am. Chem. Soc.*, **76**, 2952 (1954).
13. Walling, C., *Free Radicals in Solution* Wiley, New York, 1957, p. 516.
14. Bellamy, L. J., *The Infrared Spectra of Complex Molecules*, Wiley, New York, 1958, Chap. 12.

KWEI-PING SHEN KWEI

Department of Chemistry
Newark College of Engineering
Newark, New Jersey

Received December 6, 1963

Revised December 15, 1964

*The Mechanism of Emulsion Polymerization. II. Branching in
Polymers Prepared by Emulsion Polymerization Techniques**

INTRODUCTION

In a free radical polymerization the number of branches per monomer unit incorporated in the chain ($1/\gamma$) is a function of the polymer concentration at the site of polymerization and the constant for transfer of a growing radical to an already existent backbone, C_p . The relationship for bulk polymerization is given by eq. (1).¹

$$1/\gamma = -C_p [1 + (1/\theta) \ln (1 - \theta)] \quad (1)$$

where θ is the fractional conversion of monomer to polymer. For a bulk polymerization, the concentration of polymer at the reaction site (the whole volume) goes up linearly with conversion, as shown in Figure 1. Therefore, the likelihood of branching increases greatly with conversion.

In the Harkins-Smith-Ewart^{2,3} picture of emulsion polymerization, the whole monomer-polymer particle, which is the site of polymerization, is accessible to the radical. It is generally assumed that on the average the polymer concentration is approximately 50% from the time monomer-polymer particles are formed until the monomer reservoir droplets disappear at 50-70% conversion. From then on the concentration of monomer goes down and the polymer concentration goes up exactly like a bulk polymerization. This is graphically shown in Figure 1 by means of a dashed line. If this picture is correct, more branching should take place between 0 and 50% conversion in emulsion systems than in bulk systems. This has led to the postulation that polymers prepared in emulsion should be especially highly branched.⁴

With a surface reaction, postulated by Medvedev,⁵ most of the polymer in the monomer-polymer particle is segregated into the core of the particles. Most of the monomer is at the surface of the particles, which is the main locus of polymerization. Thus, there is probably very little polymer at the site of reaction, at least until the monomer droplets disappear at about 60% conversion. If we assume 10% polymer at the surface during this initial phase of the reaction, we obtain the graphical representation shown on Figure 1. Therefore, throughout the course of the reaction, we have less polymer present at the site of reaction than in bulk polymerization, and, in fact, we should expect very little branching below 80-90% conversion. Emulsion polymer produced by this mechanism would be less branched than polymers produced by bulk polymerization.

On the basis of these considerations, we can choose between the two loci of emulsion polymerization, if we can find some technique for estimating the degree of branching of emulsion polymers relative to the degree of branching of a bulk polymer of the same composition, molecular weight, and conversion. Such a technique has been developed by Zimm and Stockmayer and their coworkers.⁶⁻⁹

Their theory relates the intrinsic viscosities and the mean square end-to-end distances of polymer molecules to their extent of branching. In their treatment, the degree of branching is found from a factor, g , which is defined by the following equation.

$$g = (\bar{r}^2)_{br}/(\bar{r}^2)_{st} = ([\eta]_{br}/[\eta]_{st})^2 \quad (2)$$

* Presented at the 147th Annual Meeting of the American Chemical Society, Philadelphia, April 1964.

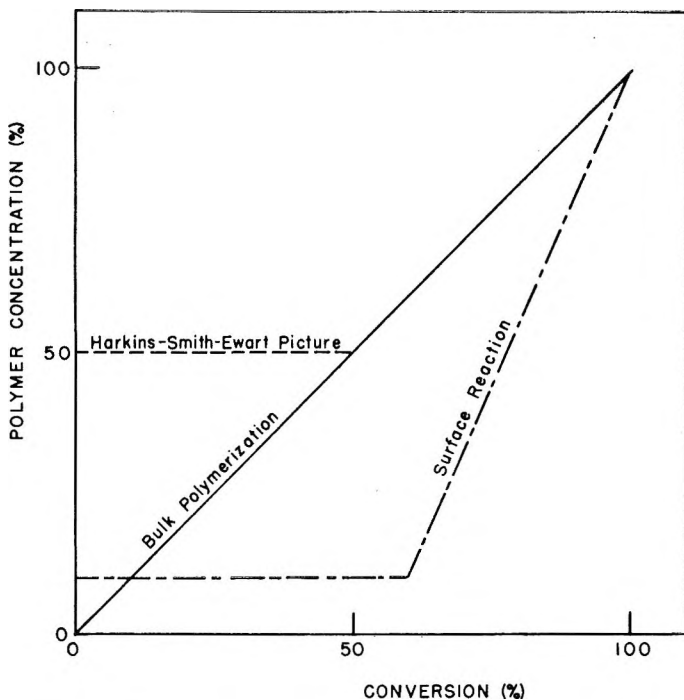


Fig. 1. Polymer concentration as a function of conversion for three model systems.

where $(\bar{r}^2)_{br}$ and $[\eta]_{br}$ are the measured mean square end-to-end distance and intrinsic viscosity, respectively, of a fraction of the branched polymer and $(\bar{r}^2)_{st}$ and $[\eta]_{st}$ are the mean square end-to-end distance and intrinsic viscosity that a straight chain fraction of the same molecular weight would have. A recent article¹⁰ utilized this technique to assess the amount of branching in poly(methyl methacrylate) by measurements of the dilute solution properties.

In this note, we present a study of the branching in emulsion systems utilizing the measurements of the dilute solution properties of the emulsion polymerization prepared polymers. Because fractionation is very time consuming, we did not investigate fractions but rather whole polymers. In that case, the ratio of the distances, $(\bar{r}^2)_{br}$ and $(\bar{r}^2)_{st}$, overestimates g and the ratio of the intrinsic viscosities underestimates g .¹⁰ These two values, however, should give us the extreme values of the number of branches found, i.e., the upper and lower bounds on the number of branches. Because a small change in g is often equivalent to a large change in the number of branches calculated, our values are relatively crude estimates. They are significant, however, in that they are the first attempts to quantitatively estimate branching in emulsion polymers, and the results are consistent with the viewpoint that the surface is the main locus of polymerization.

EXPERIMENTAL METHODS

Sample Preparation

Latices of poly(styrene) and poly(methyl methacrylate) were prepared using ammonium persulfate as initiator and sodium lauryl sulfate as emulsifier. The precautions observed previously¹¹ were followed. The complete recipes of these latices are given in Table I.

TABLE I
Recipes for the Emulsion Polymer Samples

| Sample | Con., % ^a | Initiator system | Solids, % |
|------------|----------------------|------------------------------|-----------|
| Styrene I | 5 | 0.5% ^a APS, 40°C. | 45 |
| Styrene II | 10 | 0.5% ^a APS, 50°C. | 16 |
| MMA I | 5 | 0.75% APS, 30°C. | 16 |
| MMA II | 0.25 | 0.75 APS, 30°C. | 16 |

^a Based on monomer.

The latices were coagulated by freezing (Dry Ice was dropped into a beaker containing the latex) after the emulsifier had been removed by a mixed bed ion-exchange resin. The coagulated polymer was then washed, dried, and dissolved in benzene. All the solutions of polymer in benzene were freeze-dried to obtain samples suitable for intrinsic viscosity and light-scattering measurement.

Intrinsic Viscosities

The intrinsic viscosities were run in Cannon-Ubbelohde viscometers. Reagent grade acetone and butanone were used for all the viscosity determinations. The equations for calculating the intrinsic viscosities of the unbranched polymer are:

$$[\eta] = 4.73 \times 10^{-4} M^{0.56}, \text{ polystyrene in butanone (20-35°C.)} \quad (3)$$

$$[\eta] = 1.40 \times 10^{-4} M^{0.654}, \text{ poly(methyl methacrylate) in acetone}^{10} \quad (4)$$

Equation 3 is the least squares best fit to the experimental data of a number of investigators¹²⁻¹⁵ using fractionated low conversion polymer. This compilation and correlation was done by Mrs. M. Duden of our laboratories. It covers the molecular weight range of 3000 to 1.8×10^6 .

In the investigations of the high molecular weight poly(methyl methacrylate) using eq. (4), we used the same viscometers that were used to obtain that equation. Thus, any shear thinning corrections to be applied to the data cancel out when the intrinsic viscosity ratios are calculated. The molecular weight range here was 1×10^6 to 11×10^6 .

Light Scattering

Light-scattering measurements were made as described earlier.^{10,16} From the measurements, the mean square end-to-end distance and weight-average molecular weights were obtained. They were compared to the values for unbranched polymer obtained from the following equations:

$$(\bar{r}^2)^{1/2} = 0.47 M^{0.55}, \text{ poly(styrene) in butanone, 20°C.}^{17} \quad (5)$$

$$(\bar{r}^2)^{1/2} = 0.114 M^{0.64}, \text{ poly(methyl methacrylate) in acetone}^{10} \quad (6)$$

Fractionation

To determine the effect of a rough fractionation on the value of g obtained by the two techniques for our samples, Styrene II was roughly fractionated using benzene as solvent and methanol as nonsolvent. Out of 12.1 g., a center cut of 9.55 g. was obtained. The low molecular weight cut contained 1.65 g. and the high molecular weight cut contained 0.90 g.

EXPERIMENTAL RESULTS

The intrinsic viscosities and light-scattering properties of the four emulsion polymers described in Table I were determined. By comparison with the expected values of $[\eta]$ and (\bar{r}^2) for unbranched polymers at the same weight average molecular weight, M_w , the parameter g was obtained. From g the number of branches, N , was calculated using the curve of Zimm and Stockmayer⁶ for trifunctional branching. From the molecular weight and the total number of branches the number of branches per monomer unit incorporated in the chain ($1/\gamma$) is obtained.

TABLE II
Experimental Determination of Branching in Emulsion Prepared Polymers

| Sample | $M_w \times 10^{-6}$ | $g[\eta]$ | $g[(\bar{r}^2)]$ | θ | $1/\gamma \times 10^4$ | | Calculated g |
|------------|----------------------|-----------|------------------|----------|------------------------|--------------|----------------|
| | | | | | Calculated | Experimental | |
| Styrene I | 4.51 | 0.57 | 0.80 | 0.979 | 5.9 ± 1.5 | 0.6-2.2 | 0.40 |
| Styrene II | 3.98 | 0.82 | 1.10 | 0.946 | 4.0 ± 1.0 | 0.00-0.53 | 0.50 |
| MMA I | 19.9 | 0.47 | 0.58 | 0.976 | 0.63 ± 0.20 | 0.48-0.93 | 0.53 |
| MMA II | 15.0 | 1.08 | 1.00 | 0.869 | 0.29 ± 0.09 | 0.00 | 0.72 |

All of the quantities of interest, i.e., g , θ , and $1/\gamma$, are listed for the emulsion prepared polymers in Table II. The ratio of $g[(\bar{r}^2)]$ to $g[\eta]$ is the same for the unfractionated Styrene I as it is for the crudely fractionated Styrene II. Thus, the crude fractionation was of little help in bringing about agreement between the two types of measurement. We do know¹⁶ that a good fractionation would bring them into better agreement but not coincidence so further fractionation appeared to offer no immediate advantage. Inserting the values of C_p of $2.0 \pm 0.5 \times 10^{-4}$ ¹⁸ and $2.2 \pm 0.7 \times 10^{-5}$ ¹⁹ reported for styrene and methyl methacrylate, respectively, in eq. (1), we obtain the values expected for bulk polymerization; they are also listed in Table II as calculated values with the error based on estimates given by the experimenters who obtained the C_p values.^{18,19}

Since the experimental estimates of $1/\gamma$ are based on the extreme values possible,¹⁰ it seems unlikely that the branching in emulsion polymerization is greater than that found in bulk polymerization. In fact, the data obtained with polystyrene indicate that the branching in emulsion polymerization is less than in bulk polymerization.

It should be noted that we obtained values of g greater than one, a theoretically impossible result, in two out of the eight determinations and in one instance $g[\eta]$ was greater than $g[(\bar{r}^2)]$ which is also impossible. These results indicate that there is some experimental error; a decrease of 10% in $(\bar{r}^2)_{br}$ or increase of the same amount in the calculated $(\bar{r}^2)_{st}$ for Styrene II, however, would have eliminated one discrepancy. A change of 4% in either $[\eta]_{br}$ or $[\eta]_{st}$ for MMA II would account for the other discrepancy. Much of this error may be contained in the extrapolation of $[\eta]_{st}$ and $(\bar{r}^2)_{st}$ values from 1.8×10^6 to 4.51×10^6 for polystyrene and from 1.1×10^7 to 1.99×10^7 for poly(methyl methacrylate) in estimating g .

Errors of the order given above, however, do not invalidate the differences observed. For example, compare the calculated, i.e., expected, values of g for Styrene I and II (Table II). They are lower than the $g[\eta]$ values by 43 and 64%, respectively. Since $g[\eta]$ is a function of the intrinsic viscosity squared, the errors in intrinsic viscosity measurements or estimations must be of the order of 105 and 170%, respectively, to invalidate the conclusion that there is less branching in emulsion prepared styrene than in bulk polymerized styrene.

CONCLUSIONS

The experimental results indicate, but do not prove conclusively, that there is less branching in emulsion polymerization than in bulk polymerization. Certainly, one does not find significantly more branching. This result lends support to the thesis that the surface of the monomer-polymer particles is the main locus of polymerization and in turn the results of our previous investigation¹¹ increase the reliance that can be placed on this study.

The authors would like to acknowledge the many helpful discussions held with Drs. S. Krause and D. L. Glusker.

References

1. Flory, P. J., *J. Am. Chem. Soc.*, **69**, 2893 (1957).
2. Harkins, W. D., *J. Amer. Chem. Soc.*, **69**, 1428 (1947); *J. Polymer Sci.*, **5**, 217 (1950).
3. Smith, W. V., and R. H. Ewart, *J. Chem. Phys.*, **16**, 592 (1948).
4. Gerrens, H., *Advan. Polymer Sci.*, **1**, 234 (1959).
5. Medvedev, S. S., *International Symposium on Macromolecular Chemistry, Prague*, Pergamon, New York, 1959, pp. 174-190.
6. Zimm, B. H., and W. H. Stockmayer, *J. Chem. Phys.*, **17**, 1301 (1949).
7. Stockmayer, W. H., and M. Fixman, *Ann. N. Y. Acad. Sci.*, **57**, 334 (1953).
8. Thurmond, C. D., and B. H. Zimm, *J. Polymer Sci.*, **5**, 477 (1952).
9. Zimm, B. H., and R. W. Kilb, *J. Polymer Sci.*, **37**, 19 (1959).
10. Krause, S., and E. Cohn-Ginsberg, *J. Polymer Sci.*, **A2**, 1393 (1964).
11. Brodnyan, J. G., J. A. Cala, T. Konen, and E. L. Kelley, *J. Colloid Sci.*, **18**, 73 (1963).
12. Outer, P., C. I. Carr, and B. H. Zimm, *J. Chem. Phys.*, **18**, 830 (1950).
13. Bawn, C. E. H., A. R. Freeman, and R. F. J. Kamaliddin, *Trans. Faraday Soc.*, **46**, 1107 (1950).
14. Flory, P. J., and T. G. Fox, *J. Am. Chem. Soc.*, **73**, 1915 (1951).
15. Frank, H. P., and J. W. Breitenbach, *J. Polymer Sci.*, **6**, 609 (1951).
16. Cohn-Ginsberg, E., T. G. Fox, and H. F. Mason, *Polymer*, **3**, 97 (1962).
17. Oth, and Desreux, *Bull. Soc. Chim. Belgrade*, **63**, 285 (1954).
18. Henrici-Olivé, G., and S. Olivé, *Advan. Polymer Sci.*, **2**, 496 (1961).
19. Henrici-Olivé, G., S. Olivé, and G. V. Schulz, *Makromol. Chem.*, **23**, 207 (1957).

JOHN G. BRODNYAN
ELIZABETH COHN-GINSBERG
THOMAS KONEN*

Rohm and Haas Research Laboratories
Spring House, Pennsylvania

Received June 26, 1964
Revised December 17, 1964

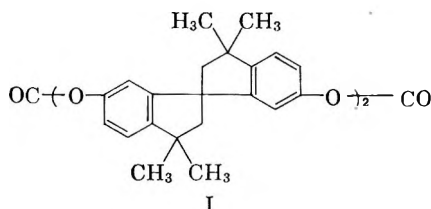
A Dimeric Cyclic Aromatic Carbonate

The formation of cyclic oligomers as by-products of condensation polymerization reactions is a widespread occurrence.¹ Cyclic carbonates of aromatic dihydroxy compounds, however, have only recently been prepared.^{2,3} In both reported instances, it was

* Present address: Franklin Institute Laboratories for Research and Development, Philadelphia, Pennsylvania.

necessary to resort to high dilution techniques in order to obtain these compounds. Thus, Schnell and co-workers² were able to prepare tetrameric cyclic aromatic carbonates by reacting bischloroformates with dihydroxy compounds at high dilution. The alternate route involving the acid or base catalyzed thermal cyclization of the polycarbonate was attempted² but was unsuccessful, possibly due to the decomposition of the bisphenol moiety.⁴ During some recent attempts to prepare a polycarbonate via the lithium hydroxide catalyzed melt reaction of diphenyl carbonate (0.00275 *M*) with 6,6'-dihydroxy-3,3',5,5'-tetramethyl-1,1'-spirobiindane⁵ (0.0025 *M*) a sublimate was observed to form in the final stages of reaction (270–300°C. <0.1 mm.). The sublimate was allowed to accumulate over a twelve hour period until a total of 0.3 gm., m.p. 287–338°C., had been collected. After washing the sublimate with benzene and crystallization from tetrachloroethane, its m.p. increased to >340°C. Analytical data indicated the substance to be the cyclic dimer (I). The carbonyl absorption of the dimer appeared at 1784 cm.⁻¹ (KBr) in the infrared as compared to 1770 cm.⁻¹ for the polycarbonate indicating the presence of strain in the former. The ability to isolate the dimer (I) under such vigorous conditions is felt to be due to the thermal stability of the spirobiindane nucleus.

Anal. Calc. for (C₂₂H₂₂O₃)₂: C, 79.01%; H, 6.63%; O, 14.36%; m.w., 668. Found: C, 79.43%; H, 6.34%; O, 14.20%; m.w., 625 (vapor phase osmometer).



References

1. Zahn H., and G. B. Gleitsman, *Angew. Chem. Intern. Ed.*, **2**, 410 (1963).
2. Schnell H., and L. Bottenbruch, *Makromol. Chem.* **57**, 1 (1962).
3. Belg. patent 643,250 (Allied Chemical), January 31, 1964.
4. Schnell H., and H. Krimm, *Angew. Chem.* **75**, 662 (1963).
5. Curtis R. F., *J. Chem. Soc.*, **1962**, 415.

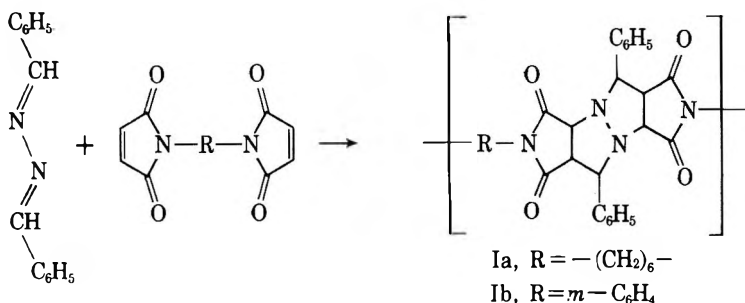
KENNETH C. STUEBEN

Plastics Division
Research and Development Department
Union Carbide Corporation
Bound Brook, New Jersey

Received December 16, 1964

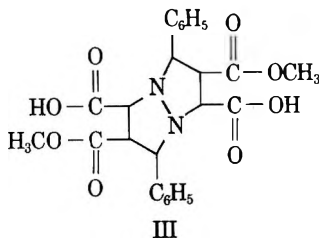
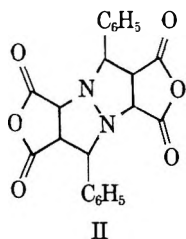
A Novel Polyimide

Most of the reported synthesis of polyimides¹ rely on the prior formation of a polyamide acid and a subsequent ring closure reaction. A novel polyimide system (I) has been reported from the reaction of benzalazine and bis-maleimides as a result of a double 1,3-addition across benzalazine.²



The polyimides obtained by this method had low inherent viscosities (0.13–0.30) for the various bis-maleimides employed. The independent synthesis of these polyimides by conventional polyimide forming techniques was undertaken to further verify the structure of the polymers formed from the 1,3-addition and to attempt to obtain higher molecular weight polymers.

The double 1,3-addition of maleic anhydride to benzalazine has been reported to give 4-8-diphenyl-1-1,5-diazabicyclo[3.3.0] octane-2,3,6,7-tetracarboxylic acid bis-anhydride (II) in low yield.³⁻⁵



When the reaction was carried out in a hydrocarbon solvent such as benzene or xylene, the product obtained has been found to be a mixture of two isomers, one melting at 233°C. and the other at 284°C.⁵ Running the reaction in the absence of solvent affords one compound with a melting point of 298°C.⁴ We found that when the reaction was run in acetic anhydride the product obtained in a 30% yield had a melting point of 296°C. By several recrystallizations from acetic anhydride or glacial acetic acid, this high melting compound could be isolated in a 23% yield from the reaction in xylene.

TABLE I

| Polymer | Method | % Yield | $[\eta]_{\text{inh}}^{\text{a}}$ | $[\eta]_{\text{inh}}^{\text{a}}$ |
|---------|--------|---------|----------------------------------|----------------------------------|
| | | | Polyamide Acid ^b | Polyimide |
| Ia | 1 | 95 | 0.10 | 0.20 |
| | | | 0.58 | 0.91 |
| Ia | 2 | 100 | — | 0.60 |
| Ib | 1 | 85 | 0.08 | 0.10 |

^a Inherent viscosities were run on dilute solutions of the polymers (0.50 g./100 ml. for the polyamide acids and 0.11–0.41 g./100 ml. for the polyimides) in dimethylformamide at 26°C.

^b The values shown for viscosities are those of the polyamide acid samples which were converted to the polyimides, whose viscosities are listed.

The formation of polyimides from II (Table I) was accomplished by two different methods, both of which have been widely employed with other polyimide systems.

The first method involved the direct reaction of the anhydride with a diamine, either hexamethylene diamine or *m*-phenylene diamine, to give the polyamide acid, which was then heated to afford the polyimide. A solution of the diamine in dimethylformamide (DMF) was added in a single portion to a slurry of an equimolar amount of the anhydride (II) in DMF. A total solute concentration of 5–10% was employed. The mixture was stirred at room temperature for 2–5 hr. and then heated for 0.25 hr. on a steam bath to complete the polymerization. The solution was then filtered and poured into a 5-fold volume of ether to precipitate the polyamide acid. Reprecipitation gave the pure polymer. The dry polyamide acids were heated to 200–210°C. in a vacuum oven for 1 to 1.5 hr. and finally the polymer was heated at 300–310°C. under a current of nitrogen to complete conversion to polyimide.

The second method required the preparation of the diacid diester III. This was accomplished by heating a solution of the anhydride in methanol to the reflux temperature for 1.25 hr. Evaporation to a small volume and cooling precipitated the product which was recrystallized from methanol. The reaction between III and the diamines to form the corresponding salt was carried out in methylene chloride. The equimolar mixture was stirred for 10 hr. under nitrogen at room temperature. The methylene chloride was then evaporated leaving the white salt as a residue. The salt was washed with hot dry benzene and cold methylene chloride. Only starting material was obtained from the reaction of III with *m*-phenylene diamine. The salt prepared from hexamethylene diamine was heated under the same conditions given for the polyamide acids.

The polyimides were dark brown, insoluble, and high melting (over 350°C.). Heating over 350°C. for any extended length of time led to polymer decomposition.

The polymers prepared by these methods showed the same infrared spectra as the polymers prepared by the 1,3-addition reaction. The lower viscosity of Ib as compared to Ia when prepared via the polyamide acid and the failure of *m*-phenylene diamine to react with III can probably be ascribed to differences in the base strength of the two amines. The viscosity of the polyimide prepared from hexamethylene diamine showed some improvement over that prepared by the 1,3-addition while that prepared from *m*-phenylene diamine was somewhat less.

References

1. Coffman, D. D., G. J. Berchet, W. R. Peterson, and E. W. Spangel, *J. Poly. Sci.*, **2**, 305 (1947); Bower, G. W., and L. W. Frost, *J. Poly. Sci.*, **A1**, 3135 (1963); Jones, J. I., F. W. Ochynski, and F. H. Rackley, *Chem. Ind.*, 1686 (1962); Bower, G. W., and L. W. Frost, *Preprints of Papers, Division of Polymer Chemistry, American Chemical Society*, **4**, 357 (1963); Sroog, C. E., S. V. Abramo, C. E. Berr, W. M. Edwards, A. L. Endrey, and K. L. Oliver, *Preprints of Papers, Division of Polymer Chemistry, American Chemical Society*, **5**, 132 (1964).
2. Stille, J. K., and T. Anyos, *J. Poly. Sci.*, **A2**, 1487 (1964).
3. Wagner-Jauregg, T., *Ber.*, **63**, 3224 (1930).
4. Van Alphen, J., *Rec. Trav. Chim.*, **61**, 892 (1942).
5. Kovacs, J., V. Bruckner, and I. Kandel, *Acta Chim.*, **1**, 230 (1951–1952).

J. K. STILLE
RICHARD A. MORGAN

Department of Chemistry
University of Iowa
Iowa City, Iowa

Received December 17, 1964

Observations of Polyethylene Forming on Large $TiCl_3$ Crystals

We have observed polyethylene forming on large crystals of titanium trichloride. The most active crystals were the thin sheets which had buckled a short time after the start of polymerization.

Observations were made using an optical microscope focused on the crystals contained in a reactor with special windows. Aluminum triethyl as a 25% solution in hexane was used as the co-catalyst. The crystals were prepared by subliming anhydrous, hydrogen-reduced titanium trichloride in an electric-gradient furnace. The crystals formed at the cold end of the subliming tube.

THOMAS B. LYDA
HOWARD F. RASE

Department of Chemical Engineering
University of Texas
Austin, Texas

Received December 17, 1964

A Manual of X-Ray Diffraction Patterns of Polymers

One hundred and fifty-six wide angle x-ray diffraction patterns of various synthetic polymers and a few modified natural polymers have been collected and published as a manual for use in routine diffraction analysis of polymers. The accompanying text includes a section on diffraction theory, a description of current views on the existence and nature of crystalline and noncrystalline regions in bulk polymer, and a discussion of the kinds of information available from the diffraction patterns. Scans were taken over a 2θ range of 5–60° using a Norelco diffractometer with filtered $CuK\alpha$ radiation ($\lambda = 1.5418$ Å.) and a Varian G-10 strip chart recorder. The patterns were reduced photographically to allow two per page. Each page has 2θ and d -spacing scales, and each pattern is identified with a chemical name, trade name if any, manufacturer's name, and a drawing of the idealized chemical structure.

Send requests for copies of the manual to the author at the address given below.

JUNE W. TURLEY

Chemical Physics Research Laboratory
The Dow Chemical Company
Midland, Michigan

Received March 10, 1965